

# **Fisheries Acoustics**

# **Fish and Aquatic Resources Series**

**Series Editor: Tony J. Pitcher**

*Fisheries Centre, University of British Columbia, Canada*

The *Blackwell Publishing Fish and Aquatic Resources Series* is an initiative aimed at providing key books in this fast-moving field, published to a high international standard.

The Series includes books that review major themes and issues in the science of fishes and the interdisciplinary study of their exploitation in human fisheries. Volumes in the Series combine a broad geographical scope with in-depth focus on concepts, research frontiers and analytical frameworks.

It is the aim of the editorial team that books in the *Blackwell Publishing Fish and Aquatic Resources Series* should adhere to the highest academic standards through being fully peer reviewed and edited by specialists in the field. The Series books are produced by Blackwell Publishing in a prestigious and distinctive format. The Series Editor, Professor Tony J. Pitcher is an experienced international author, and founding editor of the leading journal in the field of fish and fisheries. The Series Editor and the Publisher at Blackwell Publishing, Nigel Balmforth, will be pleased to discuss suggestions, advise on scope, and provide evaluations of proposals for books intended for the Series. Please see contact details listed below.

**Titles currently included in the series** (full details at [www.blackwellfish.com](http://www.blackwellfish.com)):

1. *Effects of Fishing on Marine Ecosystems and Communities* (S. Hall) 1999
2. *Salmonid Fishes* (Edited by Y. Altukhov *et al.*) 2000
3. *Percid Fishes* (J. Craig) 2000
4. *Fisheries Oceanography* (Edited by P. Harrison & T. Parsons) 2000
5. *Sustainable Fishery Systems* (A. Charles) 2000
6. *Krill* (Edited by I. Everson) 2000
7. *Tropical Estuarine Fishes* (S. Blaber) 2000
8. *Recreational Fisheries* (Edited by T.J. Pitcher & C.E. Hollingworth) 2002
9. *Flatfishes* (Edited by R. Gibson) 2005

---

For further information concerning books in the series, please contact:

**Nigel Balmforth, Blackwell Publishing, 9600 Garsington Road,**

**Oxford, OX4 2DQ, UK**

**Tel: +44 (0)1865 776868**

**e-mail: [nigel.balmforth@oxon.blackwellpublishing.com](mailto:nigel.balmforth@oxon.blackwellpublishing.com)**

# **Fisheries Acoustics**

## **Theory and Practice**

**Second Edition**

**John Simmonds**

*FRS Marine Laboratory, Aberdeen, Scotland*

**David MacLennan**

*FRS Marine Laboratory, Aberdeen, Scotland*

**Blackwell**  
Science

© 2005 by Blackwell Science Ltd  
a Blackwell Publishing company

Editorial offices:

Blackwell Science Ltd, 9600 Garsington Road, Oxford OX4 2DQ, UK

Tel: +44 (0) 1865 776868

Blackwell Publishing Professional, 2121 State Avenue, Ames, Iowa 50014-8300, USA

Tel: +1 515 292 0140

Blackwell Science Asia Pty Ltd, 550 Swanston Street, Carlton, Victoria 3053, Australia

Tel: +61 (0)3 8359 1011

The right of the Authors to be identified as the Authors of this Work has been asserted in accordance with the Copyright, Designs and Patents Act 1988.

All rights reserved. No part of this publication may be reproduced, stored in a retrieval system, or transmitted, in any form or by any means, electronic, mechanical, photocopying, recording or otherwise, except as permitted by the UK Copyright, Designs and Patents Act 1988, without the prior permission of the publisher.

First edition published by Chapman and Hall 1992

Second edition published by Blackwell Science 2005

ISBN-10: 0-632-05994-X

ISBN-13: 978-0-632-05994-2

Library of Congress Cataloging-in-Publication Data

Simmonds, E. John, 1952–

Fisheries acoustics: theory and practice/John Simmonds, David MacLennan. – 2nd ed.

p. cm.

Rev. ed. of: Fisheries acoustics/David N. MacLennan, E. John Simmonds. 1992.

Includes bibliographical references and index.

ISBN-10: 0-632-05994-X (hardback: alk. paper)

ISBN-13: 978-0-632-05994-2 (hardback: alk. paper)

1. Fishes – Detection. I. MacLennan, D. N. II. MacLennan, D. N. Fisheries acoustics III. Title.

SH344.2.S56 2005

639.2–dc22

2005005881

A catalogue record for this title is available from the British Library

Set in 10/13 pt TimesTen

by Newgen Imaging Systems (P) Ltd, Chennai, India

Printed and bound in Great Britain

by TJ International, Padstow, Cornwall

The publisher's policy is to use permanent paper from mills that operate a sustainable forestry policy, and which has been manufactured from pulp processed using acid-free and elementary chlorine-free practices. Furthermore, the publisher ensures that the text paper and cover board used have met acceptable environmental accreditation standards.

For further information on Blackwell Publishing, visit our website:

[www.blackwellpublishing.com](http://www.blackwellpublishing.com)

# Contents

<i>Series Foreword</i>	xii
<i>Preface</i>	xv
<i>Acknowledgements</i>	xvii
<b>1 Introduction</b>	<b>1</b>
1.1 A brief history	2
1.2 Synopsis	6
1.3 Acoustic terminology and symbols	9
<b>2 Underwater Sound</b>	<b>20</b>
2.1 Introduction	20
2.2 Sound waves	21
2.2.1 Pressure and displacement	22
2.2.2 Energy and intensity	23
2.2.3 Units	24
2.2.4 The decibel	24
2.3 Transducers and beams	26
2.3.1 The equivalent beam angle	32
2.3.2 Controlling the beam shape	33
2.3.3 End-fire transducer arrays	35
2.3.4 Limits to power transmission in water	35
2.4 Acoustic propagation	38
2.4.1 Beam spreading	38
2.4.2 Absorption	40
2.4.3 The sound speed	42
2.4.4 Pulses and ranging	46
2.5 Acoustic scattering	47
2.5.1 Targets large and small	48
2.5.2 Target strength	51
2.5.3 Standard targets	53
2.5.4 Target shape and orientation	56
2.5.5 Multiple targets	58
2.5.6 Volume/area scattering coefficients	59

2.5.7 Radiation pressure on targets	60
2.5.8 The inverse scattering problem	61
2.6 Echo detection	61
2.6.1 Reverberation	63
2.6.2 Noise	63
2.7 The operating frequency	65
Appendix 2A: Calculation of the acoustic absorption coefficient	67
Appendix 2B: Calculation of the speed of sound in water	68
<b>3 Acoustic Instruments</b>	<b>70</b>
3.1 Introduction	70
3.2 Echosounders	71
3.2.1 Scientific echosounders	74
3.2.2 The echo-integrator	74
3.2.3 The basic netsonde	76
3.2.4 The scanning netsonde	77
3.3 Instruments for measuring the target strength	79
3.3.1 The dual-beam echosounder	80
3.3.2 The split-beam echosounder	82
3.3.3 Resolution of single targets	84
3.4 Sonars	84
3.4.1 Searchlight sonar	85
3.4.2 Side-scan sonar	85
3.4.3 Sector scanners	88
3.4.4 Three-dimensional sonar systems	93
3.4.5 The Doppler effect	97
3.5 Wideband systems	98
3.6 Sound source location: pingers, transponders and hydrophone arrays	100
3.7 Installation of acoustic systems	102
3.7.1 Transducers on or near the vessel	102
3.7.2 Deep-towed bodies	104
3.7.3 Vessel noise performance	107
3.8 Calibration	108
3.8.1 The on-axis sensitivity	111
3.8.2 Experimental procedure	113
3.8.3 The TVG function	118
3.8.4 The equivalent beam angle	119
3.8.5 Overall sensitivity and the sound speed	120
3.8.6 Direction-sensing echosounders	121
3.8.7 Calibration of multi-beam sonars	124
3.8.8 Good calibration practice	126

---

<b>4 Biological Acoustics</b>	<b>127</b>
4.1 Introduction	127
4.2 Biological sounds	128
4.3 Hearing	129
4.3.1 Auditory detection capability	130
4.3.2 Masking and the critical bandwidth	133
4.3.3 Ultrasound and infrasound	137
4.4 Biological sonar	139
4.5 Environmental impacts	145
4.5.1 High-energy sound sources	145
4.5.2 Noise pollution	154
4.5.3 Limiting the damage	157
4.6 The swimbladder	158
<b>5 Observation and Measurement of Fish</b>	<b>163</b>
5.1 Introduction	163
5.2 Simple observation methods	164
5.2.1 Interpreting the echogram	164
5.2.2 Echosounder mapping	166
5.2.3 Side-scan sonar	171
5.2.4 Multi-beam sonar	174
5.3 Echo-counting	176
5.3.1 Single-target echoes	177
5.3.2 Range compensation	180
5.3.3 Single-beam echosounders	181
5.3.4 Direction-sensing echosounders	184
5.3.5 Thresholding and the sampled volume	185
5.3.6 Applications	186
5.4 Echo-integration	187
5.4.1 Range compensation	188
5.4.2 The echo-integrator equation	189
5.4.3 The linearity principle	191
5.4.4 Non-linear effects	194
5.4.5 Integration near the seabed	198
5.4.6 The threshold problem	201
5.4.7 Applications	202
5.5 Other techniques	203
5.5.1 Fixed sonar installations	203
5.5.2 Horizontal sonar for shallow water applications	205
5.5.3 Target tracking	209
5.5.4 Doppler sonar	210
5.5.5 Forward scattering	211

Appendix 5A: The true size distribution of fish schools	212
Appendix 5B: Calculation of the TVG error	215
<b>6 Target Strength of Fish</b>	<b>217</b>
6.1 Introduction	217
6.2 Target strength measurement techniques	218
6.2.1 Immobile fish	219
6.2.2 Live fish in cages	220
6.2.3 Wild fish	225
6.2.4 Modelling	229
6.3 Experimental results	233
6.3.1 Immobile fish	233
6.3.2 Live fish in cages	235
6.3.3 Wild fish	240
6.3.4 Size-dependence of target strength	243
6.3.5 Modelling	245
6.4 Discussion	246
6.4.1 Comparison of target strength measurement techniques	247
6.4.2 Classification of fish targets	248
6.4.3 Variation with fish size	250
6.4.4 Behaviour and physiology	253
6.5 Collected target strength data for survey applications	255
<b>7 Plankton and Micronekton Acoustics</b>	<b>262</b>
7.1 Introduction	262
7.2 Acoustic classification of plankton	264
7.3 Scattering models	266
7.3.1 FL class (soft fluid-like tissues)	268
7.3.2 ES class (elastic shell)	271
7.3.3 GB class (gas bearing)	273
7.3.4 Acoustic properties of fluid-like bodies	274
7.4 Target strength	276
7.5 <i>In situ</i> observation techniques	280
7.5.1 Abundance estimation	280
7.5.2 Size determination – the inverse problem	284
7.5.3 Species identification	290
7.5.4 Other methods of <i>in situ</i> observation	293
<b>8 Survey Design</b>	<b>294</b>
8.1 Introduction	294
8.2 Survey strategic decisions	295
8.2.1 The geographical area	296
8.2.2 Working time	297

---

8.3	Survey design options	299
8.3.1	Survey objectives	299
8.3.2	Stratification of effort	300
8.3.3	Proportions of time allocated to transects and trawls	301
8.3.4	Pre-planned track options: systematic or random designs	303
8.3.5	Pre-planned track options: parallel or triangular designs	309
8.3.6	Number of transects	311
8.3.7	Transect direction	311
8.3.8	Mapping the cruise track	312
8.4	Riverine surveys	314
8.5	Adaptive surveys	318
8.5.1	The outline survey	318
8.5.2	Variable transect length	319
8.5.3	Increased transect density	319
8.5.4	Randomized extra transects	320
8.6	Multi-ship surveys	322
8.7	The EDSU	324
8.8	More specialized surveys	324
8.9	Performance tests	325
8.9.1	Live-fish calibration	325
8.9.2	Inter-ship comparison	326
<b>9</b>	<b>Data Analysis</b>	<b>329</b>
9.1	Introduction	329
9.2	Processing the echograms	331
9.2.1	Classifying or partitioning the echo-integrals	331
9.2.2	Quality control of echogram data	336
9.3	Species composition	337
9.3.1	Analysis of fishing samples	338
9.3.2	Length-frequency distributions	339
9.3.3	Proportions by species	340
9.3.4	Selection of homogeneous regions	341
9.4	The echo-integrator conversion factor	343
9.4.1	Single species	344
9.4.2	Mixed species	345
9.4.3	Number-weight relationships	345
9.5	Abundance estimation	346
9.5.1	Spatial estimates and statistical concepts	347
9.5.2	Contour and distribution maps	349
9.5.3	Estimation with a rectangular grid	351
9.5.4	Transform methods	352
9.5.5	Geostatistics	354

9.6	Precision of the abundance estimate	355
9.6.1	Repeated surveys	356
9.6.2	Stratified random transects	357
9.6.3	Geostatistical variance	358
9.6.4	The degree of coverage	359
9.6.5	Bootstrap or resampling methods	361
9.6.6	Relative importance of various random errors	362
9.7	Sources of systematic error	363
9.7.1	Equipment sensitivity	363
9.7.2	Transducer motion	363
9.7.3	The surface bubble layer	365
9.7.4	Hydrographic conditions	367
9.7.5	Fish migration	368
9.7.6	Diurnal behaviour rhythms	370
9.7.7	Avoidance reactions	371
9.7.8	Precision of the estimated species proportions	373
9.8	Accuracy of the abundance estimate	374
9.8.1	Intrinsic error analysis	375
9.8.2	Comparison with other methods	377
<i>References</i>		380
<i>Species Index</i>		417
<i>Author Index</i>		420
<i>Subject Index</i>		429

*Colour plate section falls after page 238*

# Series Foreword

*'... The sound must seem an echo to the sense'*  
(*Sound and Sense* by Alexander Pope, 1688–1744)

Fish researchers (a.k.a. fish freaks) like to explain, to the bemused bystander, how fish have evolved an astonishing array of adaptations, so much so that it can be difficult for them to comprehend why anyone would study anything else. Yet, at the same time, fish are among the last wild creatures on our planet that are hunted by humans for sport or food. As a consequence, today we recognize that the reconciliation of exploitation with the conservation of biodiversity provides a major challenge to our current scientific knowledge and expertise. Even evaluating the trade-offs that are needed is a difficult task. Moreover, solving this pivotal issue calls for a multidisciplinary convergence of fish physiology, biology and ecology with social sciences such as economics and anthropology in order to probe the frontiers of applied science. In addition to food, recreation (and inspiration for us fish freaks), it has, moreover, recently been realized that fish are essential components of aquatic ecosystems that provide vital services to human communities. Sadly, virtually all sectors of the stunning biodiversity of fishes are at risk from human activities. In fresh water, for example, the largest mass extinction event since the end of the dinosaurs occurred as a result of the introduction of Nile perch to Lake Victoria, which eliminated over 100 species of endemic haplochromine fish. But, at the same time, precious food and income from the Nile perch fishery was created in a miserably poor region. In the oceans, we have barely begun to understand the profound changes that have accompanied a vast expansion of human fishing over the past 100 years. The Blackwell Publishing *Fish and Aquatic Resources Series* is an initiative aimed at providing key, peer-reviewed texts in this fast-moving field.

How many fish are in the sea? This question has always been important, but today has added relevance as we realize how fishing has devastated ocean resources. Most standard methods of counting fish end up killing them with nets, traps or hooks. Photography or visual counts can be used, but the clear waters necessary are rare. Examining the characteristics of reflected sound waves in an analogous way to radar is a smart alternative because it is non-lethal, works in turbid waters, covers vast areas and can be very cost-effective compared to catching the fish. To use the words of Douglas Adams (1979), analysing echoes is ‘mostly harmless’, and so ways of encouraging its use should be supported.

This book on *Fisheries Acoustics*, written by two of the world's leading practitioners, reviews the fundamental principles and practical techniques by which acoustic echoes are transformed into measurements of fish schools and stock biomass, with descriptions of the various types of hardware and software employed.

A brief review of the use of underwater sound, going back to Leonardo da Vinci listening down a tube for the sound of distant ships, is followed by a history of how acoustics came to be used to estimate the biomass of fish. Echograms were used for locating fish schools in the 1930s, but rapid improvements in sonar technology during the Second World War led to the first quantitative estimates of fish abundance in the 1950s. Echo integration methods, split-, dual- and multi-beam devices soon followed. The book goes on to provide an explanation of the theory of sound underwater, presenting rigorous and standardized descriptors of its characteristics. It contains a valuable synoptic review of how fish species, size and behaviour can affect target strengths and outlines calibration procedures for fisheries acoustic gear. Two chapters thoroughly review the fundamentals of geostatistical analysis for the design and interpretation of fisheries acoustic surveys.

It is not only fish that may be studied with underwater acoustics. At one end of the size spectrum, small plankton, which have a wide range of acoustic properties due to whiskers, elastic or gelatinous bodies and gas-filled buoyancy bladders, are measured using variations in sound speed rather than target strengths. Multi-beam sonar can provide three-dimensional images for recording behaviour. At the very large end of the size spectrum, marine mammals, which are extremely mobile and produce their own complex acoustic signals, have also been studied using acoustics.

Underwater acoustic devices are not only valuable for quantifying the amount of fish present; acoustic records that are almost as detailed as optical film have been employed to support behavioural and evolutionary studies. For example, high resolution multi-beam, side-scan sonar enabled the documentation of the anti-predator tactics of Norwegian herring schools under attack by cod and saithe (Pitcher *et al.* 1996), by orcas (Nøttestad and Axelsen 1999) and even by fin whales (Nøttestad *et al.* 2002). In the future, this book suggests that developments in sonar will make the seas even more transparent.

The first version of this book, published in 1992, rapidly became the standard resource text for anyone considering the use and application of acoustics in fisheries. Thirteen years later, this revised, expanded, reorganized and updated text will surely soon be regarded as the definitive reference work on fisheries acoustics.

Professor Tony J. Pitcher  
*Editor, Blackwell Publishing Fish and Aquatic Resources Series*  
*Fisheries Centre, University of British Columbia, Vancouver, Canada*

## References

- Adams, D. (1979) *The Hitchhiker's Guide to the Galaxy*. Heinemann, London.
- Nøttestad, L. and Axelsen, B.E. (1999) Herring schooling manoeuvres in response to killer whale attacks. *Canadian Journal of Zoology* **77**, 1540–46.
- Nøttestad, L., Fernö, A., Mackinson, S., Pitcher, T.J. and Misund, O.A. (2002) How whales influence herring school dynamics in a cold front area in the Norwegian Sea. *ICES J. Mar. Sci.* **59**, 383–400.
- Pitcher, T.J., Misund, O.A., Fernö, A., Totland, B. and Melle, V. (1996) Adaptive behaviour of herring schools in the Norwegian Sea as revealed by high-resolution sonar. *ICES J. Mar. Sci.* **53**, 449–52.

# Preface

This book has been written primarily for postgraduate students, professional scientists active in fishery research and administrators concerned with fishery management. It provides a broad description of the underlying theory and practical considerations in the use of underwater sound for the study of fish (and other lifeforms) in water. We present it hopefully as a comprehensive introduction particularly for those starting in the field of fisheries acoustics who might want a broad basis from which to move their careers forward.

It is now more than 12 years since the publication of our first textbook on fisheries acoustics (MacLennan and Simmonds 1992). That seemed at the time to say everything that should be said on the subject. However, as in most areas of technology, much has changed since then. It has taken much more work and time than we would have imagined to provide this volume. Modern sonars are now highly sophisticated compared to the earlier generation, computer processing has provided great opportunities, new applications have emerged for the study of plankton and mammals as well as fish, and there is now much better understanding of how to interpret acoustic observations of aquatic life in a rigorously scientific manner.

These developments are reflected in the large bibliography (around 770 references) which will be found at the end of the present volume. Some of the citations are in what is commonly known as the 'grey' literature. These can be rather variable in quality, but in some cases important findings have emerged from scientific working groups and meetings which were only documented informally. We felt the bibliography should be a comprehensive record, for the benefit of readers who wish to explore the subject in more detail than has been possible here, within the constraints of producing a volume of reasonable size. Therefore, we have cited various informal documents (which should nevertheless be accessible through institutional libraries or other sources), in cases where important findings have been reported but not in the peer-reviewed literature. While providing the necessary links to the literature, we have tried to restrict references to the key texts, giving readers a good place to start rather than a long string of references to choose from. Modern bibliographic systems allow simpler and faster means of information retrieval, but the drive to publish has greatly increased the volume of text that the reader must sift through. Our references are therefore provided as an introduction to the literature rather than a fully comprehensive review.

Notwithstanding the many developments and innovations that have arisen in recent years, some aspects of fisheries have not changed that much. Many fish stocks continue to be over-exploited and the goal of sustainable fishery management remains elusive (though in some cases, particularly the herring which are surveyed with acoustics, the stocks are doing better than many e.g. the gadoids which are not accessible to acoustics). There is much concern about the environmental impact of fishing and other human activities in the sea. Proper attention to these problems calls for scientific knowledge that must come from well designed and competently executed research programmes. To the extent that acoustic methods can and do make an important contribution, we hope this book will help to promote better understanding between the scientists and others concerned with fisheries, recognizing that they have many objectives in common.

*John Simmonds  
David MacLennan*

# Acknowledgements

A large number of people have provided material to help with this book. In particular, many of the illustrations and photographs from papers were helpfully provided in original form by the authors. We would like to thank the staff at the Marine Lab, especially those actively involved in acoustics – Paul Fernandes, Dave Reid, Phil Copland and Eric Armstrong – who all helped us so much with discussion and advice over the years. Also Barbara Laurence and Jackie Brown who extracted and copied references, typed the older references into our (very large) citation index and helped with the indexing file. Others who assisted with specific pieces of work or illustrations are acknowledged throughout the book. We also extend general thanks to the members of the ICES Fisheries Acoustics Science and Technology Working Group who have contributed so much to the ongoing development and understanding of fisheries acoustics, in particular the recent chairpersons Dave Demer, Francois Gerlotto, Kjell Olsen and the sadly missed Jim Traynor who died prematurely in 1998. We greatly appreciate the specific assistance of three others, John Horne who provided artistic illustrations of the KRM model output but also offered his students as a sure way of critically evaluating our drafts (though we never managed to take up the offer), Van Holliday who explained the mysteries of plankton acoustics, and Ron Mitson who collated and provided the data on vessel noise at a time when he was feeling rather unwell. Finally, we acknowledge the fact that this book would not have been written without the steadfast support and encouragement of our long-suffering families who never complained about the cost of the midnight oil.

# Chapter 1

## Introduction

The living resources of the sea and fresh waters have long been an important source of food and, more generally, of economic activity in both industrial and artisanal societies. Their exploitation in a rational manner is rather problematical, to say the least. Too often, fisheries have suffered from boom-and-bust cycles, or even worse, catastrophic failures when fish stocks collapse (Beveton 1990). The environmental impact of fishing is another area of increasing concern, raising issues of species diversity, habitat destruction and damage to non-target populations (notably the marine mammals). Further discussion of these problems is not appropriate here, except for one important factor: long-term success in fishery management depends on knowledge of the exploited population, the size and distribution of which may change unpredictably from year to year. Much of this knowledge comes from the investigation of fish in their natural environment. This book is primarily about acoustic techniques which have been developed for the remote observation and monitoring of aquatic lifeforms.

At the wavelengths of human vision, light does not penetrate more than a few metres below the water surface, and much less when the medium is loaded with suspended solids or biota such as plankton. However, sound waves travel much longer distances through water. Thus acoustic instruments which transmit and receive sound waves can be used to detect fish or other objects far beyond the range of vision. Consequently, acoustic technology has had a major impact on fishing. The information provided by sonars and echosounders is an important factor in the efficiency of modern fishing operations. Purse seining and pelagic trawling are two methods which depend on the skilful interpretation of acoustic images to ensure success.

In fisheries research too, acoustic techniques have become increasingly sophisticated and useful over the years. With sonar it is possible to search a large volume of water in a short time; other sampling methods such as trawl fishing are very slow by comparison. Acoustic echoes may be observed from fish anywhere in the water column, except in the near-surface region and just above the seabed. Sonar has contributed greatly to our understanding of life in the sea and fresh waters, especially how wild populations are distributed in space and how they change with time. There is a large and expanding literature in fisheries acoustics. Practical applications are many and varied. For general background on particular topics, see Gunderson (1993) on survey methods, Fréon and Misund (1999) on fish behaviour, Mitson (1983)

on fishing technology, Medwin and Clay (1998) on acoustical oceanography (which includes *inter alia* much on plankton acoustics) and Richardson *et al.* (1995) on marine mammals.

The measurement of fish abundance is an especially important application of acoustics in fisheries research (Gunderson 1993). Fishery management, as currently practised by most authorities, depends on controlling the quantity caught in relation to the size of the exploited population (Gulland 1983). To do this, it is necessary to estimate the current size (abundance) of the population, or that in the recent past. One approach to this problem is to conduct an acoustic survey. This involves running transects of some area while recording the echoes from fish detected by echosounder or sonar, and the abundance is estimated as the quantity of fish which would be expected to produce such echoes. However, the technique of acoustic survey is useful only when the fish of interest are conveniently located. They must not be too close to the surface or the bottom, where the fish echoes are obscured by much stronger reflections from these boundaries. Thus acoustic methods of observation are unsuited to the flatfish and other species which live in close association with the seabed, but many important species are found in midwater, far enough away from interfering boundaries. These include the herring family (Clupeidae), the mackerels (Scombridae), the anchovies (Engraulidae) and the salmonids (Salmonidae). In appropriate circumstances, an acoustic survey provides a synoptic estimate of the abundance which is independent of the fishery.

Sound also has a natural importance for the fish and mammals that live in water. They use it as a means of communication, navigation, the detection of prey and the avoidance of predators. It is therefore pertinent to consider the extent to which anthropogenic noise disturbs the natural behaviour of aquatic animals. These aspects of underwater acoustics have also been the subject of much research (Hawkins 1993; Richardson *et al.* 1995; Heathershaw *et al.* 2001).

## 1.1 A brief history

References to underwater sound can be traced back as far as mediaeval times. Urick (1983) mentions a notebook, dated 1490, in which Leonardo da Vinci observed that by listening to one end of a long tube, with the other end in the sea, ‘you will hear ships at a great distance’. The speed of underwater sound, about  $1450 \text{ m s}^{-1}$  in fresh water, was first measured by Colladon and Sturm in 1827. They simultaneously transmitted a flash of light and the sound of an immersed bell across Lake Geneva in Switzerland, and deduced the sound speed from the time delay between the received signals. However, practical applications had to await more advanced technology, notably the piezo-electric transducer which was invented by the French physicist Langevin in 1917. As a result of research motivated by the First World War, it was discovered that submarines could be detected by listening for the echo of a sound transmission. The term ‘echosounding’ first appeared in the 1920s, referring to the technique of

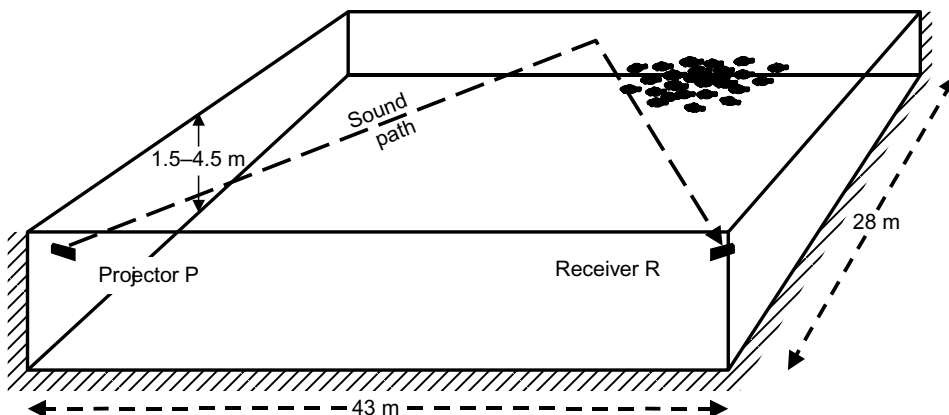


**Fig. 1.1** Apparatus used by Kimura (1929) in the first acoustic detection of fish. Sound from the projector P is reflected by the far side of the pond (1.5–4.5 m deep) and detected by the receiver R. Fish passing through the beam cause the amplitude of the received signal to fluctuate.

measuring water depth from the time delay of a two-way transmission between the surface and the bottom (Anon 1925).

The French navigator Rallier du Baty (1927) described unexpected sounder signals originating in midwater, which he attributed to echoes from fish schools, a possibility first mentioned by Portier (1924). The first successful experiment on the acoustic detection of fish was reported by Kimura (1929). He installed a transmitter and a separate receiver in a fish-cultivation pond. The sound was transmitted in a 20° beam and detected after reflection from the opposite side of the pond as illustrated in Fig. 1.1. The transmission was continuous at 200 kHz frequency, with the amplitude modulated at 1 kHz so that the rectified signal was audible. The pond contained a school of *Pagrosomus major*, about 25 fish of length 40–50 cm. Kimura recorded the received sound by photographing the waveforms displayed on an oscilloscope (Fig. 1.2). He found that the amplitude was noticeably disturbed when fish were in the beam, although reliable detection depended on the surface of the pond being flat calm. In this experiment, the fish were detected by the fluctuation of the forward transmission caused by their movement. However, it soon became obvious that the alternative ‘monostatic’ arrangement, with the same transducer used for transmission and reception, is a more practical way to observe fish in the wild.

Further advances came with the development of the recording echosounder which produced echograms on paper (Wood *et al.* 1935). Once this device became commercially available at a reasonable cost, it had obvious potential as a fishing aid. From 1933 onwards, the British skipper Ronnie Balls experimented with an echosounder on his herring drifter ‘Violet and Rose’, though he only reported the work later (Balls 1946; 1948). The Norwegian Reinert Bokn, skipper of the seiner ‘Signal’, was conducting similar investigations at much the same time. Bokn is credited with the first example of a fish echogram to be published (Fig. 1.3). He fished on the near-surface

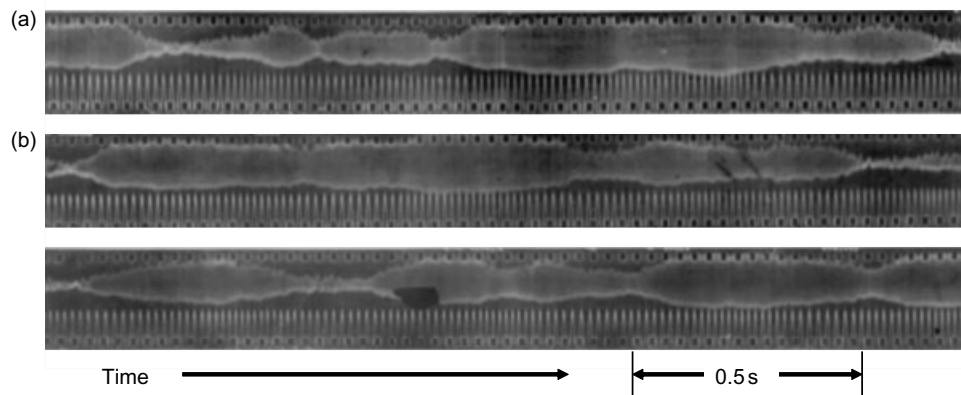


**Fig. 1.2** Three sections of photographed oscillosograms, from Kimura (1929). Each section shows two traces; the upper one (a) is the received acoustic signal, perturbed by the passage of fish through the beam; the lower one (b) is a constant 60 Hz signal giving a time reference.

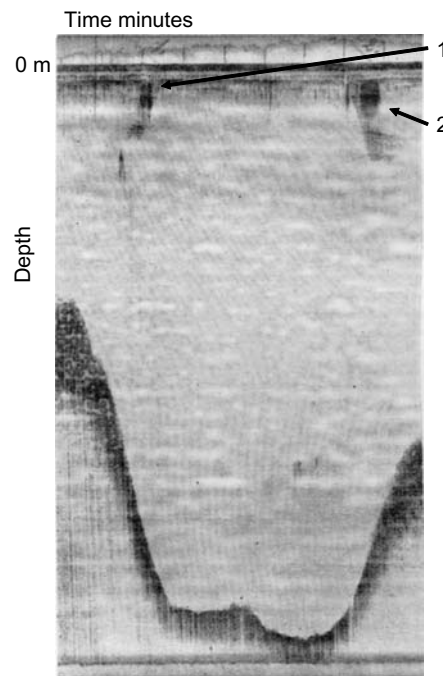


**Fig. 1.3** Early example of fish detection by an echosounder, from Anon (1934), recorded by Reinert Bokn in Frafjord, Norway. The horizontal line at the top is the sea surface. A near-surface fish school is first detected at position (1). Then the boat turns and re-locates the same school at position (2). A seine cast at this location gave a catch of 400 bushels (15 tonnes) of sprat.

marks and showed they were schools of sprat *Sprattus sprattus* (Anon 1934). Other Norwegian investigators made notable contributions, especially Sund (1935) who published echograms of the cod, *Gadus morhua*, using a 16 kHz echosounder with a magneto-strictive transducer on the research vessel 'Johan Hjort'. This equipment revealed many unsuspected features of the fish distribution, notably that the cod

were confined to a narrow layer 10 m thick at a constant depth below the surface. Two years later, the Norwegians were even conducting acoustic surveys to chart the geographic distribution of herring schools (see Runnstrom 1937).

There was another period of rapid development during the Second World War, after which fishers soon discovered the civilian potential of the acoustic techniques developed by the military (Hodgson 1950; Hodgson and Fridriksson 1955). The power and resolution of sonars continued to improve as new instruments were designed specifically for fish detection. Many different kinds of sonar are now employed in fishing, from the simple echosounder to scanning sonars which provide radar-like images of detected targets, and transducers on trawls which locate the net relative to the seabed and fish schools. The multi-coloured echogram gives a clearer perception of the signal strength, compared to the original monochrome display, while the concurrent use of two or more frequencies gives the user more information about the detected targets. Fishers have exploited these developments with great skill, especially in pelagic fishing where efficient searching for schools and accurate deployment of the gear are essential to success.

Acoustic methods of fish abundance estimation were first investigated in the 1950s. Initially these were based on simple ideas of counting individual echoes (Tungate 1958; Mitson and Wood 1962), or summing the echo amplitudes (Richardson *et al.* 1959). The latter is essentially the technique of echo integration, attributed to the Norwegian Ingvar Hoff, as described by Dragesund and Olsen (1965). However, Scherbino and Truskanov (1966) showed that the correct approach is to integrate the echo intensity, not the amplitude, and that remains a fundamental principle of fish abundance estimation. In the early days, the results that could be obtained were subject to large errors. The calibration methods of the time were imprecise, and the target strength of fish was uncertain. Intensive theoretical and experimental investigations in the 1970s and 1980s led to a better understanding of what acoustic techniques could and could not do. High-performance scientific echosounders were introduced with digital signal processing, giving larger dynamic range, more stable gain characteristics and better compensation of the propagation losses. Calibration is no longer a limiting factor, provided it is done in the recommended way (Foote *et al.* 1987). New techniques evolved for measuring the target strength of fish *in situ* (i.e. in their natural environment), notably the dual-beam and split-beam echosounders, although it has to be said that the uncertainty of target strength is still a significant error factor (among others) in acoustic abundance estimation. Nevertheless, the progressive development of scientific instrumentation, scattering theory and data analysis techniques brings us to the present state of the art: acoustic methods have greatly advanced our understanding of fish and fisheries. In particular, surveys using echo integrators or echo counters are in many cases an essential part of fish stock assessment.

Much of the fisheries-related work on acoustics, over the past 50 years or more, has been promoted by the International Council for the Exploration of the Sea (ICES) through various working groups and conferences that brought together experts from

the many disciplines involved. Historical reviews that highlight the ICES contribution will be found in Fernandes *et al.* (2002) and Rozwadowski (2002).

## 1.2 Synopsis

This book is an update of our previous text on fisheries acoustics (MacLennan and Simmonds 1992) and it follows a similar structure. A major addition is the new Chapter 7 which recognizes the importance of recent developments in plankton acoustics. Chapters 2 and 5 cover the basic principles of fish detection which are largely unchanged. Chapter 3 describes modern acoustic instruments whose capabilities have advanced by leaps and bounds over the past decade. Chapter 4 on biological acoustics contains new material on the environmental impact of anthropogenic noise. The changes to Chapter 6 reflect the considerable work done on modelling the target strength of fish, and the many experimental investigations conducted over the past 15 years. Chapters 8 and 9 are concerned with, respectively, the design of acoustic surveys and the subsequent analysis of the results. Again, there have been substantial advances to report, especially in the evaluation of errors in acoustic estimates of fish density and abundance.

We have described the physics of underwater sound to the extent necessary to show the advantages and disadvantages of acoustic methods in fishery investigations. Bearing in mind that many readers will have a background in the biological sciences, and may be less familiar with mathematics, we have tried to explain the subject in words and illustrative graphics, to reduce the reliance on mathematical shorthand which is rather too common in acoustic publications. However, some theory is essential for the proper understanding of underwater sound, the nature of fish as acoustic targets and the statistical problems which are common to any kind of survey. A collected list of symbols is provided in Section 1.3. Throughout this book, the emphasis is on acoustics as an applied science. Practical advice is given on the use of acoustic instruments in the field and the solution of problems which are often ignored by those who prefer the purely theoretical approach.

Chapter 2 is an introduction to the concept of energy transmission by sound waves and the remote detection of targets. We discuss the generation of sound by transducers, the propagation of waves, the scattering properties of targets and the formation of echoes. The competing requirements of resolving close targets and detection at long range are considered in relation to the frequency of the sound waves and the limits imposed by ambient noise in the ocean.

The operating principles of modern acoustic instruments are described in Chapter 3. The basic echosounder or sonar transmits sound in a single beam. This permits the range but not the direction of targets to be determined, although two-dimensional mapping is achieved when the sonar is on a moving vessel. More sophisticated devices are capable of angular resolution. They include the dual-beam, split-beam, multi-beam and sector-scanning sonars that are now used extensively.

The full three-dimensional imaging of targets is possible using new types of sonar that are currently progressing from the experimental stage to full commercial implementation. The multi-frequency sonar is another important development. This offers the possibility of identifying targets from the spectrum of echoes, however, truly wideband systems are still at an early stage of development. The calibration of acoustic instruments is discussed with reference to scanning sonars as well as echosounders. Practical advice is given on how to perform the calibration in accordance with internationally accepted standards.

In Chapter 4, we review various topics to do with the physiology and the behavioural importance of sound for life in the sea and fresh waters. We discuss the sensitivity of hearing, the production of sound by animals and the remarkable sonar capability of the aquatic mammals. These natural phenomena must be understood to assess the environmental impact of anthropogenic sounds which range from low-amplitude noise pollution to the shock waves produced by explosive devices. The biological consequences of noisy human activities are discussed, and we show how the impacts in terms of behavioural changes and physiological damage can be assessed. Theoretical models for predicting the strength of shock waves and the mortality of exposed fish are reviewed. Another biological topic (of a less sensitive nature) is the phenomenon of swimbladder resonance. This has potential as a means of determining fish size from the echo spectra observed at low frequencies.

Chapter 5 is concerned with the observation and measurement of fish, or in other words how to interpret the information provided by acoustic instruments. We begin with the simple echogram and the technique of school-counting. The measurement of fish density calls for more advanced techniques, notably echo-counting and echo-integration. The density is supposed to be proportional to the integral of the echo energy returned from the depth channel of interest. This assumption depends on the linearity principle which is central to the theory of fisheries acoustics. The evidence in support of linearity is discussed, and the particular conditions (e.g. very dense aggregations of fish) in which it might not apply. We describe various other acoustic techniques which can provide useful information on the behaviour, distribution and abundance of fish.

The target strength of fish is reviewed in Chapter 6. Experimental techniques for measuring the target strength are described. In addition, theoretical models of acoustic scattering have given useful insights through better interpretation of experiments and understanding the physical principles that determine the target strength. The swimbladder is the dominant sound reflector in those species which have one. Accordingly, fish targets may be classified in groups of species having similar acoustic properties, according to the type of swimbladder possessed. Within each category, fish of the same size have similar target strengths on average, but there is much residual variation which emphasizes the stochastic nature of target strength. The dependence of the target strength on the fish size is an important consideration. This is normally expressed in terms of the fish length, through the so-called target-strength function. The importance of fish behaviour and physiology in explaining

the variability of target strength is discussed. Published experimental results are presented in tables arranged to provide easy means of reference.

Chapter 7 begins with the classification of plankton as acoustic targets. Three broad classes are identified – FL (fluid-like), ES (elastic shell) and GB (gas bearing). Theoretical scattering models are especially important here; without these it is difficult to relate the target strength to the size of very small animals. Various models and approximate solutions are described. For the FL plankton, model calculations depend on the density and sound speed contrasts in the body. Measurement techniques and current knowledge of these parameters are reviewed. The target strength is still a useful descriptor of large plankton like the Antarctic krill, and the results of theoretical and experimental studies are presented. The traditional method of abundance estimation (based on the size dependence of target strength) has been applied to krill, but more sophisticated methods are generally required for plankton. The concurrent use of several frequencies gives information on the size distribution as well as the abundance, provided the model assumptions are reliable. Some progress has been made on the identification of species from their echo characteristics, but in many cases this still depends on the collection of samples by fishing. Various acoustic methods for observing the behaviour of plankton are discussed, particularly the use of multi-beam sonar to provide three-dimensional images.

The last two chapters (8 and 9) deal with the practice of acoustic surveying to measure the abundance and distribution of fish. The emphasis is on the practical problems that arise in applying the theoretical principles discussed earlier. In Chapter 8, we consider the design of the cruise track and the sampling strategy to make the best use of the available time. We discuss the balance of time between running transects to record acoustic data and other activities such as fishing to identify the echo traces. We give examples of inter-ship comparisons which test the overall performance of the survey equipment in the field, although they are not a substitute for the recommended calibration procedure. In Chapter 9, we discuss the analysis of the data collected during the survey. The aim is to calculate abundance estimates within defined confidence limits. First, the echo-integrals must be partitioned between species, and the surveyed area may be stratified depending on the stationarity of the fish density. An echo-integrator conversion factor is calculated for each species and stratum from which the density samples are obtained. The total abundance is estimated from the observed densities. There are a number of approaches to this problem, which is complicated by the statistics of spatial correlation. We describe contour mapping, geostatistics and numerical methods based on rectangular grid strata. The various factors which contribute error are discussed and we show how the overall accuracy of the abundance estimate can be assessed. The results obtained from acoustic surveys are compared with those of alternative methods, again to indicate the accuracy that can be expected in typical circumstances.

In compiling the references, we have concentrated on the many publications which have appeared in the past 35 years or so, avoiding obsolete material but including key references to earlier work that laid the foundations of modern fisheries acoustics.

A useful source of earlier reference material can be found in Venema (1985) which is a selected bibliography of publications relating to fisheries acoustics.

### 1.3 Acoustic terminology and symbols

There has been much confusion over the years about the precise meaning of terms such as the ‘acoustic cross-section’ of a target. In this book, we use the standard terminology and symbols for fishery applications recommended by MacLennan *et al.* (2002). In particular, readers should note that the acoustic reflectivity of a target is normally described by the backscattering cross-section,  $\sigma_{\text{bs}}$ . This is an important change from the treatment in MacLennan and Simmonds (1992) which was based on the spherical scattering cross-section,  $\sigma_{\text{sp}}$ . Thus some of the equations in this book have a different formulation, but they accord with what is now regarded as standard practice in fisheries acoustics. If formulas or data from older publications are being used, it is important to be clear about the units relevant to acoustic scattering parameters. Mistakes in this area can result in very large errors.

This following list defines the mathematical symbols used in this book. They mostly follow current practice and should have a similar interpretation elsewhere in the acoustics literature (MacLennan *et al.* 2002). Some are uniquely defined and may occur in several chapters (the common symbols). Others are specific to one chapter and are listed as such. Occasionally, the same symbol has alternative definitions, but the meaning in each case is always defined in nearby text.

#### **Common symbols**

c	Sound speed in water
CV	Coefficient of variation (the standard error divided by the mean)
EBA	Equivalent beam angle of a transducer, in dB relative to 1 steradian
f	Frequency (cycles per second)
$\bar{g}$	Time-varied-gain (TVG) correction factor
I	Intensity of a sound wave (power transmitted per unit area)
J	Flux of a sound or shock wave (energy transmitted per unit area)
k	The wavenumber, equal to $2\pi/\lambda$
L	Body length of a scatterer (normally the total length in the case of fish)
$L_{\text{bs}}$	Backscattering length of a target (a complex variable, $\sigma_{\text{bs}} =  L_{\text{bs}} ^2$ )
p	Instantaneous pressure amplitude of a sound wave
$s_a$	Area scattering coefficient (units $\text{m}^2/\text{m}^2$ )
$s_A$	Nautical area scattering coefficient, equal to $4\pi(1852)^2 s_a$
$s_v$	Volume backscattering coefficient (linear measure)
$S_v$	Volume backscattering strength (log measure, in dB re $1 \text{ m}^{-1}$ )
S	Salinity of water

SE	Standard error (the standard deviation of the sample mean)
SNR	Signal-to-noise ratio (expressed in dB)
SL	Source level, dB measure usually re $1 \mu\text{Pa}$ at 1 m from the source
t	Time (exception in Chapter 9)
T	Water temperature
TS	Target strength of one scatterer, a logarithmic measure of $\sigma_{\text{bs}}$
TS <sub>kg</sub>	Target strength normalized to 1 kg weight of scatterers
v	Particle velocity associated with a sound wave
Z	Acoustic impedance of a medium, equal to the density times the sound speed
$\alpha$	Acoustic absorption coefficient in dB per unit distance
$\beta$	Acoustic absorption coefficient in nepers (1 Np = 8.686 dB) per unit distance
$\Phi$	The impulse (integral of pressure w.r.t. time) transmitted by shock waves
$\eta$	Phase difference between two signals
$\lambda$	Wavelength, distance between successive peaks of a sound wave
$\rho$	Density of water
$\sigma(\theta, \phi)$	Differential scattering cross-section, defines scattering in direction $(\theta, \phi)$
$\sigma_{\text{bs}}$	Backscattering cross-section, same as $\sigma(\theta, \phi)$ for $\theta = -\pi$ and $\phi = 0$
$\sigma_{\text{sp}}$	Spherical scattering cross-section, equal to $4\pi \sigma_{\text{bs}}$
$\sigma(\omega)$	Backscattering cross-section at frequency $\omega$
$\tau$	Duration of a sonar transmission pulse, time from start to finish
$\psi$	Equivalent beam angle of a transducer in steradians
$\omega$	Angular frequency (radians per second)

## ***Chapter 2***

a	Radius of a sphere, or the side of a square
b	The beam pattern; function of direction describing the amplitude sensitivity
B	Bandwidth of the sonar receiver
c <sub>1</sub>	Speed of longitudinal sound waves in a solid
c <sub>2</sub>	Speed of transverse sound waves in a solid
d	Characteristic linear size of a target
E	Energy
f <sub>0</sub>	Frequency of the sine waves within a pulse
f <sub>1</sub>	Frequency of the lowest resonance in a solid target
F	Form function (ratio of spherical scattering and geometric cross-sections)
I <sub>0</sub>	Intensity normalized to 1 m range
I <sub>bs</sub>	Intensity of the backscattered wave
I <sub>i</sub>	Intensity of the incident wave
I <sub>m</sub>	Mean intensity
L <sub>p</sub>	Pulse length in water

---

N	Number of targets, cycles etc.
$ p $	Amplitude of the sound pressure variation
$ p_0 $	Sound pressure amplitude normalized to 1 m range
$P_0$	Ambient pressure in the water
$p_{\text{rad}}$	Radiation pressure in the water (at a target)
$p_{\text{rms}}$	Root-mean-square (average) of the instantaneous sound pressure
$P(\omega)$	Power response of the sonar at frequency $\omega$
$r_b$	Reflection coefficient; proportion of incident energy reflected at a boundary
$r_{\text{dB}}$	Ratio of two intensities expressed in decibels
R	Range or distance
$R_b$	Range at the boundary between the near and far fields
$t_e$	Time between the transmitter pulse and the echo being received
$ v $	Amplitude of the particle velocity variation
$V_0$	Sampled volume
x	Distance along the propagation path, or a general variable
z	Depth below the water surface
$Z_r$	Acoustic impedance of a reflector
$Z_w$	Acoustic impedance of water
$\theta$	Angle from the acoustic axis
$\phi$	Azimuthal angle in the transducer plane
$\rho_1$	Density of a solid target
$\theta, \phi$	Angular coordinates of the scattering direction relative to the incident wave

### Chapter 3

a(t)	Ideal TVG function for exact range compensation
$A(t)$	Actual TVG function of an echosounder
$b_n$	One-way amplitude sensitivity of the narrow beam
$b_w$	One-way amplitude sensitivity of the wide beam
B	Two-way energy sensitivity of the transducer
$C_a$	Calibration factor for the on-axis sensitivity
$c_1$	Longitudinal sound speed in a standard target
$c_2$	Transverse sound speed in a standard target
$c_f$	Sound speed at the fish depth
$c_o$	Assumed sound speed (as entered in the sounder settings)
$c_s$	Sound speed at the transducer
$c_z$	Mean sound speed along the path between the transducer and the fish
d	Linear size of the transducer face
E	Echo-integral
$E_t$	Echo-integral of a standard target
$E_0$	Echo-integral of a target on the acoustic axis

$f_0$	Frequency of the echosounder or sonar transmission
$f_r$	Frequency of the received signal
$f_1$	First resonance frequency of the standard target
$F$	Area fish density (number or weight of fish per unit area of a depth layer)
$G_E$	Transducer gain when receiving
$G_T$	Transducer gain when transmitting
$I_n$	Echo intensity on the narrow beam of a dual-beam echosounder
$I_w$	Echo intensity on the wide beam of a dual-beam echosounder
$n$	Number of fish per unit volume
$P_o$	Output transmission power at the transducer terminals
$P_r$	Received power at the transducer terminals
$R$	Range of any target
$R_{opt}$	Optimum distance between the transducer and the standard target
$R_t$	Actual range of the standard target
$t_{del}$	Electronic delay in the receiver
$t_e$	Echo time delay corrected for $t_{del}$
$t_h$	Time at which the echo amplitude is half the peak value
$t_o$	Optimum start time of the ideal TVG function
$TS_t$	Target strength of the calibration sphere
$v_R$	Radial speed of a target relative to the sonar transducer
$V_B$	Variance of $B$ over the transducer beam
$V_s$	Sample variance of the observed backscattering cross-section
$V_\sigma$	True variance of $\sigma$ in the target population
$w_i$	Weight given to the $i$ 'th sensitivity measurement
$\Delta K$	Proportional change in the overall calibration factor (F/E)
$\Delta t$	Increment of time between successive elements of a time-delay scanner
$\Delta R_{ab}$	Difference in the path lengths from a target to receivers a and b
$\Delta \eta$	Phase difference between successive elements of a modulation scanner
$\Delta \omega$	Frequency shift between successive elements of a modulation scanner
$\Delta \Omega$	Element of solid angle
$(\theta, \phi)$	Angular coordinates of a direction w.r.t the transducer axis
$\theta_t$	Split-beam angle between the target and along-ship directions
$\phi_t$	Split-beam angle between the target and athwart-ship directions
$\eta_\theta$	Split-beam phase difference corresponding to $\theta$
$\eta_\phi$	Split-beam phase difference corresponding to $\phi$
$\langle \sigma_{bs} \rangle$	Mean backscattering cross-section per fish

## **Chapter 4**

a	Equilibrium radius of a gas bubble
ESR	Radius of a sphere having the same volume as the fish swimbladder
B	Critical bandwidth for noise masking of a pure tone
$B_r$	Critical ratio, an approximation to B

---

$f_i$	i'th frequency of narrow-band noise in a sequential presentation ( $i = 1, 2$ etc.)
$f_r$	Resonance frequency of the swimbladder or a gas bubble
$f_{\max}$	Upper frequency limit of hearing range
$f_0$	Frequency of sound for maximum hearing sensitivity
$f_{vp}$	Transition frequency between velocity and pressure hearing dependence
$K$	Species-dependent constant factor in equation for $f_r$
$P_0$	Ambient (undisturbed) pressure
$P_{\max}$	Peak pressure of an explosive shock
$P_{\min}$	Minimum pressure in the rarefaction after the shock front
$P_n$	Noise power per unit bandwidth
$P_t$	Power of a tone signal at the hearing threshold
$P_{rad}$	Radiation pressure on a reflecting surface
$P_{rms}$	Root-mean-square of the sound pressure
$Q$	Quality factor of the swimbladder resonance
$R$	Distance between two points
$R_{50}$	Distance from point of explosion within which at least 50% of fish die
$t_c$	Duration of a cetacean sonar click
$t_s$	Time constant for decay of the pressure shock
$t_b$	Arrival time of the first bubble pulse after the shock front
$W_f$	Weight of a fish
$W_e$	Weight of an explosive charge
$Y$	Mortality parameter in Baxter's model
$Y_{50}$	Value of $Y$ for 50% mortality
$z_f$	Depth of fish below the surface
$\Phi_{50}$	Pressure impulse causing 50% mortality of fish
$\gamma$	Ratio of the specific heats of a gas
$\sigma_r$	Backscattering cross-section of a target at frequency $f_r$
$\xi$	Swimbladder oscillation parameter

## Chapter 5

$a_o(t)$	Exact time-varied-gain (TVG) function at long range
$A_o$	True cross-sectional area of a fish school
$A_R$	Apparent cross-sectional area of a school at range $R$
$A_s$	Area covered by the survey
$A_1, A_2$	Amplitudes of sine waves
$A(t)$	Actual TVG function of the echosounder
$b$	Signal due to a scatterer of unit strength
$B$	Width of the observation band (for school-counting)
$B_r$	Transducer sensitivity in region $r$ of the beam pattern
$C$	Echo-integrator calibration factor
$d_i$	Apparent area-density of fish in layer $i$

---

D	Distance travelled
$e_j$	Echo-integral from the $j^{\text{th}}$ fish in isolation
$\bar{e}$	Average of several $e_j$
$E_i$	Echo-integral from one transmission
E	Echo energy, or the echo-integral averaged over many pings
$\bar{E}$	Average (sample mean) of the $E_i$
$\langle E \rangle$	Ensemble average (true mean) of $E_i$
F	Area fish density (number or weight of fish per unit area of a depth layer)
$F_v$	Volume fish density (number or weight of fish per unit volume of water)
$F_m$	True value of the area fish density (F) in the $m^{\text{th}}$ depth layer
$F_{(\text{obs})m}$	Observed value of $F_m$ (reduced by shadowing)
$F_{vc}$	Volume fish density ( $F_v$ ) when it is constant throughout a depth layer
$g(R)$	Time-varied-gain error at range R
$H_L$	Thickness of a fish layer
$H_m$	Height of a fish school observed on the echogram
$H_t$	True height of a fish school
$G(R)$	Range-dependent echosounder gain function
$G_e(R)$	Exact range-dependent function
$K_i$	Number of echoes in size-class i
$K_{rs}$	Constant coefficients for school-size calculation
$L_m$	Length of a school parallel to the survey track, as observed on the echogram
$L_t$	True length of a school parallel to the survey track
M	Number of echo-size classes, layers in a depth interval etc.
$n_i$	True number of schools or fish in class i
$n, N$	Number of transmissions, fish, schools etc.
$N_i$	Observed number of schools in size-class i
$N_{sch}$	Total number of observed schools
$N(x)$	Expected frequency of trace length x
$P_{sch}$	Proportion of surveyed area occupied by schools
Q	Quantity of fish in the surveyed area
$r_{cr}$	Critical school size above which multiple scattering is possible
R	Range from the transducer
$R_1, R_2$	Limits of a range interval
$R_b$	Range of the strongest echo, usually the seabed
$S_{vo}$	Threshold value of $S_v$ (signals less than $S_{vo}$ are not detected)
$t_1, t_2$	Limits of the time interval
u	Echo amplitude
$v(t)$	Echosounder output signal at time t
$v_1(t)$	Echosounder output with constant gain (no TVG)
$v(R, t)$	$v(t)$ due to one target at range R

---

V	Ship speed
$V(t)$	Transmitter output at time t
$V_{sch}$	Estimated total volume of fish schools
W	True width of a fish school
$W_i$	Width (or diameter) of a school in size-class i
$w_E(u)$	Probability of echo amplitude u
$w_F(u)$	Probability function for backscattering by fish
$w_T(b)$	Probability of observing b from a unit scatterer
z	Depth below the water surface
$z_1, z_2$	Limits of a depth interval
$Z_r$	r'th sensitivity region of the transducer beam pattern
$\varepsilon$	Width of a size class
$\phi$	Angle between the directions of first and last contact with a fish school
$\phi_0$	Nominal beam width (angle between the half-power points of the beam pattern)
$\phi_a$	Attack angle, direction (re acoustic axis) of first contact with a fish school
$\phi_d$	Detection angle, effective beam width for a fully insonified fish school
$\Gamma(x)$	Frequency of schools of trace-length x or more
$\Gamma_i$	Observed number of schools in class i or larger
$\langle \sigma_{bs} \rangle$	Mean backscattering cross-section per fish (ensemble average)
$\sigma_e$	Extinction cross-section of one fish
$\Omega_r$	Solid angle covering directions in region $Z_r$ of the transducer beam pattern

## Chapter 6

b	Constant in formulas relating target strength to fish length
$b_{20}$	Constant in formulas which assume '20 log L' length dependence
m	Constant multiplying 'log L' in formulas for target strength
$m_f$	Constant multiplying 'log f' in Love's formula for target strength
N	Number of independent measurements
$N_v$	Number of fish per sampled volume
$P(\sigma_{bs})$	Probability density function (PDF) of $\sigma_{bs}$
$TS_0$	Target strength of surface-adapted fish
V	Volume of the swimbladder
z	Depth of the fish
$\gamma$	Factor describing the contraction of swimbladder volume with pressure
$\gamma_r$	Ratio of 'concentrated' and 'distributed' components of a signal
$\phi$	Angular direction in the horizontal plane relative to the head-tail axis of a fish
$\bar{\sigma}_{bs}$	Sample mean (average of several measurements of $\sigma_{bs}$ )
$\langle \sigma_{bs} \rangle$	True mean (i.e. the expected value) of $\sigma_{bs}$
$\sigma_n$	Measured values of $\sigma_{bs}$ ( $n = 1, 2$ etc.)

***Chapter 7***

a	Typical dimension of a scatterer (for plankton, same as ESR)
$a_j$	Value of a at the mid point of the $j$ 'th size class
b	Constant in TS-length functions
$c_1$	Sound speed in the body tissue of a plankter
$c_{\text{mix}}$	Sound speed in a mixture of water and plankton
ESR	Equivalent spherical radius of a discrete target
$f_i$	i'th frequency of a multi-frequency sonar
$F_j$	Plankton density (number per unit volume) in the $j$ 'th size class
<b>F</b>	Column vector of the $F_j$ ( $N \times 1$ matrix)
g	Density contrast of a body, $(\rho_1 - \rho)/\rho$
h	Sound-speed contrast of a body, $(c_1 - c)/c$
$k_j$	Wavenumber corresponding to the $j$ 'th frequency
$(k_1)_1$	Incident wave vector evaluated inside the plankter body
$L_{\text{bubble}}$	Backscattering length ( $L_{bs}$ ) of a gas bubble
$L_{\text{Lamb}}$	Part of $L_{bs}$ due to Lamb waves
$L_{\text{spec}}$	Part of $L_{bs}$ due to specular scattering
$L_{\text{tissue}}$	Part of $L_{bs}$ due to the body tissue
m	Constant multiplying 'log L' in formulas for target strength
M	Number of frequencies in a multi-frequency sonar
$N, N_1, N_2$	Number of size classes in a plankton aggregation
q	Compressibility contrast, $(\kappa_1 - \kappa)/\kappa$
$\mathbf{r}_v$	Position vector of a body element
<b>R</b>	Matrix of backscattering cross-sections $[\sigma_{ij}]$ , M rows, N columns
$s_i$	Measurement of $s_v$ at the i'th frequency
$\delta S_v$	Difference in $S_v$ between two frequencies
$\delta S_v(38-120)$	$S_v$ at 120 kHz minus $S_v$ at 38 kHz
$\delta S_v(120-200)$	$S_v$ at 200 kHz minus $S_v$ at 120 kHz
V	Volume of a plankter body
<b>X</b>	Column vector of the $s_i$ ( $M \times 1$ matrix)
$\Phi_{\text{pl}}$	Fraction of total volume occupied by plankton
$\kappa$	Compressibility of water
$\kappa_1$	Compressibility of body tissue
$\rho_1$	Density of body tissue
$\sigma_{ij}$	$\sigma_{bs}$ for the i'th frequency and j'th size class

***Chapter 8***

a1, a2	Side lengths of a rectangular element of area to be surveyed
A	Size of the area to be surveyed
D	Total length of the cruise track
$D_{\text{tr}}$	Average distance between successive transects

---

$t_C$	Time for calibrating the acoustic instruments
$t_F$	Fishing time
$t_H$	Time for hydrographic stations
$t_L$	Time for loading and unloading the ship
$t_M$	Time for travelling to and from the survey area
$P_d$	Proportion of the day when echo integration is useful
$t_T$	Total time available for surveying and related activities
$V$	Speed of the survey vessel
$V_R$	Variance of the rectangular design estimator
$V_T$	Variance of the triangular design estimator
$\Lambda$	Degree of coverage, equal to $D/\sqrt{A}$
$\xi$	Random number in the interval 0 to 1

## Chapter 9

$a, b$	Constants in the formula for CV as a function of the degree of coverage
$a_x, b_x$	Constants in formulas relating target strength to the fish length ( $x = i, n$ or $w$ )
$a_f, b_f$	Constants in the weight-length relationship of fish
$A$	Size of the surveyed area
$A_b$	Extra attenuation due to the bubble layer
$A_k$	Area of the $k$ 'th elementary statistical sampling rectangle (ESSR)
$A_p$	Probability factor in the equation for $D_p$
$A_i$	Area of the $i$ 'th region
$c_1$	Assumed value of the sound speed in water
$C_E$	On-axis calibration factor for echo-integration
$C_i$	Echo-integrator conversion factor for species $i$
$D$	Total length of the cruise track
$D_I$	Minimum length of the elementary distance sampling unit (EDSU)
$D_{\max}$	Maximum difference between two cumulative probability distributions
$D_p$	Value of $D_{\max}$ exceeded with probability $P$
$D_v$	Distance between two sampled locations
$E$	Echo-integral, usually the mean of many measurements
$E_i$	Partitioned echo-integral of species $i$
$E_m$	Echo-integral of a species mixture
$E_k$	Mean echo-integral near trawl-station $k$
$E_{ik}$	Mean echo-integral of species $i$ near trawl-station $k$
$E(\hat{Q})$	Expected value of $\hat{Q}$
$F$	Area fish density (number or weight of fish per unit area of a depth layer)
$F_i$	Area density ( $F$ ) of species $i$ , or the $i$ 'th density observation
$F_{ji}$	$j$ 'th observation of the area density in the $i$ 'th stratum
$\bar{F}_k$	Arithmetic mean of the area densities observed in stratum $k$
$\bar{F}_k$	Arithmetic mean of the area densities observed along transect $k$

$L_{ij}$	Fish length at the mid-point of size class j for species i
$\Delta L$	Interval between successive size classes
M	Number of trawl-stations, regions etc.
$M_i$	Number of catches containing species i
n	Number of fish, samples etc.
$n_{ijk}$	Number of species i in length-class j caught at station k
N	Number of surveys, samples etc.
$N_{ik}$	Number of species i caught at station k
$P_{ij}$	Mean frequency of length-class j for species i
$P_z$	Probability of observing zero density
$P_{KS}$	Probability (Kolmogorov-Smirnov test)
$P(F)$	Probability density function (PDF) of F
$P_{\text{all}}$	Set of all possible locations within the surveyed area
$P_{\text{sam}}$	Set of locations (within $P_{\text{all}}$ ) at which samples are collected
$q_k$	Quantity of catch at station k
$q_{ik}$	Quantity of species i caught at station k
Q	Quantity (abundance) of fish
$\hat{Q}$	Estimate of the true abundance Q
$s^2$	Sample variance
t	Multiplier of the standard error (SE) in the calculation of confidence limits
$t_k$	Time spent fishing at station k
$TS_1$	Target strength of one fish
$TS_w$	Target strength of unit weight of fish
$v_c$	Cruising speed of the survey vessel through the water
$v_f$	Migration speed of fish
$v_s$	Speed at which the survey progresses in the direction of migration
$v_w$	Wind speed
$\hat{V}$	Estimated variance of $\hat{Q}$
$w_i$	Weighted proportion of species i in fish samples
W	Weight of one fish
$W_t$	Total weight of fish sample
$X_i$	Variable in the error analysis
$\Delta X_i$	Error in $X_i$
$z_o$	Mean depth of the integration channel
$\beta_1$	Assumed value of $\beta$ , the acoustic absorption coefficient (in nepers m <sup>-1</sup> )
$\varepsilon_i$	Standard deviation of $\Delta X_i/X_i$
$\gamma$	Spatial correlation parameter used to construct the variogram
$\Lambda$	Degree of coverage, equal to $D/\sqrt{A}$
$\mu$	Population mean (in the statistical sense)
$\phi$	Angular rotation of targets relative to the transducer
$\phi_a$	Value of $\phi$ due to pitching and rolling
$\phi_f$	Value of $\phi$ due to linear movement of the transducer
$\theta_{3dB}$	Off-axis angle for transducer sensitivity 3 dB below the maximum

- $\Theta$  Parameter in formula for power data transforms.
- $\rho_L$  Serial correlation coefficient of paired samples at positions  $(i, i + L)$  in the sequence of observations
- $\sigma$  Square root of the population variance
- $\langle \sigma_i \rangle$  Mean backscattering cross-section of species  $i$
- $\omega_t$  Rotation rate of the transducer

# Chapter 2

# Underwater Sound

## 2.1 Introduction

The theory of sound is similar in many respects to that of light. Both phenomena consist of waves which propagate through a medium. Both are subject to scattering, reflection and absorption, which complicate the simple idea of waves transmitting energy through a homogeneous, lossless medium as it is explained in elementary physics textbooks. In water, sound can be transmitted over much longer distances than light, but water is nevertheless an imperfect acoustic medium. Energy is removed (scattered) from the sound wave by suspended solids, biota or entrained gas, or simply converted to heat by physical absorption. All these effects need to be considered in fishery applications, where the usual intention is to deduce features of remote targets from the acoustic signals detected by a sonar or some other instrument.

This chapter provides a largely qualitative view of the generation, transmission and detection of sound in water. Mathematical descriptions are kept to the minimum necessary as background for the discussion of practical applications later on. We begin with the concept of sound waves and their physical properties – pressure, particle velocity and intensity. Next we consider the transducers which generate sound from electrical energy, and the manner in which the sound is projected in particular directions as a beam. The transmission of sound is discussed with particular reference to energy losses through beam spreading and absorption. Empirical equations are given for calculating the sound speed and absorption coefficient in water. We go on to deal with acoustic scattering and the nature of echoes reflected by various kinds of target. Apart from the ordinary physics of low-level acoustic fields, two special effects of some interest in fishery acoustics are discussed, firstly the radiation pressure generated by pulsed transmissions, and secondly the non-linear propagation which occurs when the transmitted intensity is very high. Finally, we consider the detection of acoustic signals and the importance of noise as the limiting factor in the performance of acoustic instruments.

The reader who wishes to know more about the physics of sound may consult one or more of the following historic references. Rayleigh (1945) is the classic and still much quoted work on the subject; see also Morse (1948), Officer (1958) and Mason (1964). The classic work by Urick (1967), now in its third edition (Urick 1983), and

Tucker and Gazey (1966) are still excellent textbooks on underwater acoustics. Clay and Medwin (1977) wrote the major text on acoustical oceanography, now updated as Medwin and Clay (1998), while Forbes and Nakken (1972), Burczynski (1982), Johannesson and Mitson (1983) and Mitson (1983) have dealt with applications specific to fishery acoustics.

## 2.2 Sound waves

Sound is transmitted by the periodic compression and expansion which is permitted by the elasticity of water. This results in a travelling pressure wave as illustrated in Fig. 2.1 for the case of sinusoidal variations at one frequency. At any point in space, the pressure  $p$  relative to the ambient level varies as  $\sin(\omega t)$  where  $t$  is the time and  $\omega$  is the angular frequency of the oscillation.  $f = \omega/2\pi$  is the frequency in Hertz (Hz), the number of cycles per second. When the wave is plane, this means that changes occur in one direction only, the direction in which the wave propagates.  $p$  is the same everywhere in any plane perpendicular to this direction.

The wave-fronts are those planes in which  $p$  is maximal. More generally, each wave-front is a surface joining continuous loci of the peak pressures. If  $x$  is the distance along the direction of propagation of a plane wave, then at any instant

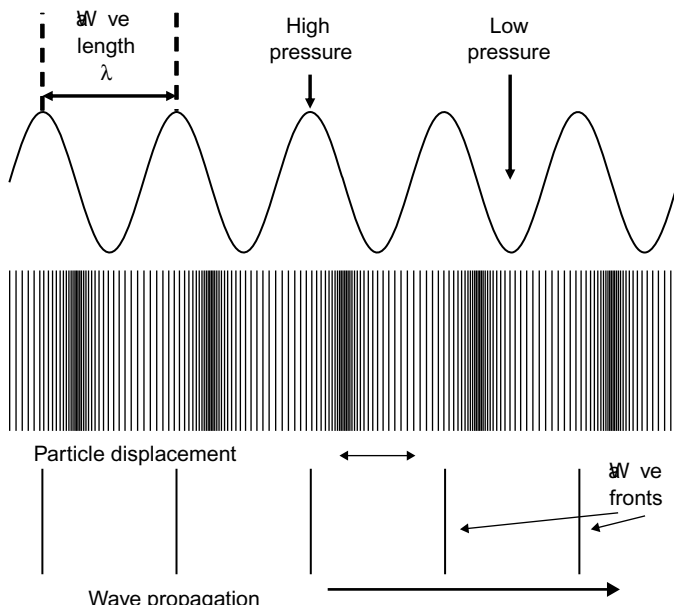


**Fig. 2.1** Illustration of a propagating sound wave. Top: the pressure varies cyclically as a sine wave;  $\lambda$  is the wavelength. Middle: the particle displacement is out of phase with the pressure. Bottom: the wave-fronts are lines which follow the maximum pressure.

$p$  changes as  $\sin(kx)$ .  $k$  is called the wavenumber. The pattern of pressure changes in space is also cyclical and it repeats at intervals of the wavelength  $\lambda = 2\pi/k$ . Thus  $\lambda$  is the distance between successive wave-fronts (Fig. 2.1). Combining the changes in space and time, we can say that the pressure  $p$  varies as  $\sin(kx - \omega t)$ . This implies that the wave-fronts move forward at the sound speed  $c = \omega/k$ . Another important relationship which immediately follows from these definitions is that the sound speed is equal to the product of the wavelength and the frequency:

$$c = \lambda f \quad (2.1)$$

The sound speed describes the movement of the pressure peaks (wave-fronts) through the medium and should not be confused with the particle velocity, which applies to the local oscillation of molecules. For water,  $c$  is generally in the range  $1450\text{--}1550\text{ m s}^{-1}$ , depending on the temperature, ambient pressure and the salinity. The wavelength is important as the fundamental limit on the spatial resolution of targets. The smaller the wavelength, or the higher the frequency, the easier it is to discriminate targets that are close together. If  $c$  is  $1500\text{ m s}^{-1}$ , a typical value in the sea, then sound of  $10\text{ kHz}$  frequency has a wavelength of  $15\text{ cm}$ . If the frequency is  $500\text{ kHz}$ , the wavelength is reduced to  $3\text{ mm}$ .

The continuous sine wave is a convenient and simple description of sound, but in practice we need to consider more complicated waveforms such as pulses and echoes, the amplitude of which changes with time. However, any sound wave may be conceived as the sum of continuous sine waves over a spectrum of frequencies. The pulses transmitted by sonars comprise a few cycles of a sine wave which lasts for a finite time, the pulse duration. The frequency of the sonar as quoted by the manufacturer is that of the sine wave,  $f_0$ , but some of the energy is transmitted at other frequencies within a band centred on  $f_0$ . The width of the band depends on the pulse duration. The shorter the pulse, the wider is the spectrum of frequencies transmitted by the sonar. For example, if the pulse duration is  $\tau = 1\text{ ms}$ , the bandwidth is about  $B = 1\text{ kHz}$ ; if the pulse length is longer, say  $\tau = 2\text{ ms}$ , then the bandwidth reduces to  $B = 500\text{ Hz}$ .

### 2.2.1 Pressure and displacement

In addition to the pressure changes, the wave causes the water molecules to vibrate. The amplitude of the molecular movement is called the particle displacement, and the rate of change is the particle velocity. In a plane wave, the particle velocity and the sound pressure are in phase, meaning that the maximum values coincide in time and space. They both vary as  $\sin(kx - \omega t)$ , and the amplitudes are proportional. If  $\rho$  is the density of the water, then pressure  $p$  and particle velocity  $v$  are related by:

$$p = \rho cv \quad (2.2)$$

Now consider a small source which generates sound at one frequency. If the source is remote from any reflecting objects or surfaces, the waves are said to propagate in free-field conditions. The wave-fronts are now spherical and they travel away from

the source in all directions. The curved wave-fronts result in a more complicated relationship between the pressure and the particle velocity, compared to the plane wave (Harris 1964; Siler 1969). At distance  $R$  from the source:

$$|p| = \rho c |v| / \sqrt{(1 + (\lambda / 2\pi R)^2)} \quad (2.3)$$

Here the modulus symbols are used to indicate the amplitude of a sinusoidal variable. Thus the amplitude ratio  $|p|/|v|$  changes with wavelength  $\lambda$  and range when  $R$  is the order of a wavelength or less. This phenomenon, known as the near-field effect, has implications for the hearing ability of fish (Section 4.3). At greater ranges the pressure is asymptotic to  $1/R$ , as discussed further in Section 2.4 on propagation.

Since water is a fluid, it cannot sustain shear forces, and the particle displacement is always in the direction of sound propagation. This type of sound wave is described as longitudinal. More complicated sound fields occur in solids where transverse (shear) waves can propagate in the direction normal to the particle displacement. The speeds of the two waves caused by the transverse and longitudinal vibrations in solids are not generally the same. This gives rise to more complex sound fields as described in Section 2.5.

## 2.2.2 Energy and intensity

An important feature of the travelling wave is that it transports energy from one place to another. The flux  $J$  is the energy of the waves passing through a unit area perpendicular to the wave-front. The intensity  $I$  is the energy flux per unit time. It is convenient to use the intensity to describe the power of continuous waves, or long pulses within which the amplitude is constant for many cycles. In the case of short pulses, the intensity may change from one cycle to the next and it is better to describe the pulse in terms of the total energy transmitted over the finite pulse duration (Craig 1983).  $J$  is simply the integral of  $I$  with respect to time. The total energy carried by the wave,  $E$ , is the integral of  $J$  with respect to area over the surface of the wave-front. In the case of the scattered waves spreading outwards from a small target, the wave-fronts are spherical or nearly so, and  $E$  is finite. The definition of the echo strength in terms of the total energy, rather than the intensity, is better suited to the modern theory of echo integration as discussed in Chapter 5.

The instantaneous intensity is the product of the pressure and the particle velocity. In a plane wave, combining the definition with Equ. (2.2), we find that the intensity is proportional to the pressure squared:

$$I = p^2 / \rho c \quad (2.4)$$

More usually, it is the average intensity over one or more cycles that is required, in which case Equ. (2.4) still applies if the mean squared sound pressure is substituted for  $p^2$ . The quantity  $Z = \rho c$  is called the acoustic impedance, which is constant within a few percent over the sound path in typical oceanic or freshwater

environments. If the variation of  $Z$  is ignored, the echo energy obtained by integrating Equ. (2.4) is proportional to  $p^2$ . This is the reason why the echo integrator operates by first squaring the voltage at the echosounder output (which is proportional to the sound pressure at the transducer) before the integration is performed. It is the echo energy, not the pressure amplitude, which is believed to be proportional to the observed quantity of fish. This continuity or conservation of energy is a fundamental principle in the propagation of sound.

When the pressure amplitude is quoted, there are three ways of expressing this: peak-to-peak, peak, or RMS (root-mean-square). If we observe a pure-tone signal on an oscilloscope, we should see a wave like that shown at the top of Fig. 2.1, with the horizontal axis now being the time  $t$ . The absolute pressure  $P(t)$  cycles between high and low limits,  $P_{\max}$  and  $P_{\min}$  say, and the mean over a cycle is  $P_0$ . The peak-to-peak amplitude is  $(P_{\max} - P_{\min})$ . The peak value is exactly half that, i.e.  $(P_{\max} - P_0)$  or  $(P_0 - P_{\min})$ , and the RMS value ( $p_{\text{rms}}$ ) is the square root of the mean of  $\{P(t) - P_0\}^2$ . The RMS measure is most suited to continuous waves, but it is also used to express the mean amplitude of a burst of waves or a pulse. The peak-to-peak value is used for highly variable pulse shapes such as the transmissions of marine mammals (see Chapter 4). Strictly speaking, when dealing with energy, power or intensity expressed in dB (see below), referred to a base level that includes pressure, the RMS measure is the correct one to use. The three measures are related in the following manner:

$$I_{\text{rms}} = I_{\text{peak}} / 2 = I_{\text{peak-peak}} / 4 \quad (2.5)$$

Conventionally, man-made sonar transmissions are usually described using RMS measures, as are fish hearing capabilities. However, dolphin sonar transmissions are often quoted as peak-to-peak levels. In this book, unless explicitly stated otherwise, numerical values of the sound pressure and intensity are always based on the RMS definition.

### **2.2.3 Units**

Sound pressures and intensities have been measured in various units over the years. Current practice is to use only the Système International (SI) scheme, as we do throughout this book. The SI unit for pressure is the Pascal (Pa) which, depending on the magnitude, can have the usual decadal multipliers e.g.  $1 \mu\text{Pa} = 10^{-6} \text{ Pa}$ . Table 2.1 lists some of the more diverse units often seen in older texts, and their equivalent value in Pascals.

### **2.2.4 The decibel**

Acoustic measurements are often quoted in decibel (dB) units rather than the more formally correct SI units for pressure, intensity etc. This is done because the numbers involved can be very large or very small, covering many orders of magnitude. The decibel is a logarithmic measure of the ratio of two intensities, e.g.  $I_1$  and  $I_2$ .

**Table 2.1** Some uncommon units and their Pascal equivalent.

Pressure unit – long description	Short form	Conversion to Pascals (Pa)
Newton per square metre	N m <sup>-2</sup>	1.0
Dyne per square centimetre	dyne cm <sup>-2</sup>	0.1
Microbar	μbar	0.1
Standard atmosphere	atm	101 325
Pounds per square inch	psi	6894.8

The ratio is expressed in dB by the formula:

$$r_{\text{dB}} = 10 \log(I_2 / I_1) \quad (2.6)$$

'Log' means the logarithm to the base 10, as elsewhere in this book. A change in the sound level covering many orders of magnitude may be expressed within a modest range of decibels. Because the dB unit is so commonly used in acoustics, it is important to understand how it is applied.

In principle,  $I_1$  should be a reference level of intensity against which  $I_2$  is measured. For example, suppose a transducer generates a source level of 200 000 Pa. The source level is defined as the sound pressure at 1 m distance from the transducer. The reference pressure used for transducer measurements is commonly 1  $\mu$ Pa. Because the intensity is proportional to the pressure squared, the source level in dB is:

$$\begin{aligned} \text{SL} &= 10 \log(200 000 / 0.000001)^2 \\ &= 226 \text{ dB relative to } 1 \mu\text{Pa} \end{aligned} \quad (2.7)$$

It is important to include the reference pressure or intensity when describing the measurement of an absolute quantity such as the source level. Otherwise the dB number is meaningless. The above source level might equally be referenced to 1 Pa, in which case it would be written as '106 dB relative to 1 Pa'. This long description is commonly shortened to '106 dB re 1 Pa' or '106 dB//1 Pa'.

It is also necessary to specify which pressure amplitude is intended, since this can be measured in different ways (see above in Section 2.2.2). In this book, unless explicitly stated otherwise, numerical values of the sound pressure and intensity are always based on the RMS definition.

The decibel unit is also used to describe the acoustic reflectivity of targets, namely the target strength (TS). The reflectivity is defined by the ratio of the reflected intensity at 1 m from the target ( $I_2$ ) and the incident intensity ( $I_1$ ). Since  $I_2$  is proportional to  $I_1$ , the target strength is a true ratio and there is no need to quote a reference level in this case. For example, if  $I_2$  is 0.0002  $I_1$ , then:

$$\text{TS} = 10 \log(I_2 / I_1) = 10 \log(0.0002 I_1 / I_1) = -37 \text{ dB} \quad (2.8)$$

We discuss the important subject of target strength in more detail in Section 2.5 and Chapter 6.

## 2.3 Transducers and beams

The transducer supplied with fishery sonars has two functions. Firstly, it converts electrical energy into the transmitted acoustic pulse, sometimes called the ping. Secondly, when targets reflect the ping, the transducer converts the acoustic echoes to electrical signals which are applied to the receiving amplifier. The most common type of transducer is made from ceramic materials which are piezo-electric. When pressure is applied to this material, a voltage is generated, and the effect is reversible. Thus, when an oscillating external voltage is applied, the ceramic expands and contracts, radiating sound as it does so. The magneto-strictive transducer is another type, found particularly in low-frequency applications. However, the ceramic transducers have a higher efficiency, and they are preferred for fishery applications. More complete descriptions of the physics of transducers are given by Mason (1964) and Tucker and Gazey (1966).

There have been considerable advances in transducer design in recent decades. The production of materials with greater energy-conversion efficiency improved both the performance and the predictability of transducers. Better understanding of mechanical bandpass filters and the propagation of sound in solids led to more complex constructional designs in which several components vibrate in a coupled fashion, allowing wider bandwidths to be achieved and better coupling to the water. In addition, the use of composite ceramics (see below) has improved both the efficiency and the bandwidth of the transducers. All these developments, and especially the better matching of acoustic impedances between the transducer material and the water, have resulted in more powerful sonar transmissions (i.e. higher source levels) than were previously possible. A good reference on the practical and theoretical issues of transducer design is Stansfield (1991). This book concentrates on rather low frequencies in the context of fishery applications, i.e. 2–20 kHz. Stansfield does include some discussion of higher frequencies (up to 500 kHz), but his book deals best with the fundamental principles of transducer design. Unfortunately, published references on designs for higher-frequency applications are limited due to the commercial sensitivity of the information.

Ceramic and magneto-strictive transducers project modest amounts of energy into the water. Various other techniques have been used to produce the high-energy pulses required for geophysical surveys, such as the airgun and explosive charges. These devices are described in Chapter 4.

Transducers are often constructed as an array of individual elements. Figure 2.2 illustrates the traditional design of a ceramic element, and the arrangement of multiple elements (34 in this example) which form the transducer array. Each element consists of four ceramic tubes fitted between two steel masses, one at the head and one at the tail of the element. The masses are designed to ensure efficient transfer of energy into the water. The ceramic tubes are held together by a pre-stressing bolt. The low-density backing material ensures that most of the acoustic energy is transmitted in the forward direction into the water. This type of transducer is reversible: it

may be used either to transmit or to receive sound waves. More recently, transducer elements have been designed with a layer of different material on the transmitting face. This layer is close to a quarter of a wavelength thick (at a frequency near the centre of the bandwidth), and it is included to better match the acoustic impedances of the ceramic piston and the water. More precisely, the layer has an acoustic impedance ( $Z$ ) which is the geometric mean of the impedances of the main part of the element and the water. Such a layer, when it is  $\lambda/4$  thick, greatly improves the transfer of acoustic energy into the water, compared to a conventional transducer design in which there is only one boundary with a substantial impedance mismatch between the solid and liquid media.

These techniques have been applied by Foote (1998a) in the design of wideband transducer elements. He used seven transducers to cover the frequency range 25 kHz to 3.3 MHz. The 25 kHz transducer is the standard ‘tonplitz’ design discussed by Stansfield (1991) and has a construction similar to that in Fig. 2.2. The next two frequency bands are covered by more sophisticated element designs, each having three resonances which are associated, respectively, with the thickness mode, the flapping mode and a  $\lambda/4$  layer on the transducer face for the upper resonance.

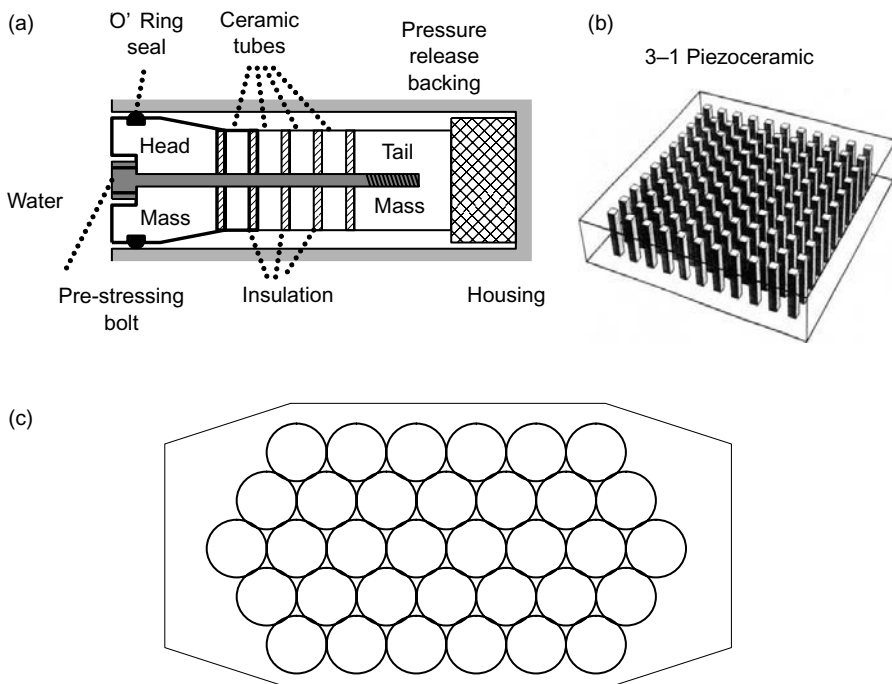


**Fig. 2.2** Transducer design and construction. (a) A low-frequency element formed from four ceramic tubes and head and tail masses for mechanical damping; (b) 3-1 composite piezoceramic element, this material is highly efficient and allows wide bandwidth transmissions; (c) an array of 34 elements arranged in a row-echelon matrix.

All three transducers have multiple elements arranged in small arrays. The higher-frequency units have even more complex matching faces such that each one can operate over an octave of frequency. They are made from a composite ceramic which is illustrated in Fig. 2.2. This has several advantages compared to the conventional uniform type of piezo-electric material used in sonar transducers. Composites have a higher acoustic efficiency and a wider bandwidth. They also reduce the cross-talk (interference) between the elements, thus the beam patterns of composite transducers can be more accurately predicted. The transducers described by Foote (1998a) typically have between 5 and 10 dB change in sensitivity over the octave bandwidth.

A transducer that is used to listen to underwater sound, like a microphone in air, is called a hydrophone. This device is often a single piece of piezo-electric ceramic. If the ceramic is shaped as a spherical shell or a small cylinder, then in theory the hydrophone is equally sensitive to sound waves coming from any direction. However, the sensitivity of most transducers is strongly dependent on the wave direction because of the phase differences between the signals produced by the elements or parts of the transducer. The effect is illustrated in Fig. 2.3 for the simple case of a transducer consisting of two spherical hydrophones. When the wave-fronts are parallel to the line joining the hydrophones, the two signals are in phase and their sum (the transducer output) is maximal (Fig. 2.3a). The direction of propagation in this case is called the acoustic axis. As the sound source moves away from the axis (Fig. 2.3b), the phase difference increases and the amplitude of the sum is less than the maximum. In Fig. 2.3c, the path lengths between the sound source and the hydrophones differ by nearly half a wavelength. The two signals cancel each other and the amplitude of the sum is very small. As the sound source moves yet further from the axis, the summed amplitude increases once again (Fig. 2.3d). This effect may be used to determine the direction of a sound source, by comparing the phases of the signals produced by the individual elements of a transducer.

The function  $b$  which describes the change of sensitivity with direction is called the beam pattern. The same beam pattern normally applies both to transmission and to reception of sound. By convention,  $b$  is unity in the direction of greatest sensitivity, the acoustic axis. For a point source or receiver, one whose size is much smaller than the wavelength,  $b = 1$  everywhere and the sensitivity is omni-directional. In the case of a square transducer of side length  $a$ , the acoustic axis is perpendicular to the radiating surface. To describe the sound field produced by such a transducer, consider the plane through the acoustic axis and parallel to one side of the transducer. If  $\theta$  is any angle from the acoustic axis in this plane, the beam pattern in that direction is:

$$b(\theta) = \sin[(\pi a / \lambda) \sin(\theta)] / [(\pi a / \lambda) \sin(\theta)] \quad (2.9)$$

When transmitting, the sound pressure at a fixed range  $R \gg a$  is proportional to  $b(\theta)$ , and the intensity varies as  $b^2(\theta)$ . We see from Equ. (2.9) that  $b$  is zero in directions where  $\sin(\theta) = n\lambda/a$ ,  $n$  being a non-zero integer. These directions

are said to be ‘nulls’ in the beam pattern. The region of higher sensitivity between adjacent nulls is called a lobe. The larger the face of the transducer (in terms of wavelengths  $\lambda$ ), the more lobes there are and the more directional is the sensitivity. The beam pattern is normally represented as a polar diagram of sensitivity against direction (Fig. 2.4).

If the transducer is a circular disc of diameter  $a$ , the beam pattern is symmetrical.  $\theta$  is now the angle from the axis in any plane normal to the disc, and:

$$b(\theta) = 2J_1[(\pi a / \lambda) \sin(\theta)] / [(\pi a / \lambda) \sin(\theta)] \quad (2.10)$$

where  $J_1(x)$  is the first-order Bessel function of the argument  $x$  (Abramowitz *et al.* 1964). Again,  $b$  goes through a pattern of maxima and nulls as  $\theta$  increases from zero. The first null occurs when  $\sin(\theta) = 1.2\lambda/a$ .

Any transducer, even if it is actually a continuous structure, may be considered as if it were made from a number of elements. If the beam pattern of each element is known, that for the complete transducer is obtained by adding the signals from each element, taking account of the phase differences between them (Tucker and Gazey 1966). The signal phase is determined by the path length from the element to the sound source (or the target in the case of transmission). The elements

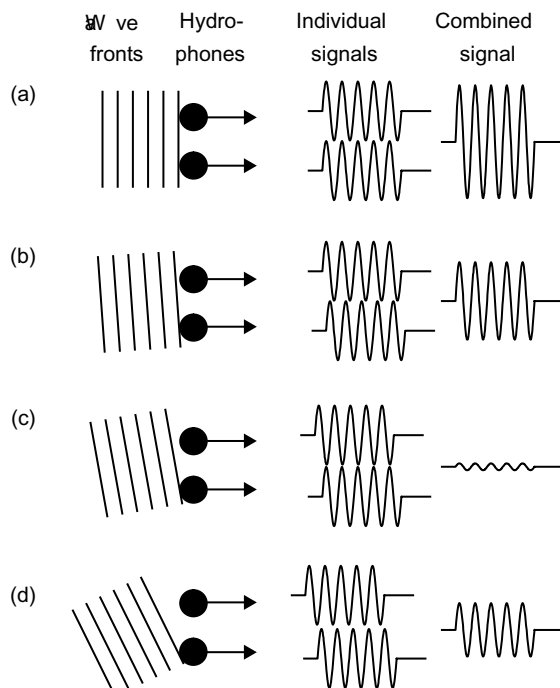


**Fig. 2.3** Combination of signals from two hydrophones. (a) The signals are in phase and the summed amplitude is maximal; (b) the amplitude is reduced as the source moves off the acoustic axis; (c) the signals nearly cancel at the null; (d) after the null the amplitude rises again.

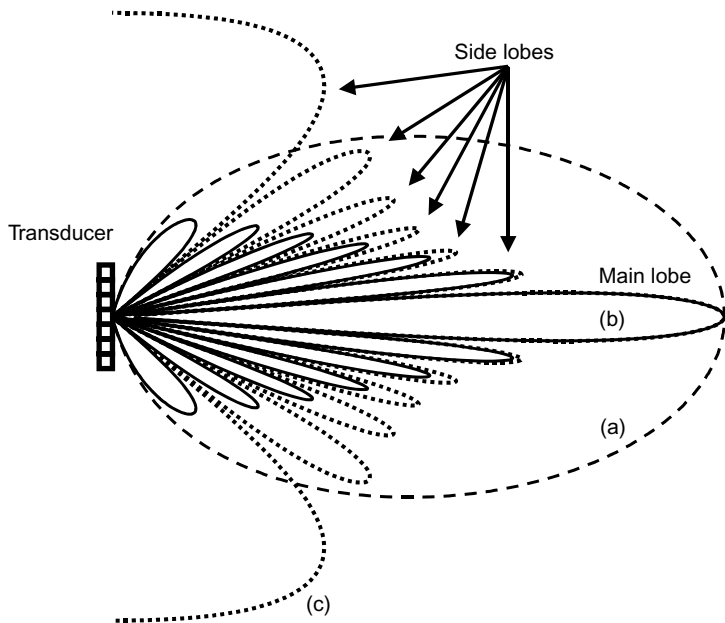


**Fig. 2.4** Examples of beam patterns (shown as cross-sections) for a transducer that is seven wavelengths long. The sensitivity is proportional to the distance of the pattern from the centre of the transducer. Broken oval pattern (a) is for a single square element one wavelength long. Dotted pattern (c) is formed from seven point sources one wavelength apart. The solid curve (b) is the full transducer with seven touching one-wavelength elements, or a single element seven wavelengths across.

may be individual units as in Fig. 2.2, but the same principle may be applied to a transducer whose radiating surface is large and continuous, however complicated its shape may be. The irregular surface is considered as a network of simple contiguous elements which might be flat squares, in which case the elemental beam pattern is given by Equ. (2.9).

Referring to the three patterns in Fig. 2.4, curve (a) shows a section through the beam pattern of a square element which is one wavelength long. In this case there is only one null, at  $\theta = 90^\circ$ . Now consider a larger transducer which consists of seven of these elements side by side. The interference between the signals at the seven elements results in the beam pattern of the complete transducer having the more complicated shape shown in curve (b). It is most sensitive in a narrow cone centred on the acoustic axis, called the main lobe, and there are six side lobes at larger values of  $\theta$ , separated by nulls. Curve (c) shows the beam pattern of a transducer whose elements are point sources in a line, again spaced one wavelength apart. In this case the side lobes are larger and there is no null at  $\theta = 90^\circ$ . The ‘filled’ transducer pattern in curve (b) can be obtained as the product of curves (a) and (c), or directly from Equ. (2.9) extended to the case of a rectangular transducer. The results are the same.

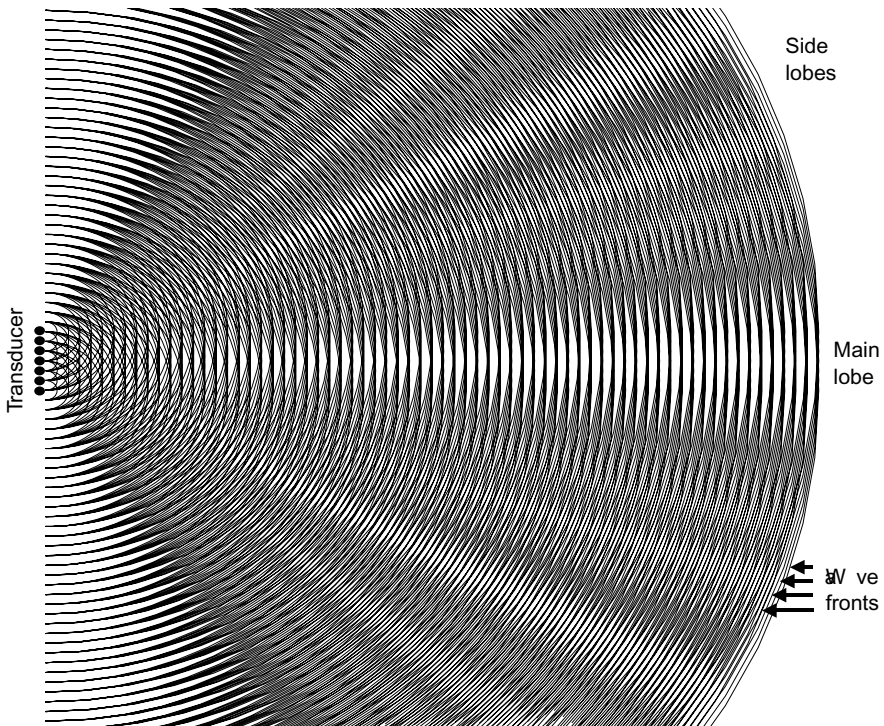


**Fig. 2.5** Illustration of how the beam is formed by a transducer consisting of seven point sources at one-wavelength spacing. The wave-fronts associated with each source are drawn as black curves. When they coincide (e.g. in the main lobe) the sound intensity is maximum.

Figure 2.5 is a pictorial representation of the wave-fronts generated by the point sources when the transducer is used as a transmitter. It illustrates how the seven omni-directional sound sources combine to produce the lobe structure of the beam pattern. The main lobe is evident as the near coincidence of the wave-fronts when they are far from the transducer. The picture is more confused in the region close to the transducer face, due to the near-field effect which we discuss later (p. 39). The coincidence of the wave-fronts is less complete in the side lobes, except for the one at 90°. The pattern corresponds directly to curve (c) of Fig. 2.4.

The beam width of a transducer is commonly described by the angle between the directions on opposite sides of the main lobe where  $b = 1/\sqrt{2}$ , or expressed in decibels, the intensity is 3 dB less than that on the acoustic axis. Numerical methods for calculating the beam width are given by Urick (1975). The beam width depends on the frequency and the size of the transducer (e.g. Table 2.2). It is important to remember that all the measures of a beam pattern will scale in a consistent way. For a given shape of transducer, if the 3 dB beam width is known or measured, we can immediately determine the effective size of the transducer and other parameters such as the equivalent beam angle (see below).

**Table 2.2** Examples of the beam width (angle between 3 dB-down directions) for square transducers according to their size (side length) and operating frequency; calculated values based on a sound speed of 1500 m s<sup>-1</sup>.

Frequency (kHz)	Size (mm)	Beam width (degrees)
19	300	16
38	300	8
76	300	4
76	150	8
150	150	4
1	22 500	4

### 2.3.1 *The equivalent beam angle*

Another measure of the beam pattern is the equivalent beam angle,  $\psi$ , which is sometimes called the reverberation angle of the transducer.  $\psi$  is the solid angle at the apex of the ideal conical beam which would produce the same echo-integral as the real transducer when the targets are randomly distributed in space. Such a conical beam would be like an ideal searchlight with  $b = 1$  for any direction within the cone, and  $b = 0$  elsewhere (Simmonds 1984a).  $\psi$  is a useful quantity to evaluate, but it must be remembered that the ideal beam is not physically realizable in practice. To describe the beam pattern in space, we use spherical polar coordinates which require two angles,  $\theta$  and  $\phi$ , to determine the direction of any point P relative to the transducer at the origin O.  $\theta$  is the angle of OP from the acoustic axis, and  $\phi$  is the azimuthal angle of OP projected onto the plane of the transducer face.  $\psi$  is defined mathematically as:

$$\psi = \int_{\theta=0}^{\pi} \int_{\phi=0}^{2\pi} b^4(\theta, \phi) \sin(\theta) d\theta d\phi \quad (2.11)$$

The integral is taken over the entire beam pattern, which is normally supposed to be the hemisphere in front of the transducer ( $\theta = 0$  to  $\pi/2$ ;  $\phi = 0$  to  $2\pi$ ). The fourth power of b appears in the definition because  $\psi$  is defined in terms of the echo intensity, involving the combined transmitting and receiving sensitivities, whereas b is defined in terms of pressure. The importance of  $\psi$  in the theory of echo-integration is discussed in Chapter 5. In effect, the equivalent beam angle is a measure of the width of the volume insonified by the transducer (p. 47). It takes account of the signals from all targets, including those in the side lobes. However, for most transducers less than 1% of the transmitted energy is projected outside the main lobe. Thus the side lobes have very little effect on the value of  $\psi$ .

$\psi$  is a solid angle which is measured in steradians. Some writers use logarithmic units for the equivalent beam angle, defined as EBA = 10 log( $\psi$ ), which is expressed in dB relative to 1 steradian. There are other ways of describing the beam pattern by one parameter, such as the Directivity Index (Urick 1983) which expresses

the difference between the actual beam pattern of the transducer and that of an omni-directional receiver. However, for most fisheries applications, we consider the EBA to be the most useful measure of transducer directivity.

### 2.3.2 Controlling the beam shape

We have already described how a number of similar elements may be combined to determine the beam pattern of the complete transducer. In the examples shown in Fig. 2.4, the elements are connected in parallel. When transmitting, the same signal is applied to all the elements, and when receiving, the element signals are summed to produce one output. It is possible to modify the resultant beam pattern by controlling the electrical gain applied to the signal at each element. This technique is called shading. For a given size of transducer, shading may be used to reduce the strength of the side lobes, in which case the width of the main lobe increases. Figure 2.6 shows an example of a BioSonics 200 kHz transducer beam pattern. The main element is 8.2 cm diameter in an 18 cm housing, designed to give a 6° beam

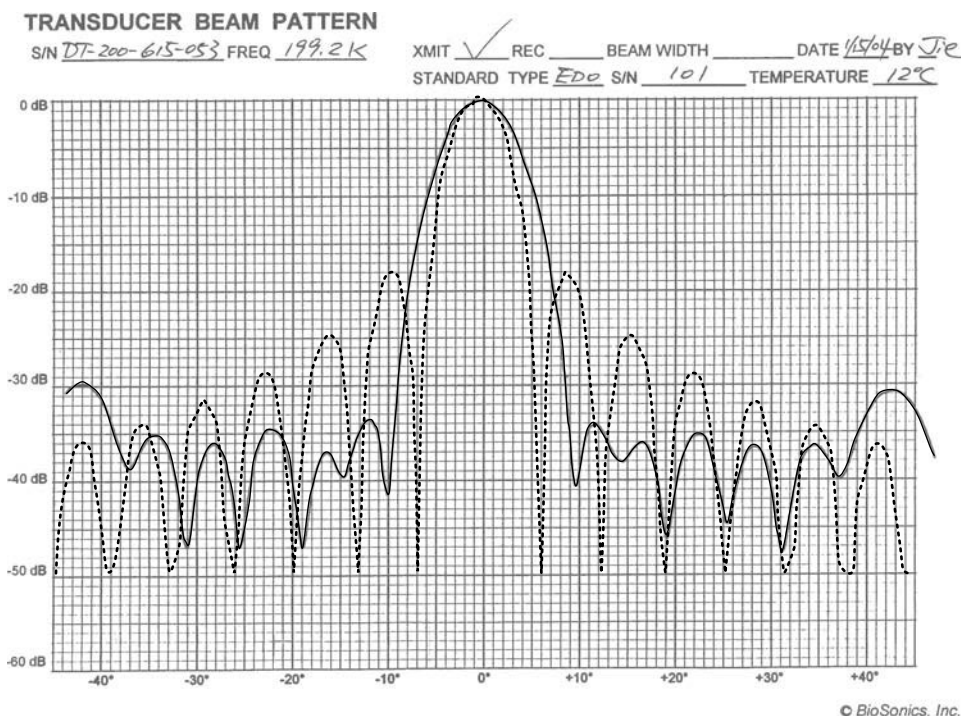


**Fig. 2.6** Example of a measured transmission beam pattern. BioSonics 200 kHz transducer with an 8.2 cm radiating face, 6° beam width and –30 to –35 dB side lobes (solid line). This transducer is designed to have low side lobes; a simple piston of the same dimensions would have a beam width of 5.5° and side lobes around –18 dB (superimposed dotted line). The modest increase in beamwidth gives a worthwhile reduction in the side lobes.

and side lobes between  $-30$  and  $-35$  dB below the on-axis sensitivity. The same size of transducer element used as a piston without side lobe suppression would have a beam width of approximately  $5.5^\circ$  and side lobes up to  $-18$  dB. The theoretical beam pattern is superimposed on the measured values supplied by the manufacturer. The increase in beam width due to shading is modest considering the useful reduction of the side lobes.

Conversely, a shaded transducer may be designed to reduce the beam width if larger side lobes can be accepted. In the case of a transducer array, the strength of the side lobes also depends on the proportion of the transducer surface that is filled by the radiating parts of the elements. In a good transducer design, this proportion should be at least 70%, and in addition the spacing of adjacent elements should be less than a wavelength.

A simple form of shading is to separate the signals from two or more parts of the transducer. The transducer is used as though it were several independent devices having different beam patterns. This technique is the basis of the dual-beam and split-beam echosounders which are described in Chapter 3.

The scanning sonar is another useful application of shading. In this device the signals from adjacent elements are delayed before they are summed, so that the beam is tilted from the acoustic axis. By varying this delay rapidly, the beam is made to rotate within the pulse duration and targets may be viewed in azimuth as well as in range, i.e. in two dimensions as on a radar display.

As an obvious extension of this idea, targets may be located in three dimensions by varying both angles of the beam. The transducer is now constructed as a matrix of elements, and different delays are applied to the (mutually perpendicular) columns and rows of the transducer elements. Then a single beam can be made to scan a two-dimensional raster or, if multiple receiver channels are provided, several beams may be formed simultaneously. Various instruments based on these concepts are described in Chapter 3.

The principles of shading functions have been well understood for many years. For any one transducer size operating at one frequency, there is always a trade-off between various performance options. For example, the narrowest beam will have the largest side lobes; this can be achieved by using only the outside elements on a transducer, effectively a toroidal design which gives a narrow beam but has side lobes equal to the main lobe. At the opposite extreme, shading with binomial coefficients (e.g. 6 elements with gains proportional to 0.1, 0.5, 1, 1, 0.5 and 0.1) gives the broadest beam. In theory, the binomial design has no side lobes; in practice the side lobes do not vanish although they will be small. Another option, known as Dolph–Chebyshev shading, provides steeper-sided beams with flatter tops and low side lobes, again at the expense of a wider main lobe. This subject is too extensive for further examination here, but the key points are that the beam shape can be controlled through shading the element signals and, provided a large enough transducer can be used, considerable benefits in directional performance are possible. The practical limits to what can be achieved arise in matching the performance of

the transducer elements, and ensuring that the face of each element is constructed to move like a rigid piston.

### 2.3.3 *End-fire transducer arrays*

There is another method of forming an acoustic beam, involving a rather different type of transducer design. This is the end-fire array in which the transducer elements are arranged in a line, spaced at half-wavelength intervals. On transmission, alternate elements of the array are driven in antiphase, meaning that, in effect, the terminals on successive elements are reversed. The transducer can be used both for transmission and reception. This type of design has a much simpler near field than that of planar transducers. The beam has a main lobe along the line of the array and the directional pattern is almost fully formed at the end of the array, thus the near-field distance is relatively small. The end-fire transducer is uncommon in man-made sonars, but it has been implicated in the reception of sound by dolphins, whose teeth are said to form the elements of such an array (see Chapter 4).

### 2.3.4 *Limits to power transmission in water*

Most of this book is concerned with linear acoustics, meaning small-amplitude first-order effects which obey simple rules, such as waves propagating independently and inverse-square spreading of energy in the far field. Two exceptions are the shock waves generated by explosions (Chapter 4) and high-order scattering in dense fish schools (Chapter 5). Here we discuss another phenomenon which is a potential cause of non-linearity. When the acoustic power levels are very high, there are several problems to be considered. Firstly, the transducer converts electrical energy into the pressure waves which propagate in the water. The transducer can accept driving voltages only up to some maximum, though for a well-designed system this is unlikely to be the limiting factor. High power and long pulses heat the transducer, causing a change in temperature depending on how fast this heat can be dissipated. Very large voltages can stress the materials used in the transducer construction, leading to mechanical fatigue and possibly failure after extended use. However, a good transducer design should avoid all these problems.

More importantly, there are limits on the acoustic pressure amplitude that can be sustained in the water. There are two mechanisms to be considered. Firstly, for transducers operating near the surface, the static pressure is 1 atm. The maximum wave that can exist is limited by the fact that the minimum pressure (acoustic plus static) cannot be negative. If the wave is very strong, the trough pressure approaches zero and a vacuum can ensue. Formation of the vacuum and its later collapse result in explosive sounds called cavitation. The likelihood of this problem reduces rapidly with the transducer depth as the static pressure increases. However, cavitation is more readily induced when there are air bubbles in the water, as can occur near the surface in bad weather. On the other hand, cavitation takes some time to develop,

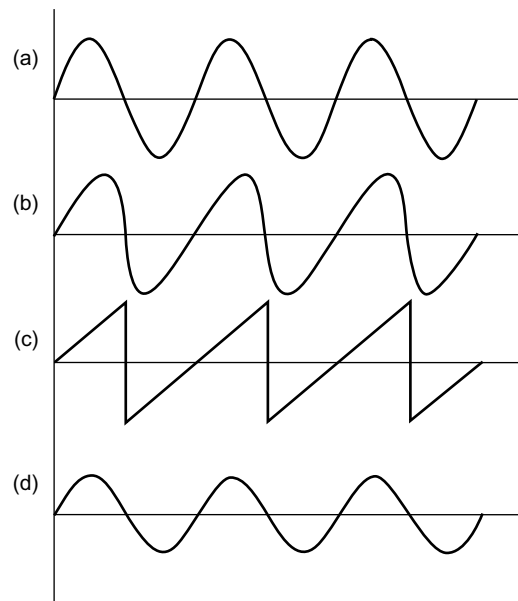


**Fig. 2.7** Non-linear propagation. (a) A high-amplitude sine wave is produced; (b) the peak moves faster than the trough, distorting the wave. (c) In the limit this becomes a triangular wave in which the  $n$ th harmonic has intensity  $1/n^2$ ; (d) the distorted wave propagates further at lower amplitude and the higher frequency harmonics are absorbed faster (cf. Section 2.4).

and is therefore less of a problem with shorter pulses and higher frequencies due to the more transient periods of low pressure.

The second non-linear mechanism is associated with the large pressure changes in so-called finite-amplitude waves. This can occur at any depth. As the amplitude of the wave increases, so does the pressure difference between the peak and the trough. The speed of sound depends on the pressure (Appendix 2B). Consequently, the trough of a finite-amplitude wave propagates more slowly than the peak. Consider a wave that starts as a pure sinusoid (Fig. 2.7a). This contains energy at only one frequency – the fundamental. As the wave propagates, it distorts progressively with the peaks advancing relative to the troughs (Fig. 2.7b). Eventually, if the amplitude is high enough for long enough, each peak overtakes the following trough and the waveform is now triangular (Fig. 2.7c). The effect of this is to transfer energy from the fundamental frequency into harmonics. Using a Fourier analysis to determine the spectral components, we find that when the wave is fully triangular, the  $n$ th harmonic has an intensity  $1/n^2$  that of the fundamental. Thus energy is transferred from low to higher frequencies. This happens more rapidly when the fundamental frequency is higher. The peak–trough difference in sound speed is the same, thus the shorter the wavelength, the less time is required for a peak to advance to the following trough. Once these harmonics have been created, the triangular wave continues to propagate but the high-frequency components are absorbed more rapidly (as explained in the

next section). Eventually, at a large distance from the source, only the fundamental component remains but it is weaker than would be expected from the linear theory of small-amplitude waves. Furthermore, energy is removed preferentially from the high-intensity region in the main lobe of the beam, with the result that the side lobes become more prominent in a finite-amplitude wave.

This process is used productively in so-called non-linear sonars where two powerful high-frequency beams are superimposed in the water. The non-linear interactions transfer energy into two new waves, one at the sum and the other at the difference of the original frequencies. The sum frequency attenuates rapidly, but the lower difference frequency can have useful applications, although it contains only a small proportion of the total energy transmitted. For example, two beams at 375 kHz and 400 kHz generate a signal at the 25 kHz difference frequency. By sweeping one of the original frequencies over a small range, the difference signal has a proportionately much wider bandwidth. Thus, if the first beam is 375 kHz and the second sweeps from 380 to 420 kHz (a fractional change of 10%), the difference signal sweeps from 5 to 45 kHz. This 9-fold change of frequency is not easily achieved with linear acoustic techniques.

The intensity at which non-linear effects become significant is frequency dependent, and may be calculated by the method of Shooter *et al.* (1974). Figure 2.8 shows the limiting source levels for (a) the onset of non-linearity and (b) the formation of

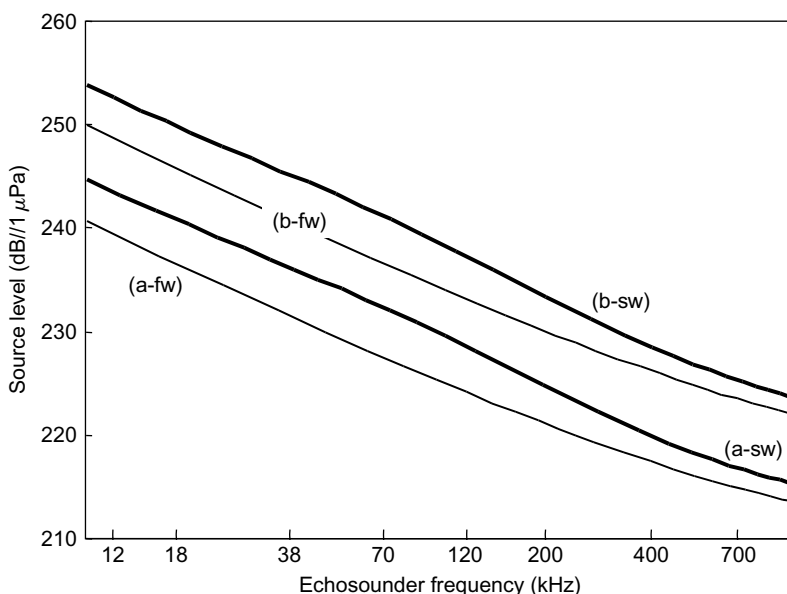


**Fig. 2.8** Limits to sound intensity in water. Frequency dependence of the onset of non-linear attenuation vs source level in fresh water (fw, thin line) and sea water (sw, thick line). Lines show the source level necessary for (a) the onset of non-linear losses and (b) fully formed saw-toothed waves (cf. Fig. 2.7).

fully triangular waves. Shooter *et al.* (1974) compare their theoretical results with measurement at 450 kHz. Their observations suggest that at the lower limit shown in Fig. 2.8, there may be about 1 dB of extra attenuation due to non-linear effects. We consider that a further 3 dB reduction in the source level should be sufficient to ensure the propagation is entirely linear.

Tichy *et al.* (2003) report measurements using a 200 kHz echosounder which they compare with theoretical plane-wave propagation. At very short range they found more attenuation than that expected from the work of Shooter *et al.* (1974), but the observed waveforms were strangely asymmetrical, suggesting that other factors might have influenced the results of Tichy *et al.* At ranges greater than 5 m, however, there was agreement between the two investigations. Notwithstanding these difficulties of interpretation, Tichy *et al.* demonstrated that there are non-trivial non-linear effects to be considered in fishery acoustics. The limited experimental work published confirms that when using source levels of more than 222 dB//1  $\mu$ Pa at 1 m, and frequencies at or above 200 kHz, non-linear effects can be important. When echo-integrating at high frequencies and power levels, it is preferable to calibrate with the sphere at greater ranges than those determined on near-field criteria alone (see below and Chapter 3). Figure 2.8 provides guidance on the frequency/power limits above which non-linear distortions might be expected.

Further details of the physics and applications of non-linear acoustics are given in Hamilton and Blackstock (1997).

## 2.4 Acoustic propagation

Here we consider the sound field in the water between the transmitting transducer and any target which generates an echo. Much of the literature on acoustic propagation is concerned with horizontal transmission over long distances, when reflections from the sea surface and the bottom are important. There is also the phenomenon of refraction, which causes the direction of propagation to change if the sound speed varies across the wave-front. In fisheries applications, however, we are more often concerned with short-range or vertical transmission in which refraction is relatively unimportant.

### 2.4.1 Beam spreading

As the wave-fronts travel outwards from the transducer, they spread over a larger area. The total energy of the transmission is fixed, so the intensity (power transmitted through unit area) decreases as the beam spreads (Fig. 2.9a). At ranges much larger than the transducer size, said to be in the ‘far field’, the intensity varies with the range  $R$  in accordance with the inverse-square law:

$$I = I_0 / R^2 \quad (2.12)$$

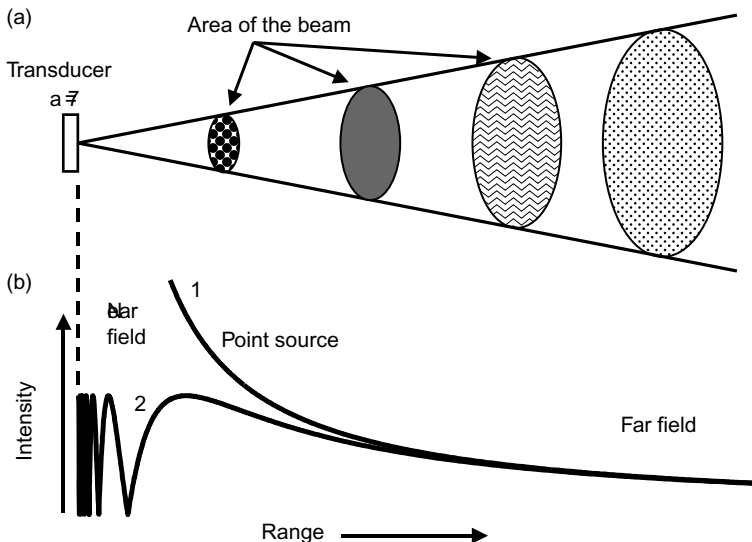


**Fig. 2.9** Illustration of acoustic energy propagating away from a transducer. (a) Spherical spreading reduces the intensity at large ranges. (b) This causes the intensity of a point source to follow the inverse-square law (curve 1) at any range. The near-field effect limits the intensity near the face of a finite transducer (curve 2), one of size  $7\lambda$  in this case.

It follows that the pressure amplitude is inversely proportional to the range:

$$|p| = |p_0| / R \quad (2.13)$$

The constants  $I_0$  and  $|p_0|$  are respectively the intensity and the peak-pressure amplitude normalized to unit range. However, the actual intensity at unit range may not be the same as  $I_0$ . There is a region immediately in front of the transducer where the range dependence of the intensity is more complicated, called the near field or the Fresnel zone. This occurs at ranges where the wave-fronts produced by the transducer elements are not parallel, a state which alters the phase relationships compared to the far field as illustrated in Fig. 2.5. In the near field, the intensity varies rapidly with the range in an oscillatory manner (Fig. 2.9b). It is only in the far field (also known as the Fraunhofer zone), where the element wave-fronts are nearly parallel, that the beam is properly formed and the inverse square law applies. If  $a$  is the linear distance across the transducer face, the boundary between the near and far fields is approximately at the range:

$$R_b = a^2 / \lambda \quad (2.14)$$

For example, the wavelength in sea water is about 3.95 cm at 38 kHz. If  $a = 7\lambda$  as in Fig. 2.5, the near field extends to  $R_b = 1.89$  m. A higher-frequency transducer designed to have the same beam width would have a smaller near field. The transition from near- to far-field conditions occurs gradually around  $R_b$ . For this reason,

acoustic measurements that depend on the assumption of far-field conditions should be done at ranges of at least  $2R_b$ .

It is possible to calculate the spatial variation of the intensity in the near field as described by Rschevkin (1963). This reference is out of print and there is no current replacement; however, such calculations are likely to be inaccurate when applied to real transducers, because small and unpredictable differences between the elements can result in large changes of the intensity. Acoustic measurements to calibrate the transducer must be performed in the far field where the intensity is more predictable.

## 2.4.2 Absorption

As sound propagates through water, acoustic energy is lost through the process of absorption; it is converted to heat. This causes the pressure of a plane wave to decrease exponentially with the distance  $x$  along the propagation path.

$$|p(x)| = |p_0| \exp(-\beta x) \quad (2.15)$$

$\beta$  is the absorption coefficient in nepers per unit distance, which means that the amplitude decreases by the factor  $\exp(1) = 2.718$  over the distance  $1/\beta$ . Since the intensity is proportional to the amplitude squared, we have:

$$I(x) = I_0 \exp(-2\beta x) \quad (2.16)$$

It is more usual to express the absorption coefficient as the energy loss in dB per unit distance, for which we use the symbol  $\alpha$ . Thus an alternative formula for the intensity loss is:

$$I(x) = I_0 10^{(-\alpha x/10)} \quad (2.17)$$

Comparing Equ. (2.16) and Equ. (2.17), the two measures are simply related as  $\alpha = 8.69\beta$ .

Several mechanisms contribute to the absorption. Viscous (frictional) losses occur in both fresh and saline water. This part of the absorption coefficient is proportional to the square of the frequency. Conceptually, higher frequencies involve faster particle velocities and thus higher friction losses. In the sea, there are additional losses owing to the molecular relaxation of certain compounds. For each compound, there is a critical ‘relaxation’ frequency below which the losses occur. Relaxation is a pressure-induced reduction of molecules to ions which takes a certain time to complete. At high frequencies, the sound pressure cycles too quickly for the reduction to occur and thus no energy is absorbed by this process. The magnesium sulphate relaxation dominates the absorption in the frequency range 2–500 kHz, and at lower frequencies there is a further loss associated with boric acid. The frequency is the main determinant of the absorption, but  $\alpha$  also depends on the water temperature and salinity (Fig. 2.10).

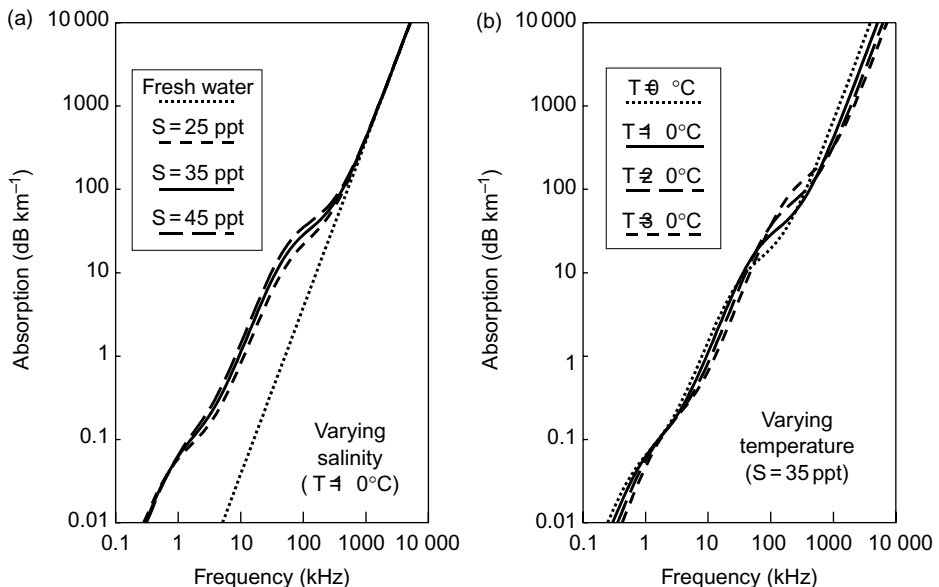


**Fig. 2.10** Acoustic absorption coefficient in water vs frequency, calculated from Francois and Garrison (1982). S is salinity and T is temperature. (a) Variation with salinity at  $T = 10^\circ\text{C}$ ; (b) variation with temperature at  $S = 35 \text{ ppt}$ .

Various equations have been developed for predicting  $\alpha$  at a given frequency, temperature, salinity and depth, notably by Shulkin and Marsh (1963) and Fisher and Simmons (1977). The later equations of Francois and Garrison (1982a; 1982b) are the most accurate currently available (Appendix 2A). Francois and Garrison maintain that the predicted  $\alpha$  is within 5% of the true value, assuming that the temperature and other parameters are known exactly. More recently, Ainslie and McColm (1998) proposed a simplified formula for the absorption coefficient, based on the same hydrographic data, which is much easier to evaluate. However, for most purposes, and particularly when high accuracy is required, the original Francois–Garrison equations should be used despite their complicated formulation.

The rapid increase of absorption with frequency is the limiting factor which determines the highest useful frequency for the detection of targets at a given range. Above this limit, the absorption loss is so great that the received signal is below the noise level and cannot be detected. Some examples of the absorption loss are shown in Table 2.3. For targets at 100 m range in the sea, absorption is unimportant below 10 kHz, but at 1 MHz the useful range is only a few metres. The absorption in freshwater is relatively small at low frequencies, up to 200 kHz or so, since the molecular relaxation loss is absent. In that case, the same target should be detectable at greater ranges in freshwater applications than could be achieved in sea water. Above this frequency, however, the absorption is dominated by friction losses which are the same in fresh water and sea water.

**Table 2.3** Examples of the acoustic absorption coefficient ( $\alpha$ , dB km $^{-1}$ ) at selected frequencies relevant to fishery acoustics. The absorption depends on the water temperature, salinity and depth. Calculated values are shown for near-surface water at a temperature of 10°C, pH = 8 and salinity S, based on the formulas of Francois and Garrison (1982a; 1982b) which are given in Appendix 2A.

Frequency (kHz)	Absorption coefficient (dB km $^{-1}$ )	
	Sea water (S = 35 ppt)	Fresh water (S = 0 ppt)
18	2.76	0.10
38	10.1	0.45
70	23.6	1.52
120	38.7	4.48
200	54.3	12.4
420	101.2	54.8
1000	358.4	310.8

### 2.4.3 The sound speed

As with the absorption coefficient, the sound speed  $c$  depends on the water temperature, salinity and depth. It can also be predicted by empirical equations. Historically, the algorithms developed by Del Grosso (1974) and Chen and Millero (1977) are the usual basis for estimating sound speed from hydrographic measurements in the ocean. These equations are still considered to be the international standard. Speisberger and Metzger (1991) examined sound-travel times across 3000 km tracts of ocean, and found some deviations which suggested corrections of up to 0.7 m s $^{-1}$  in the results of Del Grosso (1974). More recently, Dunshaw *et al.* (1993) and Wong and Zhu (1995) re-examined these discrepancies and concluded that Del Grosso's equations do provide the best agreement with measurements of long-range propagation. The sound speeds predicted by all these equations match to within 0.025 m s $^{-1}$ , reinforcing the view that  $c$  can be estimated from physical parameters to better than 1%.

Simpler formulas for the sound speed are good enough for most fishery applications, notably Mackenzie (1981) who claims a standard error of 0.07 m s $^{-1}$  for his nine-term equation. Leroy (1969) provides a simpler version that is adequate in many cases. The relevant formulas are given in Appendix 2B. The variation of  $c$  with temperature and salinity is illustrated in Fig. 2.11 using Mackenzie's formula to give the predicted values of  $c$ .

In the case of sonars which transmit horizontally, refraction is important because the sound speed changes with depth. The temperature is normally highest at the surface, so the sound speed decreases with depth and the rate of change is most rapid at the thermocline. As a result, waves propagating near the surface bend downwards because the lower part of the wave-front is in cooler water where it travels more slowly (Fig. 2.12). When considering this effect, it is easier to understand what happens to the sound if we think of the acoustic signals as travelling along rays. A ray is a line which is everywhere perpendicular to the wave-front. The downward bending caused

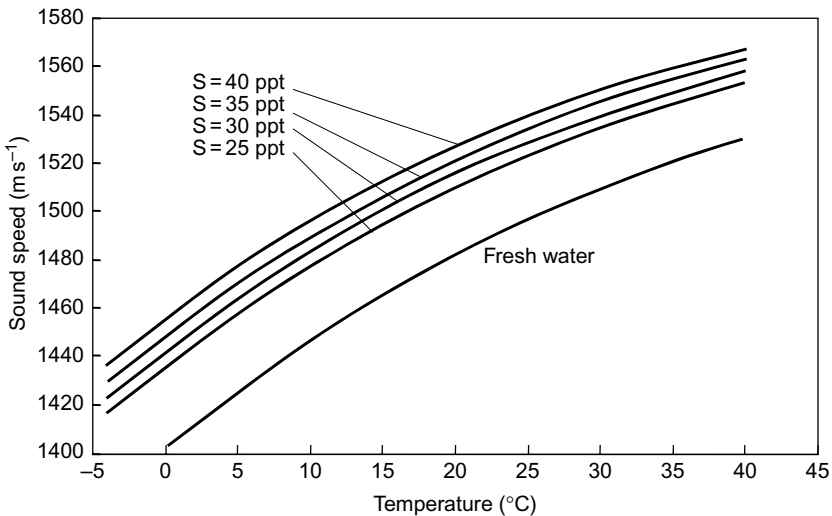


**Fig. 2.11** Variation of the sound speed in water as a function of temperature and salinity (S).

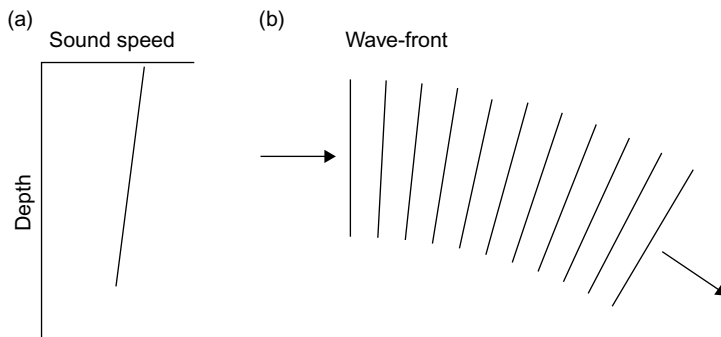


**Fig. 2.12** Refraction of sound waves. (a) In this example the sound speed decreases with depth, and (b) this causes the wave-fronts to incline progressively along the propagation path (arrowed) resulting in a downward deflection.

by refraction limits the horizontal range at which a target can be detected. This is seen by drawing rays in various directions from the sonar transducer (Fig. 2.13). At each point on the diagram, the ray is shown as a circular arc whose radius is proportional to the gradient of  $c$  across the wave-front. This means that the centre of the arc is at a point where  $c$  would be zero if the gradient were constant along the radius. Note that the arc centre could be below the seabed or above the water surface, depending on how the sound speed changes with depth. The gradient of  $c$  versus depth can be positive or negative (see below).

When a ray meets the surface or the bottom, it continues as a reflection. The angles from the surface to the incident and reflected rays are the same. Some

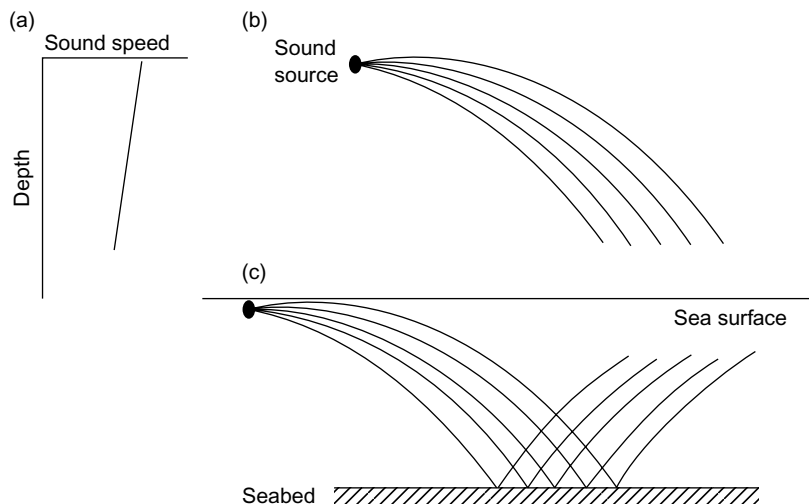
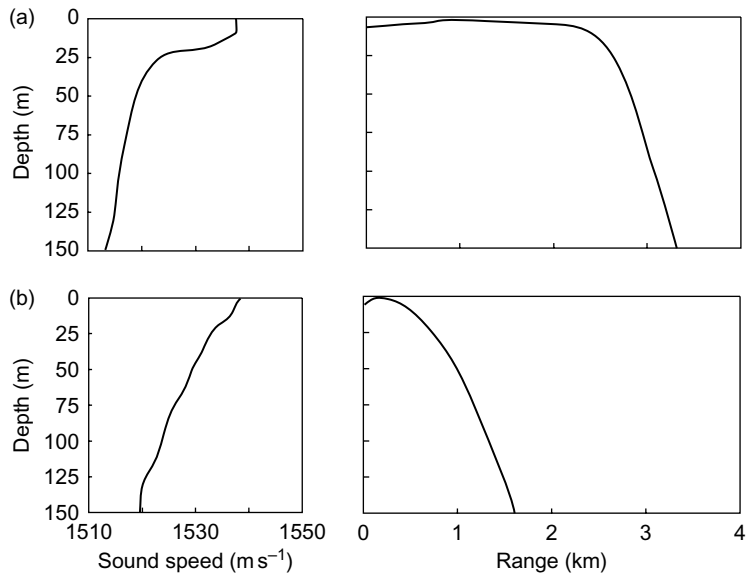


**Fig. 2.13** Ray tracing. (a) When the sound speed decreases with depth; (b) the rays are projected in a horizontal beam which is deflected downwards by refraction, limiting the maximum range in free-field conditions. (c) Reflection from the seabed can increase the effective range.

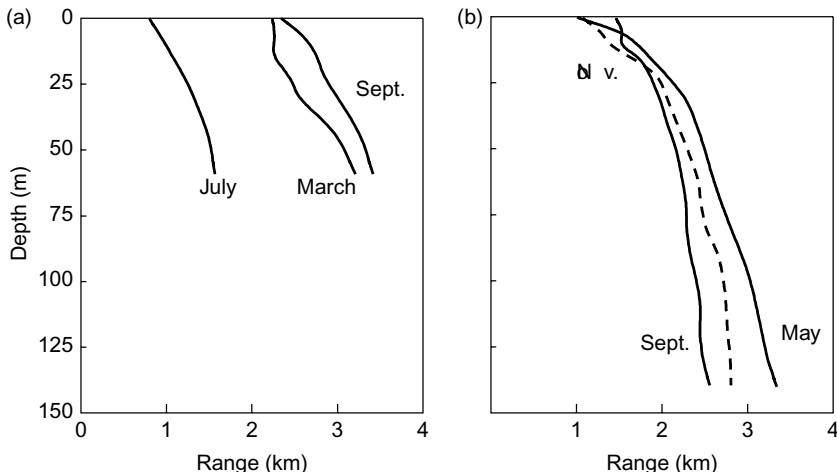
energy will be reflected (scattered) in other directions, especially at the seabed if it is rough, but the simple reflection law is good enough for the ray diagram to show any ‘hidden zone’ where targets will not be detected. It is possible for bottom-reflected rays to penetrate a zone which is inaccessible to the direct unreflected rays (Fig. 2.13c).

Figure 2.14 shows two examples of measured sound-speed profiles and the calculated surface-grazing ray which defines the maximum horizontal range of sonar detection. The transducer is 5 m below the surface and the range depends on the depth of the target. When the gradient of the sound speed is uniform (Fig. 2.14b), the ray-bending is particularly severe. In Fig. 2.14a, most of the change in  $c$  occurs at the strong thermocline above 25 m and the maximum range is greater. The position and strength of the thermocline changes with the time of year, and so does the performance of sonar. Figure 2.15 shows the maximum range that can be achieved in different months. In the Persian Gulf (Fig. 2.15a), the surface water becomes very hot in summer, up to 35°C, while the temperature below 50 m is less variable. Thus the thermocline is strongest in the summer, when the conditions for sonar observations are much worse than in other seasons.

Deep oceanic water is nearly isothermal, and below 500 m the depth (or pressure) dependence of  $c$  is the dominant factor and the sound speed increases with depth. Thus the negative gradient which occurs near the surface, caused by the strong influence of declining temperature, changes to a positive gradient further down. The refraction within these gradients has the strange effect of bending shallow waves downwards and deep waves upwards, confining the acoustic energy to an interval of depth known as the SOFAR channel. Low-frequency sound propagates



**Fig. 2.14** Observed variation of the sound speed with depth and the corresponding maximum range for sonar detection. (a) Persian Gulf; (b) Gulf of Oman.



**Fig. 2.15** Maximum range for sonar detection at different times of year vs the depth of targets. (a) Persian Gulf; (b) Gulf of Oman.

in the SOFAR channel with little change over hundreds of kilometres, since the propagation is two-dimensional and no energy is lost in reflections from boundaries. It is said that the great whales use the SOFAR channel to communicate over very long distances (Schevill *et al.* 1964).

### 2.4.4 Pulses and ranging

The pulsed sonar transmits a short burst of sound, called the pulse or the ping, consisting of several cycles at the sonar operating frequency. Figure 2.16 shows a pulse of 19 cycles generated by a 38 kHz sonar. The pulse duration (time from start to finish) is  $\tau = (19/38) = 0.5$  ms. If the sound speed is  $1500 \text{ m s}^{-1}$ , the pulse length in the water at any instant is  $L_p = c\tau = 75 \text{ cm}$ . The envelope of the pulse is the curve which shows the amplitude of the oscillations. Thus the envelope in Fig. 2.16 is a rectangle because the amplitude is constant during the transmission.

The transmitted pulse travels away from the transducer. When it encounters a target, some energy is reflected as the echo, which travels back to the transducer (Fig. 2.17). The echo is received at time  $t_e$  after the transmission. The distance  $R$  between the target and the transducer is estimated by measuring  $t_e$ . The two-way path length is  $2R$ , so:

$$t_e = 2R / c \quad (2.18)$$

$$R = ct_e / 2 \quad (2.19)$$

Suppose there are two targets at ranges  $R_1$  and  $R_2$ . In order to resolve the targets and measure them individually, the range difference ( $R_2 - R_1$ ) must be large enough

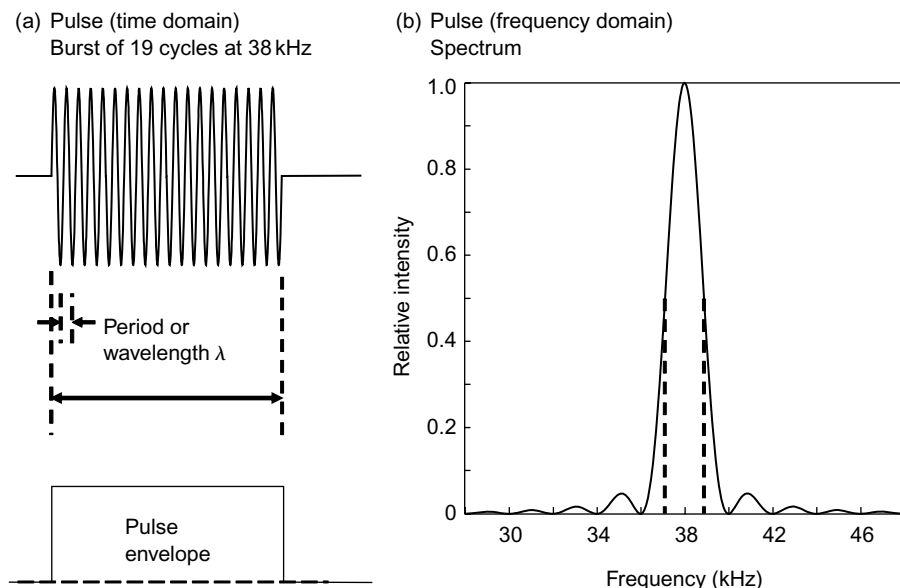


**Fig. 2.16** Illustration of a transmitted sonar pulse. As observed at the transmitter output, (a) the pulse is 19 cycles at 38 kHz (duration is 0.5 ms) in the time domain. In water the pulse length is 0.75 m when  $c = 1500 \text{ m s}^{-1}$ . The envelope is the curve joining the maximum amplitudes. (b) In the frequency domain, the spectrum shows the frequency composition as the intensity or power relative to the peak value. The broken lines indicate the bandwidth between half power points, 1.8 kHz in this case.

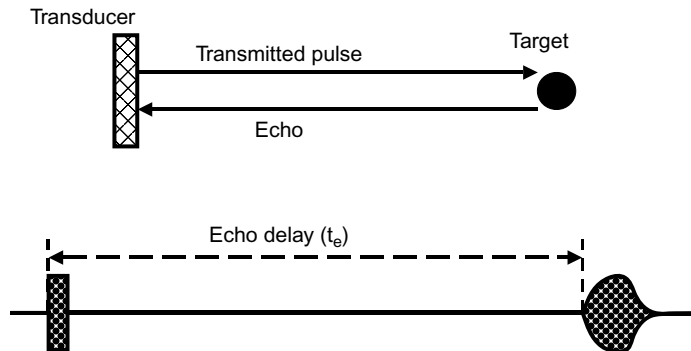


**Fig. 2.17** The target range ( $ct_e/2$ ) is estimated from the time delay between the transmitted pulse and the echo. The lower figure illustrates the pulse waveform that would be seen on an oscilloscope.

for the two echoes not to overlap. The echo from the nearer target is detected first, at time  $t_1 = 2R_1/c$ , and it continues for the pulse duration, that is until time  $(t_1 + \tau)$ . The second echo produces a signal which begins at  $t_2 = 2R_2/c$ . To resolve the targets, we must have  $t_2 > (t_1 + \tau)$  or:

$$R_2 - R_1 > c\tau / 2 \quad (2.20)$$

Thus targets must differ in range by at least  $c\tau/2$ , half the pulse length in water, to produce separate echoes. Another way of looking at this problem is to say that if there are many targets at all ranges, then at a given time, echoes are being received from those targets within a shell whose thickness is half the pulse length. Furthermore, the width of the shell is limited by the transducer beam because targets outside the beam produce no echo. This leads to the concept of the sampled volume  $V_0$ , which is the shell thickness multiplied by the effective cross-sectional area of the beam. The latter is equal to the equivalent beam angle times the square of the range, so:

$$V_0 = c\tau\psi R^2 / 2 \quad (2.21)$$

The sampled volume indicates the space that is contributing echoes at any instant. It is a useful measure for comparing the performance of different sonars.

## 2.5 Acoustic scattering

When acoustic waves encounter a target, some of the incident energy is scattered, generating a secondary wave which propagates in all directions away from the target. The reflection which occurs at a large smooth surface is a special kind of scattering, in which the secondary (reflected) wave is confined to one direction such that the incident and reflected wave-fronts are at the same angle to the surface.

More generally, scattering occurs wherever there is a spatial change of the acoustic impedance  $Z = \rho c$ . The proportion of the incident energy in the reflected wave is determined by  $r_b$ , the coefficient of reflection at a boundary (Tucker and Gazey 1966). If  $Z_w$  and  $Z_r$  are respectively the acoustic impedances of the water and of the reflector, then:

$$r_b = (Z_r - Z_w) / (Z_r + Z_w) \quad (2.22)$$

The greater the change of  $Z$  across a boundary, the stronger is the scattered wave. The remaining energy passes through the boundary as the transmitted wave. The strength of the scattered wave is determined by boundary conditions such as the continuity of the sound pressure. The theory of scattering by simply-shaped reflectors is well established and need not be repeated here. A more detailed treatment will be found in Morse (1948) and Officer (1958). The important and more complicated problem of scattering by fish and plankton is discussed at length in Chapters 6 and 7, respectively. Here we consider only the basic principles of acoustic reflection.

The energy reflected back towards the sound source is said to be backscattered. This component of the total scattering provides the sonar echo, in the monostatic case which means that the same transducer is used for transmission and reception. Small targets reflect energy in all directions, while large targets reflect most strongly in one direction. The component that propagates in the same direction as the incident wave is called the forward scatter. When the transmission is a short pulse, the incident and backscattered pulses occur at different times in the region between the source and the target, and there is no interference. This applies to almost all active echosounders and sonars. On the far side of the target, the sound field is the sum of the incident and forward-scattered waves, and they do coincide in time. After passing the target, the incident wave continues to propagate but the amplitude (pulse shape) is distorted by the addition of the forward scatter.

### 2.5.1 Targets large and small

A target is any object with a boundary across which there is a discontinuity in the acoustic impedance. If the target is very small compared to the wavelength, then as the incident wave arrives, the whole target is subjected to the same sound pressure. The target contracts and expands in response to the pressure oscillation in the incident wave, and it acts as a point source of the scattered waves, which spread spherically in all directions (Fig. 2.18). However, the scattered intensity is not usually the same in all directions. It is the volume rather than the shape of the target that determines the scattering. If  $d$  is the characteristic size, i.e. the cube root of the volume, then the scattered energy is proportional to  $(d/\lambda)^4$  when  $d \ll \lambda$ . This is the Rayleigh scattering law, which applies to light as well as to sound.

Now consider the other extreme, when the target is much larger than the wavelength. In this case the incident sound is scattered by the surface rather than the volume of the target. When the surface is smooth, the scattering is simply a reflected

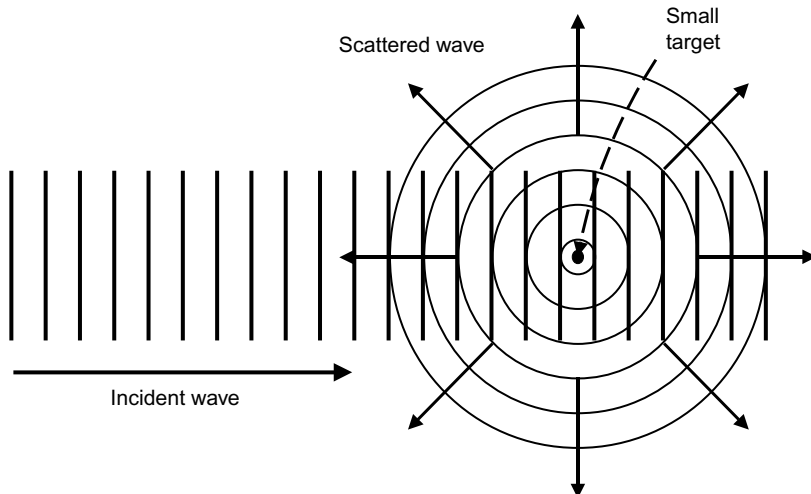


**Fig. 2.18** Scattering of sound by a small target. The scattered wave propagates outwards from the target in all directions.

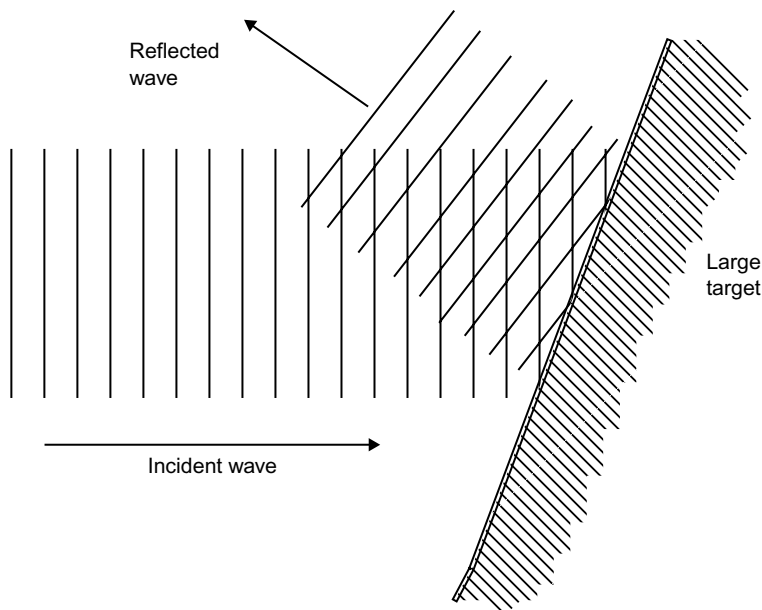


**Fig. 2.19** Scattering by a large target. The scattered waves form a specular reflection in one direction such that the angles of incidence and reflection are the same.

wave whose direction is determined by the usual rule that the angles of incidence and reflection are equal (Fig. 2.19). If the target is spherical, the scattered energy increases approximately as the square of the sphere radius. When this relationship applies, we say that the scattering is geometric or, for a plane surface, specular. The

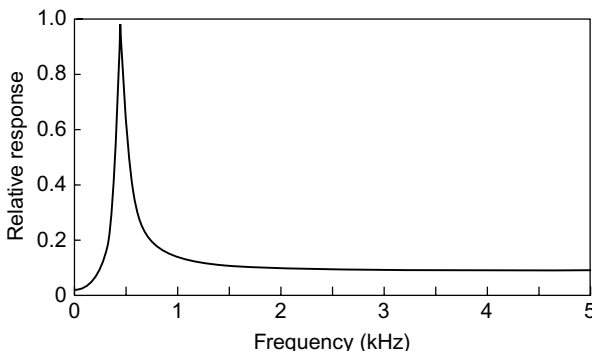


**Fig. 2.20** Frequency dependence of scattering by a gas bubble. The scattered intensity (normalized to 1 at the resonance) increases rapidly to a peak at the resonant frequency of the bubble, then it falls to a constant level at high frequencies.

reflection from a plane surface is sometimes referred to as the Lloyd's mirror effect. The shape of the target is important as well as the size. Thus a flat disc and a sphere of the same radius have different scattering properties.

Reflections at the sea surface and the bottom are of particular interest. The surface is a good reflector because the impedance mismatch between water and air is very great, and  $Z_r \ll Z_w$ . For this condition, Equ. (2.22) gives the result  $r_b \approx -1$ . This means that the intensities of the incident and reflected waves are nearly the same, but the negative coefficient of reflection indicates that the two waves are in antiphase; the reflected pressure is minimal when the incident pressure is maximal, and vice versa. In the case of the bottom reflection, the acoustic impedance is higher in the ground than the water ( $Z_r > Z_w$ ). Referring again to Equ. (2.22),  $r_b$  is now positive and the reflected and incident waves are in phase. If the bottom is rough, meaning that it is uneven on the scale of the wavelength, some energy is scattered in directions other than that of the specular (mirror-like) reflection.

At intermediate sizes where the target dimensions and the wavelength are similar, the scattering depends on the geometric structure and the material properties of the target in a rather complicated way. Resonances occur which cause the strength of scattering to change rapidly with frequency. In the case of gas bubbles in shallow water, there is one resonance near the high-frequency limit of the Rayleigh scattering region (Fig. 2.20). At higher frequencies, in the geometric region, the scattering strength of the gas bubble is almost constant. The resonance behaviour of solid targets is more complicated. Many sharp resonances occur at intervals above a certain frequency which is normally within the geometric scattering region. This phenomenon is discussed further below.

In summary, scattering by a small target increases rapidly with frequency; for large targets the frequency has little effect; at intermediate sizes of the order of a wavelength, resonances occur which make it difficult to predict the scattering accurately.

## 2.5.2 Target strength

Most fisheries applications involve only one transducer which is used both to transmit acoustic pulses into the water and to detect echoes from targets within the transducer beam. In that case, only the backscattered waves are important, namely those travelling in exactly the opposite direction to the incident waves generated by the transmitter.

The target strength is a logarithmic measure of the proportion of the incident energy which is backscattered by the target. To understand the nature of target strength, it is better to begin with the related quantity  $\sigma_{bs}$ , the backscattering cross-section, which is a more meaningful parameter in physical terms.  $\sigma_{bs}$  is measured in units of area, square metres in SI units. It is defined in terms of the intensities of the incident and the backscattered waves.

Suppose  $I_i$  is the intensity of the incident waves at the target. The fact that the transmission is a pulse complicates matters, but suppose for the present that the pulse is long and  $I_i$  refers to the intensity at the midpoint of the pulse.  $I_{bs}$  is the intensity at the midpoint of the backscattered pulse.  $I_{bs}$  will depend on the distance  $R$  from the target at which the intensity is measured. If  $R$  is large enough to be outside the near field of the target, which means that  $R$  has to be much greater than the linear size of the target, but not so large that absorption losses are important, then the backscattering cross-section  $\sigma_{bs}$  is defined by the relationship:

$$\sigma_{bs} = R^2 I_{bs} / I_i \quad (2.23)$$

The inverse-square law of energy spreading means that  $(R^2 I_{bs})$  is the same at any range, thus Equ. (2.23) gives  $\sigma_{bs}$  as a constant for a given target. Various other cross-sections are used to describe the acoustic scattering properties of targets (MacLennan *et al.* 2002). The most general is the differential scattering cross-section  $\sigma(\theta, \phi)$  which covers the bistatic case, i.e. the transmitter and receiver are separate, and the angles  $(\theta, \phi)$  define the direction of the receiver relative to the transmitter as seen from the target (Medwin and Clay 1998). This is defined in the same way as Equ. (2.23), in terms of the intensity  $I_{scat}(\theta, \phi)$  measured by a receiver at a distance  $R$  from the target in the stated direction. The distance to the transmitter is not relevant since  $I_i$  is the actual intensity at the target position.

$$\sigma(\theta, \phi) = R^2 I_{scat}(\theta, \phi) / I_i \quad (2.24)$$

$\sigma_{bs}$  is the same as  $\sigma(\theta, \phi)$  in the backscattered direction for which  $\theta = -\pi$  and  $\phi = 0$ . Another measure of the same quantity is the so-called spherical scattering cross-section, written as  $\sigma_{sp}$  (MacLennan *et al.* 2002) which is equal to  $\sigma_{bs}$  multiplied by  $4\pi$ .  $\sigma_{sp}$  is an older concept which derives from the over-simplified idea that the scattered intensity is the same in all directions. That is true for very small targets, and then  $\sigma_{sp}$  has a specific physical meaning as the area which intercepts transmitted power equal to the total power in the scattered wave. The  $4\pi$  factor arises because the surface area of a sphere,  $4\pi R^2$ , is multiplied by the intensity to obtain the scattered power.

The spherical scattering cross-section is sometimes used to describe backscattering by targets which are not omni-directional, although the strict physical meaning of the parameter is then lost.

There has been much confusion over the years due to  $\sigma_{bs}$  and  $\sigma_{sp}$  not being clearly distinguished in the literature. The term ‘acoustic cross-section’ and the symbol ‘ $\sigma$ ’ have been used for both parameters, especially in older publications, but they are not adequate descriptors. When numerical values are quoted, it is essential to state which cross-section is intended. In this book, all references to backscattering cross-sections mean  $\sigma_{bs}$  defined by Equ. (2.23). Fortunately, this difficulty does not apply to the target strength which has a unique and universally accepted definition (see below).

Equ. (2.23) is rigorously correct only for the case of continuous transmission at constant amplitude and in the absence of absorption. It is also assumed that the target is isolated; no other targets or reflecting boundaries are close enough to perturb the scattered sound field at the position where  $I_{bs}$  is measured. The problem with continuous transmission is that the incident and scattered waves coexist, so it is not possible to measure them separately. When the transmission is a pulse of finite duration, this problem is overcome because the incident and backscattered pulses are separated in time. If the pulse is long enough, intensity measurements in mid-pulse will be a good approximation to the continuous-wave case. If the pulse is short, however, the definition of  $\sigma_{bs}$  is more complicated. It involves the frequency response of the sonar as well as scattering properties of the target, because a short pulse may be conceived as the sum of many continuous waves covering a spectrum of frequencies (MacLennan and Forbes 1984). Suppose that  $\sigma(\omega)$  is the backscattering cross-section as defined by Equ. (2.23) when the transmission is continuous at frequency  $\omega$ , and  $P(\omega)$  is the power response of the sonar.  $P(\omega)$  is the signal power which would be observed at the output of the sonar receiver if the transmissions were applied directly to the receiving transducer. According to the definition of Foote (1982a),  $\sigma_{bs}$  is a weighted average of  $\sigma(\omega)$  over the bandwidth of the sonar. The formal definition is:

$$\sigma_{bs} = \int_0^{\infty} \sigma(\omega)P(\omega) d\omega / \int_0^{\infty} P(\omega) d\omega \quad (2.25)$$

Note that the frequency response of the sonar is unimportant if  $\sigma(\omega)$  is constant over the bandwidth, in which case Equ. (2.25) reduces to  $\sigma_{bs} = \sigma(\omega)$ . One complication is the absorption loss which is ignored in the defining equations. However, a simple correction can be made if necessary. The measured  $I_{bs}$  is multiplied by the factor  $\exp(\beta R)$  to give the intensity that would be observed in a lossless medium.

The target strength is the backscattering cross-section expressed in decibels, according to the formula:

$$TS = 10 \log_{10}(\sigma_{bs}) = 10 \log_{10}(\sigma_{sp} / 4\pi) \quad (2.26)$$

When this formula is used, the value substituted for  $\sigma_{bs}$  or  $\sigma_{sp}$  must be in  $m^2$ . Note that TS has the same numerical value whichever cross-section is used. TS,  $\sigma_{bs}$  and  $\sigma_{sp}$  are

simply alternative ways of describing the same physical property of the target, namely the strength of backscattering. The logarithmic TS is convenient because of the great difference between aquatic organisms at opposite ends of the size scale, which covers many orders of magnitude, from microscopic plankton to the great whales. A modest span of decibels is sufficient to describe the target strengths of all these creatures. For almost all fish, TS is within the range  $-60$  dB to  $-20$  dB. The equivalent back-scattering cross-sections span four orders of magnitude, from  $0.000001$  to  $0.01\text{ m}^2$ . To calculate  $\sigma_{\text{bs}}$  equivalent to a given target strength, the formula is:

$$\sigma_{\text{bs}} = 10^{(\text{TS}/10)} \quad (2.27)$$

The concept of logarithmic units may seem rather strange to those not familiar with fields such as electrical engineering where their use is common. Comprehension is not helped by the fact that in the case of fish, TS is always negative, and  $-60$  is a smaller number than  $-20$ . In thinking about the nature of acoustic scattering and its theoretical description, it is easier to work with the backscattering cross-section  $\sigma_{\text{bs}}$ , which can be conceived as a physical area which is related to the size of the target. Target strength is more often used in practical work which involves calculations with real data, to provide numerical values within a convenient range. The important point to remember is that the decibel is a measure of ratio. To say that one target is  $3$  dB more than another means that the stronger target scatters twice as much energy; if the difference were  $6$  dB, the scattered-energy ratio would be four times, and so on. The  $-20$  dB target, a large tuna perhaps, produces an echo 10 000 times as strong as one at  $-60$  dB, such as a small sprat around  $4$  cm in length.

### 2.5.3 Standard targets

One method of calibrating the sonar is to measure the echo from a standard target whose acoustic scattering properties are known. Early proposals for standard targets included table tennis balls (Welsby *et al.* 1972) and solid spheres made from various materials such as steel or brass (MacLennan 1982). However, subsequent work showed that spheres made from tungsten carbide (MacLennan and Armstrong 1984; MacLennan and Dunn 1984) or copper (Foote 1982a; Foote and MacLennan 1984) give the best results.

The scattering properties of the homogeneous sphere do not change as the target rotates. Thus the orientation of the sphere is unimportant, and the echo is determined only by the position of the centre relative to the transducer. There is a well-established theory for calculating the backscattering cross-section from the material properties of the sphere expressed as proportions of those in water (Hickling 1962; Dragonette *et al.* 1974; Neubauer *et al.* 1974; MacLennan 1981a). The functional dependence is:

$$\sigma_{\text{bs}} = (a^2 / 4) F(\omega a / c, \rho_1 / \rho, c_1 / c, c_2 / c) \quad (2.28)$$

There are two sound speeds within the sphere,  $c_1$  and  $c_2$ , which are the speeds of longitudinal and transverse waves respectively.  $\rho_1$  is the sphere density and  $a$  is the

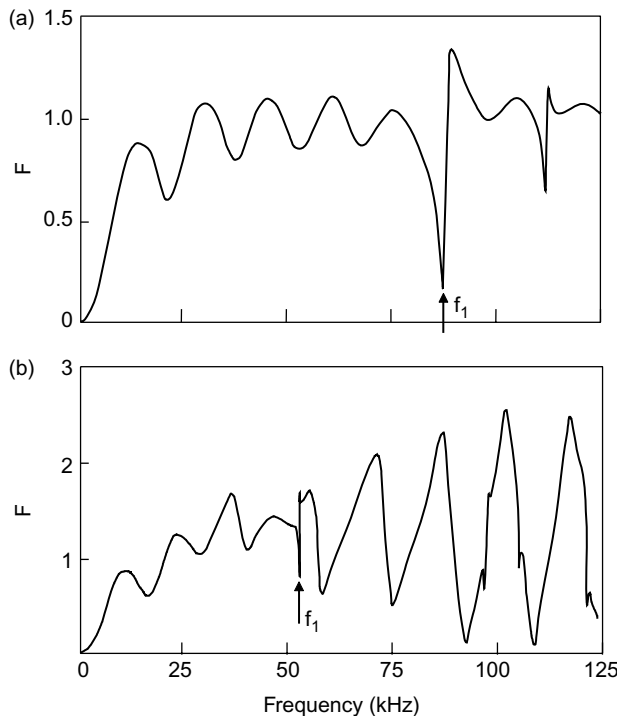


**Fig. 2.21** Frequency dependence of scattering by a homogeneous solid sphere of radius  $a$ . (a) Tungsten carbide,  $a = 19.05 \text{ mm}$ ; (b) copper,  $a = 30.0 \text{ mm}$ . The vertical axes (note different scales) show the form function ( $F$ ) which is the ratio of the spherical and geometric cross-sections (cf. Eqn. 2.28). The arrows indicate the lowest resonant frequency ( $f_1$ ) of each sphere.

radius.  $\rho$  and  $c$  are respectively the density and sound speed in the surrounding water. Thus changes in the medium influence the scattering properties.  $F$  is the so-called form function, defined (for historical reasons) as the ratio of the spherical scattering and geometric cross-sections, i.e.  $F = \sigma_{\text{sp}}/\pi a^2 = 4\sigma_{\text{bs}}/a^2$ .

The variation of  $\sigma_{\text{bs}}$  with frequency is shown in Fig. 2.21 for tungsten carbide and copper spheres. At very low frequencies, Rayleigh scattering applies and  $\sigma_{\text{bs}}$  varies as  $f^4$ . Once the wavelength is commensurate with the sphere size,  $\sigma_{\text{bs}}$  varies cyclically and smoothly at first, but extreme variations occur at frequencies above a certain limit  $f_1$ . In the high-frequency region, there are sharp maxima and minima which correspond to resonances between the elastic vibrations of the sphere and the sound field in the water. The resonances occur at discrete frequencies which depend on the sound-speed ratios. The density ratio also has an influence but this is small. Since the parameter  $\omega a/c = 2\pi a/\lambda$ , the frequency dependence is controlled by the number of wavelengths across the sphere. This means that for the same material and sound speed, the resonance frequencies are inversely proportional to the sphere radius. The larger the sphere, the lower is the frequency  $f_1$  which marks the beginning of the resonance region.

The standard target must be large enough to provide a strong echo well above the background noise level and of similar amplitude to the echoes that would be received by the sonar in the intended application. This dictates the approximate cross-section of the target. To meet this requirement, the sphere may have to be so large that the sonar frequency  $f_0$  is greater than  $f_1$ . It is important to ensure that no resonance is within the frequency band of the transmission. Otherwise the target strength will be sensitive to small changes in the environmental conditions, notably the water temperature, which determines  $c$ , in which case the sphere will be unsuitable as a standard for calibration purposes. More generally, the optimum sphere size for a particular application can be determined as follows (Foote 1982a; Foote *et al.* 1983). A first approximation to the radius  $a$  is the size which gives the required target strength at frequency  $f_0$  on the assumption that the form function  $F = 1$ . The nominal value of the target strength is much less important than the need to avoid resonances. Calculations are performed for a range of sizes around the approximate value, to determine how the target strength changes with the expected variability of the sound speed in water, the pulse duration and other parameters. The optimum sphere size is the one whose target strength is least sensitive to changes in the parameters. However, it should not be necessary for the users of acoustic instruments to perform these rather complicated calculations. The manufacturers of scientific echosounders will normally recommend optimum spheres for the calibration of their own equipment.

The harder the material of the standard target, the higher  $f_1$  is for the same size of sphere. For this reason tungsten carbide is particularly suitable for standard targets. It is durable and does not corrode in the sea. The spheres are manufactured by sintering the tungsten carbide with a small amount (about 6%) of cobalt as a binder. The density varies slightly with the proportion of cobalt, but  $\rho$  is easily measured. MacLennan and Dunn (1984) determined the sound speeds in tungsten carbide spheres from which the target strength for any size and frequency may be calculated precisely. The sound speeds  $c_1$  and  $c_2$  are checked by comparing the expected and measured frequencies of particular resonances. The theory works well even at quite high frequencies. Figure 2.22 compares the observed and measured resonances on a sphere designed for use at 455 kHz. The measurements are noisy, as the narrow bandwidth limits the energy transmitted at frequencies distant from the centre frequency of the sonar, but there is a clear match between the measured and predicted resonances. From this diagram it is also easy to see that small changes in the size of the sphere can move the response from a region where the form function is relatively flat to one where a resonance occurs within the frequency band of the sonar. In our example (Fig. 2.22), a sphere only 1 mm larger or smaller than the optimum would be useless as a reference target. The design of optimum spheres becomes more difficult as the frequency increases, and is therefore particularly challenging in the case of broadband sonars which transmit frequencies well above those discussed so far. The selection of spheres for use at various frequencies between 850 kHz and 3.6 MHz is discussed in detail by Foote *et al.* (1999). This involves several dissimilar spheres,

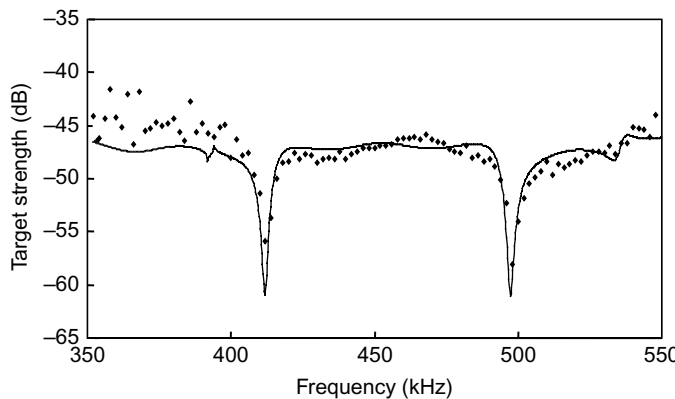


**Fig. 2.22** Comparison of measured and theoretical target strengths of a 16 mm diameter tungsten carbide sphere. There is good agreement especially around the resonance frequencies. The measurements distant from the design frequency (455 kHz) are noisy as the sonar generates little energy in that part of the spectrum.

each assigned to one or a few operating frequencies, of sizes that ensure the resonances have minimal influence on the target strength. The calibration technique may also require a different type of transmitted waveform (e.g. a chirp instead of a mono-frequency pulse) to ensure a good enough signal-to-noise ratio. This topic is discussed by Foote (2000).

#### 2.5.4 Target shape and orientation

With the exception of a perfectly spherical target, or one that is very small compared to a wavelength, the scattered sound field depends on the shape of the target and how it is positioned relative to the incident wave direction. The target strength is still defined in the same way, but in general it is a function of shape and orientation as well as the material properties of the target. In this book we are particularly interested in fish-like shapes, namely objects which are long compared to their width and height. This description is relevant to the swimbladder (as the dominant reflecting organ) as well as the fish body. The target strength of such an object is strongly influenced by the tilt angle. This is defined as the angle between the long axis of the object and the incident wavefront. In the case of asymmetric targets like a fish, it is necessary to distinguish head-up and head-down orientations for which the tilt angles are, respectively, positive and negative (Fig. 2.23). In this context, since fish are usually insonified from above, head-up means that the transducer is closer to the head than to the tail.

We shall see later, in Chapter 6, that the tilt behaviour of fish is an important determinant of the target strength. Figure 2.24 suggests an explanation as to why the tilt angle should have such a pronounced effect on acoustic scattering. When the transmitted pulse interacts with a long and thin target such as a swimbladder,

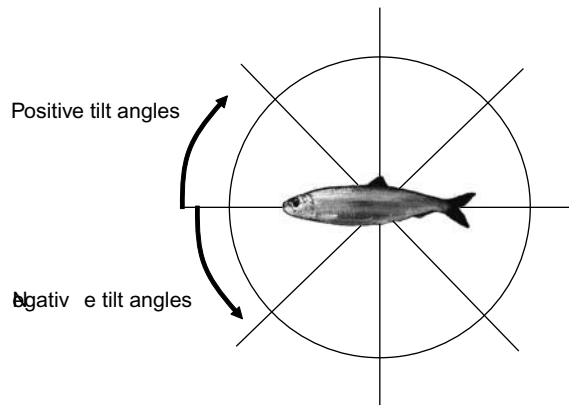


**Fig. 2.23** Definition of the tilt angle of a fish. The angle is positive with the fish head up and negative with the fish head down.

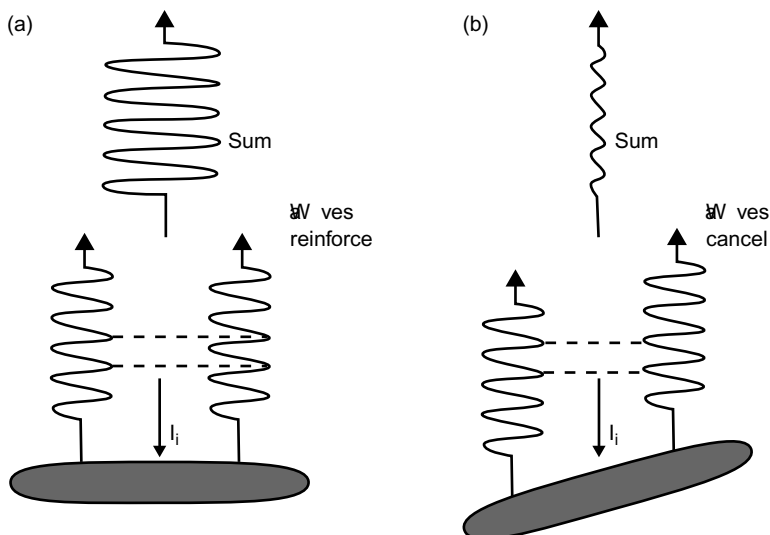


**Fig. 2.24** Effect of tilt angle on the echo from an oblong target, e.g. a fish swimbladder. Destructive interference reduces the echo amplitude when the path difference between opposite ends of the target is a substantial fraction of a wavelength.

the energy in the reflected wave changes as the target tilts. There are two reasons for this effect. Firstly, the apparent size of the target, as seen from the transmitting transducer, decreases as the tilt increases. Secondly, while the apparent size varies as the cosine of the tilt angle, the echo energy may change even more rapidly because of interference between wavelets reflected from different parts of the target. When the target is parallel to the incident wavefront, as in Fig. 2.24a, all the reflected wavelets are in phase and reinforce each other. When the target tilts, the wavelets

originating at opposite ends of the target become progressively out of phase and the summed amplitude is reduced, eventually to zero in the case of two wavelets that are exactly out of phase. This interference effect is only important when the acoustic wavelength is comparable to, or smaller than, the length of the target. In the case of very long wavelengths, the path difference is never great enough to produce a large phase difference.

### 2.5.5 *Multiple targets*

We have seen that to resolve the echoes from two targets, they must be separated in range by at least  $c\tau/2$ , half the pulse length in water. We have also seen how the orientation of a long thin target affects the target strength as different parts of the object reflect signals at slightly different ranges. More generally, in the case of a layer containing many small scatterers in close proximity,  $c\tau/2$  is the width in range of the sampled volume from which echoes are being received at any instant.

The echo waveform produced by an isolated small target is rather similar to the waveform of the incident pulse. The echo is modified by the frequency response of the target, but if the sonar has a narrow bandwidth (10% of  $f_0$  or less), the frequency response of the target can generally be ignored, unless  $f_0$  happens to be close to a resonance. However, when the received signal contains the superimposed echoes from many targets, the different phases of each echo cause the signal amplitude to fluctuate. The echoes are said to interfere with one another. Furthermore, the targets may move (this is certainly true of fish) and the amplitude fluctuations are not consistent from one ping to the next. Examples of this effect are shown in Fig. 2.25. Because of the interference, one sample of the signal amplitude provides little information about the density of targets in the sampled volume.

If the targets are positioned randomly on the scale of a wavelength, the phases are random and the instantaneous amplitudes are described by the Rayleigh distribution (Rayleigh 1945) for which the probability that the instantaneous intensity (amplitude squared) exceeds  $I$  is  $\exp(-I/I_m)$ , where  $I_m$  is the mean intensity. Furthermore, the mean and standard deviation of the intensity are equal. The Rayleigh distribution has the important property that the shape of the probability density function (PDF) is independent of  $N$ , the number of scatterers contributing to the received signal. The mean intensity is proportional to  $N$ , but the proportional fluctuation of the signal is virtually the same for  $N = 10$  or  $N = 100$ . However, if the target density is low ( $N < 5$ ), the shape of the PDF deviates from the true Rayleigh distribution and there is a possibility of estimating the target density (or the number of targets as the density multiplied by the sampled volume) from the statistics of the echo intensities. If  $N$  is more than 5, the statistical properties for different  $N$  are too similar for the target density to be inferred from the statistics of the amplitude distribution alone.

When the density of targets is very high, the received signal is further modified by acoustic extinction and multiple scattering, which remove energy from the direct path of the incident and backscattered waves. These problems are discussed in Chapter 5.

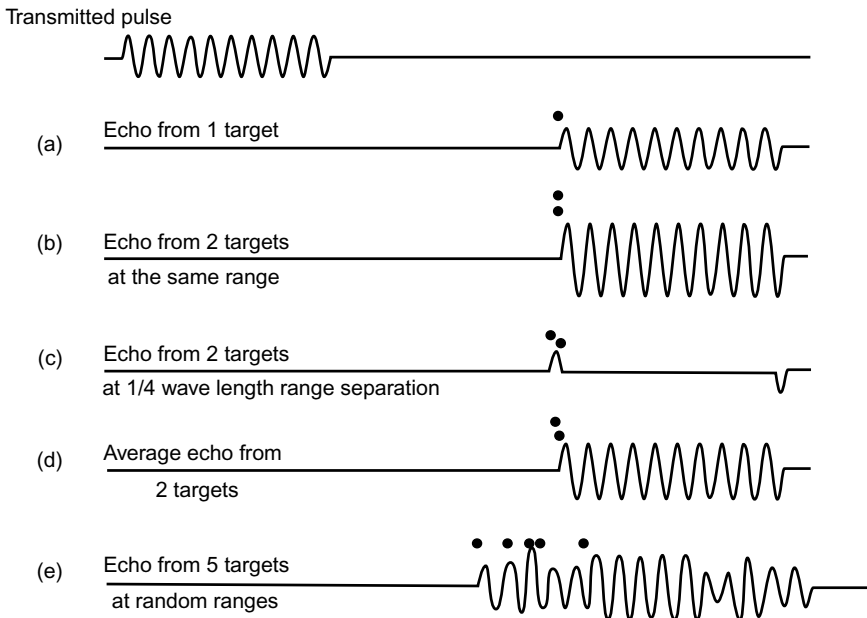


**Fig. 2.25** How the echoes from multiple targets combine. (a) An isolated target simply reproduces the transmitted pulse; (b) when two targets are at the same range, the amplitudes sum; (c) for two targets  $\lambda/4$  apart in range, the echoes largely cancel with residuals separated by  $\lambda/2$ ; (d) for two targets at random ranges, the average energy is summed; (e) five targets at random ranges produce irregular signal amplitudes and phase changes.

### 2.5.6 Volume/area scattering coefficients

When the individual targets are very small and there are many in the sampled volume, their echoes combine to form a received signal which is continuous with varying amplitude. It is no longer possible to resolve individual targets, but the echo intensity is still a measure of the biomass in the water column. The basic acoustic measurement is the volume backscattering coefficient,  $s_v$ , which is obtained from the echo-integral (cf. Section 5.4).  $s_v$  is formally defined as:

$$s_v = \Sigma \sigma_{bs} / V_0 \quad (2.29)$$

where the sum is taken over all the discrete targets contributing to echoes from  $V_0$ , the sampled volume. The equivalent logarithmic measure is the volume backscattering strength,  $S_v = 10 \log(s_v)$  whose units are dB re  $1 \text{ m}^{-1}$ . When  $s_v$  is averaged over a volume much larger than  $V_0$ , covering a larger range interval and several pings, the logarithmic equivalent is called the mean volume backscattering strength or MVBS. This measure of the scattering strength is common in studies of plankton aggregations.

The area backscattering coefficient ( $s_a$ ) is a measure of the energy returned from a layer between two depths in the water column. It is defined as the integral of  $s_v$

with respect to depth through the layer.  $s_a$  is an important parameter in fisheries acoustics because most echo-integrators provide data in terms of the integration over one or more layers. Since  $s_a$  is the product of  $s_v$  (units  $\text{m}^{-1}$ ) and distance, it is dimensionless. This makes it difficult to express numerical values clearly when different scaling factors are applied. The basic SI unit for  $s_a$ , as defined above, should be written as ( $\text{m}^2/\text{m}^2$ ) meaning the integrated  $\sigma_{\text{bs}}$  per square metre of the layer surface. There are various scaled versions of  $s_a$  in common use, notably the nautical area scattering coefficient (NASC) for which we use the symbol  $s_A$ . For historical reasons, this is defined in terms of the spherical scattering coefficient ( $\sigma_{\text{sp}}$ ) and the nautical mile (1852 m). The conversion formula is  $s_A = 4\pi(1852)^2 s_a$ . Although  $s_a$  is dimensionless, it is essential to indicate the scaling when quoting numerical values. This is done by adding e.g. ( $\text{m}^2/\text{m}^2$ ) for the basic SI unit, or ( $\text{m}^2/\text{km}^2$ ) as another differently-scaled parameter. Thus the NASC unit is written as ( $\text{m}^2/\text{nmi}^2$ ). However, the unit statement does not indicate which cross-section is involved in the parameter definition, nor does it mention the  $4\pi$  factor. This may be clarified by using definitive symbols as recommended by MacLennan *et al.* (2002). In their scheme, symbols for the area scattering coefficient are subscripted in lower or upper case when the parameter is based on  $\sigma_{\text{bs}}$  and  $\sigma_{\text{sp}}$ , respectively. In particular, the NASC should always be accorded the symbol  $s_A$ .

### **2.5.7 Radiation pressure on targets**

When a pulsed transmission is reflected from a density discontinuity, such as the swimbladder surface in a fish, the phenomenon of radiation pressure generates a force on the reflecting boundary. This effect has important implications for the ability of fish to detect sonar transmissions (cf. Chapter 4). Radiation pressure occurs because the incident and reflected waves carry momentum in opposite directions. Newton's second law of motion states that force equals the rate of change of momentum, thus the reflection generates a pressure on the boundary which is proportional to the intensity of the incident wave. If the transmission is an ultrasonic pulse incident on a perfectly reflecting boundary (the swimbladder surface is close to this ideal), and the root-mean-square pressure of the incident wave at the boundary is  $p_{\text{rms}}(t)$  at time  $t$ , the radiation pressure is:

$$p_{\text{rad}} = p_{\text{rms}}^2(t) / (\rho c^2 / 2) \quad (2.30)$$

The important point to note is that  $p_{\text{rad}}$  is always positive. It follows the envelope of the incident intensity. The spectrum of  $p_{\text{rad}}$  includes ripple at twice the modulation frequency, but the principal frequency components are those of the pulse envelope. The spectrum of a rectangular unmodulated signal of duration  $\tau$  is maximum at zero frequency, reducing to half the maximum level when  $f = 0.3/\tau$ . If  $\tau = 0.5 \text{ ms}$  for example, this means the spectrum of the radiation pressure is strongest in the range 0–600 Hz. As we shall see in Chapter 4, many fish species have sensitive hearing at such low frequencies. However, if the signal is a pure tone, for which  $\tau$  is very long,

the cut-off frequency is very low. In that case the  $p_{\text{rad}}$  spectrum should be insignificant at frequencies within the typical hearing range of fish.

The term  $(\rho c^2/2)$  is called the internal cohesive pressure of the medium. For values typical of water, say  $\rho = 1000 \text{ kg m}^{-3}$  and  $c = 1500 \text{ m s}^{-1}$ , this is 301 dB re 1  $\mu\text{Pa}$  or rather more than 3000 atmospheres. To illustrate the potential effect of radiation pressure, consider an echosounder transmitting a source level of 220 dB re 1  $\mu\text{Pa}$  at 1 m, and a fish swimbladder within the beam at 50 m range. It is convenient to use the decibel notation due to the large numbers in the calculation.  $p_{\text{rms}}$  is then 186 dB re 1  $\mu\text{Pa}$ , and Equ. (2.30) gives  $p_{\text{rad}}$  as  $(2 \times 186 - 301) = 71 \text{ dB re } 1 \mu\text{Pa}$ . Although some of the  $p_{\text{rad}}$  spectrum may be outside the normal hearing range, this signal is strong enough to be detectable by many fish species (cf. Chapter 4).

### 2.5.8 *The inverse scattering problem*

Much of sonar theory is formulated in terms of the so-called forward problem. The transmitted energy propagates through the water and is scattered by one or more targets, producing echoes which propagate back to the transducer where they combine to form the received signal. The standard theory describes the received signal as a unique result of the scattering properties of the targets, their location in space, the propagation losses and so forth. The forward problem presumes that the target properties are known. In practice, however, a sonar measures the acoustic signal received from one or more unidentified targets. The performance of the sonar is determined by calibration and the propagation losses are calculated from knowledge of the sound speed and absorption coefficient. The question then is, what do these measurements tell us about the unknown targets? This is the inverse scattering problem. In general, it does not have a unique solution because different sets of targets might produce the same signal.

Much of this book is concerned with establishing the rules and assumptions required to solve the inverse scattering problem in fisheries applications, in particular to identify and quantify the aquatic organisms which have generated the signals observed by sonar.

## 2.6 Echo detection

The receiver is an electronic amplifier between the transducer and the sonar output. The transducer converts the acoustic echoes to small electrical signals which must be amplified many times before they can be measured or displayed. The receiver has two other functions. Firstly, it may include time-varied gain (TVG, Section 3.8) to compensate the signal for spreading and absorption losses, providing a sonar output that is independent of the target range. Secondly, the receiver filters the transducer signal, rejecting components of the signal at frequencies outside the pass-band of

the amplifier. The filtering is described by the bandwidth  $B$ , which normally means that signals at frequencies  $f_0 \pm B/2$  are attenuated by 3 dB relative to the response at the central sonar frequency,  $f_0$ .

The transmitted pulse is a number of cycles at frequency  $f_0$ . The frequency spectrum of this pulse depends on the pulse duration  $\tau$ . The shorter the pulse, the wider is the spectrum; there is more energy at frequencies further from  $f_0$ . The same is true of the echo. Thus  $B$  must be large enough to pass most of the echo energy. On the other hand, a narrow bandwidth reduces the broadband noise in the signal and makes it easier to detect small echoes. The signal-to-noise-ratio (SNR) is a common measure of the performance of a sonar system. It is the ratio of the signal energy to that of the noise in the bandwidth of interest, usually expressed in dB.

The width of the transmitted spectrum is inversely proportional to  $\tau$ . As a general rule, to avoid significant loss of echo energy, the bandwidth should be such that the product  $B\tau = 3$ . For example, if  $\tau = 1$  ms, then  $B$  should be 3 kHz. If the echo detection is limited by broadband noise, then the bandwidth might be reduced to  $B\tau = 1$ . Some of the echo energy would then be removed by the filter, but the SNR would nevertheless be increased to its optimum level. The best SNR is obtained by using a ‘matched’ filter. This type of filter exactly duplicates the complete frequency response (often described as the transfer function) of the transmitted signal, water path and target characteristics combined. In many practical circumstances, a matched filter maximizing the SNR will give the best detection results. However, in some applications we need to preserve features of the pulse shape and/or signal phase which are relevant to, for example, algorithms for target identification. In that case a good SNR is not the only consideration, and a non-matched filter may be required for the best performance.

In modern sonars, both the range correction (time-varied-gain) and band-pass filtering are implemented by digital signal processing. Compared to the earlier analogue methods, digital techniques allow more complex signal filters at less cost, and much better stability of operation may be achieved. Nevertheless, care must always be taken to ensure that the sonar design is fully compatible with user needs. Another advantage of digital processing is that the time-varied-gain for range compensation by use of a TVG can be implemented exactly, thus removing one of the major limitations of analogue technology.

The SNR is a fundamental limitation on the detection of small targets in deep water (cf. Section 5.3.5). The reduction of electronic noise through careful exclusion of electromagnetic radiation from sensitive parts of the sonar, and limiting the self-generated noise in the water can make a considerable difference to SNRs. In the case of echosounders on ships, Mitson (1995) noted that the noise radiated by a vessel above 5 kHz, although unimportant for fish which do not hear such frequencies (cf. Chapter 4), can still degrade the performance of the onboard acoustic instrumentation. Thus attention to the vessel-noise specification above 5 kHz is still important if the best signal-to-noise performance is to be achieved.

### 2.6.1 *Reverberation*

Reverberation is a general term used to describe the echoes from unwanted targets. Thus it depends on the purpose of the observation. If the intention is to detect fish, the echoes from plankton are part of the reverberation. Conversely, in studies of plankton, there could still be interference from solid particles in suspension, and of course the large echoes from fish are no longer wanted. It is important to remember that one person's reverberation may come from targets that another might wish to observe.

The design of the sonar has little bearing on the reverberation problem. Increases in transmitted power or receiver gain will change the target echoes and reverberation to the same extent, with no improvement in discrimination. Changes of pulse duration or the transducer beam width may help, but only if the targets of interest are spatially distributed in a manner different from the sources of reverberation. However, the sonar frequency is important in this context because the relative scattering strength of two targets is unlikely to be the same at widely separated frequencies, especially if the targets are very different in size. As a general proposition, if the intention is to detect large targets among reverberation caused by small targets, a relatively low frequency should be considered, such that the targets of interest scatter geometrically while the reverberation echoes are in the Rayleigh region (and thus very small). Conversely, if small targets are the primary interest, then a higher frequency might give better results.

### 2.6.2 *Noise*

Noise comes from unwanted signals that are present in the medium but independent of the echosounder transmission. In other words, it is any unwanted signal other than the reverberation. This noise is caused by independent effects and is present in the receiver output even when the transmitter is switched off. There are many sources of noise in the sea which may be classified as (a) physical – wind, breaking waves, turbulence; (b) biological – animal sounds and movement; or (c) artificial – shipboard machinery, the propeller, water flow around the hull. These few examples are not intended to be a complete list. The mechanisms and sources of acoustic noise are detailed in Urick (1986). There is also the electrical noise in the receiver which adds to the acoustic sources, although the latter are likely to dominate in fishery sonars.

It is important to ensure that sonars and echosounders are properly earthed electrically. Failure to install the equipment correctly, in accordance with the best electrical practice (e.g. with double-screened transducer cabling) can negate all the hard work done to reduce the self-generated noise.

It is usual to describe noise in terms of its frequency composition. The spectrum level is the noise power per unit frequency interval, as would be observed by passing the signal through an ideal filter of bandwidth 1 Hz. If the spectrum level is constant at all frequencies, the noise is said to be white, but more generally there is

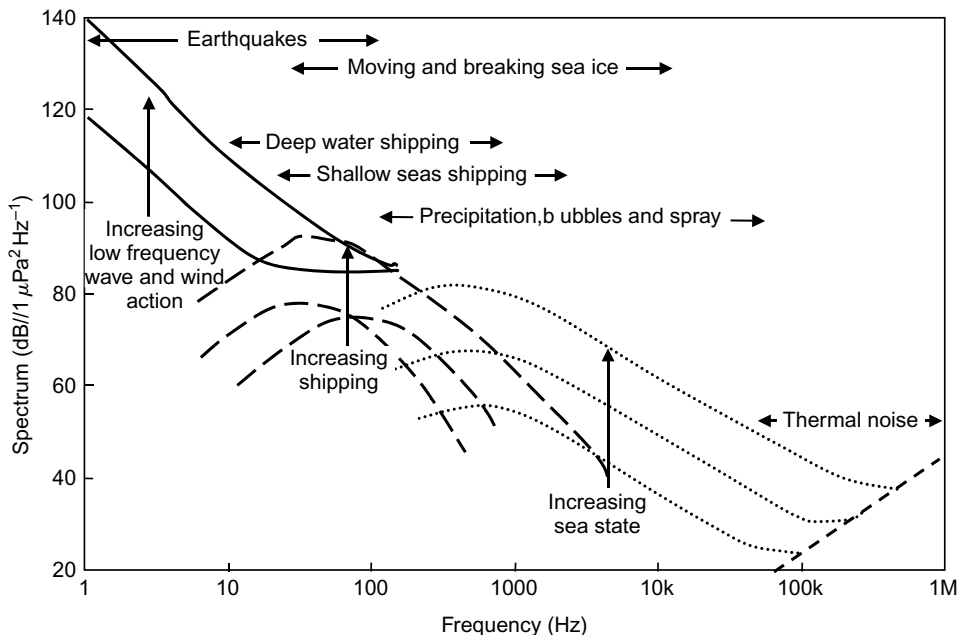


**Fig. 2.26** General characteristics of ambient noise in the sea, from data in Wenz (1962; 1972) and Anon (2003). The spectrum level is the noise per 1 Hz bandwidth. The separated curves represent the variation of ambient noise according to weather conditions and the level of shipping activity.

a systematic variation with frequency. Peaks in the noise spectrum may occur due to narrow-band sources such as rotating machinery. The seminal work of Wenz (1962), and the updated version in Wenz (1972), still provide the core references on general background noise in the ocean. Anon (2003), in a report on the effects of sound in the ocean, provided an extensive review of noise and a few additions to Wenz's original diagrams.

Figure 2.26, combining data from Wenz (1962) and Anon (2003), illustrates features of the ambient acoustic noise which is always present in the sea. The spectrum level decreases with frequency to a minimum at a few tens of kHz. At very low frequencies, below 20 Hz, the noise is mostly caused by large-scale oceanic turbulence, while at middle frequencies (0.5–25 kHz), wind-induced waves are the main source and the noise level depends on the sea state. At high frequencies, it increases again due to the thermal motion of the water molecules. Anthropogenic contributions come from shipping (5–500 Hz); seismic exploration with air guns that have broadband explosive characteristics; sonars which are military (from <1 kHz to >10 kHz) or civilian (10–400 kHz). In addition, biological sources can dominate locally, producing a variety of sounds ranging from blue whale tones at 20 Hz, sperm whales at around 1 kHz to dolphin sonar transmissions at 100 kHz or more. The aquatic mammals, as a general rule, employ a frequency band inversely related to body size. Detailed reviews of oceanic mammals and the sounds they produce can

be found in Richardson *et al.* (1995) and Anon (2003). Fish also ‘vocalize’, while the sound of snapping shrimp can be an important source of noise particularly in shallow water.

Noise is usually expressed in one of two forms, as the power in a reference bandwidth which is either 1 Hz or some fraction of an octave wide. A common standard is the 1/3 octave band. To convert from the former to the latter requires the power in all the 1-Hz intervals within the 1/3 octave to be summed. The effect of this is to add a slope of 10 dB per decade of frequency to the graphical representation. The resulting conversion from  $I_{1\text{Hz}}$  (the intensity in a 1-Hz band) to  $I_{\text{octave}/3}$  (that in a 1/3 octave band) may be expressed in dB as:

$$10 \log(I_{\text{octave}/3}) = 10 \log(I_{1\text{Hz}}) + 10 \log(f) - 5.4 \text{ dB} \quad (2.31)$$

where  $f$  is the centre frequency (harmonic mean) of the 1/3 octave band. For other octave-based bandwidths, different constant factors apply but the change in slope is the same. For example, if the reference bandwidth is 1/12 octave, the constant in Equ. (2.31) becomes  $-11.0$  dB. Conversion between two fractional-octave measures is simpler; the frequency dependence is now the same and the numerical values differ by the bandwidth ratio expressed in dB. Thus, to convert from 1/12 octave to 1/3 octave noise levels, we add the constant  $10 \log(4) = 5.6$  dB.

For an echo to be detected, it must appear in the output signal at a power level which is at least commensurate with the combined power of all noise sources. There are several ways of improving the signal-to-noise ratio should that be necessary. The transmitter power might be increased – a simple remedy, but there is a physical limit to the power which can be handled by a given transducer. The pulse duration might be increased in conjunction with a narrower bandwidth. This reduces the noise while the echo strength is maintained (in the case of single targets) or increased (when the targets are distributed). However, the benefit is achieved at the cost of a larger sampled volume which makes it less easy to distinguish targets at nearly the same range. The background noise in the sea is omni-directional. Thus a transducer with a narrower beam will suffer less from extraneous sources, although noise generated within the sonar (the self-noise) is unaffected. If machinery noise is a problem, moving the transducer to another position on the hull or deploying it on a towed body might improve matters, but isolating noisy machinery e.g. with anti-vibration mounts is likely to be more effective. We discuss the idea of noise-reduced vessel design in Chapter 3.

## 2.7 The operating frequency

Depending on the application, sonars currently operate at frequencies extending from 1 kHz to 5 MHz. Several factors need to be considered in deciding the most suitable frequency for a particular application. This is a major topic in fishery acoustics

that we shall revisit many times in later chapters. Here we provide a broad overview of the main factors that have to be considered.

There is always an element of compromise in choosing the sonar frequency. It is necessary to balance the competing requirements of long range and the resolution of close targets. As the frequency increases, so does the absorption which limits the maximum range of observations. On the other hand, high-frequency sonars can transmit short pulses because the normal requirement is for the pulse to consist of a certain number of cycles. The shorter the pulse, the better is the resolution. Furthermore, higher frequencies allow narrower beam patterns since there are practical limits on the maximum transducer size. For the same beam width, the transducer size decreases as the frequency goes up. Low-frequency transducers are large and heavy. Special handling machinery has to be installed on the ship to deploy the largest transducers safely.

The target strength of the species of interest is another consideration. If this has been measured in experiments at one frequency, it cannot be assumed that the same value will apply in a survey conducted with equipment operating at a different frequency. More generally, high frequencies are necessary when the targets are small, to avoid the Rayleigh scattering region where TS increases rapidly with frequency. The scattering is more predictable when the wavelength is similar to or smaller than the

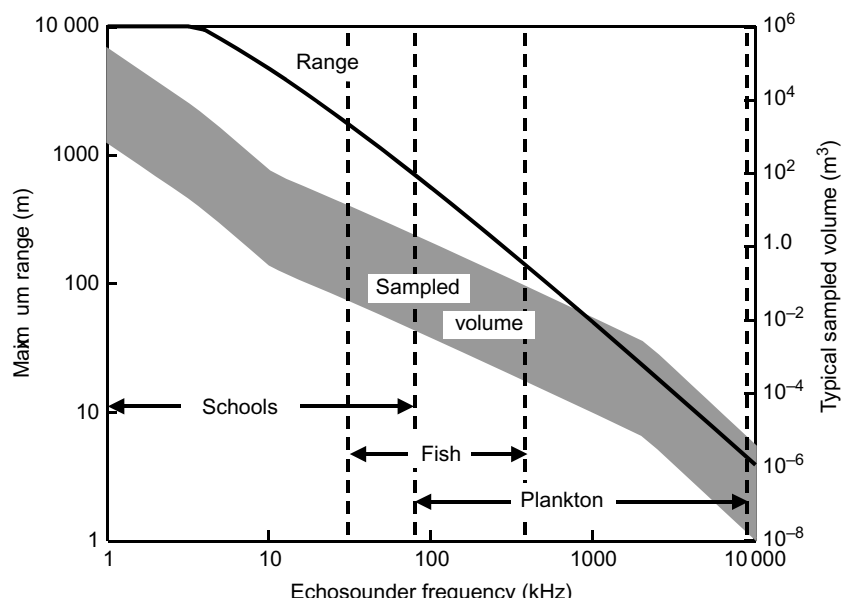


**Fig. 2.27** Frequency dependence of the operating parameters of sonars. Range is the maximum distance at which targets might be distinguished from noise. The sampled volume (shaded region) is  $c\tau\psi/2$ . Suitable frequencies for the observation of schools, individual fish and plankton are indicated.

target size, excepting the problem of resonance (p. 160). Thus sonars for detecting fish might operate in the range 30–200 kHz, while those designed for plankton studies generally work at high frequencies, perhaps 100–5000 kHz. Very-low-frequency sonars (1–10 kHz) are unsuitable for resolving individual fish, but they can be used to observe schools at a range of many kilometres, or to detect swimbladder resonances which can be related to the fish size (cf. Section 4.6).

The various factors to be considered in choosing the operating frequency are illustrated in Fig. 2.27, which gives an indication of the practical performance to be expected from sonar equipment in terms of the maximum range and the sampled volume.

## Appendix 2A: Calculation of the acoustic absorption coefficient

The recommended method for calculating the absorption coefficient  $\alpha$ , given knowledge of the environmental conditions in the water, is the formula developed by Francois and Garrison (1982b).  $\alpha$  is obtained as the sum of three frequency-dependent components representing the absorption due to boric acid, magnesium sulphate and viscosity in the order shown below:

$$\alpha = \frac{A_1 P_1 f_1 f^2}{f^2 + f_1^2} + \frac{A_2 P_2 f_2 f^2}{f^2 + f_2^2} + A_3 P_3 f^2 \quad (\text{A2.1})$$

Here  $f$  is the frequency in kHz. In fresh water, the first two components are negligible and may be ignored; the absorption is then entirely viscous and  $\alpha = A_3 P_3 f^2$ . In sea water, all the factors in Equ. (A2.1) have to be evaluated as functions of the temperature  $T$  ( $^{\circ}\text{C}$ ), salinity  $S$  (parts per thousand or ppt), depth  $z$  (m) and the acidity pH. The sound speed  $c$  in  $\text{m s}^{-1}$  is also required and may be calculated separately (see Appendix 2B). The following expressions are evaluated first, and the results are substituted in Equ. (A2.1) giving  $\alpha$  in units of  $\text{dB km}^{-1}$ .

$$A_1 = (8.86 / c) 10^{(0.78\text{pH}-5)}$$

$$f_1 = 2.8(S / 35)^{0.5} 10^{[4 - 1245 / (T+273)]}$$

$$P_1 = 1$$

$$A_2 = 21.44 (S / c)(1 + 0.025T)$$

$$P_2 = 1 - 1.37 \times 10^{-4}z + 6.2 \times 10^{-9}z^2$$

$$f_2 = 8.17 \times 10^{[8 - 1990 / (T+273)]} / [1 + 0.0018(S - 35)]$$

$$P_3 = 1 - 3.83 \times 10^{-5}z + 4.9 \times 10^{-10}z^2$$

$$(\text{A2.2})$$

The value of  $A_3$  depends on the temperature. If  $T \leq 20^\circ\text{C}$ ,

$$A_3 = 4.937 \times 10^{-4} - 2.59 \times 10^{-5}T + 9.11 \times 10^{-7}T^2 - 1.5 \times 10^{-8}T^3$$

and if  $T > 20^\circ\text{C}$ ,

$$A_3 = 3.964 \times 10^{-4} - 1.146 \times 10^{-5}T + 1.45 \times 10^{-7}T^2 - 6.5 \times 10^{-10}T^3$$

The alternative absorption coefficient  $\beta$ , giving the amplitude loss in nepers per kilometre, is equal to  $\alpha$  divided by 8.69. The Francois–Garrison formula is claimed to predict  $\alpha$  to an accuracy of 5% for temperatures from  $-1.8$  to  $30^\circ\text{C}$ , salinities from 30–35 ppt, and frequencies from 400 Hz to 1 MHz.

The pH of sea water is normally in the range 7.8–8.2. If the precise value is unknown, it is reasonable to assume pH = 8 for the purpose of calculating  $\alpha$ .

## **Appendix 2B: Calculation of the speed of sound in water**

### ***Speed of sound in sea water***

The recommended method for accurate calculation of the sound speed  $c$ , from knowledge of the environmental conditions in sea water, is the following nine-term equation described by Mackenzie (1981):

$$\begin{aligned} c = & 1448.96 + 4.591T - 0.05304T^2 + 2.374 \times 10^{-4}T^3 \\ & + 1.34(S - 35) + 0.0163z + 1.675 \times 10^{-7}z^2 \\ & - 0.01025T(S - 35) - 7.139 \times 10^{-13}Tz^3 \end{aligned} \quad (\text{A2.3})$$

where  $T$  is the temperature ( $^\circ\text{C}$ ),  $S$  is the salinity (parts per thousand or ppt), and  $z$  is the depth (m), giving  $c$  in  $\text{m s}^{-1}$ . Mackenzie's equation is valid for temperatures from  $-2$  to  $30^\circ\text{C}$ , salinities from 25–40 ppt and depths from 0–8000 m. Within these ranges, the standard error of the predicted sound speed is  $0.07 \text{ m s}^{-1}$ . In depths less than 1000 m, the final term of Equ. (A2.3), the one in  $Tz^3$ , is very small and may be ignored.

For many fishery applications, a less accurate but simpler formula will be good enough. The following formula devised by Leroy (1969) is suggested for rapid evaluation of the sound speed:

$$\begin{aligned} c = & 1492.9 + 3(T - 10) - 0.006(T - 10)^2 - 0.04(T - 18)^2 \\ & + 1.2(S - 35) - 0.01(T - 18)(S - 35) + D / 61 \end{aligned} \quad (\text{A2.4})$$

Leroy's formula predicts  $c$  correctly to within  $0.1 \text{ m s}^{-1}$  for temperatures from  $-2$  to  $23^\circ\text{C}$ , salinities from 30–40 ppt and depths not exceeding 500 m.

### ***Speed of sound in fresh water***

The above equations are not valid for fresh water. Del Gross and Mader (1972) have described the following equation which predicts the sound speed in pure water at atmospheric pressure, to an accuracy of  $0.015 \text{ m s}^{-1}$  over the temperature range 0–95°C.

$$\begin{aligned} c = & 1402.388 + 5.03711T - 0.0580852T^2 \\ & + 0.3342 \times 10^{-3}T^3 - 0.1478 \times 10^{-5}T^4 + 0.315 \times 10^{-8}T^5 \end{aligned} \quad (\text{A2.5})$$

There is a slight depth dependence of  $c$  (Chen and Millero 1977). At 10°C and 10 m depth,  $c$  is  $0.161 \text{ m s}^{-1}$  greater than the near-surface value given by Equ. (A2.5).

# Chapter 3

## Acoustic Instruments

### 3.1 Introduction

Sonar is a general term for any device that uses sound for the remote detection or observation of objects in water. The echosounder is a particular kind of sonar, one whose acoustic beam is directed vertically downwards. Many types of sonar and echosounder are used for the detection and observation of fish. We shall consider the practical application of these devices later. Here we discuss the principles of operation and the facilities for underwater observation provided by modern acoustic instruments.

This chapter begins with the single-beam echosounder and the display of echoes on the echogram as a pictorial representation of the insonified water. We describe various other instruments in common use: the netsonde, whose transducer is remotely attached to a fishing gear; dual-beam and split-beam echosounders, which measure the target strength directly; the sector scanner and multi-beam sonars, which produce radar-like displays in two dimensions; and recent developments of these techniques that provide three-dimensional views of the detected targets. The Doppler sonar allows us to measure the speed as well as the position of targets. Another development with potential for the future is wideband sonar, a technique which provides more information about targets from the frequency composition of echoes. Then there are pingers and transponders, useful ancillary devices which are attached to fish or other objects to make them more visible on the sonar display, and to improve the accuracy of target-tracking in space.

We briefly review best practice for sonar installations and platforms, covering particular solutions to more demanding applications: noise-reduced vessels, deep- and shallow-towed transducer bodies. The calibration of acoustic instruments is another important topic. Practical advice is given on how to perform the calibration of echosounders and echo-integrators in accordance with internationally accepted standards.

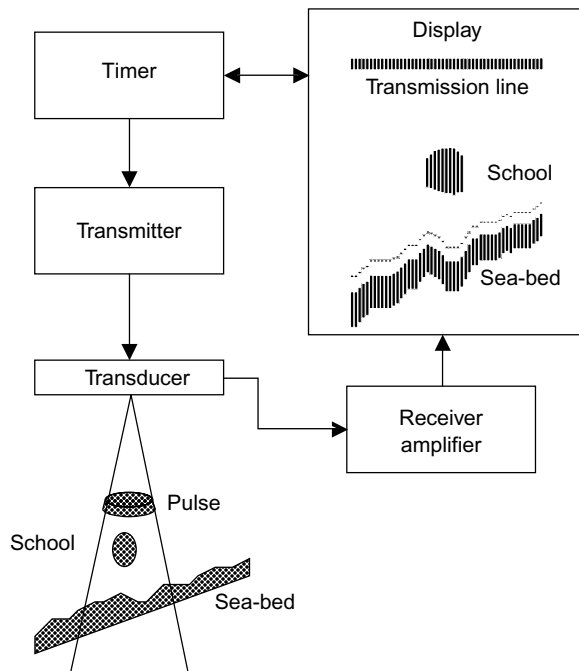


**Fig. 3.1** Concept of echosounding. The transmitted pulse generates echoes from the fish school and the seabed below the transducer which are displayed on an echogram.

## 3.2 Echosounders

Figure 3.1 shows the basic components of the echosounder. The transmitter produces a burst of electrical energy at a particular frequency. Typical frequencies of the echosounders used in fisheries applications are 38 kHz (i.e. 38 000 cycles per second), 120 kHz, 200 kHz or 420 kHz. The transmitter output is applied to a transducer which converts the electrical energy to acoustic energy propagating through the water. The transducer projects sound in a directional beam, similar to the beam of light produced by a searchlight, as described in Section 2.3. The width of the beam is inversely proportional to the frequency of the sound. Thus, for the same physical size of transducer, a 400 kHz echosounder would have a beam width one-tenth that of a 40 kHz echosounder. Conversely, to produce the same beam width, a transducer one-tenth of the size would be required at 400 kHz compared to that needed at 40 kHz. The beam from a typical fishing echosounder is normally 5°–15° wide, but it is not necessarily symmetrical; the along-ship and athwart-ship beam widths might be different.

The transmitted pulse of sound propagates through the water away from the transducer. It may encounter various targets, e.g. fish or the seabed. These targets reflect or scatter the pulse, and some energy returns towards the transducer. This back-scattered sound (the echo) is detected by the transducer and converted to electrical

energy as the received signal. As described in Section 2.4, the time when the echo is received determines the distance of the target from the transducer. The received signal is amplified by electronic circuits in the receiver and displayed on the echogram. On the traditional greyscale display, detected signals appear as dark traces on a white background. However, most echograms now use a range of colours to give a better visual contrast; in this case the strongest signals are (usually) presented in black/red, descending through various colours and hues to blue/grey for the weakest signals. Whichever type of display is used, a ‘picture’ of the targets is generated which shows their depth or range as the distance from the transmission mark on the echogram (Fig. 3.1).

After some time, the transmitter produces another pulse and the whole process is repeated. This results in a two-dimensional picture of targets as connected echo traces. The images in this picture are called marks. The vertical extent of a mark indicates the height of the object concerned, a fish school or scattering layer for instance, while the horizontal position shows changes in time if the echosounder is stationary, or in space if the echosounder is mounted on a moving vessel. Figure 3.1 shows how particular objects like a fish school and the rising seabed appear as the echosounder moves.

Early types of display used mechanically-operated pens which marked paper to provide the recording. Two types of paper were used, firstly a dry paper on which dark recordings indicated the strength of targets as a grey scale on a white background, but this paper had poor dynamic range meaning there was little difference between dense and diffuse fish traces. Secondly, there was a wet paper which had better dynamic range. More recently, sonar systems have made extensive use of computers to pre-process the signals. Thus echograms are now shown mostly on computer monitors, while a peripheral printer provides a hard-copy version if required. Figure 3.2 shows a greyscale example. Near the top of this figure we see the transmitter mark which corresponds to the depth of the transducer, close to the surface. The diffuse marks between 20 and 40 m depth are caused by plankton. The slight increase in density seen at 40 m is associated with the thermocline. A few small fish schools can be seen as black traces well below the plankton layer, just clear of the broad dark line at about 140 m which indicates the seabed. Fishing on these schools established that they were herring of mean length 27.5 cm. In addition to the representation of real targets, various artificial marks are included to annotate the echogram. There is a horizontal depth marker at 50 m intervals, vertical time markers at 06.30 and 06.45 hrs, and a line 1 m above the seabed contour. The latter is a reference for bottom-following channels which can be selected in addition to the usual depth intervals required for echo integration.

Inexpensive colour printers permit permanent records to be made if required. Plates 3.1 and 3.2 show coloured paper representations of two very different kinds of marks, both recorded in Norwegian fjords. In Plate 3.1, many individual small targets are seen around 80 m depth, while Plate 3.2 shows a very large school of overwintering herring which is so dense that the individual fish cannot be distinguished.

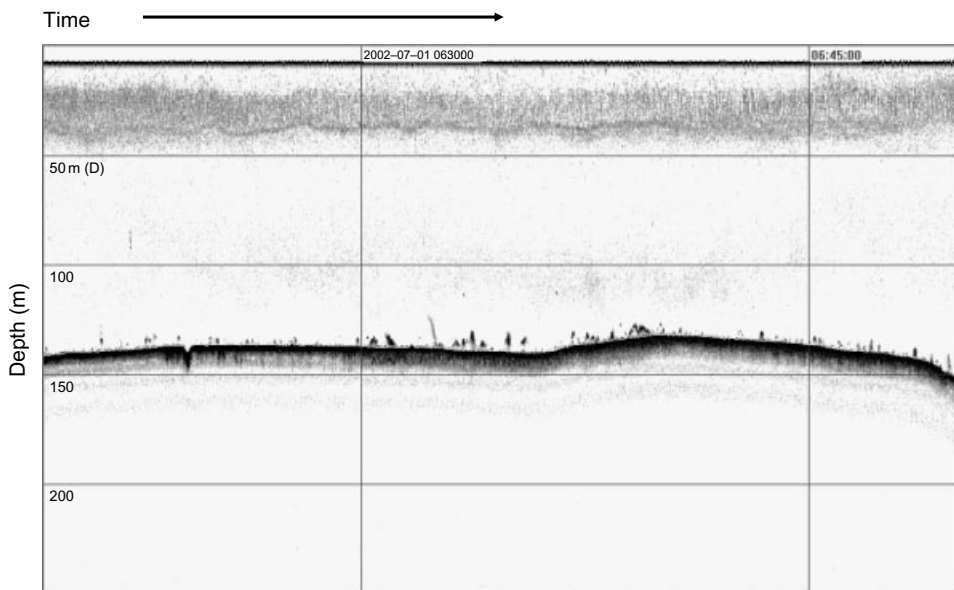


**Fig. 3.2** Example of an echogram. The transmitter mark at 7 m corresponds to the depth of the transducer. The diffuse marks 20–40 m deep are caused by plankton. A few small fish schools can be seen as black traces well below the plankton layer, just clear of the broad dark line at about 140 m which indicates the seabed. Fishing on these schools established that they were herring of mean length 27.5 cm.

The simplest echosounders are used primarily to locate aggregations of fish and to determine the depth of the seabed. They provide little information about the quantity of targets detected as echoes, for which purpose more sophisticated instruments have been developed: the scientific echosounders and other devices described later in this chapter.

There are some general considerations in designing echosounders to obtain the best performance. The absorption of sound in water increases rapidly with frequency (Section 2.4), so the maximum range of an echosounder is determined by the frequency of operation. High-frequency echosounders are limited to short ranges. We can improve the detection capability of the echosounder by reducing the width of the beam, but the physical size of the transducer is a problem if a very narrow beam is required at low frequency. We can improve the range resolution by reducing the pulse duration. This is easier to do at higher frequencies because the duration is shorter for the same number of cycles within the pulse. If the pulse is very short, the receiver must have a wide bandwidth to receive the echoes and it is more vulnerable to noise. To overcome noise it is helpful to generate more power in the transmission, but there are limitations in both the electronics and the sound levels that can be transmitted in the water. It is easier to generate higher power levels at lower frequencies. From these general considerations we see that long range is obtained at low frequencies, but high definition requires high frequency, and for any specified

requirement there will be an optimum frequency. This compromise was illustrated in Fig. 2.27. We find in practice that echosounders used over continental shelves, at water depths up to 400 m, operate in the 20–50 kHz range. Work in the deep ocean requires lower frequencies, down to 10 kHz, while the echosounders used in shallow lakes or to observe plankton near the surface normally operate at frequencies between 100 and 450 kHz.

### **3.2.1 *Scientific echosounders***

The scientific echosounder is constructed from the same basic components as those shown in Fig. 3.1. However, the electronics have been designed with amplitude stability in mind and with many additional features. Most notably, the received signal is converted from analogue to digital form early in the processing. This allows greater flexibility in use and stability of operation. Analogue amplifiers suffer from variable performance due to ageing of the electronic components and/or changes with the temperature. This is no longer a problem once the signal is digitized. The problem then is to ensure that the computer software (or firmware) is free of bugs and that it correctly models the echo integration. Nevertheless, digital signal processors are relatively cheap and they have improved the accuracy and repeatability of sonar measurements. The previous problem of compensating the beam-spreading and absorption losses, described in Section 2.4, is now solved by a simple software calculation. However, the requirement for accurate processing of very different signal levels, from a shallow seabed at one extreme to weakly scattering fish or diffuse plankton in deep water at the other extreme, still needs to be addressed. There are various methods for dealing with this, such as simple fixed-step gain control, or non-linear amplification to compress the signal range. For example, the Simrad EK500 and the newer EK60 scientific echosounders (Fig. 3.3) have several fixed-gain channels, with automatic selection of the one that best matches the signal level being received. Plate 3.3 shows a typical echogram generated by the Simrad EK500. The output of such an echosounder is sufficiently accurate to count individual fish or to measure the density of major fish aggregations. The echo-integrator function may be included within the instrument firmware, or it may be implemented as a program in a separate computer, providing an output proportional to the fish density. Some echosounders reveal the direction or location of targets in the beam, and they provide outputs proportional to the target strength when individual fish are detected. Two kinds of instrument have been employed for this purpose, the dual-beam and the split-beam echosounders, as described later (Section 3.3).

### **3.2.2 *The echo-integrator***

Historically, the echo-integrator was a separate electronic instrument connected to the output of an echosounder. Now it is normally implemented in software within the echosounder or an ancillary computer. In essence, what the integrator does is to

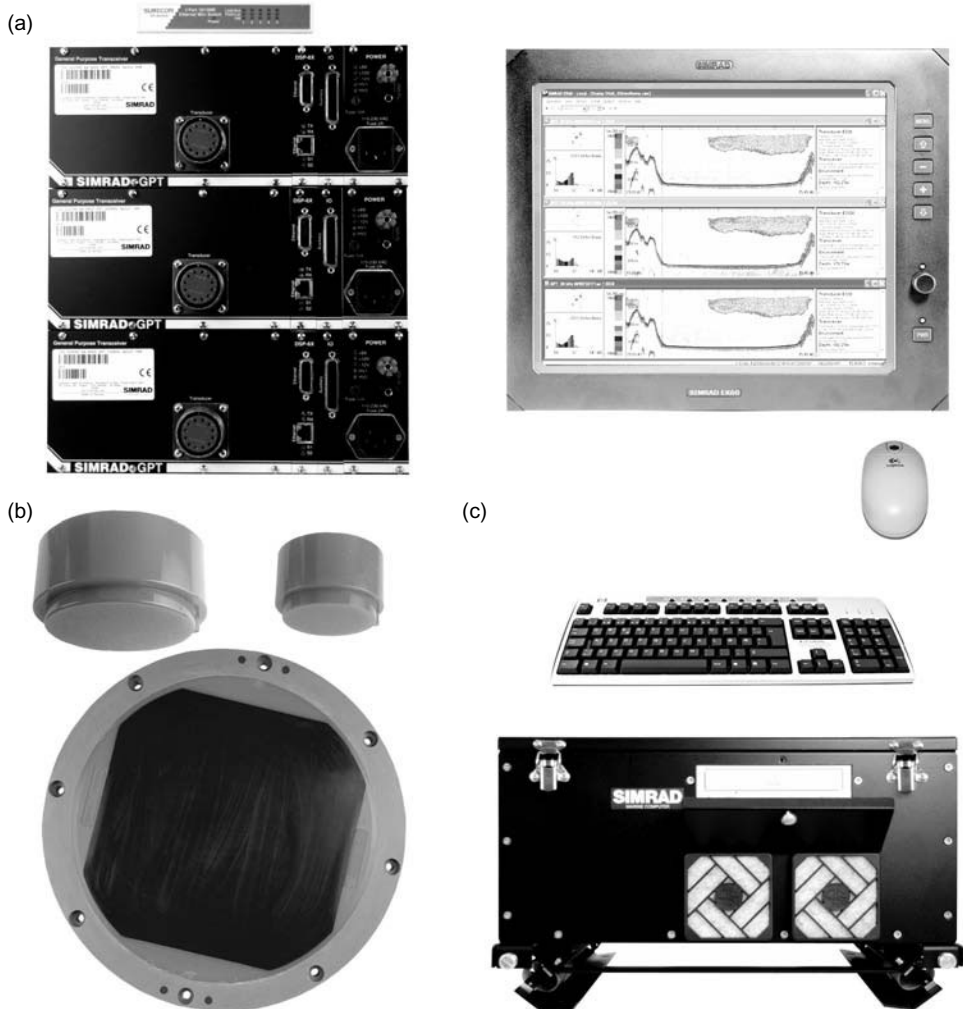


**Fig. 3.3** The Simrad EK60 echosounder showing (a) a stack of transceiver units for operating at three frequencies, (b) 7° beamwidth transducers for the 120, 200 and 38 kHz channels, (c) ruggedized computer and display. (With thanks to Simrad Norge AS.)

sum or integrate the energy in echoes returned from selected parts of the echogram. These may be pre-selected depth channels, or polygons drawn free-hand by the operator around marks that are selected manually or automatically. It is important to remember that the integrator sums the echo energy. In practice, this is done by first squaring the digitized voltages sampled by the echosounder, then summing the results with respect to time or distance, over depth intervals corresponding to the depth channels or polygons. An example of the integrator records from a section of an echogram is given in Plate 3.3. The theory of echo integration is discussed in Section 5.4 and the principles involved are illustrated in Fig. 5.15.

It is necessary to exclude the bottom echo from the integration when fish are being surveyed. Some fish may be in dense schools close to the ground; if the discrimination of the bottom is poor, there will be large errors in the estimated fish density. Analogue or digital discriminators may be used to detect the bottom echo, but their adjustment is critical and failures may occur when the ground suddenly rises or deepens. Currently there is no completely automatic solution to this problem, and some manual intervention is usually required to ensure that no contribution from bottom sediment is included within the echo-integral.

### **3.2.3 *The basic netsonde***

The netsonde is an echosounder whose transducer is remote from the receiver electronics. As used in trawl fishing, the transducer is attached to the headline of the net, and echoes are transmitted to the receiver in the towing vessel through an electrical cable or by means of an acoustic link. In the latter case, the netsonde on the trawl contains its own power supply and two transmitters, one to pulse the transducer and the other to drive the acoustic link, transmitting signals to a hydrophone in the water near the ship. The frequencies of the echosounder and the acoustic link must be sufficiently different to avoid interfering with each other. On the ship, the received signals are displayed as an echogram in the normal way. The beam width of the headline transducer is typically 15–30°. This ensures that a good proportion of the netmouth can be observed, and the footrope of the trawl may be detected even when it is not directly below the headline.

Figure 3.4 illustrates how the headline transducer is located on a pelagic trawl to detect fish traces and the bottom. An example of the echogram as recorded on the ship is shown in Fig. 3.5. The transmission line at the top of the echogram marks the transducer position on the headline. Thus the ‘depth’ of a mark indicates the distance below the headline, not the distance below the surface as would be the case if the transducer were on the ship. On the left we see the footrope rising towards the headline at the beginning of the haul, as the net accelerates to the fishing speed (A). In the normal fishing condition, the vertical opening of the net is 12–16 m depending on the towing speed. The higher the speed, the smaller is the opening. The net descends initially and the bottom soon appears as the strong trace rising from the foot of the echogram (D). The distance between the echoes from the footrope and the bottom indicates the height of the gear above the ground. Thus the netsonde allows the fishing skipper to control the depth of the gear with great precision, to place the net within one or two metres of the bottom while avoiding damage through contact with the ground (B). The apparent rise and fall of the bottom marks in Fig. 3.5 mainly indicate the vertical movement of the net rather than any real change of water depth. Several fish schools can be seen just above the bottom as the net descends (E), and on the right of the figure, fish are observed entering the net between the headline and the footrope (F). At the end of the haul, the towing warps are wound in, accelerating the net which reduces the vertical opening, and at the same time lifting the gear away

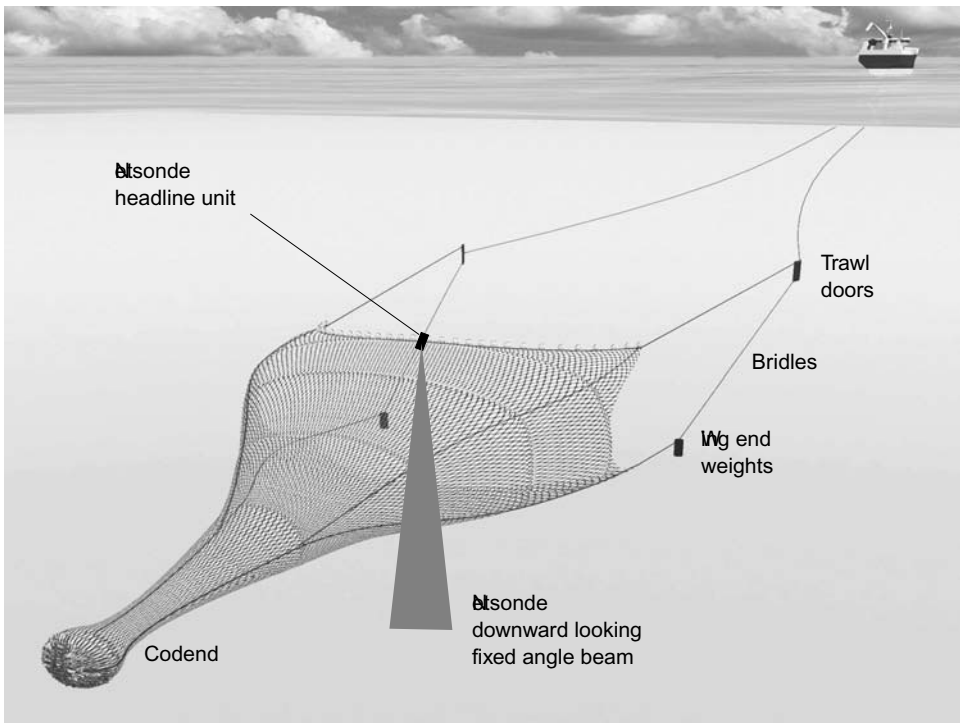


**Fig. 3.4** Netsonde attached to a pelagic trawl. The transducer is on the centre of the headline. Echoes received by the transducer are transmitted to the ship via a cable connection or an acoustic link (not shown). (With thanks to Alvan Rice who provided the pelagic trawl illustration.)

from the bottom (C). This particular netsonde includes a sensor to measure the water temperature, which is indicated by the position of artificial marks appearing as a line on the echogram. This facility might be used to position the net at the thermocline (a region where the temperature changes suddenly with depth) if it is expected that fish might aggregate there.

Some netsondes have two transducers so that one beam is directed downwards, like the basic instrument described above, and a second beam is directed upwards. The combined echogram then covers the water column from the surface to the seabed. As for any echosounder, the netsonde echogram may be recorded on paper or displayed in colour on a monitor screen.

### 3.2.4 *The scanning netsonde*

Ona and Eger (1987) first described this interesting device which works on the same principle as a one-axis searchlight sonar (p. 85), but the transducer is on the headline of a trawl, connected by a long electrical cable to the other parts of the instrument on the towing vessel, as is done with conventional netsondes. The acoustic axis of

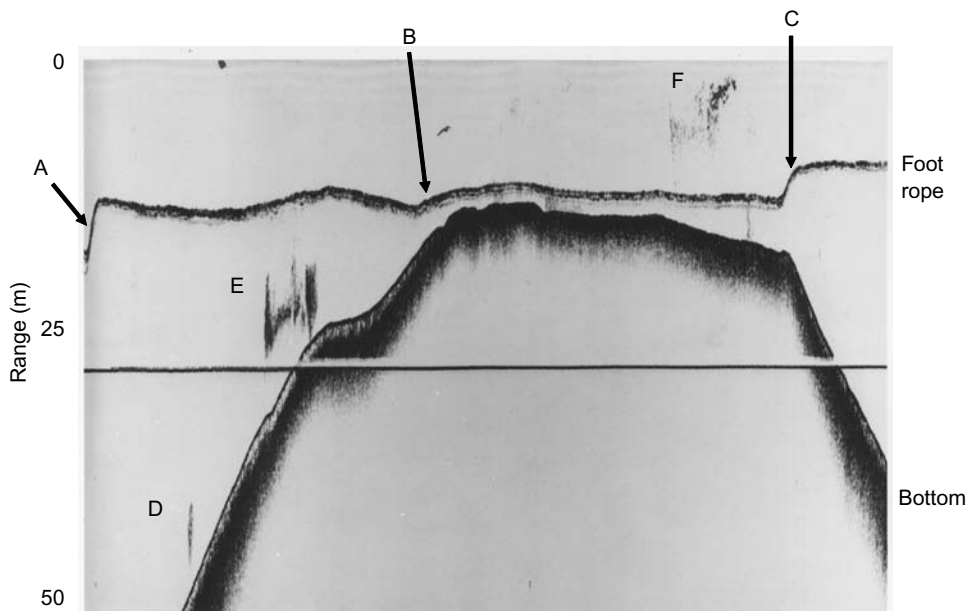


**Fig. 3.5** Echogram from a netsonde attached to a pelagic trawl. The vertical scale indicates the range in metres below the headline, not the true depth. See text for explanation of the sequence.

the transducer may be set by the operator to point in a particular direction, or it may be rotated automatically like a radar aerial so that the acoustic beam sweeps around the vertical plane perpendicular to the towing direction. Alternatively, if the net is near the bottom, it may be preferable to repeatedly scan across a sector. After a short period of time, the combined images give a composite view of the netmouth, the bottom and any fish entering the net.

Four examples taken from a single tow are given in Fig. 3.6. They show a small pelagic trawl whose netmouth is approximately 24 m wide by 12 m high. In Fig. 3.6a the net is shown approaching the bottom and the oval shape of the net opening is clearly seen. If the net were damaged or twisted in some way (a common problem with pelagic trawls if they are mishandled in shooting), then the distorted opening on the netsonde image should reveal the problem. In Fig. 3.6b the net is shown fishing with the footrope about 2 m above the seabed. The net is not in ground contact. Note that the seabed echoes are unclear when the transducer points to the side about  $30^\circ$  from the vertical. With the beam centred in such a direction, echoes from the shortest path to the seabed (vertically down) are received on the side lobes, and they interfere with the slant on-axis return which arrives slightly later. Although the echo from the netting appears to merge with the seabed at this point, the gear is still towing well clear of the bottom. Figure 3.6c shows a school of herring being caught. Note how the herring stay clear of the netting as they are herded into the net. Finally, in Fig. 3.6d we see the net lifting off the seabed as hauling begins. The increased strain on the

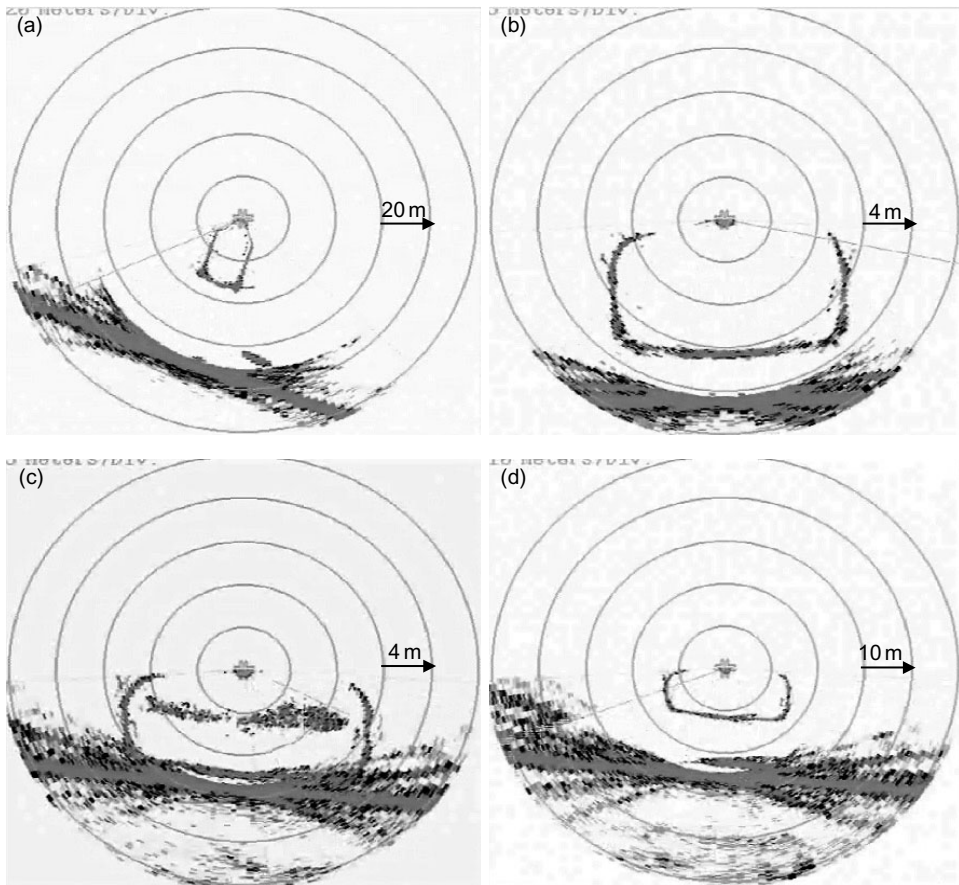


**Fig. 3.6** Observations with a scanning netsonde on a pelagic trawl in 120 m of water: (a) the gear descending through the water column with very little strain on the net which is hanging with starboard side lower – 20 × 30 m opening; (b) coming close to the seabed under strain – opening now 24 × 12 m; (c) catching herring which are herded by the netting, the footrope is 1 m off the seabed and the wing-end weights are on the ground – 24 × 10 m opening; (d) pulling clear at the end of the haul with increased strain – 30 × 11 m opening. (a) and (d) both show small herring schools below the net close to the seabed.

towing warps now spreads the trawl doors further apart, causing the net to become wider and more box-like in shape.

### 3.3 Instruments for measuring the target strength

The signal produced by the single-beam echosounder depends on the direction of the target as well as the backscattering cross-section. The measurement of target strength is an important application of acoustic instruments. When this is done by the so-called ‘direct’ method (Sections 5.3 and 6.3), we must determine the direction

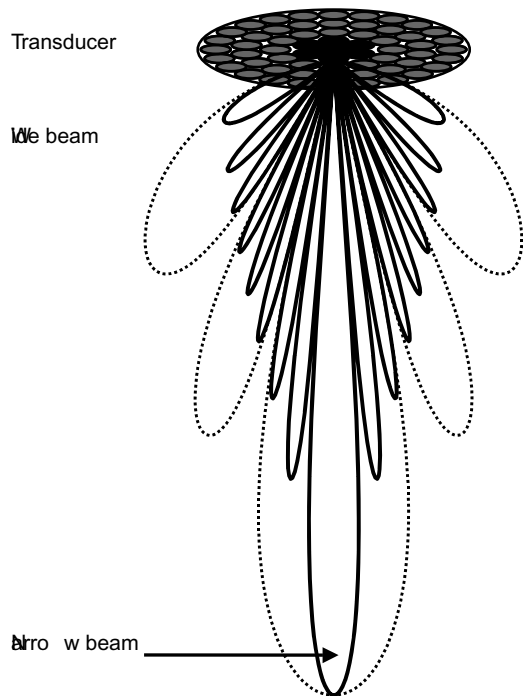


**Fig. 3.7** Dual-beam transducer and beam pattern. The solid and dotted lines show the narrow and wide beam patterns, respectively. The logarithmic radial scale emphasizes the side lobes.

of the target so that the observed echo strength may be compensated for the effect of the transducer beam pattern. The dual-beam and split-beam echosounders are two instruments which have been developed (and are commercially available) for the direct measurement of target strength (Ehrenberg 1974a; Carlson and Jackson 1980). Ehrenberg (1983) maintains that the split-beam technique has a slight theoretical advantage, however, the practical problems of transducer design, signal processing and accurate resolution of single targets (Soule *et al.* 1996) are more important limitations on the accuracy of these measurements.

### 3.3.1 *The dual-beam echosounder*

Figure 3.7 illustrates the transducer and the two beam patterns of a dual-beam echosounder. The transducer consists of 73 elements arranged in four concentric circles around one element at the centre. If all the elements are used as one large transducer, they form a narrow beam. The seven central elements (the black ones in Fig. 3.7) may be controlled independently of the others. When used alone as a smaller transducer, the central elements form a wide beam. The sizes of the two transducers are such that the narrow beam has three side lobes to each one in the wide beam, and the nulls coincide.

The transmitter pulse is applied to all the elements, so the transmission is on the narrow beam only. The signals received by the elements are separately processed to form two output signals, giving intensities  $I_n$  and  $I_w$  corresponding to the narrow and wide beams respectively. These intensities are measured after time-varied-gain has been applied to compensate for the range-dependent propagation losses (cf. Section 3.8).

Assuming that the received signals come from one target, the ratio  $I_n/I_w$  (called the beam factor) depends on the direction of the target. Suppose that  $b_n$  and  $b_w$  are the one-way amplitude sensitivities in the target direction, for the narrow and wide beams respectively, normalized to  $b_n = b_w = 1$  on the acoustic axis. Earlier calibration of the instrument (by the methods described in Section 3.8) has determined  $b_n$  and  $b_w$  as functions of direction, and  $C_a$  which is the on-axis power sensitivity factor. If  $\sigma_{bs}$  is the backscattering cross-section of the target, and remembering that the transmission is on the narrow beam only, the observed intensities are formulated as:

$$I_n = C_a \sigma_{bs} b_n^2 \quad (3.1)$$

$$I_w = C_a \sigma_{bs} b_n b_w \quad (3.2)$$

Solving these equations for  $\sigma_{bs}$  and the beam factor, we get:

$$I_n / I_w = b_n / b_w \quad (3.3)$$

$$\sigma_{bs} = (1 / C_a)(1 / b_w^2) I_w^2 / I_n \quad (3.4)$$

In principle, the target direction and therefore  $b_w$  are functions of  $I_n/I_w$ , and an estimate of  $\sigma_{bs}$  follows from Equ. (3.4). Unfortunately, the indicated direction is ambiguous because it is not a single-valued function of  $I_n/I_w$ . The same beam factor might result from targets on the main lobe or the side lobes. This problem is illustrated in Fig. 3.8.

The ambiguities of direction may be greatly reduced by the following techniques. Firstly, we should accept only those echoes having a beam factor greater than some limit. Secondly, if  $I_n$  or  $I_w$  is less than some threshold, the echo is again ignored. Suppose the limit on  $I_n/I_w$  is the arc shown in Fig. 3.8c. The ambiguities attributable to the smaller lobes of the beam factor (which must not be confused with the different lobes of the transducer beam pattern) are thus removed, since targets in the relevant directions are not detected. In this case the larger lobes of the beam factor (Fig. 3.8c) correspond to nulls of the beam patterns (Fig. 3.8a and b). In directions around these nulls, the sensitivity of the transducer is relatively low, and most targets in these directions will be ignored because  $I_n$  or  $I_w$  does not exceed the threshold. Almost all the detected targets are now in directions within the central lobe of the beam factor and the main lobe of the narrow beam. A few strong targets elsewhere may still be wrongly located by these techniques, but the error rate will be acceptably small if the thresholds are well chosen.

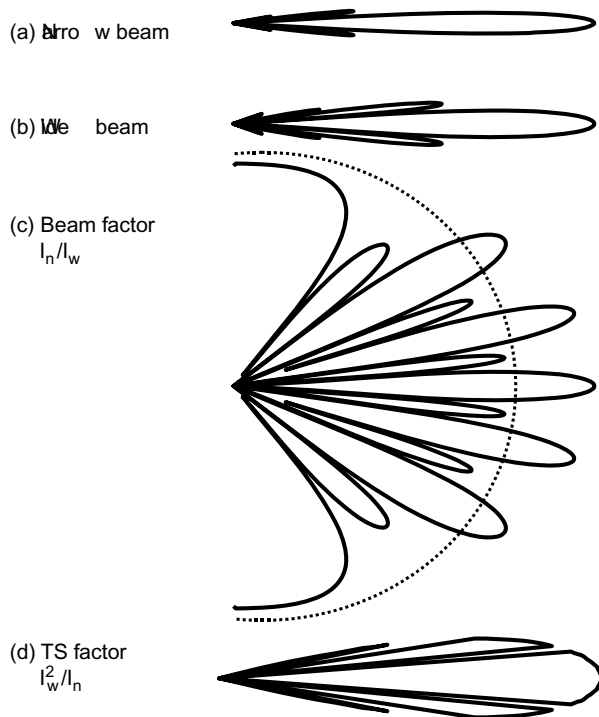


**Fig. 3.8** Directional properties of the dual-beam echosounder. (a) Narrow beam pattern, (b) wide beam pattern, (c) the beam factor. The dotted arc in (c) represents a threshold applied to exclude the smaller side lobes of the beam factor. (d) The target-strength (TS) factor is relatively independent of direction over both the main lobes.  $I_w$  and  $I_n$  are, respectively, the intensities of the wide and narrow beams.

### 3.3.2 The split-beam echosounder

The split-beam echosounder has a transducer which is divided into four quadrants (Fig. 3.9). The target direction is determined by comparing the signals received by each quadrant. In Section 2.3 we explained how the phase difference between the signals received by two hydrophones depended on the direction of the source. The same principle is applied in the split-beam technique. The transmission pulse is applied to the whole transducer but the signals received by each quadrant are processed separately. Suppose the four quadrants are labelled 'a' to 'd' as in Fig. 3.9. The angle  $\theta_t$  of the target in one plane is determined by the phase differences  $(a - b)$  and  $(c - d)$ , which should be the same. In practice, the summed signal  $(a + c)$  is compared with  $(b + d)$  to give a phase difference  $\eta_\theta$ . The angle  $\phi_t$  in the plane perpendicular to the first is similarly determined by the phase difference, this time between  $(a + b)$  and  $(c + d)$ , which we write as  $\eta_\phi$ . The two angles define the target direction uniquely. The target strength is estimated from the transducer sensitivity in the relevant direction, namely the beam pattern and the on-axis sensitivity which are determined by calibration as described in Section 3.8. The split-beam design illustrated here has four

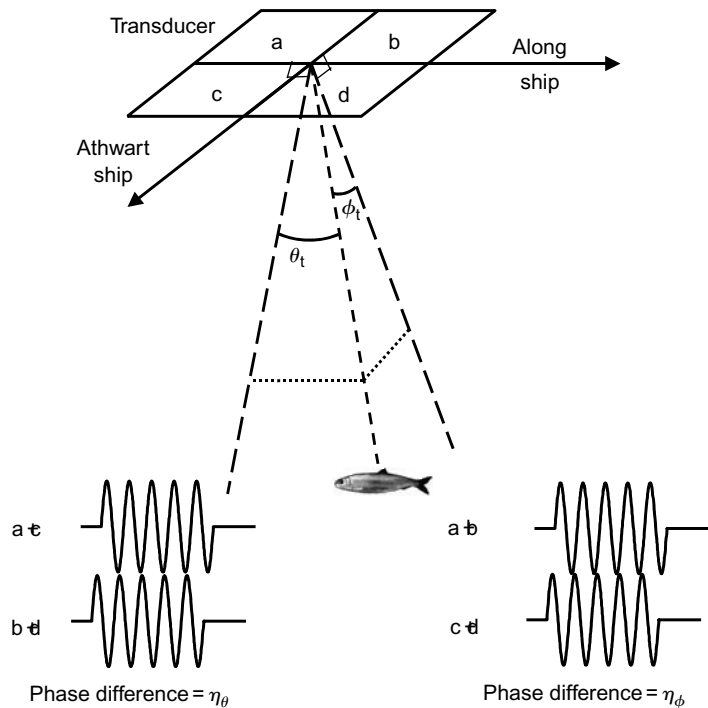


**Fig. 3.9** Principles of the split-beam echosounder. The target direction is determined by  $\theta_t$  and  $\phi_t$  which are, respectively, the angles from the along- and athwart-ship axes. Signals from the four transducer quadrants (a–d) are combined in pairs giving phase differences  $\eta_\theta$  and  $\eta_\phi$  which determine these angles directly.

symmetrical elements, as implemented in the Simrad EK60 for example. The symmetrical design is not an essential feature of the split-beam method. In the BioSonics DT 200, there is one large element whose signal determines the echo amplitude with a narrow beam, while three smaller elements are used to measure the off-axis angles.

The directional ambiguity noted earlier (p. 81) occurs also in the split-beam echosounder. Suppose the difference in the path lengths from quadrants ‘a’ and ‘b’ to a particular target is  $\Delta R_{ab}$ . If the path-length difference for another target were  $\Delta R_{ab} + \lambda$ , then the relative phase of the two signals would be the same. Again, this problem can be avoided to a large extent by good transducer design and well-chosen thresholds which the detected signals must exceed.

An example of the visual output from a split-beam echosounder (Simrad EK60) is shown in Plate 3.4. The echogram shows data collected in the Indian Ocean at approximately 10.30 local time. The vessel is moving slowly past a fish aggregation device (FAD) that is used to attract tuna. These devices can be complex instrumented buoys, or simple wood or palm structures and may be drifting or moored. In this case the vessel fished around the FAD and caught 50 tonnes of tuna comprising 95% skipjack (*Katsuwonus pelamis*) of size 40–70 cm overall length and 5% bigeye tuna

(*Thunnus obesus*) of 40–60 cm in length. The display shows the distribution of target strengths, as a histogram containing values mostly from the skipjack which have no swimbladder, while the larger values are probably from the bigeye which do have a swimbladder. The sounder also provides the distribution of targets across the beam in the bottom left of the display. The vertical display and the horizontal distribution of detected targets come from the central part of the echogram which shows a dramatic vertical excursion which is typical of tuna in this situation. The exact reason for these vertical movements is not known but they may be motivated by feeding behaviour.

### 3.3.3 Resolution of single targets

The dual-beam and split-beam echosounders determine the target strength directly for each echo. There is also the indirect method, based on echo statistics, which can be used with single-beam instruments (cf. Sections 5.3 and 6.3). In either case, an important requirement is to identify those echoes that have come from one fish. If the echoes from two or more fish are received at the same time, it is not possible to determine a useful target strength, and such echoes must be ignored.

The presence of overlapping echoes may be detected by examining the shape (envelope) and/or the phase coherence of the received signal. Both methods are used concurrently in modern target-strength measuring instruments. Figure 3.10 illustrates how these criteria are used to distinguish single and multiple targets.

It is not possible by acoustic measurement alone to say whether a particular echo (satisfying the shape and phase criteria) has come from one fish, or from two fish very close together which happen to reflect echoes which are nearly coincident. In practice, it is difficult to set single-target recognition criteria that are good enough to accept a wide range of echo amplitudes while rejecting a sufficiently large proportion of multiple targets, see Ona and Barange (1999) for a detailed analysis of this problem. Demer *et al.* (1999) have proposed a multi-frequency, and perhaps more importantly a multi-location method for improving single-target detection. When many echoes have been detected and measured, some proportion of the estimated target strengths will be wrong because of coincident multiple targets. Nevertheless, good estimates of the target strength are obtained if the mean density of the observed fish is low enough, and the width of the target-strength distribution is sufficiently narrow to ensure that the proportion of such errors is acceptably small. The reader is referred to Sections 2.5 and 5.3 for further discussion of this problem.

## 3.4 Sonars

There are two kinds of sonar: active and passive. The active sonar transmits an acoustic signal and detects the reflections from objects in the surrounding water. The passive sonar transmits no signal, but it detects the sounds or noise produced

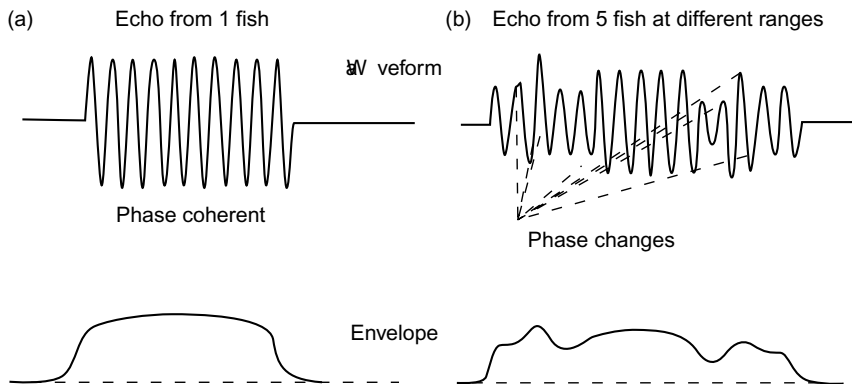


**Fig. 3.10** Resolution of single-target echoes based on the pulse shape and phase coherence of the received signal. (a) The echo from one fish is well defined; (b) the echo from several fish has an irregular envelope and incoherent phase.

elsewhere, by ships or submarines for example. There are few applications of passive sonar in fisheries research, and here we shall confine attention to the active instruments which are the most useful for the remote observation of fish.

### 3.4.1 *Searchlight sonar*

This instrument is a single-beam device used mainly by fishermen when searching for schools of fish. It works on the same principles as the echosounders described in Section 3.2, and employs similar sizes of transducer and beam widths. However, the transducer is mounted on a stalk extending about 1 m below the hull of the vessel. The transducer may be rotated and tilted to point the beam in any direction (Fig. 3.11).

Searchlight sonars allow manual or automatic control of the beam direction. For example, with the transducer tilted slightly below the horizontal, it might be rotated in steps through 360°, transmitting once at each step so that near-surface schools are detected in any direction around the ship. The display may be an echogram, or a plan view presented on a monitor screen with targets shown both in range and direction relative to the ship's position at the centre of the display. The mechanical movement of the transducer is slow, and it takes tens of seconds to construct the complete picture of targets around the ship.

### 3.4.2 *Side-scan sonar*

The side-scan sonar is a single-beam instrument with the transducer mounted in a towed body so that the beam is directed sideways, perpendicular to the cruise track (Fig. 3.12). The transducer has a highly asymmetrical beam pattern which is narrow in the fore-aft direction and wide in the vertical plane perpendicular to the cruise track, typically 1° by 40°. Side-scan sonars are most often used to map static features of the

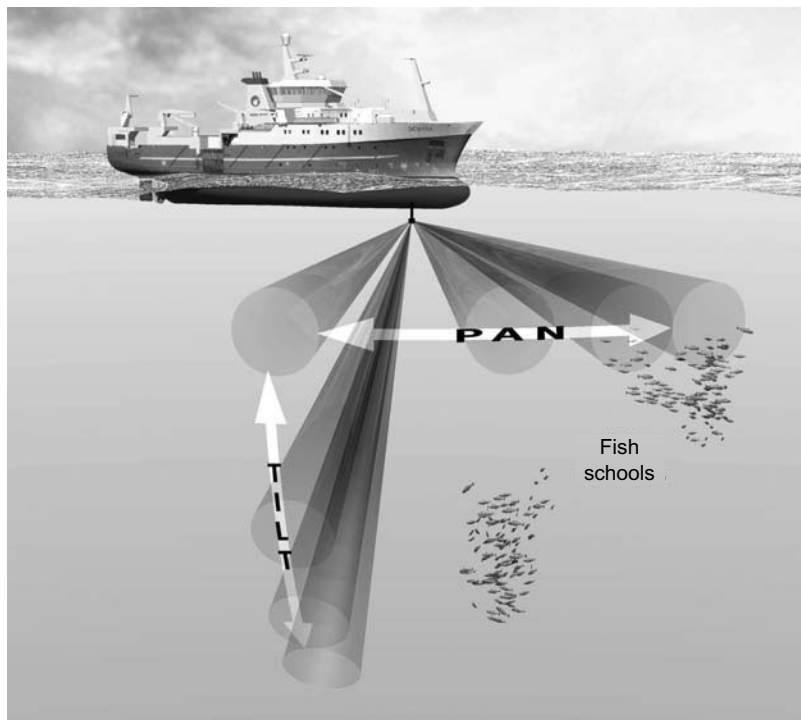


**Fig. 3.11** Searchlight sonar. The transducer is rotated mechanically to pan and tilt the beam towards any direction. (Illustration drawn by Alvan Rice.)

seabed and solid objects thereon. In this application, the pulse duration is short and the towed body is on a long cable so that the transducer is close to the bottom. After each transmission, the marks on the echogram show rising features of the bottom topography, which reflect the transmission strongly, whereas the valleys behind these features are shielded from the transmission and therefore produce no marks on the echogram. As the ship proceeds along the cruise track, successive transmissions are displayed on the echogram, which shows a two-dimensional picture of the seabed to one side of the ship.

An example of a side-scan echogram is shown in Fig. 3.13. The transmission mark is at the top of the figure. A short distance below this we see the start of the seabed echoes. In this example the seabed is sandy and smooth. The picture shows a prawn trawler rigged with two trawls deployed from towing booms amidships. Both nets, the vessel and its wake are visible on the echogram. Any object can be seen in plan view using a side-scan sonar, but it insonifies only the leading edges of large targets, thus any objects in areas shadowed by the largest targets will not be seen.

One fishery application of the side-scan sonar is the mapping and counting of fish schools (Section 5.2). Smith (1970; 1977) used a side-scan sonar to map small

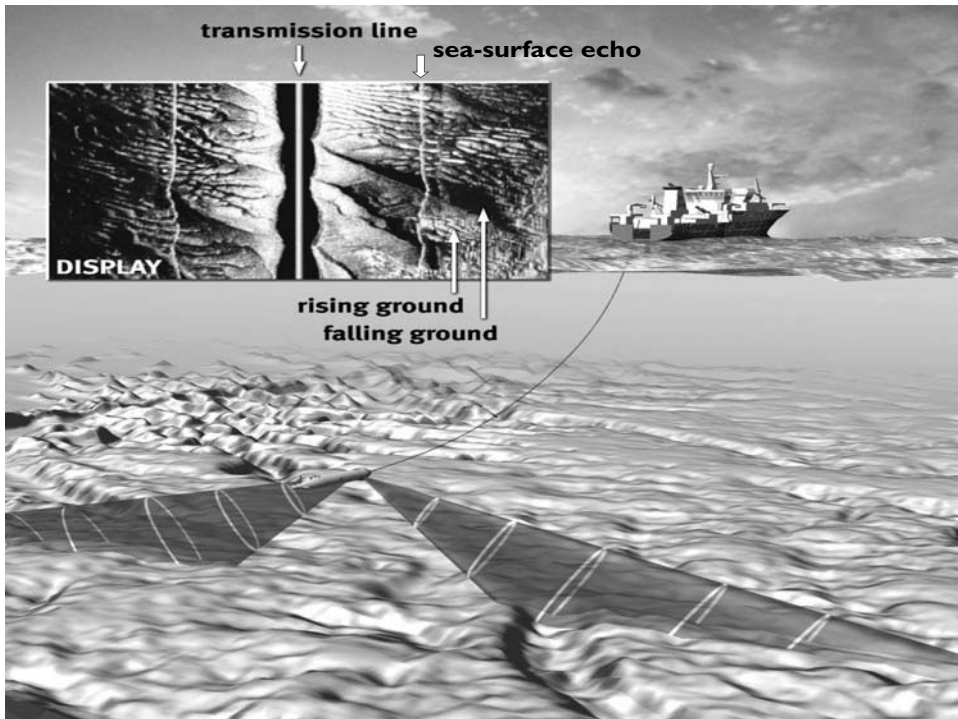


**Fig. 3.12** Side-scan sonar. The transducer is in a towed body not far above the seabed. Two transducers are used to observe both sides of the track simultaneously. Marks on the display (inset) indicate topographical features of the seabed, showing rock and sand ripples in this example. (Illustration drawn by Alvan Rice.) The strong white echoes (marked) are sea-surface reflections from side lobes.

pelagic fish schools off the coast of California. Rusby (1977) showed how a low-frequency side-scan system might be used for counting herring schools. More recently, Trevorrow (2001) described side-scan sonar observations of single fish in shallow water, while O'Driscoll and McClatchie (1998) applied the school-mapping method in their surveys of schooling fish off the coast of New Zealand. More generally, the side-scan sonar reveals the bottom topography which is useful in studies of demersal fish and shellfish, whose behaviour and distribution may depend on the type of habitat which is available.

Sophisticated techniques for the classification of seabed types using side-scan data have been developed since this idea was proposed by Reut *et al.* (1985). For example, Hurst and Karlson (2004) used automated texture analysis of side-scan sonar data from an area near the Galapagos Islands. They found good agreement between the acoustic identification based on four classifiers and the ground-truth data obtained from samples collected by submersible vehicles. However, good-quality classification of the seabed does require care with the data collection. Bell *et al.* (1999) raise concerns about the apparent texture difference which may depend on the

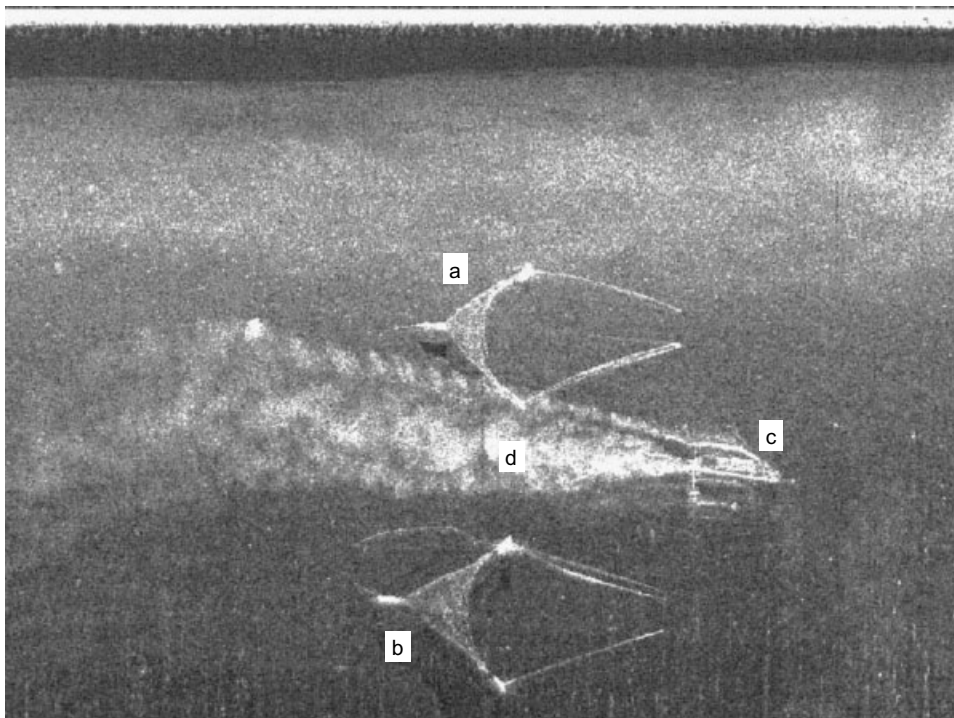


**Fig. 3.13** Side-scan sonar image of a prawn trawler towing two gears (a and b) from port and starboard booms. The trawler (c) and its wake (d) can be seen between the gears. The side-scan was deployed from an adjacent vessel travelling faster on a parallel course. The transducer location is at the top of the picture. (With thanks to NOAA and Klein Associates Inc. for permission to reproduce this image.)

observation direction. They suggest there is a high probability of the seabed being wrongly classified if the direction of observation is ignored.

### 3.4.3 Sector scanners

In the searchlight and side-scan sonars, the transducer moves or it rotates so that each transmission insonifies different volumes of water, and the eventual result is a two-dimensional display of targets in the vicinity. The sector scanner does this much more rapidly and without the instrument moving. A broad beam is transmitted so that echoes are returned from targets in any direction. The receiver forms a narrow beam which is steered or scanned electronically, covering a sector in one plane. The full sector is scanned in less time than the pulse duration. Thus the range and direction of targets within the sector are both determined after each transmission.

The transducer is constructed as an array of many elements in a line (Fig. 3.14). The transmitter pulse is applied to one central element, generating a wide beam on transmission. Alternatively, a separate transmitting transducer can be used. Suppose

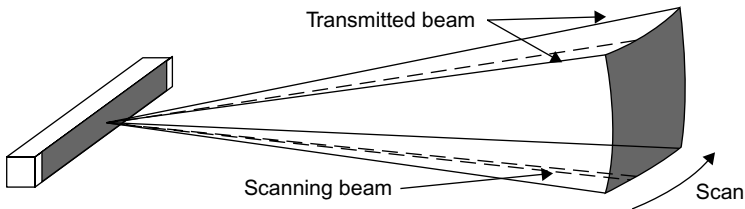


**Fig. 3.14** The sector scanner. The transmission beam covers a wide sector which is swept by the narrow scanning beam to locate targets in any direction.

for the present that the line of elements is horizontal and the transducer face is vertical. The sector is the horizontal cross-section of the transmitted beam. The signals received by the elements are processed in such a way that the receiving (or scanning) beam is a thin vertical section of the transmitted beam. Furthermore, the scanning beam is moved under electronic control and it sweeps from one side of the sector to the other within the pulse duration.

The scanning technique makes use of the phase differences between the echoes detected by the elements. As discussed earlier (p. 82), the phase differences depend on the direction of targets within the sector. More generally, the ranges and angles of all targets in the sector are determined uniquely by reference to the time dependence of the received signals (Tucker and Gazey 1966). Unlike the split-beam echosounder, the sector scanner can detect and correctly locate many targets in different directions, even when they are at the same range.

There are two kinds of electronic scanner, which differ in the method of processing the received signals to steer the beam across the scanned sector, see Mitson (1983) for a detailed description of these techniques. The modulation scanner (Fig. 3.15) depends on the fact that when a sine wave of frequency  $\omega$  is multiplied (modulated) by another of frequency  $\omega_1$ , the result is the sum of two signals with frequencies  $(\omega + \omega_1)$  and  $(\omega - \omega_1)$  respectively. The lower-frequency component is removed by means of a high-pass filter, leaving one signal which has been shifted to the higher frequency  $(\omega + \omega_1)$ . The frequency shift  $\omega_1$  is incremented by a constant amount  $\Delta\omega$  in modulating the signals from successive transducer elements. This introduces a phase difference  $\Delta\eta$  between the signals from successive elements;  $\Delta\eta$  is proportional to  $\Delta\omega$  and both increase linearly with time. The direction of the receiving beam depends on  $\Delta\eta$ , thus the beam rotates and the sector is scanned. However, the modulation technique has limited power to resolve targets in range, because it requires a pulse long enough to ensure that for targets at the edge of the sector, the echoes received by all the transducer elements overlap to some extent. If the pulse duration is reduced to improve the range resolution, the discrimination of targets at extreme angles will deteriorate. There may also be ambiguity between the extreme angles of the sector, as the phase differences at the sector edges differ by  $2\pi$  radians and are thus indistinguishable.

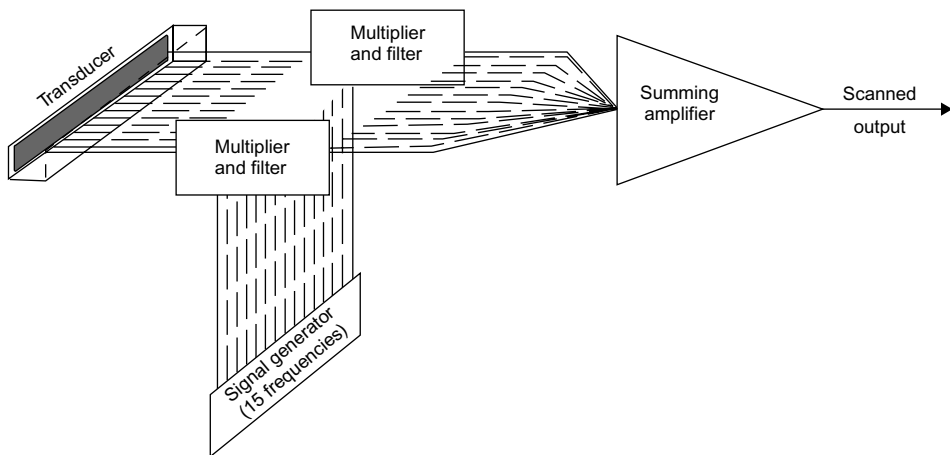


**Fig. 3.15** Modulation scanning technique. The received signals are multiplied (modulated) by internally generated signals with a frequency difference  $\Delta\omega$  between those applied to successive transducer elements. After the modulated signals are filtered to select the higher frequency component, the summed output corresponds to targets in a particular direction which sweeps as  $\Delta\omega$  increases with time.

The time-delay scanning technique is illustrated in Fig. 3.16. In this case the received signals are delayed for variable periods before they are summed to form the output signal. The delays are incremented in steps  $\Delta t$  between successive transducer elements. This is equivalent to introducing a phase shift ( $\omega\Delta t$ ). Thus by changing  $\Delta t$  the receiving beam is made to move across the sector. Although the time-delay processor is more difficult to implement in hardware, it correctly determines the angle of any target, and the same resolution can be achieved with shorter pulses compared to the modulation scanner. However, digital signal processing greatly simplifies the implementation of both techniques, and most scanners are now based on the time-delay method. The performance of the sector scanner is limited by noise and the need for a large bandwidth to include the full frequency spectrum of echoes, and in these respects the modulation and time-delay scanning techniques are similar.

Tucker and Gazey (1966) have described the theory of sector scanning which we need not repeat here. Mitson (1983) provides a good description of the design and operation of scanners. These instruments have been applied in studies of fish behaviour and migration, see for example Cushing (1977) and a more general review by Arnold *et al.* (1990).

Over the past decade, scanning sonars of various kinds have been used more extensively in fisheries. In the swathe sounder for instance, the scanned sector is in the vertical plane normal to the track of a survey vessel. This device is used by hydrographers to map the seabed. A swathe width around twice the water depth is achieved using typically between 60 and 120 beams. On each transmission the signal processor determines the depth of the seabed in a section normal to the path of the vessel. Simple versions of the swathe sounder obtain just one estimate of

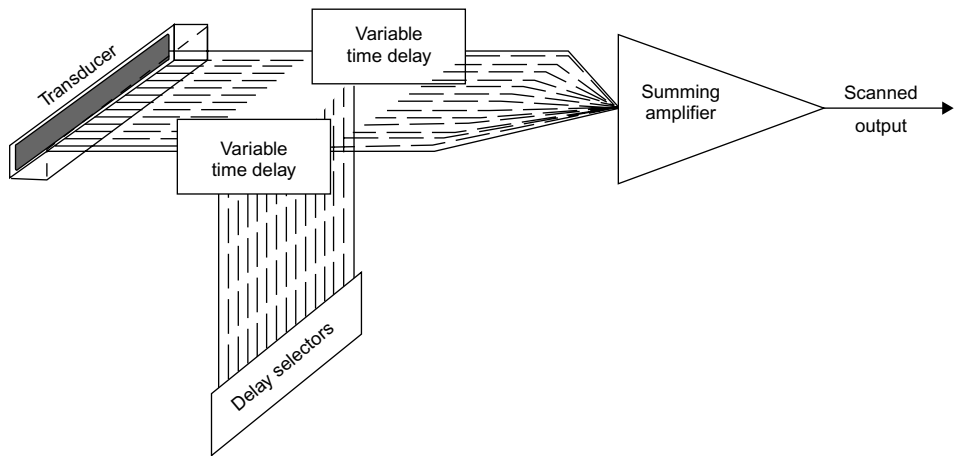


**Fig. 3.16** Time-delay scanning technique. The received signals are delayed by an amount which increments in steps  $\Delta t$  between successive transducer elements. The summed output corresponds to targets in a particular direction which sweeps as  $\Delta t$  increases with time.

depth per beam for each ping. More sophisticated versions use the phase of the bottom echo in a manner similar to the split-beam technique, to estimate the range to the seabed and thus the depth several times over the width of each outer beam. A complete map of the seabed may be obtained by surveying an area in a series of evenly spaced transects. An example of such a map, obtained using a 95 kHz 60-beam swathe sounder (Simrad SM950), is given in Fig. 3.17. This shows a map of the seabed structure formed by the volcanic caldera around the island of St Kilda to the west of Scotland, presented with little post-processing of the swathe data. On the smoother area in the foreground, a furrow-like structure can be seen parallel to the vessel track. This is due to the assumed sound-velocity profile being incorrect, resulting in wrong depth indications in the outer beams. Thus adjacent transects show ridges or dips at the swathe edges, hence the furrow effect. Very close inspection of the central area shows a fast ripple along the track. This is another artefact, due to imperfect heave compensation in bad weather which adds false undulations to the bottom depth. All these artefacts can be removed by post-processing of the swathe data. This procedure should include the correction of other known errors, notably the effect of changes in the tidal height over the duration of the survey.

These seabed-survey instruments have been applied in fishery applications by recording pelagic as well as bottom echoes. Melvin *et al.* (1998; 2003) pioneered the idea of sector scanning in acoustic biomass surveys using a Simrad SM2000 sonar. Gerlotto *et al.* (1994; 1998; 1999) have developed a pseudo-3D (three-dimensional) system for mapping fish schools and evaluating their avoidance reactions to survey vessels. Figure 3.18 provides an illustration of how the system works. The scanned sector is in a vertical plane normal to the vessel track. Each transmission provides a two-dimensional image of targets in this plane, and successive transmissions build

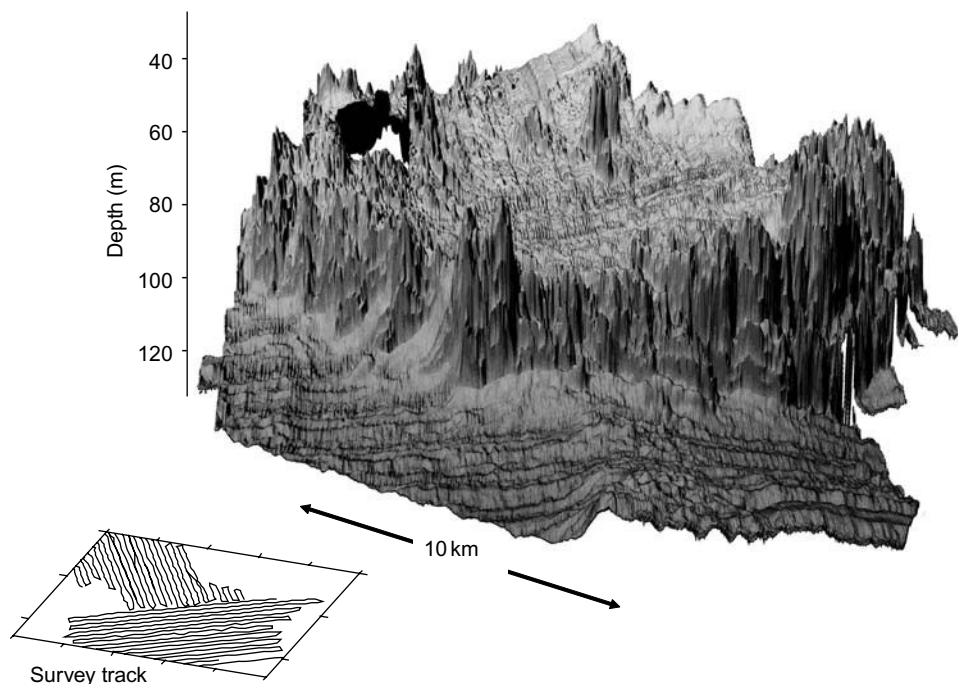


**Fig. 3.17** Swathe sounder map of the St Kilda caldera (50–60 m deep, 15 × 15 km area) located on the continental shelf (120 m deep) to the west of Scotland. The rim of the crater has steep walls with rocky outcrops. The uncorrected acoustic measurements show spurious irregularities (1–2 m depth variation) due to imprecise sound-speed profiles and the tidal rise and fall.

the full 3D view of the water column. If the scanned sector is 90°, then the water on only one side of the vessel is examined, as illustrated in Fig. 3.18. With a 180° sector, of course, the water column on both sides of the vessel can be mapped. The 3D image can be processed to view the detected objects in various ways. An example of a single fish school is given in Plate 3.5. Three planes through the school are illustrated along with a 3D representation of the surface and some of the descriptors that can be used to characterize schools. The choice of parameters for this purpose and their relative merits are discussed by Scalabrin *et al.* (1996) and Reid *et al.* (2000). Plate 3.6 illustrates the capabilities of such systems for 3D viewing. It has been necessary to develop new calibration procedures for these long-range high-frequency scanners, as discussed later in this chapter.

The concept of the ‘acoustic camera’ has been around since the 1960s (Smyth *et al.* 1963; Jacobs 1965). This is a sonar which can provide images approaching the quality of optical pictures, based on the usual principles of multiple beams and scanning to generate an array of visualized points (i.e. pixels). The operating frequency is typically 0.5–2 MHz, which limits the range to a few metres, but that is still much better than optics can achieve in dark or turbid water. Very-high-frequency systems with almost photographic capability have been developed using more complex

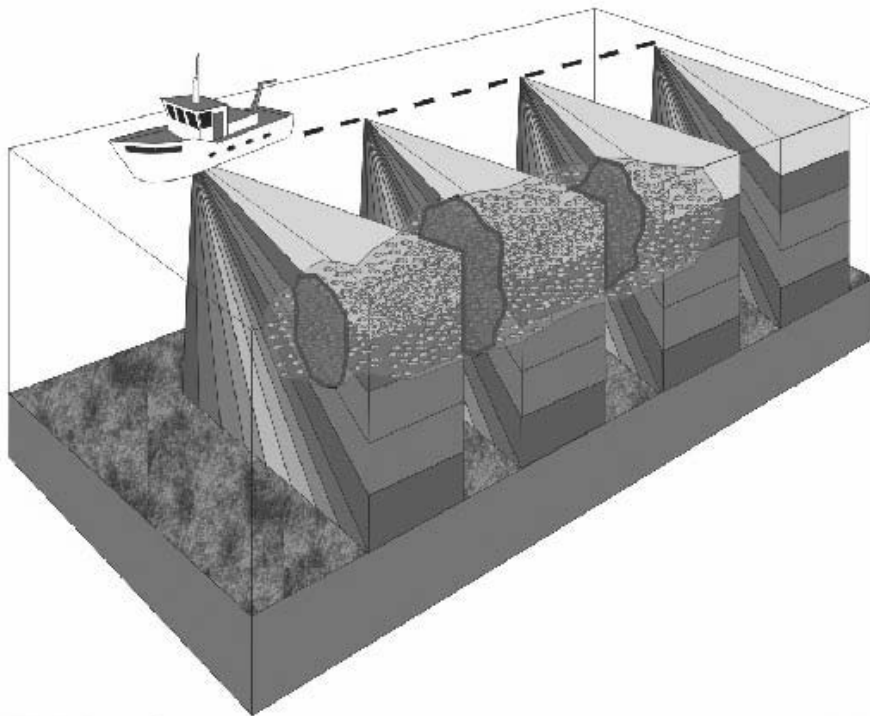


**Fig. 3.18** Example of three-dimensional data collection. Successive pings from a scanner provide 2D images of sideways cross-sections and the third dimension comes from the forward movement of the vessel. The illustration shows four idealized 2D images through a near-surface fish school recorded by a 13-beam scanner. (With thanks to Stratis Georgakarakos for the artwork.)

beam-forming techniques involving acoustic lenses. Moursund *et al.* (2003) used an acoustic camera to observe fish in a passageway at a hydro-electric power station. They compared images obtained at 1 and 1.8 MHz. The higher frequency gave much better results, with images containing 50 000 pixels formed from 96 beams. Despite the noisy environment, 18–68 cm fish could be observed clearly up to 12 m distant from the camera. Figure 3.19 shows an image of several salmon obtained with the 1.8 MHz camera. The advantage of acoustic instruments over optical cameras is that the former provide views that are almost unaffected by water turbidity and do not require any light. Both high- and low-frequency instruments have been deployed on fishing gear to study the behaviour of fish entering the net. Figure 3.20 shows how the equipment is deployed, and an example view near the netmouth obtained from a single frame (or ping).

#### 3.4.4 Three-dimensional sonar systems

We have already discussed some aspects of three-dimensional (3D) acoustic observations. The split-beam echosounder, for example, can locate targets in 3D, but only

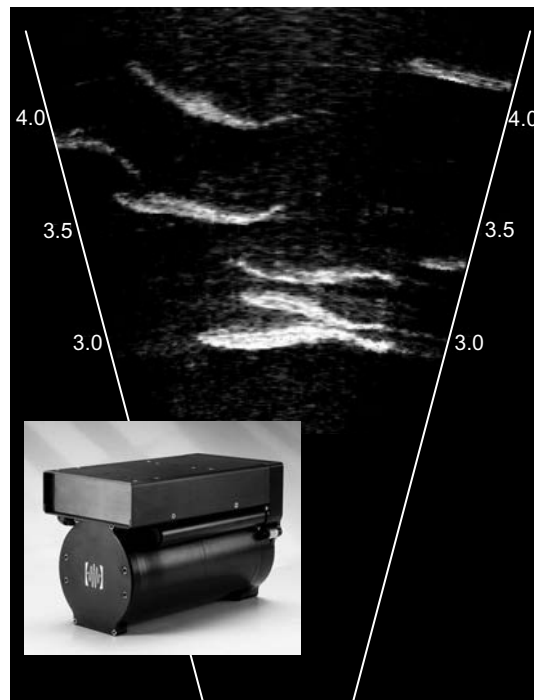


**Fig. 3.19** The DIDSON acoustic camera is a multi-beam scanning sonar operating at 1.8 MHz. This example of a DIDSON image shows chinook salmon (*Oncorhynchus tshawytscha*) of 80–100 cm in length swimming in a pond at the University of Washington. The numbers are distances in metres; the resolution at 4 m is approximately 2 cm. The camera (inset) is 30.7 cm long, 20.6 cm wide and 17.1 cm high. (With thanks to Ed Belcher for permission to use the illustration.)

if they are small and isolated. The pseudo-3D display mentioned above builds a 3D picture from a series of two-dimensional images obtained in several pings. However, a sonar that can be said to be fully 3D does not have these limitations. In principle, for each ping, such sonars should provide the echo intensities coming from known positions within a finite volume, irrespective of the type of target. Here we consider some examples of advanced sonar techniques for 3D imaging. These are mostly still at the experimental stage, at least as far as fishery applications are concerned, and it is likely that further developments will lead to even more sophisticated instruments becoming available in the near future.

The omni-sonar is an older but nevertheless versatile instrument which uses electronic scanning to locate targets in two dimensions within various sections of the hemisphere below the ship. This is not completely 3D, but it has two sector scanners operating concurrently, so that single objects or small schools can be located in space where the two sectors coincide. The transmitted beam insonifies one-half of a thin conical shell (Fig. 3.21). The receiving beam scans the 180° sector formed by the half-shell to determine both the direction and the range of any targets within the sector. The shape (apex angle of the cone) and the orientation of the shell may be

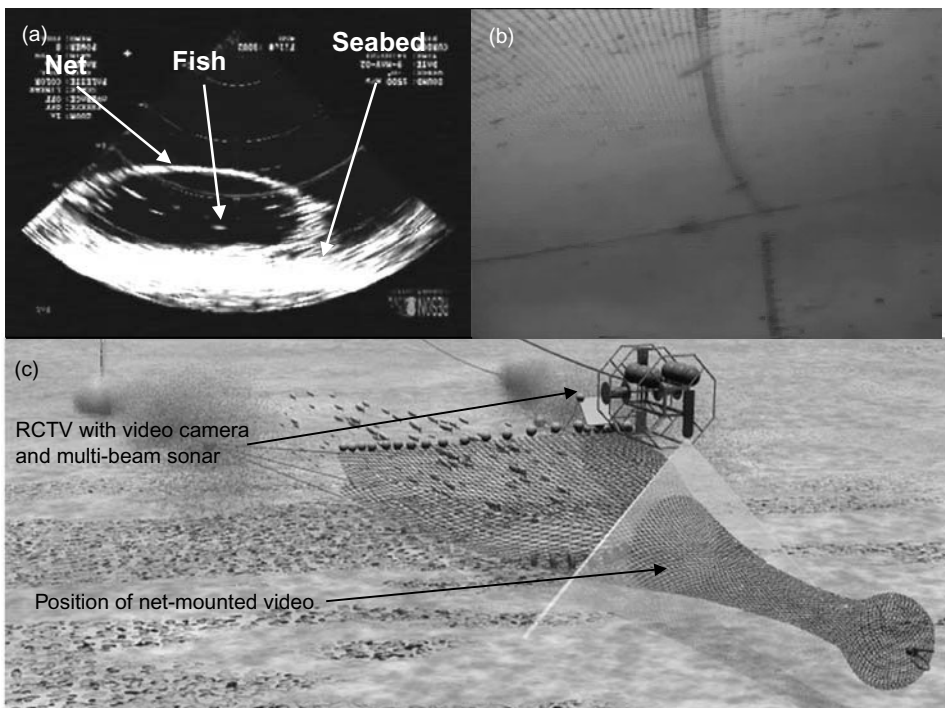


**Fig. 3.20** Use of a multi-beam sonar (Reson Seabat, 455 kHz) to observe fish behaviour in a bottom trawl: (a) sonar image showing the oval outline of the net, in contact with the seabed, just behind the headline; (b) video image recorded further down the net; and (c) diagram showing the instrumentation and the trawl. The video camera and sonar are deployed on a remote-controlled towed vehicle (RCTV). (With thanks to Emma Jones and Alvan Rice for the illustration.)

altered to inspect any part of the downward hemisphere. Two particular shells are shown in Fig. 3.21, one with a forward-looking sector and tilted slightly below the horizontal, and the second in a vertical plane, but many others may be selected by the sonar operator.

By connecting navigational instruments to the sonar, it is possible to view the ship's track and the movement of schools over a period of time, on what is called a 'true motion' display. Another useful facility is the automatic tracking of schools. In this mode, the omni-sonar adjusts the inclination of the shell automatically as the ship moves so that a particular target (selected by the operator) is always within the transmitted beam.

Plate 3.7 shows the display of an omni-sonar, recorded on a vessel which is fishing with a purse seine. There is a school of tuna to the left of the vessel, marked by the white arrow. The white curve is the track of the vessel which has circled the school while shooting the purse seine. The track of the vessel is shown by the echoes coming from the aeration in its wake. The comprehensive facilities of the omni-sonar are achieved by means of microprocessors or computers which access the acoustic

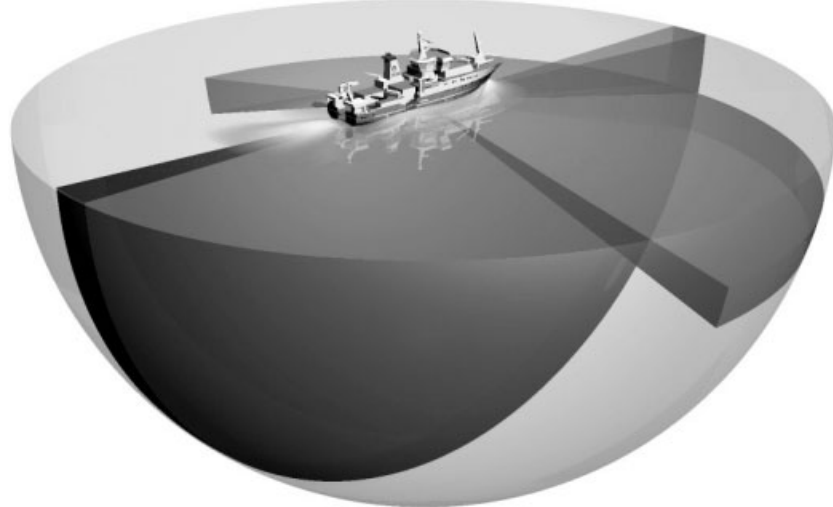


**Fig. 3.21** Omni-sonar showing two examples of transmitted beams formed as conical shells (heavy shading), one vertical in the fore-aft plane, the other directed forward and tilted slightly downwards. The direction of targets within the shell is determined by scanning a narrow receiving beam through a 180° sector. The beams may be rotated and/or tilted to inspect the complete hemisphere below the ship (light shading). (Illustration drawn by Alvan Rice.)

and other data, perform the necessary calculations, control the transmitted beam and generate the display.

Current designs of fully-3D sonars are limited to small sectors, short ranges and high frequencies. McGehee (1994) provides a description of one such instrument, while the performance and results achieved in practice have been described by Jaffe *et al.* (1995), McGehee and Jaffe (1996) and Jaffe (1999). Another interesting development is the 3D Omnitech system. This has been used to observe fish entering a demersal trawl, and it generates spatial images in real time that can be visualized by means of appropriate software (Plate 3.8). The sonar was mounted on the headline, looking backwards into the mouth of the trawl. The ground gear of the trawl can be seen as a raised ridge along the lower leading edge of the images. The sequenced, post-processed tracks of two fish entering the trawl can be seen just in front of the ground gear. One of the fish appears to swim upwards towards the top netting panel, while the other remains closer to the belly of the trawl. The images, provided by Norman Graham of the Bergen Institute of Marine Research, were recorded in the Barents Sea during November 2003, on board the Norwegian research vessel ‘Sarsen’. Based on the composition of the trawl catch, it is likely that the imaged fish are cod. The recorded positions of the fish, in combination with visual techniques for identifying sonar targets, are being used to elucidate species-specific behaviours which might assist the design of more selective fishing gear.

A great deal of development is required to provide comprehensive object tracking in 3D, and experimental work in this field is at an early stage. Currently, new systems

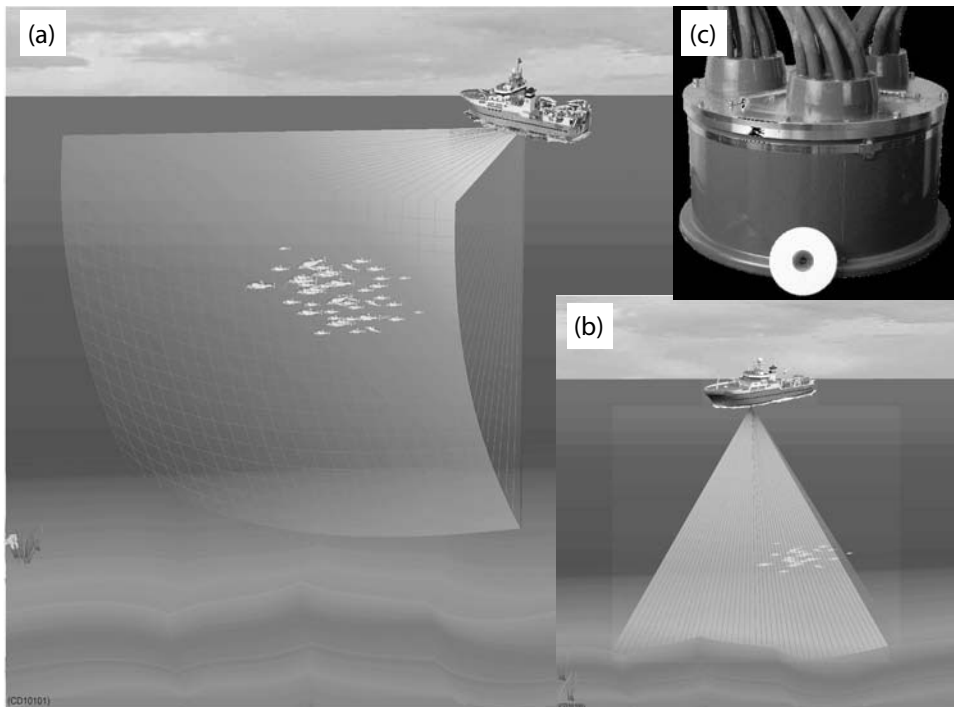


**Fig. 3.22** The Simrad SMS sonar (70–120 kHz) shown operating in two modes: (a) as a fully 3D sector scanner and (b) as a multi-beam vertical sounder. These systems can be used to study fish behaviour, distribution and scattering properties both around (a) and directly under (b) the vessel. The transducer (c) is shown with a CD in front to give scale. The configuration can be changed at will from 3 to 45 beams, with transmission over the full sector, or a partial sector which improves the signal in relation to noise and reverberation levels. (With thanks to Simrad Norge AS for the illustrations.)

for longer-range 3D observation are under development. The aim is to reduce the sonar frequency to around 100 kHz, which would allow observation ranges of several hundred metres. Figure 3.22 illustrates the main operational modes of the 70–120 kHz Simrad SMS sonar, which can work as a fully-3D sector scanner or as a multi-beam vertical sounder. The beam configuration can be changed to any number from 3 to 45 beams. The transmission can be over the full sector, or it may be restricted to a narrower range of angles which improves the signal-to-noise ratio and reduces the reverberation. In conclusion, we believe that 3D-sonar technology offers good prospects for future advances in our understanding of fish behaviour and distribution in the sea.

### 3.4.5 The Doppler effect

Suppose a sonar transmits sound of frequency  $f_0$ , and an echo is received from a moving target whose range is increasing at speed  $v_R$ . The frequency of the received

signal is not  $f_0$ , but the slightly different  $f_r$  which is given by the formula:

$$f_r = f_0(1 - 2v_R / c) \quad (3.5)$$

The change of frequency is caused by the Doppler effect (Kinsler and Frey 1951). For example, if  $c = 1500 \text{ m s}^{-1}$ ,  $v_R = 5 \text{ m s}^{-1}$  and  $f_0 = 100 \text{ kHz}$ , then  $f_r$  is 660 Hz less than  $f_0$ . Conversely,  $v_R$  may be estimated by measuring  $f_0$  and  $f_r$ , provided that the pulse duration ( $\tau$ ) is long enough to ensure that the bandwidth of the echo is less than  $|f_0 - f_r|$ . More generally, the change of frequency may be determined to an accuracy of about  $(1/\tau)$ . Rearranging Equ. (3.5), we see that  $v_R$  may be estimated from the formula:

$$v_R = c(f_0 - f_r) / 2f_0 \quad (3.6)$$

Note that  $v_R$  is the radial component of the relative velocity. Sideways components of the velocity do not change the frequency. One useful application of this effect is the Doppler log. This instrument measures the speed of the ship relative to the seabed or to the water at some depth. The log may have four transducers, whose beams are inclined to the vertical in the fore, aft, port and starboard directions respectively. The speeds in the forward and sideways directions are determined by resolving the radial (along-beam) speeds indicated by the changes in frequency.

A Doppler sonar is one that measures the frequency of the received signal, but otherwise it operates in much the same way as any other sonar. Doppler sonars have been used by Holliday (1977a) to study the movement of schooling fish and by Johnston and Hopelain (1990) to measure the migration speeds of salmon in rivers. Interest in this technique seems to have lapsed in the 1990s. More recently, Tollefson and Zedel (2003) tested a Doppler system, again on migrating salmon, in the Fraser River (British Columbia). Their results were preliminary, but showed promise for future applications of this technique in fresh water.

### 3.5 Wideband systems

A major problem in fisheries acoustics is how to determine the species and size of targets whose echoes have been detected. Early attempts to do this by acoustic means had limited success. Holliday (1977b) suggested that the size of fish relates to the resonance frequency of the swimbladder, and this frequency may be determined from the spectrum of echoes generated by a broadband source such as an explosive charge. There are considerable difficulties in this approach (cf. Section 4.5). Rose and Leggett (1988) reported that the probability distribution of the echo amplitude from a school depended on the species, perhaps because of different packing densities in the schools. However, Denbigh *et al.* (1991) suggest that the echo amplitude distribution is largely independent of the packing density if there are more than five fish per sampled volume.

In principle, the more frequencies there are in a signal (or the wider the spectrum) the more information is conveyed from the source to the receiver. This leads to the concept of the wideband sonar, which has a much larger bandwidth than that of conventional sonars and echosounders. Simmonds and Copland (1989) described such an instrument whose bandwidth covers an octave (i.e. a factor of two) from 27–54 kHz. An important requirement for the measurement of fish is that the transducer beam width should be the same at all frequencies. This is achieved by means of the spherical-cap transducer which was first described by Rogers and Van Buren (1978). The transducer consists of a number of independent elements on a spherical surface, and the beam width is controlled by ‘shading’ the signals from the individual elements (cf. Section 2.3).

The spectrum of the echoes received by the wideband sonar is a useful indicator of the target identity, provided that the target strength of each species expected to be present changes with frequency in a characteristic way. Thus for one species, the target strength might increase between 27 and 54 kHz, and in another the change might be in the opposite direction. Simmonds and Copland (1989) and Simmonds *et al.* (1996) conducted experiments with cod, herring and mackerel in cages. Having first measured the frequency dependence of the target strength for each species, they derived algorithms for deciding which species had produced the particular spectrum of echoes observed with the wideband sonar. Simmonds *et al.* (1996) found that the success rate in identifying the species depended on the number of independent samples on which the decision was based. With 100 and 1000 samples, the decision was correct 90% and 95% of the time respectively. Their method could also identify mixtures of two species, although the success rate in this case was lower, 75% and 90% respectively for 100 and 1000 samples. Other wideband experiments have been reported by Zakharia and his co-workers (Zakharia *et al.* 1989, 1996). They studied tethered individual fish and showed that the spectrum of echoes depended on both the species and the activity of the fish which might be swimming or stationary. Good results were obtained in that individual species were found to have characteristic acoustic properties that indicated their identity. What was less clear from these studies, however, was how well generic species identification could be achieved in the field. Unfortunately, these investigations ceased before the results of the experimental studies could be supported with the necessary validation in the circumstances relevant to acoustic surveys. The failure to realize the potential of this work was mostly due to the lack of funds needed to develop reliable survey instruments from the experimental prototypes.

Thompson and Love (1996) used a low frequency (0.5–10 kHz) wideband echosounder to obtain estimates of fish size and density. The fish species were not identified directly, but rather the size distribution was inferred from the echo spectrum and swimbladder scattering models (see Chapter 6). Blue whiting (*Micromesistius poutassou*) and redfish (*Sebastes* spp.) were identified in the Norwegian Sea, while Pacific hake (*Merluccius productus*) and grenadiers (*Coryphaenoides* spp.) were separately estimated in two layers off the west coast of the USA. The same equipment

was used in the Gulf of Oman to investigate myctophids (*Benthosema pterotum*). The indications were that the system could identify such small fish (1.5–4.5 cm overall length) among others, but the results were tentative.

There are commercial wideband sonars on the market; however, their capabilities for target identification in fisheries applications are uncertain. In summary, it seems that the classification and/or identification of species based on the echo signatures recorded during acoustic surveys is a tractable problem, and wideband sonar can assist here. However, the concept of species identification from wideband spectra, which can vary geographically and among seasons, is perhaps too ambitious at present. It must be appreciated that satisfactory identification of a species depends not only on the acoustic characteristics of that species, but also on the features of any other targets whose echoes may confound the identification process. Nevertheless, this is a promising area for future development and there is a real need for fully operational and supported systems which can be used to develop libraries of scientifically-based criteria for the identification of detected targets.

### **3.6 Sound source location: pingers, transponders and hydrophone arrays**

All the instruments discussed so far are active sonars. They rely on the reflection of their own transmission to detect targets. Echo detection may be unreliable if the targets are small, at great range or close to a strong reflector such as the seabed. However, a much stronger (and more easily detected) signal can be obtained by attaching a pinger or transponder to the target. When attached to a fish, these devices are commonly called acoustic tags.

The pinger has no receiver but it transmits a pulse of sound at regular intervals. The pulses are detected by one or more hydrophones located in the vicinity. If there are three receiving hydrophones in a triangular array, the pinger can be located in two dimensions (in the plane of the array). This is done by measuring the arrival times of the pinger pulses at the hydrophones, see for example Hawkins *et al.* (1974). If there are four hydrophones, one at each apex of a tetrahedron, the pinger can be located in three dimensions. Furthermore, the frequency of the pinger transmission or the pulse interval may be changed in response to some variable, such as the water depth or the temperature, to transmit additional information. In contrast, the transponder is a device which transmits a signal when it receives one. The transponded signal is much stronger than the echo, but both arrive simultaneously at the sonar receiver and the target may be located in the usual way. It is possible to detect bottom-living fish that have been tagged with transponders, even against the strong seabed echo, and this technique has been widely used in the study of fish behaviour near nets (review, Arnold *et al.* 1990).

Smith *et al.* (1998) analysed the errors in acoustic position fixes. They showed how the variance of the position estimate depended on the location and speed of

the tracked pinger relative to the hydrophone array. The position is normally estimated on the assumption that the pinger transmission follows the direct path to each hydrophone. This assumption may fail, for instance when the pinger is close to an undulating seabed. Further, multi-path transmissions can occur with the received signal being a combination of propagating waves on the direct path and others through the sediment, especially when the bottom is soft. This effect confuses the arrival-time measurements and substantial position errors can result. When tracking near-bottom pingers, the hydrophones should be located on higher ground, not in valleys, and slightly above the bottom to reduce the effect of signals other than the direct path.

Further advances in acoustic tracking technology have been reported by Ehrenberg and Steig (2003). Sophisticated tags and signal processing methods have been developed to allow tracking of fish in three dimensions with a spatial resolution better than 1 m. The use of frequency-modulated (chirp) transmissions can reduce multi-path errors and gives options for tracking several tags concurrently (Ehrenberg and Torkelson 2000). Arrays with many hydrophones (i.e. more than the minimum required for a unique position fix) allow more accurate tracking, and the positional errors can be estimated through statistical analysis of redundant measurements. The system described by Ehrenberg and Steig (2003) can have up to 16 hydrophones. It receives and automatically stores the tag detections for each hydrophone, and plots the resulting positions in three dimensions. Thus the movement of each pinger can be observed in real time. This technique has been used to study the behaviour of salmonids and many other species in various aquatic environments.

In the ocean, we note the work of Dagorn *et al.* (2000a) on bigeye tuna (*Thunnus obesus*) and Dagorn *et al.* (2000b) on yellowfin tuna (*Thunnus albacorus*), in their studies of how these species behave when they are concentrated around FADs. Bach *et al.* (2003) used the same telemetry technique with external pingers attached to bigeye tuna. They compared observations of the depth distribution seen in the catches from a longline fishery with the observed behaviour of the tagged fish. Both methods gave similar results for the vertical distribution of the tuna.

Pingers and transponders used to study the behaviour of fish must be small to avoid disturbing the natural behaviour of the animal. Modern microelectronic circuits are very compact; most of the volume is required for the transducer and the battery which powers the device. The size of battery is determined by the transmission power, the pulse duration and the period of time for which the device is required to continue working. The device may be attached externally to a fin, in the same way as a Pedersen tag, or it may be internal i.e. inserted through the mouth into the gut or the body cavity through an incision in the body. In both cases, the fish must be anaesthetized to minimize the stress of the operation.

Some animals (notably the aquatic mammals) emit sufficiently clear sounds in their natural vocalization to allow tracking by hydrophone arrays without any artificial signals from pingers or transponders. This passive tracking technique has the obvious advantage that the natural behaviour is in no way disturbed by the

experimental procedure. It depends on the vocalizations being pulses with a wide enough bandwidth for the arrival times at the hydrophones to be measured precisely. Many applications of passive tracking have been reported in recent years. Morphett *et al.* (1993) and Connolly *et al.* (1997) obtained good results in tracking dolphins near submarine structures and moving fishing gears such as midwater trawls. Møhl *et al.* (2001) proposed a system of independent recorders forming a large-aperture array for tracking marine mammals. The errors associated with this method have been analysed by Wahlberg *et al.* (2001). Brening *et al.* (2001) tracked bottlenose dolphins (*Tursiops truncatus*) using four closely-spaced hydrophones arranged in two pairs. The sound source was located from the intersection of the two directions determined from the phase differences in the signals received by each hydrophone pair. Although the method was tested using recordings, it clearly has potential for real-time tracking. These systems are still under development; however, passive tracking has been the subject of extensive study in the military field and development of these techniques for biological research should prove a rich source of interesting developments in the future.

### **3.7 Installation of acoustic systems**

The advice presented here is not intended to replace or even to supplement the installation instructions supplied by the manufacturer of an echosounder or sonar. Sonar installations vary from the extensive systems on major research vessels to the minimal portable equipment deployed on small dinghies (Fig. 3.23). Whatever the application, careful attention to the electrical installation is critical to good performance. Most manufacturers provide detailed descriptions of how to connect, screen and earth the acoustic equipment to protect it from electrical interference. This is particularly difficult in a shipboard environment. These instructions may seem elaborate, but they must be followed if the system is to be used to its full potential. The basic rules are that transceivers should be located as close as possible to the transducers, and they should be multiple screened to protect sonar signals from sources of electrical interference. Here we discuss more general questions like where, on or off a vessel, will be the best location for deployment of the transducer. We also discuss important issues concerning the vessel noise specification.

#### **3.7.1 Transducers on or near the vessel**

The traditional echosounder installation has the transducer on a pod extending a short distance below the hull. The pod is usually fitted some 5–15% of the vessel width to the side of the keel. It is an oval- or boat-shaped block extending about 0.3–0.5 m below the hull. The transducer is often located above the keel to provide protection in the event of grounding. Such installations have disadvantages for scientific use. When operating in adverse weather conditions, the simple pod installation suffers from

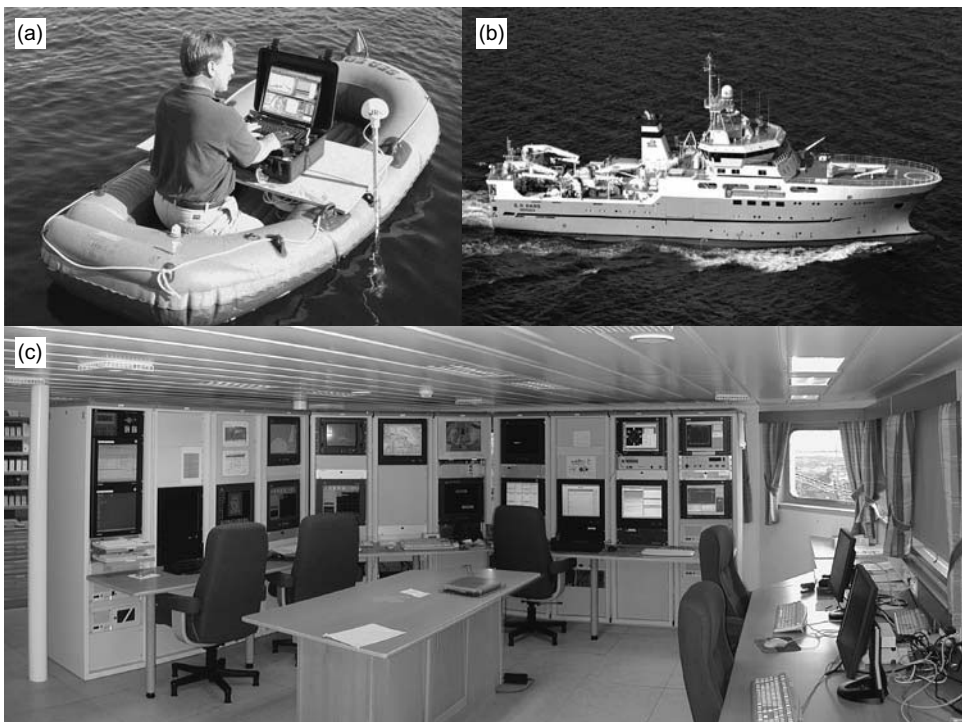


**Fig. 3.23** Various acoustic installations. (a) Self-contained BioSonics DT 420 split-beam echosounder ( $6^\circ$  beam width, 420 kHz) deployed in a dinghy with the transducer and a GPS antenna on a pole mounting; (b) The Norwegian research vessel 'G.O. Sars'; she has two independent drop keels, a six-frequency EK60 echosounder, two ADCPs, acoustic telemetry from trawl instrumentation, two multi-beam sonars, a side-looking sonar (MBS) with 500 beams, two hydrographic swathe sounders and a sub-bottom profiler. She can also deploy a dual-frequency sonar on a deep-towed vehicle with 7500 m of fibre-optic cable. (c) The instrument room on 'G.O. Sars'. (With thanks to Janusz Burczynski at BioSonics and Hans-Petter Knudsen IMR Bergen.)

signal loss due to motion-induced bubbles forced downwards by the shape of the hull (cf. Chapter 9). To overcome this problem, given that some (especially commercial) vessels which are used for acoustic surveying do not have sophisticated facilities like the drop keel (see below), the transducer can be deployed on a shallow-towed body. This is towed on a short cable alongside the vessel as seen in Fig. 3.24. Illustrations of typical shallow-towed bodies are shown in Fig. 3.25. When the transducer must be located on the hull, some reduction in the roll may be possible through stabilization of the vessel, or both pitching and rolling can be reduced by dynamic stabilization of the transducer platform.

In recent times, many new fishery research vessels have been built with a special facility for sonar, the drop keel, following the design pioneered in RV 'Miller-Freeman'. The transducers are mounted on the lower face of a retractable housing which forms part of the vessel keel. Some of these installations are designed

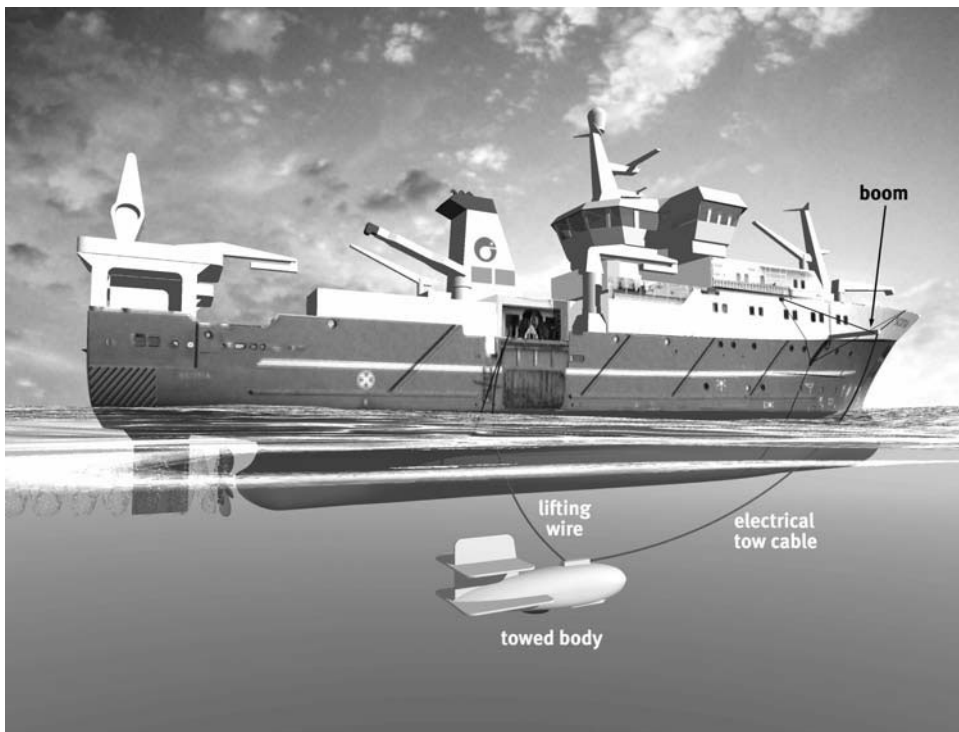


**Fig. 3.24** Deployment of a shallow-towed transducer platform. The body is towed on a fixed length of cable from a forward towing boom. It is launched and retrieved on the stern quarter using a separate lifting cable which is slack during towing. (Illustration drawn by Alvan Rice.)

to allow access without the need to drydock the vessel, since the transducer housing can be lifted clear of the water inside the vessel. A typical example is the Scottish fisheries research vessel ‘Scotia’ which has a drop keel 6 m long that can be lowered to a depth 3 m below the fixed part of the vessel keel. Figure 3.26 illustrates this installation and a view of the drop keel taken during construction. A transducer deployed in this way is well protected from weather-induced bubbles, even better than one in a shallow-towed body.

### 3.7.2 Deep-towed bodies

Some fish live in very deep water, up to 1000 m depth or more. Acoustic abundance estimation at such depths has a number of problems. If the transducer is deployed near the surface in the usual way, then:

- at this range only low frequencies may provide sufficient signal-to-noise ratio;
- seabed discrimination may be difficult due to the large cross-section of the acoustic beam;

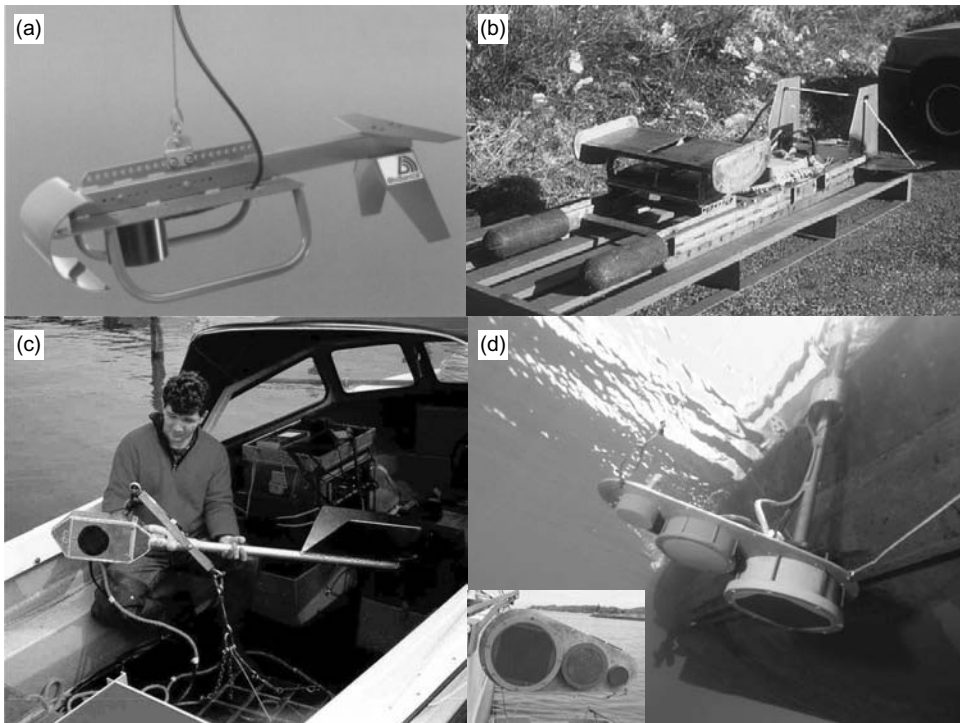


**Fig. 3.25** Examples of transducer deployments on shallow-towed bodies and poles. (a) BioSonics towed body 1.3 m long and 0.5 m wide, weighing 36 kg with an additional 4.5 kg for the 200 kHz transducer shown. (b) FRS Aberdeen towed body (on transporting pallet) which has 38, 120 and 200 kHz transducers below the central wing; it is 2.5 m long, 1.3 m wide and weighs 350 kg. (c) Side-looking transducer on a thin towed body intended for work in rivers (Mous *et al.* 1999). (d) Removable pole mounting of a three-frequency EK60 echosounder (inset shows the transducers). (With thanks to Janusz Burczynski, Paul Fernandes and Erwan Josse.)

- high frequencies which might help with species identification are unusable due to acoustic absorption;
- target strength cannot be estimated *in situ* due to the large sampled volume (which is unlikely to contain only one target);
- correction of the echo intensity for absorption losses is inaccurate over the long transmission paths.

The reasons for these limitations have been explained in Chapter 2. They can be avoided to a large extent by using a deep-towed body which places the transducer much closer to the fish. Dalen and Bodholt (1991) were the first to describe this technique which is illustrated in Fig. 3.27. Development has been slow but the results have been productive. Dalen *et al.* (2003) compared the performance of deep-towed and hull-mounted transducers during surveys of pelagic redfish. They found that the deep-towed method greatly improved the spatial resolution of fish in scattering

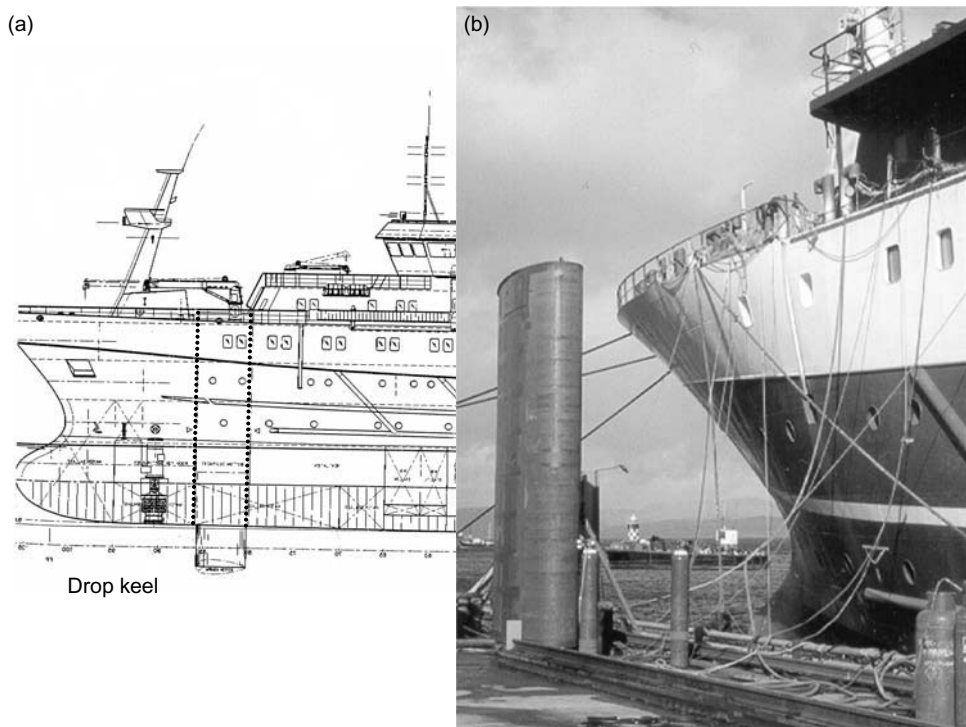


**Fig. 3.26** (a) Drop keel for housing acoustic instruments on FRV 'Scotia'. (b) The keel is 9 m high and is seen on the quayside next to the bow of the vessel while fitting out.

layers, it suffered less from noise interference and gave clearer echograms which allowed the target species to be identified more confidently. On the other hand, the transducer performance was depth-dependent and this caused some uncertainty in the fish density indicated by the deep-towed system. Measurements showed that, between the surface and 500 m, the sensitivity of the 38 kHz transducer increased by 2.5 dB while that of the 120 kHz transducer decreased by 1.5 dB. Even allowing for this effect, however, different abundances were indicated by the deep-towed and hull-mounted systems, particularly for the deepest fish. Dalen *et al.* (2003) thought this was a consequence of the different signal-to-noise ratios, but their analysis was insufficient to support or refute this explanation. The overall conclusion was that deep-towing the transducer was a substantial improvement over the traditional hull-mounted installation. Kloser (1996) and Kloser *et al.* (2000) had similarly encouraging results in deepwater surveys of benthopelagic fish off Tasmania and New Zealand. Their deep-towed system (Fig. 3.27) was used down to 600 m. The transducer sensitivity at 38 kHz was again seen to change in the manner described by Dalen *et al.* (2003). In this case, the main benefit derived from the deep-towed transducer was said to be improved seabed discrimination on the edges of the seamounts and canyons around which the species of interest were located.

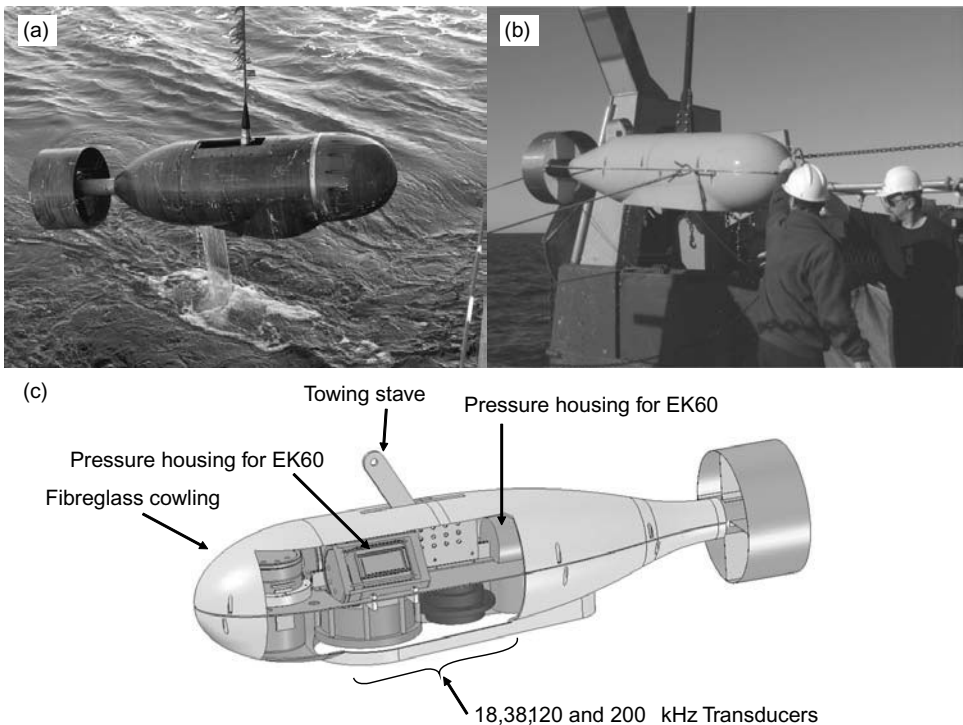


**Fig. 3.27** Two similar deep-towed bodies described by (a) Dalen *et al.* (2003) and (b, c) Kloser (1996). (With thanks to John Dalen and Rudy Kloser for the illustrations.)

### 3.7.3 Vessel noise performance

Over the past 30 years, it seems that technological change in marine engineering has resulted in two rather complementary developments. Firstly, the increasing demands for power and performance led to vessel designs that could be particularly noisy, both at the low frequencies heard by fish (Chapter 4) and in the ultrasonic bands used by echosounders. Secondly, the isolation of this noise to reduce its emission into the water was becoming technically and financially feasible. Low-frequency noise is mostly produced by rotating machinery. This consists of a fundamental frequency (corresponding to the rotation rate) and harmonics thereof. High frequencies are generated by hydrodynamic effects like the flow noise around the hull and, most importantly, cavitation at the tips of the propeller blades. However, there are other sources of energy in ships that cause vibrations, such as the alternating current in electrical cables and the diode-switching devices used to control motors.

As a general scientific principle, it is important to ensure that the measurement technique does not perturb the object being observed. Thus, in acoustic surveys of fish from a moving vessel, the radiated noise is an important factor. Garnier *et al.* (1992) conducted a noise survey of European fisheries research vessels. They found wide disparity, greater than 50 dB, in the noise performance of the vessels investigated.

Some had been designed with a noise specification and some had not. They briefly reviewed the reasons for including a noise specification in the design criteria, and presented preliminary ideas on how this should be done.

There is limited scope for reducing the noise of existing vessels. However, when a new vessel is to be built with acoustic surveying in mind, the design should ensure that the radiated noise level is below some limit. This question was addressed by an ICES Study Group, leading to a report on the acceptable noise performance of research vessels (Mitson 1995). This study examined data on ambient noise, fish hearing and sound-induced behaviour to provide an objective methodology for setting noise levels in the audio range appropriate to fish observation. In addition, limits on the ultrasonic noise were specified to avoid degradation of echosounder performance. A case study for herring surveys was used as a worked example to describe the procedure; the resulting specification is a noise signature that should not disturb herring 20 m below the vessel. This signature is the line shown in Fig. 3.28, and it has become known as the ICES standard. However, it is the method rather than this particular line that is recommended by Mitson (1995). The low-frequency noise specification depends on the species to be surveyed, its hearing capability, reaction behaviour and depth. Herring was chosen for the worked example as an often-surveyed species and because they were perceived as having particularly sensitive hearing (Chapter 4). The range limit of 20 m arose because, closer to the surface, visual stimuli are likely to be as important and there is little point in further noise reduction. The closer one is to a vessel, the more difficult (and expensive) it is to meet a given ambient noise specification.

The important point is this: to design a research vessel without any attention to the noise specification is not a good policy. Noise reduction is now a well established procedure. The method is simple in concept; each item of equipment needs to be supplied with documented details of the noise radiated to air and through the mountings to the ship's hull, the latter being most important. We then develop a noise budget, and by checking critical machinery on installation we ensure that the budget is maintained. Recent experience has shown it is possible to set a scientifically-based noise specification that is achievable in modern vessel designs. Figure 3.28 shows the radiated noise performance of several fishery research vessels, five of which were designed to be noise reduced and evidently did achieve their design objectives. It is worth noting that the worst vessels, built without any noise specification, are likely to disturb herring schools up to 400 m distant (Diner and Massé 1987), while the corresponding limit for the best is around 15 m. This difference shows that noise reduction is both achievable and effective (Fernandes *et al.* 2000).

### **3.8 Calibration**

The need for careful and accurate calibration of the acoustic instruments cannot be emphasized too strongly. Calibration provides the quality control that is crucial to reliable surveys. In the early days of acoustic surveys, before 1980 perhaps,

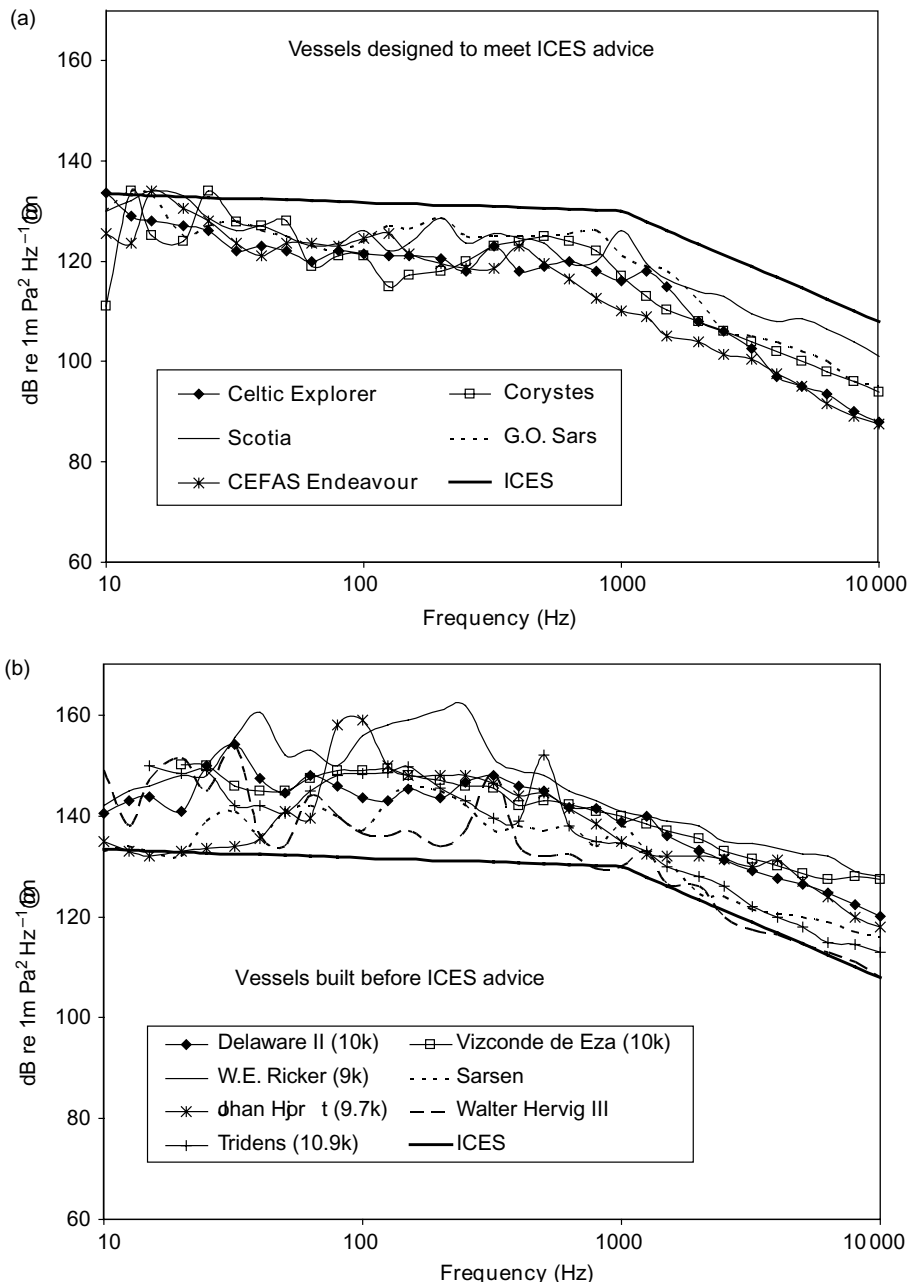


**Fig. 3.28** Vessel noise signatures. Comparison of (a) five vessels designed to the ICES specification and (b) other vessels designed without particular attention to noise reduction. The (a) signatures are around 20 dB better than (b) at frequencies in the hearing range of fish. (With special thanks to Ron Mitson for assembling all the data.)

calibration was a major source of error in the fish abundance estimate, amounting to a factor of two or worse (Blue 1984). If the calibration is wrong, the abundance estimate will be consistently different from the true value; a bias is introduced. However, much better calibration techniques were developed in the 1980s. Errors arising from uncertainty about equipment performance are now of minor significance, provided the calibration is performed in accordance with international practice (Simmonds *et al.* 1984; Foote *et al.* 1987). The calibration procedure recommended by Foote *et al.* (1987) is still regarded as the standard approach. Since then, more sophisticated instruments have evolved requiring different experimental methods. Nevertheless, though some practical aspects of the calibration have changed, the fundamental principles described by Foote *et al.* (1987) are still valid.

What is a calibration? In traditional physics or engineering, it is an experiment conducted to determine the correct value of the scale reading of an instrument, by measurement or comparison with a standard. In the case of the acoustic instruments used for echo integration, the ‘correct value’ is the backscattering cross-section of targets in the transducer beam, and the ‘scale reading’ is the corresponding output of the echosounder. Other definitions apply to directional sonars when the objective is partly to locate targets in space, but we shall start with the calibration of the single-beam echosounder. This is a difficult instrument to calibrate because it does not measure the target direction. The calibration must take account of the distribution of targets across the acoustic beam as well as the physical response of the instrument. Here we restrict attention to the physical calibration of acoustic instruments, that is to say the calibration of the transducer and electronic equipment as independent pieces of hardware, but excluding the acoustic properties of particular targets which are discussed in Chapter 6. We also briefly consider the calibration of multi-beam sonars of the kind described in Section 3.4.

The sensitivity of the single-beam echosounder is determined by reference to the echo from a target in a particular direction, normally the acoustic axis of the transducer, which is the direction of maximum sensitivity and therefore more easily identifiable. Targets in this direction are said to be on-axis. The receiver incorporates time-varied gain (TVG), which is intended to ensure that the same fish density will produce the same signal at any range. The gain changes with time after the transmitted pulse; this dependence is described by the TVG function. Another factor to be considered is the change in sensitivity with direction, known as the beam pattern. Thus the physical calibration of the single-beam echosounder involves three separate measurements, to determine (1) the on-axis sensitivity, (2) the TVG function and (3) the beam pattern.

The echo-integrator output, E, is assumed to be proportional to the number of fish per unit area, F, according to the equation:

$$F = [C_a \bar{g} / (\psi \langle \sigma_{bs} \rangle)]E \quad (3.7)$$

This is the echo-integrator equation which is discussed further in Section 5.4. To apply it, we need to determine the values of the several factors within the square brackets.

$\langle\sigma_{bs}\rangle$  is the expected value of the backscattering cross-section of the targets, which are assumed to be randomly distributed over the acoustic beam. This is a major topic in its own right, to which we return in Chapter 6. For the present, it is the three other parameters which have to be measured in the physical calibration of the equipment, corresponding to the three aspects of performance noted above. They are:  $C_a$ , the on-axis sensitivity;  $\bar{g}$ , the TVG correction factor; and  $\psi$ , the equivalent beam angle of the transducer.

### 3.8.1 *The on-axis sensitivity*

The acoustic axis of the transducer is the direction in which the transmitted energy is greatest, and from which the largest echo is returned for a given target at constant range. The calibration is performed to determine the combined transmit and receive sensitivity in this direction, from which the value of  $C_a$  is calculated. Three standard methods might be used to measure the on-axis sensitivity:

- the reciprocity technique due to Foldy and Primakoff (1945; 1947); this method is absolute but time consuming and suited mainly to laboratory conditions;
- the calibrated hydrophone; this is a secondary transducer of known performance which is used as a reference;
- the standard target.

The first two methods are mentioned only for the sake of completeness, and neither is recommended. In modern practice, the standard target method is preferred as the one that gives the most accurate results. The basic methodology is explained in Foote *et al.* (1987), although practical details have been updated over the years as new types of instrumentation have become available. This method of calibration employs a standard (or reference) target, one whose acoustic scattering properties are known. The target is normally a homogeneous solid sphere which is suspended below the transducer. The echosounder is operated in the normal manner with the same pulse length, TVG and power level as would be used during the survey. The echo produced by the target is measured, and also the time delay between the echo and the transmitted pulse. These measurements are sufficient to estimate both the range of the target and the combined transmit–receive sensitivity of the transducer in the direction of the target. By moving the target across the beam, the position at which the echo is strongest for a given range can be found. The target is then on the acoustic axis, and  $C_a$  is determined from the corresponding echo measurements. For split-beam or dual-beam systems, the direction of the target relative to the transducer axis is known from the measurements, thus greatly simplifying the alignment of the target within the beam. The standard-target technique is both accurate and simple to apply in practice. A particular advantage is that the echosounder transmits and receives signals exactly as it would during the survey, so the one calibration takes account

**Table 3.1** (a) Physical properties of two spheres used to calibrate 38 kHz echosounders, and (b) their target strengths. Calculated values assuming continuous wave (zero bandwidth) transmission;  $c$ , speed of sound in water;  $c_1$  and  $c_2$ , longitudinal and transverse sound speeds in the spheres;  $\rho_1$ , sphere density. Water density 1000–1030 kg m<sup>-3</sup>.

(a)	Sphere material	Diameter (mm)	$\rho_1$ (kg m <sup>-3</sup> )	$c_1$ (m s <sup>-1</sup> )	$c_2$ (m s <sup>-1</sup> )
	Copper	60.0	8945	4760	2288
	Tungsten carbide	38.1	14 900	6853	4171

(b)	$c$ (m s <sup>-1</sup> )	TS (dB) in spheres made from	
		Copper	Tungsten carbide
	1430	−34.0	−41.8
	1450	−33.8	−42.1
	1470	−33.6	−42.3
	1490	−33.6	−42.4
	1510	−33.6	−42.4
	1530	−33.6	−42.4
	1550	−33.8	−42.2

of the transducer sensitivity, the electrical gain and the frequency response of the band-pass filters in the receiver.

Two limitations of the standard-target technique should be mentioned. Firstly, since the transmitter and receiver are measured simultaneously, it is less easy to identify the cause of peculiar results, for example if the sensitivities determined from two successive calibrations were greatly different. In that event, however, a few additional electrical measurements of the transmitter power and the receiver gain should quickly reveal the cause of the problem. Secondly, some modern echosounders have several fixed-gain receiver channels operating in parallel, each designed to match a particular signal amplitude. In practice, the particular target being used will match only one receiver channel, and the others are not included in the calibration. However, it is a simple matter to measure the electrical gain of each channel should that be required. Foote (1982a) and Foote and MacLennan (1984) have examined various materials which might be used for standard targets. They concluded that tungsten carbide or copper spheres give the best results in practice. The acoustic properties of these targets have been discussed in Section 2.5, in particular the factors that determine the optimum size of target for calibrating a particular echosounder. The target strength depends on the sound speed in the water as well as the echosounder frequency, so the environmental conditions must be known to determine the target strength correctly. Table 3.1 gives details of particular copper and tungsten carbide spheres which are commonly used to calibrate 38 kHz echosounders. Of the two materials, tungsten carbide is the more versatile because it is harder and resonates at higher frequencies. A few examples of suitably-sized spheres covering frequencies up to 0.5 MHz are specified in Table 3.2.

**Table 3.2** Target strengths of tungsten carbide spheres for sound speeds of  $1450\text{ m s}^{-1}$  (fresh water) and  $1490\text{ m s}^{-1}$  (sea water). Calculated values for an ideal receiver (constant gain inside the passband, zero outside); sound speeds in the sphere are (longitudinal)  $c_1 = 6853\text{ m s}^{-1}$  and (transverse)  $c_2 = 4171\text{ m s}^{-1}$ ; sphere density  $\rho_1 = 14900\text{ kg m}^{-3}$ .

Frequency (kHz)	Diameter (mm)	Bandwidth (kHz)	TS in fresh water (dB)	TS in sea water (dB)
18	38.1	1	-43.0	-42.7
30	38.1	3	-39.8	-39.8
38	38.1	3	-42.0	-42.3
50	36.4	5	-40.9	-40.4
50	38.1	5	-41.4	-40.9
70	33.2	7	-41.3	-41.0
70	38.1	7	-40.6	-41.1
120	33.2	12	-41.0	-40.9
120	38.1	12	-40.1	-40.0
200	36.4	20	-39.8	-39.7
200	38.1	20	-40.0	-39.9
250	23.0	25	-43.7	-43.7
420	21.2	40	-44.3	-44.1
455	24.8	50	-42.9	-42.8

Below 100 kHz, with a sphere that has no resonance close to the echosounder frequency, the calibration should be accurate to better than 2.5% in the value of  $C_a$ . These targets are best suited to calibrations at low frequencies. At very high frequencies, the target strength is less certain because of the close spacing of the resonances.

### 3.8.2 Experimental procedure

The standard target is suspended below the transducer, supported by the minimum amount of additional material to avoid unwanted reflections. This is normally done by encasing the target in a web of monofilament nylon (Fig. 3.29). The influence of the support system is more important at higher frequencies. At low frequencies the effect of any trapped air is reduced if the frequency is low enough, and in any case spheres for low frequencies are usually physically larger with higher target strengths. Three suspension lines are attached to the web, and by adjustment of the lengths of the lines, the sphere can be moved to any point in the transducer beam. Before it is put into the water, the sphere should be soaked in a soap solution – a mixture of one part household detergent to four parts fresh water is adequate – to wet the surface thoroughly so that air bubbles on the web are eliminated.

In the case of a hull-mounted transducer, the sphere is suspended by two lines on one side of the ship and a third line on the other side (Fig. 3.29). Booms are fitted to the ship's rails to lead the lines clear of the hull. A small winch or angling reel on each boom is used to adjust the lengths of the support lines, to move the sphere to any required position.

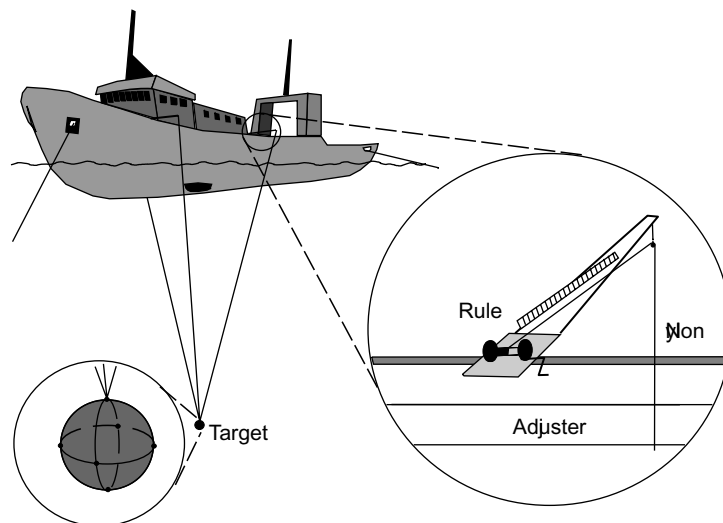


**Fig. 3.29** Apparatus for calibrating a transducer mounted on the hull or in a drop keel. The standard target is suspended below the ship by three lines. The line lengths are adjusted and measured against marks on the rule to locate the target relative to the transducer.

When the transducer is in a towed body, the sphere can be suspended from three horizontal arms in a frame attached to the top of the body (Fig. 3.30). The entire apparatus (transducer, body, sphere and frame) is lowered into the water, hung from a wire attached to the top of the vertical arm. This is lowered until the transducer is at its normal depth. The three support lines from the sphere can be led up the vertical arm so that they are accessible for adjustment at the surface. Alternatively, the line lengths may be adjusted by remote control of motors on the frame.

Whether the transducer is in a towed body or on the ship's hull, the conduct of the calibration is much simpler if remotely-controlled motors are used to adjust the lengths of the target suspension lines. The support lines must run from the adjusting mechanism to the sphere with the minimum of friction to allow free movement of the lines. Yacht fairleads may be used as a cheap and durable method of leading the support lines with little friction at any point where they have to change direction.

If the calibration is being performed from a vessel anchored in a current or swinging in the wind, the hydrodynamic force on the sphere may cause it to move unpredictably. This is less likely to occur when the support lines are short. On the other hand, the sphere must be far enough from the transducer to be outside the near field. Thus the optimum position of the sphere is just outside the near field, at a distance from the transducer which may be estimated from the formula:

$$R_{\text{opt}} = 2d^2 f_0 / c \quad (3.8)$$

where  $d$  is the greatest width of the transducer face,  $f_0$  is the echosounder frequency and  $c$  is the sound speed in water. For example, suppose that the transducer to be

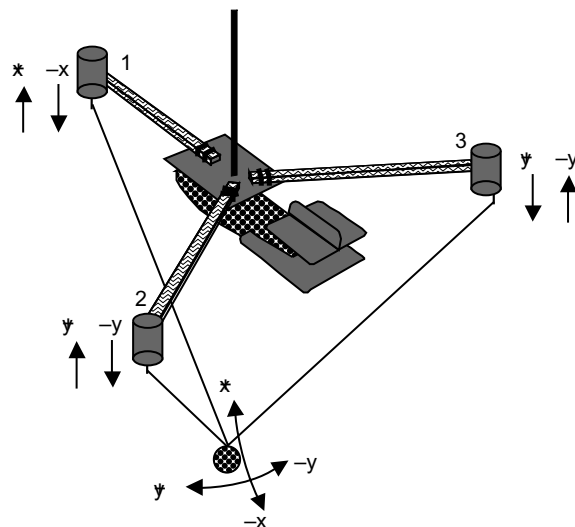


**Fig. 3.30** Adjusting the target position on mutually perpendicular axes (x and y). In this case the transducer is in a towed body and the lines are adjusted by remotely-controlled motors on the three arms of the attached frame. Motor 1 controls x while motors 2 and 3 work together but in opposite directions to control y.

calibrated has a rectangular face of size  $45 \times 30$  cm. Thus the larger dimension is 0.45 m. If the frequency is 38 kHz and the sound speed is  $1500 \text{ m s}^{-1}$ ,  $R_{\text{opt}}$  is  $2 \times (0.45)^2 \times 38000 / 1500$ , or 10.26 m. In performing this calculation, remember that all the parameters must be expressed in the same units (metres and seconds in this case). If the range of the sphere is  $R_{\text{opt}}$  or more, the bias in the on-axis sensitivity measurement resulting from the near-field effect will be less than 1% and can be ignored.

The echo strength is measured as the energy (integral of the squared amplitude), and is recorded by the echo-integrator which is normally included in the calibration. The sphere is moved across the beam to find the position where the echo is strongest for the same range, at which point the sphere is on the acoustic axis. This might be done by adjusting the length of each line in turn until the strongest echo for that movement is observed. With each adjustment the sphere will move progressively closer to the acoustic axis, but this procedure is rather slow. A faster method is to adjust one line first, and then the other two by equal amounts in opposite directions (Fig. 3.30). This procedure moves the sphere successively in two directions at right angles to each other. The one-line and two-line adjustments are repeated until the maximum echo energy during each adjustment achieves a steady value. Three or four adjustment cycles are usually sufficient to locate the sphere on the acoustic axis. For a hull-mounted system, it is a good idea to mark the line lengths on completion of the calibration, so that the sphere can quickly be deployed near the same position on subsequent occasions.

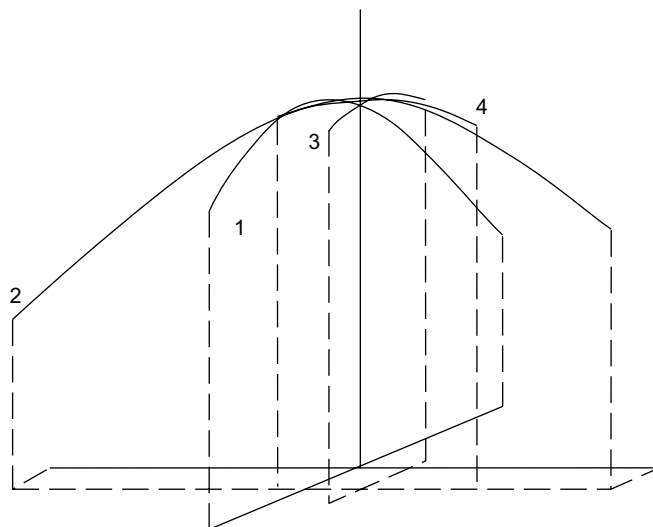


**Fig. 3.31** Estimation of the on-axis sensitivity of a single-beam transducer. Each curve is a quadratic fitted to the measurements made in one plane. Successive curves (1–4) are in planes at right angles to one another. The maxima of the curves converge to the on-axis sensitivity.

It is normal practice but not essential to move the sphere precisely onto the acoustic axis. An alternative procedure is to measure the echo energy with the sphere at a series of points in a section extending from one side of the beam to the other. The echo increases in amplitude from the first point onwards, then it decreases after the sphere passes the centre of the beam. At each point, the echo energy is measured as the average from several transmissions, perhaps 10 or 20. The length of the moving support line is recorded as a determinant of the sphere position in the section, and the maximum echo energy is estimated by fitting a quadratic curve to the measurements at the several points (Fig. 3.31). As before, the sphere is moved successively across two perpendicular sections of the beam until the overall maximum of the echo energy is determined. For the best results, the quadratic curve is fitted to the fourth root of the energy measurements, which matches the fitted curve to the theoretical beam shape, and the sphere is moved over a small portion of the centre of the beam, between points at which the echo energy is within 30% of the maximum.

Since the sphere is a single target, the echo amplitude depends on the range  $R_t$  which therefore has to be measured independently.  $R_t$  is estimated by measuring the time delay between the transmitter pulse and the echo. This method is easier and more accurate than attempting to measure the distance physically in the water. The arrival time of the echo depends on the target range and the sound speed in the water, but a small additional delay is introduced by the receiver electronics and this must be included in the calculation. Some echosounders provide a range indication which is already compensated for the receiver delay, but others do not. The user should ensure that the distance recorded in the calibration is the true range of the sphere.

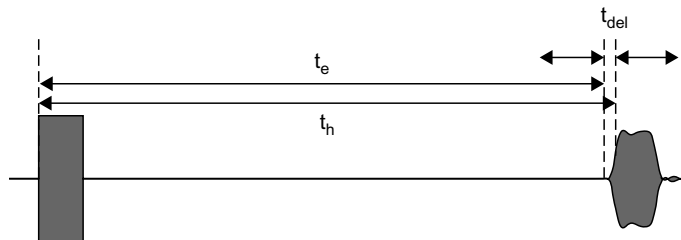


**Fig. 3.32** Estimation of the target range. The echo delay  $t_h$  is measured at the half-amplitude point on the envelope.  $t_{del}$  is the electronic delay in the receiver. The range is  $R = ct_e/2$  where  $t_e = t_h - t_{del}$  (cf. Table 3.3).

**Table 3.3** Values of the delay parameter  $t_{del}$  for standard targets used with a 1.0 ms pulse at 38 kHz, a receiver bandwidth of 3.0 kHz and 20 log R time-varied-gain function.

Target material	Sphere diameter (mm)	Receiver delay $t_{del}$ (ms)
Copper	60.0	0.47
Tungsten carbide	38.1	0.45

Another problem is that the echo may have a rounded shape when it is viewed, and it is not immediately obvious which point on the waveform should be timed. The recommended procedure is to measure the time between the start of the transmit pulse and the point on the leading edge of the echo at which the amplitude has risen to half the peak value (Fig. 3.32). If this time is  $t_h$ , and  $t_{del}$  is an additional delay correction, the target range is:

$$R_t = c(t_h - t_{del}) / 2 \quad (3.9)$$

The delay  $t_{del}$  may be determined from the theory of echo formation and knowledge of the receiver electronics. Some examples are given in Foote *et al.* (1987). The calculations are not simple, but in some cases the value may be known from published data (Table 3.3).

The echo delay  $t_h$  must be measured against an accurate time reference; however, most modern echosounders provide good enough timing for this purpose. If the time delays are automatically converted to display  $R_t$ , it is important to ensure this is based on the correct sound speed at the site of the calibration. If a different sound speed is applicable to the subsequent survey, the echosounder settings must be adjusted accordingly.

Suppose  $E_t$  is the measured echo energy when the sphere is on the acoustic axis. It is also necessary to know  $TS_t$ , the target strength of the sphere in decibels (Table 3.1). The sensitivity factor  $C_a$  can now be estimated as:

$$C_a = E_t R_t^2 / [10^{(TS_t/10)}] \quad (3.10)$$

If a different echo-integrator is to be used during the survey, or the echosounder is set to a receiver gain or transmitter power level different from those employed during the calibration, then additional electrical measurements would be necessary to derive the correct value of  $C_a$ . It is much preferable to perform the calibration with the same equipment and control settings as will be used during the survey, repeating the calibration for different settings if required.

If the echosounder is to be used for counting single-fish echoes, the appropriate time-varied gain function is  $40 \log R$ , which removes the range dependence of the standard-target echo.  $E_t$  is now the echo-integral or the square of the peak echo amplitude, depending on how the echo-counter works, and the formula for  $C_a$  reduces to:

$$C_a = E_t / [10^{(TS_t / 10)}] \quad (3.11)$$

### 3.8.3 *The TVG function*

The purpose of the time-varied-gain (TVG) function is to compensate the range dependence of the echo. Here we consider the echo integration of distributed targets, when the appropriate TVG function is nominally  $20 \log R$ . However, the same principles may be applied to the calibration of the  $40 \log R$  function which is required for echo-counting. As most scientific echosounders now implement the TVG by digital signal processing, the TVG error should be negligible, provided that the function has been programmed correctly. Sadly this has not always been the case, because some instrument designers have ignored the effect of the transmitted pulse length and the receiver bandwidth. The programmed function will then provide adequate range compensation at large distances from the transducer, but can introduce substantial errors at the short ranges needed for the calibration.

Suppose the voltage gain of the receiver is proportional to  $A(t)$  where  $t$  is the time after the start of the transmitter pulse.  $A(t)$  is the actual TVG function of the echosounder, but in general it will not compensate the range dependence exactly and the purpose of the calibration is to estimate the resulting error. To do this, measurements of  $A(t)$  are compared with the ideal TVG function,  $a(t)$ , which does compensate the range dependence exactly. MacLennan (1987) has shown that the following function, although not completely exact, is a good enough representation of  $20 \log R$  TVG for all practical purposes:

$$a(t) = c(t - t_0) \exp(\beta ct / 2) \quad (3.12)$$

Here  $c$  is the speed of sound,  $\beta$  is the acoustic absorption coefficient and  $t_0$  is the optimum start time of the TVG.  $t_0$  depends on the pulse duration and the bandwidth of the receiver; it is always more than half the pulse duration. In the past, manufacturers generally ignored (or were unaware of) the need for the start time of the TVG (at  $t = t_0$ ) to be delayed for an interval after the beginning of the transmitter pulse. However, this deficiency is overcome provided that  $A(t)$  is compared with the correct

**Table 3.4** The optimum start time of the ideal TVG function (nominally  $20 \log R$ ) for range compensation of distributed targets according to the transmitted pulse duration and the receiver bandwidth.

Bandwidth (kHz)	Pulse duration (ms)	TVG start time $t_0$ (ms)
1	1	1.21
1	3	2.18
3	1	0.95
3	3	1.94

ideal function, that given by the above equation. Values of  $t_0$  for a particular echosounder are given in Table 3.4. For the same pulse duration and bandwidth, other echosounders may have slightly different values of  $t_0$  but the differences are unlikely to be important. The calculation of  $t_0$  is rather complicated (details, MacLennan 1987). If users are in any doubt about the correct form of the TVG function, they should contact the manufacturer and confirm how the implemented function changes with the pulse and bandwidth settings.

### 3.8.4 *The equivalent beam angle*

The third part of the calibration procedure is the measurement of  $\psi$ , the equivalent beam angle of the transducer, which is a measure of the beam width.  $\psi$  has been formally defined in Section 2.3.1, see Equ. (2.11).

Simmonds (1984a; 1984b) described how  $\psi$  can be determined experimentally. He showed that in most cases, less than 1% of the transmitted energy appears in the side lobes of the transducer beam. To determine  $\psi$  therefore, it is normally sufficient to measure the beam pattern in detail only within the main lobe, adding a small correction which is calculated from theory to take account of the energy in the side lobes. However, a few measurements should be made in directions beyond the main lobe to check that the side lobes are as expected. Gross changes in the beam pattern might occur, for example, if the transducer had been damaged.

It is possible to calculate  $\psi$  from theory and the known geometry of the transducer face. Early measurements by Simmonds (1984b) revealed that the theoretical predictions could be wrong by more than 20%, and the  $\psi$  of different transducers that were supposed to be identical showed variations of the same order. Later investigations using the same methodology have been more encouraging. It seems that transducer manufacture is now a much more reliable and consistent process, and theoretically-derived values of  $\psi$  are now considered to be good enough. It is therefore sufficient to check that the manufacturer's measurement of the 3-dB-down beam angle does conform to transducer theory, and then the theoretical  $\psi$  value can be used directly in the echo-integrator equation (cf. Section 5.4).

Measurements of the same ceramic transducer by Simmonds (1990) repeated at intervals over several years revealed that  $\psi$  remains nearly constant, provided the

transducer does not suffer damage. However, if a sudden change in the on-axis sensitivity were to be observed between two successive calibrations, this might suggest a mechanical failure or deterioration of the transducer, in which case the beam pattern should be measured again. Ideally, the manufacturer should provide a certified empirical value for  $\psi$  to go with each transducer, avoiding the need for users to undertake this measurement which, at least for single-beam transducers, is a difficult and time-consuming procedure.

Since the split-beam technique provides acoustic measures of the target direction as well as TS, some manufacturers provide dedicated software that estimates  $\psi$  from the data recorded as a standard target is moved to various positions covering the beam. However, to be reliable, this procedure requires some independent (i.e. non-acoustic) measure of the target direction. The provision of such data is non-trivial for most installations.

### **3.8.5 Overall sensitivity and the sound speed**

The calibration is performed at a particular location where the local sound speed (assumed or measured) is  $c_0$ . If the echosounder settings are matched to  $c_0$ , then the instrument is correctly calibrated. The sound speeds encountered during the survey may be different, however, and some adjustment of the factors in Equ. (3.7) may be necessary to obtain the correct conversion factor in the subsequent analysis. To understand the effect of sound-speed changes on  $C_a$ , we begin with the following formula for  $P_r$ , the power received by an echo-integrator (without TVG) from distributed targets at range  $R$ :

$$P_r = P_o G_T R^{-2} 10^{-2\alpha R/10} \psi(c\tau/2) n \langle \sigma_{bs} \rangle G_E \quad (3.13)$$

Here  $P_o$  is the transmitted power,  $\alpha$  is the acoustic absorption coefficient ( $\text{dB m}^{-1}$ ),  $c$  is the true sound speed,  $\tau$  is the pulse duration and  $n$  is the number of fish per unit volume.  $G_T$  and  $G_E$  are, respectively, the on-axis transducer gains when transmitting and receiving.

If the sound speed increases, so does the wavelength, and the echo delay decreases. The apparent range  $R$  also decreases because it is calculated as  $c_0$  times half the echo delay ( $t_h$ ). Thus changes in the sound speed affect the various factors in Equ. (3.13) in different ways. For small beam widths,  $\psi$  varies as  $c^2$  because it is inversely proportional to the numbers of wavelengths across and along the transducer face.  $G_T$  and  $G_E$  vary as  $1/c^2$ . This is the ‘array gain’ effect which is related to the change in  $\psi$ ; since  $P_o$  is constant, the narrower the beam width the greater is the on-axis transducer gain. The pulse length in the water ( $c\tau/2$ ) obviously varies as  $c$ . In addition, the transducer efficiency may vary a little with  $c$ , and also with the temperature, and  $\langle \sigma_{bs} \rangle$  may vary with  $c$  in an uncertain way, but we do not consider these factors here (for  $\langle \sigma_{bs} \rangle$  cf. Chapters 6 and 7).

Suppose that during the calibration, the local sound speed  $c_0$  and the corresponding equivalent beam angle are incorporated in the echosounder and these settings are not

changed during the survey. Noting that the sound speed is often depth dependent, suppose that in the survey area it is  $c_s$  at the transducer,  $c_f$  at the depth of the fish and has a mean value  $c_z$  in the water column from the surface to the fish. The factors in Equ. (3.13) will change as follows:  $G_T$  and  $G_E$  as  $c_0^2/c_s^2$ ; spreading loss ( $r^2$ ) as  $c_0^2/c_z^2$ ; absorption loss as  $10^{5\alpha(c_z-c_0)t_h}$ ;  $\psi$  as  $c_s^2/c_0^2$  (though there will be some dependence on  $c_z$  and  $c_f$  due to refraction in the water which is ignored here); and the pulse length  $c\tau/2$  as  $c_f/c_0$ . This results in the overall calibration factor (F/E) changing by the proportion:

$$\begin{aligned}\Delta K &= (c_0^2 / c_s^2) \cdot (c_0^2 / c_s^2) \cdot (c_0^2 / c_z^2) \cdot \{10^{(\alpha/10) \cdot (c_z - c_0)t_h}\} \cdot (c_s^2 / c_0^2) \cdot (c_f / c_0) \\ &= (c_0^2 / c_s^2) \cdot (c_0^2 / c_z^2) \cdot \{10^{(\alpha/10) \cdot (c_z - c_0)t_h}\} \cdot (c_f / c_0)\end{aligned}\quad (3.14)$$

If the sound speed  $c_z$  is used within the sounder to correct for depth dependence, then  $c_0^2/c_z^2$  and  $10^{5\alpha(c_z-c_0)t_h}$  are both unity and  $\Delta K$  becomes  $\{c_0^2/c_s^2 c_f/c_0\} = c_0 c_f / c_s^2$ . In the simplest case, if  $c_s = c_f = c_z$ ,  $\Delta K$  is  $c_0/c_z$ . This indicates that, if the depth dependence is corrected, then for echo integration, the overall calibration factor is inversely proportional to the sound speed.

Different sound-speed dependences arise in the case of single targets (and the measurement of their target strength). The relevant equation for the received power from an isolated target is:

$$P_r = P_o G_t(\theta, \phi) R^{-4} 10^{2\alpha R/10} \langle \sigma_{bs} \rangle G_r(\theta, \phi) \quad (3.15)$$

where the transducer gains are now functions of the target direction  $(\theta, \phi)$ . In this case  $\psi$  is not relevant and the result of the analysis is:

$$\Delta K = (c_0^2 / c_s^2) \cdot (c_0^2 / c_s^2) \cdot (c_0^2 / c_z^2) \cdot \{10^{(\alpha/10) \cdot (c_z - c_0)t_h}\} \quad (3.16)$$

If the range is correctly accounted for by using  $c_z$ , then  $\Delta K = \{c_0^2/c_s^2 c_0^2/c_s^2\} = \{c_0^4/c_s^4\}$ . This indicates that for echo-counting, the overall calibration factor is inversely proportional to the fourth power of the sound speed.

In some modern echosounders, these sound-speed dependences are automatically incorporated in the on-axis sensitivity factor whenever a different mean sound speed is entered in the settings. Before manually correcting the acoustic measurements for changes in the sound speed, it is important to know whether that feature has been implemented in the signal processor. If the sounder is to be used where there are important differences in sound speed between the transducer and the fish aggregation, then the more complete correction factor required can be calculated from Equ. (3.14) for echo-integration or Equ. (3.16) for echo-counting.

### 3.8.6 Direction-sensing echosounders

The signals produced by the split-beam and dual-beam echosounders determine the direction of targets as well as the range and the echo amplitude. When the instrument is to be used for echo-counting or the measurement of target strength, the appropriate

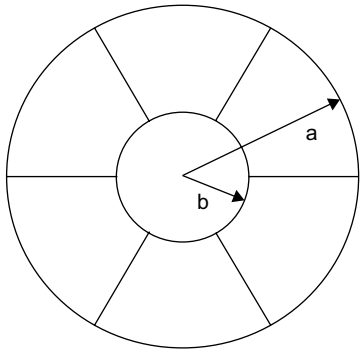


**Fig. 3.33** The cross-section of a transducer beam divided into seven equal sub-areas. The radius of the inner circle (b) is  $1/\sqrt{7}$  times that of the outer circle (a). (Redrawn from MacLennan and Svellingen 1989.)

TVG function is  $40 \log R$ . The TVG is calibrated by the method described above for the single-beam echosounder. The TVG calibration should be performed first, and the results used to correct the subsequent sensitivity measurements for any residual range dependence of the echoes. As before, the sensitivity in various directions may be measured by reference to the echo from a standard target which is placed at a number of representative positions over the active part of the beam. The on-axis direction is not especially important in this case. The usual requirement is to determine the average sensitivity weighted by the area of the beam cross-section, and the additional variation of the output signal caused by inexact compensation for the target direction. These issues have been discussed in detail by Degnbol and Lewy (1990).

The sensitivity calibration is simply a matter of recording the echo energy while the standard target is placed at a number of positions distributed across the beam. It is not necessary to measure the target position independently since the direction of the echo is determined by the instrument itself. Figure 3.33 illustrates the method proposed by MacLennan and Svellingen (1989). The cross-section of the beam is divided into seven regions of equal area, a circle in the centre and six segments on the periphery. The target is moved so that the number of measurements is about the same in each region, ensuring that all parts of the beam receive the same attention.

Suppose that  $n$  measurements are made and  $B_i$  is the observed sensitivity at the  $i^{\text{th}}$  position of the target. The mean sensitivity is estimated by weighting each measurement in proportion to the area it represents. To a first approximation, the weighting factor  $w_i$  is proportional to the angular distance of the  $i^{\text{th}}$  measurement position from the acoustic axis at the centre of the beam. The mean  $\bar{B}$  and variance  $V_B$  of the sensitivity are obtained from the formulas:

$$\bar{B} = \sum_{i=1}^n B_i w_i / \sum_{i=1}^n w_i \quad (3.17)$$

$$V_B = \sum_{i=1}^n (B_i - \bar{B})^2 w_i^2 / \left\{ (n - 1) \left( \sum_{i=1}^n w_i \right)^2 \right\} \quad (3.18)$$

There is a simpler but perhaps less precise method for charting the directional sensitivity of a split-beam echosounder. In this case the standard target is suspended on one line below the transducer so that it is free to swing around. Over time, assuming enough movement is induced by water currents etc., the sphere should be detected in various directions covering, more or less, the whole beam. Statistics of the sensitivity can then be estimated as described above, or a theoretical model can be fitted to the data to estimate the beam pattern. This is not a completely rigorous procedure, since some parts of the beam will be sampled more than others and the relative weightings are uncontrolled.

The direction-sensing echosounder is often used to determine the distribution of target strengths in the fish population which is to be surveyed. The results may be considered in terms of the target strength or the equivalent backscattering cross-section of the detected fish. Suppose that  $\bar{\sigma}_{bs}$  is the true mean and  $V_\sigma$  is the corresponding variance. To estimate these statistics, many observations are required of individual targets as a representative sample of the population. It is also assumed that the detected targets are randomly distributed over the active area of the beam. This implies that if  $\bar{E}$  is the mean of the observed echo energy, then  $(\bar{E} \bar{B})$  is an unbiased estimate of  $\bar{\sigma}_{bs}$ . However, any variation of the sensitivity across the beam will increase the spread of the observed distribution.  $V_B$  is a measure of the sensitivity variation, and this quantity as determined from the calibration may be used to correct  $V_s$ , the sample variance of the observed cross-sections. On the reasonable assumption that the variations of sensitivity and target strength are not correlated, an unbiased estimate of  $V_\sigma$  is given by:

$$V_\sigma / \bar{\sigma}_{bs}^2 = (V_s / \bar{\sigma}_{bs}^2 - V_B / \bar{B}^2) / (1 - V_B / \bar{B}^2) \quad (3.19)$$

So far we have considered only the mean and variance of the target strength distribution. Other statistics such as the skewness may also be distorted by the variation of sensitivity across the beam. It is possible to reconstruct the true target strength distribution from the histogram of observations, given a large number of measurements of target strengths and the sensitivity as a function of the target direction. This may be done by the deconvolution method described by Clay (1983). Although originally developed for the treatment of signals from the single-beam echosounder, deconvolution is equally applicable to direction-sensitive instruments. However, it is not necessary to consider the complexities of deconvolution if the compensation for the target direction is good enough, that is to say if  $V_s / \bar{\sigma}_{bs}^2$  is much larger than  $V_B / \bar{B}^2$ .

Figure 3.34 shows some measurements obtained during the calibration of a dual-beam echosounder. The same target has been moved to different positions across the beam. The TS factor,  $I_w^2 / I_n$  is proportional to  $\sigma_{bs}$ , the backscattering cross-section of the target, and is essentially constant if the beam factor  $I_n / I_w$  is large enough. A threshold is applied to the beam factor (cf. Section 3.3), to reject echoes in the anomalous region for which  $I_n / I_w$  is less than about 0.3.

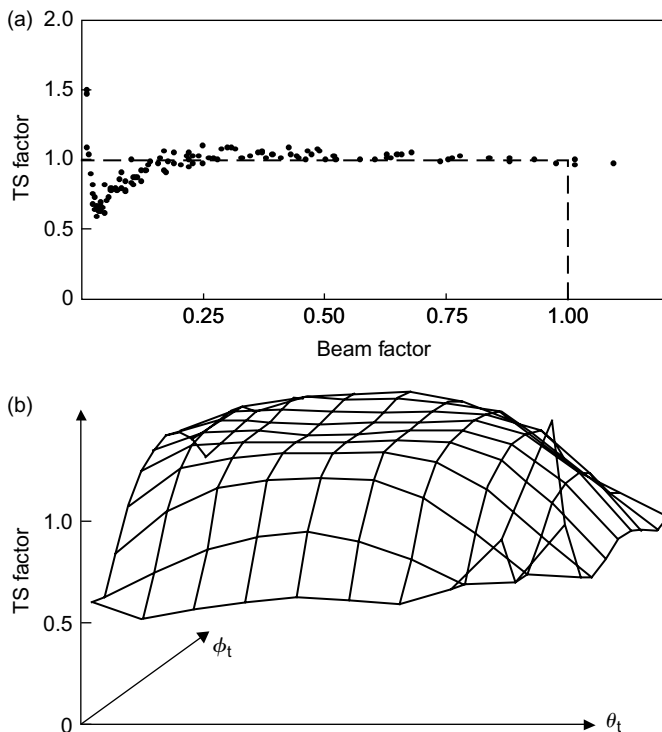


**Fig. 3.34** Calibration of a dual-beam echosounder. The TS factor  $I_w^2/I_n$  is proportional to the backscattering cross-section of the standard target. The beam factor is  $I_n/I_w$ . The vertical scales are arbitrary. (a) Measurements of the same target in various directions; (b) landscape plot of the TS factor versus direction.  $\theta_t$  and  $\phi_t$  are respectively the fore-aft and athwartship angles of the target direction relative to the acoustic axis.

The measured sensitivity of a split-beam transducer is illustrated in Fig. 3.35. The upper plot is a landscape showing the directional sensitivity after the echo amplitude has been compensated using the measured phases of the received signals. There is some residual variation of sensitivity with direction, but it is much less than that of the uncompensated beam pattern shown in Fig. 3.35b.

### 3.8.7 Calibration of multi-beam sonars

Multi-beam sonars are rapidly developing as tools for fish observation and measurement. Melvin *et al.* (2003) provide the formal equations applicable to one such device, the Simrad SM2000 sonar, while Simmonds *et al.* (2000) have developed a calibration procedure for another example, the RESON Seabat 6012 sonar. The latter has a fan of 60 beams with nominal  $1.5^\circ$  spacing. Each beam is  $1.9^\circ$  by  $15^\circ$  wide, thus forming a  $90^\circ$  sector. The calibration of this sonar involves a series of scans around the  $90^\circ$  sector to determine the beam pattern for each of the 60 beams, which

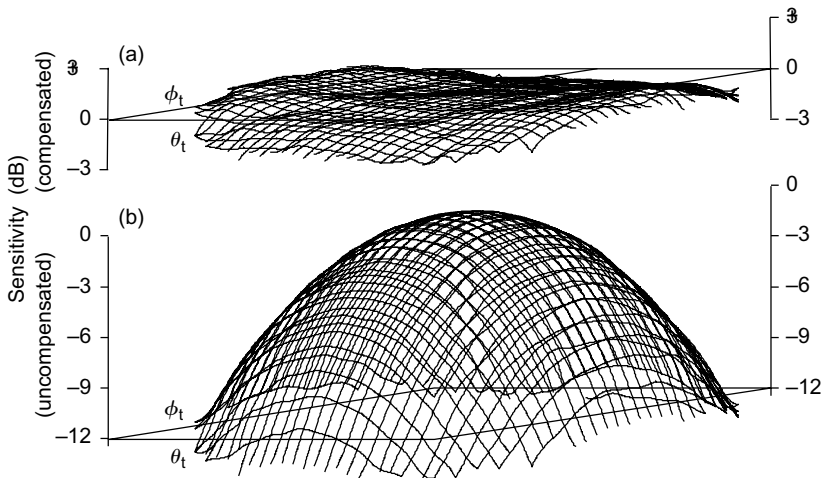


**Fig. 3.35** Calibration of a split-beam echosounder presented as landscape plots of the combined transmit-receive sensitivity. (a) Results with compensation for the beam pattern, normalized to the mean; (b) uncompensated sensitivities, normalized to the (on-axis) maximum.  $\phi_t$  and  $\theta_t$  are respectively the fore-aft and athwartship angles of the target direction relative to the acoustic axis.

are combined to obtain the overall transmit-receive sensitivity and  $\psi$ . Figure 3.36 shows the relative sensitivity of the 60 beams. The Reson sonar has about 3 dB of broad variation across the sector, with the local variability (over 3 or 4 beams) being rather less, around 1.5 dB.

One serious difficulty was encountered in calibrating the Reson sonar. It has a very short pulse ( $60\ \mu\text{s}$ ) to give fine range resolution, and this allows only two samples within each target echo (meaning 2 per beam = 120 in total). In consequence, the sample values depend on where they are measured on the received echo waveform. This has finite rise and fall times. If both samples are close to the peak, the largest value is obtained, but the integral is reduced if either sample is on the initial or final slopes. This affects the calibration because the sonar samples each of the 60 beams sequentially. The echo occurs at the same range on each beam, but the timing of the samples relative to the echo changes with beam number. The result is an artificial cyclic change of around 1 dB in the beam-to-beam measurements, which appears as a smooth ripple when the sensitivities are plotted against the beam number. Simmonds *et al.* (2000) estimated the ripple by matching the exact sample timings to points on the echo waveform, and so were able to compensate their results for this unwanted effect. This type of practical problem is an unfortunate feature of digital sampling techniques, and is most likely to occur during calibrations since the standard target is held at a fixed range. Care must always be taken to determine how a digital processor samples acoustic data, to ensure that such problems are avoided or adequately corrected.

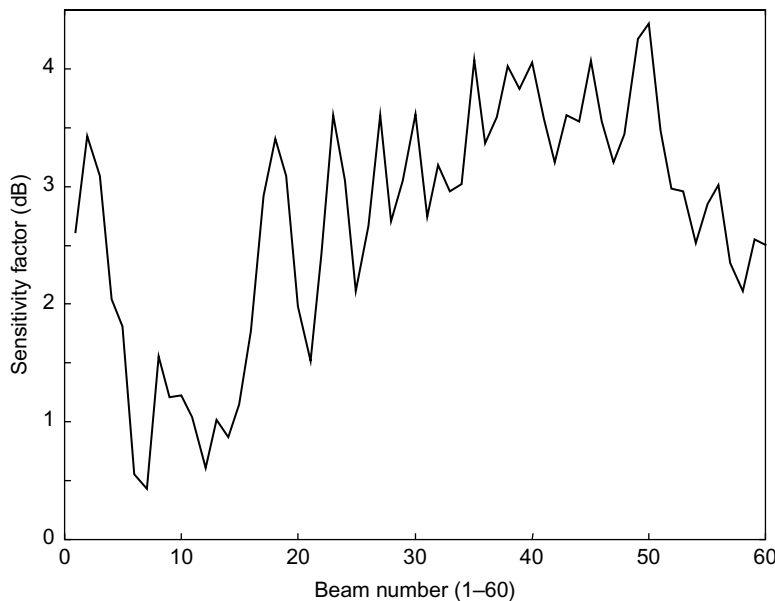


**Fig. 3.36** Sensitivity variation across the 60 beams of a 455 kHz Reson Seabat 6012 multi-beam sonar, measured using a 24.8 mm tungsten carbide calibration sphere. These sensitivities take account of the two-way on-axis response and the equivalent beam angle and are therefore the appropriate calibration factors when the sonar is used for echo integration.

### 3.8.8 *Good calibration practice*

To achieve satisfactory results, the calibration of acoustic instruments must be performed with careful attention to detail, using equipment that is capable of the required accuracy, and in accordance with the recommended procedures described here. It is all too easy to make mistakes, and they are costly because any error in the calibration will bias the estimate of fish abundance derived from the survey. Simmonds (1990) investigated the accuracy to be expected from a calibration. He concluded that good practice should determine the performance of the echo-integration system to within 7%. The aim should be to develop a routine or protocol for calibration which will achieve this accuracy consistently. Many problems arise in the interpretation of acoustic survey results, but there is no need for the calibration error to be one of them.

# Chapter 4

# Biological Acoustics

## 4.1 Introduction

Sound is important for the fish and other animals that live in water. On the most general level, propagating sound waves and their reflections by objects offer possibilities for remote sensing of the environment. Most aquatic animals have organs which are sensitive to acoustic waves, and they may in addition produce sounds as a deliberate act. Underwater sound has a key role in several kinds of animal behaviour. These include communication between individuals, mating behaviour, detection of prey, escape from predators and navigation.

This chapter is primarily concerned with the significance of sound to living things, including the physiology of sound production and reception, and behaviours which are motivated by hearing. We begin by describing the many different sounds of biological origin that are produced under water. Then we discuss the hearing mechanisms of fish, invertebrates and mammals. The acoustic sensitivity of different species is compared, and their ability to detect signals in background noise. This leads to a discussion of the critical bandwidth, namely the frequency range of noise that interferes with a signal through ‘masking’. Next, we consider the intriguing ability of some aquatic mammals to navigate and detect prey by echolocation. These animals have evolved a sophisticated form of active sonar. The frequency composition and directional properties of their sonar ‘clicks’ are discussed in relation to the information content of the returning echoes and the signal processing required to extract this information.

These natural phenomena must be understood to assess the environmental impact of human activities in the aquatic environment. Anthropogenic sounds range from low-amplitude noise pollution to the shock waves produced by explosive devices. We discuss the impacts in terms of behavioural changes and physiological damage to the exposed animals which may be temporary, permanent or lethal. Equations for predicting the strength of shock waves are presented, and theoretical models for predicting the mortality of exposed fish are reviewed.

Finally, we discuss the phenomenon of swimbladder resonance which is relevant to acoustic propagation and scattering at low frequencies, typically well below 10 kHz.

To some extent this anticipates the subject matter of the next two chapters, but it is included here because we shall later concentrate on the much higher frequencies used in fisheries work.

## 4.2 Biological sounds

Compared with light, sound has several advantages as a means of communication in water. It can propagate over hundreds of metres, it is easily generated and the frequency composition of the signal may convey useful information from the sender to the receiver. In contrast, light waves attenuate very rapidly with distance, especially when the water contains suspended solids as often occurs in fast-flowing rivers, lakes and estuaries. It is not surprising, therefore, to find that many aquatic animals have evolved sensitive hearing organs, and that many of the background sounds heard under water are biological in origin (Tavolga *et al.* 1981; Hawkins and Myrberg Jr 1983; Fay 1988).

Aquatic lifeforms produce a great variety of sounds. These can be heard by listening to the output from a hydrophone placed judiciously in the water, provided the noise from non-biotic sources such as boat engines is not too great. There are three groups of animals that produce sounds with distinctive characteristics. These are (a) some crustaceans, especially shrimp, (b) teleost fish with swimbladders and (c) the aquatic mammals, notably the whales and dolphins.

When the hydrophone is placed close to the bottom, the snaps, clicks and rustles produced by benthic crustaceans may be heard (Fish 1964; Cato 1993). These sounds may be caused simply by the movement of the creatures over the ground, or more deliberately by the rubbing or impact of hard parts of the body against each other, a mechanism called stridulation. When many individuals do this within a localized colony, the sounds merge into a continuous noise which has been described variously as crackling, sizzling and frying.

The snapping shrimp (Crangonidae e.g. *Synalpheus parneomeris*) are widespread inhabitants in seas which are warm enough ( $>11^{\circ}\text{C}$ ) and less than 55 m deep (Everest *et al.* 1948). They are perhaps the best known of the invertebrate sound producers. Each shrimp has one enlarged claw which is snapped shut to produce a loud ‘click’. The spectrum of this sound is very broad. It peaks typically between 2 and 5 kHz, but the energy level is within 20 dB of the maximum up to 200 kHz or more (Readhead 1997; Au and Banks 1998). The sound is intense, with a source level around 180–190 dB re 1  $\mu\text{Pa}$  at 1 m. This is the same order as the source levels produced by singing whales, a remarkable comparison considering the huge size difference between these creatures. The high intensity combined with the short duration of the clicks offers the possibility of locating the shrimp concentrations by passive ranging techniques (cf. Chapter 3), and thus to determine their source levels. Ferguson and Cleary (2001) describe how this can be done by correlating the signals received on a wide-aperture hydrophone array.

Teleost fish are able to produce sounds by vibrations of the swimbladder induced by muscular force. The aptly-named croaker, *Micropogon undulatus*, is well known in this respect (Fish 1964). It produces a tapping sound like that of the woodpecker, containing frequencies mainly in the range 350–1500 Hz. Groups of fish may sound in concert, giving rise to the ‘croaker chorus’ which occurs in the evening, a diurnal behaviour similar to the evensong of birds. The catfish, *Galeichthys felis*, also produce evening choruses, in this case at somewhat lower frequencies resulting in a sound like the bubbling of a percolator (Tavolga 1962). On a more local scale, sounds variously described as knocks, grunts and growls are associated with fish spawning (Hawkins and Amorim 2000) or competitive feeding (Amorim *et al.* 2004). Some fish generate sounds by mechanisms not involving the swimbladder. They may produce squeaks and rasps by rubbing hard parts of the body together (stridulation), crunching due to feeding, and low-frequency noise by the hydrodynamic turbulence associated with swimming. The latter effect is particularly evident near schools of fast swimmers such as tuna (Fine *et al.* 1977).

The aquatic mammals produce many different kinds of sound. At the one extreme, there are the high-frequency clicks which whales and dolphins use for echolocation, a topic to which we shall return later. At the other end of the spectrum, there are the powerful sounds of the great whales, narrow-band signals at 20 Hz which can be detected at distances of several hundred kilometres (Schevill *et al.* 1964; Walker 1963; Watkins *et al.* 1987). Other sounds of the mammals among an extensive repertoire have been described as moans, knocks, pulses, screams and grunts (Clark 1990; Stafford *et al.* 1999). The ‘song’ of the humpback whale, *Megaptera novaeangliae*, is worthy of special note in this context. It is perhaps the most fascinating acoustical phenomenon in nature. These vocalizations are loud, up to 190 dB re 1  $\mu$ Pa at 1 m (Thompson *et al.* 1986), and can be detected as far as 160 km from the source (Clark 1994). Each song is characterized by a series of themes and phrases within a unique sequence which is the signature of an individual whale (Smith 1991; Frankel 1995; Tyack 1999). The song may last for more than 30 minutes, and is repeated exactly (Payne and McVay 1971; Helweg *et al.* 1992). Bowhead, fin and blue whales are also known for their singing behaviour (Watkins *et al.* 1987; Thompson *et al.* 1992; 1996).

### 4.3 Hearing

Fish and mammals have various organs which might sense an acoustic stimulus. The swimbladder is especially important in this context for those fish which possess one. Movements of the bladder wall in response to sound waves are transmitted to the earbones (otoliths) whose function has been described by Fay and Popper (1980). There are also the hair cells of the lateral line and the labyrinthine structures which respond to movements in the surrounding fluid relative to the fish body (Hawkins and Myrberg Jr 1983; Hawkins 1993). In the aquatic mammals, the ear is

constructed on similar principles to that of their terrestrial relatives, with sound being transmitted to the cochlea via the tympanic membrane and the auditory ossicular mechanism.

### **4.3.1 Auditory detection capability**

The sensitivity of fish and other animals to sound has been the subject of many investigations, cf. reviews by Fay (1988) and Nachtigall (2000). Classical conditioning techniques have generally been employed, in which the animal is first trained to respond to a sudden burst of sound whose intensity is high enough to be easily detected. The intensity is then reduced in successive trials until the response fails. The auditory threshold is the sound level at which the animal responds in 50% of the trials. The response may be induced by presenting a food reward which the animal associates with the stimulus. This method has been particularly successful with mammals (Johnson 1967; Terhune and Ronald 1975; Gerstein *et al.* 1999). In the case of fish, more reliable results have been obtained by the cardiac conditioning technique, first proposed by Otis *et al.* (1957) and subsequently applied in experiments with many species, see for example (Chapman and Sand 1974; Hawkins and Johnstone 1978; Jerkø *et al.* 1989). In this technique, a mild electric shock is applied shortly after the sound burst. This quickly establishes a conditioned change in the cardiac rhythm which is detected by means of electrodes attached to the body of the fish. When the sound is heard, the heart misses a beat immediately; when it is not heard, the heart rate remains the same until the shock arrives.

More recently, there has been increasing interest in alternative methods which are less stressful to the subject animal, particularly one known as the auditory brain-stem response (ABR) approach (Enger and Anderson 1967; Sand 1974; Kenyon *et al.* 1998). This involves subcutaneous electrodes which detect the signals (a.c. currents) from neural activity in response to the sound stimulus. Kenyon *et al.* (1998) showed that, compared to the classical methods, the ABR approach gave similar results in fish-hearing experiments. However, it is unsuitable for work at frequencies below 100 Hz.

By observing the responses of the same fish to tone bursts at different frequencies, we can construct the audiogram which is a graph of the auditory threshold against frequency. The threshold is the minimum audible sound, usually expressed in terms of the pressure amplitude. Some examples are shown in Fig. 4.1. In most cases the threshold changes slowly at the lower frequencies, but there is a sharp deterioration of hearing performance at the high-frequency end of the audiogram. The maximum sensitivity (or the minimum auditory threshold) and the corresponding frequency are of particular interest in comparing audiograms. The results of hearing experiments are summarized in Table 4.1, from which it will be seen that there is a wide spread of the sensitivity and the frequency range of hearing among species. Note that the numerical results are expressed in terms of the root-mean-square (rms) of the pressure amplitude. The rms is the normal measure in hearing studies, as opposed

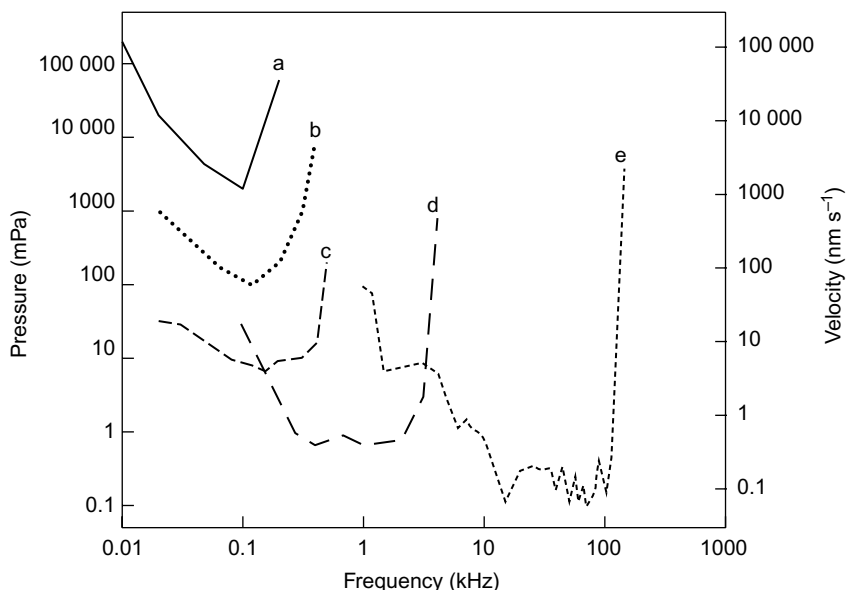


**Fig. 4.1** Audiograms of hearing sensitivity for five species: (a) lobster, *Homarus americanus*; (b) Atlantic salmon, *Salmo salar*; (c) soldier fish, *Myripristis kuntee*; (e) bottlenose dolphin, *Tursiops truncatus* (references, Table 4.1). Vertical axes are (left) sound pressure amplitude at the auditory threshold; (right) corresponding particle velocity for plane-wave free-field transmission.

to peak or peak-to-peak pressure amplitudes, although the distinction is not always made clear in the literature (cf. Section 2.2.2).

Figure 4.1 shows that the aquatic mammals have particularly good hearing. The invertebrates are very insensitive by comparison (Offutt 1970), while most fish have intermediate capabilities. Some fish such as the carp, *Cyprinus carpio*, are said to be ‘hearing specialists’ because they are especially sensitive to sounds over a wide frequency range (Popper 1972). The specialists have an intimate connection between the otoliths and the swimbladder which acts as an efficient aid to hearing. Species in which the connection is made by soft tissue have relatively poor hearing, although the swimbladder still has an auditory role by amplifying the particle velocity of the sound waves near the otoliths. The Atlantic cod, *Gadus morhua*, is one example of fish which are ‘non-specialist’ as regards their hearing ability (Chapman and Hawkins 1973).

An important question is whether the hearing organs of fish respond primarily to the pressure or to the particle velocity of sound waves (Hawkins and MacLennan 1976). The distinction between these variables does not matter when the animal is remote from the sound source or any boundary, since the ratio of the particle velocity and pressure amplitudes is constant in free-field conditions. When the distance to the source is comparable to the acoustic wavelength, however, the velocity amplitude is relatively large due to the near-field effect (cf. Section 2.4.1). The velocity–pressure ratio is also affected by nearby boundaries such as the water surface, where the

**Table 4.1** Auditory thresholds and the frequency range of hearing, typical values by species. Thresholds are given as the sound pressure amplitude and the corresponding particle velocity for free-field propagation.  $f_0$  is the frequency of maximum sensitivity;  $f_{\max}$  is an upper hearing limit defined by the threshold being 20 dB above the minimum.

Species	Minimum threshold (mPa)	Minimum threshold (nm s <sup>-1</sup> )	$f_0$ (kHz)	$f_{\max}$ (kHz)	Reference
<b>Invertebrate</b>					
Lobster ( <i>Homarus americanus</i> )	1260	820	0.07	0.16	Offutt (1970)
<b>Non-specialist fish</b>					
Oscar (Cichlidae) <sup>(1)</sup> ( <i>Astronotus ocellatus</i> )	<106	<69	<0.1	<1.1	Kenyon <i>et al.</i> (1998)
Atlantic salmon ( <i>Salmo salar</i> )	100	65.0	0.16	0.31	Hawkins and Johnstone (1978)
American shad ( <i>Alosa sapidissima</i> )	100	65.0	0.6	1.8	Mann <i>et al.</i> (1998)
Dab ( <i>Limanda limanda</i> )	35.0	23.0	0.1	0.2	Chapman and Sand (1974)
Herring ( <i>Clupea harengus</i> )	5.6	3.7	0.2	2.9	Enger (1967)
Cod ( <i>Gadus morhua</i> )	5.1	3.3	0.16	0.45	Chapman and Hawkins (1973)
<b>Specialist fish</b>					
Goldfish ( <i>Carassius auratus</i> )	1.6	1.0	0.6	1.7	Kenyon <i>et al.</i> (1998)
Carp ( <i>Cyprinus carpio</i> )	0.79	0.52	0.46	1.5	Popper (1972)
Soldier fish ( <i>Myripristis kuntee</i> )	0.32	0.2	1.3	3.1	Coombs and Popper (1979)
<b>Mammals</b>					
Ringed seal ( <i>Pusa hispida</i> )	2.6	1.7	40.0	55.0	Terhune and Ronald (1975)
Hawaiian monk seal ( <i>Monaculus schauinslandi</i> )	1.8	1.2	16.2	30.0	Thomas <i>et al.</i> (1990)
West Indian manatee ( <i>Trichechus manatus</i> )	0.38	0.25	18.0	30.0	Gerstein <i>et al.</i> (1999)
River dolphin ( <i>Inia geoffrensis</i> )	0.32	0.21	30.0	100	Jacobs and Hall (1972)
Bottlenose dolphin ( <i>Tursiops truncatus</i> )	0.1	0.06	50.0	115.0	Johnson (1967)
Killer whale ( <i>Orcinus orca</i> )	0.02	0.013	15.0	31.0	Hall and Johnson (1972)

<sup>(1)</sup> Results at 0.1 kHz which was above  $f_0$ . The method used (ABR) was impractical at lower frequencies.

acoustic impedance is mismatched and the correct ratio is difficult to predict; this problem should be borne in mind when considering studies of sound or hearing in small aquaria or tanks. On the other hand, the near-field effect (which is predictable) provides a neat method for demonstrating the relative importance of pressure and

particle velocity in hearing (Hawkins 1993). This is done by conducting auditory threshold experiments with the sound source at different distances from the fish. The controlling parameter is the one which shows the most consistent thresholds at any distance.

Both the hair cells of the lateral line and the otoliths are sensitive primarily to the particle velocity. However, the gas-filled swimbladder generates a scattered wave in response to the incident pressure. The velocity amplitude of the scattered wave at the otolith may exceed that of the incident sound, at least at frequencies below some limit (de Munck and Schellart 1987). Thus the swimbladder functions as a pressure–velocity converter. This explains why some fish whose hearing depends on the otoliths are nevertheless sensitive to the sound pressure, notably the hearing specialists but also the cod. Other non-specialists have been shown to be more sensitive to the particle velocity, which is to be expected in fish that depend on the unaided otolith for hearing (Chapman and Sand 1974; Hawkins and Johnstone 1978). Finneran *et al.* (2002) have reported similar investigations of marine mammals. It seems that for both fish and mammals, the frequency of the sound stimulus is the key to the velocity–pressure question. The particle velocity is the controlling factor below some frequency  $f_{vp}$ , otherwise it is the sound pressure. In practice, the dominant factor will depend on whether the hearing is most sensitive above or below  $f_{vp}$ .

Some fish are able to sense the direction of sound waves (Schuijf and Buwalda 1980). Myrberg *et al.* (1972) found that the predatory sharks are particularly good at locating sound sources. Conditioning experiments have shown similar if less acute ability in teleost species such as the cod (Chapman and Johnstone 1974; Hawkins and Sand 1977). Sorokin *et al.* (1988) observed the effect of airgun pulses on schools of the sardine, *Sardinops sagax melanosticta*. The airgun releases a volume of compressed air which creates a shock wave, similar to an underwater explosion (cf. Section 4.5.1). The fish reacted by swimming away from the airgun at ranges up to 150 m. Not surprisingly, it appears that the directional sensitivity is strongest for sounds well above the auditory threshold and at frequencies near the middle of the hearing range.

There are two mechanisms that might provide fish with an awareness of direction. Firstly, the otolith vibrates in the direction of propagation of the resultant sound field. This is the combination of the incident wave and that scattered by the swimbladder (see above). Secondly, the phase difference between the signals at two spatially-separated receptors partly locates the source (i.e. one angular coordinate is determined). Neither mechanism is sufficient on its own to determine the direction uniquely, but this ability is explained if both are involved, or if the fish is able to compare the signals from several receptors.

### **4.3.2 Masking and the critical bandwidth**

The audiogram is not a complete description of the sound detection capability. It takes no account of the background noise which is always present, whether the

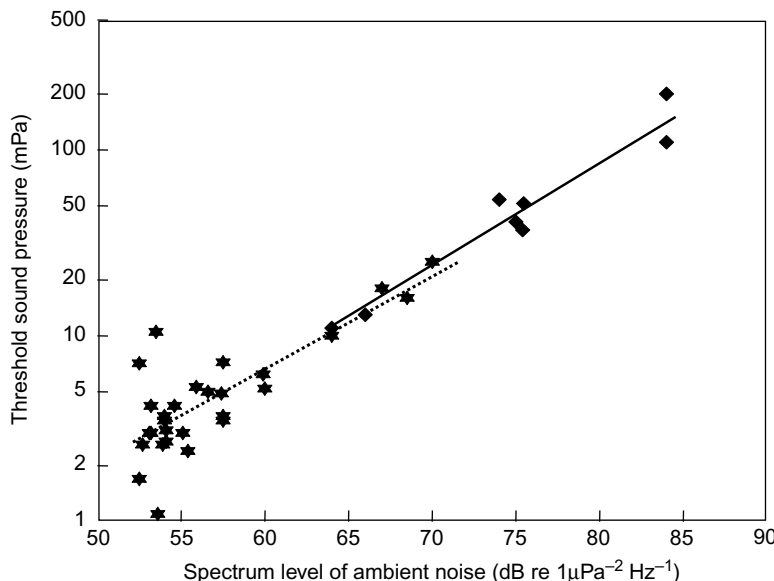


**Fig. 4.2** How the auditory threshold of cod, *Gadus morhua*, at 160 Hz changes with the spectrum level of background noise (per 1 Hz bandwidth). Comparison of thresholds obtained in natural sea noise (★, dotted line) and artificial white noise (◆, solid line). Each point is the result of one experiment. The lines are linear regressions on the experimental data. (Redrawn from Chapman and Hawkins 1973.)

experiments are done in the laboratory or in the field. When a signal such as a tone burst is presented to an animal in a noisy environment, the threshold for hearing the tone depends on the intensity of the noise. As the noise increases, so does the threshold, because the noise impairs the ability of the animal to detect the tone (Fig. 4.2). This phenomenon is called masking (Tavolga 1974; Coombs and Fay 1989). According to Chapman and Hawkins (1973), the natural background noise in the sea is sufficient to cause noticeable masking. Given that the noise is highly variable, depending on the sea state for instance, this could explain some of the variation found in auditory threshold experiments.

The frequency components of broadband noise are not all equally effective in masking a tone signal. The tone is most severely masked by noise at the same and nearby frequencies. In experiments where the noise is produced artificially, permitting the frequency content to be controlled by electronic filtering, it is found that noise frequencies well separated from that of the tone do not mask the signal (Hawkins and Chapman 1975). This observation leads to the concept of the critical bandwidth,  $B$ , which is the effective range of noise frequencies that do mask a tone.

In principle,  $B$  may be determined experimentally as follows. Suppose that a tone of frequency  $f$  is presented to a fish along with a noise signal which is filtered to include only frequencies in the band  $f \pm \Delta f/2$ . The noise power per unit frequency is constant within the bandwidth  $\Delta f$ . The auditory threshold is measured in a series of trials with

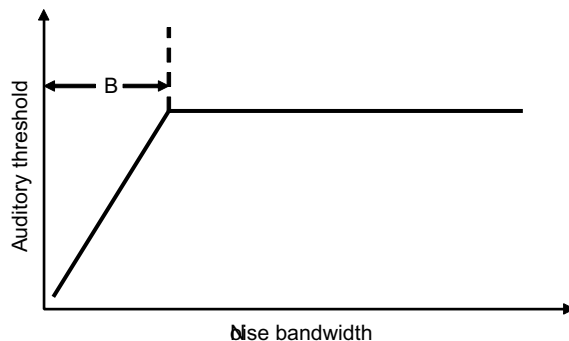


**Fig. 4.3** Auditory threshold for a tone presented with noise of various bandwidths centred on the tone frequency. The critical bandwidth  $B$  is indicated by the inflection of the threshold curve.

different noise bandwidths. The results should follow the curve illustrated in Fig. 4.3. The threshold increases with  $\Delta f$  at first, up to some limit after which it is constant.  $B$  is estimated as the bandwidth at which the threshold stops increasing, the implication being that frequencies beyond  $f \pm B/2$  do not mask the tone (Fletcher 1940). Unfortunately, this experimental technique has not been successful when applied to fish. In experiments with cod, Hawkins and Chapman (1975) developed a more accurate method, in which the noise is presented in a constant narrow bandwidth centred on different frequencies,  $f_i$ . The masking is greatest when  $f_i = f$ , and reduces with the separation of the noise and tone frequencies. The masking curve is the graph of the auditory threshold against  $f_i$ , normalized to 1 when  $f_i = f$  (see Fig. 4.4). For each tone frequency,  $B$  is estimated as the width of the ideal rectangular filter which encloses the same area as the actual masking curve. Using this method, Hawkins and Chapman (1975) showed that the critical bandwidth of the cod increased with the tone frequency (Fig. 4.5).

A simple but approximate method for estimating  $B$  is to measure the auditory threshold for a tone signal in the presence of white noise. If  $P_t$  is the power of the tone signal at the threshold, and  $P_n$  is the noise power per unit bandwidth, which is the same at all frequencies for white noise, then  $B_r = P_t/P_n$  is an estimate of  $B$ . The assumption is that when white noise just masks a signal, the noise power in the critical band is equal to the signal power. This assumption is not generally true, however, and  $B_r$  is called the critical ratio, to distinguish it from  $B$  (the critical bandwidth) which is not necessarily the same. Note that  $B_r$  and  $B$  are expressed in the same units (Hz). Thus, in principle, both measures may be determined for the same animal. Experimental comparisons have shown that  $B_r$  is generally less than  $B$  (Hawkins and Chapman 1975; Au and Moore 1990). Nevertheless, the white-noise technique has been widely applied in studies of marine mammals (for example Johnson *et al.* 1989; Schlundt *et al.* 2000; Southall *et al.* 2000).

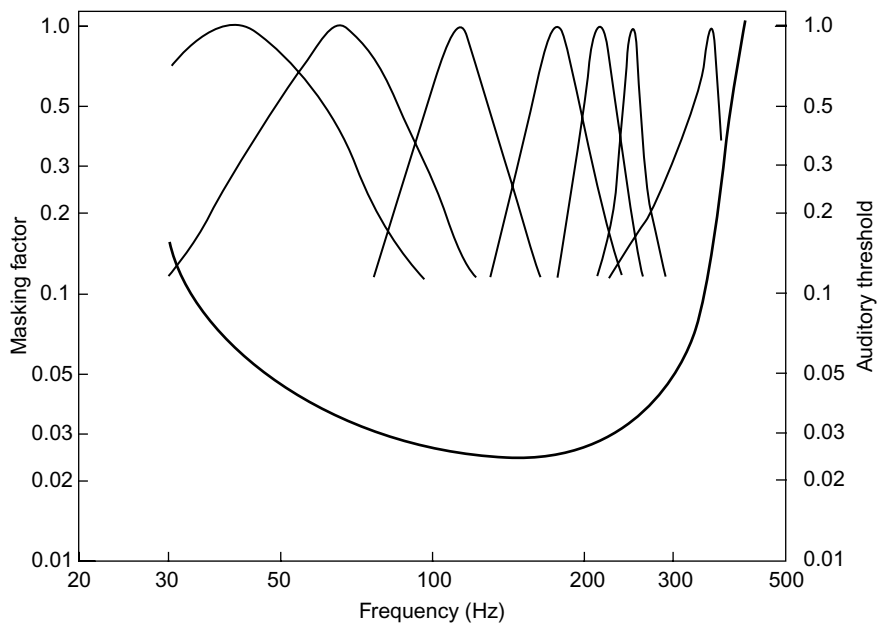


**Fig. 4.4** Masking effect of 10-Hz-wide noise bands on pure tone signals at different frequencies for the cod, *Gadus morhua*. The auditory threshold increases in proportion to the masking factor, which is normalized to unity when the noise and tone frequencies coincide (upper curves, masking factor vs noise frequency). The cod audiogram (lower curve, auditory threshold vs tone frequency, arbitrary units) is included to show the hearing range. (Redrawn from Hawkins and Chapman 1975.)

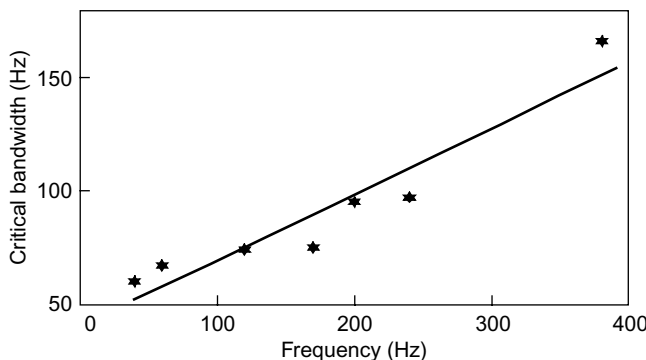


**Fig. 4.5** Values of the critical bandwidth for various tone frequencies presented to the cod, *Gadus morhua*. The least-squares fitted line is  $B = 38.85 + 0.29f$ . (Redrawn from Hawkins and Chapman 1975.)

The ratios  $B/f$  and  $B_r/f$  are measures of the ability to discriminate against noise. The smaller these ratios, the better is the ability of the animal to discriminate signals from their frequency composition. Some examples are given in Table 4.2, including comparisons of  $B$  and  $B_r$  in the few cases where both measures have been determined.

**Table 4.2** Experimental results for noise masking of a tone at frequency f, in terms of the critical bandwidth (B) and/or the critical ratio ( $B_r$ ).

Species	f (Hz)	B (Hz)	$B_r$ (Hz)	B/f	$B_r/f$	Reference
Atlantic salmon ( <i>Salmo salar</i> )	160	183	—	1.14	—	Hawkins and Johnstone (1978)
Cod ( <i>Gadus morhua</i> )	160	85	68	0.53	0.42	Hawkins and Chapman (1975)
Goldfish ( <i>Carassius auratus</i> )	500	100–200	—	0.2–0.4	—	Tavolga (1974)
Ringed seal ( <i>Pusa hispida</i> )	10 000	—	1700	—	0.17	Terhune and Ronald (1975)
California sea lion ( <i>Zalophus californianus</i> )	1 200	—	158	—	0.13	Southall <i>et al.</i> (2000)
Harbour seal ( <i>Phoca vitulina</i> )	1 200	—	100	—	0.08	Southall <i>et al.</i> (2000)
Bottlenose dolphin ( <i>Tursiops truncatus</i> )	60 000	22 800	3400	0.38	0.06	Au and Moore (1990)

### 4.3.3 Ultrasound and infrasound

So far we have concentrated on sounds at frequencies near the minimum threshold of the audiogram (Fig. 4.1). It is nevertheless possible that fish might be able to detect acoustic waves at extreme frequencies outwith the normal hearing range. These are called ultrasound and infrasound which correspond, respectively, to very high and very low frequencies. In the context of fish hearing, ultrasound means transmissions above 10 kHz, while infrasound is below 20 Hz.

There is strong evidence that some fish species can detect ultrasound, while others have no capability in this respect. Nestler *et al.* (1992) reported that various clupeoids (herrings, sardines and shads) reacted to echosounder transmissions by swimming away from the source. The same behaviour has been observed in cod (Astrup and Møhl 1993). Mann *et al.* (1997) found that the American shad, *Alosa sapidissima*, can detect pure tones at 180 kHz. Gregory and Clabburn (2003) report that the clupeoid *Alosa fallax fallax* avoided a monitoring site where there was a 200 kHz echosounder, but not when this was replaced by one operating at 420 kHz. On the other hand, hearing experiments have shown that several species are unable to detect ultrasound, notably the Spanish sardine (*Sardinella aurita*) and the goldfish (*Carassius auratus*). The results of Mann *et al.* (2001) suggest that ultrasound detection by clupeiforms is restricted to one sub-family, the Alosinae.

The thresholds reported for ultrasound detection by fish are much higher than those applicable to low-frequency hearing. Some examples are given in Table 4.3.

**Table 4.3** Ultrasound detection by fish. Auditory thresholds (rms sound pressure) determined experimentally at frequencies above 30 kHz. For comparison with Table 4.1, 100 dB re 1  $\mu$ Pa is equivalent to 100 mPa.

Species	Frequency (kHz)	Threshold (dB re 1 $\mu$ Pa)	Reference
Clupeoids	125	145	Nestler <i>et al.</i> (1992)
Cod	38	195	Astrup and Møhl (1993)
( <i>Gadus morhua</i> )	50	198–202	Astrup and Møhl (1993)
American shad ( <i>Alosa sapidissima</i> )	50–100	139–156	Mann <i>et al.</i> (1998)
Menhaden ( <i>Brevoortia patronus</i> )	40–80	180	Mann <i>et al.</i> (2001)

It is unclear what sensory mechanism is involved. In the case of clupeoids, Mann *et al.* (2001) surmise that specializations such as the air-filled bulla in the utricle of the inner ear could be responsible. However, it is not known why some species with apparently similar physiology are unable to detect high-frequency sound.

It is not necessarily the case that specialized organs are required for fish to detect ultrasound. As explained in Chapter 2, when a pulsed ultrasonic transmission is reflected from a discontinuity such as the swimbladder surface, the radiation pressure can result in a low-frequency signal within the normal hearing range. The effect is unimportant in the case of the pure tones normally used in hearing experiments, but it could allow fish to detect short ultrasonic pulses such as echosounder transmissions or the sonar clicks of aquatic mammals.

Mann *et al.* (1998) speculate that ultrasonic hearing might have evolved as an aid to predator avoidance. They showed that American shad could hear simulated dolphin echolocation clicks, and that the fish should be able to detect a hunting *Tursiops truncatus* at a range of more than 180 m. Astrup and Møhl (1998) found that the cod could discriminate different repetition rates of ultrasonic pulses. This capability may also be relevant to predator avoidance. Some dolphins, having detected a prey, increase the transmitted click rate as they close in. This interesting behaviour is discussed in the following section.

Infrasound could also be important to fish. There is a lot of low-frequency noise in the aquatic environment, from both natural causes (e.g. waves and currents) and anthropogenic sources (e.g. ships and fishing gear). Fish audiograms generally start at a few tens of Hz and suggest the sensitivity to sound pressure declines at the bottom end of the spectrum. However, Enger *et al.* (1993) say that the pressure audiogram gives the wrong impression, since low-frequency hearing depends on the kinetic sound components (i.e. the particle displacement, velocity or acceleration). When the fish audiogram is replotted to show the sensitivity to particle acceleration, the low-frequency part becomes much flatter. This suggests that hearing could still be important at frequencies below those normally displayed in audiograms. Enger *et al.* (1993) found that juvenile salmon exhibited strong avoidance reactions to a

10 Hz signal, while no such responses were seen at 150 Hz (which is near the upper end of the hearing range).

Infrasound perception down to 1 Hz or less has been demonstrated in several other species, e.g. cod *Gadus morhua* (Sand and Karlsen 1986), perch *Perca fluviatilis* (Karlsen 1992a) and plaice *Pleuronectes platessa* (Karlsen 1992b). Myrberg Jr *et al.* (1976) showed that wild sharks were attracted to sounds in the band 10–20 Hz. Higher frequencies (up to 80 Hz) were also attractive to the sharks, but less strongly than the infrasound.

It is interesting to note the different behaviour of large sharks and small teleosts, the first being attracted and the second repelled by infrasound. This suggests that the ability of fish to detect and react to infrasound could have evolved through the natural selection pressures on both predators and prey.

#### 4.4 Biological sonar

Some animals use active sonar as a means of sensing objects in their environment, notably the bats (Microchiroptera) in air and the whales and dolphins (Cetacea) in water. This ability is seldom observed in fish, although Tavolga (1976) reported a simple form of echo detection in the catfish, *Arius felis*. The aquatic mammals have the most advanced forms of biological sonar. Living in a world dominated by sounds and echoes, where long-range vision is relatively useless, these animals can ‘see’ their surroundings to a remarkable extent by interpreting the reflections of self-generated sounds (Purves and Pilleri 1983; Au 1993). It has to be said that many of the whales and dolphins can sense prey and their environment using sound waves rather better than we can, even with the most advanced man-made sonar and signal processing technology. Aquatic mammals can successfully echolocate in environments that are difficult – if not impossible – for electronic sonars (e.g. in shallow water or under ice sheets, noisy places that are full of clutter). The study of mammalian sonar is interesting in its own right, and has produced an extensive literature, but in addition it can provide clues to guide the future development of our sonar technology.

Cetaceans produce many different sounds over a broad spectrum extending to more than 100 kHz; these are described as whistles, screams or clicks according to their amplitude and frequency components. The clicks are one type of sonar transmission, consisting of short pulses with a frequency content at the upper end of the phonation range (Diercks *et al.* 1971; Au 1993). Key features of the clicks produced by several species are compared in Table 4.4. Some animals click at widely different frequencies (Pilleri *et al.* 1976). The clicks can be very strong, comparable to our sonar transmissions, but the animals have some control over the amplitude which may be adjusted according to environmental noise and the target range. Then there is the whistle which is another kind of transmission. Evans (1973) described the whistle as a frequency-modulated pulse which can last up to 3 s, sweeping a frequency range of 2–30 kHz; see also Buck *et al.* (2000) and Thomsen *et al.* (2001). The ability

**Table 4.4** Examples of cetacean sonar clicks characterized by f, the dominant frequency;  $t_c$ , the click duration; and SPL, the transmitted source level in decibels re  $1 \mu\text{Pa}$  at 1 m (peak-to-peak amplitude unless otherwise stated). See Au (1993) for the click behaviour of many other species.

Species	f (kHz)	$t_c$ ( $\mu\text{s}$ )	SPL (dB)	Reference
Amazon dolphin ( <i>Inia geoffrensis</i> )	65–100	40–60	166	Purves and Pilleri (1983)
Bottlenose dolphin ( <i>Tursiops truncatus</i> )	50–60 110–130	50–250 50–70	170 204–216	Evans (1973) Au (1993)
Atlantic spotted dolphin ( <i>Stenella frontalis</i> )	40–50 <sup>a</sup> 110–130 <sup>a</sup>	ca 50	200–210 (max. 223)	Au and Herzing (2003)
Indus river dolphin ( <i>Platirista indi</i> )	ca 63 <sup>a</sup> 160–200 <sup>a</sup>	40–70		Pilleri <i>et al.</i> (1976)
Killer whale ( <i>Orcinus orca</i> )	14	500–1500	178	Diercks <i>et al.</i> (1971)
Sperm whale ( <i>Physeter catodon</i> )	3–12	ca 3000	175–231 <sup>(1)</sup>	Møhl <i>et al.</i> (2000)
Beluga ( <i>Delphinapterus leucas</i> )	1.2–1.6 <sup>b</sup> 30–40 <sup>b</sup>	2000–4000 75–250	205–225	Turl and Penner (1989)
Harbour porpoise ( <i>Phocoena phocoena</i> )	2 <sup>b</sup> 10–150 <sup>b</sup> 147	500–5000 100 ca 80	93–108 132–149 144–166 <sup>(1)</sup>	Møhl and Andersen (1973) Goodson and Sturtivant (1996)
		—	157 ± 7	Au <i>et al.</i> (1999)

<sup>(1)</sup> Root-mean-square amplitude, averaged over the whole pulse.

<sup>a</sup> Clicks with a bi-modal spectrum.

<sup>b</sup> Different click trains produced by the same animal.

to transmit (and to receive) over a wide frequency range increases the information content of echoes, compared to the man-made sonars (cf. Chapter 3) which are mostly limited to narrow-band transmissions. However, it is unclear whether the whistles are generally intended for inter-animal communication rather than echolocation; possibly they serve both purposes.

Sometimes the clicks are emitted at a low rate, when each one can be distinguished by a human listener with a hydrophone. In this mode, the animal appears to be maintaining a general awareness of its surroundings. The repetition rate may change, however, and at times is so high that the clicks merge into a creaking or crackling sound, presumably when a particular object has excited the animal's interest. The much studied bottlenose dolphin, *Tursiops truncatus*, adjusts the click interval according to the range of the target, transmitting shortly after the receipt of each echo (Fig. 4.6). The time delay between receiving one echo and the next transmission is about 20 ms, suggesting it takes that long for the dolphin to process the echo and decide what to do next. Au *et al.* (1999) report similar behaviour in the harbour porpoise, *Phocoena phocoena*, but this adjustment behaviour is not universal. The beluga, *Delphinapterus leucas*, has a different strategy (Turl and Penner 1989).

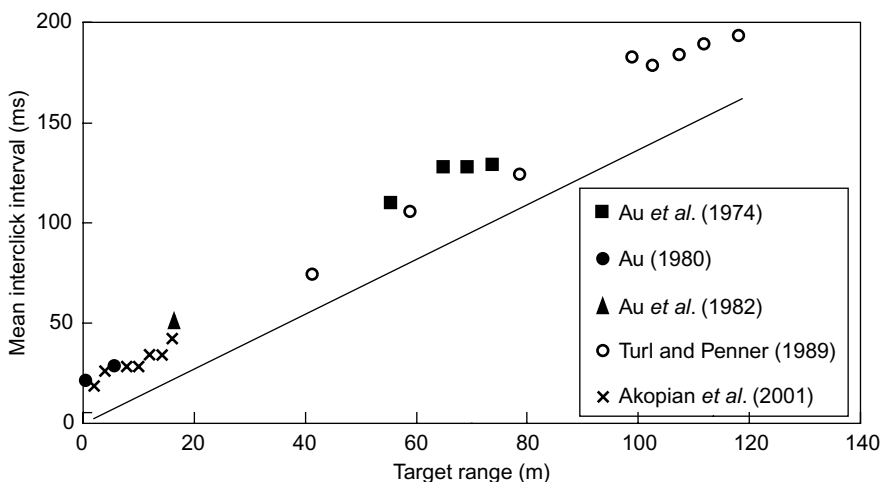


**Fig. 4.6** Click interval as a function of target range for the bottlenose dolphin, *Tursiops truncatus*. Points are the results from various experiments. The solid line shows the time delay between the click transmission and the target echo (the two-way transit time).

In one mode (among several), the clicks occur at a relatively constant rate, even when the echo delay exceeds the click interval. Evidently the beluga can extract useful information from echoes while transmitting and receiving concurrently.

The experimental results reported here were obtained from *in situ* observations in the wild or from experiments with captive animals in aquaria or tanks. Clearly there are better prospects for observing natural behaviour when the animals are free in open water. It is then necessary to locate the animals so that, for instance, the source level can be calculated from measured click amplitudes taking account of the range-dependent spreading loss (Au 1992). This can be done using hydrophone arrays to locate the source of clicks from arrival-time measurements as described in Chapter 3. Of course, the directionality of the click transmissions can confuse source-level measurements in the wild, since the orientation of the animal relative to the receiver is unknown. Dolphin sonar is more easily investigated with captive animals, and much of the reported work has been done in confined enclosures. It is important to note that the background noise in an enclosure is likely to be very different from that in the sea. Since dolphins can adjust the click amplitude according to the noise level, that could explain some of the differences seen in source levels between tank and *in situ* measurements of the same species.

Nevertheless, the finer details of dolphin sonar and echolocating performance can only be studied in specially designed facilities where the animal and target geometry is known precisely. It is not essential to use a real target for this work. Aubauer and Au (1998) describe an interesting technique called phantom echo generation. Some distance in front of the subject animal is a small receiver connected to a nearby projector via a signal processor controlled by the experimenter. When a dolphin click

is detected, it is processed to produce a phantom echo which simulates the reflection by a particular target, at an adjustable range since the echo can be delayed, and this signal is transmitted by the projector for consideration by the subject animal. The phantom echo technique allows quite complicated scenarios (e.g. moving targets) to be simulated without the inconvenience of having to physically move one or more pieces of equipment.

The physiology of sound production by the cetaceans is not completely understood, although Aroyan (2001) and Aroyan *et al.* (1992) have successfully modelled beam formation by the common dolphin, *Delphinus delphis*. Several organs are believed to be involved, in particular the larynx, the diverticuli associated with the blowhole, and the muscular plugs that seal the internal nares (Purves and Pilleri 1983). Simultaneous sound production by different organs could explain the ability to transmit signals with spectrum peaks at widely separated frequencies. Another important factor is the reflection and refraction of the transmitted sound by the bones, air spaces and fatty tissues of the animal's head (notably the melon) and the rostrum. As a result, the sound is focused into the water as directional beams (see Fig. 4.7). Normally the sound is projected in a single beam in the forward direction. For example, the Amazon dolphin, *Inia geoffrensis*, projects a beam 30° wide in vertical section and a few degrees narrower in the horizontal plane (Pilleri *et al.* 1979). Some species generate more complicated sonar fields. In the Indus river dolphin, *Platinista indi*, the forward direction is blocked by the cristae maxillares, a pneumatized bony structure in the frontal part of the skull. The sound transmission is thus divided into two beams, one above and one below the head (Purves and Pilleri 1983). It is possible that searching with a null between two beam lobes is better than searching with a single broad lobe; this technique is used in direction finding by radar. Yet another mechanism is found in the beluga, which produces superimposed low (LF) and high frequency (HF) clicks, with dominant spectral components at 1.6 and 35 kHz respectively. The HF field is the more powerful in the forward direction. The LF field is angled slightly downwards and has a wider beam. Thus the LF field is the more powerful in the ventral direction. Frequency analysis of the received echoes could therefore provide additional directional clues to the beluga. The sonar field of the harbour porpoise, *Phocoena phocoena*, has a similar characteristic based on dual-frequency clicks (Møhl and Andersen 1973; Goodson and Sturtivant 1996).

In addition to their remarkable ability to locate objects in space, the cetaceans can interpret the echoes well enough to have a good awareness of the size, shape and material composition of targets (Au and Martin 1989; Au and Pawloski 1989). For example, Au *et al.* (1980) and Nachtigall (1980) have shown that *Tursiops truncatus* can distinguish: (a) spheres and cylinders; (b) aluminium and copper discs, for the same target strength; (c) objects 1 dB different in target strength but similar in shape; (d) hollow cylinders of different wall thickness (Au and Pawloski 1991); and (e) cylinders of different material composition and aspect angles (Au and Turl 1991). This performance in target classification exceeds the capability of most man-made

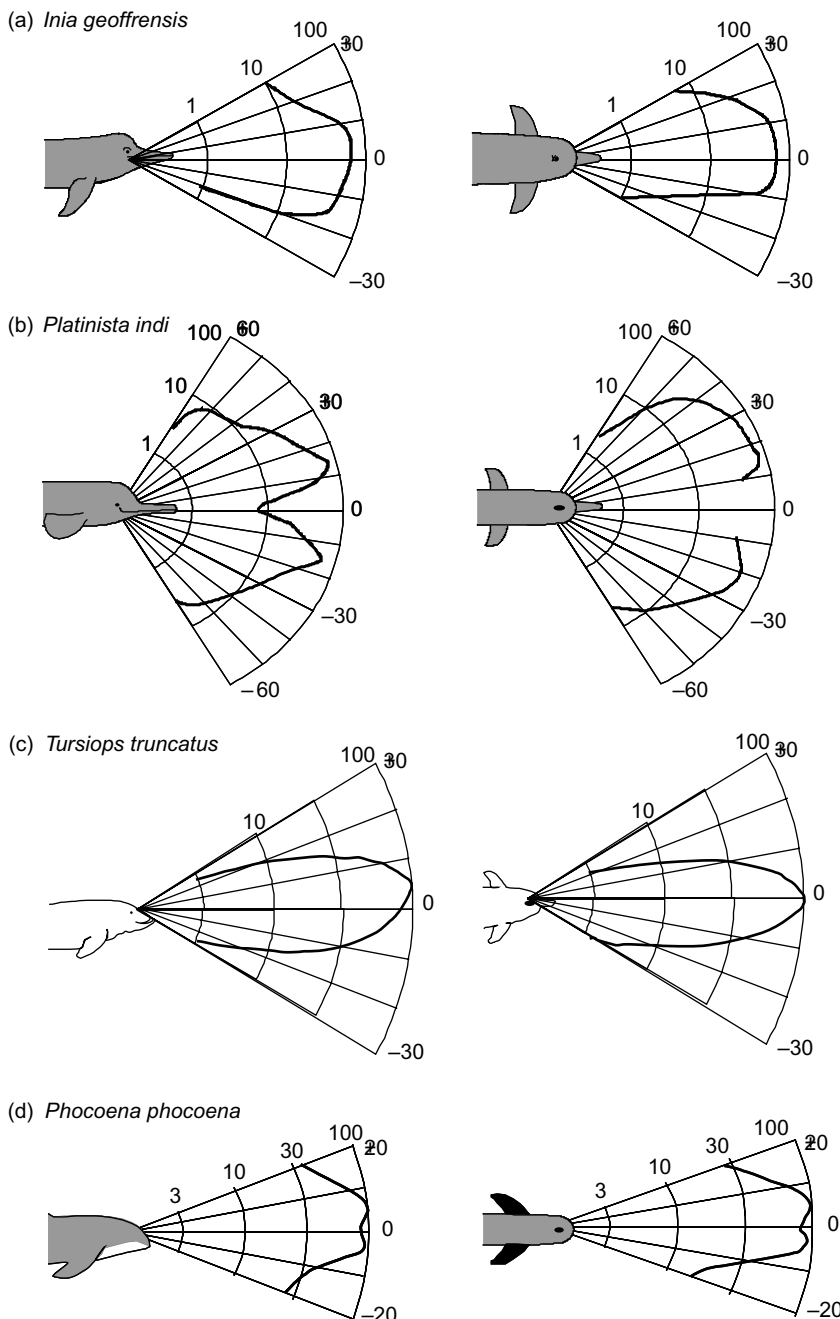


**Fig. 4.7** Directivity of dolphin sonar. Typical beam patterns of the clicks transmitted by four species. Each diagram shows the sound pressure amplitude on the radial axis (log scale, arbitrary units) vs direction (azimuthal angle, degrees) in one plane. Left, dorsal-ventral sections; right, lateral sections viewed from the dorsal aspect. Dominant frequencies of the clicks are (a, b) 80 kHz; (c, d) 120 kHz. (Redrawn from (a, b) Pilleri *et al.* (1976); (c) Au (1993); (d) Au *et al.* (1999)).

sonars. *T. truncatus* has a large acoustic nerve which connects the auditory sensors to the cerebral cortex, which suggests that a substantial proportion of the brain is involved in the interpretative function.

The transmitted beam patterns of the cetacea are quite wide, around 30°, yet many species are capable of much finer angular resolution when echolocating. This implies that the receiving beams are narrow, which is difficult to explain since we normally associate narrow beams with transducers somewhat larger than the cetacean head. Goodson and Klinowska (1990) suggest that the uniformly spaced teeth in the jaw act as an end-fire array, and Dobbins (2001) describes the physics of how this might assist directional hearing. The end-fire array has a beam pattern determined by the length rather than the diameter (cf. Chapter 2). There are other possibilities for focusing echoes passing through the various structures and tissues in the cetacean head. Although the evaluation of the resultant sound field is complicated, Aroyan (2001) has successfully modelled the three-dimensional hearing capability of the dolphin *Delphinus delphis*; see also Flint *et al.* (1997).

The Indus river dolphin, *Platinista indi*, is perhaps the most specialized of all the cetaceans as regards the use of biological sonar. This animal is blind and therefore relies entirely on acoustic information to navigate and to capture prey. We have already mentioned some important features of the *P. indi* sonar, notably the broadband clicks and the complex shape of the transmitted beam, which has a null in the direction of the rostrum axis (Fig. 4.7). While this null is present in both sexes, it is more pronounced in the male, which also exhibits greater asymmetry between the dorsal and ventral sectors of the beam. Purves and Pilleri (1983) suggest that the larynx is the only source of acoustic energy in *P. indi*. The dorsal field is due to direct transmission in directions constrained by the air spaces and bony tissues of the head, while the ventral field is the same larynx signal reflected downwards by the cristae maxillares. The maximum intensities occur in forward directions about 25° above and below the rostrum axis.

Pilleri *et al.* (1976) describe the behaviours adopted by *P. indi* according to whether the animal is exploring its surroundings, locating an object in space or inspecting an already-located object. *P. indi* normally swims on its side, and when exploring, nods its head back and forth as the animal moves forward. The head movement causes the sonar beam to sweep horizontally, and echoes are returned from all directions, despite the 'blind spot' on the rostrum axis. Moreover, the changing echo strength as the beam sweeps, and the comparison of signals from the dorsal and ventral sectors, allows the direction of targets to be determined precisely. When an echo is detected that the dolphin wishes to locate, it swims in an arc until the position of the target is established. Finally, if the target is considered worthy of further investigation, the dolphin stops swimming but remains on its side with the head bent and the throat directed at the target one or two metres distant. The ventral sector of the sonar beam is used exclusively during this inspection behaviour. Figure 4.8 is a splendid example of this behaviour, with *P. indi* inspecting a small piece of lead shot at close range.



**Fig. 4.8** Dolphin sonar in action. The blind *Platista indi* inspects a piece of lead shot (arrowed) 3 mm in diameter. (Reproduced with permission from Purves and Pilleri 1983.)

## 4.5 Environmental impacts

Most of the animals living in the aquatic environment are sensitive to sound in one way or another. This means that any anthropogenic disturbance of the acoustic environment could have adverse effects on life in the sea. Here we discuss the potential problems for aquatic life associated with man-made sounds, which range from shipping noise (relatively low level but always present in some areas) to more occasional catastrophic events like underwater explosions. The environmental impact of any such activity has been a matter for increasing concern in recent years. A precautionary approach is often suggested, meaning that no-risk strategies should be adopted, although it is doubtful if this idea in its strictest sense could ever be applied across the full range of man's activities in the sea. Nevertheless, anyone (or any organization) operating underwater sound-producing equipment owes a 'duty of care' to account for the effect of these activities on aquatic lifeforms (Heathershaw *et al.* 2001).

### 4.5.1 High-energy sound sources

There are several applications, in fields other than fisheries, which involve the sudden release of large amounts of energy into the water (Cole 1948; Greene *et al.* 1985). In seismic surveying, for example, the transmitted pulse of acoustic energy must be sufficient to penetrate the deep subterranean structures where oil or gas may be found. Construction work close to rivers or in shallow seas involving pile drivers

produces short pressure pulses of high amplitude that will propagate some distance into the surroundings. Then there is the use of explosives to excavate soil and rock during construction work. Even when the excavations are on land, again shock waves can be transmitted through the ground into nearby bodies of water.

It is important to understand the biological effects of underwater explosions, so that fishery scientists can give an informed view on the consequences for aquatic animals, and advice on how the work should be done to minimize the risk of damage or even mortality. As a first step, it is necessary to understand the physical nature of the shock waves produced by explosives (Weston 1960), or devices such as the airgun which is commonly used in seismic surveys (Duncan 1985; Goold and Fish 1998). The damage which exposed animals may suffer depends on the nature of the shock wave and the distance from the explosion site. Even at long range, however, beyond the area where physical damage is likely, continuous exposure to high-energy pulses could have detrimental effects on the animals concerned, or their behaviour might be influenced in an undesirable way. For example, fishermen often complain that the disturbance created by seismic surveying ‘drives the fish away’. Again, the opinion of scientists may be sought in resolving disputes between fishermen and seismic surveyors who are to some extent competitive users of the sea.

### *Shock waves*

When a large amount of energy is suddenly released within a small volume of water, the immediate effect is the generation of a shock front, which travels away from the explosion site, initially at a speed greater than that of low-amplitude sound waves. As the front passes, the pressure at a particular location rises sharply to a peak value, then decays exponentially with time (Fig. 4.9). At the explosion point, there is a bubble of gas which first expands, creating the shock front, then it contracts and continues to oscillate in size. During the first contraction, the pressure at the bubble surface falls below the ambient (undisturbed) level. Thus the shock front is followed by a rarefaction, and then by a series of pulses caused by the bubble oscillations. The bubble pulses are relatively small and their speed is close to that of low-amplitude sound. The shock front attenuates more rapidly as it travels than do the bubble pulses. This means that the shape of the pressure-time waveform, which is called the ‘signature’ of the explosion, changes with distance from the explosion site. As the range increases, the time-delay between the shock front and the first bubble pulse lengthens and a larger proportion of the transmitted energy is contained in the bubble pulses.

The signature illustrated in Fig. 4.9 applies when the shock wave is propagating in free-field conditions, at any range  $R$  more than a few times the bubble radius but less than the distance to the water surface or the bottom. The qualitative features of the signature are similar for all high-energy sources which produce gas bubbles – sparkers, airguns or explosive charges; see Duncan (1985) for technical details of these sources. They differ in the amount of energy which can be released in practical

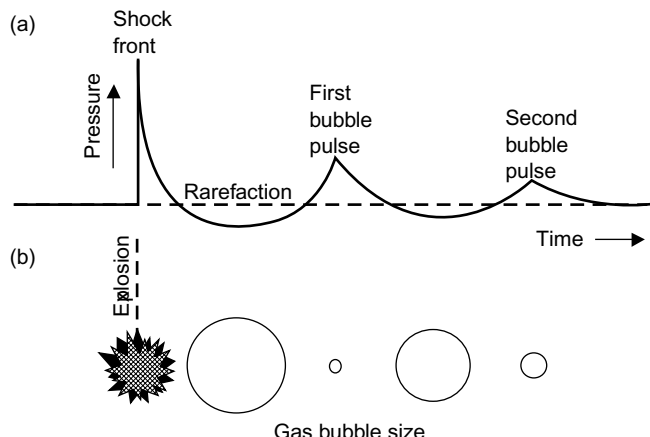


**Fig. 4.9** Sequence of events following an underwater explosion. (a) Pressure waveform at distance  $R$  from the explosion, assuming free-field propagation. The peaks and troughs about the ambient level are produced by oscillations of the gas bubble at the explosion site; (b) the bubble size is shown against the corresponding time on the pressure waveform.

applications (Table 4.5), and in the rate of energy release which determines the amplitude of the shock front. For example, there are two types of chemical explosive in common use – propellants such as gunpowder, and high explosives such as TNT. The high explosives are more energetic than the propellants and they detonate more rapidly. Of all the high-energy sources mentioned above, the high explosives produce the strongest shocks and are most likely to have adverse biological consequences.

In free-field conditions, when the shock front propagates far from the surface or other boundaries, the physical effects of detonating a charge of high explosive can be predicted by empirical equations (Cole 1948; Staal 1985). Of particular interest from the biological point of view are:  $P$ , the pressure relative to the ambient level ( $P_0$ ) and how it changes with time;  $J$ , the energy flux transmitted by the shock waves; and  $\Phi$ , the impulse, which is the integral of the pressure with time over the duration of the initial shock (definitions, Marshall 1996). When the shock front arrives at a given point, the pressure rises almost instantaneously to  $P_{\max}$ , the peak value, then it decays more slowly. The time constant  $t_s$  is a measure of the width of the shock pulse.  $t_s$  is the time at which the pressure has dropped to  $\exp(-1) = 0.37$  of the peak value. These parameters are illustrated in Fig. 4.10. Predictive equations are given in Table 4.6 for TNT and Pentolite, two types of high explosive in common use. To illustrate the scale of Fig. 4.10, suppose 10 kg of TNT explodes at 100 m depth. At 30 m distance,  $P_{\max}$  is 2.7 MPa,  $P_{\min}$  is 53 kPa below ambient,  $t_s$  is 0.36 ms and the first bubble pulse arrives 90 ms after the shock front.

The rarefaction which follows the initial shock is much smaller than  $P_{\max}$ . On the other hand, fish are more resistant to the compressive forces implied by positive pressures. The expansion caused by a sudden reduction in pressure can be very

**Table 4.5** Properties of high-energy sound sources. The stated values refer to the shock front observed at distance R from the explosion centre, propagating in free-field conditions; calculations based on Cole (1948) and Duncan (1985).

Source	Specification	R (m)	Max. pressure (kPa)	Time constant (μs)	Energy flux (J m <sup>-2</sup> )	Impulse (Pa s)
Pentolite	10 kg charge at depth >R	10	135 000	258	8730	3190
TNT	10 kg charge at depth >R	10	9 250	284	7600	3160
Black powder	40 kg charge at depth >R	10	190	—	70	1100
Airgun	82 litres at 14 MPa 8 m depth 32-gun array, size 100 m by 21 m	100	31	—	9	90
Airgun	37 litres at 14 MPa 7 m depth 16-gun array	10	225	—	40	570
Airgun	1.6 litres at 14 MPa 1 gun at 8 m depth	10	17	—	<1	90
Sparker	3 kJ discharge	10	5	—	<1	<10

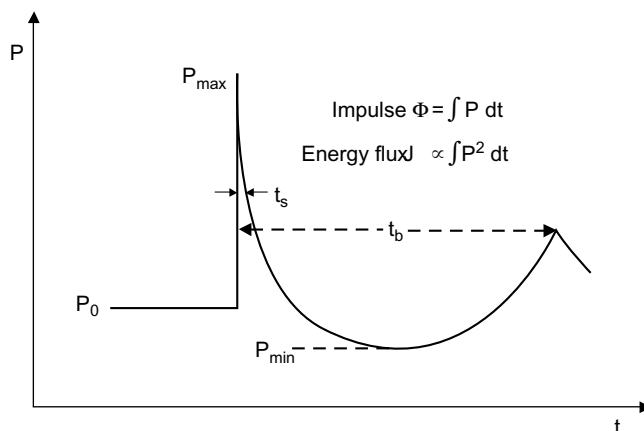


**Fig. 4.10** Physical parameters of the pressure signature (not to scale). P, pressure at time t at the fixed point where the signature is observed;  $P_{\max}$ , peak pressure which coincides with the shock front;  $P_{\min}$ , greatest rarefaction;  $P_0$ , ambient pressure;  $t_s$ , time constant of the decaying shock;  $t_b$ , time delay of the first bubble pulse.

**Table 4.6** Equations for predicting the characteristics of explosive shock fronts propagating in free-field conditions.  $W_e$  is the charge weight (kg);  $R$  is the distance of the observation point from the explosion centre (m);  $P_{01}$  and  $P_{02}$  are the ambient undisturbed pressures at, respectively, the explosion centre and the observation point (Pa).

Parameter	Explosive material	
	TNT	Pentolite
Peak pressure, $P_{\max}$ (Mpa)	$52.4 (W_e^{1/3}/R)^{1.13}$	$56.3 (W_e^{1/3}/R)^{1.14}$
Energy flux, $E$ ( $\text{kJ m}^{-2}$ )	$82.1 W_e^{1/3} (W_e^{1/3}/R)^{2.05}$	$105 W_e^{1/3} (W_e^{1/3}/R)^{2.12}$
Impulse, $\Phi$ (Pa s)	$5750 W_e^{1/3} (W_e^{1/3}/R)^{0.89}$	$7410 W_e^{1/3} (W_e^{1/3}/R)^{1.05}$
Time constant, $t_c$ ( $\mu\text{s}$ )	$92.5 W_e^{1/3} (W_e^{1/3}/R)^{-0.22}$	$84.0 W_e^{1/3} (W_e^{1/3}/R)^{-0.23}$
Min. pressure, $P_{\min}$ (Pa)	$P_{02} - 69 W_e^{1/3} P_{01}^{2/3}/R$	$P_{02} - 74 W_e^{1/3} P_{01}^{2/3}/R$

destructive, especially to gas-filled organs such as the swimbladder. This effect depends on  $P_{\min}$ , the lowest pressure relative to the ambient level during the rarefaction, and on the time scale of the pressure changes. Formulas for predicting  $P_{\min}$  are included in Table 4.6.

When the distance of the observation point from the explosion ( $R$ ) is more than the charge depth below the surface or height above the seabed, the pressure waveform is modified by reflections from the two boundaries, especially the pressure-release condition at the water surface (Chapman 1985; 1988). Since the shock front precedes the reflections, which have longer path lengths, the peak pressure is unaffected. However, the free-field equations cannot be used to predict the energy flux nor the impulse in the presence of boundary reflections.

The changes in pressure for the surface reflection are the reverse of those in the direct wave, because the sum of the two must be zero at the surface. On the other hand, the pressures in the bottom reflection and the direct waves change in the same way (Fig. 4.11). Note that the inverted reflection from the surface can result in a substantial rarefaction when it combines with the direct wave. In the absence of any other boundaries, the resultant pressure is the sum of contributions from the direct wave and the two reflections. Rather complicated waveforms can arise from these interactions. Nevertheless, it is possible to calculate important parameters, such as the impulse and the minimum pressure, if reasonable assumptions can be made about the magnitude of the bottom reflection.

The classical theory applies to an explosion at a point, whose free-field shock wave spreads with equal intensity in all directions. The end-fired line charge has quite different features. Here the total charge is in a continuous length of cord, or it may be divided into a number of smaller packages spaced at intervals. The detonation starts at one end and proceeds along the line with increasing delay. This results in a focused shock wave. The blast is concentrated in particular directions (called the maximum response axis). Thus the line charge can be designed to reduce collateral damage by directing the explosive force where it is wanted, and away from where it

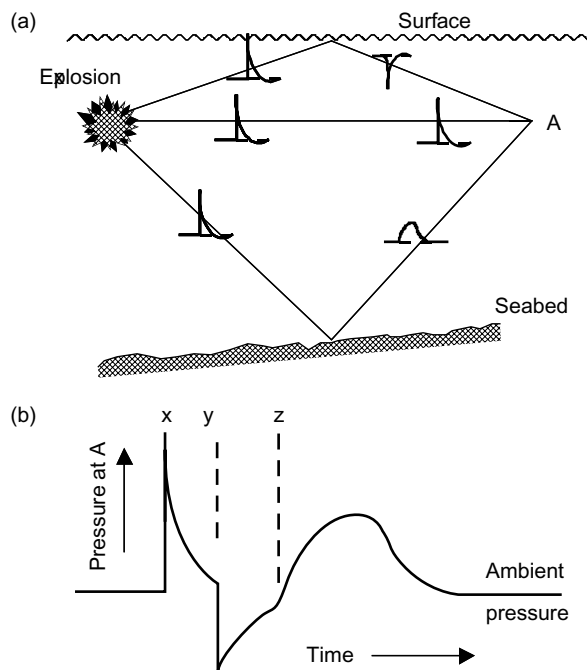


**Fig. 4.11** Effect of boundary reflections. (a) Direct and reflected transmission paths to the observation point A, showing the individual pressure waveforms. (b) The pressure signature observed at A: x, the shock front arrives first by the direct path; y, the surface reflection reverses the pressure change; z, the bottom reflection arrives last.

is not wanted. Marshall (1998) has described a model for predicting the acoustical properties of line charges, backed by experimental results obtained with three types of explosive cord (known commercially as HLX, PETN and RDX).

An alternative practical approach is to experiment with the detonation of a very small charge at the intended explosion site, and to record the resulting shock by means of several hydrophones placed at different locations in the area. The measurements may be scaled to predict what will happen when the ‘big bang’ occurs, by reference to the similarity principle, which states that the parameters of the shock wave are the same when distances are measured as the number of charge radii (Cole 1948). In the case of spherical charges, the radius is proportional to the cube root of  $W_e$ , the weight of the explosive material. Thus the maximum pressure, for example, is a function of the ratio  $(W_e^{1/3}/R)$  and has no other dependence on  $W_e$  or  $R$ .

#### *Biological effects of explosions*

The damage to aquatic life caused by underwater explosions has been the subject of many investigations from the time, just after the Second World War, when surplus munitions had to be disposed of (e.g. Aplin 1947; Hubbs and Rechnitzer 1952;

Teleki and Chamberlain 1978). The shock fronts described above may injure nearby fish. The damage depends on several variables apart from the size of the explosion, notably the relative positions of the source, the fish, the water surface and the seabed. Fish close to the blast may be killed instantly by the shock wave, while those at greater distances suffer less damage. Depending on such factors, death is not necessarily immediate but may still occur a day or two later.

The damage to exposed animals may include scale loss, the tearing of muscle tissue, haemorrhaging, and rupturing of internal organs such as the liver or spleen. The swimbladder, in those fish which possess one, is particularly responsive to pressure changes. Fish that have no swimbladder, and shellfish, are much more resistant to the stress of explosive shock, size for size. For the same species, large animals are less susceptible to damage than small ones.

Mortality in the vicinity of an explosion is revealed by the dead fish which float to the surface following the blast. However, counting them provides no indication of the mortality rate: the number of live fish will be uncertain, and some of the corpses may sink. A more scientific technique is to place fish in cages at different distances from the centre of the explosion. The proportion of mortalities in each cage can then be related to the physical parameters of the shock wave, to describe the biological effect in quantitative terms.

The proportion of mortalities is one measure of the biological effect of the explosion. For example, we may describe an explosion in terms of  $R_{50}$ , the range at which 50% of the exposed fish are expected to die, or  $\Phi_{50}$ , the corresponding size of the impulse. Yelverton *et al.* (1975) conducted experiments on several different species and sizes of freshwater fish, including both physostomes and physoclists, held in cages exposed to the detonation of 0.45 kg Pentolite charges. They found that the mortality correlated well with the impulse but not with the peak pressure. When the experimental results are plotted on a logarithmic graph, the data lie close to a straight line (Fig. 4.12). This suggests that  $\Phi_{50}$  is proportional to some power of  $w_f$ , the weight of one fish, and a simple empirical formula can be derived by log-log regression. If  $W_f$  is in kilograms, the Yelverton formula giving  $\Phi_{50}$  in Pascal seconds (Pa s) is:

$$\Phi_{50} = 371 W_f^{0.32} \quad (4.1)$$

However, Yelverton *et al.* (1975) only observed fish close to the surface. Following the initial shock, the pressure reversal in the surface reflection results in a strong rarefaction which is particularly damaging to fish. As the depth increases, the surface rarefaction is reduced by the ambient pressure; it is unimportant at depths greater than 10 m. Furthermore, fish near the surface are exposed in ventral aspect, from which direction they are most vulnerable to damage from shock waves (Sakaguchi *et al.* 1976). We therefore consider that the Yelverton model can only be applied to fish within a few metres of the surface. For deeper fish, Equ. (4.1) greatly underestimates  $\Phi_{50}$ .

Wiley *et al.* (1981) suggest that the mortality of fish at any depth depends primarily on the expansion and contraction of the swimbladder in response to the explosive

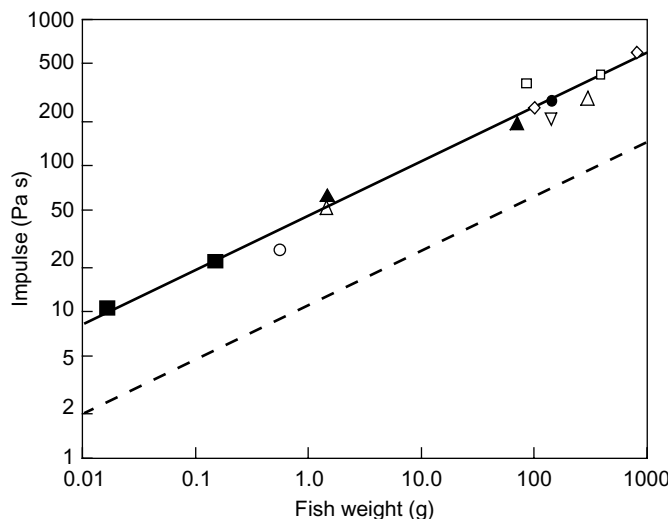


**Fig. 4.12** Mortality of fish exposed to underwater explosions as a function of the explosive impulse and the fish weight. Points are the observed 50% mortalities. Physoclists: ■ guppy, *Lebistes reticulatus*; ▲ bluegill, *Lepomis macrochirus*; ● black bass, *Micropterus salmoides*. Physostomes: ○ minnow, *Gambusia affinis*; Δ goldfish, *Carassius auratus*; ▽ rainbow trout, *Onchorynchus mykiss*; □ channel catfish, *Ictalurus punctatus*; ◇ carp, *Cyprinus carpio*. Solid line, log-log regression of the 50% mortality data (Equ. 4.1); dashed line, impulse level for no injury. (Redrawn from Yelverton *et al.* 1975.)

forces. They define a ‘bladder oscillation parameter’ ( $\zeta$ ) in terms of changes in the equivalent spherical radius (ESR, the radius of a sphere having the same volume as the swimbladder). This parameter is:

$$\zeta = 100 \ln(\text{ESR}_{\max} / \text{ESR}_{\min}) \quad (4.2)$$

where the subscripts ‘max’ and ‘min’ refer, respectively, to the maximum and minimum ESRs as the swimbladder volume oscillates. From experiments with spot, *Leiostomus xanthurus*, and white perch, *Morone americana*, Wiley *et al.* (1981) found that for fish at different depths, the mortality correlates well with  $\zeta$  but not with  $\Phi$ . Goertner (1978) has shown how  $\zeta$  may be calculated from the observed pressure waveform, leading to a model which predicts the mortality for any positions of the charge and the fish relative to the surface. He suggests that the mortality is 50% when  $\zeta = 125$ . However, this model shows that  $R_{50}$  depends on the fish size and depth in a complicated way. In certain circumstances, perhaps owing to resonance between the bladder oscillation and the pressure changes, the mortality is more than that expected from simple theory. When the shock front is propagating in free-field conditions, distant from the surface, the Goertner model predicts that  $\Phi_{50}$  is more than 10 times the value suggested by Yelverton *et al.* (1975).

The Goertner model seems to be the most accurate of those developed to date. However, it is complicated and difficult to apply in practice, since it requires detailed

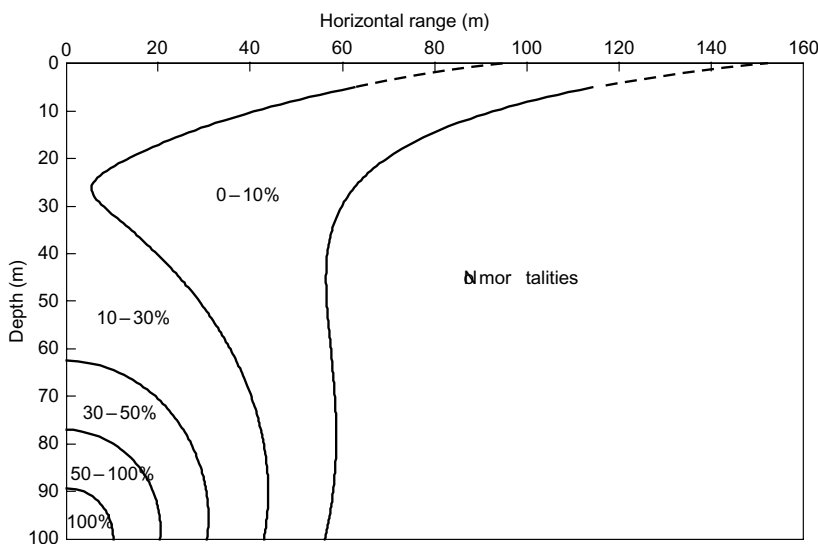


**Fig. 4.13** Predicted mortalities according to the Baxter model; example of a 90 g fish exposed to 11 kg of TNT detonated at 100 m depth. Due to pressure release at the surface, the mortality above 5 m (broken curves) will be less than predicted here.

knowledge of the pressure signature throughout the volume affected by the explosion. Baxter (1985) proposed a simpler method for predicting the fish kill, which nevertheless takes account of the fish weight and depth. He suggests that the energy flux ( $J$ ) rather than the impulse, provides the best correlation with the mortality. The Baxter model determines the mortality as a function of the parameter  $Y$  defined by the formula:

$$Y = J / [W_f^{1/3} (1 + 0.1 z_f)] \quad (4.3)$$

where  $z_f$  is the depth of the fish in metres and the term  $(1 + 0.1 z_f)$  is the ambient pressure in atmospheres. When  $J$  and  $W_f$  are expressed in SI units as previously, comparison with experimental data shows that 50% mortality is likely when  $Y = Y_{50} = 400$ . Also, the values of  $Y$  corresponding to 0% and 100% mortality are  $Y_0 = 49$  and  $Y_{100} = 1860$  respectively. These criteria can be used to draw contour maps of the region where fish are likely to be killed. An example is shown in Fig. 4.13, using the relevant formula from Table 4.6 to estimate the energy flux. This calculation does not take account of the pressure release at the surface, so the Baxter model should only be used to predict the fish kill at depths of several metres or more.

So far we have only considered fish with swimbladders. The fate of marine mammals is another area of concern. O'Keefe (1985) extended the Goertner model to mammals on the assumption that changes in the volume of the lungs will be a major factor, and including a margin for intestinal injury which is caused primarily by the peak pressure. For example, suppose a 4500 kg charge of TNT is detonated at 400 m

depth. The model predicts that a 6 m whale at the same depth would be uninjured at a range of 330 m or more. For the same whale at 100 m depth, however, the safe range is 820 m. Again, contours of the damage risk may be drawn to show how the danger zone depends on the depth and size of exposed animals.

High-energy sources other than the high explosives appear to cause little mortality, although Kostyuchenko (1971) found that airguns are capable of destroying fish eggs within a few metres' range. Non-lethal effects might also have important consequences. In a study of caged pink snapper (*Pagrus auratus*), exposed to an operating airgun over some two hours, McCauley *et al.* (2003) showed that the fish suffered extensive damage to the sensory epithelia of the ears. This appeared to be a long-term if not permanent injury; 58 days after the exposure, when the observations ended, there was no sign that the damaged sensory cells were being repaired or replaced. Hastings *et al.* (1996), working with pure tones at low frequencies, also found that intense sounds (>180 dB re 1  $\mu$ Pa) can damage the hair cells of the fish ear.

Even if there is no physiological damage, airgun pulses might disturb fish sufficiently to modify their behaviour (Pearson *et al.* 1992). In wild fish, this would very likely be a flight response away from the area of the survey. This behaviour seems to depend on the type of fish involved. Engås *et al.* (1996) report that the catch rates of bottom trawls declined by some 50% in the vicinity of seismic survey operations in the Barents Sea, and did not recover to the previous levels during several days of fishing after the survey ended. In the case of pelagic species, Slotte *et al.* (2004) suggest that both vertical and horizontal reactions are involved, since the fish were seen in deeper water during the seismic operations, and the fish abundance was less inside compared to outside the survey area.

#### **4.5.2 Noise pollution**

Apart from the occasional high-energy shocks discussed above, man is responsible for more widespread acoustical disturbance of the aquatic environment, covering a wide range of frequencies and intensities, which is reasonably described as 'noise pollution'. This comes from the many different sounds generated by shipping, military, research, recreational and industrial activities (review, Richardson *et al.* 1995). Anthropogenic noise in the sea has increased dramatically over the past century (Ross 1976; Curtis *et al.* 1999). It is important to understand the consequences of this contamination for fish and mammals (including human swimmers and divers), as a basis for mitigation measures which might be adopted to minimize any harm.

The biological effects of noise pollution can be broadly classified as follows, in descending order of severity: (a) immediate traumatic death, normally occurs only with local explosive shocks; (b) physiological damage e.g. hearing impairment, non-lethal in the first instance but may affect long-term survival prospects; (c) no physical injury, but behavioural changes occur which may have adverse consequences for the animal itself, or for other human activities such as fishing.

The important parameter to be considered is the noise level at the exposed animal. Thus, even strong noise sources will have negligible effect if the animal is far enough away. We should also remember that the sea is naturally a noisy place (Wenz 1962). Fish and aquatic mammals have evolved with adaptations for their survival in a permanently noisy environment. There is no reason to be concerned about man-made sounds unless they are somewhat above the normal ambient level at frequencies detectable by biological hearing mechanisms.

Exposure to loud sounds over a period of time can alter the hearing ability. This can be demonstrated by measuring the auditory thresholds before and after the exposure, with reference to pure tones (in the absence of noise) at frequencies near the centre of the hearing range. Hearing impairment is indicated by a positive threshold shift ( $\sim TS$ ) which is deemed to be temporary (TTS) or permanent (PTS) according to whether the animal recovers its former sensitivity by some time limit (normally many days) after the exposure (Richardson 1997). There is no auditory threshold shift if the noise is minimal, but we suppose there is some level of intensity above which TTS is likely, and a higher level associated with the onset of PTS. It would be logical to evaluate noise impacts by reference to these critical limits. If the noise source is localized, a drilling rig for instance, the intensity of the exposure decreases with distance. Thus it should be possible to define risk zones around the source, bounded by the intensity contours corresponding to the mentioned criteria for TTS or PTS effects (Heathershaw *et al.* 2001). These zones would not be the same for all species, but the precautionary principle suggests that the impact assessment should be based on the largest zones, i.e. those relevant to the animals with the most sensitive hearing. The difficulty with this approach, at present, is the shortage of experimental data on the TTS/PTS criteria relevant to fish and marine mammals. Only a few species have been investigated so far – the bottlenose dolphin (Ridgway *et al.* 1997; Schlundt *et al.* 2000); the harbour seal (Kastak and Schusterman 1996); the beluga whale (Erbe and Farmer 2000b) and a variety of fish (Popper and Clarke 1976; Scholik and Yan 2001; 2002). Scholik and Yan found that hearing-specialist fish were more likely to suffer TTS/PTS than non-specialists exposed to the same noise signal.

Behavioural changes may still occur in response to sounds below the TTS criterion. Hearing ability is again the main factor to be considered. We suppose that any such effect depends on the difference between the noise level and the auditory hearing threshold. However, many species with different hearing abilities may be involved, for instance if the requirement is to write a general environmental impact statement for some installation or activity. Heathershaw *et al.* (2001) suggest that noise evaluation should be based on a generic threshold value (GTV). This is a curve following the hearing thresholds of the most sensitive species at any frequency (Fig. 4.14). The GTV is constructed by grouping audiograms in three frequency bands: 10–300 Hz (fish); 300–1500 Hz (humans) and 1.5–100 kHz (marine mammals). The duration of exposure to the noise is also important. For the same sound pressure amplitude, we expect many hours to be more damaging than a few seconds of exposure. This leads to the concept of the sound dosage which is well known in human studies.

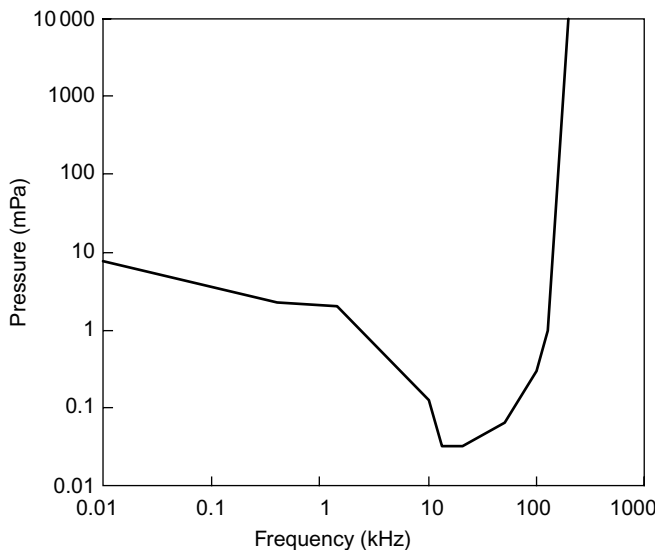


**Fig. 4.14** A generic threshold curve of hearing ability vs frequency. The curve follows the most sensitive auditory thresholds of fish (10–300 Hz), humans (300–1500 Hz) and aquatic mammals (1.5–100 kHz). (Redrawn from Heathershaw *et al.* 2001.)

The dosage is a logarithmic measure (expressed in dB) that increases with both the amplitude and the duration of the noise. In principle, critical dosage levels might be established which should not be exceeded if effects like PTS or TTS are to be avoided. There is insufficient knowledge to do this properly for fish and aquatic mammals, however, Heathershaw *et al.* (2001) suggest that the sound dosage criteria developed for humans might be applied to other species. This approach may seem doubtful, but it has some scientific justification given the basic similarity of the audiological response and inner-ear transduction mechanisms among species of particular interest (Richardson *et al.* 1995; Hastings *et al.* 1996).

There is an extensive literature on the behaviour of fish and mammals in response to intermittent or continuous noise. The tendency of animals to move away from high-energy sources has already been mentioned. Mitson and Knudsen (2003) have reviewed the noise radiated by vessels in relation to the hearing ability of fish; their bibliography includes many references describing the avoidance behaviour of fish near a moving vessel and/or fishing gear. While the mean noise level is the main factor to be considered, other characteristics such as amplitude variation can also influence the behavioural response (Engås *et al.* 1995). Vessel noise is mostly at low frequencies within the normal hearing range; however, high-frequency sonar pulses may cause a similar response. Gregory and Clabburn (2003) report that the clupeoid *Alosa fallax fallax* avoided a monitoring site where there was a 200 kHz echosounder, but not when this was replaced by one operating at 420 kHz.

The behaviour of exposed animals (apart from any avoidance reaction) can be disturbed even when the noise level is below the TTS criterion. Erbe and

Farmer (2000b) suggest that the risk zone for altered behaviour is only slightly less than that corresponding to the auditory threshold. It is well known that cetaceans can adjust their acoustic behaviour according to the ambient noise, whether it is natural or anthropogenic (Richardson *et al.* 1995; Richardson and Wurtsig 1997). For example, Foote *et al.* (2004) found that killer whales increase the duration of their vocalizations in the presence of boat noise. The significance of such effects is unclear. Hearing ability is hugely important to aquatic mammals for the detection of predators, prey and potential mates. Therefore, it has to be said, any interference which degrades the acoustic performance of aquatic mammals could be harmful to an uncertain extent. Clearly there is need for further investigation of this topic.

Not all noise is harmful, indeed, acoustic devices can be beneficial in motivating helpful behaviours in some cases. For example, high-power transmitters are often used in aquaculture to repel dolphins or seals which would otherwise attack the farmed fish (Richardson 1997). Similar devices attached to fishing gear have had some success in reducing the bycatch of marine mammals (Goodson 1997; Kraus *et al.* 1997). Knudsen *et al.* (1994) describe an acoustic barrier to control the movement of salmon smolts in a river. A continuous 10-Hz sound field provided an effective barrier, but transmissions at 150 Hz were ineffective even at intensities 114 dB above the hearing threshold. Maes *et al.* (2004) showed that 20–600 Hz sound could repel estuarine fish away from the cooling water inlet of a power station. Among the various species present during this study, those with a swimbladder (especially clupeoids) showed a strong avoidance response, but the scaring device had little effect on fish without a swimbladder.

### 4.5.3 *Limiting the damage*

Man-made noise is an inevitable consequence of many social and commercial activities, but we should consider what can be done by way of mitigation measures, to reduce or eliminate the least desirable impacts on the environment. This may be a specific requirement imposed by law, as in the United States where strict regulations are in force to protect marine mammals. These are expressed in terms of the harrassment at different levels, e.g. physical damage or behavioural disturbance, although Richardson (1997) notes that there is some doubt as to the exact definition of harrassment and what constitutes a ‘biologically significant disturbance’ in the legal context.

We have already discussed the biological effects on exposed animals in relation to the noise they experience. The next step in the impact assessment is to determine the amplitude, frequency content and temporal structure of the noise at different locations within the area affected by the sound source. This might be done by physical measurement if an existing activity is being investigated. Alternatively, an acoustic propagation model can be used to show how the noise level depends on the range from the source, reflections from boundaries and so forth. The theory for this calculation is reasonably well developed (Jensen *et al.* 1994; Erbe and Farmer 2000a; 2000b).

Of course, the modelling approach is essential when proposed new activities are being investigated, or if the need is to evaluate different mitigation measures that might be adopted.

Various precautions may be considered to minimize the risks of noise exposure. In the case of seismic surveys or other deployments of high-energy sources, the work might be done in a season when fish are least likely to be present. A scouting ship could be used to search the area by sonar, to ensure that no large schools were near the work site. When explosives are to be used in seabed excavations, the deeper the charge is buried the better, and the burial hole should be properly backfilled to reduce the energy transmitted into the water. The use of linear explosives instead of a point charge might achieve the same mechanical effect but with a reduced shock wave, especially at short distances from the detonation. More generally, mitigation measures might include any or all of the following options. Further details will be found in Richardson (1997).

- (1) Equipment design modification, e.g. to reduce the source level to the minimum compatible with the work objective.
- (2) Restrictions on the season, time of day and geographic location of the work, to avoid sensitive areas and periods when the damage risk is unacceptably high.
- (3) Revised operational procedures, e.g. a seismic survey might start with low-level emissions which ramp up to the maximum required. The idea here is to induce nearby animals to flee the area before the disturbance becomes harmful.
- (4) Real-time monitoring of the risk zones so that, if animals are detected there, operations can be suspended until it is safe to resume.

## 4.6 The swimbladder

Most fish have a swimbladder, a gas-filled organ within the body cavity. Due to the large density contrast between the gas and the fluid medium, the swimbladder has a number of important acoustical properties. It can act as a hearing aid (cf. Section 4.3) and contributes most of the energy in fish echoes. The high-frequency scattering properties of fish are discussed later, in Chapters 5 and 6. Here we confine attention to the generally lower frequencies around the resonance which is a characteristic feature of gas bubbles in water.

It is often assumed, as a first approximation, that the swimbladder behaves acoustically like a free gas bubble of the same volume. A bubble surrounded only by water is nearly spherical, and a well-established theory describes how it responds to insonification from a distant source (Minnaert 1933; Weston 1967). When undisturbed, the gas pressure inside the bubble equals the ambient pressure in the water. If the size of the bubble is changed from this equilibrium by an external force such as acoustic waves, the gas pressure will also change, in accordance with Boyle's Law which states

that, if the temperature of the gas does not change, the pressure is inversely proportional to the volume or the cube of the bubble radius. The disturbed bubble has a natural oscillation frequency as it alternately expands and contracts about the equilibrium. This frequency is determined by the compressibility of the gas (the bubble acts like a spring) and the inertia of the water which must move to accommodate the changing volume of gas. If the frequency of the external force is close to the natural oscillation frequency, the bubble is said to resonate. The motion of the bubble wall is then greater, and the radiated acoustic waves are stronger than at other frequencies (cf. Fig. 2.20).

The resonance frequency of the free bubble depends on the ambient pressure  $P_0$ , the water density  $\rho$  and the equilibrium bubble radius  $a$ , according to the equation:

$$f_r = \frac{1}{2\pi a} \sqrt{\frac{3\gamma P_0}{\rho}} \quad (4.4)$$

where  $\gamma$  is the ratio of the specific heats of the gas (1.4 for air). Other formulas have been derived for more realistic structures, with the gas bubble contained by a membrane (the bladder wall) and surrounded by fish flesh (Andreeva 1964; Ye and Farmer 1994). The swimbladder generally has an elongated shape with an irregular surface (Whitehead and Blaxter 1989). The natural tendency of the contained gas to form a sphere is resisted by the bladder wall and the surrounding tissues. Thus the acoustic properties of the swimbladder are unlikely to match those of the equivalent free bubble. Another complication arises when many fish (e.g. a school) are insonified at the same time. Then, multiple scattering within the school results in different scattering amplitudes and resonance frequencies compared to those observed with isolated fish (Ye and Farmer 1994; Feuillade *et al.* 1996).

Despite these complications, Equ. (4.4) is a simple approximation which is good enough for some investigations. To apply it to fish swimbladders, we must first decide on the appropriate value for  $a$ . There is likely to be much variation among species, and even between individual fish of the same size and species, but we can say that  $a$  is typically 5% of the total fish length. For example, consider a 10 cm fish near the surface where  $P_0$  is 1 atmosphere ( $10^5 \text{ Nm}^{-2}$ ). The density of seawater is  $1029 \text{ kg m}^{-3}$  and  $a$  is 0.005 m. Substituting in Equ. (4.4),  $f_r$  is estimated to be 640 Hz. This is much lower than the frequencies typical of fishery sonars. However,  $f_r$  increases with depth and is greater for smaller fish. In the case of fish larvae,  $f_r$  could be as much as 40 kHz.

The resonance frequency changes with depth in a manner which depends on the mass of gas in the swimbladder. If this mass remains constant, as is likely for physostomes such as the clupeoids, which are unable to secrete gas into the swimbladder, then the equivalent bubble radius is proportional to  $P_0^{-1/3}$  and  $f_r$  will vary as  $P_0^{5/6}$ . However, some fish adjust the amount of gas in the swimbladder. Physoclists such as the cod, *Gadus morhua*, do this to maintain the same volume (and the same buoyancy) against changes in the ambient pressure. If the volume is constant, so is the equivalent bubble radius and  $f_r$  should then vary as  $P_0^{1/2}$ . Both the  $P_0^{1/2}$  and

$P_0^{5/6}$  dependences have been observed in measurements of the resonance frequency of species which undergo vertical migrations (Hersey *et al.* 1962; Mozgovoy 1986). These migrations usually occur as a diurnal rhythm, in response to changes in the light level between night and day.

In experiments where cod are moved rapidly from one depth to another, so that the fish do not have time to adapt by secreting or absorbing gas, it is found that the  $P_0^{5/6}$  law is followed while the swimbladder is compressed below its normal volume (Sand and Hawkins 1973). However, the resonance frequency is then about 25% higher than that predicted by Equ. (4.4). For fish close to the adaptation depth, with fully inflated swimbladders, the difference is much greater. The observed resonance frequency can be as much as six times the predicted value. These results are explained by the elasticity of the bladder wall and the surrounding tissues, which have a greater effect on the resonance frequency than the non-spherical shape of the organ.

When fish are insonified at frequencies near the resonance, more energy is scattered out of the incident wave. This has important consequences for long-range sonars and underwater communication devices, which operate at relatively low frequencies, since the transmission loss can be much increased when the propagation path is through aggregations of fish. See Ye (1996) and Diachok (1999) for a theoretical analysis of this problem.

In principle, the spectrum of low-frequency echoes from fish can be used to determine their size, on the assumption that peaks in the spectrum correspond to the resonance frequencies of swimbladders (Hawkins 1977). Løvik and Hovem (1979) showed that for several species adapted to surface pressure, including both physoclists and physostomes, the resonance frequency in Hz is related to the fish length  $L$  in metres, according to the empirical formula:

$$f_r = 120 / L \quad (4.5)$$

The frequency predicted by this formula is too low for herring and too high for cod (Fig. 4.15). This is perhaps unsurprising, since the swimbladders of the two species are dissimilar in structure and function (Blaxter and Batty 1990). It would be more accurate to apply Equ. (4.5) with a different constant multiplier for each species. This should be 170 for herring and 80 for cod, according to Løvik and Hovem (1979).

The variation with depth complicates the calculation of fish size from the observed resonance frequency. For fish that are adapted to surface pressure and then move quickly downwards, without changing the amount of gas in the swimbladder, the 5/6 pressure law applies and we suppose that:

$$f_r = K(1 + z / 10)^{5/6} / L \quad (4.6)$$

where  $K$  is a constant for each species, typically 120, and  $z$  is the depth in metres. This equation should apply to physostomes in the course of vertical migration as a natural behaviour. However, in the case of physoclists which have been at depth for some time, the resonance frequency is expected to be less than that predicted by

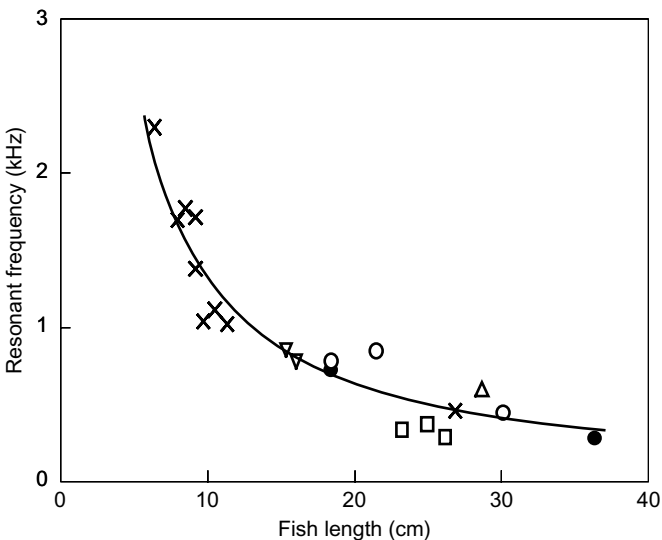


**Fig. 4.15** Relationship between swimbladder resonance frequency and length of surface-adapted fish:  $\times$  saithe, *Pollachius virens*;  $\circ$  pollack, *Pollachius pollachius*;  $\square$  cod, *Gadus morhua*;  $\bullet$  trout, *Salmo trutta*;  $\Delta$  herring, *Clupea harengus*;  $\nabla$  sprat, *Sprattus sprattus*. The fitted curve is  $f_r = 120/L$ . (Redrawn from Løvik and Hovem 1979.)

Equ. (4.6). Depending on how much gas the fish has secreted to reinflate the bladder,  $f_r$  could be reduced by as much as  $(1 + z/10)^{1/3}$  times.

In practice, the received signal will normally consist of the superimposed echoes from many fish or other scatterers at similar ranges. The ability to distinguish targets of different size depends on the sharpness of the resonance peak. This is described by the Q factor. If  $f_1$  and  $f_2$  are the frequencies on either side of the peak at which the echo intensity is half the peak value, Q is defined as the ratio  $f_r/(f_2 - f_1)$ . For fish swimbladders, Q is generally in the range 2–5. When fish move rapidly downwards from the adaptation depth, so that the swimbladder is compressed, Løvik and Hovem (1979) report that Q increases linearly with depth. However, in the case of physoclists that remain at the new depth for some time and are able to restore the bladder volume, Q gradually decreases to the original value. This implies that for a fully inflated swimbladder, Q is independent of the ambient pressure.

As a general rule, it should be possible to distinguish two peaks in the echo spectrum which are more than  $(f_r/Q)$  apart. Figure 4.16 shows an echo spectrum which Holliday (1977b) obtained by detonating small explosive charges near the surface. Two peaks are evident at the low-frequency end of the spectrum, and can be associated with particular species by comparison with catches of schooling fish in the same area. The lower resonance is due to jack mackerel, *Trachurus symmetricus*, of mean length 180 mm, and the other is northern anchovy, *Engraulis mordax*, of lengths (from a small sample) in the range 97–146 mm. Holliday confirmed that the

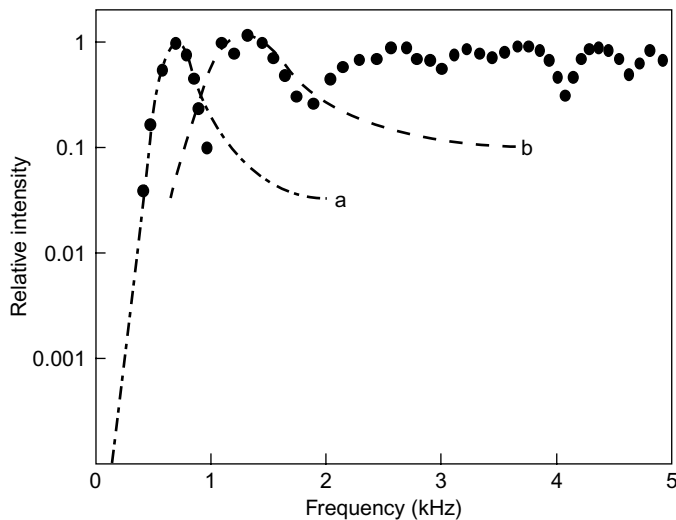


**Fig. 4.16** Spectrum of echoes from schooling fish. Points are measured intensity per unit bandwidth, relative to the maximum spectrum level. Theoretical curves fitted to the peaks: (a) jack mackerel, *Trachurus symmetricus*; (b) northern anchovy, *Engraulis mordax*. (Redrawn from Holliday 1977b.)

higher resonance is associated with the anchovy by means of other experiments when only that species was present. Thompson and Love (1996) applied the same method in different regions – Arabia, Europe and North America. In each case, they showed that the combination of broadband scattering measurements below 5 kHz and swimbladder-model calculations could reveal important features of the abundance and size composition of fish stocks. This approach depends on the fish being in layers which can be identified on echograms. A different analysis is required for each layer so identified.

The resonance technique for fish sizing is difficult to apply in practice because of the strong dependence of the resonance frequency on the depth as well as the size of targets. To obtain useful results, it is necessary to know the history of vertical movements of the observed fish. This information has to be inferred from prior knowledge of fish behaviour, such as the vertical migrations regularly undertaken by certain species of fish.

# Chapter 5

## Observation and Measurement of Fish

### 5.1 Introduction

Active sonars and echosounders are devices which transmit an acoustic pulse through a transducer into the water. The pulse travels away from the transducer, but the transmitted energy is concentrated in certain directions, within a beam whose width depends upon the size of the transducer. Any fish or other targets within the beam are said to be ‘insonified’ by the transmission, just as they would be ‘illuminated’ by a beam of light. The insonified targets scatter the transmitted energy, producing echoes which are subsequently detected by the receiving part of the instrument. The received signal will contain some information about the targets which generated the echoes, and the aim is to extract as much of this information as possible, by deciphering the signal as it were. This deciphering is known as the inverse scattering problem. It is relatively simple to calculate the signal generated by a known target (the forward scattering problem), but it is more difficult to work backwards, to say what targets might have caused the observed signal.

The information available to the observer depends on the type of equipment in use. A simple echosounder with a single-beam transducer is capable of detecting the presence or absence of targets, but little else, whereas modern echo-integrators, multi-beam sonars and the like can be much more revealing. Ideally, we want to identify the detected targets, to say what species and sizes of animals are present in the water, and to measure quantities such as the biomass or the number of fish in the acoustic beam. The more information that is required from the received signal, the more sophisticated the acoustic instrument has to be (Mitson 1983).

In this chapter, we consider first what can be achieved using simple echosounders of the type commonly found on fishing vessels, and how to interpret the visual representation of targets as displayed on the echograms produced by such equipment. We describe how echosounders and sonars can be used to measure the dimensions of fish schools. To do this, the observed width of marks on the echogram must be corrected to take account of the finite beamwidth. We show how the true size distribution of schools may be estimated from a set of two-dimensional sections as might be recorded by an echosounder along a transect. We go on to discuss the measurement of fish abundance which relies on more sophisticated survey techniques, intended

primarily for applications in fisheries research and management (Gunderson 1993). The alternative techniques of echo-counting and echo-integration are compared. Their advantages and limitations are discussed with reference to practical applications. The theory of fish abundance estimation is presented, to the level necessary for the calculation of fish densities from acoustic measurements. In the case of echo-integration, there is a simple relationship between the fish density and the backscattered energy, called the echo-integrator equation. The theory depends on a major assumption about the distribution of targets within the transducer beam, known as the linearity principle. We discuss the experimental evidence in support of linearity. We also consider the circumstances in which it might not apply, most importantly through the shadow effect which may occur in dense fish concentrations. Finally, we describe various other techniques and acoustic instruments which can provide useful information on the behaviour, distribution and abundance of fish.

## 5.2 Simple observation methods

The single-beam echosounder is the simplest and cheapest of acoustic instruments. Nevertheless, it is capable of detecting any target that produces an echo above the background noise level. The detection of an echo indicates little more than the presence of some unidentified object, but one way to learn more is to view the signals received over a period of time or a number of transmissions. This is done by means of the echogram, which is a pictorial representation of the echosounder output. Figure 5.1 is a typical example of the monochrome display which shows a pattern of dark marks on a light background.

### 5.2.1 Interpreting the echogram

Following each transmission, the receiver output is displayed as marks along a vertical line. The dark horizontal line at the top of Fig. 5.1 is the transmission signal. The lower marks indicate echoes; the heavier the mark, the stronger is the received signal. When the echo from a particular target arrives at the receiver, the corresponding mark appears at a distance below the transmission line which is proportional to the range of the target from the transducer. Of course, the echoes from many targets, fish in a school for example, may combine to produce strong marks extended in depth. The picture is built up by displaying the signals from each transmission along successive vertical lines which are separated horizontally by a small distance. If the transducer is stationary, the display represents a time series of observations of the same volume. In the case of Fig. 5.1, the signals are from a downward-looking echosounder on a ship which is travelling at constant speed in one direction. The display may then be viewed as a vertical cross-section of the water column. The transducer is close to the sea surface which corresponds nearly enough to the line of transmission marks. The strong echo from the seabed is evident in the middle of the

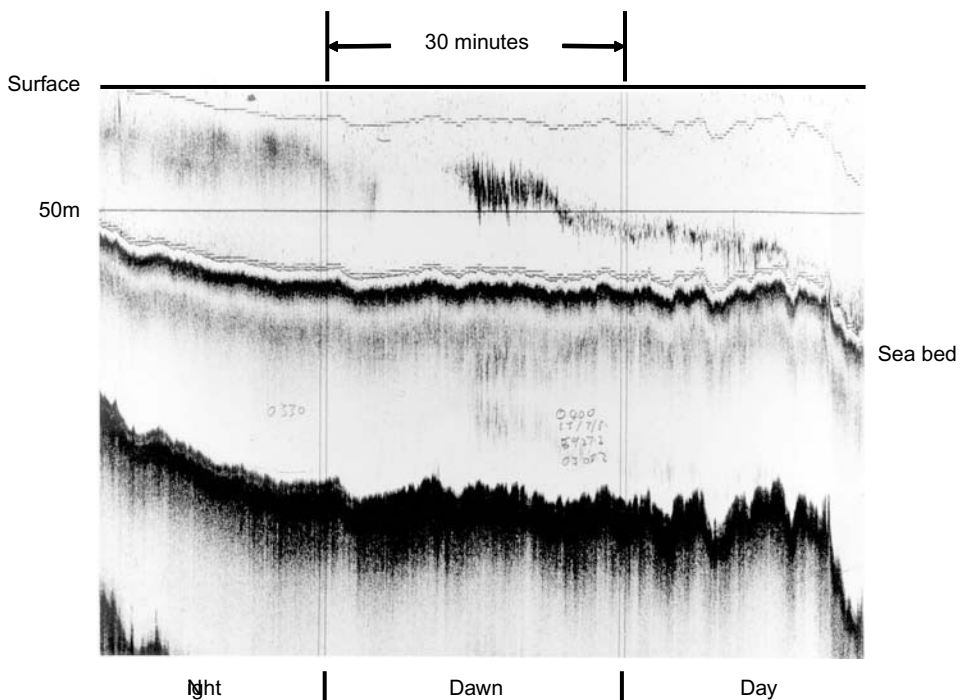


**Fig. 5.1** Example of an echogram recorded on a ship which is moving at 10 knots in a straight line. The echogram represents a vertical cross-section of the water column below the ship and shows the changing behaviour of the fish layer between night and day.

figure. The marks in between are due to fish or other targets such as plankton which have produced detectable echoes. A sequence of contiguous marks from successive transmissions is called a trace. The important point is that by examining the traces displayed on the one echogram, we gain additional information about the targets and their distribution in space and time. Fish may be observed as scattered individuals, or clumped in schools or aggregations, which may themselves have characteristic features. In Fig. 5.1, the echogram covers the period through dawn. The fish are seen to be dispersed as diffuse traces at night, then they aggregate in denser concentrations and descend as daylight comes.

The monochrome echogram has a limited range of contrasts as far as the human eye is concerned, and some of the information associated with the echo intensity will be lost. This limitation is overcome to a large extent when the echogram is displayed in colour, as is normally the case with modern echosounders. The signal intensity controls the colour. In the example shown in Plate 5.1, red indicates very strong echoes, the green marks are less strong, the blue ones are weak and the white areas are empty. On fishing vessels, this type of display is often shown on a cathode ray tube (CRT) without a permanent record. If a permanent record is required, a colour printer may be connected to the echosounder. Plate 5.1 shows marks in several layers

separated by depth. We can infer from the varied strength and structure of the marks that the layers contain different species and/or sizes of targets. The echogram on its own, however, does not provide sufficient information to determine the species or the size composition of the layers.

The underlying principles of colour and monochrome echograms are the same: they show how the acoustic reflectivity varies over a cross-section of the water column. The colour display provides a much better visual impression of the echo strength. However, for the particular task of comparing the size and shape of traces, when this is done by eye, it is easier to work with a monochrome display because the trace boundaries are more obvious.

Echograms may not provide sufficient information to identify the target species with certainty. Two species having similar gross anatomical features and occurring in similar school sizes could produce the same traces. In many cases, however, the size and shape of different traces on the echogram, and also their location in the water column, may suggest which species are present. To interpret the echogram in this way, the observer needs a good understanding of the local fish populations and their behaviour, especially as regards schooling. Even then, it is desirable to collect independent evidence (such as trawl samples) to be sure about the identification of targets.

### **5.2.2 Echosounder mapping**

When the fish are in schools, the echogram displays a ‘mark’ for each school, formed by the combined echoes from successive pings while the school is insonified. The shape of the mark provides useful information about the school size and structure, although some interpretation is required to deduce the true school geometry from what is seen on the echogram.

The simple concept of mapping fish schools with an ordinary downward-looking echosounder was pioneered by S. Olsen (1969). This can be done with very basic equipment – a cheap echosounder, a ship or boat to move over the area being surveyed, and some means of estimating the speed of travel. It is necessary to have a printer or another way of recording the echogram, so that the school marks can be examined at any time and previous measurements may be checked.

#### *School dimensions*

Figure 5.2 illustrates what happens as the survey vessel crosses a school. The mark shows all the echoes received while the beam intersects the school. The first step in the analysis is to measure the dimensions of each mark. The observed height  $H_m$  is determined directly from the echogram scale. The observed length  $L_m$  (along the ship’s track) is calculated from the distance travelled by the ship as it passes the school. If  $V$  is the ship’s speed and  $t$  is the time between the first and last detections of the mark, then  $L_m = Vt$ . However, the true length  $L_t$  is rather less than  $L_m$ , due to the finite size of the beam.

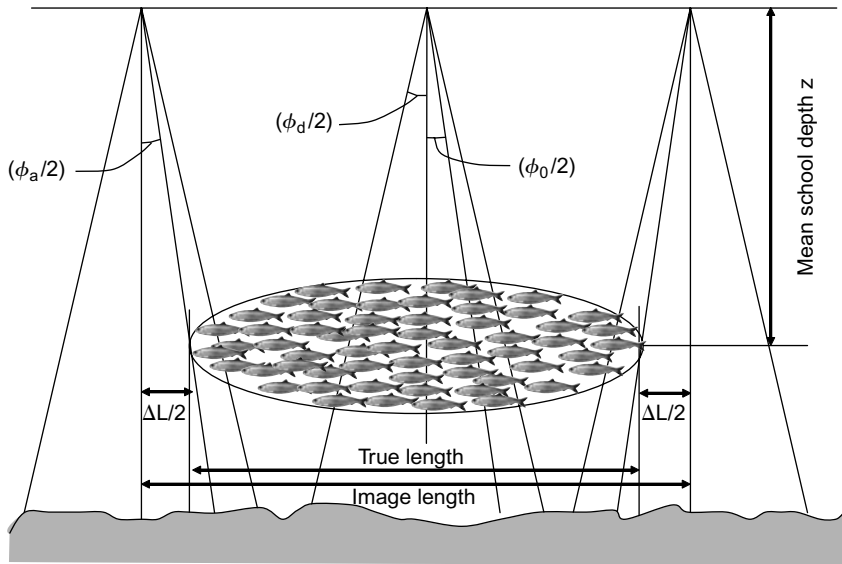


**Fig. 5.2** Illustration of various beam angles relevant to the detection of fish schools.  $\phi_o$  is the nominal beam width defined by the half-power points of the directivity function. The detection angle  $\phi_d$  defines the sampled volume for echo integration when the beam fully intersects the school. The attack angle  $\phi_a$  gives the directions of first and last points of contact. The image length and the true length differ by  $\Delta L = 2z \tan(\phi_a/2)$ . (Redrawn from Diner 1999.)

Suppose that  $\phi$  is the angle between the directions from the transducer to the points of first and last contact with the school. For an ideal beam,  $\phi$  is simply the angle across the apex of the insonified cone. If the first and last points of contact are at depth  $z$ , then the length correction is:

$$L_t = L_m - 2z \tan(\phi/2) \quad (5.1)$$

For a real transducer,  $\phi$  is traditionally assumed to be the nominal beam width specified by the manufacturer, namely the angle between the half-power points of the beam pattern,  $\phi_o$  say. For the purposes of school measurement, this is a crude approximation. The school is first detected as and when enough fish enter the beam to give an echo above the signal threshold (see below). This occurs at some off-axis angle  $\phi_a/2$  which is different from  $\phi_o/2$ . Diner (1999) calls  $\phi_a$  the ‘attack angle’ to make the distinction clear. He also defines a ‘detection angle’,  $\phi_d$  which is relevant once the beam fully intersects the school. It is the top angle of the cone that includes all the fish contributing to the school echo at a given time. The attack and detection angles depend on other factors apart from the beam pattern, notably the volume scattering strength inside the school ( $S_v$ ) and the signal threshold ( $S_{vo}$ ) which is set by the operator. The three measures –  $\phi_o$ ,  $\phi_a$  and  $\phi_d$  – are identical in the case of an ideal beam, but not for any realistic beam pattern. Misund *et al.* (1995), from their work on herring schools in the North Sea, say that  $\phi_a$  can be as much as 50% more

than  $\phi_o$ . The various calculations give quite different results. Consider a school which is observed on the echogram for 20 s at a mean range of 150 m while the ship passes at a speed of  $5 \text{ m s}^{-1}$ . The mark length is 100 m. Suppose  $\phi_o = 7^\circ$  and  $\phi_a = 10^\circ$ . The estimated lengths based on the nominal and attack angles are, respectively, 81.6 and 73.7 m.

The apparent height of the school should also be corrected to take account of  $\tau$ , the pulse duration. This correction is more important for small schools, although it is generally less important than that of length. If  $c$  is the sound speed, the true height is:

$$H_t = H_m - c\tau / 2 \quad (5.2)$$

Diner (1999) has developed a comprehensive theory of how the observed marks derive from the true dimensions. The signal threshold is another source of error which we have not yet discussed. This is applied to remove noise and small planktonic echoes from the fish marks, so that the school boundaries can be seen more clearly. If the signal-to-noise ratio is small, meaning that the school  $S_v$  is close to the threshold, the echoes from the few fish in the beam at first contact with the school may be too weak to be detected. This reduces the observed mark length, sometimes by more than the increase due to the beam width (i.e.  $L_m$  becomes less than  $L_t$ ). Diner (1999) suggests that the threshold effect is likely to be important if  $(S_v - S_{vo})$  is 3 dB or less. Clearly, to avoid this problem, the threshold should be set at the minimum level which allows satisfactory detection of the school boundaries.

#### *Size distribution of schools*

Having surveyed an area along a set of transects, observing many schools in the process, we may wish to know their size distribution. The school heights have been determined directly, and their distribution is easily expressed as a histogram of the height measurements. The horizontal dimensions are more complicated because only one has been measured, namely the length of some vertical cross-section of the school. If the school is large, most of the fish will be to the side of the survey track, beyond the transducer beam. Only a small proportion of the fish will have contributed to the echogram marks, and the histogram of school lengths, even after correction for the beam width, is not the true size distribution. The root of the problem is that the survey track crosses each school along a line which lies at an unknown distance from the centre of the school. The track is unlikely to cross the middle of the school. Consequently, the observed length will be less than the school diameter, supposing for the present that the schools are circular in the horizontal cross-section. Since the track crosses a particular school just once, all we know about the diameter of that school is that it is probably greater than the observed length.

A statistical analysis of many school observations can be done to obtain more quantitative results. The true size distribution may be expressed in terms of the

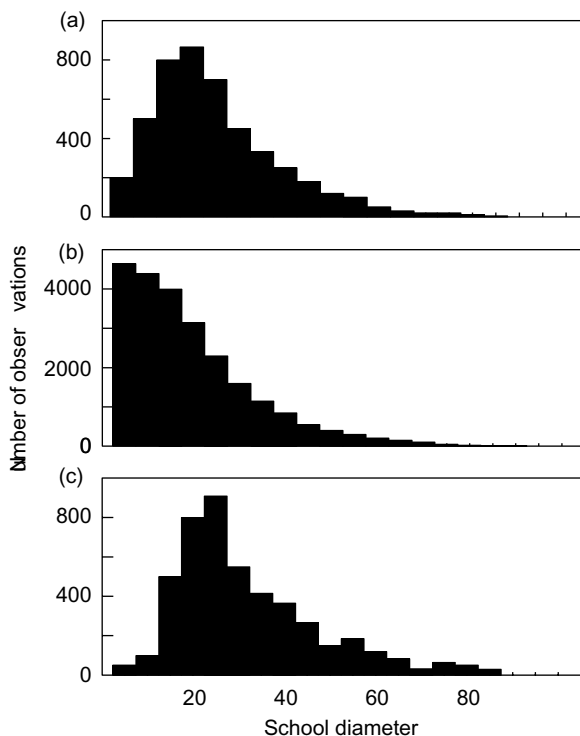


**Fig. 5.3** Estimation of the true distribution of school sizes from measurements of echogram marks. Example with hypothetical data. (a) Histogram of the observed mark lengths after correction for the beam width; (b) the cumulative distribution shows the number of schools larger than the indicated diameter; (c) the true size distribution estimated by the method in Appendix 5A.

frequencies of school diameters by size class, using the method described in Appendix 5A to convert the observed histogram of school lengths. An example of the results which can be obtained from this approach is shown in Fig. 5.3. The calculated histogram of school diameters will generally be a crude representation of the true size distribution. The method assumes that the beam width is small compared to the school diameter, so it is not applicable to very small schools. The results for the largest schools may also be anomalous. They are generally so few in number that an accurate estimate of the size distribution is impossible. Nevertheless, the frequencies of schools in the middle size classes can be predicted accurately, provided many schools have been detected within each size class. When the occasional large school is encountered, the best plan is to map the true dimensions directly, by crossing the school several times from different directions. Furthermore, the largest schools are most likely to have an irregular shape, in which case the simple theory based on circular cross-sections is not applicable. See Fréon *et al.* (1992) for examples of the complicated structures which can occur in nature, such as 'vacuoles' which are empty spaces within the school.

### *Fish density and abundance*

The echogram records locate fish concentrations and provide some information on the structure of schools. Beyond that, another objective might be to estimate the abundance of the target species which is the total volume occupied by schools multiplied by the mean packing density of the fish (i.e. the number of fish per unit volume). Consider the volume calculation first. It may be assumed that the survey track is equally likely to cross any part of the school. If many schools are observed and the mean observed length is  $\bar{L}_m$  it can be shown that on average the school diameter is  $(4/\pi)\bar{L}_m$ . Furthermore, the average school area is  $(3\pi/8)\bar{L}^2$ . These results are explained in Appendix 5A. If  $H_r$  is the height of the  $r$ 'th school as seen on the echogram, assumed to be representative of the entire school and not just the observed part, and  $L_r$  is the observed length of the same school (corrected for the beamwidth), an unbiased estimate of the volume of all the detected schools is:

$$V_{sch} = (3\pi / 8) \sum_r L_r^2 H_r \quad (5.3)$$

There are several possibilities for estimating the packing density. Firstly, the  $S_v$  of the school can be measured by echo-integration, and converted to fish density if the target strength is known. This method is complicated by the fact that all pings contributing to the mark do not fully intersect the school, see Diner (1999) for an analysis of this problem. Secondly, given the school volume which can be measured by sonar, the corresponding quantity of fish might be determined by capturing the whole school with a purse seine (Misund and Beltzstad 1996). Thirdly, general knowledge of fish behaviour may indicate natural limits on the separation of fish within schools. There is an extensive literature on this topic. Blaxter and Hunter (1982) have reviewed field observations of the packing density which Pitcher and Partridge (1979) suggest is typically one fish per cubic body length. Even for the same species in the same area, however, the packing density can be highly variable as reported by Misund *et al.* (1995) and Gauthier and Rose (2002).

When the area to be surveyed is large, many schools remote from the cruise track will not be detected. To estimate the total abundance, we need to know the area which has been sampled. This area may be estimated as the mean school diameter times the length of the cruise track; suppose it is a proportion  $P_{sch}$  of the whole area being surveyed. The total abundance is then estimated as  $V_{sch}/P_{sch}$ .

An unbiased measure of the fish abundance can also be obtained by noting the proportion of the cruise track over which schools are detected. For example, if the distance covered while schools are observed is 5% of the track, it may be assumed that regardless of the school shape or size, 5% of the surveyed area is occupied by similar schools. In the case of irregularly shaped schools, this technique should be more accurate than the alternative based on Equ. (5.3) which depends on the assumption that the cross-section of the average school is circular.

Echosounder mapping is particularly well suited to studies of the depth distribution and vertical structure of schools, as reported by Massé *et al.* (1996) and Fréon *et al.* (1996). It is not useful when the schools are mostly close to the surface, since the downward-looking echosounder does not detect fish in the near field or above the transducer. In that case, we require different techniques using other kinds of sonar equipment.

### 5.2.3 Side-scan sonar

When the fish are predominantly in the near-surface zone, good results can be obtained with a side-scan sonar. The original version of this instrument consists, essentially, of a single-beam transducer turned to point sideways, so that the beam is almost horizontal and perpendicular to the ship's track. Thus a wide area to the side of the ship can be observed.

Side-scan sonar is mostly used to image hard objects on the seabed like wrecks and oil pipelines. It has also proved useful in fisheries work, notably in the school-counting technique pioneered by Smith (1970; 1977). This method of school-counting is called sonar mapping. It has been successfully applied in studies of near-surface pelagic fish by Hewitt *et al.* (1976) and O'Driscoll and McClatchie (1998). The horizontally projected beam is also advantageous in shallow water, where it allows a greater volume to be sampled than would be possible with a vertical echosounder (Trevorow 1998; Trevorow and Pedersen 2000).

When sonar mapping with a towed side-scan, the ship moves in a straight line and the received signals are displayed on an echogram which now represents a rectangular area to one side of the survey track. Schools may be seen anywhere in this area, but they are included in the count only when they appear entirely within the 'observation band' which is a range interval,  $R_1$  to  $R_2$  say (Fig. 5.4). This is done to avoid bias in the results. At long range the echoes can be distorted by inhomogeneities in the transmission path, or hidden in background noise, while at short range the beam may not be deep enough to detect all the schools (Fig. 5.5). The observation band should be chosen so that the number of detected schools per unit area is the same at all ranges, within the margin of statistical error. The width and length of each school are derived in the same way as echosounder detections, by correcting the observed mark dimensions for the effect of beam width and pulse duration.

Smith (1970) used a 30 kHz sonar with  $10^\circ$  vertical beam width. He observed schools most frequently in the range interval 250–500 m, while few were seen close to the ship and beyond 750 m. He therefore chose 200–450 m as the observation band within which the probability of school detection was assumed to be independent of the range. However, the spatial distribution of detected schools may also depend on non-acoustic factors. O'Driscoll and McClatchie (1998) counted very few schools near the vessel track, suggesting that avoidance behaviour by the fish as well as the beam width determines the probability of school detection at close range. They used

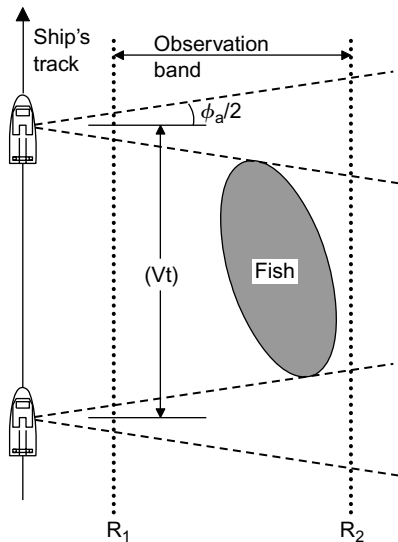


**Fig. 5.4** Geometry of the side-scan sonar beam. Schools are observed within the observation band between ranges  $R_1$  and  $R_2$ . The distance travelled while in contact with the school,  $Vt$ , is again greater than the actual school length due to the finite beam width.

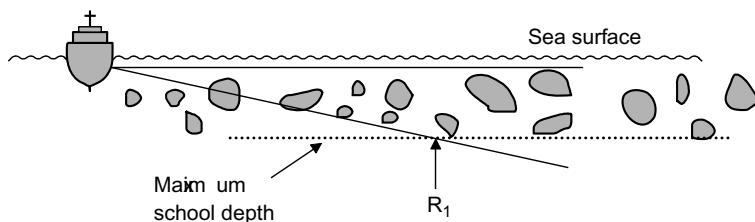


**Fig. 5.5** Horizontal view in the direction of the survey track. The schools are in a near-surface layer whose depth determines the near side of the observation band. At ranges less than  $R_1$ , some schools are outside the beam.

a 130 kHz side-scan sonar. The higher frequency restricted the useful range to 100 m, but it allowed better resolution of school shapes and sizes.

Even for one species, fish schools often occur in a wide range of sizes, and a particular school is likely to be irregular in shape. The width and length will be different, but we may suppose that the long axis of the school lies in any direction with equal probability. This is a reasonable assumption unless the schools adopt a preferred orientation owing to migration behaviour or reactions to the survey vessel. If we assume that the orientation is random, the frequency of school numbers among size classes should be the same whether it is the widths or the lengths that are used to determine the distribution. If many schools were to be superimposed, the irregularities would tend to cancel one another, leaving a circular shape as the mean cross-section of the ensemble (this term is defined on p. 191). If  $W^2$  is the mean squared width of the schools, then the expected cross-sectional area is simply  $\bar{A} = \pi W^2/4$ . If the area of

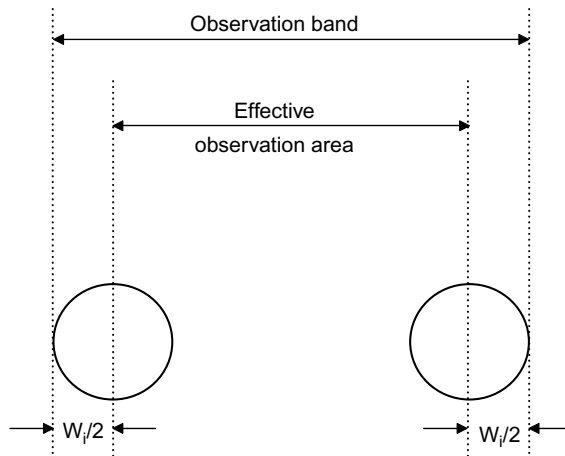


**Fig. 5.6** Correcting the school count for edge bias. The effective observation area is narrower than the observation band by an amount equal to the school diameter,  $W_i$ .

a particular school of width  $W_1$  and length  $L_1$  is required directly, then the formula for an ellipse should be used, namely  $A_1 = \pi W_1 L_1 / 4$ .

The results of school-counting are normally presented as a histogram of the number by size class. Suppose  $N_i$  schools are counted in size class  $i$ , and  $W_i$  is the width (or the diameter) at the class midpoint. It is necessary to correct the count for the edge effect, which reduces the apparent frequency of large schools. The problem arises because of the rule that schools are counted only when they are entirely within the observation band. If any part of a school is outside the band, the school is ignored. In Fig. 5.6, the area corresponding to the counted schools is within the dashed lines. The larger the school, the smaller is the effective observation area. If  $B$  is the width of the observation band, and  $N_{i(\text{cor})}$  is the corrected count which refers to the same area irrespective of the size class, then:

$$N_{i(\text{cor})} = N_i B / (B - W_i) \quad (5.4)$$

This formula depends on the assumption that  $N_i$  is large enough for the average school to be sensibly circular in shape. We suppose that sufficient schools have been measured to be reasonably certain of the mean and other statistics of  $W$ . Figure 5.7 shows the size distribution of northern anchovy schools counted by Smith (1970). The histogram is skewed to the left. Most of the schools are small, but a few are very large. The occasional large school which is the only one in a size class ( $N_i = 1$ ) should be examined individually to take account of the irregular shape in calculating the school volume or biomass.

The single-beam side-scan sonar gives no information on the school height, which is of course required to calculate the volume. However, Squire (1978) showed that the vertical size may be inferred from the horizontal cross-section if the schools are known to have a characteristic three-dimensional shape. The proportion of the

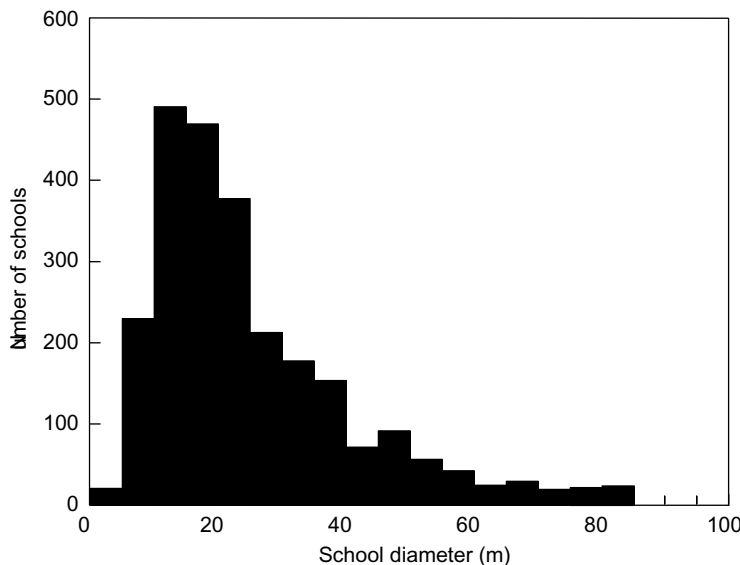


**Fig. 5.7** The size distribution of schools of northern anchovy, *Engraulis mordax*, from side-scan sonar counts corrected for edge bias. (After Smith 1970.)

surveyed area occupied by schools is:

$$P = \sum_i N_i \pi W_i^2 / (4BD) \quad (5.5)$$

The volume occupied by the schools is their total area times the mean height, and given the packing density, the fish abundance can now be estimated in the manner described for echosounder mapping.

The side-scan arrangement is also useful in surveys of near-surface dispersed fish, by means of echo-counting (see Section 5.3). This requires the echoes from individual fish to be identified and measured. Successful work on migrating salmon *Oncorhynchus* spp. has been reported by Tarbox and Thorne (1996) and Trevorrow (2001) using, respectively, dual-beam and sector-scanning sonars.

#### 5.2.4 Multi-beam sonar

A more complete picture of school shapes can be obtained using instruments which are sensitive to the direction as well as the range of targets, such as the multi-beam sonars described in Chapter 3. The direct measurement of school dimensions will be more accurate than the statistical treatment required in the case of measurements made with single-beam instruments (Misund and Beltestad 1989; Misund *et al.* 1992; 1995; 1996).

Misund *et al.* (1995) discussed the application of multi-beam sonar to the measurement of herring schools. They used a 95 kHz sonar (Simrad SA950) which has

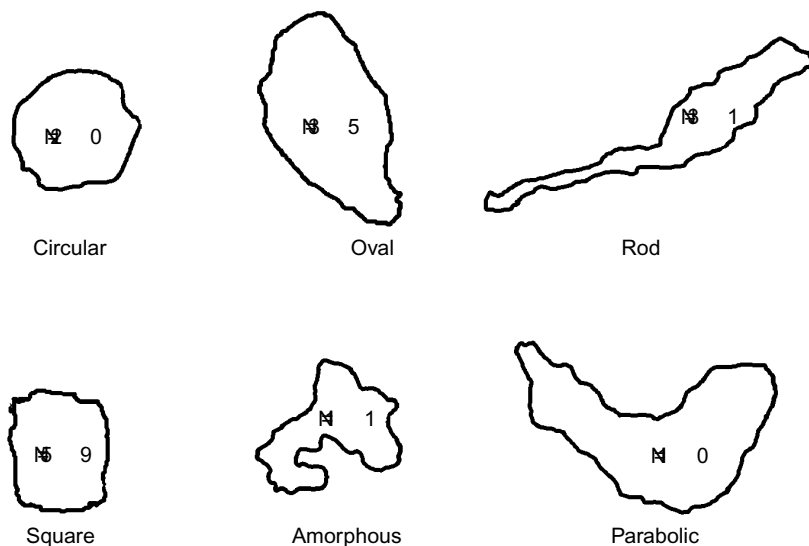


**Fig. 5.8** Horizontal cross-sections of herring schools revealed by multi-beam sonar. In total 166 schools were observed at 100 m range and 10–30 m depth. The outlines here are examples of six types of school identified by their approximate morphology. N is the number of schools of each type. (Redrawn from Misund *et al.* 1995.)

32 beams, each  $1.7^\circ$  wide, covering a sector of  $45^\circ$ . The beams were projected ahead of the vessel in a plane tilted  $5^\circ$  below horizontal to maximize the vertical coverage of near-surface schools. Thus schools could be observed continuously from the first detection (at a few hundred metres) until past the vessel. Provided the school is large enough to cover several beams, the two-dimensional images presented by this kind of sonar reveal the actual shape which is often irregular (Fig. 5.8). It is still necessary to correct the images for errors due to beam width, although in this case the errors occur only in the two  $1.7^\circ$  beams at the transverse limits of the school. The fact that the same school is seen at different ranges allows a novel approach to this problem. The apparent width is the full distance across all the beams intersecting the school. The true width is less than that, by up to two beam widths. The beam width (as a distance) is proportional to the range R. Thus the apparent cross-section of the school ( $A_R$ ) should decrease as the vessel approaches, tending towards the true value  $A_0$  at zero range. Measurements at close range are unsatisfactory once the beams no longer cover the full height of the school; however, Misund *et al.* (1995) did a linear regression of  $\sqrt{A_R}$  against R which they extrapolated to estimate  $A_0$ . This method has the advantage that it can be applied to one school, and the corrected area does not depend on any assumptions about the effective or nominal beam width. Anomalous results can occur (e.g.  $A_0 < 0$ ), due to the school shape or the proportion insonified changing with range. In that event, the traditional method of beam-width correction (see above, echosounder-mapping) should be applied to the particular schools concerned.

Multi-beam sonar can also be used in side-scan mode. The beams are now in a vertical fan directed sideways from the vessel track. This technique provides direct measurement of the full three-dimensional morphology of any observed school. The height and the athwartship coordinates come from the echogram of each ping, while comparison of successive pings along the vessel track gives the third dimension as illustrated in Fig. 3.18. Gerlotto *et al.* (1999) used this technique to study tropical clupeoid schools. Their 455 kHz sonar (RESON Seabat model 6012) had 60 beams, each  $1.5^\circ$  by  $15^\circ$ , covering a  $90^\circ$  sector. Thus the athwartship fan extended from the surface to the vertical below the vessel. The maximum range for school detection was 100 m, rather less than in the other sonar applications discussed above, due to the higher operating frequency of the Seabat (which, on the other hand, provides better spatial resolution). Gerlotto and Paramo (2003) found that fish schools have an irregular morphology which is poorly approximated by ellipsoids or cylinders. They were able to show consistent proportionalities between the height, width and length, and noted that the dimensions were rather unequal, with the height being normally less than the other two, confirming the general conclusions of earlier work e.g. Soria *et al.* (1996). These relationships may differ between species, suggesting the use of shape measurements to assist the acoustic identification of the schooling fish.

Traditional ideas of schooling behaviour suggest that the fish density should be rather uniform throughout the school volume (Pitcher and Partridge 1979). However, Gerlotto and Paramo (2003) found that the structure of large schools (but not small ones) was more heterogeneous than expected. They use the terms ‘nuclei’ and ‘vacuoles’ to describe these structures. The vacuoles are empty spaces while the nuclei are zones of uniform density somewhat greater than the school average.

Acoustic mapping and school-counting techniques work best when the fish form many distinct schools which are not too different in size and shape. The techniques determine the volume occupied by the schools, from which the abundance can be deduced if the packing density is known from other sources. When the fish are dispersed or in poorly defined aggregations, however, much better results can be obtained by the acoustic measurement of fish densities in a structured survey design, as described in the following sections.

### **5.3 Echo-counting**

When fish are well separated from one another, it may be possible to detect the echoes from individual fish, as first suggested by Trout *et al.* (1952). The count of these echoes might be used to determine the density of fish within the acoustic beam. This was first attempted by Midttun and Saetersdal (1957), although they did not determine the sampled volume within which targets are counted. The sampled volume depends on the size of the target among other factors identified

by Foote (1991a). Thus the conversion of the target count to an estimate of fish density must take account of the size distribution of the surveyed population. Several theoretical approaches to this problem have been developed over the years e.g. Craig and Forbes (1969); Ehrenberg (1972); Kieser and Mulligan (1984); Kieser and Ehrenberg (1990); Mulligan and Chen (1998).

The amplitude of the echoes can be measured to provide information about the fish size distribution. In general, larger fish give bigger echoes, but the relationship between fish size and echo amplitude is not simple. Suppose that a number of echoes from the same fish are measured. The echo amplitude will depend on the position of the fish within the acoustic beam and the beam pattern of the transducer. But even if the effect of the beam pattern is removed, which can be done directly using an echosounder of the split-beam or dual-beam type, or indirectly from the echo statistics (p. 182), the observed echo amplitudes will very likely cover a range of values. The reasons for this variation are discussed more fully in Chapter 6. For the present, the important point is that the echo amplitude from a given fish must be considered as a stochastic variable, one that can have a range of values described by a probability distribution. The same is true of the backscattering cross-section and the target strength, since these variables are defined in terms of the echo amplitude.

The observed echo-amplitude distribution is further complicated when the echoes have come from a range of fish sizes, and more than one species may be present. Moreover, in the case of the single-beam echosounder, the target direction is unknown, so the beam pattern also contributes to the observed variation.

### 5.3.1 Single-target echoes

The echo-counter has to distinguish those echoes coming from isolated fish, which we call single-fish echoes, and those which result from two or more fish being detected concurrently. Before proceeding, we must define what constitutes an echo. Any part of the received signal whose amplitude is always above a pre-determined threshold is considered to be an echo from one or more targets (Fig. 5.9). Signals below the threshold are ignored. The reason for applying the threshold is to reject noise and signals from very small targets which are of no interest.

It is only the single-fish echoes which are useful in echo-counting. Fortunately, it is often possible to determine whether the echo has come from one or more fish by the shape of the echo-envelope, which depends on the number of targets contributing to the received signal. The original pulse generated by the transmitter has an ideal rectangular envelope (Fig. 5.10a), but the echo-envelope has a more rounded shape owing to the electronic filters in the receiver and the frequency dependence of the transducer sensitivity.

In the case of the echo from an isolated fish, the envelope might look like the example shown in Fig. 5.10b. The precise shape will depend on the characteristics of the echosounder, notably the bandwidth of the receiver. When two or more fish

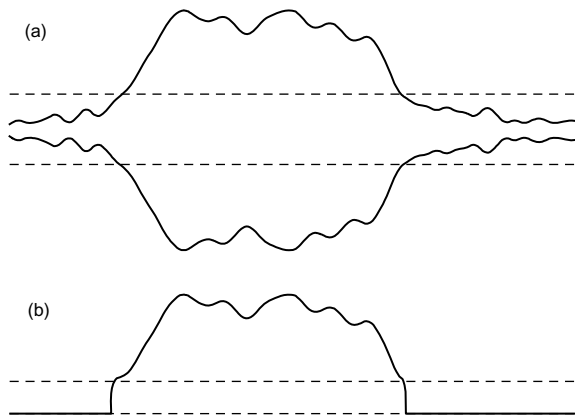


**Fig. 5.9** Echo detection. (a) Envelope of the received signal; dashed lines indicate the threshold applied to reject noise. (b) The detected echo is the part of the received signal which is above the threshold level.

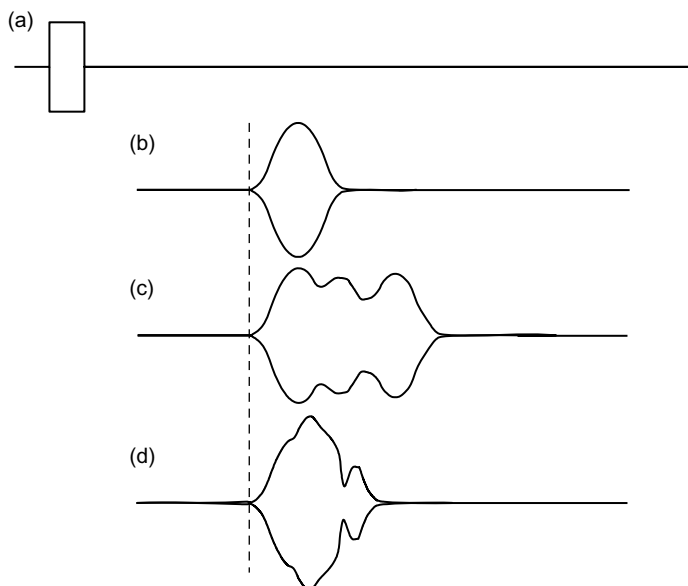


**Fig. 5.10** Examples of signal envelopes. (a) The transmission pulse; (b) echo from an isolated fish; (c) overlapping echoes from targets at different ranges; (d) several targets at nearly the same range.

are contributing to the received signal, however, the echo is likely to be distorted by two effects. Suppose  $\tau$  is the duration of the transmitter pulse. Firstly, if there are targets at different ranges within a pulse length, the echo duration may be much more than  $\tau$  (Fig. 5.10c). Secondly, in the case of targets at nearly the same range

but in different directions, the individual target echoes may interfere, causing the envelope to fluctuate, as in Fig. 5.10d.

One criterion is to accept only those echoes whose duration is within some interval around  $\tau$ . For example, it might be decided to reject echoes longer than  $1.5\tau$ . This would eliminate the echoes from diffuse targets or aggregations spread over a quarter of the pulse length or more in range. Other criteria are necessary to eliminate echoes from multiple targets at nearly the same range. The decision may be based on measurement of the echo rise-time or the phase coherence within the echo, factors which will remain within known limits for single-fish echoes.

These simple techniques for detecting single-fish echoes are not perfect. Some of the detected echoes may not be from isolated fish, for example if two fish were close together but far from other neighbours. This problem is discussed at length in Chapter 6. The main requirement, however, is to ensure that the amplitude distribution of the detected echoes is representative of the echoes from isolated fish, and that the error rate is low enough not to distort the statistics of the distribution.

The best conditions for echo-counting occur when the fish are randomly distributed at a low average density. The worst conditions occur when the fish are in dense schools or layers. It is possible to determine whether the fish distribution is suitable for echo-counting, by examining certain features of the received signal such as the distribution of peak amplitudes, a technique originally proposed by Spindel and McElroy (1973). According to Stanton (1985), there are fewer peaks at small amplitudes when the signal is predominantly multiple-fish echoes (Fig. 5.11). Practical applications of this effect have been discussed by Stanton and Clay (1986) and Trevorrow (1996).

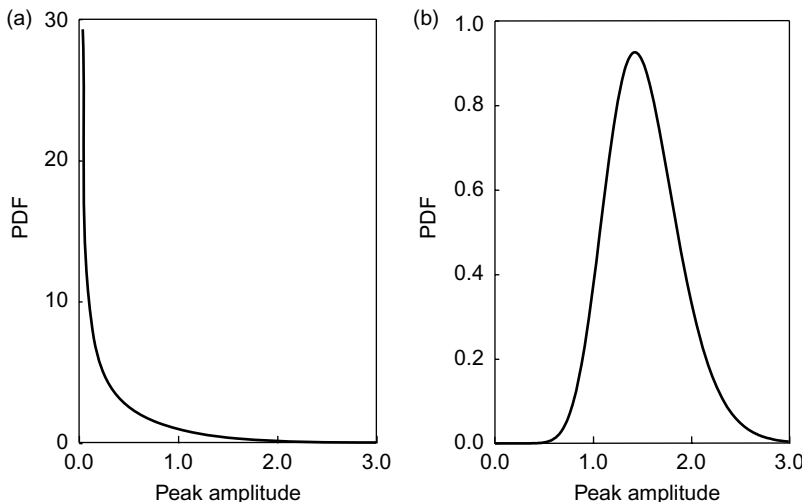


**Fig. 5.11** Probability distribution of peak amplitudes in the signal received from (a) isolated targets; (b) multiple targets with overlapping echoes. PDF = probability density function. (Redrawn from Stanton 1985.)

### 5.3.2 Range compensation

The echo amplitude decreases with the range of the target due to beam spreading and absorption as the sound waves propagate through the water. The receiver includes a time-varied-gain (TVG) amplifier to compensate the output signal for these propagation losses. The gain is increased in proportion to the TVG function  $a(t)$ , where  $t$  is the time from the start of the transmitter pulse (Fig. 5.12).

In the case of one isolated target whose range is much greater than the pulse length, the appropriate TVG function is:

$$a_o(t) = (ct)^2 \exp(\beta ct / 2) \quad (5.6)$$

where  $c$  is the sound speed and  $\beta$  is the absorption coefficient. This function is commonly known as ‘40 log R’ TVG. The range dependence is obtained by substituting the range  $R = ct/2$  as an approximation, and calculating  $20 \log[a_o(t)]$ , which is the TVG expressed in decibels.

The spreading losses increase with the range, as does the time delay until the echo is received. The echo amplitude is multiplied by the TVG function and the result should be an output signal which does not depend on the target range. Note that  $a_o(t)$  is an approximation to the exact function,  $a(t)$ , which was formally derived by MacLennan (1986). However, Furusawa *et al.* (1999) showed that the exact TVG function is only required for targets at ranges of less than a few pulse lengths.  $a_o(t)$  is a

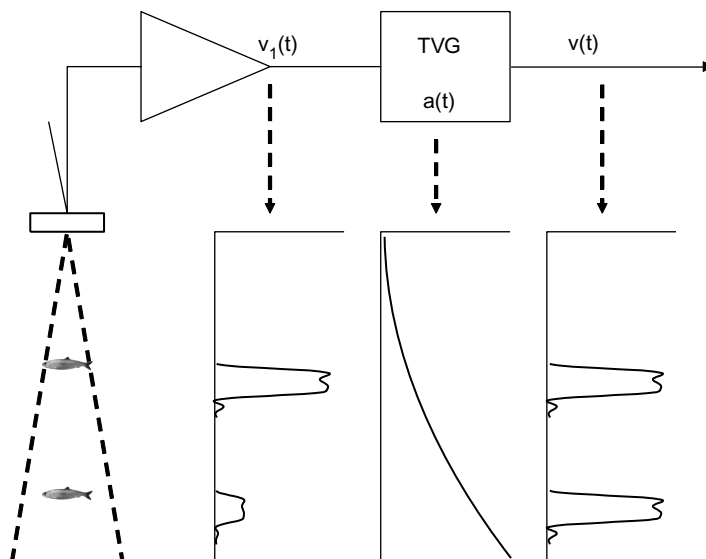


**Fig. 5.12** Range compensation by TVG, single target case.  $v_1(t)$  is the uncompensated signal proportional to the echo amplitude. The receiver gain  $a(t)$  increases with time so that the output  $v(t) = a(t)v_1(t)$  is independent of range for similar targets. This is ‘40 log R’ TVG.

good enough approximation for the ranges at which most fish targets will be observed, since the echoes are received at times  $t \gg \tau$ .

### 5.3.3 Single-beam echosounders

The count of single-fish echoes is not useful by itself, even when the range dependence has been removed, because the sensitivity of the single-beam transducer depends on the direction of the target relative to the acoustic axis. The received signal provides no intrinsic information about the target direction. The same signal might result from a small fish on the acoustic axis or a large one near the edge of the main lobe. It is usual to accept only those signals which exceed some threshold. Since the threshold is the same for targets in any direction, the sampled volume (that within which all fish are counted) depends on the target strength of the observed fish. The larger the fish, the greater is the portion of the beam that can ‘see’ it (Fig. 5.13). An important problem is how to determine the fish density from the count and other measurements of the received signal. The solution is not immediately obvious because the echo-count relates to some unknown average of the sampled volumes.

The first step is to determine the distribution of target strengths among the observed fish. Since the sampled volume is a known function of the backscattering cross-section,  $\sigma_{bs}$ , the fish density (and its dependence on  $\sigma_{bs}$ ) then follows immediately. The target strength is defined in terms of the energy in the echo produced by the target (Chapter 6). The energy is the integral of the square of the echo amplitude, and it is the appropriate measure of the size of echoes in the present context (cf. Section 2.2).

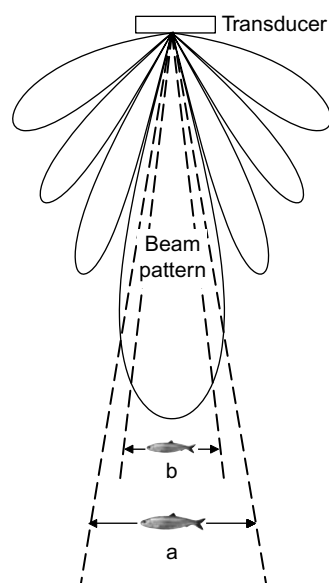


**Fig. 5.13** Dependence of the sampling volume on the target size. The beam pattern is shown as a polar plot of the sensitivity against direction. Echoes larger than the signal threshold are detected. Thus large fish (a) are detected over a greater volume than small fish (b).

### *Indirect target-strength estimation*

It is important to recognize that the target strength of a fish depends on many factors apart from the size. In particular, the echo energy is likely to fluctuate between wide limits as the orientation of the fish changes. We return to this problem in Chapter 6. For the present, the key point is that the target strength must be considered a stochastic variable. To estimate the fish density from the acoustic measurements, one first has to determine the probability distribution of the target strength. In the case of single-beam echosounders, the echo energy also varies due to the random position of the target in the beam. This effect has to be removed to reveal the residual variation due to the distribution of target strengths among the observed fish. The target strength distribution can be derived from statistics of the observed echo energies, as first suggested by Raitt (1948). This is the so-called ‘indirect’ method of which there are several variants. Those of Craig and Forbes (1969), Ehrenberg (1972) and Clay (1983) are described in the following sections. The indirect methods all have the disadvantage that many echoes have to be measured to yield satisfactory results. The problem arises from the assumed random distribution of targets. The actual number of fish in a given volume is subject to statistical fluctuation, so the observed echo energy includes stochastic errors. The solution is sensitive to these errors. Anomalous results can occur if the dataset is not large enough, such as negative frequencies being predicted for certain target strengths.

#### *Craig–Forbes algorithm*

The method of Craig and Forbes (1969) is an early approach to the problem of target strength estimation. An echosounder is used to measure the energies of  $N$  echoes which are counted in  $M$  consecutive classes ( $e_i$  to  $e_{i+1}$ , for  $i = 1, 2, \dots, M$ ), and ‘ $40 \log R$ ’ time-varied gain is applied to remove the range dependence.  $e_1$  corresponds to the smallest detectable echo, so any smaller than  $e_1$  are excluded from the count. No echoes are detected larger than  $e_{M+1}$ . Suppose that  $K_i$  echoes are counted in the  $i$ 'th class. The  $N = \sum K_i$  echoes have come from fish of various target strengths located in different parts of the beam. The echo energy varies due to the change in sensitivity across the beam as well as the stochastic target strength. It is assumed that the target strength and the position of the fish are uncorrelated.

Next, we consider the cross-section of the beam to be divided into regions of different sensitivity (Fig. 5.14). The central region  $Z_1$  is the most sensitive,  $Z_2$  is the second most sensitive and so on. Suppose there are  $n_j$  fish per unit volume with target strengths in the interval  $TS_j$  to  $TS_{j+1}$ .  $TS_j$  is defined as the target strength of a fish which produces an echo energy between  $e_j$  and  $e_{j+1}$  when it is in  $Z_1$ . The  $K_M$  echoes in the largest energy class have been produced exclusively by the strongest targets ( $TS_M \leq TS < TS_{M+1}$ ) in  $Z_1$ . However, the  $K_{M-1}$  echoes in the second largest energy class comprise the strongest targets in  $Z_2$  and the second strongest class of target in  $Z_1$ . It follows that none of the  $K_i$  echoes in the  $i$ 'th energy class can be associated with target strengths below  $TS_i$ .

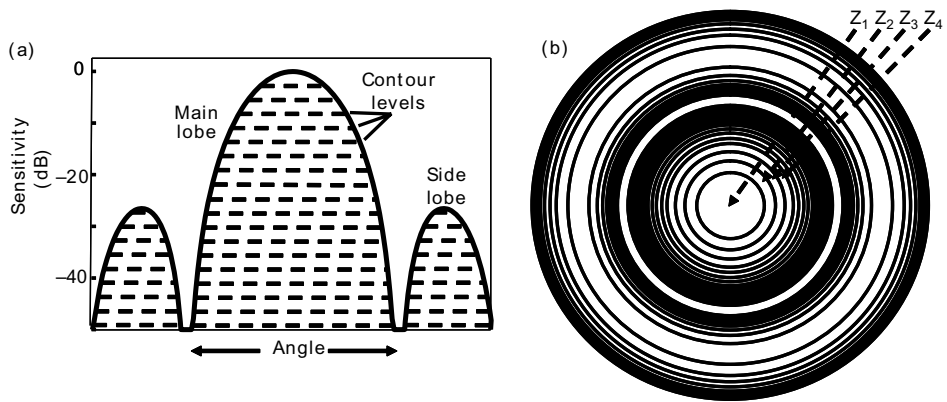


**Fig. 5.14** Cross-section of an acoustic beam divided into regions by contours of equal sensitivity: (a) sensitivity vs angle from the acoustic axis; (b) the central region  $Z_1$  is the most sensitive. In this hypothetical example, the beam is symmetrical and the contours are circles.

It is assumed that for all  $j$ , the  $n_j$  fish are randomly distributed over the beam cross-section. The transducer sensitivity and its dependence on the target direction (i.e. the beam pattern) must be known. The sensitivity factors  $B_r$  are calculated from the beam pattern. If  $R_1$  and  $R_2$  are the range limits between which echoes are counted, and  $\Omega_r$  is the solid angle of directions in region  $Z_r$ , then:

$$B_r = \Omega_r (R_1^3 - R_2^3) / 3 \quad (5.7)$$

The  $K_i$  may now be expressed as a linear combination of the  $n_j$ , ignoring those targets which are too weak to produce the required echo energy.

$$K_i = B_i n_i + B_{i+1} n_{i+1} + \dots + B_M n_M \quad (5.8)$$

There are  $M$  such equations, obtained by substituting  $i = 1$  to  $M$ , and they are easily solved for the  $n_j$  to determine the target strength distribution.

#### *Ehrenberg's method*

Ehrenberg (1972) derived an integral equation which describes the echo-energy distribution in terms of probability functions for the target strength and the location of targets. Unfortunately, numerical computation of the target strength distribution is likely to be unsatisfactory because of ill-conditioned simultaneous equations. The indirect methods all suffer from this problem. Various techniques have been suggested to overcome the difficulty, such as the polynomial-fitting technique of

Robinson (1982) which smoothes the observed echo-energy distribution, but with limited success.

#### *The deconvolution technique*

Clay (1983) proposed a different approach, see also Stanton and Clay (1986) and Jacobson *et al.* (1990). If  $w_E(u)$  is the probability of observing the echo-amplitude  $u$ , then:

$$w_E(u) = \int_0^1 w_T(b) w_F(u/b) (1/b) db \quad (5.9)$$

where  $w_T(b)$  is the probability of observing  $b$ , the signal from a scatterer of unit strength;  $w_T(b)$  may be deduced from the beam pattern of the transducer, which is assumed to be known. Equ. (5.9) now has to be solved for  $w_F$ , the probability function which describes the scattering properties of the fish.  $w_F(u)$  is equivalent to the target strength distribution. Clay applied the substitutions  $b \rightarrow \exp(-x)$  and  $u \rightarrow u_0 \exp(-y)$ , leading to the simpler expression:

$$w_E(u) = \int_0^\infty w_T(x) w_F(y - x) dx \quad (5.10)$$

which in mathematical language is called a convolution integral. It may be solved (or deconvolved) numerically to determine  $w_F$ . Algorithms for this purpose will be found in Clay (1983). According to Rudstam *et al.* (1988), the deconvolution technique for removing the beam-pattern effect has certain theoretical advantages over the traditional Craig–Forbes method, although the latter offers greater computational simplicity.

#### **5.3.4 Direction-sensing echosounders**

The precision of the target strength measurement can be improved by using instruments which determine the direction as well as the range of the target. Knowledge of the target direction allows the signal to be compensated for the beam pattern. One target strength value is obtained directly from each echo that is identified as coming from a single target, hence the term ‘direct method’. The problem of how to identify the single-fish echo is unchanged, however, and the target strength must still be considered as a stochastic variable described by a distribution of values. The same rules for rejecting echoes from multiple targets are applied in both the direct and indirect methods.

Two kinds of direction-sensitive equipment are commonly used for echo-counting, namely the dual-beam and split-beam echosounders whose working principles were described in Chapter 3. In addition to the direct measurement of target strength, these instruments allow the sampled volume to be fixed at a constant value. An ‘acceptance cone’ may be defined, and echoes from directions outside this cone are

rejected, so that the volume from which echoes are recorded does not depend on the target size.

Ehrenberg (1983) has compared the theoretical performance of split-beam and dual-beam echosounders. While the split-beam technique is more difficult to implement, it is superior in the presence of noise. It also locates the target in three dimensions, a facility not provided by the dual-beam method. This additional information has been incorporated in echo-counting models which allow for a non-random distribution of targets within the beam. As regards the specific task of target strength measurement, however, there is probably little to choose between the two methods in practical terms. Both have given useful results in experimental work, see for example Traynor and Williamson (1983), Foote (1987) and numerous other citations in Chapter 6.

### 5.3.5 Thresholding and the sampled volume

As explained earlier (Section 2.6.2), one consequence of removing noise by means of a signal threshold is that the sampled volume increases with the target size. If the insonified fish cover a range of sizes, then the larger targets will be over-represented in the echo count. Thus the mean target strength calculated from measurements on fish of different sizes will be too high (Weimer and Ehrenberg 1975). The bias increases with the spread of the target strength distribution. Kieser and Ehrenberg (1990) have described a statistical model which provides unbiased results from echo-counting, given knowledge of the target strength distribution, the beam pattern and a well-calibrated echosounder.

Another approach is the duration-in-beam technique (Thorne 1988) which does not require prior knowledge of the target strength. If the fish density is sufficiently low, successive echoes known to be from the same target may be observed, and the transit time required for each fish to traverse the beam can be measured. Weaker targets will have shorter transit times since they are only detected in the central part of the beam. If the fish speed relative to the transducer is known, the effective sampled volume may be estimated from the distribution of transit times, with some statistical treatment to avoid bias (Crittenden *et al.* 1988; Crittenden and Thomas 1992). The duration-in-beam technique was originally developed for single-beam echo-counting. Essentially the same idea can be used with split-beam echosounders, by tracking the target in space as well as time, which much reduces the stochastic error.

The threshold bias is more important in echo-counting than in echo-integration. The signal reduces more rapidly with range (as  $r^4$  instead of  $r^2$ ). Further, the target strength is a stochastic variable, thus even for the same fish there is a possibility of some echoes being below the threshold, and these are ignored. Again, the observed echoes represent only part of the probability distribution, and the observed mean target strength is larger than it should be. Another problem is that the algorithms used to detect single targets can be perturbed by noise, resulting in fewer correct

detections when the signal-to-noise ratio is low. However, the adverse effects of noise can be reduced by using range-dependent thresholds, in the manner described by Watkins and Brierly (1996) and Korneliussen (2000).

Although the sampled volume can in principle be determined for any target and threshold setting, echo-counting works best with large fish which are strong scatterers. In these circumstances, the threshold can be set well below the smallest fish echo, and the sampled volume is then much the same for any size of fish.

### **5.3.6 Applications**

Echo-counting as originally conceived was a method for estimating the abundance of fish. For this purpose it is necessary to know firstly the number of insonified fish, and secondly the sampled volume relevant to these fish. The ratio gives the fish density, and the total abundance is estimated from the mean density multiplied by the volume of water in the area of interest.

The echoes being counted are only those from fish well enough separated from neighbours to avoid overlapping echoes, and this is an important limitation of echo-counting. The technique is most useful for fish which behave independently and whose mean density is low. If the statistics of their spatial distribution are known (a Poisson model will be appropriate for a strictly random distribution), then it is possible to estimate the proportion of fish which are sufficiently isolated to be counted. The recorded count may then be corrected, to include those fish which are not isolated. The correction will be small when a large proportion of the fish are separated (a) vertically by more than half the pulse length and (b) horizontally by more than the width of the main lobe of the beam pattern. The width of the lobe cross-section increases with distance from the transducer. Hence the critical fish density, above which echo-counting will not give satisfactory results, is lower for targets further from the transducer. We shall return to this later, in Section 6.2, since the direct method of target-strength measurement is subject to similar restrictions as regards the fish density.

Notwithstanding these problems, many successful applications of echo-counting have been reported, mainly from work on freshwater fish and migratory salmonids, in lakes (Thorne 1979; 1983; Lindem 1981; Kubecka *et al.* 1994; Romare 2001) and rivers (Skalski *et al.* 1993; Bannehaka *et al.* 1995; Kubecka and Duncan 1998; Nealson and Gregory 2000; Burwen *et al.* 2003). In confined shallow water like a river, the normal technique of surveying an area with mobile equipment can be difficult (review, Thorne 1998). Another approach is to install one or more transducers in fixed positions so that the passage of fish may be monitored as they migrate upstream or downstream (Gaudet 1990; Mesiar *et al.* 1990; Ransom *et al.* 1992; Pedersen and Trevorrow 1999; Fleischman and Burwen 2003). The sonar beam is projected horizontally, sometimes in combination with vertical echosounding to provide additional data on the fish distribution (Gauthier *et al.* 1997; Knudsen and Saegrov 2002). The problem of single-fish detection is somewhat different in rivers, since the main

sources of unwanted echoes are the boundary reflections and the passage of inanimate objects, such as logs or lumps of ice. Stables and Kautsky (2000) used electric and light stimuli to startle the fish, whose energetic reaction ensured their echo traces were clearly distinguishable from those of logs etc. Johnston and Hopelain (1990) have described a method for discriminating fish moving upstream from other targets, based on the Doppler effect, which causes the frequency of the echo to change with the velocity of the target relative to the transducer (Section 3.4.5).

Satisfactory conditions for abundance estimation by echo-counting are found more often in fresh water than in the sea. However, the echo-counting technique is also used to measure the target strength of fish in the wild, and for that purpose it is applicable to schooling marine species. The measurements are limited to individual fish detected on the edges of dense concentrations. It does not matter that the fish contributing to the observed target strength distribution are a small sample from the population, provided that the sample is unbiased.

## 5.4 Echo-integration

For fish aggregated in schools or layers, the density is usually too high for echo-counting to give reliable estimates of fish abundance. The alternative technique of echo-integration, first described by Dragesund and Olsen (1965), has proved to be more generally applicable as a means of estimating the quantity of fish or other scatterers in the acoustic beam, whether or not the received signal contains overlapping echoes. The theoretical ideas behind echo-integration developed over some 20 years from the mid 1960s, notably through the work of Scherbino and Truskanov (1966), Thorne (1971), Moose and Ehrenberg (1971), Ehrenberg (1973; 1974b), Bodholt (1977), Foote (1982b; 1983) and Aksland (1986).

The echo-integrator is simply an echosounder whose output is connected to a device which accumulates the energy in the received signal (Fig. 5.15). If  $v(t)$  is the voltage produced by the echosounder at time  $t$  after the transmit pulse, the energy is the integral of the squared amplitude of  $v(t)$  with respect to time. Thus the echo-integrator output due to one transmission is:

$$E_i = \int_{t_1}^{t_2} |v(t)|^2 dt \quad (5.11)$$

and  $E_i$  is called the echo-integral. In practice, the echo-integrator accumulates the echo-integrals from many transmissions. The fish density is calculated from the mean echo-integral, written as  $\bar{E}$ . If there are  $N$  transmissions, then:

$$\bar{E} = \sum_{i=1}^N E_i / N \quad (5.12)$$

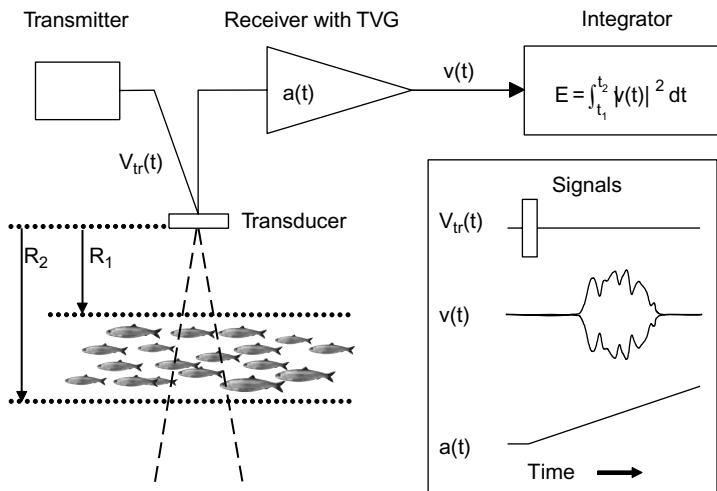


**Fig. 5.15** Principles of echo integration. Signals in the preset range channel  $R_1$  to  $R_2$  contribute to the integrator output  $E$ . The integral is performed between the times  $t_1 = 2R_1/c$  and  $t_2 = 2R_2/c$  after the beginning of  $V_{tr}(t)$ , the transmitter pulse.  $a(t)$  is the TVG function and  $v(t)$  is the receiver output.

In the following discussion,  $\bar{E}$  is abbreviated to  $E$ . The time gate  $t_1$  to  $t_2$  is chosen to correspond to the depth channel which is to be sampled. If  $(t_2 - t_1)$  is much longer than the pulse duration, almost all the targets contributing to  $E$  will be in the channel bounded by the depths  $ct_1/2$  and  $ct_2/2$ . We shall now consider the relationship between  $E$  and the quantity of insonified targets in the depth channel. A simple version of the theory is presented here; for a more rigorous treatment of the statistical theory of echo-integration, the reader is referred to the classic dissertation on the subject by Ehrenberg (1973).

#### 5.4.1 Range compensation

The TVG function appropriate to a single target,  $40 \log R$ , has already been described. In the case of many targets which are distributed randomly over the beam, whose mean density is to be derived by echo-integration, a different function is required. Suppose the targets are fish in a thin layer extending sideways well beyond the beam (Fig. 5.16). As the range of the layer increases, so does the number of fish in the acoustic beam. The larger number of targets compensates the transmission losses to some extent. We want the signal from the layer to be independent of the range, assuming the fish density is constant. To achieve this in the case of randomly distributed targets, if the range is much greater than the pulse length, the approximate TVG function is:

$$a_o(t) = (ct) \exp(\beta ct/2) \quad (5.13)$$

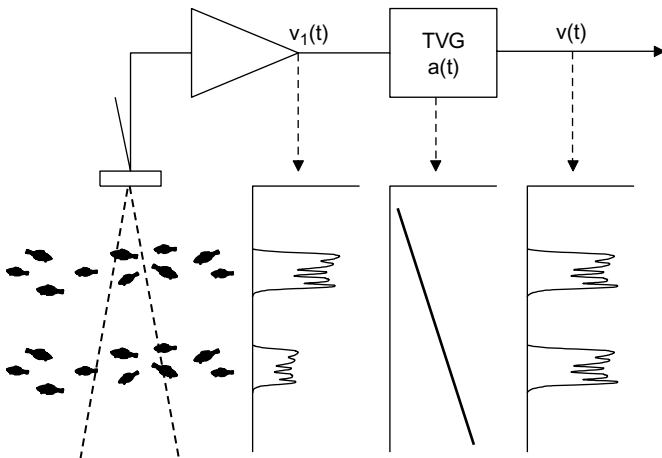


**Fig. 5.16** Range compensation by TVG for targets distributed in layers.  $v_1(t)$  is the uncompensated signal proportional to the echo amplitude. The receiver gain  $a(t)$  increases with time so that the output  $v(t) = a(t) v_1(t)$  is independent of range for similar layers. This is '20 log R' TVG.

which is the same as Equ. (5.6) but without the square in the  $(ct)$  term. This function is known as '20 log R' TVG. The range dependence is obtained by substituting  $R = ct/2$  and expressing the result in decibels, as before. Again,  $a_o(t)$  is a good enough approximation at the ranges of most fish targets. The exact functions may be required for targets close to the transducer, in particular the standard target which is suspended below the transducer when calibrating the equipment (Section 3.8).

When echo-counting, 40 log R is the correct type of TVG; when echo-integrating, 20 log R is always required and the controls on the echosounder should be set accordingly. It does not matter that the population being integrated may be so sparse that only one fish at a time is in the beam. The 20 log R function is still appropriate. The echo-integrator accumulates the integrals from many transmissions, and therefore from many fish which are detected at random positions throughout the beam.

#### 5.4.2 The echo-integrator equation

The integration is performed between times  $t_1$  and  $t_2$ , corresponding to the depth channel  $R_1$  to  $R_2$  as in Fig. 5.15, and  $E$  is the average integrator output over many transmissions. While the integration is in progress, the transducer may be on a moving ship and the fish are also mobile. Thus many different fish will contribute to  $E$ . If the number of detected fish is very large, and if they are randomly distributed over the beam cross-section, then  $E$  is proportional to  $F$ , the number of fish per unit area of the depth channel. This is the primary assumption of echo-integration theory. The relationship may be written in the form:

$$F = [C\bar{g} / (\psi \langle \sigma_{bs} \rangle)]E \quad (5.14)$$

This is known as the echo-integrator equation (MacLennan 1990).  $E$  is the measurement produced by the echo-integrator. To calculate  $F$ , we need to measure or to estimate the four terms within the square brackets.  $\langle \sigma_{bs} \rangle$  is the expected value of the backscattering cross-section which describes the scattering properties of the insonified fish. This is a major topic in its own right, and we shall postpone further discussion of  $\langle \sigma_{bs} \rangle$  until Chapter 6.  $C$  is a calibration factor which depends on the sensitivity of the transducer and the electronic components of the echo-integrator.  $\psi$  is the equivalent beam angle, a measure of the beam width, and  $\bar{g}$  is the TVG correction factor. The measurements of  $C$ ,  $\bar{g}$  and  $\psi$  come from the equipment calibration (Section 3.8).

The equivalent beam angle has been defined in Section 2.3. It may be visualized as the solid angle at the apex of the ideal conical beam which would produce the same echo-integral as the real beam from a large number of randomly distributed targets (Fig. 5.17). In this context, an ideal beam is one whose sensitivity is constant inside a cone, and zero outside.

$\bar{g}$  is the average TVG error over the depth channel. It arises because the actual TVG applied to the signal, as generated by the receiver, is likely to differ from the function required for exact range compensation.  $\bar{g}$  is determined from electrical measurements of the actual TVG function, and the waveform of the signal at the echosounder output. The formal definition of  $\bar{g}$  is given in Appendix 5B.

When the range compensation is exact,  $\bar{g} = 1$  and there is no TVG error. Some error is likely in practice, for three reasons. Firstly, the actual TVG may deviate from the intended function due to inaccuracy in the circuits which control the gain, however, this problem is unimportant in modern echosounders whose

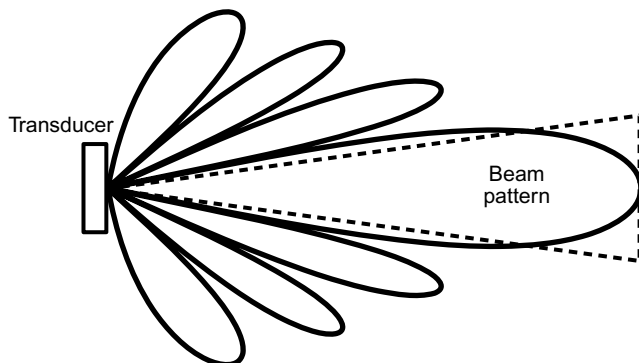


**Fig. 5.17** Section through a transducer beam pattern (solid curve) and the equivalent ideal conical beam (broken curve). The ideal beam has constant sensitivity within the cone and zero sensitivity outside. The equivalent beam angle  $\psi$  is the solid angle enclosed by the apex of the cone. The beam pattern has a log scale on the radial coordinate which emphasizes the side lobes.

TVG is digitally controlled. Secondly, particular values of the sound speed and the absorption coefficient have to be assumed in implementing the intended function; both these parameters vary with the hydrographic conditions, notably the water temperature, and any deviation from the assumed values will result in the wrong TVG being applied. Thirdly, there can be an error at short ranges due to incorrect timing of the TVG function just after the transmission pulse (Furusawa *et al.* 1999).

### 5.4.3 *The linearity principle*

Much of the foregoing theory has been founded on the assumption that echo integration is a linear process. In other words, it is supposed that the output of the echo-integrator is proportional to the quantity of targets having similar acoustical properties.

#### *Definitions and assumptions*

More formally, the linearity principle may be stated as follows. Consider an aggregation of targets which are insonified over a period of time by N transmissions (pings) generated by an echosounder. At any instant, the received signal consists of the overlapping echoes from targets within the sampled volume, sometimes called the pulse shell (Burczynski 1982; Foote 1991a). This volume has been defined in Section 2.4. It extends to half the pulse length in range, and across to include the equivalent beam angle. Suppose that n targets ( $n > 1$ ) are present in the sampled volume. Linearity requires that the mean sampled value of the echo energy from the n targets will be the same as the sum of all the echo energies that would have been observed if each target were insonified separately. The two main assumptions required for linearity are that (1) the targets are randomly distributed in the insonified space, ensuring that the phases of the echoes from each target are randomly distributed relative to each other, and (2) the targets move so that a new random set of phases is generated from each transmission. The echo energy from a single sample from the i'th ping is  $E_i$ . All the  $E_i$  will be different because of the changing echo phases and target locations within the beam and, at least for live targets free to behave naturally, the variability of the echoes from each target arising from the stochastic nature of the target strength.

The  $E_i$  come from an ‘ensemble’, which is a statistical term defined strictly as ‘the infinite set of realizations of a stochastic process’ (Kendall and Buckland 1971). In the case of fish targets, the stochastic process is the random movement of the fish. The concept of the ensemble is frequently extended to apply to a sample set of realizations, as we do here in considering a large but finite number of pings. Between successive pings, the fish must move randomly relative to one another if a new independent member of the ensemble is to be obtained. An alternative applicable to a survey would be successive independent samples from different sampled volumes on the same ping, or for the transducer to move and observe a new set of n randomly

distributed targets. The echo amplitudes from such an ensemble are described by the Rayleigh distribution (Skudrzyk 1971), while the echo energies follow the exponential distribution. The true mean of the  $E_i$  is written as  $\langle E \rangle$ , the angle brackets being the usual way of denoting these ‘ensemble averages’. The actual mean of the  $N$  observations,  $\bar{E}$ , is an estimate of  $\langle E \rangle$ . In the limit of a large number of observations,  $\bar{E}$  tends to the true mean  $\langle E \rangle$ , which is the expected value of the echo-integral. Note that the ensemble average is derived from observations of a number of different random realizations, not just a number of observations of one realization (even if the targets are randomly positioned) or a single observation of a large number of targets.

Now suppose that all the targets except the  $j$ 'th one are removed, but it continues to behave as before.  $e_j$  is the expected echo-integral from this target in isolation, that is to say the mean value taking account of random positioning and other stochastic effects which, except for the echo phase, apply equally to one or many targets. This ‘thought experiment’ is repeated for each target in turn, giving the average result  $\bar{e} = \sum_j e_j/n$ .

The linearity principle states that the expected value of  $\bar{E}$  (i.e.  $\langle E \rangle$ ) is equal to the sum of the  $e_j$ . This implies the mathematical condition:

$$\lim_{N \rightarrow \infty} [\bar{E}] = n\bar{e} \quad (5.15)$$

which holds for any value of  $n$ . The key feature of this equation is that  $\bar{e}$  is a property of the individual targets and does not depend on their density (number per unit volume). Thus if  $N$  is very large,  $\bar{E}$  is proportional to the quantity of targets (Fig. 5.18a), and this is an essential requirement for the echo-integration technique to be valid. Typically,  $N$  should be 20 or more to achieve a reasonably accurate asymptotic value of  $\bar{E} \approx \langle E \rangle$ .

The linearity principle follows from the statistical properties of the Rayleigh distribution. The central hypothesis is that the randomness of the ensemble causes the individual-target echoes to be incoherent. Two echoes are said to be incoherent when their phases are completely unrelated. Any value of the phase difference is equally probable. Conversely, the echoes are coherent when the phase difference is constant over a series of pings. When the echoes are incoherent, the expected energy returned from the ensemble is the sum of the echo energy from the individual targets. The energy is proportional to the square of the echo amplitude, and to the echo integral, so Equ. (5.15) follows immediately. As a simple illustration of this result, consider two echoes of angular frequency  $\omega$  and phase difference  $\eta$  which are received individually as the signals  $A_1 \sin(\omega t)$  and  $A_2 \sin(\omega t + \eta)$ , where  $A_1$  and  $A_2$  are the amplitudes and  $t$  is the time. When the echoes are received together, the signal is:

$$v(t) = A_1 \sin(\omega t) + A_2 \sin(\omega t + \eta) \quad (5.16)$$

which is a sine wave whose squared amplitude is:

$$A_T^2 = A_1^2 + A_2^2 + 2A_1A_2 \cos \eta \quad (5.17)$$

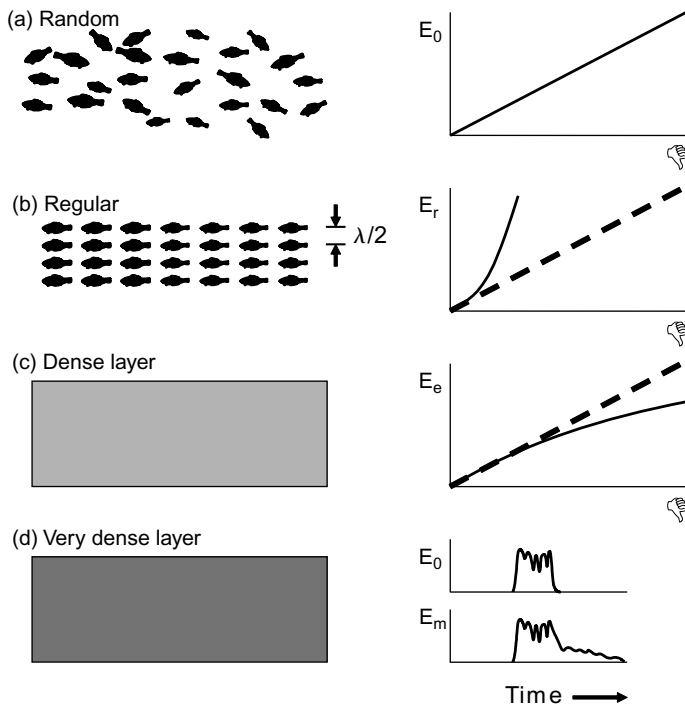


**Fig. 5.18** Types of fish distribution. (a) Random, low density: the echo energy  $E = E_0$  is proportional to the target density  $F$ , and linearity applies. (b) Regular, half-wavelength spacing:  $E = E_r$  increases more rapidly than  $F$ . (c) Shadow effect:  $E = E_e$  increases less rapidly than  $F$ . (d) Multiple scattering:  $E = E_m$  is extended in time compared to  $E_0$ .

Suppose now that many pairs of echoes are observed which have random phases. Any value of  $\eta$  is equally likely, so on average  $\cos \eta$  is zero. When Equ. (5.17) is summed over many observations, the  $\cos \eta$  terms cancel out. Thus the mean squared amplitude from the ensemble is:

$$\overline{A_T^2} = \overline{A_1^2} + \overline{A_2^2} \quad (5.18)$$

The truth of the linearity principle is not self-evident in the case of fish targets, although Stanton (1985) has published echo data which match the Rayleigh distribution. It is possible, for example, that the alignment of fish in a school might be sufficiently regular for coherent scattering to occur. If the echoes were all in phase, as in the special case of targets spaced at half-wavelength intervals in range, the amplitude of the school echo would be the sum of the amplitudes from the individual targets. The echo energy returned from the school would then increase as the square of the number of targets (Fig. 5.18b).

A further assumption required for linearity is that acoustic extinction and multiple scattering are negligible. These phenomena are discussed below (pp. 195–197). Linearity supposes that second-order echoes, which occur when the primary echo

from one target is scattered by another target, contribute little to the echo-integral of the aggregation. This will certainly be true at low densities, but it has to be asked whether the highest packing densities observed in fish schools are above the level at which multiple scattering becomes important (Lytle and Maxwell 1983; Stanton 1983).

#### *Experimental evidence*

The experimental verification of linearity is an essential test of the echo-integration method and the validity of Equ. (5.14). The experiment is difficult to perform because of the need to measure the ensemble and the individual targets under identical conditions, and for long enough to obtain precise means of the echo-integrals. Hamilton *et al.* (1977) described an early attempt to verify the linearity principle, known as the MP-1 experiment. They measured the echoes from sets of 10-cm spherical polystyrene floats moored at randomly-selected positions in a tank of water. The results did not support the linearity assumption; however, it is now believed that the design of the MP-1 experiment was flawed (Swingler and Hampton 1981). The positions of the floats were randomized, but the results for each target density were obtained using *the same* set of positions. This provided just one realization of the ensemble for that density, however many echoes were averaged. In the case of a fish aggregation, the fish move and present different realizations from one ping to the next. Thus the mean echo-integral of a fish aggregation is an average over many realizations of the ensemble, while that of the MP-1 experiment was the ‘mean’ of only one sample.

Subsequently, Foote (1983) conducted a definitive test of linearity with live fish. He measured the echo-integral from caged, free-swimming aggregations of herring, *Clupea harengus*, and pollack, *Pollachius pollachius*, at densities up to 57 fish m<sup>-3</sup>. At the same time, he observed the behaviour of the fish (notably the tilt-angle distribution) by photography. Finally, he anaesthetized the fish and measured the target strength of individuals as a function of the tilt angle, using the method of Nakken and Olsen (1977).  $\langle \sigma_{bs} \rangle$  is estimated as the mean cross-section over the tilt-angle distribution. An acoustic estimate of the fish density now follows from Equ. (5.14) and may be compared with the true density, which is the number of fish divided by the cage volume. The estimated and true densities agreed within the bounds of experimental error; Fig. 5.19 shows the results obtained at four frequencies – 38, 50, 70 and 120 kHz.

The Foote experiment demonstrates that the linearity principle is applicable to fisheries acoustics. The conditions which he tested cover the range of frequencies, transmitted power levels and the normal fish densities likely to be encountered during acoustic surveys.

#### **5.4.4 Non-linear effects**

There remains the question of whether linearity fails at very high fish densities. In experiments with caged fish, Røttingen (1976) found that the echo-integral is

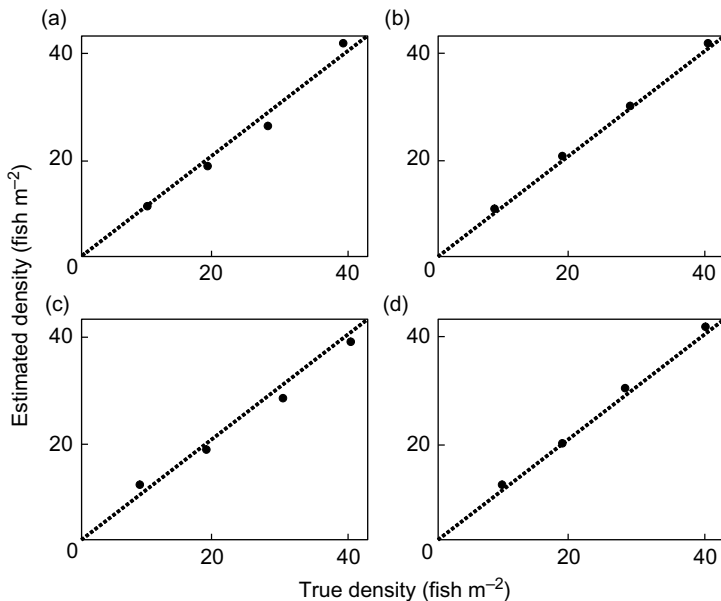


**Fig. 5.19** Comparison of the estimated and true densities of caged fish. Linearity requires that within experimental error, the observations should be on the 1 : 1 line. Results at four frequencies: (a) 38, (b) 50, (c) 70 and (d) 120 kHz. (Redrawn from Foote 1983.)

proportional to the fish density up to a certain limit, after which the relationship becomes non-linear. As the density is further increased,  $E$  continues to rise but at a slower rate (Fig. 5.18c).

### Shadowing

Foote (1978) suggests that changes in fish behaviour with packing density might alter the scattering properties of the aggregation, causing some non-linearity. However, we believe the main cause of non-linearity is the so-called shadow effect. The fish nearest the transducer attenuate the acoustic energy so that the more distant fish contribute less to the received signal. The amount of the signal reduction is determined by the area density of the intervening fish and  $\sigma_e$ , the extinction cross-section, which is a measure of the energy removed from the beam by each fish. Lytle and Maxwell (1983) considered the estimation of fish density in the presence of significant shadowing. They described various approximate solutions based on different theoretical models. The best solution depends on the ‘optical thickness’, which is the distance over which the transmitted intensity is reduced by the factor  $\exp(1) = 2.718$  due to shadowing, over and above the losses arising from spreading and acoustic absorption. The extinction cross-section can be measured *in situ* from the attenuation of the bottom echo observed through a school (Toresen 1991; Foote *et al.* 1992; Foote 1999) or by comparing the signals from hydrophones located above and below the school (Furusawa *et al.* 1992).

Foote (1983) maintains that first-order scattering theory, with the addition of an attenuation term to allow for shadowing, will be adequate for the fish densities found in the wild. In this model, for the case of constant fish density within an aggregation, the strict linearity condition (Equ. 5.15) is modified to become:

$$\lim_{N \rightarrow \infty} [\bar{E}] = n\bar{e} [1 - \exp(-2H_L F_v \sigma_e)] / (2H_L F_v \sigma_e) \quad (5.19)$$

where  $F_v$  is the density as the number of fish per unit volume, averaged over the thickness  $H_L$  of the aggregation. If the factor  $(2H_L F_v \sigma_e)$  is very small, shadowing is not important and conditions (5.15) and (5.19) are nearly identical.

An approximate method of estimating the fish density in the presence of shadowing, assuming that  $\sigma_e$  and  $\langle \sigma_{bs} \rangle$  are both known, is to calculate the density in steps of increasing range (Foote 1990a; MacLennan *et al.* 1990a). Suppose the fish are observed in the depth interval  $z_1$  to  $z_2$ . This interval is divided into  $M$  consecutive layers of thickness  $(z_2 - z_1)/M$ . The layers are numbered 1, 2, ...,  $M$  sequentially downwards.  $E_m$  is the echo-integral from the  $m$ 'th layer, and Equ. (5.14) is used to calculate  $F_{(obs)m}$ , the apparent area density of fish in that layer. The true area density  $F_m$  will be greater than  $F_{(obs)m}$  if shadowing is important. However, in the case of the first layer, which is at the top of the aggregation, there is no shadowing and  $F_1 = F_{(obs)1}$ . The apparent density of the second layer is corrected to take account of shadowing by the first layer, and so on down through the aggregation. The formula for the layer  $m$  is:

$$F_m = F_{(obs)m} \left( 2\sigma_e \sum_{n=1}^{m-1} F_n \right) / \left[ 1 - \exp \left( -2\sigma_e \sum_{n=1}^{m-1} F_n \right) \right] \quad (5.20)$$

This approach has been applied to the estimation of fish held in sea pens (Furusawa *et al.* 1984; Burczynski *et al.* 1990). Very high densities are common in the enclosures used by fish farmers. The enclosures are large and there is need for accurate and unobtrusive methods of determining the quantity of the captive fish. Echo-integration is one such method, but it is necessary to take account of the high-order scattering problem at the densities found in fish farms.

The accuracy of Equ. (5.20) depends on the layers being thin enough for shadowing within one layer to be neglected. For satisfactory results, the factor  $(2\sigma_e F_m)$  should be much less than unity. It is possible to derive more complicated formulae which are theoretically correct when  $(2\sigma_e F_m)$  is large, but they are not much use in practice. When shadowing is very strong, the echoes returned from the bottom of the aggregation are so weak that accurate density estimation is impracticable.

The shadow effect depends on the area density  $F$  rather than the volume density  $F_v$ . Røttingen (1976) reports that for caged sprat of mean length 12.1 cm, shadowing becomes significant at  $F_v = 1900 \text{ m}^{-3}$ , corresponding to  $F = 4560 \text{ m}^{-2}$  over the 2.4-m depth of the cage. This volume density is much greater than that observed in wild schools, which is typically one fish per cubic body-length (Pitcher and Partridge 1979). For 12.1-cm sprat, that would be equivalent to  $F_v = 560 \text{ m}^{-3}$ , and a school

8.1 m thick would have an area density of  $4560 \text{ m}^{-2}$ . The implication is that if a school of sprat or similar fish were thicker than this limit, the apparent density should be corrected for the shadow effect.

### *Multiple scattering*

The acoustic field at a given target is produced by the incident wave and the scattering fields of all the other targets. When the scattering fields dominate the total field, high-order multiple scattering becomes important. If this occurred in a school of fish, acoustic energy from the incident wave would be retained inside the school by repeated scattering between the fish. The energy would gradually escape, and the echo would continue for longer than predicted by first-order scattering theory (Fig. 5.18d). In effect, the school would ring like a bell.

The presence of high-order multiple scattering may be indicated by the appearance of the echogram. The lengthened echo shows as a diffuse ragged tail below the more solid mark of the school. Some examples are shown in Fig. 5.20, and the tail is arrowed in Fig. 5.20a. Multiple scattering is not necessarily the main cause of this effect. After the main lobe of the beam pattern has passed the school, the side lobes might still show echoes at apparently greater range due to the slant angle of the side lobe transmission. However, that effect would be expected to produce a shorter tail than the example in Fig. 5.20a. Of course, the tail might be due to a few fish scattered below the school, but that idea seems unlikely, especially in Fig. 5.20b where a tail is seen on the seabed echo as well. Both the downward transmission pulse and the returning bottom echo are subject to multiple scattering while passing through the school.

Stanton (1983; 1984) considered higher-order scattering in aggregations of randomly distributed targets. He showed that second-order scattering partially offsets the shadow effect, and predicted an upper bound for the echo-integral of a dense school. This was confirmed by Andreeva and Belousov (1996) who suggested that multiple scattering was only important in schools above a critical size,  $r_{\text{cr}}$ . For swimbladdered fish and frequencies typical of fishery sonars,  $r_{\text{cr}}$  is a few tens of metres. It increases with the fish length (due to the higher packing density) and with the sonar frequency.

Multiple scattering is certainly a feature of the high fish densities involved in aquaculture. De Rosny and Roux (2001) have addressed the problem of estimating the quantity of fish in a dense aggregation confined within a reflecting cavity such as a tank. The standard theory of echo-integration is not applicable in these circumstances. Instead, De Rosny and Roux (2001) used multiple scattering theory to determine correlations between coherent and incoherent components of the received signals. These represent, respectively, echoes from the tank and the fish, and the ratio of the two quantifies the scatterer density. This concept has been further advanced by Conti and Demer (2003) who studied the scattering properties of anchovy *Engraulis mordax* and sardine *Sardinops sagax caerulea* in an echoic tank.

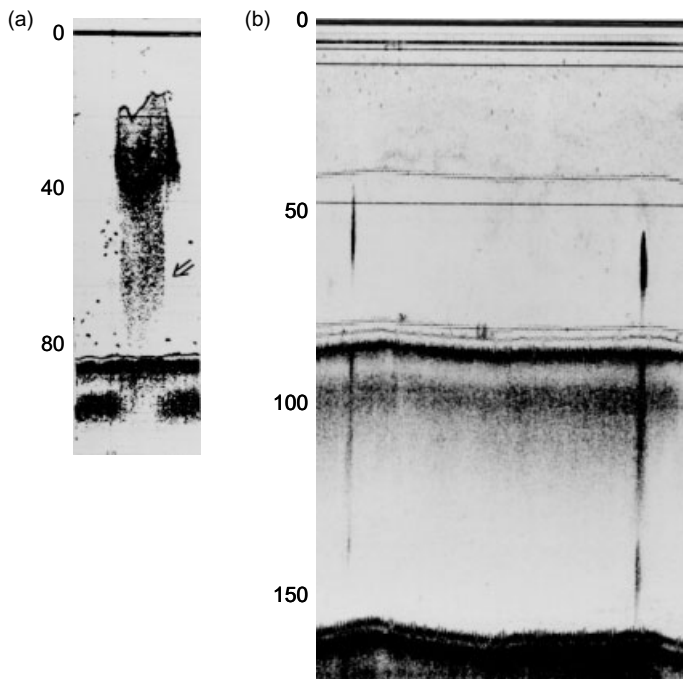


**Fig. 5.20** Examples of multiple scattering in fish schools: (a) herring, Alaska, 105 kHz, reproduced from Stanton (1984); the multiple-scatter tail is arrowed; (b) herring, North Sea, 38 kHz showing multiple reflections in the seabed and surface. Vertical scales show depths (m) below the surface. Not all such ‘tails’ seen below schools on the first echo are due to multiple scattering. Echosounder images are horizontally compressed and the long tails can be caused by sidelobe echoes off horizontally extended schools.

#### 5.4.5 Integration near the seabed

The echoes from fish close to the bottom are liable to coincide with the much stronger echo from the seabed. It is important to ensure that the seabed echo is excluded from the integration. If the seabed is even partly integrated, the result is a large overestimation of the fish density (MacLennan *et al.* 2004). To avoid this problem, the echosounder incorporates an automatic bottom detector. This determines  $R_b$ , the range of the strongest echo, which is normally that from the seabed. The fish integration is terminated at  $R_b$  or, in some instruments, at a range  $R_2$  which is less than  $R_b$  by a small distance called the backstep (Fig. 5.21). The backstep is a safety margin to reduce the chance of the initial rise of the seabed echo being integrated. Of course, any fish beyond  $R_2$  are also excluded in the process. Thus, to obtain an unbiased estimate of the total fish abundance, the observed echo-integrals need correction to allow for the ‘lost’ fish (Ona and Mitson 1996). As well as the backstep, the pulse duration and the beam width are important in this context.

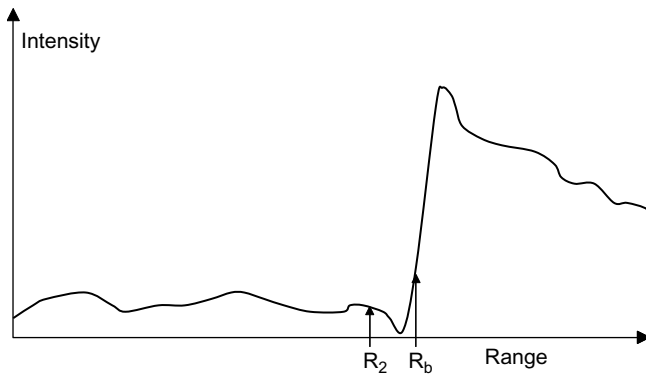


**Fig. 5.21** Echo integration near the seabed. The bottom depth,  $R_b$ , is assumed to be the start of the largest echo. The integration ends at  $R_2$  which is  $R_b$  less the backstep. The backstep ensures that no part of the bottom echo is integrated.

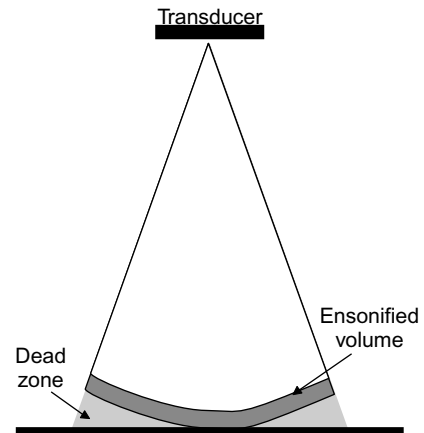


**Fig. 5.22** Cross-section of a conical beam at the instant of first contact with the bottom. The curved wavefront results in a ‘dead zone’ within which fish echoes are lost in the strong bottom signal.

For pulse duration  $\tau$  and sound speed  $c$ , the seabed return overlaps the echo from any fish less than  $c\tau/2$  above the bottom. The backstep eliminates the overlapping part of the echo; however, it follows that fish in the range interval  $(R_2 - c\tau/2)$  to  $R_2$  are not completely integrated. Ona and Mitson (1996) call this the partial integration zone (PIZ). The significance of the PIZ depends on the uniformity of the near-bottom fish distribution. Suppose the bottom integration layer covers ranges  $R_1$  to  $R_2$ . It is important to note that any fish above the layer, within  $c\tau/2$  of  $R_1$  are partially integrated just like those above  $R_2$ , and the calculation of fish abundance should take account of any anomalies at the top as well as at the bottom of the integration layer.

The finite beam width further limits the observation of demersal fish. Figure 5.22 illustrates an ideal conical beam at the instant when the leading wavefront contacts a flat bottom at normal incidence. The curved wavefront is above the bottom at the

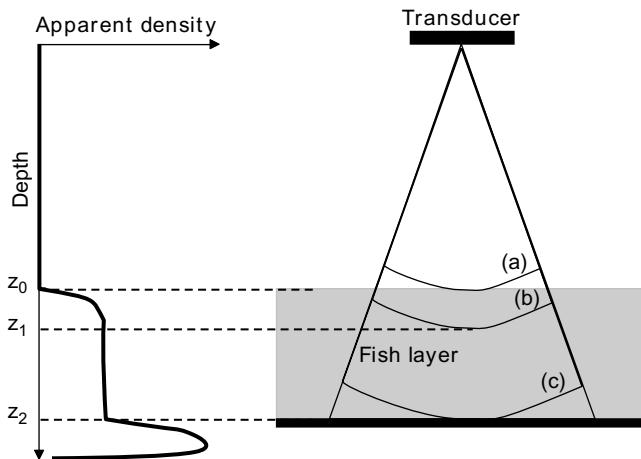


**Fig. 5.23** Integration of a fish layer, shown in grey, extending from depth  $z_0$  to the bottom at  $z_2$ . The transmitted wavefronts are shown at successive times: (a) on first contact with the layer; (b) when the wavefront is fully in the layer; and (c) on first contact with the bottom. The chart on the left shows how the volume fish density as measured by the echo integrator varies with depth.

sides of the beam. The region between the wavefront and the bottom is called the ‘dead zone’ because echoes from fish there are totally lost in the seabed return. How should the abundance estimate be corrected to account for these undetected fish? At first sight this seems straightforward. If we assume that the fish density in the dead zone is the same as that observed in the last integrator sample, the correction might simply be that density multiplied by the volume of the dead zone (Ona and Mitson 1996). This assumption is not exactly correct. Consider a fish layer of constant density from depth  $z_0$  to the bottom at  $z_2$ , with empty water above  $z_0$  (Fig. 5.23). The transmitted pulse contacts the layer at range  $R = z_0$ . The initial echo comes from a small central part of the beam and is therefore small. The echo intensity,  $I$ , increases with  $R$  to a constant level at  $z_1$  when the beam is wholly in the layer. We suppose the layer is thick enough for the beam to be wholly in the layer at some point. In echo-integration, we assume that the backscattered intensity is proportional to the volume fish density  $F_v$  (fish  $m^{-3}$ ), and the abundance is obtained from the area fish density  $F$  (fish  $m^{-2}$ ). If  $F_{vc}$  is the (constant) volume density in the layer, then the true area density is  $F_{(true)} = F_{vc}(z_2 - z_0)$ , but the observed value ( $F_{(obs)}$ ) is the integral of the apparent  $F_v$  with range, over the interval  $z_0$  to  $z_2$ .

Write  $F_{(obs)} = F_{(true)}(1 - P_{err})$ , where  $P_{err}$  is the proportional error in the measurement. For an ideal conical beam, one with constant sensitivity over the beam width  $\phi$ , the geometry of Fig. 5.23 leads to the result:

$$P_{err} = \frac{z_0}{(z_2 - z_0)} \cdot \frac{\log\{\sec(\phi/2)\}}{\{1 - \cos(\phi/2)\}} \quad (5.21)$$

or approximately, if  $\phi$  is small,

$$P_{\text{err}} = \frac{z_0}{(z_2 - z_0)} \sin^2(\phi/4) \quad (5.22)$$

The traditional correction based on the dead zone volume gives the same result if  $(z_2 - z_0) \ll z_2$ , i.e. for the integration of a narrow layer in deep water. Otherwise, Equ. (5.22) indicates a smaller correction.

So far we have only considered the case of acoustic beams perpendicular to the seabed. When the seabed slopes or the transducer axis is not vertical, due to vessel motion for instance, the apparent depth is the range of the first bottom detection which is less than the vertical distance to the seabed, thus increasing the volume of the dead zone. This effect may be compensated by estimating the bottom slope from the observed depths on successive pings (MacLennan *et al.* 2004).

It is not difficult to extend the above results for an ideal beam to the general case of a realistic beam pattern, although the relevant formulas are rather complicated. See Ona and Mitson (1996) for further details of the theory involved.

#### 5.4.6 The threshold problem

We have already mentioned the importance of thresholding in connection with school measurements (Section 5.2) and the sampled volume (Section 5.3.5). The signal threshold is applied to remove ‘noise’, which here means any unwanted signal produced by the echosounder, whether it is electrical noise in the equipment, acoustic reverberation or the merged echoes from non-target species e.g. plankton in the case of fish surveys. Whatever the source, the noise obscures the smaller echoes that we wish to measure. When a signal threshold is applied, any echo smaller than the threshold is also ignored. The observed density is therefore biased because some proportion of the target population has not been detected. The bias depends on the ratio of the signal and noise amplitudes (SNR).

It is not always necessary to apply a signal threshold. In favourable circumstances, the unthresholded echogram may show clear marks from schools or large fish against a negligible planktonic background. On the other hand, if the plankton echoes dominate the complete echo-integral, being more numerous though individually weaker than those from fish, a well-chosen signal threshold may be the only way of rejecting the plankton echoes. Surveys in the tropics often suffer from strong plankton reverberation. It is less of a problem elsewhere, excepting the occasional short-lived bloom.

Weimer and Ehrenberg (1975) studied the threshold bias by simulating the signals from an assumed distribution of target strengths. When the SNR was 30 dB, the bias was about 25%. Foote *et al.* (1986) performed similar calculations incorporating measurements of the noise and empirical target-strength functions. They found no bias in the echo-integration of large gadoids ( $L > 50$  cm), but for smaller fish ( $L = 10$ –30 cm; SNR = 15–20 dB) the bias could be as much as 50%. The problem

is more severe at higher frequencies when the acoustic absorption reduces the signal level at long range. In that case, the steeper TVG function amplifies the (constant) background noise and the signal-to-noise ratio is reduced considerably.

Nunnallee (1990) proposed an alternative to the signal threshold for dealing with noise in echo-integration. He measured the noise level at the echosounder output with the transmitter switched off. Subsequently, this estimate of the noise contribution is subtracted from the complete echo-integrals (i.e. those recorded with no threshold applied). This procedure does not allow for reverberation, but it has the advantage that the threshold bias is eliminated or at least reduced. The noise in the complete echo-integral is subject to random variation, but this should average to zero over a long period of integration.

If the echo PDF of the target species is known, the threshold bias may be calculated and a correction may be applied to the estimated abundance. Unfortunately, the true PDF is seldom known well enough for this purpose. The problem is best avoided if at all possible, by using quiet vessels or deep-towed transducer platforms for example.

#### **5.4.7 Applications**

Echo-integration has become well established as a practical technique for the measurement of fish abundance. It can provide quick results and up-to-date information about the pelagic fish distribution in the area covered by the survey. The technique is more widely applicable than echo-counting because it does not depend on having to identify single-fish echoes.

Echo-integrators are in widespread use by fishery research institutions throughout the world. Many applications have been reported from work in tropical, temperate and Arctic waters (Everson *et al.* 1993; Toresen *et al.* 1998; Aglen *et al.* 1999; Getabu *et al.* 2003). Echo-integrators have been used to study many kinds of fish, notably clupeoids (Aksland 1986; Bailey *et al.* 1998), gadoids when they are found in mid-water (Dalen and Smedstad 1983; Rose 2003), occasionally salmonids (Mulligan and Kieser 1986) although echo-counting is more usual in this case, and various species in fresh water (Duncan and Kubecka 1996; Rudstam *et al.* 1999).

Echo-integration has a number of important limitations. It is not possible to detect fish close to the seabed because of the obscuring effect of the bottom echo, and fish close to the sea surface are similarly inaccessible to integration. When the fish occur in dense concentrations, non-linear effects (notably shadowing) may degrade accuracy. At the other extreme, small fish which are not close to one another, some of the echoes might fall below the signal threshold. If the fish-size distribution spans the limit set by the threshold, the echo-integration will exclude any fish too small to be detected. The consequent error in the fish-density estimate is called the ‘threshold-induced bias’ (Kloser 1996; Reynisson 1996).

A major problem is that the echo-integrator by itself provides no information to identify the species or the size composition of targets. When the aim is to measure the abundance of one species and it is known that others are present in the survey area,

the species composition has to be determined by other means such as trawl samples. The collection of unbiased samples is difficult. Also, the accuracy of echo-integration depends critically on having well-calibrated instruments with a stable performance, good data on the scattering properties of fish and knowledge of acoustic propagation losses in the water. We shall return to these and other practical problems in later chapters.

## 5.5 Other techniques

So far we have covered fish abundance estimation by echo-counting and echo-integration, and the more visual observations e.g. of schooling behaviour made possible by various kinds of sonar. The concept of imaging fish with an ‘acoustic camera’ was discussed in Chapter 3. Here we consider some other techniques and specialized adaptations, all concerned with the use of active sonars for the remote observation of fish. There is a rapidly expanding literature in this field, and the following overview is unlikely to be complete, but it does illustrate the versatility and potential of acoustics for experimental studies of fish.

### 5.5.1 Fixed sonar installations

As an alternative to the mobile sonar carried on a ship, the equipment may be installed at a fixed location near to a base on land, and fish may be observed as they move through the sonar beam. The fixed installation offers the possibility of continuous observation over a long period – months or even years. Furthermore, large and heavy transducers, which would be impractical on a ship but which are capable of high powers and low frequencies, can be deployed to detect targets at distances of many miles.

The fixed installation has already been mentioned as a useful option for work in confined shallow waters, notably lakes and rivers (cf. Section 5.3.6). It has also given interesting results in the open sea. Weston and Andrews (1988; 1990) made a long series of observations with an installation off the Cornish coast. The sonar transmissions were directed horizontally to seaward, and the returning echoes were received by a hydrophone array 18 m long. The operating frequency was 1 kHz at first, later changed to 2 kHz, giving horizontal beam widths of 4° and 2°, respectively. Fish traces could be distinguished from the background reverberation by the change of their range with time as the fish migrated or drifted back and forth with the tide. Useful records were obtained at ranges up to 40 km or so from the transducer, depending on the propagation conditions and disturbance by the wind. The observations continued over a period of 5 years, giving a remarkable long-term record of fish concentrations in the area. The schools could be counted, although the size of individual schools could not be estimated reliably. Nevertheless, the school count

(assumed to be *Sardina pilchardus*) showed a strong seasonal dependence which correlated with the catch rate of the local fishery. The numerical school density was greatest in the summer, typically three per km<sup>2</sup>. The sonar images revealed patterns of fish behaviour, particularly the dispersal and re-forming of the schools at dusk and dawn respectively.

Farmer *et al.* (1999) have described similar experiments with a 12-kHz side-scan sonar. They deployed the sonar at 8.4 m depth in the Drogden Channel between Denmark and Sweden, an area where herring *Clupea harengus* migrate in spring and autumn, with a cable connection to a nearby lighthouse. The horizontal and vertical beam widths were, respectively, 2.8° and 122°. Interference from the surface and the seabed was minimized by combining signals over frequency-modulated transmissions in the range 11.2–12.8 kHz, and by averaging the echoes over a long time to identify those from stationary targets. The sonar transducer could be rotated mechanically, thus providing two-dimensional images of the herring schools up to several kilometres from the sonar installation (Fig. 5.24).

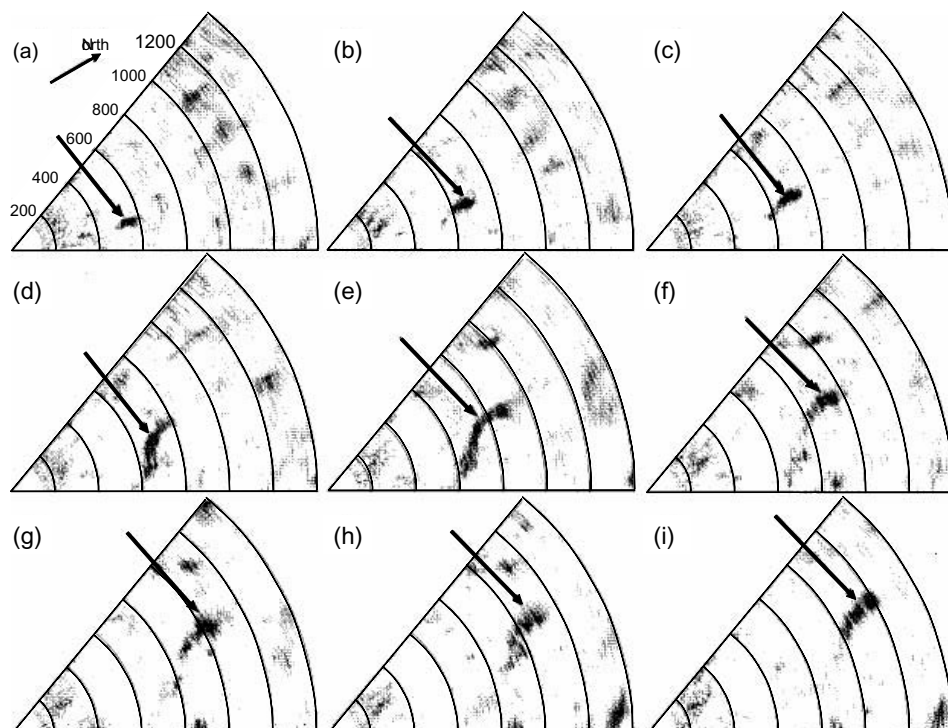


**Fig. 5.24** Records from a fixed sonar installation in the Drogden Channel between Denmark and Sweden, showing the movement of a herring school (arrowed) at night. Each scan is compiled from 25 transmissions at 6 s intervals and shows a 50° sector up to 1400 m from the transducer. The range divisions are 200 m. (Redrawn from Farmer *et al.* 1999.)

### 5.5.2 Horizontal sonar for shallow water applications

It is often difficult to obtain good results with traditional echosounding methods in shallow waters (e.g. rivers and lagoons), when vertical sampling misses areas near the surface and the bottom that are rather important. This leads to the idea of directing the sonar beam horizontally, observing targets in side aspect. Several groups have developed methods for side-aspect surveys e.g. Kubecka *et al.* (1992), Tarbox and Thorne (1996), Kubecka and Wittingerova (1998), Trevorrow (1998) and Knudsen and Saegrove (2002).

There are two circumstances in which this approach is most appropriate, firstly in lakes or seas where the fish are predominantly within a few metres of the surface, and secondly in rivers where the width is within normal acoustic range and greatly exceeds the depth. This applies both to the fixed installations used for migration studies (Chen *et al.* 2004) and mobile acoustic surveys for abundance estimation (Hughes 1998). While there are distinct advantages in increasing the sampled volume by horizontal beaming, the technique has many practical problems that do not occur in vertical sampling of deep water. Each case presents specific difficulties relating to the site and the fish being studied, such that simple general recommendations are not appropriate. A range of issues need to be considered in each application to ensure that horizontal beaming will give good results. These issues can be summarized in two categories as follows: distributional effects and boundary echoes.

*Distributional effects:* If the species of interest naturally occupies specific regions in the water, assumptions about target location cannot be assumed to be independent of the observation method. This may influence the results in several ways. The fish may actively avoid a moving craft or static objects, though the former is more likely. This may affect the horizontal distribution of the fish, decreasing the densities observed at short range. Changes in the orientation of the fish may be part of the avoidance reaction. The vertical distribution may be strongly depth dependent so that the common assumption of a uniform distribution of targets over the beam cross-section is invalid. The vertical profile of the beam may be distorted by stratification of the water (e.g. by a thermocline) though this is normally only a problem for observations at long range. The natural horizontal distribution may be non-stationary in the statistical sense, for example if there are systematic variations in the spatial density across a river associated with water flows or the bottom topography.

*Boundary echoes:* There are two types of boundary echo to be considered. Primarily there is the direct reverberation from the bottom and/or the surface. This generates a noisy background that obscures weaker fish echoes more than stronger ones thus potentially biasing the results. In open-water conditions this effect will be dominated by the surface reverberation which is worse in bad weather. In shallow water the bottom will contribute most of the range-dependent reverberation. In the case of static installations, the bottom reverberation should be apparent (and should be measurable) as echoes which are relatively invariant in time, even though the range dependence may be rather unusual due to irregular boundary conditions.

In the case of mobile surveys, the general level of this reverberation may still be determined and used to set a threshold with a safety margin, though we would expect this to be higher than the margin required for a comparable static installation. The irregular nature of the bottom, particularly in rivers and reservoirs that may be flooded valleys with submerged buildings and trees, adds to the variability of the bottom reverberation. Secondly, there may be multi-path reflections from targets of interest. These occur when the signal received from one target contains two echoes with a time delay, one on the direct path from the target to the receiver, and the other via the longer path that includes a boundary reflection. This is particularly a problem for fish located near the water surface in calm conditions.

At first sight this catalogue of problems may appear insurmountable, but this is too pessimistic. While early studies with horizontal beaming ignored some of these problems, they still produced better results compared to vertical sounding (Kubecka and Wittingerova 1998). However, we have reservations about accepting such results at face value. It is possible that different effects might operate in a compensating manner, giving more reasonable results than might otherwise be expected. For example, the use of a threshold to remove bottom reverberation certainly leads to small targets being underestimated, but any multi-path echoes due to boundary reflections will compensate the overall measurement. This can result in an over-optimistic view of the capabilities of the technique, unless the underlying principles are properly understood. Most of these issues have been discussed in the cited literature, and some practical solutions have been proposed.

The type of beam used in horizontal sonar depends on the desired results. A wider beam in the vertical plane insonifies the water column more uniformly at the expense of vertical resolution and, in shallow water, more surface and bottom reverberation. Trevorrow (2001) evaluated a side-scan sonar with an elliptical beam whose major axis was horizontal while a vertical sector was scanned by rotating the transducer. He examined many of the problems mentioned above, and suggested methods for estimating and correcting the consequent errors.

Trevorrow (1998) also evaluated a side-scan sonar deployed in a fixed installation. He showed how the reverberation from the river bed could be removed by means of a complex range-dependent threshold. There was some indication of bias in fish detection due to the loss of small echoes, since the mean TS appeared higher at ranges where there was more reverberation. On the other hand, the reference target (a homogeneous solid sphere) followed a predictable TS-range relationship (Fig. 5.25). While there was no surface reverberation in calm conditions, this increased with the wind speed and sometimes exceeded the bottom reverberation (Fig. 5.25). The additional surface reverberation would mask some echoes that would have been detectable in calm conditions.

Pedersen and Trevorrow (1999) describe how ray tracing can be used to estimate sound intensity at longer ranges, and consider the detection of targets under different propagation conditions i.e. in stratified and unstratified water. They refer to the concept of a wave guide to explain the acoustic propagation, but that is not really

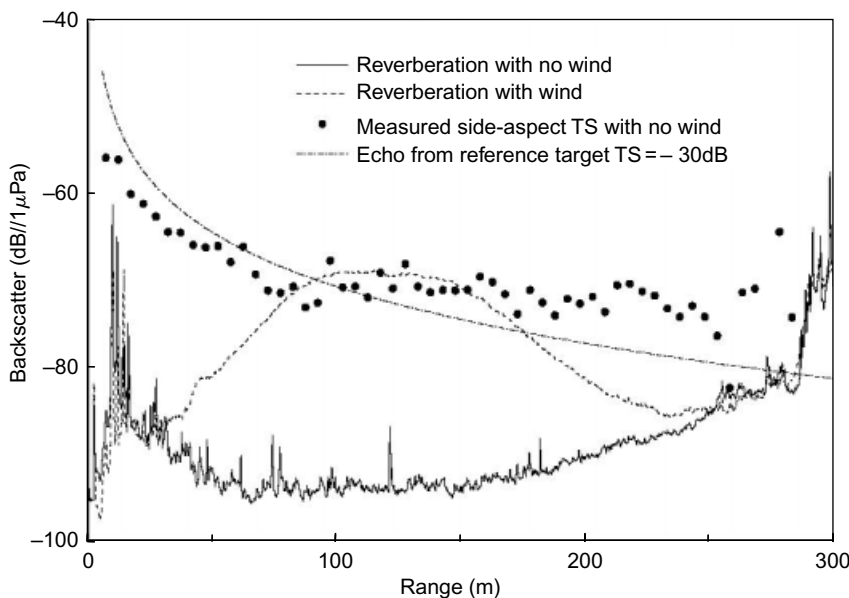


**Fig. 5.25** Reverberation and echo levels from a 100 kHz side-scan sonar in a fixed installation on the Fraser River. The TVG was  $20 \log R$ . The graphs illustrate the consistent background reverberation from the bottom and the increased reverberation when wind disturbs the water surface. The echo level from a  $-30$  dB reference target is shown, and the apparent lateral-aspect target strength (TS) determined from single-fish echo traces, averaged in 5 m range bins. The apparent TS decreases with range because the TVG is 20 (not 40) times  $\log R$ . (Redrawn from Trevorrow 1998 with permission of Elsevier.)

appropriate in this case. Their method for predicting the intensity at range is quite appropriate but it is more correctly described as ray tracing. The theory of wave guides is useful only in long-range acoustic propagation over a very flat bottom, and has little relevance to most fisheries work in shallow water. Farmer *et al.* (1999) adopted a similar approach to the reverberation problem in their work with a fixed sonar installation (see above).

Gerlotto *et al.* (1998) used a multi-beam sonar, configured as a sector scanner (Section 3.4.3), to insonify the whole water column at the same time. Their images show a fish school and its reflection by the water surface as separate marks. When the sonar has good enough angular resolution, as in this case, reflections that would otherwise overlap the direct-path echoes are seen as separate marks and they are known as ghost echoes. The ghost is a mirror image of the school but is weaker than the primary mark (Fig. 5.26a). Trevorrow (1998) describes similar multi-path echoes from salmon in the Fraser River which were visible even among a large number of targets at both long and short range, with the ghost echo following the primary one at a few metres further range (Fig. 5.26b). In the case of a simple single-beam sonar, however, marks that appear to be ghosts might be caused by two real fish that happen to be suitably near one another, and we cannot know for sure which

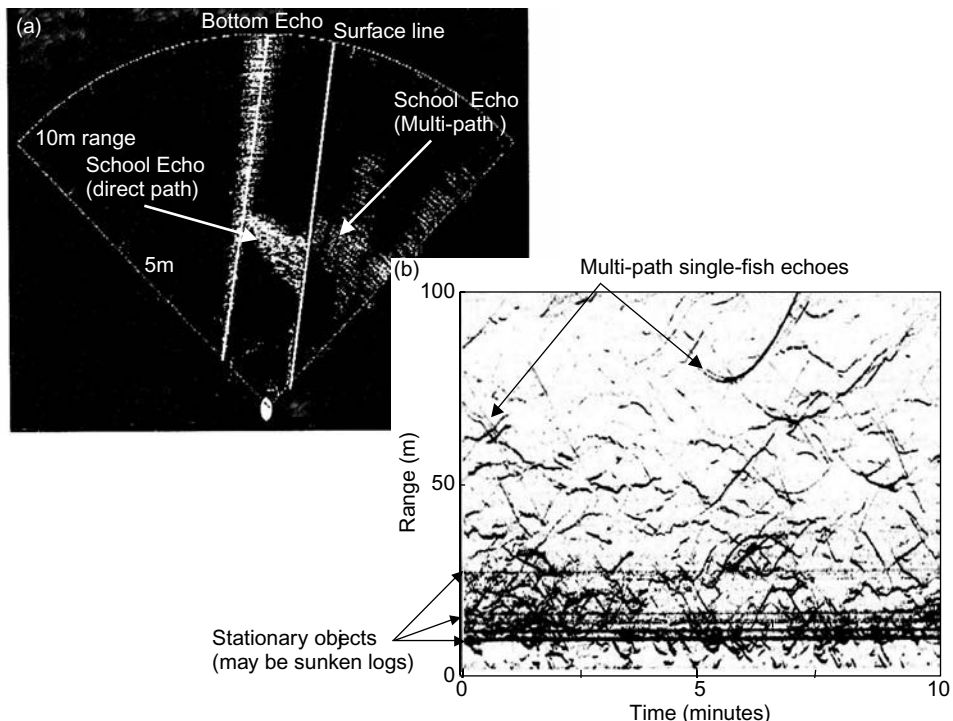


**Fig. 5.26** Examples of multi-path echoes. (a) Echoes from a fish school in a lagoon off Cuba are seen by a multi-beam sonar both within the water column and as multi-path reflections above the water surface (Gerlotto *et al.* 1998); (b) a few possible multi-path returns are seen as ghost echoes from salmon in the Fraser River (Trevorow 1998).

explanation is correct. Trevorow (1998) also presents a single-beam image of a herring school, recorded under similar circumstances to those described by Gerlotto *et al.* (1998), but in the former case any ghost would be merged with the primary school echo. The more sophisticated (and expensive) equipment of Gerlotto *et al.* allows the ghost effect to be quantified, but that is not generally possible in any simple way. If the observed fish are well separated in space, we might test the equipment performance with artificial targets at known positions to reveal the characteristics of any multi-path echoes; however, these will be greatly influenced by the weather conditions. In the case of fish schools, the propagation methods of Pedersen and Trevorow (1999) may provide some useful information but, again, predictions of the echo intensity at long range in shallow water are very sensitive to disturbance of the water surface. It is for this reason that echo-counting is often preferred to echo-integration in horizontal beaming. However, a split-beam transducer deployed horizontally can achieve fine angular resolution of single-target (including ghost) echoes, together with information on the target locations and their movements in two dimensions (Mulligan and Kieser 1996; Steig and Johnston 1996). This is essentially

target tracking, a technique described more fully in the following section. For the present, we note that such information can assist the identification of targets in the presence of multi-path echoes.

Hughes (1998) provides an example of perhaps the most difficult application, namely the mobile river survey, conducted in a shallow river 1.5–5 m deep. The diverse topography meant that variable rather than fixed reverberation thresholds had to be used. The survey was carried out in both upstream and downstream directions, giving two estimates for each section of the river. However, the consequences of the varying threshold and possible differences in fish size were not evaluated, and there was no analysis of the avoidance problem. Yule (2000) compared estimates of salmonid densities and fish size in eleven lakes obtained, respectively, by purse-seine fishing and acoustic measurements with a split-beam sonar. Here the bottom topography and other conditions were more favourable than in the above-mentioned river survey. The split-beam sonar was used to check that echo-counted fish were within the depth range sampled by the purse-seine. There was good agreement between the two sets of results. The mean fish lengths determined by fishing and horizontal beaming were similar. Yule did not determine the complete size distribution of the fish based on the acoustic data (which would involve a deconvolution procedure, cf. Section 5.3.3), but he notes that the stochastic nature of the echo strengths resulted in a smoother TS histogram compared to the multi-modal fish size distribution revealed by the purse-seine catches.

As a general conclusion, we emphasize that it is important to evaluate the spatial and amplitude characteristics of the acoustic measurements, and especially the limited dynamic range available in shallow reverberant or noisy environments. With careful attention to these details, good results can be achieved with the horizontal beaming technique.

### 5.5.3 Target tracking

When exactly one fish is in the sampled volume of a split-beam echosounder, the signal phases locate the fish in the plane perpendicular to the transducer axis, at coordinates  $x$  and  $y$ , say. The along-axis coordinate ( $z$ ) is simply the target range, or  $ct/2$  where  $t$  is the arrival time of the echo. Thus a three-dimensional position is determined for each ping. Over a series of pings, the successive positions mark the path of the fish as it moves through the insonified volume. This technique is called target tracking (Brede *et al.* 1990; Ehrenberg and Torkelson 1996). It has been applied extensively in fish behaviour studies (e.g. Pedersen 1996; Cech and Kubecka 2002; McQuinn and Winger 2003), especially for the measurement of fish swimming speeds (Huse and Ona 1996; Arrhenius *et al.* 2000; Pedersen 2001). Compared to the alternative of stereo photography, acoustic target tracking allows fish to be observed in greater volumes, in more turbid water and at lower light levels. In fact it is possible to track fish over distances much greater than the beam width. Hedgepeth *et al.* (2000) describe a transducer assembly which automatically rotates to point the transducer

axis at the fish. The rotation is controlled by feedback of the off-axis angle measured by the split-beam echosounder.

The indicated positions are subject to measurement error, thus each one will be some distance away from the true path of the fish (Kieser *et al.* 2000). In the split-beam method, the accuracy of x and y (from phase angles) is likely to be worse than that in z (from timing). We suppose the errors in the three coordinates are independent of one another and between pings. Thus the fish might appear displaced from the true path in any direction. This implies that the estimated distance the fish has moved from one ping to the next is larger than it should be, and the indicated swimming speed will also be too high. Mulligan and Chen (2000) have described the statistics of this problem, and noted that the bias could be substantially removed by appropriate smoothing of the observed positions. If the correct track is a straight line, then linear regression of the x and y data against time (or the ping number) will give good results. If the track is curved, a different treatment is required. A good method is the Kalman filter which, for each ping, compares the observed location with that predicted by extrapolation of the earlier track (Jones 1993).

#### **5.5.4 Doppler sonar**

The speed of a target (or, more correctly, the radial component of the velocity) causes a proportional difference in frequency between the transmission and the echo. This is the Doppler effect, well known from the changing pitch of engine noise as an automobile speeds past a stationary observer. In the case of sonar, the radial speed (along the transducer axis) can be estimated directly from the spectrum of the echo, which suggests interesting possibilities for the study of fish behaviour (Hester 1967). Holliday (1974; 1977a) showed how the speed of fish schools could be measured, and in another experiment where individual salmonids were insonified in side aspect, he found features in the echo spectrum which could be related to tail beats and swimming movements. Despite the early interest in the use of Doppler sonar in fisheries, there have been few developments since the 1970s, although there have been considerable advances in hydrographic applications. The work of Johnston and Hopelain (1990) on salmonids has already been mentioned (Section 5.3.6). Tollef-sen and Zedel (2003) have described a novel approach based on phase rather than frequency measurements, again for salmonid observations. Their sonar transmitted two pulses in quick succession, and the target speed was estimated from the phase difference between the two echoes. This is called the coherent Doppler method, while the traditional technique of spectral analysis is described as incoherent.

In oceanography and fisheries, the Doppler effect is probably best known through its application in the Acoustic Doppler Current Profiler (ADCP). This is a sonar with four beams each pointing some 30° off the vertical, as illustrated in Fig. 5.27 for a shipboard installation. The frequencies of the echoes from a particular depth give four radial velocity components which are then resolved into north, east and vertical speeds for the layer at that depth. This assumes that the layer has a uniform velocity



**Fig. 5.27** The Acoustic Doppler Current Profiler (ADCP) as a shipboard installation. Four beams are projected, each about 30° off the vertical, giving radial velocity components from the echoes at each depth. (Redrawn from Demer *et al.* 2000.)

relative to the sonar over the sampled volumes of the four beams. The ADCP was originally developed for water current measurements; however, Demer *et al.* (2000) showed that it could also be applied to fish, in their study of large sardine schools in False Bay, South Africa. They found interesting results such as fish occasionally swimming against the prevailing current. This technique depends on the schools being large enough to be fully intersected by the four beams. It will not work if the schools are too small for that condition to be satisfied.

### 5.5.5 Forward scattering

Small targets scatter sound in all directions. Normally we think only of the echo reflected back to the sound source (the monostatic case), but measurements of the sound field at locations distant from the transducer (the bistatic case) can provide useful information about targets in the transmission path. If a hydrophone is placed on the acoustic axis some distance from the transducer, the signal comprises the

transmission pulse perturbed by the forward scattering of any intervening targets. If these are swimbladdered fish, the forward scattering is quite strong, some 14–17 dB more than the backscattering strength according to Ding (1997). The theory of this effect has been described by Ye (1995) who suggested that the forward scattering technique could be useful for counting fish in rivers, using a sonar transmitter and two receivers located on opposite banks. The receivers are a short distance apart but both are within the sonar beam. The received signals are perturbed by water turbulence as well as any fish migrating through the beam. Ye (1995) showed that forward scattering by fish and the turbulent fluctuations could be distinguished by correlating the signals from the two receivers.

Ye and Farmer (1996) have described a comprehensive theory of forward scattering which takes account of the fish body as well as the swimbladder. However, they conclude that further experimental evidence and validation of the technique is needed before it can be usefully applied to fish abundance estimation.

## Appendix 5A: The true size distribution of fish schools

We assume that the schools are circular in horizontal cross-section, but the size (as measured by the school diameter) is variable.  $N_{\text{sch}}$  is the number of schools detected by the echosounder, and  $n(y) \Delta y$  is the number whose diameter is in the interval  $(y \pm \Delta y/2)$ . If  $N_{\text{sch}}$  is very large and  $\Delta y$  is very small,  $n(y)$  is the true size distribution of the schools.

When a school is observed on the echogram,  $L$  is the trace length corrected for the effect of the beam shape.  $L$  is less than the diameter because the survey track projected onto the horizontal cross-section crosses the school on a chord which is off-centre (Fig. A5.1).  $N(x) \Delta x$  is the expected frequency of trace lengths in the interval  $(x \pm \Delta x/2)$ . The cumulative function  $\Gamma(L)$  is the frequency of schools with trace-lengths of  $L$  or more. Thus:

$$\Gamma(L) = \int_L^\infty N(x) dx \quad (\text{A5.1})$$

The true size distribution is to be estimated from the observed frequencies of traces in consecutive size classes.  $\varepsilon$  is the class interval, which is not necessarily small.  $N_r$  is the observed frequency of the  $r$ 'th class, which includes trace lengths in the range  $(r - 1)\varepsilon$  to  $r\varepsilon$ . The largest observed trace is in class  $M$ . The observed cumulative frequencies are:

$$\Gamma_r = N_r + N_{r+1} + N_{r+2} + \dots + N_M \quad (\text{A5.2})$$

By definition,  $\Gamma_1 = N_{\text{sch}}$  is the total number of observations, and  $\Gamma_{M+1} = 0$ .

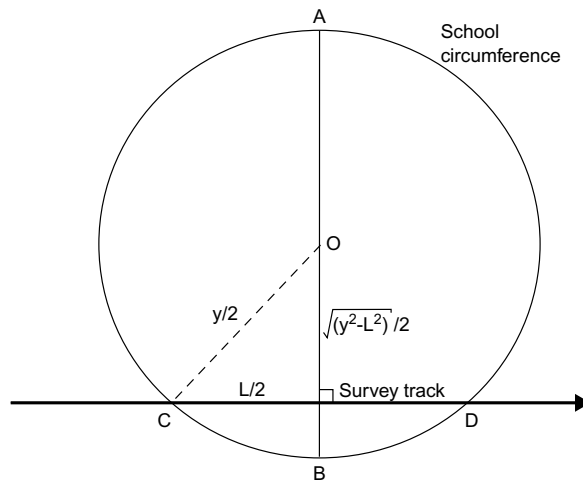


**Fig. A5.1** Geometry of the survey track projected onto the horizontal cross-section of a circular school.  $y$  is the school diameter and  $L$  is the length of the chord  $CD$ .  $AOB$  is the diameter perpendicular to  $CD$ .

The school diameters are considered within the same size classes. If  $n_r$  is the frequency of schools with diameters in the  $r$ 'th class, then:

$$n_r = \int_{(r-1)\varepsilon}^{r\varepsilon} n(y) dy \quad (\text{A5.3})$$

The school centres are assumed to be randomly located with respect to the survey track. The chord  $CD$  (Fig. A5.1) may cross any point on the perpendicular diameter  $AOB$  with equal probability. This implies that of all the schools with diameters close to  $y$ , the proportion  $\sqrt{[1 - (L/y)^2]}$  will produce trace lengths of  $L$  or more. Thus  $\Gamma(L)$  and  $n(y)$  are related through the integral equation:

$$\Gamma(L) = \int_L^\infty n(y) \sqrt{1 - (L/y)^2} dy \quad (\text{A5.4})$$

Substituting  $y = ex$  and  $L = (r - 1)\varepsilon$ , this equation can be expressed as a sum over the class intervals:

$$\Gamma_r = \sum_{s=r}^M \left\{ \int_{s-1}^s n(ex) \sqrt{1 - \{(r-1)/x\}^2} dx \right\} \quad (\text{A5.5})$$

An approximate numerical solution is obtained by neglecting the variation of  $n(y)$  within each size class.  $n(ex)$  is replaced by the constant  $n_s$  as the true frequency by

**Table A5.1** Values of the coefficients  $K_{rs}$  used to estimate the true distribution of school diameters from the observed cumulative frequencies of echo-trace lengths.

r	s = 1	s = 2	s = 3	s = 4	s = 5	s = 6	s = 7	s = 8	s = 9	s = 10
10									0.300	
9								0.316	0.536	
8							0.335	0.564	0.674	
7						0.359	0.596	0.707	0.774	
6					0.388	0.635	0.744	0.808	0.850	
5				0.426	0.682	0.786	0.845	0.882	0.907	
4			0.478	0.741	0.836	0.886	0.916	0.935	0.949	
3		0.554	0.816	0.894	0.931	0.951	0.964	0.972	0.978	
2	0.685	0.913	0.957	0.975	0.983	0.988	0.991	0.993	0.994	
1	1.000	1.000	1.000	1.000	1.000	1.000	1.000	1.000	1.000	

diameter class, leading to the following set of linear equations:

$$\begin{aligned} \Gamma_M &= K_{MM}n_M \\ \Gamma_{M-1} &= K_{M-1M-1}n_{M-1} + K_{M-1M}n_M \\ \Gamma_r &= K_{rr}n_r + K_{rr+1}n_{r+1} + \dots + K_{rM}n_M \\ \Gamma_1 &= K_{11}n_1 + K_{12}n_2 + \dots + K_{1M}n_M \end{aligned} \quad (\text{A5.6})$$

Values of the coefficients  $K_{rs}$  up to  $r = 10$  are given in Table A5.1. They are obtained from the formulas:

$$\begin{aligned} K_{rs} &= \int_{s-1}^s \sqrt{[1 - (1/x)^2] dx} \\ &= \sqrt{s^2 - (r-1)^2} - \sqrt{(s-1)^2 - (r-1)^2} \\ &\quad + (r-1)\{\cos^{-1}[(r-1)/(s-1)] - \cos^{-1}[(r-1)/s]\} \end{aligned} \quad (\text{A5.7})$$

To solve Equ. (A5.6), first calculate  $n_M = \Gamma_M/K_{MM}$ . This is substituted in the next equation which is solved for  $n_{M-1}$ , then by repeated substitutions through the set, the true frequencies ( $n_1 n_2 \dots n_M$ ) are obtained explicitly.

### **Statistics of the distribution**

Suppose there are many schools of diameter  $y$ . The trace lengths associated with these schools could have any value between 0 and  $y$ . Chord CD crosses the school diameter at a distance  $q$  from the centre, and  $L = \sqrt{(y^2 - 4q^2)}$ . Any value of  $y$  between 0 and  $y/2$  is equally probable, so the mean length is:

$$\bar{L} = (2/y) \int_0^{y/2} \sqrt{(y^2 - 4q^2)} dq = (\pi/4)y \quad (\text{A5.8})$$

The overall mean of the traces due to all schools of any size is obtained by integrating Equ. (A5.8) over the size distribution. It is:

$$\overline{L_0} = (\pi / 4) \int_0^{\infty} y [n(y) / N_{sch}] dz \quad (A5.9)$$

The integral in Equ. (A5.9) is simply the mean school diameter,  $\bar{y}$ . Thus:

$$\bar{y} = (4 / \pi) \overline{L_0} \quad (A5.10)$$

The cross-sectional area of each school is  $A = \pi(y/2)^2$  and the mean can be derived by a similar analysis. In this case it is the squared trace lengths which have to be considered. For schools of diameter  $y$ ,

$$\overline{L^2} = (2 / y) \int_0^{y/2} (y^2 - 4q^2) dq = (2 / 3)y^2 \quad (A5.11)$$

and for all the schools, irrespective of size,

$$\overline{L_0^2} = (2 / 3) \int_0^{\infty} y [n(y) / N_{sch}] dz \quad (A5.12)$$

Again, the integral in Equ. (A5.12) is the mean of the squared diameters, or  $(4/\pi)$  times the mean area which is estimated as:

$$\overline{A} = (3\pi / 8) \overline{L_0^2} \quad (A5.13)$$

## Appendix 5B: Calculation of the TVG error

$A(t)$  is the actual TVG function of the echosounder, i.e. the amplitude gain at time  $t$  after the start of the transmitter pulse. It may differ from the intended ‘ $20 \log R$ ’ function.  $\bar{g}$  is the error in the echo-integral due to the imprecise TVG. The error depends on the depth channel being sampled, say  $R_1$  to  $R_2$ .

Suppose that  $v(R, t)$  is the signal at the echosounder output at time  $t$  due to an isolated target at range  $R$ . We define the range-dependent gain function to be:

$$G(R) = \int_{t_1}^{t_2} |v(R, t)|^2 dt / \int_{t_1}^{t_2} |v(R, t)/A(t)|^2 dt \quad (B5.1)$$

where the integrals are taken over the duration of the echo,  $t_1$  to  $t_2$ . When the range is much greater than the transmitted pulse length, so that  $A(t)$  is nearly constant over the echo duration, the integrals of  $v(R, t)$  cancel.  $(2R/c)$  is substituted for  $t$ , giving the approximate form which does not include the time explicitly.

$$G(R) \approx A^2(2R / c) \quad (B5.2)$$

The more complicated relationship, Equ. (B5.1), is important only at short ranges. For exact range-compensation,  $G(R)$  should equal the exact function, which is:

$$G_e(R) = R^2 \exp(2\beta R) \quad (B5.3)$$

Since  $g(R)$ , the TVG error at range  $R$ , is the ratio of the exact and actual range-dependent gain functions, we get:

$$g(R) = [R^2 \exp(2\beta R)] / [G(R)] \quad (B5.4)$$

Finally, the correction factor for the echo-integrator equation is obtained from the average of the reciprocal of  $g(R)$ :

$$\bar{g} = (R_2 - R_1) / \int_{R_1}^{R_2} [1 / g(R)] dR \quad (B5.5)$$

At long range, when Equ. (B5.2) is a good approximation, this becomes:

$$\bar{g} = (R_2 - R_1) / \int_{R_1}^{R_2} \{A^2(2R/c) / [R^2 \exp(2\beta R)]\} dR \quad (B5.6)$$

# Chapter 6

## Target Strength of Fish

### 6.1 Introduction

When a fish is insonified by a sonar which transmits acoustic energy into the water, some of the transmitted energy is reflected as an echo which is subsequently detected by the sonar receiver. The target strength of the fish is a number which indicates the size of the echo. The greater the target strength, the stronger is the echo relative to the transmission. When acoustic instruments are used to observe fish, the objective is usually to learn as much as possible about the fish or other targets whose echoes have contributed to the signal at the receiver output. It is relatively easy to measure electrical features of this signal, such as the amplitude of echoes when they are clearly separated from one another, or the energy content of the signal when it consists of superimposed and indistinguishable echoes. The problem then is, what do these measurements tell us about the insonified targets? In order to deduce quantitative information about fish targets, such as the number per unit volume, an important requirement is to know the value of target strength appropriate to those fish that have contributed to the received signal.

In this chapter, we first describe three experimental techniques for investigating the target strength of fish or other aquatic animals. The techniques differ in the state of the animals being examined, according to whether they are (1) immobilized and unconscious, (2) active but confined within a cage, or (3) wild and free to behave normally in their natural environment. In addition, theoretical modelling of acoustic scattering by fish has given useful insights, through better interpretation of experiments and understanding of the underlying physical processes. Much research has been conducted using all these techniques, and we discuss what can be learned and the limitations of each one. Examples of the results obtained from target strength experiments are presented. Collected results show that target strength depends on fish size, but there are differences between species for the same size of fish. The importance of fish behaviour and physiology in explaining the variability of target strength is discussed. Fish are classified in groups of species having similar acoustic properties, according to the type of swimbladder possessed. Finally, published experimental results are presented in a form suitable for easy reference.

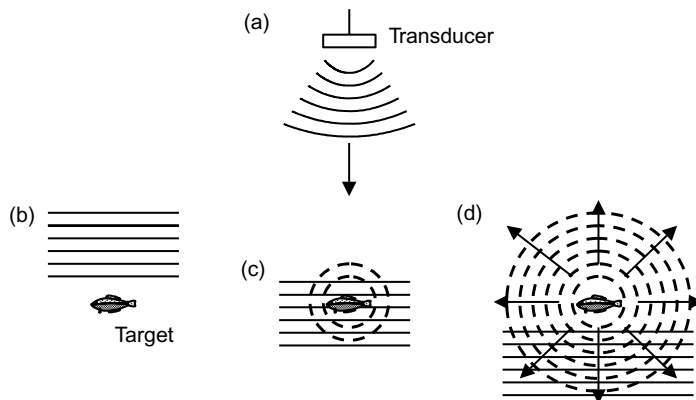


**Fig. 6.1** Scattering of acoustic waves. (a) The transducer transmits a sinusoidal pulse which propagates in the direction arrowed; solid curves indicate wave fronts. (b) At long range the wave fronts are almost plane. (c) The incident pulse interacts with the target and scattering generates spherical wave-fronts (broken curves) centred on the target. (d) After the incident pulse has passed, the scattered waves continue to propagate in all directions.

## 6.2 Target strength measurement techniques

Sound waves propagating through water are scattered by any object whose density is different from that of the surrounding medium. The scattered waves travel away from the object in all directions (Fig. 6.1), and their intensity decreases with the distance from the object owing to spherical spreading and the absorption of energy by the water. Most echosounders and sonars have one transducer which is used both to transmit acoustic pulses into the water and to detect echoes. In that case it is only the backscattered waves that are important, namely those travelling in exactly the opposite direction to the incident waves generated by the transmitter.

The target strength is defined by the intensities of the incident and the backscattered waves, as is the backscattering cross-section; these equivalent quantities are defined formally in Section 2.5. In principle it is possible to compute the target strength of a particular fish from acoustical theory and knowledge of the parts of the fish body which contribute to the echo, notably the swimbladder (Clay and Heist 1984; Foote 1985; Foote and Ona 1985; Furusawa 1988; Clay and Horne 1994; Ye and Farmer 1994; Jech *et al.* 1995). According to Foote (1980b), the swimbladder (in species that possess one) reflects 90% or more of the backscattered energy. There is considerable variation between individual fish, however, even those of the same size and species. The strength of the echo depends on the internal physiology – the shape of the swimbladder, for example, which can be very different between fish which are similar in external appearance. Furthermore, target strength depends also on fish behaviour, especially the orientation of the body with respect to the transmitted beam (MacLennan *et al.* 1990b). The scattering of sound by fish is too complicated for accurate target strength values to be derived from theoretical considerations alone.

For practical purposes, it is necessary to measure the target strength by experiment. A good theoretical understanding of how sound is scattered by fish is, nevertheless, important for interpreting experimental results which are often highly variable.

The essential requirements for target strength experiments are (1) a calibrated echosounder, and (2) knowledge of the species, quantity and size distribution of the insonified fish. The target strength is highly variable. Even for the same fish, the target strength is unlikely to be constant, owing to changes in the orientation of the body and the physiological state of the swimbladder among other factors. It is best to think of target strength as a stochastic variable, a quantity having a distribution of values and a mean value which is the average of a large number of measurements, while individual measurements will be widely scattered around this mean. During an experiment, a large number of echoes must be measured to establish the statistics of the target strength distribution, and in particular, the mean value for the observed fish. Results from many experiments with different fish will be required to determine the target strength properties of the population as a whole, the size dependence for example.

It is important to note that the ‘mean target strength’ must be calculated in the linear domain, namely from the average of the backscattering cross-sections, and not from the average of the individual target strengths. Suppose we have  $N$  independent measurements of  $\sigma_{bs}$ . The measurements are  $\sigma_n$  for  $n = 1, 2, \dots, N$ . The average is:

$$\bar{\sigma}_{bs} = (\sigma_1 + \sigma_2 + \dots + \sigma_N) / N \quad (6.1)$$

and the appropriate mean target strength is  $10 \log(\bar{\sigma}_{bs})$ . This is not the same result as would be obtained by first calculating the individual target strength values, namely  $10 \log(\sigma_n)$ , and then their arithmetic average.

Three experimental techniques have been used extensively for the measurement of target strength. They differ mainly in the state of the targets which are being studied. In the case of fish, they may be (1) immobilized and unconscious, (2) active but confined by a cage or (3) wild and free to behave normally (Midttun 1984). The terms *ex situ* for the first two and *in situ* for the third are common descriptors for the respective techniques, indicating whether or not the fish are in their natural environment. Foote (1991b) has classified these methods with further subdivisions according to the number of fish in an experiment (one or several) and the type of analysis for converting acoustic measurements to target strengths.

### 6.2.1 *Immobile fish*

The earliest experiments were performed on dead or stunned fish, which are held by thin wires so that the body does not move, except when the wire lengths are adjusted. Many investigations have been reported from pioneering work in several countries, notably Midttun and Hoff (1962), Haslett (1970), Love (1971) and Shibata (1972). We shall describe the technique by reference to the comprehensive experiments conducted by Nakken and Olsen (1977), whose apparatus is illustrated in Fig. 6.2.

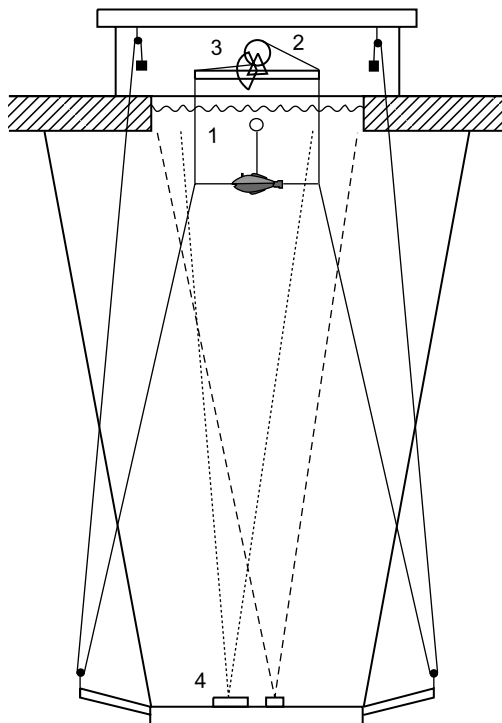


**Fig. 6.2** Apparatus for TS measurements on immobilized fish. (1) Fish suspension wires; (2) hoisting system; (3) tilting system; (4) two transducers, 38 and 120 kHz. A small float holds the fish upside-down. (Redrawn from Nakken and Olsen 1977.)

Only one fish is observed at a time. It is positioned upside-down, and near to the water surface for ease of access. Two transducers are positioned below, angled so that the fish is in the centre of both beams. The transducers are connected to separate echosounders operating at 38 kHz and 120 kHz respectively, so target strengths at both frequencies may be measured concurrently.

The lengths of wire can be adjusted to observe the change of target strength with body orientation, particularly the tilt, which is the angle between the head-to-tail line of the fish and the plane at right angles to the acoustic axis of the transducer (see Fig. 2.23). Figure 6.3 shows the kind of variations observed by Nakken and Olsen (1977). The tilt dependences at the two frequencies are different, the 120 kHz curve showing more variability, although in both cases the maximum target strength occurs when the fish is a few degrees head-down.

### 6.2.2 Live fish in cages

The variation of target strength with the tilt angle is very great. Since free-swimming fish change their orientation from time to time in their natural behaviour, the results of experiments with moribund fish are useful only with knowledge of the tilt angles adopted by fish in the wild (Foote 1980a). Experiments with active, live animals are more likely to produce results relevant to acoustic surveys, assuming that the

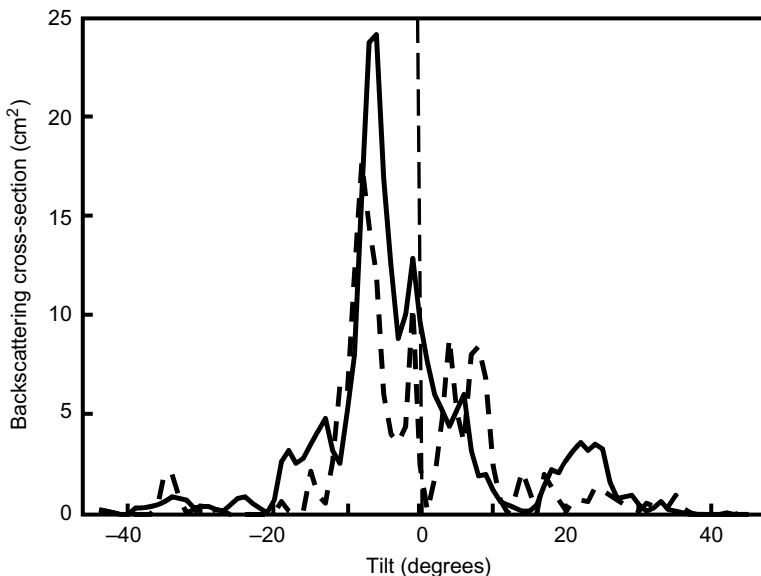


**Fig. 6.3** Backscattering cross-section ( $\sigma_{bs}$ ) of a 45 cm cod, *Gadus morhua*, in dorsal aspect at two frequencies: solid curve 38 kHz; broken curve 120 kHz. Positive tilt angles are head-up. (Redrawn from Nakken and Olsen 1977.)

treatment of the observed fish (by confining them in a cage, for example) has had little effect on their natural behaviour.

The earliest observations on live animals were made using a small cage containing only one fish. Aggregations or schools of fish are perhaps more natural subjects for study. Johansson and Losse (1977) first proposed the modern technique in which many fish were confined by a cage large enough to allow free-swimming behaviour. This technique was subsequently developed in a series of experiments reported by Edwards and Armstrong (1983; 1984).

#### Materials and methods

The apparatus used by Edwards and Armstrong is illustrated in Figs 6.4 and 6.5. The cage was suspended below a raft moored in a sheltered sea loch on the west coast of Scotland. Again, two single-beam transducers were used, operating concurrently at different frequencies and mounted on a gimbal table which could be rotated to align the acoustic beams and the fish cage. A reference target, such as a tungsten carbide sphere of known target strength, was suspended on monofilament nylon twines below the gimbal table to calibrate the echosounder and thus the signal from the fish.

The raft was connected by cables (1000 m long) to a shore station which housed the ancillary electronic equipment – the electronic parts of the echosounder, recording devices and so forth. Both the transmitter and the receiver were located in

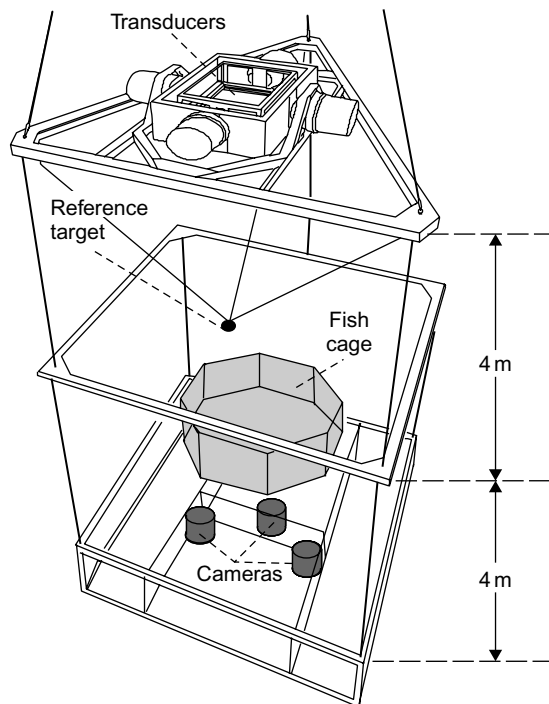


**Fig. 6.4** Apparatus for TS measurements on live fish in a cage. The reference target provides continuous calibration of the fish echo. The cage is typically 2 m in diameter, 1 m deep and 5 m below the transducer.

the shore station. The loss of signal amplitude in transmission over the long cable was not small, but the accuracy of the results was unaffected because the signals from the reference target and the fish were attenuated to exactly the same extent. Television and still cameras were located below the fish cage, firstly to observe the horizontal distribution of the fish, which might be random or structured in some way, and secondly to measure the orientation of individual fish by means of stereo photography.

Cameras positioned below the fish cage, as in Fig. 6.4, do not interfere with the fish echoes. Alternatively, Foote (1983) has described how the work can be done with the cameras to the side of the cage, in a position corresponding to a minimum of the transducer beam pattern, so that the cameras produce very small echoes. This arrangement improves the precision of the tilt angle measurement, but it requires very careful positioning of the cameras, which must not be allowed to move into the main lobe of the beam pattern.

The sensitivity of the echosounder to a group of fish depends on the horizontal distribution of the fish within the cage, since the fish direction as seen from the transducer changes with the distance from the centre of the cage. In calculating the mean target strength of the caged fish, it is usually assumed that the fish are

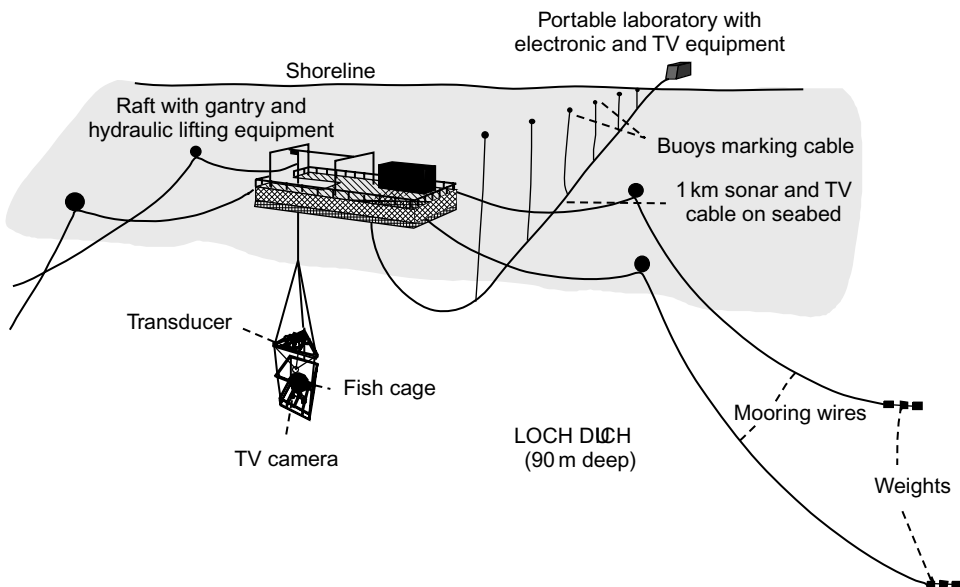


**Fig. 6.5** Sketch of a typical setup used for TS experiments. The fish cage is suspended from a moored raft which is connected by signal cables to an onshore station.

randomly distributed over the horizontal cross-section of the cage. If this is not true, for example if the fish prefer to swim around the cage circumference (a behaviour known as wheeling), the results will be biased. Visual observation of the horizontal fish distribution will indicate whether a correction is necessary to take account of non-random behaviour such as wheeling.

The horizontal sensitivity can be made more uniform by increasing the distance between the cage and the transducer, so that the acoustic beam is wider at the cage. If the beam is too wide, however, the received signal may include echoes from wild fish and other unwanted targets outside the cage.

The received signal will include echoes from the cage as well as from the enclosed fish, and the cage contribution must be subtracted from the measured data. This may be done by recording the echo-integral from the empty cage before the fish are introduced, and preferably again once the fish have been removed at the end of the experiment. The cage should not be made from heavier material than necessary, to minimize the acoustic reflectivity. The cage contribution is not usually important in experiments with fish that have a relatively high target strength, those with a swimbladder, but for fish without a swimbladder it can be a problem. This can be avoided by using a large cage, one much wider than the beam. The amount of fish in the beam is then uncertain, but that does not matter if the target strength is being measured by one of the direct methods (see below). Ona (2003) gives an example of this approach; his experiments with herring in a large pen are described in the next section.

As an alternative to a cage, tethering is another means of holding fish under observation. The tether is a thin line attached to the fish with the other end anchored. This allows the animal essentially free movement while the tether is slack. Tethering was a common *ex situ* technique in the early days (Midttun 1984). Recent *ex situ* work mostly involves fish in cages or pens, but tethering is still used occasionally (Kubecka 1994; Jech *et al.* 1995; Horne *et al.* 2000; Ermolchev and Zaferman 2003).

### *Treatment of the fish*

The capture and handling of live fish is an important part of the experimental technique. The fish must be kept healthy and subjected to the minimum of damage and stress from the moment of capture. The difficulty is that often it is necessary to catch the fish some distance from the experimental site. The fish then have to be transported from the place of capture. The whole operation should be planned in advance, with due attention to the fragility of the species in question and the choice of equipment and techniques. There is an extensive literature on fish transport which should be consulted at the planning stage, e.g. Solomon and Hawkins (1981), Berka (1986).

Sometimes fish may be transported quickly by road, when simple containers might be adequate, such as plastic bags cooled with ice. On other occasions, slow transport by sea may be necessary, calling for more sophisticated equipment to safeguard the fish. Figure 6.6 shows a barge made from an 8 m lifeboat hull, designed by Edwards and Armstrong (1984) for the long-distance transport of clupeoid fishes. The barge contains a 10 m<sup>3</sup> tank which is continuously flushed with sea water by electric pumps.

### *Experimental procedure*

At the start of each experiment, the fish are transferred into the cage at the surface, then the transducer and cage assembly (Fig. 6.4) is lowered to the required depth, around 20 m below the raft. The cage depth must be sufficient to prevent disturbance by surface waves or the tidal flow, and to avoid the low-salinity near-surface layer which is sometimes found in enclosed sea lochs. The transfer of the fish and the descent to the working depth is likely to be stressful, and anomalous results may be observed during the first day or two. Furthermore, systematic changes in target strength are often observed according to the time of day, and are associated with changes in the light level. This phenomenon is discussed later, but the important point relevant to the design of caged-fish experiments is that to obtain a satisfactory average value of target strength, the measurements must continue for several days. Short experiments which run for hours rather than days will produce little useful information. The need for a long series of measurements again emphasizes the importance of careful handling to ensure the survival and consistent condition of the fish.

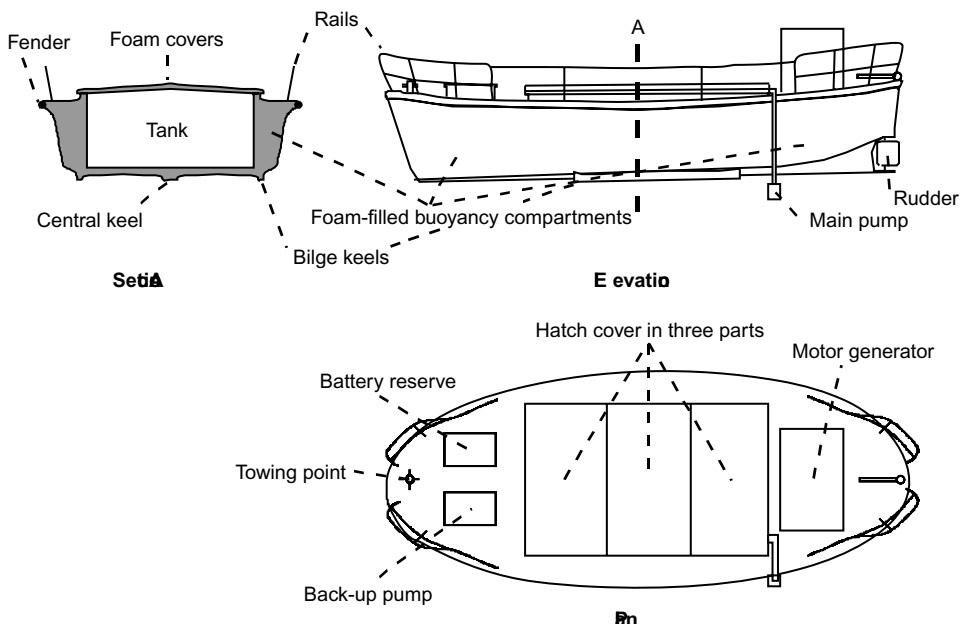


**Fig. 6.6** Barge for the transport of live fish.

At the end of each experiment, the cage is raised and the fish are recovered, at which stage their lengths and weights are measured. It is not practical to collect these data beforehand.

### 6.2.3 Wild fish

Experiments with caged fish have provided much insight into the nature of the target strength and how it depends on physiological and environmental factors. It is possible, however, that the stress of capture or confinement in the cage has some indirect effect on the target strength. For example, the captive fish might not school in the same way as wild fish, so the distribution of tilt angles might also be different. The measurements made on caged fish might not be representative of the target strength of wild fish in open water.

Ideally, target strength data should be obtained from measurements on fish that are typical of the population to be surveyed, both as regards the physiological state of the animals and their environment. The observations should be made unobtrusively, without disturbing the fish or their natural behaviour. This kind of measurement is said to be performed *in situ*, meaning that target strength is determined while the fish remain in place and, all being well, unaware of what is going on. Several techniques have been developed for the *in situ* measurement of target strength.

### *The comparison method*

The echo-integrator provides an acoustic measurement from which the fish density may be determined if the target strength is known. Conversely, if the fish density can be measured independently, the target strength may be estimated from the echo-integrator data. We call this the comparison method. Misund and Beltzstad (1996) have described how it can be applied to herring and mackerel. The fish must lie in a well-defined school which is easily captured by purse seining. First, the purse seiner crosses the school on several transects while the echo-integrator data are collected. At the same time, the dimensions of the school are mapped to determine the total volume. This can be done using an ordinary echosounder to record the vertical extent of the school along the transects, while the horizontal dimensions are determined from the distances covered by the vessel while crossing the school. It is helpful to have a scanning or multi-beam sonar operating at a shallow angle so that the horizontal extent of the school can be observed directly. The sonar display will also show whether the school is disturbed by these activities. After the acoustic measurements are complete, the purse seine is deployed to capture the whole school. The size of the catch divided by the school volume gives the density, which is required to calculate the mean target strength.

When the fish are known to be confined to a small area with limited access, it may be easier to obtain an independent estimate of the population. Mulligan and Kieser (1986) have applied the comparison method in their work on the sockeye salmon, *Oncorhynchus nerka*, in Long Lake, British Columbia. The fish migrate into the lake over a short period in the summer months, and they are counted as they pass through a weir at the single entrance. The weir count is an accurate estimate of the total population which can be compared with echo-integration or echo-counting data, provided most of the population is accessible to acoustic survey, i.e. not too close to the surface, the bottom or the shore.

Another technique is to compare the echo-integration data against the catch rate of a trawl or other fishing gear in the depth stratum that was sampled acoustically. This technique has been applied to studies of demersal fish (Hwang *et al.* 1993) and euphausiids (Pieper 1979; Sameoto 1980). It is necessary to assume that the trawl acts like a sieve, filtering a known volume of water, and that all the animals within this volume are captured. If the target species exhibits an avoidance reaction, so that some unknown proportion escapes capture, the results will not be valid.

### *Direct and indirect target strength measurement*

It is not often that an accurate independent measure of the population density is conveniently available. The more usual kind of *in situ* experiment is conducted to determine the target strength of individual fish, without prior knowledge of the population size. To do this, it is necessary to know the position of the fish in the acoustic beam as well as the echo energy, to compensate for the effect of the directivity

pattern of the transducer. This can be done with instruments like the split-beam or dual-beam echosounders described in Chapter 3, by the so-called direct method. It is also possible to estimate the distribution of target strength values when many targets are observed by a conventional single-beam echosounder. This is known as the indirect method, in which it is assumed that the detected targets are at randomly located positions within the beam. If the beam pattern is known, the target-strength distribution may be deduced from the observed echo-energy distribution using the methods discussed in Section 5.3.

There are three important limitations of the *in situ* technique as applied to individual fish. Firstly, consider the signal received after one ping. This consists of a series of 'echoes' each one comprising the signal while the amplitude is above some threshold. It is necessary to identify those echoes which come from one fish while no other is within the sampling volume. This is done automatically by the signal processor in the echosounder, using algorithms to sort the echoes according to their duration, amplitude stability or other criteria (Ona and Barange 1999). The assumption is that an echo from one fish will have a well-defined shape and the duration should be close to that of the transmitted pulse. When there are multiple targets in the sampled volume, the echo may be longer because there are similar targets at different ranges, or the amplitude may fluctuate due to interference between targets at the same range (Foote 1996). Unfortunately, current methods of single-target detection are imperfect. They are liable to accept some multiple targets as singles because the single-target criteria are satisfied by chance. This problem has been discussed in detail by Soule *et al.* (1995). The superimposed echoes from two fish near to each other will have a combined energy more than that coming from one fish, resulting in the indicated target strengths being too high. This bias can be small to negligible for a low density of large targets, solitary predators such as cod for example. The problem increases with the fish density and can be very severe in and around schools of small fish. Sawada *et al.* (1993) suggest that  $N_v$ , the mean number of fish per sampled volume, is a useful indicator of the multiple-target bias. They conclude that  $N_v = 0.04$  is the upper limit for reliable single-fish measurements. Ona and Barange (1999), however, suggest  $N_v = 1$  as the practical limit. It is unlikely that one  $N_v$  limit can be applied in all circumstances. The multiple-target bias depends on the quality of the single-target detector, and the patchiness of the fish distribution, as well as the fish density.

There is potential for the development of new algorithms to improve the rejection of multiple targets, using the phase information in split-beam signals, see for example Soule *et al.* (1995; 1996). Another possibility is the use of transducers operating at different frequencies to insonify the same fish. Multiple targets are more likely to be rejected if the echoes at two frequencies both have to pass the single-target criteria. This method has been applied successfully by Demer *et al.* (1999).

The second problem arises because the fish detected as single targets are not necessarily representative of the target ensemble. They are by definition in a low-density region where  $N_v$  is less than 1. The selection of isolated targets means that in the

case of species which form dense schools, the recorded measurements will be made on solitary fish which are on the periphery of the main concentrations. These fish may not be typical of the average school member; they may adopt a different tilt angle for example, because the visual cues from nearest neighbours will be less strong.

The third difficulty with the *in situ* method is that it is necessary to catch a representative sample of the fish which have been observed acoustically, to determine the length and species composition. Only then can the observed target strength measurements be related to specific fish targets. The sample is often taken by fishing with a trawl. Unfortunately, it is very difficult to ensure that the trawl catches fish from the same schools that have been observed acoustically. The usual procedure is to operate the acoustic equipment first, and then to deploy the trawl to collect the sample. The two operations are not concurrent. The ship must retrace the track covered during the acoustic measurements and may or may not encounter the same schools. Moreover, the trawl is not a perfect sampling tool; it is likely to catch some sizes of fish more efficiently than others. Other kinds of fishing gear such as the purse seine may be used, but there is still doubt as to whether the catch will be representative of the selected fish whose target strengths have been measured. However, the capture of representative samples is not difficult in favourable circumstances, when there are large monospecific aggregations of fish which are nearly the same size, for example in the surveys of the walleye pollock, *Theragra chalcogramma*, reported by Foote and Traynor (1988).

The direct method provides a one-to-one correspondence between the detected echoes and the target strengths. The indirect method provides the distribution of echo amplitudes modified by the unknown beam factor. The amplitude histogram has to be converted (or deconvolved) to determine the distribution of target strengths. Assuming that the echoes come from fish which are randomly located in the beam cross-section, and with knowledge of the transducer beam pattern, the deconvolution is reduced to a set of simultaneous linear equations which can be solved for the target strengths as frequencies in a histogram. Algorithms for this purpose have been described by Craig and Forbes (1969) and Clay (1983). The exact solution is often unreliable due to poor conditioning of the equations and strong dependence on outliers in the measurements. This problem can be overcome, to some extent, by smoothing the echo-amplitude distribution before it is converted to target strengths, see Rudstam *et al.* (1988) and Hedgepeth *et al.* (1999). We suggest, however, that the indirect method of target strength estimation should be used only if a single-beam echosounder is all that is available. The direct method (using split-beam or dual-beam echosounders) is much better since it completely avoids the statistical problems of deconvolution.

Notwithstanding the practical problems with the *in situ* method, measurements on fish in their wild state, covering all components of the stock being surveyed, should in principle provide the most accurate target strength data for the purpose of estimating fish abundance.

### 6.2.4 Modelling

Purely empirical target strength measurements can be highly variable, even for the same kind of fish. The observed target strength, for a given species and size of fish, is influenced by behaviour (especially the tilt angle) and/or physiology (structure of swimbladder, bones and other tissues), not to mention extraneous factors such as errors in the species/size composition which are a particular problem with *in situ* methods. Models of acoustic scattering by fish help us to interpret the experimental results, and to understand the practical limits within which the experimental findings can be applied to biomass estimation in acoustic surveys.

The swimbladder, when it is present, accounts for 90% or more of the back-scattered energy (Foote 1980b). Thus fish scattering models tend to focus on the swimbladder, with the fish body contribution as a minor addition. The structure of fish is complicated, with discrete body components having different acoustic properties. A different approach is required for large fish compared to small zooplankton which are often modelled as homogeneous fluid-filled objects without gas inclusions (see Chapter 7). Here we further restrict attention to acoustic frequencies well above the swimbladder resonance (often described in the literature as ‘rather high frequencies’), when the wavelength is small compared to the bladder dimensions. There is some interest in low-frequency modelling of the resonance region e.g. Feuillade *et al.* (1996), Feuillade and Nero (1998), but it mainly arises in non-fishery applications. The resonance frequencies of fish swimbladders are typically a few kHz, while fishery echosounders operate at tens or hundreds of kHz.

The swimbladder may be modelled as a simple shape such as a sphere (Andreeva 1964), a finite cylinder (Clay 1992) or a prolate spheroid. These models have the advantage that the acoustic equations can be solved to give exact analytical expressions for the scattered amplitudes, although the solutions may involve infinite summations which must be evaluated with careful attention to the point at which the summations are truncated. Of the simple shapes, the prolate spheroid (an ellipsoid of circular cross-section whose radius is less than the length of the major axis) is the most realistic representation of a real swimbladder. The theory of scattering by a prolate spheroid is well known, but the computation of numerical results is difficult. The exact solutions involve multiple infinite summations which, even with the power of modern computers, are difficult to evaluate. Various approximate solutions have been used to obtain practical results for prolate spheroidal and other shape models. Below we describe those most relevant to fish, with references which may be consulted to explain the mathematical intricacies.

#### *Deformed cylinder model (DCM)*

The target is modelled as a cylinder whose radius varies along the axis. Thus longitudinal asymmetry of the swimbladder is included, but not transverse asymmetry. The echo is calculated as the sum of contributions from narrow sections along the axis, as described by Stanton (1988b). The DCM was originally developed for studies of

plankton (see Chapter 7), but it has also been applied to fish. Clay and Horne (1994) describe a composite model of the Atlantic cod in which the DCM was applied only to the fish body, while a different model (the KRM, see below) was used to evaluate the swimbladder contribution. Similar work on the threadfin shad, *Dorosoma petenense*, has been reported by Jech *et al.* (1995). The DCM can also be used with prolate spheroidal models of the herring swimbladder. Gorska and Ona (2003) showed how this approach overcomes the above-mentioned computational difficulties with the exact solution for prolate spheroids.

#### *The Kirchoff ray-mode approximation (KRM)*

This model assumes that the reflection at every point on an arbitrary interface (e.g. a density discontinuity across an arbitrary closed surface) is the same as the reflection of an infinite plane wave from an infinite tangential interface (Medwin and Clay 1998). The interior of the scatterer is supposed to be homogeneous with the same acoustic properties everywhere. The three-dimensional shape of the scattering surface is conceived as a mesh of contiguous small elements, triangles or quadrilaterals, which can be represented by a digital map of the nodes where the elements connect. An example is shown in Fig. 6.7. The surface is considered in two parts, the insonified region facing the transmitter where the direct path is entirely in water, and the shadowed region where the direct path goes through the scatterer. A pressure-release surface is usually assumed. Then the boundary conditions on the insonified region are that the particle velocity is equal and opposite to that of the incident wave, while in the shadowed region, the particle velocity is zero (Francis 1993). Note that this assumption ignores diffraction effects which, in reality, would cause some of the incident energy to ‘leak’ into the shadowed region. The boundary conditions allow the scattered field to be computed for each element, and the total echo is determined by coherent summation (taking account of phase relationships) of the elemental contributions over the entire surface.

#### *Boundary element method (BEM)*

As for the KRM, the target surface (which may have any shape) is divided into small elemental areas defined by a set of nodal points. The scattered pressure amplitude is expressed through the wave equation (harmonic time dependence of all variables is assumed) converted to Helmholtz integrals, in terms of the pressures and particle velocities at each area element. The solution involves the inversion of a large matrix, and many more calculations than does the simpler KRM approach. A powerful computer (and/or a long time) is required to evaluate the BEM formulas. The BEM, however, takes account of energy diffracted into the shadow zone, an effect which is ignored in the KRM, and it allows the possibility of modelling an inhomogeneous swimbladder as an object with discrete interior inclusions having different acoustic properties (Foote and Francis 2002).

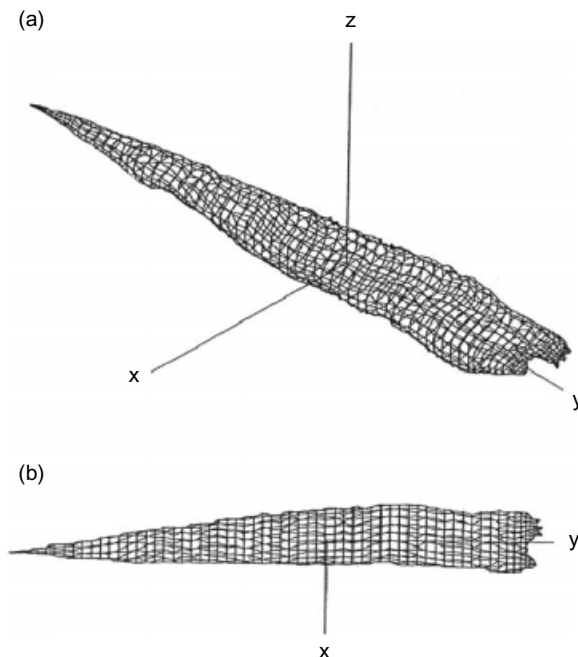


**Fig. 6.7** Example of a mesh fitted to the swimbladder surface, as used for scattering computations. The mesh has 1107 elements and 3181 nodes. The modelled swimbladder (from a 39 cm pollack) is 141 mm long. (Redrawn from Foote and Francis 2002.)

#### *Fourier matching method (FMM)*

The FMM is a sophisticated way of computing the sound scattered by an axisymmetric body, see in particular Reeder and Stanton (2004). It is based on a two-dimensional conformal mapping of the target, hence the restriction to bodies which are symmetrical about the longitudinal axis. In other respects the FMM has fewer limitations than most other models. It is valid over a wide range of frequencies (below and above the Rayleigh transition), body shapes, tilt angles and material properties.

Conformal mapping is done by transforming Cartesian space to a new coordinate system ( $uvw$ ) which has special properties relating to the body shape. Here  $v$  is the azimuthal angle (in the plane of symmetry),  $w$  is another angle and  $u$  is the (transformed) radial distance from the origin. The new system is orthogonal, it preserves the orientation (angular) features of the target and is designed so that  $u$  is constant on the body surface. This allows an analytic solution of the wave equations as a double-infinite summation of Fourier modes, even though the body shape (though axisymmetric) is otherwise irregular. The FMM is numerically efficient in the time required to compute solutions, and it avoids some (but not all) of the problems concerning slow convergence and digital precision which arise in the numerical

evaluation of double-infinite series. These problems are most likely to occur with long thin targets (high aspect ratio) which are irregular in shape.

#### *Measuring swimbladder morphology*

The first step in evaluating any model is to determine the swimbladder morphology of the subject fish. What we require are digitized positions which map the surface at sufficient resolution to represent the true shape. There are two techniques for doing this with real fish. Firstly, as described by Foote (1985), we might construct a physical replica of the swimbladder. The fish is quickly frozen in a bath of liquid nitrogen, the swimbladder is extracted and a cast of identical shape is made. The digital map is constructed by slicing the cast into thin sections with a microtome, then photographing and digitizing the outline of each section. This is a lengthy procedure. The alternative method of X-ray imaging is faster although less good in the spatial resolution. The images of the fish (normally dorsal and lateral aspects) show cross-sections of the swimbladder whose outlines can be traced (Yasuma *et al.* 2003). Recent advances in computer tomography have shown that fish body shapes and structures can be digitized in the same way (Horne *et al.* 2000; Reeder *et al.* 2004).

The nodes for swimbladder mapping must be close enough to obtain good representation of the acoustic variables. Foote and Francis (2002) suggest that, when the area elements are curved and smoothly joined, the spacing should be  $\lambda/3$  and  $\lambda/6$  for the BEM and KRM respectively. Closer spacing would be necessary for the same resolution if the area elements were flat. These criteria imply that several thousand nodes are needed for an adequate representation of the swimbladder in, for example, a 30 cm cod.

#### *Comparison of models*

It is unclear whether simple shapes can adequately represent the form of real fish swimbladders. Prolate spheroids are certainly more realistic than spheres or cylinders. The DCM and FMM allow any shape for the longitudinal section, but the transverse section is assumed to be circular. The KRM and BEM techniques have the advantage of being fully three-dimensional. They do not involve any assumptions on symmetry and can be applied to swimbladders of arbitrary shape. In that case it is necessary to map the swimbladder surface into a digital representation. The KRM is relatively simple to compute, but it is inaccurate at low frequencies and high aspect ratios i.e. in the case of fish, high tilt angles. The BEM and FMM techniques are valid over a wider range of frequencies for any orientation of the target.

Once the digital map of the swimbladder has been prepared, repeated calculations can be done to predict the target strength for any orientation of the fish. If the results are to be extended to represent the mean of many target strengths sampled from a wild-fish aggregation, it is necessary to make a further assumption about

the distribution of tilt angles adopted by the fish in the aggregation. This might be modelled as a normal distribution with a specified mean and standard deviation, or a replicate of an actual distribution observed in field experiments. The model results are weighted by the tilt-angle distribution, then averaged (this must be done in the linear domain, using backscattering cross-sections) to calculate the mean target strength of the insonified fish.

### 6.3 Experimental results

Many experimental investigations have been reported using all of the techniques described above. Each technique has advantages and disadvantages, and we shall now consider how the different approaches have contributed to our knowledge of the acoustic scattering properties of fish and other aquatic lifeforms.

Whatever the method, the target strength is determined experimentally from measurements of the echo intensity and (excepting the direct methods) the sampled volume. It is normally the case that a signal threshold is applied to eliminate noise and weak (e.g. planktonic) echoes of no interest. However, any fish echoes below the threshold are also ignored. This means that if the TS distribution begins below the threshold, the average echo intensity (calculated from the stronger signals) will be biased high. An additional problem arises with the sampled volume when that enters the equation. For a target with a given TS, increasing the threshold reduces the sampled volume because the cut-off point on the transducer beam pattern moves closer to the central axis (Foote 1991a; Reynisson 1996). The sampled volume corresponding to a given TS distribution can be estimated if the beam pattern is known, but that is problematic when the whole object of the experiment is to measure the TS distribution itself.

It is important to be aware of this problem, especially when measuring the TS of small fish which lack a swimbladder. In general, we can say that the threshold-induced bias should not be significant when the signal-to-noise ratio is good, provided the threshold is not set higher than it needs to be.

#### 6.3.1 *Immobile fish*

Among the early investigations, the comprehensive work of Love (1971; 1977) is notable. He collected data on many species from 14 families, using echosounders operating at a range of frequencies from 15–1000 kHz. The body of the fish was exposed to the acoustic beam in different aspects, from dorsal through side-on to ventral. Love supposed that the target strength would be systematically dependent on both the body length  $L$  and the frequency  $f$ . He proposed the following formula for the target strength:

$$TS = m \log L + mf \log f + b \quad (6.2)$$

where  $m$ ,  $m_f$  and  $b$  are constants for a given aspect of the fish (e.g. dorsal), to be determined by the best fit to the experimental data. However, Equ. (6.2) is now mainly of historical interest. It became apparent from later work that the determinants of the target strength are too complicated to be described by one simple relationship, applicable to all species over a wide frequency band.

Nakken and Olsen (1977) conducted experiments with many individual fish (17 species) at two frequencies: 38 and 120 kHz. In each case, the target strength was measured over a range of tilt and roll angles to observe the change with the orientation of the fish body in the acoustic beam. The results could then be presented as graphs of target strength against angle, as in Fig. 6.3, or tabulated as in Foote and Nakken (1978). It was found that the tilt angle had a much larger effect than the roll. Further, the target strength would sometimes change rapidly over a small range of tilt angles, and these changes were greater than could be explained by simple geometrical ideas of the aspect of the fish body exposed to the acoustic beam. However, there was normally a well-defined maximum in the target strength plotted against the tilt angle, and this value was called the ‘maximum dorsal-aspect target strength’. Different species and sizes of fish could be compared in terms of the maximum target strength. In general, larger fish of the same species had larger target strengths, but there was considerable scatter in the results. Foote (1983) used the Nakken–Olsen technique to determine the target strength at various tilt angles of immobilized specimens, after measurements on the same fish while they were alive in a cage, for his demonstration of the linearity principle (Section 5.4.3).

The early investigators recognized that the maximum target strength measurement would be of limited practical use, because active free-swimming fish would adopt a range of tilt angles. For wild fish, target strength would vary between individuals, and the average value would be less than the maximum recorded in dorsal aspect. Love (1971) suggested that the target strength averaged over the tilt angle range  $\pm 45^\circ$  would be representative of wild fish, but this idea was not based on any observations of natural fish behaviour. By reference to tilt-angle distributions derived from underwater photographs of live fish, Nakken and Olsen (1977) thought that the average target strength appropriate to wild fish would be 6 dB less than the maximum dorsal-aspect value. This conclusion was based on very limited data.

The observed fish are normally insonified from above. An interesting exception is the work of Kubecka (1994) on the lateral-aspect target strengths of freshwater fishes. In water too shallow for vertical echosounding, fish may still be insonified by a horizontal sonar beam. The same principles apply to target strength determination in this case, but there is the added complication of the substantial difference in the echoes from fish observed in the head–tail or side directions. Using stunned fish mounted on a rotatable frame, Kubecka measured the target strength against  $\phi$ , the horizontal angle relative to the head–tail axis. The sonar frequency was 420 kHz. He found that a cubic-cosine model gave the best fit to his data. For a 19 cm rudd, *Scardinius erythrophthalmus*, a least-squares fit gave the lateral-aspect target strength

**Table 6.1** Selected literature on target strength experiments using immobilized or dead fish. This technique is now mainly of historical interest.

Species	Frequency (kHz)	Reference
Gadoids and clupeoids (17 species)	38, 120	Nakken and Olsen (1977)
Common shiner ( <i>Notropis cornutus</i> )	220	Huang and Clay (1979)
Mummichog ( <i>Fundulus heteroclitus</i> )	220	Huang and Clay (1979)
Cod ( <i>Gadus morhua</i> )	30	Fedotova and Shatoba (1983)
Yellowtail ( <i>Seriola quinqueradiata</i> )	50, 100	Miyanohana <i>et al.</i> (1986)
Japanese horse mackerel ( <i>Trachurus japonicus</i> )	50, 100	Miyanohana <i>et al.</i> (1986)
Sea bream ( <i>Pagrus major</i> )	50, 100	Miyanohana <i>et al.</i> (1986)
Various freshwater fishes	70	Borisenko <i>et al.</i> (1989)
Kokanee ( <i>Oncorhynchus nerka</i> )	50	Mukai and Iida (1996)
Orange roughy ( <i>Hoplostethus atlanticus</i> )	38	McClatchie <i>et al.</i> (1999)
Myctophids (mainly <i>Benthosema fibulatum</i> )	200	Benoit-Bird and Au (2001)

as  $TS = -7.55 \cos^3(2\phi) - 44.3$  dB. Kubecka's model predicts equal minima of TS in the head and tail directions ( $\phi = 0$  or  $180^\circ$ ) and equal maxima in the side directions ( $\phi = 90$  or  $270^\circ$ ).

Other studies using immobilized fish have covered many species and frequencies, see Table 6.1 for a summary of this work. Bearing in mind the unusual condition of the subject fish, the target strengths measured in such experiments are now considered too inaccurate to be used directly for the interpretation of survey results. That objective requires observations on live, healthy fish. Nevertheless, studies of immobilized fish have certainly provided useful insights in more general investigations of the target strength and its variation.

### 6.3.2 Live fish in cages

The concept of target strength measurement using live fish held in a cage is well established, see Foote (1986) for a review of early work in this field. The technique was developed in a series of experiments conducted by Edwards *et al.* (1984) using a raft moored in a sea loch on the west coast of Scotland. Their equipment evolved through technical development during the course of the work, starting with simply suspended cages leading to the more sophisticated apparatus illustrated in Figs 6.4 and 6.5. The aim was to collect representative target strength data for species which might be encountered on acoustic surveys of fish populations, and to investigate the variation of target strength in relation to environmental and biological factors. Edwards *et al.* (1984) studied several species – various gadoids, clupeoids and the Atlantic mackerel, *Scomber scombrus*, among others. The experiments were conducted mostly at 38 kHz but they included some measurements at 120 kHz.

In most cases the procedure was as follows. At the start of each experiment, the cage was raised to the surface and the fish selected for measurement were transferred from a nearby holding facility. The cage was then lowered to about

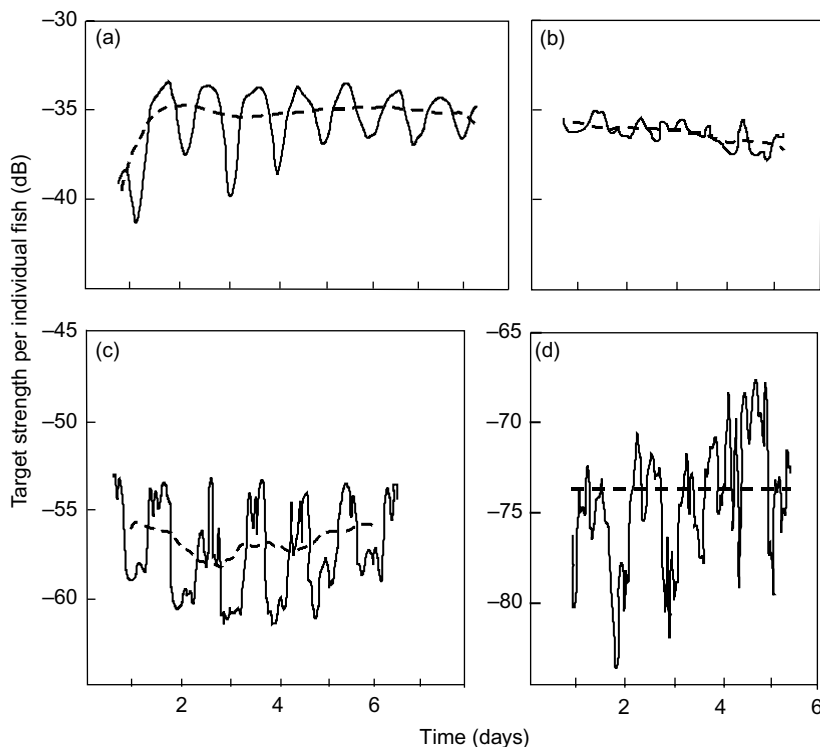


**Fig. 6.8** Target strength of caged fish at 38 kHz (solid curves). Examples of experimental results for (a) cod,  $\bar{L} = 28.5$  cm,  $N = 41$ ; (b) herring,  $\bar{L} = 24.3$  cm,  $N = 78$ ; (c) mackerel,  $\bar{L} = 32.5$  cm,  $N = 100$ ; (d) sandeel,  $\bar{L} = 12.3$  cm,  $N = 3750$ . The marks on the time axes are at midnight. The broken curves are 24-hour moving averages in (a) to (c) and the overall mean target strength in (d).

20 m depth where it remained for several days while the measurements were performed. A few examples of the results obtained at 38 kHz are shown in Fig. 6.8 as graphs of the mean target strength against time. The curves represent running averages of the measurements made during the previous hour, or some longer period as noted in the legend. The echosounder transmitted three pulses per second; however, the target strength measured from one transmission is extremely variable. By presenting the results as averages over many transmissions, the random component is reduced to reveal the systematic time dependence which is evident in Fig. 6.8.

#### Variation with time

In the case of the cod, *Gadus morhua* (Fig. 6.8a), the target strength is low at the start, then it gradually increases over the first day or two. This happens because the fish are initially acclimatized to atmospheric pressure, having been kept in a holding facility close to the sea surface. When the fish are lowered to 20 m depth,

the swimbladder is compressed to less than half its initial size. The bladder volume is gradually restored by gas secretion and, as it inflates, the target strength increases. A pronounced diurnal cycle is superimposed on this trend. The target strength is higher during the day than at night. This is probably caused by some change in fish behaviour associated with the light level. The ability of the fish to see each other could affect their orientation or schooling behaviour. The dotted line which shows the 24-hour running average of target strength is, however, steady once the initial acclimatization period is over.

This diurnal cycle in the target strength is often observed with fish in cages, but there are important differences between species. In the case of the herring, *Clupea harengus*, there is no evidence of an acclimatization period following the change in depth at the start of the experiment (Fig. 6.8b). Unlike the cod, the 24-hour average of the herring target strength shows a consistent decline. This is caused by diffusion of gas out of the swimbladder, whose volume slowly decreases with time. The effect is more pronounced in smaller fish. This is to be expected, since in approximate terms, the gas diffusion rate is proportional to the swimbladder surface area, and hence to the square of the fish length, whereas the volume of the swimbladder depends on the cube of length. Over the same time, a smaller fish will lose a greater proportion of the gas in the swimbladder through diffusion.

The Atlantic mackerel, *Scomber scombrus*, has no swimbladder and the target strength of this fish is much lower than that of clupeoids or gadoids of similar size. The problem of gas-pressure adjustment does not arise. As can be seen in Fig. 6.8c, there is no initial acclimatization period, nor is there any consistent trend in the daily average of the target strength. On the other hand, the diurnal cycle is particularly evident here. This is due to the very different swimming behaviour of mackerel by night and by day, through the consequent changes in the tilt-angle distribution. Another species with no swimbladder is the sandeel, *Ammodytes* sp. Figure 6.8d shows some evidence of diurnal changes in the sandeel target strength, although other effects are clearly contributing much random variation. Furthermore, there is a small rise in the measured target strength during the experiment. This is unlikely to represent a real change of reflectivity, and is probably due to the difficulty of measuring such low target strengths in a cage experiment. The sandeel is a much smaller fish than the mackerel and so the individual-fish target strength values are not directly comparable. The measurements may be compared, however, by adjusting target strength to represent the same weight of fish. To do this, the quantity  $10 \log(W_m/W_s)$  is added to the sandeel per-fish data, where  $W_m$  is the mean weight of the mackerel (287 g), and  $W_s$  is that of sandeel (6.75 g). The added term is  $10 \log(275/6.75) = 16.3$  dB. For the same weight of fish, the average target strength of sandeel is a few dB higher than that of mackerel, but the scatter about this average overlaps to a large extent. Although the two species are very different in many physiological respects, it appears that their acoustical properties for the same weight of fish are not too dissimilar.

### *Variation with depth*

The volume of a gas-filled swimbladder depends on the ambient pressure which increases with the water depth. If the amount of gas remains the same, then according to Boyle's law, the volume is inversely proportional to the pressure. Thus the target strength is likely to change with the depth of the fish, the amount of time it has remained at the same depth, and whether the fish arrived there by moving downwards or upwards.

Figure 6.9 compares the results from three experiments with different species, conducted by Edwards and Armstrong (1984). The fish were in a cage which was raised or lowered at intervals, the depth being held constant for some time between moves. The fish were initially acclimatized to near-surface pressures, having been held in a pen at a depth of 2–3 m for several weeks before transfer to the experimental cage. At the start of each experiment, the cage was dropped to 17.5 m depth. At intervals of several days, the cage was again lowered or raised, eventually returning to 17.5 m.

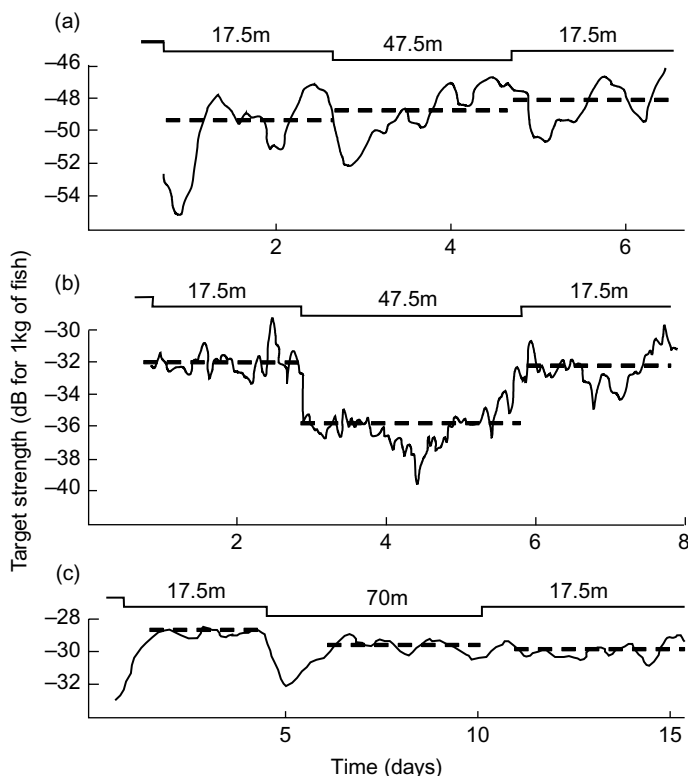


**Fig. 6.9** Depth dependence of the target strength. The fish are in a cage which is moved down and up. (a) Haddock; (b) herring; (c) mackerel. The step changes of depth are shown above each record. Broken lines indicate the mean target strength over the acclimatized period at each depth. (Redrawn from Edwards and Armstrong 1984.)

Figure 6.9a shows that the target strength of the haddock, *Melanogrammus aeglefinus*, falls when the fish are lowered from 17.5 m to 46.5 m, then recovers to its original value over 36 hours. A similar recovery can be seen at the start of the experiment following the initial drop from the surface to 17.5 m. When the fish are raised from 47.5 to 17.5 m, however, the effect on target strength is small and transient. The haddock and the cod show similar characteristics in this respect, but the response of the herring, *Clupea harengus*, to the same test is quite different (Fig. 6.9b): the mean target strength changes systematically with depth and is more or less constant at the same depth. The Atlantic mackerel, *Scomber scombrus*, does not show a consistent response to the changes in depth, as might be expected for a fish with no swimbladder (Fig. 6.9c). There are, however, large transient changes in target strength, particularly in the few hours following the trauma of the transfer to the experimental cage.

More recently, Ona (2003) made a comprehensive study of how the herring target strength changed with depth. Part of this was a 'vertical excursion' experiment. The fish were in a large cage ( $12.5 \times 12.5 \times 21$  m) deployed from a research vessel. The water depth below the moored vessel was sufficient to allow measurements down to 100 m. This cage is so large that the transducer (at the top of the cage) will insonify only a fraction of the cage volume. In the early *ex situ* work done with single-beam transducers, the fish aggregation had to be measured as a whole, thus the cage size was limited by the need to ensure that all the fish were within the beam. Ona used a split-beam transducer (38 kHz) to measure single-fish target strengths. This technique places no restriction on the cage size. The results showed a consistent reduction in the herring target strength as the cage dropped from the surface to 100 m depth.

Since the swimbladder accounts for 90% or more of the scattered energy, we expect the target strength to be determined primarily by the volume, V, and the shape of the bladder surface. Ideally we want to express the target strength as a function of depth. The ambient pressure is 1 atm at the surface and it increases by 1 atm per 10 m of depth. Thus the pressure at depth z metres is  $(1 + z/10)$  atm. If Boyle's law applies, then  $V \propto (1 + z/10)^{-1}$ . Consider first the simple case of a spherical balloon which contracts symmetrically under pressure, without change of shape. Suppose that the backscattered echo is determined by the geometric cross-section rather than the volume of the swimbladder. The cross-section of a sphere changes as volume to the power  $2/3$ , and it follows that  $\sigma_{bs} \propto (1 + z/10)^{-2/3}$ . Mukai and Iida (1996) conducted depth-excursion experiments on live kokanee, *Oncorhynchus nerka*, tethered to a frame. They showed that the balloon model satisfactorily described the target-strength changes down to 40 m depth. A real swimbladder, however, may not contract symmetrically. A more general model is  $\sigma_{bs} \propto (1 + z/10)^\gamma$ , where  $\gamma$  is known as the 'contraction-rate factor'.

Ona (2003) applied the general model to data from several sources, including his caged-fish experiments and *in situ* measurements on herring down to 500 m depth. He found that  $\gamma = -0.23$  gave the best fit to the combined dataset. This is closer to zero than the balloon  $\gamma$  (which is  $-2/3 \approx -0.67$ ), suggesting that the horizontal

cross-section of the swimbladder contracts more slowly with depth than it would in a sphere. In other words, the height is more compliant than the length as the pressure increases. In terms of the target strength, Ona's results convert to the formula  $TS = TS_0 - 23 \log(1 + z/10)$ , where  $TS_0$  is the target strength of surface-adapted fish.

### 6.3.3 Wild fish

There is an extensive and growing literature on the measurement of target strengths *in situ*. All three of the techniques described in Section 6.2.3 have been widely applied. These are the direct method with dual-beam or split-beam transducers (Foote *et al.* 1986; Barange *et al.* 1996; Lillo *et al.* 1996; Rudstam *et al.* 2003), and the indirect method for observations made with the conventional single-beam echosounder (Ehrenberg *et al.* 1981; Halldorsson and Reynisson 1983; Rudstam *et al.* 1988). Foote and Traynor (1988) describe an unusual application in which the signals from one transducer are processed in two channels, to provide dual-beam and split-beam measurements simultaneously.

These *in situ* techniques are unobtrusive inasmuch as the transducer will normally be more distant than the visibility range from the target, thus avoiding visual cues. The measurements are restricted to isolated fish. The signal processor should reject any superimposed echoes coming from neighbouring fish. In normal circumstances, when the fish occur in moderately dense concentrations, the signal processor will record the target strengths of only a small proportion of the insonified fish, those which are sufficiently isolated to pass the single-fish detector.

#### *Interpretation of in situ data*

In practice, *in situ* experiments are performed by recording many target strength measurements over a period of time while a particular layer or school of fish is under observation. The measurements usually cover a wide span of target strength values. It is convenient to display this sort of information as a histogram of target strength frequencies, as in Fig. 6.10 which shows measurements from Forbes (1985) made on a layer of fish to the west of the British Isles, using a 38 kHz dual-beam echosounder. The target strength distribution is bimodal, and we suppose that each peak is associated with one species and size category of fish. There may of course be more than one species present, or more than one year class of the same species. The important question to be answered is this: which species and/or size category is associated with which peak of the target strength histogram?

In the case of Fig. 6.10, trawl catches showed that the layer contained blue whiting, *Micromesistius poutassou*, in the size range 25–30 cm, and also the myctophid, *Maurolicus muelleri*, which is a much smaller fish. Probably the blue whiting were feeding on the myctophids. Because of the size difference between the two species, it is relatively easy to identify the modes in the target strength histogram; the right-hand peak is associated with the blue whiting, and the left-hand one is the myctophids.

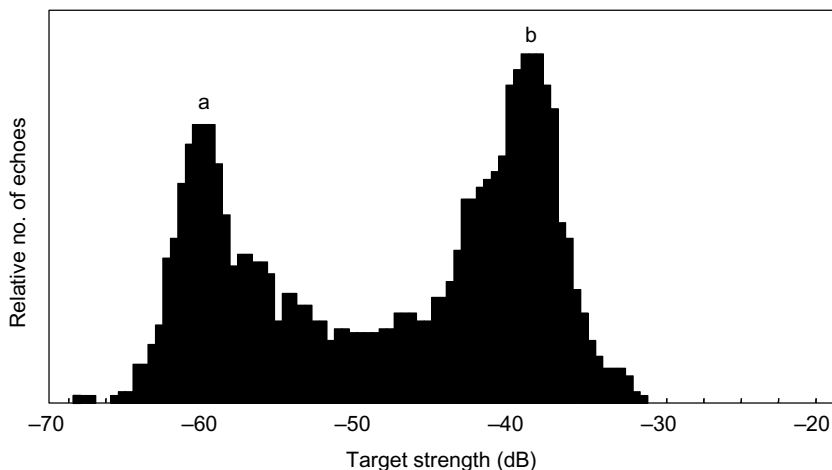


**Fig. 6.10** TS histogram from measurements on a fish layer. The data were collected using a dual-beam echosounder. The two peaks correspond to fish of different sizes, identified by trawling as (a) myctophids and (b) blue whiting, *Micromesistius poutassou*. (Redrawn from MacLennan and Forbes 1987.)

The first problem in the interpretation of *in situ* target strength data is to relate the size modes of fish from the trawl catch to the modes observed in the TS histogram. This is not difficult when there are only a few well-separated modes. Figure 6.11 shows an example which requires more careful interpretation. Again, blue whiting are known to be present in the observed layer. The trawl catch histogram in Fig. 6.11b shows three length modes which correspond to successive year classes of fish. Three target strength modes are tentatively identified in Fig. 6.11a, at the higher values appropriate to blue whiting. The latter possibly correspond to the length modes of the trawl samples, but the quality of the data is not good enough to be certain about this conclusion.

The idea of matching the modes in paired trawl and acoustic histograms is, at best, rough and ready. Only the peak values of the modes are considered; the lower values on either side of a peak are ignored. Furthermore, the target strength for a particular species and size must be considered as a stochastic variable, one which exhibits a range of values in repeated measurements of apparently similar targets. MacLennan and Menz (1996) have described a statistical method for the analysis of corresponding TS and fish-length histograms. To apply this method, we need to know (or to assume) the type of probability density function (PDF) applicable to the backscattering cross-section of a given fish ( $\sigma_{bs}$ ), and the form of the equation giving the mean target strength as a function of the fish length.

A common assumption is that fish echo amplitudes follow the Rician distribution, or the Rayleigh distribution which is a special case of the Rician (Clay and Heist 1984; Kieser and Ehrenberg 1990). The Rayleigh assumption means that  $\sigma_{bs}$  (which is proportional to the amplitude squared) has an exponential distribution. The PDF of the

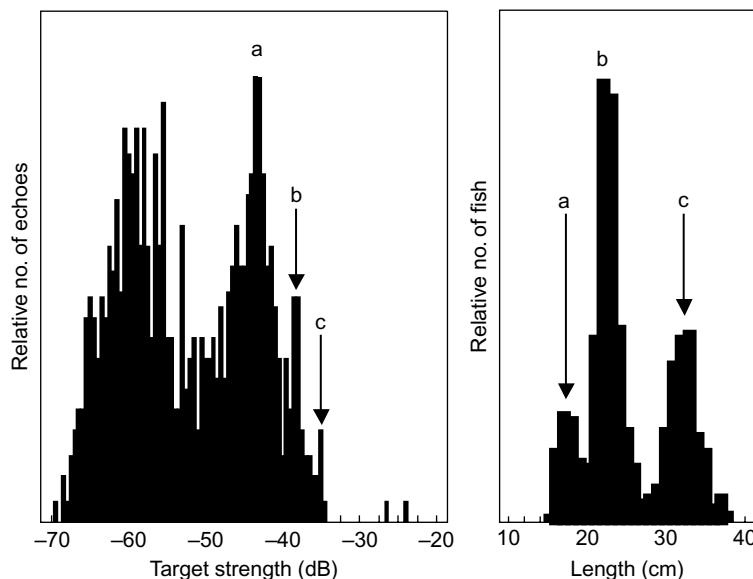


**Fig. 6.11** Comparison of TS measurements and trawl samples of blue whiting. The TS histogram (left) shows evidence of three modes (a, b and c); so do the trawl samples (right). The TS modes may be related to fish from successive year classes (a, b and c), although the correspondence is uncertain in this example. Any modes below  $-50$  dB are associated with smaller targets e.g. myctophids. (Redrawn from Forbes 1985.)

exponential distribution is  $P(\sigma_{bs}) = (1/\langle\sigma_{bs}\rangle) \exp(-\sigma_{bs}/\langle\sigma_{bs}\rangle)$ , where the parameter  $\langle\sigma_{bs}\rangle$  is the true mean, and the corresponding target strength is  $10 \log(\langle\sigma_{bs}\rangle)$ . The Rician distribution has an additional parameter,  $\gamma_r$ , which is the ratio of ‘concentrated’ and ‘distributed’ components of the signal. The limits  $\gamma_r \rightarrow 0$  and  $\gamma_r \rightarrow \infty$  correspond, respectively, to Rayleigh and Gaussian distributions. According to Clay and Heist (1984),  $\gamma_r$  depends on the fish morphology and behaviour.  $\gamma_r$  is small for large fish, in which case the Rayleigh assumption is a good approximation. Conversely, the Gaussian distribution would be better as a simple model for small fish.

In their study of *Diplotaxodon* spp., MacLennan and Menz (1996) assumed the Rayleigh distribution of echo amplitudes and the function  $TS = 20 \log L + b$ , which is equivalent to  $\langle\sigma_{bs}\rangle = 10^{b/10} L^2$ . This particular form of the length dependence is discussed below in more detail. An initial value for  $b$  is guessed, and  $\langle\sigma_{bs}\rangle_i$  is calculated for each length  $L_i$  in the catch histogram. This information is sufficient to calculate an overall TS histogram. The frequencies of the calculated and observed TS histograms are compared, see Fig. 6.12, and  $b$  is adjusted until the least-square difference between the two is minimized. The final value of  $b$ ,  $-67.4$  dB, gives the best estimate of the TS function for *Diplotaxodon* spp.

The best conditions for *in situ* target strength measurement occur when the observed fish are homogeneous, consisting of one year class of one species, and

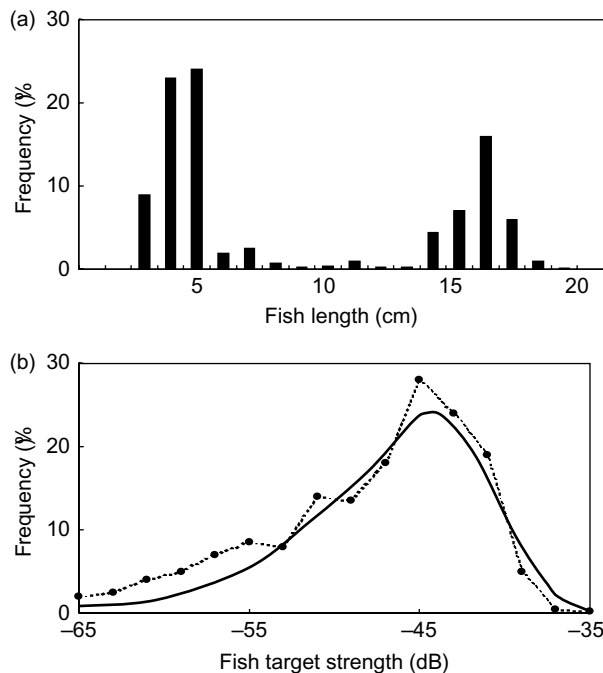


**Fig. 6.12** Estimating the TS-length relationship. (a) Fish size distribution; the larger mode is *Diplotaxodon*  $\bar{L} = 15.8$  cm, s.d. = 1.1 cm; (b) --- • --- observed TS frequencies in 2 dB intervals; —— best fit distribution ( $b_{20} = -67.4$  dB) matched to the *Diplotaxodon* mode. (Redrawn from MacLennan and Menz 1996.)

when the size distribution can be confirmed by fishing. Some examples from the literature are presented in Fig. 6.13. It is notable that the observed target strengths cover a large range, spanning 20 dB or more, even when the fish are nearly the same size. This confirms the stochastic nature of target strength, although it is reasonable to expect that the average of many TS measurements would have a systematic dependence on the size and species of the fish targets.

The results from *in situ* TS experiments need to be treated with some caution. There are many factors which can introduce substantial bias, notably the single-target echo detector and the extent to which the identified targets are representative of the whole population. The reliability of *in situ* data should be carefully considered before the relevant target strengths are used to estimate the fish abundance.

### 6.3.4 Size-dependence of target strength

The results of target-strength experiments are often expressed in terms of the body length L using the equation:

$$\text{TS} = m \log L + b \quad (6.3)$$

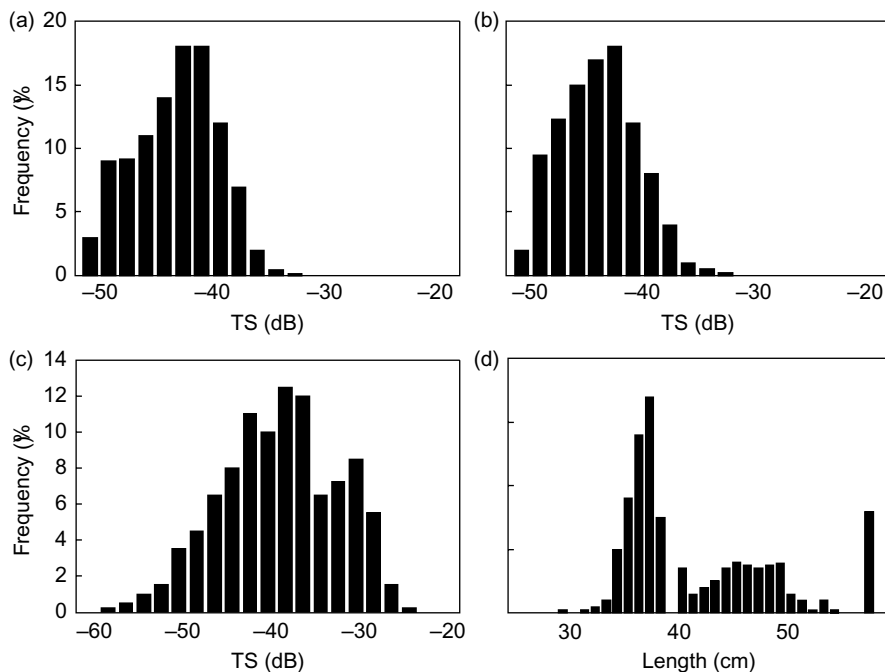


**Fig. 6.13** Target strength of wild fish at 38 kHz. Examples of experimental results with split-beam echosounders. (a) Herring, *Clupea harengus*, at 65–95 m depth,  $\overline{TS} = -43.4$  dB,  $\overline{L}$  (from trawl samples) = 28.5 cm,  $N = 6545$ ; (b) herring at 15–45 m,  $\overline{TS} = -42.6$  dB,  $\overline{L} = 28.5$  cm,  $N = 2687$ ; (c) walleye pollock, *Theragra chalcogramma*,  $\overline{TS} = -33.6$  dB; (d) trawl samples related to (c). (Herring data from Foote *et al.* 1986; others from Foote and Traynor 1988.)

where  $m$  and  $b$  are constants for a given species. This is essentially the same as Love's model (Equ. 6.2) without the frequency term. Equation (6.3) has been generally accepted as a reasonable and convenient, if not necessarily accurate, description of how the mean target strength depends on the fish length, see Foote (1979a). From observations made on a particular group of fish, we get one estimate of the mean target strength which is associated with the mean length of the fish. When data are available from several experiments of this kind, made on different groups of fish whose mean lengths cover a range of values, the slope  $m$  and the intercept  $b$  can be estimated by linear regression of target strength on  $\log L$ . Note that Equ. (6.3) does not imply a deterministic relationship which can be applied to the individual fish.  $L$  is the mean length of the observed group, and  $TS$  is the expected (i.e. mean) value of the target strength.

We normally use  $L$  to denote the total length of the fish, measured from the front of the head to the tip of the tail. Some writers describe their results in terms of the standard length (head to the end of the caudal peduncle) or the fork length (head to the notch in the tail). Here, unless otherwise stated,  $L$  is the total length.

It is convenient to summarize the results from a series of experiments by quoting the regression parameters  $m$  and  $b$ . Tabulated results are presented at the end of this chapter (Tables 6.3–6.6).  $m$  is generally between 18 and 30, and often close to 20. In the case of physostomous fish,  $m$  is consistently close to 20, the value predicted by the area scattering model (Table 6.4). This finding has resulted in the popular view that the true  $m$  is always 20. This is a simple idea which is possibly wrong, or at least not universally applicable. When  $m = 20$  is assumed in the analysis of target strength data,  $b$  is written as  $b_{20}$  and Equ. (6.3) is replaced by the ‘standard’ formula:

$$TS = 20 \log L + b_{20} \quad (6.4)$$

The parameter  $b_{20}$  is also known as the reduced target strength. It may be estimated as the mean of  $(TS - 20 \log L)$  over the experimental data. In Tables 6.3–6.6, the results are summarized sometimes by  $b_{20}$  and sometimes by  $m$  and  $b$  obtained from a proper linear regression. In the latter case, the equivalent  $b_{20}$  is given to facilitate comparison of the results. The  $b_{20}$  of fish is generally in the range –85 to –65 dB, depending on the species. The utility of the simple log-length method for describing the target strength is discussed further below.

### 6.3.5 Modelling

Foote (1985) conducted experiments on immobile pollack, *Pollachius pollachius*, in his investigation of acoustic scattering by the swimbladder. Having measured the target strength over a range of tilt angles, he constructed a digital map of the swimbladder surface as described in Section 6.2.4. He then calculated the theoretical scattered sound field of the real swimbladder, using the KRM model, as a function of the tilt angle. There was good agreement between the experimental and theoretical target strengths (Fig. 6.14). The implication is that the rapid variation of target strength with tilt is caused mainly by the irregular shape of the swimbladder, since the theoretical calculations did not take account of scattering by other organs and body tissues.

Clay and Horne (1994) developed a complete acoustic model of the cod, *Gadus morhua*, in which the swimbladder echo was determined in the same way as Foote (1985), while a different model (the DCM) was used to calculate the smaller contribution from the fish body. The complete fish echo was obtained as the coherent sum of the swimbladder and body contributions. Again, the model was validated by comparison with experimental data. Plate 6.1 is an illustration of the model results, showing how the target strength varies with the target orientation and the echosounder frequency.

There have been many similar studies on various species. Model calculations have demonstrated the important effect of fish orientation on the target strength. This effect is more significant at higher frequencies, as shown by Jech *et al.* (1995). Reeder *et al.* (2004) describe how broadband measurements (40–95 kHz) combined with high-resolution X-ray morphology can identify sound scattering features apart from

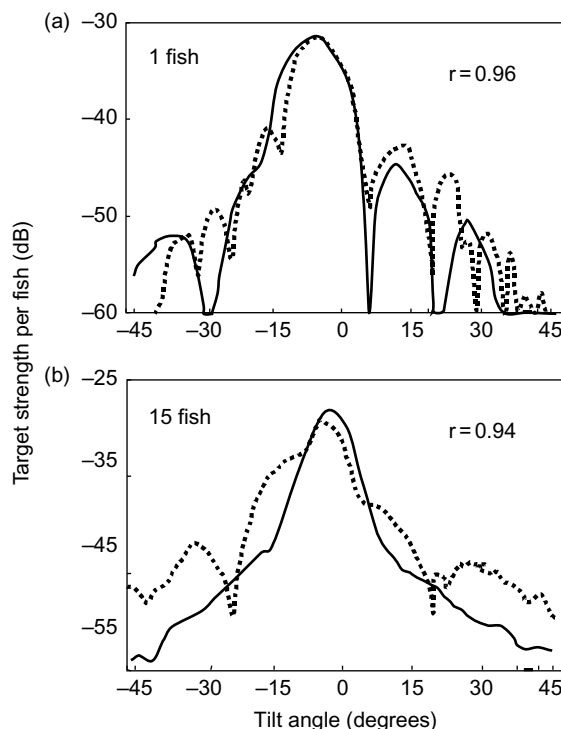


**Fig. 6.14** TS functions of pollack, *Pollachius pollachius*, in dorsal aspect at two frequencies. Positive tilt angles are head-up. Solid curves are computed functions; broken curves are measured functions. (a) Single fish,  $L = 31.5\text{ cm}$ ; (b) composite results for 15 fish,  $\bar{L} = 37.0\text{ cm}$ .  $r$  is the correlation coefficient between computed and measured functions. (Redrawn from Foote 1985.)

the swimbladder, the skull for instance. Experimental work backed by theoretical studies can improve the precision of purely empirical estimates of the target strength. See Tables 6.3–6.6 for additional citations of this combined approach.

## 6.4 Discussion

The target strength of apparently similar fish is highly variable. It may change with time or between individuals, due to behavioural or physiological reasons which are not well understood (MacLennan *et al.* 1989; 1990b). We must think of target strength as a stochastic variable, one which is described by a probability distribution. This means that the result of any one target strength measurement is unpredictable. As far as the practice of acoustic surveying is concerned, however, the inherent variability of target strength is not too important. It is the expected value (of the backscattering cross-section) that is required to calculate the fish density. The expected value is the mean of the probability distribution, and we suppose that it is determined

by observable characteristics such as the size, behaviour and species composition of targets.

#### **6.4.1 Comparison of target strength measurement techniques**

Experiments with immobile fish do not reliably estimate the target strength of active fish. Uncertain physiological changes are likely to occur after the animal is rendered unconscious, and the effect of this treatment on the acoustic properties of the body is unclear. More accurate results are obtained from studies with live fish. Nevertheless, the immobile-fish technique has the advantage of allowing the orientation of the target to be measured precisely, so that the functional dependence of target strength can be studied in detail, especially the variation with the tilt angle.

Experiments with live fish in cages have provided much insight and practical information as to how the target strength depends on the physiology of the animals, their behaviour, and environmental factors such as the ambient pressure and the light level. The technique has the advantage that the observed fish are available for examination. During the experiments, the behaviour of the fish may be observed visually, and the distribution of tilt angles or other behavioural parameters may be determined by photography. Afterwards, it is a simple matter to record precise length and weight distributions from post-mortem examination. The acoustic measurements may be related to observed features of the fish aggregation, to search for determinants of the target strength. One limitation is that the behaviour and condition of captive fish may not be representative of those in the wild, owing to the stress of capture and the restraints of captivity. If the behaviour of wild fish in their natural free state could be observed as precisely, it should be possible to deduce their distribution of target strengths by reference to the results of experiments on captive fish of similar size and species. This would require a good understanding of the relationship between the target strength and behavioural factors such as the tilt-angle distribution. Theoretical models of scattering by groups of fish, an isolated fish or even by the swimbladder on its own can usefully reveal complex functional dependences (Hazen and Horne 2003), since calculations can be repeated much faster than experiments.

In principle, the *in situ* methods should provide the most accurate estimates of the target strength of fish in their natural state, which would be directly applicable to acoustic surveys of wild populations. The data can be collected by remote instruments so that the fish need not be disturbed in any way. The comparison method avoids the need to identify single-fish targets, but it has been successful only in a few special cases. There are several practical difficulties with the other *in situ* methods. The algorithms intended to separate the echoes from single fish and multiple targets can be unreliable, and the target strength of an isolated fish may not be representative of the bulk of fish inside dense concentrations. Furthermore, it is essential to collect samples by fishing to determine the size and species composition, but it is not easy to sample the same fish that have been observed by the

acoustic instruments. In comparing the acoustic and fishing data, it is necessary to make assumptions about the randomness of the sampling which are often difficult to justify. As an alternative to fishing, underwater photography might be used to determine species or size distributions, but the unobtrusive observation of behaviour in the wild is a difficult task. Fish are easily disturbed by the sight of cameras or flashlights.

Of all the target strength measurement techniques which we have considered, the *in situ* approach is the best in theory but the most difficult to apply in practice. The indirect methods can be applied with relatively simple equipment, but the direct methods are more accurate and statistically more robust (Ehrenberg 1983). The split-beam technique performs better than the dual-beam alternative in the presence of noise (Ehrenberg 1979), but in practice, we find that satisfactory results of comparable quality have been obtained with both instruments. However, the split-beam echosounder does have a useful additional capability, in that it locates the fish in three dimensions. Thus the fish can be tracked as they move through the beam, giving information on the target strength and the tilt angle at the same time, as demonstrated by McQuinn and Winger (2003).

#### **6.4.2 Classification of fish targets**

The importance of the swimbladder in determining the target strength has already been mentioned. The bones, the liver and fatty tissues also reflect sound, but much less strongly than any gas-filled organs that may be present, because the echo energy depends primarily on the difference in density between the reflecting organ and the water surrounding the fish. It does not matter whether the density of the reflecting organ is higher or lower than that of water; the greater the absolute density difference, the stronger is the echo. The gas in the swimbladder has a very low density compared to the body tissues. That is why the target strength of fish lacking any gas-filled organ is much smaller than that of species which do have a swimbladder, comparing size for size.

There are four broad categories of fish to be considered in this context: those with gas bladders, of which there are two kinds as explained below; those with bladders filled with oil or fat instead of gas; and those which have no bladder at all.

Two kinds of gas bladder are found in fish. First, there are the physoclistous fish, those with closed swimbladders. The cod, *Gadus morhua*, and other gadoids belong to this group. They have glands through which gas extracted from the water may be secreted into the bladder. If the fish descends, it compensates for the pressure increase with depth by ‘pumping up’ the bladder to restore its volume and to maintain neutral buoyancy. In the cod, this adjustment is accomplished slowly, over one or two days following a descent from the surface to e.g. 20 m depth (involving a three-fold increase of ambient pressure) and in the meantime the fish will be heavier than water. If the fish ascends rapidly, the gas is retained by the bladder above the ambient pressure in the surrounding water, until the excess gas has been removed

by glandular action, or if the pressure difference is very large, by rupture of the bladder wall.

Second, there are the physostomous fish. They have a pneumatic duct connecting the swimbladder to the alimentary canal and thence to the surrounding water (Whitehead and Blaxter 1989). The bladder cannot sustain any excess pressure because, if the fish ascends, the excess gas is vented through the pneumatic duct. Many schooling species such as the clupeoids are physostomes. These fish are unable to secrete gas into the bladder while underwater, or if they do have such a mechanism, it acts very slowly indeed. In the case of the herring, *Clupea harengus*, Blaxter and Batty (1984) suggest that the fish replenishes the bladder gas by swallowing air during occasional visits to the sea surface. While the fish is underwater, gas is lost continuously by diffusion through the bladder wall. The effect of ambient pressure on bladder shape means that the target strength is likely to change when the fish moves up or down in the water column.

Third, fish living in very deep water often have bladders filled with oil or fatty tissue. Although there are no gas inclusions, the density contrast between oil and water is sufficient to augment the target strength to some extent. This category is less well understood than the others. Given the range of peculiar physiologies found in deep-water fish, it is probably best to consider their scattering properties on a species-by-species basis.

Fourth, several important species (e.g. the Atlantic mackerel, *Scomber scombrus*) do not have a swimbladder. The target strength of these fish will be relatively small, but it is not expected to be depth-dependent since there is no gas to be compressed. It is possible that changes in behaviour with vertical migration might indirectly cause a depth-dependence of the target strength, for example, if the tilt-angle distribution changes in response to the light level.

This broad classification is reasonable since the experimental evidence suggests that fish within each category have broadly similar acoustic properties. On the other hand, there are substantial differences in the magnitude of target strength for the same size of fish. Typical target strengths for species representative of each category are given in Table 6.2. The cod has the highest target strength, more than 4 dB (3 times) higher than that of herring, and 19 dB (80 times) higher than that of mackerel. The comparison is more striking when it is made in terms of the backscattering cross-section.

**Table 6.2** Typical values of the target strength (TS) for 30 cm fish length.  $\sigma_{bs}$  is the equivalent backscattering cross-section. The species listed are representative of four distinct types of fish, classified according to swimbladder physiology.

Species	Swimbladder type	TS (dB)	$\sigma_{bs}$ ( $\text{cm}^2$ )
Cod ( <i>Gadus morhua</i> )	Gas-filled, physoclistous	-37.9	1.64
Herring ( <i>Clupea harengus</i> )	Gas-filled, physostomous	-42.4	0.58
Orange roughy ( <i>Hoplostethus atlanticus</i> )	Wax-ester filled	-47.4	0.18
Mackerel ( <i>Scomber scombrus</i> )	No swimbladder	-56.9	0.02

### 6.4.3 Variation with fish size

A simple geometrical model of the size dependence of target strength is to suppose that the backscattered energy is proportional to the horizontal cross-sectional area of the organs contributing to the echo. This area changes as the square of the fish length  $L$ , assuming for the sake of argument that all parts of the body grow at the same rate. This implies that  $\sigma_{bs}$  is proportional to  $L^2$ , and that target strength is equal to  $20 \log L$  plus a constant term, in accordance with Equ. (6.4). Alternatively, if the echo strength depends on the volume of the scattering material rather than the cross-section,  $\sigma_{bs}$  would be proportional to  $L^3$  and the target strength would be  $30 \log L$  plus a constant term.

As a general proposition, the choice of model depends on the wavelength of the sonar transmission relative to the target size. If  $\lambda \gg L$ , Rayleigh scattering applies and the volume model is appropriate. If  $\lambda \ll L$ , the scattering is said to be geometric and then the area model might be a better description. However, the wavelengths commonly used in fisheries acoustics are commensurate with the size of discrete scatterers such as a whole fish or a swimbladder. Further, the inhomogeneous structure of fish results in more complicated variations of TS with size and frequency than are suggested by simple geometrical models. Consequently, it is not possible to decide from *a priori* reasoning whether the area-scattering or the volume-scattering approach is correct. Empirical evidence must be considered if we are to understand the size-dependence of the fish target strength, which is commonly expressed as a linear function of  $\log(L)$ , in the form of Equ. (6.3). This must be considered as a rough approximation, but it has nevertheless proved extremely useful as a general description that can easily be applied in practical calculations.

#### *Physostomes*

Foote (1987) suggested the following relationship for the target strength of clupeoids at 38 kHz, as his best estimate based on published evidence from many sources:

$$TS = 20 \log L - 71.9 \quad (6.5)$$

The line represented by this equation is shown in Fig. 6.15, together with the results of experiments on two clupeoid species at 38 kHz, the herring, *Clupea harengus*, and the sprat, *Sprattus sprattus*, reported by Edwards *et al.* (1984). Although the data are scattered, the least-squares regression of target strength on  $\log L$  gives a slope which is not significantly different from 20, the dependence assumed by Foote (1987). In the case of the clupeoids, the results of caged-fish and *in situ* experiments are consistent, and in particular they have shown the same length dependence of the target strength.

There are many reasons why the individual results of target strength experiments might differ from the average expressed by Equ. (6.5). The schooling behaviour might depend on environmental conditions or the season, especially around spawning time. Furthermore, there could be morphological differences between the swimbladders of similarly sized fish according to their condition and state of maturity. Also the

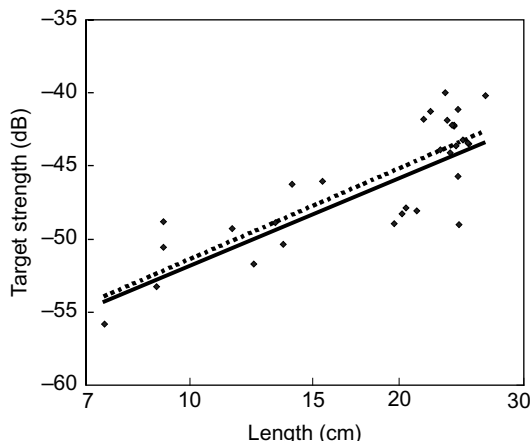


**Fig. 6.15** Variation of target strength with fish length. Results from measurements on herring and sprat at 38 kHz. ♦, each point is the mean result from one caged-fish experiment; -----, regression of TS on  $\log L$  (Edwards *et al.* 1984); —,  $TS = 20 \log L - 71.9$ , the Foote (1987) general equation for clupeoids.

experiments have been conducted at many different places and seasons of the year. Nevertheless, Equ. (6.5) has gained general acceptance as a fair description of the target strength of clupeoid-like fishes.

#### Physoclists

The results reported for physoclists have been more divergent. The target strengths from early *ex situ* experiments appeared to increase more rapidly with length, at a rate of about  $25 \log L$  (Midttun 1984). Foote (1987) considered these results along with later *in situ* measurements which suggested that  $m$  was closer to 20. He believed that more weight should be placed on the *in situ* results, and he proposed the following equation for the target strength of wild gadoids at 38 kHz:

$$TS = 20 \log L - 67.4 \quad (6.6)$$

Figure 6.16 compares the results of various *ex situ* and *in situ* studies of cod, as lines obtained from linear regression of the target strength against  $\log L$ . Several of the regression slopes are clearly greater than 20; however, these are all derived from *ex situ* experiments. It is possible that the abnormal behaviour forced on captive fish could result in the slope ( $m$ ) being too high compared to wild fish. The behaviour of small fish in a cage could be fairly natural, while large fish in the same cage might be more affected. In particular, large fish in a small cage may be forced to maintain a near-horizontal position. In that case, it is the maximum dorsal-aspect target strength which is measured, not the (smaller) mean value relevant to fish which can adopt a range of tilt angles.

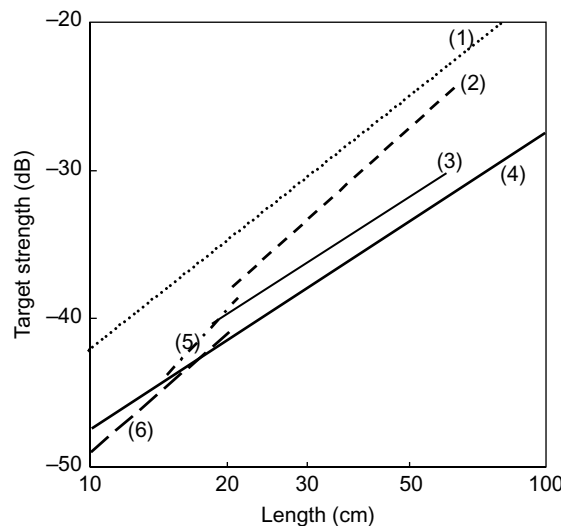


**Fig. 6.16** Variation of target strength with fish length. Collected results from experiments on cod shown as regressions of TS on  $\log L$ . (1) Nakken and Olsen (1977), maximum dorsal aspect; (2) MacLennan (1981b), caged fish; (3) Rose and Porter (1996); (4)  $TS = 20 \log L - 67.4$ , the Foote (1987) general equation for gadoids; (5) Ermolchev and Zaferman (2003); (6) Nielsen and Lundgren (1999). (5) and (6) are at 120 kHz, others at 38 kHz.

For species other than the gadoids and clupeoids, the experimental results are even more diverse. It has not been possible to obtain general functions like Equ. (6.5) and Equ. (6.6) for other large groupings of species. Target strengths for use in survey applications must be derived from the experimental and theoretical evidence, on a species-by-species basis.

The  $20 \log L$  dependence of target strength seems to work for the clupeoids, and perhaps for the gadoids, but it is not tenable as a general rule. McClatchie *et al.* (2003) have discussed the different morphologies of fish, some of which are decidedly unlike clupeoids or gadoids, and the special case of deep-water species whose swimbladders have evolved to cope with very high pressures. Of the ten species considered by McClatchie *et al.* (2003), five had  $m$  values significantly greater than 20 ( $P < 0.05$ ).

A problem arises when there is little or no evidence to suggest the form of the target strength function. Suppose that for some species being newly investigated, a few target strength measurements are available, but they cover a narrow range of sizes. The estimated regression slope can be very imprecise in that case. In this case the best approach is to accept the  $20 \log L$  dependence as a working hypothesis. Then  $b_{20}$  can be estimated as described above. If the size range of the fish to be surveyed is similarly narrow, the function  $TS = 20 \log L + b_{20}$  can reasonably be applied in the calculation of biomass. This assumption may be unreasonable if there is a wide range of sizes in the surveyed population. Nevertheless, some

size dependence is inevitable, and the simple geometry-based rule may be the best available.

#### 6.4.4 Behaviour and physiology

Hawkins (1981) described how the echo from a fish depends on the size, density and relative position of the various organs and tissues within the body. Substantial differences in the target strength of individual fish of the same length may be explained by the natural variation of the maturity state and the condition factor within the population, for the reasons suggested by Ona (1990; 2003). It is less easy to explain changes with time, e.g. between night and day, in the target strength of a particular animal or school being observed. These changes are unlikely to be caused by physiological factors, and probably some change in the behaviour of the fish is responsible, affecting the spatial distribution of the school or the orientation of the individual fish bodies relative to the acoustic axis of the transmitting transducer.

Vabø *et al.* (2002) studied the behaviour of herring in response to the approach of a survey vessel. They saw a sharp reduction of the acoustic fish density as the vessel passed. The fish reacted by swimming away from the vessel track, moving horizontally and diving at the same time. Thus some (perhaps most) of the echo loss represents a real dilution of the fish density below the vessel. However, in the transition from horizontal swimming to diving, the fish tilt from the dorsal towards the tail aspect in the beam. This causes a systematic reduction of the target strength, and it follows that the true density dilution could be much less than the acoustic measurements would suggest.

Fish within an aggregation can adopt a range of tilt angles. In the case of the herring, *Clupea harengus*, the standard deviation of the tilt-angle distribution is typically 10–15°, while the average can be off the horizontal, either head-up or head-down (Ona 2001). It is known that the diurnal change in target strength correlates well with the tilt angle of the body, while the correlation with other behavioural factors, such as the nearest-neighbour distance, is unimportant (MacLennan *et al.* 1990b; Huse and Ona 1996).

As explained in Chapter 2, the target strength of a fish-like body changes much more rapidly with the tilt angle than would be expected from geometrical considerations alone. Interference effects are undoubtedly significant, and more so at higher frequencies as seen in Fig. 6.3. Moreover, experiments have shown great differences in the TS–tilt relationship between apparently similar fish, probably owing to unseen differences in the shape of the swimbladder. Fortunately, it is the average over all the detected fish which is important for the interpretation of acoustic surveys. Thus the large changes observed for individual fish will tend to cancel when the TS–tilt functions of all the detected fish are combined (Fedotova and Shatoba 1983; MacLennan *et al.* 1989).

Changes in the horizontal distribution of the fish might explain some of the observed target strength variation in cage experiments. Figure 6.17 shows

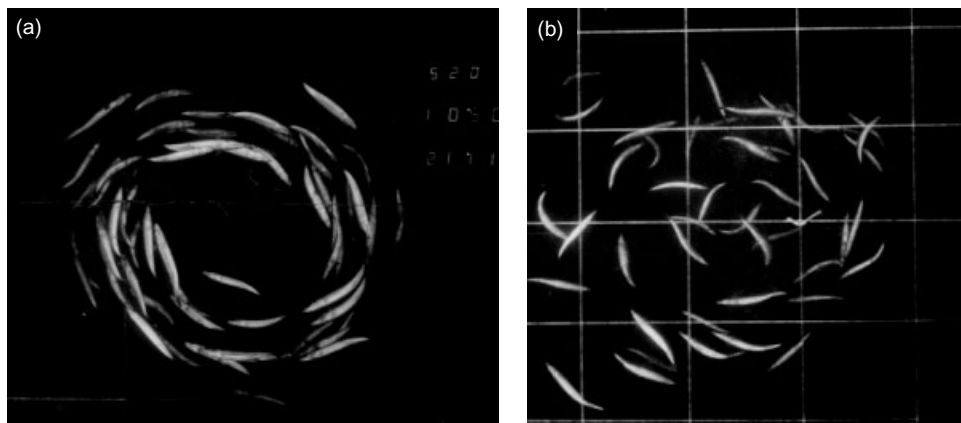


**Fig. 6.17** Herring in a cage, photographed from below. (a) During the day, the fish swim in a circular school; (b) at night, the fish swim randomly with no schooling structure.

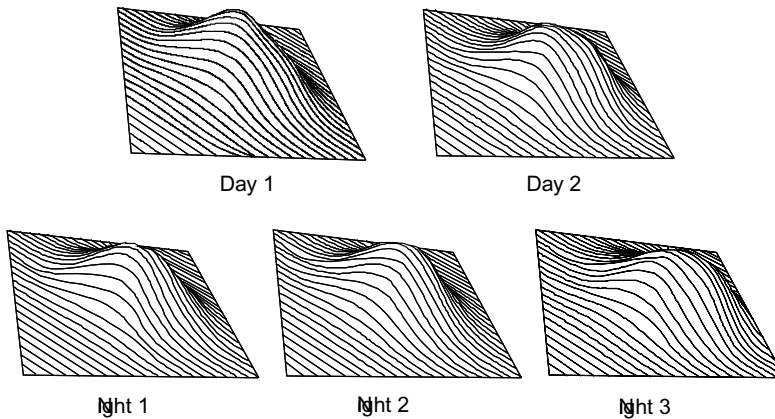


**Fig. 6.18** Landscape plots showing the horizontal distribution of herring in a cage. The height of the landscape is proportional to the frequency of fish occurrence at that point in the cage. Each landscape represents accumulated observations from different 4-hour periods around midday or midnight.

photographs of herring taken from below the cage. The fish are randomly distributed at night, but they school during the day as soon as the light level is sufficient for visual contact between nearest neighbours. Although the night and day photographs are quite different in appearance, the statistical fish distributions are rather similar. Figure 6.18 shows a series of landscape presentations in which the height indicates the frequency of fish presence at each point in the cage. The night and day landscapes look similar to the eye, and any small statistical difference between them would be insufficient to explain the substantial diurnal change in the observed target strength.

While it has been shown that the echo strength is correlated with the mean tilt angle of fish in a school, MacLennan *et al.* (1989) found that the tilt does not explain all the observed target strength variation. It is not clear what other behavioural or physiological effects contribute to the variation, but the problem does emphasize the stochastic nature of target strength, and the need to measure many fish whose behaviour and physiology can be considered representative of those observed during the survey, or in any other application for which the target strengths are required.

## 6.5 Collected target strength data for survey applications

We have seen that even for the same size and species of fish, the observed target strength can cover a wide range of values. Many experimental investigations have been reported in the literature. For some species at least, Foote (1987) suggests that consideration of the mass of published data leads to a reliable indication of the expected value of target strength and how it depends on the fish size. It is the expected value which is required for the interpretation of acoustic surveys.

It is generally accepted that, for a moderate range of sizes, the target strength depends on the fish length according to the equation  $TS = m \log L + b$ , where  $m$  and  $b$  are constants for a given species and frequency. When  $L$  is the mean length of a large number of fish, this equation gives target strength as the expected value, or the average of many observations.

The slope  $m$  is generally in the range 18–30. Exceptionally, for very young or larval fish,  $m$  can be 100 or more, see for example Chu *et al.* (2003). This is due to the non-allometric growth of the swimbladder from the gas-free egg. Some writers (but not all) assume  $m = 20$ , and then calculate the value of  $b$  (the reduced target strength, written as  $b_{20}$ ) which best fits their data. McClatchie *et al.* (2003) argue against this approach, but it has the merit of simplicity, and it is commonly adopted when the length range of the measured fish is narrow. In that case, the estimate of  $m$  may be imprecise to the point of being useless, while the estimate of  $b_{20}$  is the best indicator of the target strength at the midpoint of the length range. When there is considerable scatter in the experimental data, little precision is lost by assuming a fixed value for  $m$ .

Early experimental results for clupeoids and gadoids at 38 kHz are summarized by Equ. (6.5) and Equ. (6.6), respectively. These formulas are useful for comparison with experimental results, and as a starting assumption for species of unknown target strength which are deemed to be clupeiform or gadiform, as the case may be. Most target strength experiments, however, have been concerned with particular species and survey applications. At the species level, the behaviour, physiology, shape and size of fish are very different. One or two equations are unlikely to be adequate to describe the target strengths of all these animals.

Target strength data from the extensive literature on this subject are summarized in Tables 6.3–6.6, covering four groups of fish – gadoids and other physoclists, clupeoids

**Table 6.3** Collected results by species from target strength measurements: gadoids and other marine physoclists. The functional dependence on fish length L is  $TS = (m \log L + b)$ , or the 'standard' formula  $TS = (20 \log L + b_{20})$ . Parameters m, b and  $b_{20}$  are normally obtained from linear regression.  $b_{20}$  in brackets is a reference value  $\{(m - 20) \log L_{\text{ref}} + b\}$ , where  $L_{\text{ref}}$  is the midpoint of the length range.

Species	Location	Length		Time of day*	F (kHz)	m (dB)	b (dB)	$b_{20}$ (dB)	Methods <sup>†</sup>	Ref. <sup>§</sup>
		Range (cm)	Mean (cm)							
Cod ( <i>Gadus morhua</i> )	Newfoundland	18–60	N	38	31.6	-80.7	-66.0	CF, DB	1	
	Kola Bay, Russia	15–21	A	120	(-66.1)	CF	SB	2		
(juveniles)	Scandinavia	3–19	9.4	A	120	-76.2	(-68.9)	CF	3,4	
	Newfoundland	0.1–1.2			120	-82.4	CF, M	5		
(larvae)	Newfoundland	0.1–1.2			500	-79.8	CF, M	5		
	Norwegian Sea	45–91	57.2	N	38	-65.8	SB	6		
Saithe ( <i>Pollachius virens</i> )	Norwegian Sea	9–43	19.7	N	38		-67.1	SB	6	
	Redfish ( <i>Sebastes marinus</i> )									
Norway pout ( <i>Trisopterus esmarkii</i> )	Norwegian Sea	12–19	14.8	N	38		-68.3	SB	6	
		10–21	17.6	N	38		-67.1	SB	6	
Great silver smelt ( <i>Argentina silus</i> )	Norwegian Sea	25–50	37.2	N	38		-68.0	SB	6	
	Haddock ( <i>Melanogrammus aeglefinus</i> )						-67.9	SB	7	
Walleye pollock ( <i>Theragra chalcogramma</i> )	Bering Sea	35–52	41.7	A	38		-66.0	SB, DB	8	

Cape horse mackerel ( <i>Trachurus trachurus capensis</i> )	S.W. Atlantic	25-47	N	38	14.7	-58.7	-66.8	SB	9
Jack mackerel ( <i>Trachurus symmetricus</i> )	Chilean coast	22-40	N	38	23.3	-73.3	-68.9	SB	10
Jurel ( <i>Trachurus picturatus</i> )	Peru	36-40	A	38	-	-68.1	CF	11	
Southern hake ( <i>Merluccius australis</i> )	Chilean coast	48-80	N	38	22.0	-73.3	-68.1	SB	10
Chilean hake ( <i>Merluccius gayi</i> )	Chilean coast	37-53	N	38	23.6	-74.0	-68.5	SB	10
Pacific whiting ( <i>Merluccius productus</i> )	Pacific	47-60	51.8	N	38	-	-68.5	DB	8
Blue whiting ( <i>Micromesistius poutassou</i> )	N.E. Atlantic	21-37 <sup>(2)</sup>	31.1	N	29	-	-71.9	Ind	12
Southern blue whiting ( <i>Micromesistius australis</i> )	N.E. Atlantic	-	A	38	21.7	-72.8	-	-	13
Capelin ( <i>Mallotus villosus</i> )	New Zealand	19-53 <sup>(2)</sup>	-	38	25.0	-81.3	(-73.5)	M, SB, Ind	14
Gadoids	Iceland	11.5	N	38	-	-	-78.1	Ind	15
	Iceland	14.5	N	38	-	-	-78.8	Ind	15
	Newfoundland	9-15	A	38-49	21.1	-74.3	-73.1	DB, SB	16
	Gulf of St Lawrence	16.5	D	120	-	-	-65.3	DB	17
	Various	9-105	A	38	-	-67.4	All	-	18

Fish size measurements are: (1) standard length; (2) fork length; otherwise total length.

\* D, day only; N, night only; A, any time (D + N averaged).

† DB, *in situ* observations with dual-beam echosounder; SB, *in situ* observations with split-beam echosounder; Ind, indirect *in situ* observations. M, modelling; CF, *ex situ* measurements on captive fish.

§ References: 1, Rose and Porter (1996); 2, Ermolchev and Zaferman (2003); 3, Nielsen and Lundgren (1999); 4, Ona (1994); 5, Chu *et al.* (2003); 6, Foote *et al.* (1986); 7, Ona and Hansen (1986); 8, Traynor (1996); 9, Barange *et al.* (1996); 10, Lillo *et al.* (1996); 11, Gutierrez and MacLennan (1998); 12, Robinson (1982); 13, Monstad (1992); 14, McClatchie *et al.* (1998); 15, Halldorsson and Reynisson (1983); 16, Rose (1998); 17, Rose and Leggett (1988); 18, Foote (1987).

**Table 6.4** Collected results by species from target strength measurements: clupeoids and other marine physostomes. The functional dependence on fish length L is  $TS = (m \log L + b)$ , or the 'standard' formula  $TS = (20 \log L + b_{20})$ . Parameters m, b and  $b_{20}$  are normally obtained from linear regression.  $b_{20}$  in brackets is a reference value  $\{(m - 20) \log L_{ref} + b\}$ , where  $L_{ref}$  is the centre of the stated length range.

Species	Location	Length		Time of day*	F (kHz)	m (dB)	b (dB)	$b_{20}$ (dB)	Methods <sup>†</sup>	Ref. <sup>§</sup>
		Range (cm)	Mean (cm)							
Herring ( <i>Clupea harengus</i> )	N.E. Atlantic	7-27	18.8	A	38	20.1	-71.5	(-71.3)	CF	1
	Northern North Sea	24-34	28.5	N	38			-72.1	SB	2
	Iceland	9-33	21.5	N	38			-73.2	Ind	3
	Norwegian fjord			D	38			-71.1	Comp	4
	N. Baltic, coastal	6-24	13.0	N	70	21.7	-75.5	-69.9	Ind	5
	Norwegian fjord	22-33	28.0	D	70			-72.3	Comp	6
Sprat ( <i>Sprattus sprattus</i> )	North Sea	9-15	12.6	N	30			-69.1	Ind	7
	North Sea		7.15	N	30			-70.7	Ind	7
Mixed herring/sprat	Kattegat/Skagerrak	19-26	21.0	A	38			-72.6	Ind	8
Clupeoids	N.E. Atlantic	12-21	16.6	A	38			-73.4	CF	1
	S.E. Baltic	7-19	13.8	N	120			-73.1	Ind	8
	N.E. Atlantic	12-21	16.6	A	120			-76.0	CF	1
	Various	6-34		A	38			-71.9	All	2
	Peru	10-16	12.8	A	38			-78.9	CF	9
	Peru	10-13	11.3	A	120			-76.2	CF	9
Anchoveta ( <i>Engraulis ringens</i> )	S.E. Atlantic	7-14		N	38	19.5	-75.6	-76.1	SB	10
Anchovy ( <i>Engraulis capensis</i> )	S.E. Atlantic	15-23		N	38	17.1	-66.7	-70.5	SB	10
Pilchard ( <i>Sardinops ocellatus</i> )	Peru	12-20	16.3	A	120			-74.1	CF	9
Sardine ( <i>Sardinops sagax</i> )										

Fish size measurements are: (1) standard length; (2) fork length; otherwise total length.

\* D, day only; N, night only; A, any time (D + N averaged).

<sup>†</sup> SB, *in situ* observations with split-beam echosounder; Ind, indirect *in situ* observations; CF, *ex situ* measurements on captive fish; Comp, comparison with independent data.

<sup>§</sup> References: 1, Edwards *et al.* (1984); 2, Foote (1987); 3, Halldorsson and Reynisson (1983); 4, Misund and Beltestad (1996); 5, Rudstam *et al.* (1988); 6, Misund and Ørvredal (1988); 7, Robinson (1983); 8, Degnbol *et al.* (1985); 9, Gutierrez and MacLennan (1998); 10, Barange *et al.* (1996).

**Table 6.5** Collected results by species from target strength measurements: freshwater fish species. The functional dependence on fish length L is  $TS = (m \log L + b)$ , or the 'standard' formula  $TS = (20 \log L + b_{20})$ . Parameters m, b and  $b_{20}$  are normally obtained from linear regression.  $b_{20}$  in brackets is a reference value  $\{(m - 20) \log L_{ref} + b\}$ , where  $L_{ref}$  is the centre of the stated length range.

Species	Location	Length		Time of day*	F (kHz)	m (dB)	b (dB)	$b_{20}$ (dB)	Methods $^\perp$	Ref. $^\S$
		Range (cm)	Mean (cm)							
Sockeye salmon ( <i>Oncorhynchus nerka</i> )	Canadian lakes	51.0	N	38		-61.9	Comp	1		
	Lake Kuttara (Japan)	11–25	16.3	N	50	-66.0	DB	2		
	Canadian lakes	4.5	N	420	-65.4	DB	3			
	Canadian lakes	7.2	N	420	-66.9	DB	3			
Cisco ( <i>Coregonus artedii</i> )	Canadian lakes	19.5	N	70	21.9	-67.2	-64.7	Ind	4	
Rainbow smelt ( <i>Osmerus mordax</i> )	N. American lakes	2–16	N	120	19.9	-67.8	(-67.9)	SB	5	
Alewife ( <i>Alosa pseudoharengus</i> )	N. American lakes	2–15	N	70	20.5	-64.2	-63.6	SB	6	
Lamun ( <i>Sebastes schlegeli</i> )	Lake Kenneret (Israel)	8–15 <sup>(1)</sup>		120	25.0	-73.0	(-67.7)	SB	7	
Diplotaxodon spp.	Lake Malawi	12–20	15.0	D	120		-68.4	DB	8	
Nile perch (juveniles) ( <i>Lates niloticus</i> )	Lake Victoria	18–33	22.3	A	120		-66.0	CF	9	
Dagaa ( <i>Rastrineobola argentea</i> )	Lake Victoria	4–7	5.4	A	120		-72.0	CF	9	

Fish size measurements are: (1) standard length; (2) fork length; otherwise total length.

\* D, day only; N, night only; A, any time (D + N averaged).

$^\perp$  DB, *in situ* observations with dual-beam echosounder; SB, *in situ* measurements on captive fish; Comp, comparison with independent data.

$^\S$  References: 1, Mulligan and Kieser (1986); 2, Iida *et al.* (1991); 3, Burczynski and Johnston (1986); 4, Rudstam *et al.* (1987); 5, Rudstam *et al.* (2003); 6, Warner *et al.* (2002); 7, Walline *et al.* (1992); 8, MacLennan and Menz (1996); 9, Getabu *et al.* (2003).

**Table 6.6** Collected results by species from target strength measurements: miscellaneous species. The functional dependence on fish length L is  $TS = (m \log L + b)$ , or the 'standard' formula  $TS = (20 \log L + b_{20})$ . Parameters m, b and  $b_{20}$  are normally obtained from linear regression.  $b_{20}$  in brackets is a reference value  $(m - 20) \log L_{ref} + b$ , where  $L_{ref}$  is the centre of the stated length range.

Species	Location	Length		Time of day*	F (kHz)	m (dB)	b (dB)	$b_{20}$ (dB)	Methods <sup>†</sup>	Ref. <sup>§</sup>
		Range (cm)	Mean (cm)							
Mackerel ( <i>Scomber scombrus</i> )	N.E. Atlantic	31–35	32.7	A	38			-84.9	CF	1
	North Sea		37.8	D	38			-86.4	Comp	2
Horse mackerel ( <i>Caballa</i> )	Peru	26–30	27.9	A	38			-70.9	CF	3
( <i>Scomber japonicus</i> )	Peru	26–30	27.9	A	120			-70.8	CF	3
Sandeel	N.E. Atlantic	11–14	12.2	A	38			-93.7	CF	4
( <i>Ammodytes</i> spp.)										
Hoki	—	45–104	68.6		38	23.8	-79.6	-72.7	M	5
( <i>Macruronus novaezelandiae</i> )										
Orange roughy ( <i>Hoplostethus atlanticus</i> )	New Zealand	28–37 <sup>(1)</sup>	32.0		38	16.4	-71.6	(-77.0)	M, CF, SB	6
Rockfish	N.W. Pacific	10–24	16.1		38			-67.7	CF	7
( <i>Sebastodes schlegeli</i> )	N.W. Pacific	10–24	16.1		120			-74.3	CF	
	N.W. Pacific	10–24	16.1		200			-72.8	CF	7
Red seabream	N.W. Pacific	10–35	19.9		38			-66.8	CF	7
( <i>Pagrus major</i> )	N.W. Pacific	10–35	19.9		120			-74.0	CF	7
	N.W. Pacific	10–35	19.9		200			-74.1	CF	
Myctophids	Hawaii	2.4–8.2 <sup>(1)</sup>	5.1		200			-58.8	CF	8
(mostly <i>Benthosema filiformium</i> )										
<i>Diaphus theta</i>	Japan	2.7–7.7 <sup>(1)</sup>			38	11.8	-63.5	(-69.4)	M	9
<i>Symbophorus californiensis</i>	Japan	8.5–10.8 <sup>(1)</sup>			38			-85.7	M	9
<i>Notoscopulus japonicus</i>	Japan	12.6–13.3 <sup>(1)</sup>			38			-86.7	M	9

Fish size measurements are: (1) standard length; (2) fork length; otherwise total length.

\* D, day only; N, night only; A, any time (D + N averaged).

<sup>†</sup> SB, *in situ* observations with split-beam echosounder; Ind, indirect *in situ* observations; M, modelling; CF, *ex situ* measurements on captive fish; Comp, comparison with independent data.

<sup>§</sup> References 1, Edwards *et al.* (1984); 2, Misund and Beletstad (1996); 3, Gutierrez and MacLennan (1998); 4, Armstrong (1986); 5, Do and Surti (1990); 6, McClatchie *et al.* (1999); 7, Kang and Hwang (2003); 8, Benoit-Bird and Au (2001); 9, Yasuma *et al.* (2003).

and other physotomes, freshwater fish and miscellaneous species. Similar tables on the target strengths of non-fish species (plankton and shellfish) will be found in Chapter 7. We have not included results published before 1980. It is only since then that measurements with precisely calibrated equipment, backed by good theoretical understanding, have provided reliable numeric values for the target strengths applicable to acoustic surveying.

On some occasions we may have local information on target strengths, collected for example with a split-beam echosounder on the survey vessel. It then has to be considered whether the fish densities should be based on the local TS data, instead of using a generic formula or previously published results. This depends on the quality of the contemporary measurements. If they are reliable and precise, then they should be used in the survey analysis. On the other hand, a few scattered observations will give a mean TS with a large standard error. The abundance estimate is biased by the amount of this error, cf. Chapter 9. Thus, unless the local measurements are very good, it may be better to use a generic or published TS-length function, even if there is some doubt as to how representative that will be of the surveyed population.

The target strength data and size dependences described above may be used to give a first indication of the values required for the interpretation of acoustic surveys. Random variation of the individual-fish target strength about the expected value has little effect on the estimate of fish density. Systematic changes in target strength, however, will bias the survey results. Such changes might occur if the behaviour and the condition of the observed fish were unusual. There is a continuing need for target strength data to be collected on fish which are representative of those to be surveyed, and on other species which may be present so that their contribution to the echo integration may be deduced accurately.

Good estimates of the fish target strength are critical in many fisheries applications. This is currently a fast-developing field. We believe that further progress will be made when data from modelling, *in situ* measurement and behavioural studies are combined to give a coherent explanation of target strength relevant to particular species and environmental circumstances.

# Chapter 7

# Plankton and Micronekton Acoustics

## 7.1 Introduction

There is a huge variety of life in the sea. So far we have concentrated on the acoustic properties of post-larval teleost fish, but they are only one component of the biomass. The plankton may be less important in economic terms, but they are central to ecological research, being at or near the bottom of the food chain. Although plankton have been studied acoustically for many years, it is only recently that sonar techniques have developed to the stage of providing useful ecological insights.

Of course, plankton produce echoes by the same scattering laws as any other target. Since they are chiefly small to microscopic objects in close proximity to one another, the echoes overlap to form the diffuse cloud-like marks often seen on echograms. An example is shown in Fig. 7.1. The planktonic background can be very strong, and is one factor which limits the performance of sonars in detecting fish. As well as the ecological interest, studies of plankton acoustics have improved our ability to separate fish echoes from those of other targets seen in echograms.

The interpretation of fish and plankton echoes calls for rather different approaches. The traditional ideas of echo-counting and target-strength regressions cannot be used in the same way, if at all. The individual plankters are too small and their echoes are weak although very numerous. High frequencies (up to 10MHz) have been used to improve the spatial resolution, but the greater absorption then limits the observable range to a few metres, at least in sea water. There is a wide variety of shapes, structures and sizes of plankton. The acoustic identification of planktonic targets to species or even genera level is difficult if not impossible. Nevertheless, some progress has been made in the classification of plankton as acoustic targets (Stanton *et al.* 1996). It has become clear that single-frequency echosounders are rather limited in this application. Wideband or multi-frequency measurements are more likely to reveal the size and structure of planktonic targets. In contrast to fish, theoretical scattering models have been a primary rather than a secondary tool for interpreting plankton echoes, since the possibilities for empirical ground truthing are more limited than they are for aggregations of larger animals.

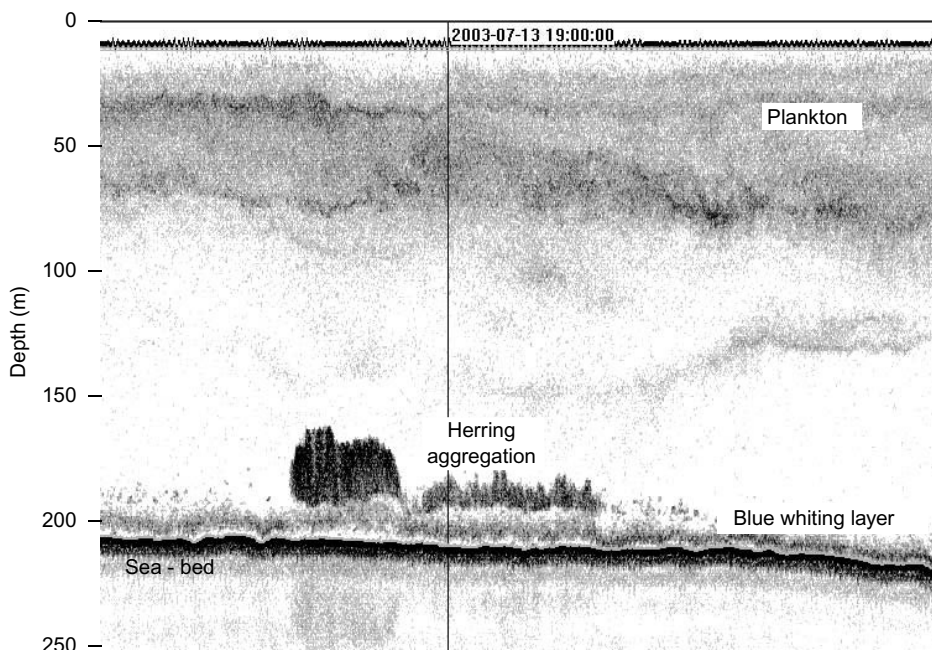


**Fig. 7.1** Echogram showing diffuse echoes from plankton and aggregations of different fish. Recorded north of Shetland in daylight. Simrod EK500 (38 kHz).

Most of the work described below concerns zooplankton which are animals. Selivanovsky *et al.* (1996) and Shenderov (1998) have discussed the acoustic properties of phytoplankton which otherwise have received little attention. Phytoplankton, like algae, are plants and are very weak scatterers except when they have gas inclusions. In general, the theory and experimental methods described in this chapter are applicable to both kinds of plankton.

In strict definition, according to the original Greek meaning of the term, the plankton are floating objects ‘that are made to wander’, implying that they move under external influences (notably water currents) rather than self-generated actions like swimming. This certainly applies to the phytoplankton, however, in this chapter we include the micronekton which are also small but, again by the Greek definition, are capable of swimming. Nevertheless, the active swimming is generally on a local scale and, while vertical migration does occur, the horizontal motion is still dominated by the effect of water currents. Zooplankton like the decapod shrimps are part of the micronekton. For simplicity in this chapter, we use the generic term plankton rather loosely, to include a variety of non-fish biota which are mostly very small and may or may not be active swimmers.

Among the zooplankton, the krill *Euphausia* spp. have been the subject of many experimental and theoretical studies. Some of these animals are relatively large, up to 4 cm long in the case of the Antarctic krill *Euphausia superba*. Since the last

two chapters focused almost entirely on fish, here we shall discuss the acoustics of crustaceans and molluscs, notably the squids for which there are important commercial fisheries. They can be very large indeed, but they are still weak targets in comparison to the same weight of most fish.

We begin with the classification of plankton as acoustic targets. Three broad classes are identified – FL (fluid-like), ES (elastic shell) and GB (gas bearing). Theoretical models which solve the forward scattering problem are important since without these it is difficult to relate the target strength (TS) to the size of very small animals. Various models and approximate solutions are described. Different approaches are required for each scattering class. For the FL plankton, model calculations depend on the density and sound-speed contrasts in the body. Measurement techniques and current knowledge of these parameters are reviewed. The target strength is a useful descriptor of large plankton, notably the Antarctic krill which has been the subject of much study. TS measurements of krill and a few other species are discussed. The traditional method of abundance estimation (based on a TS-length function) has been applied to krill, but more sophisticated methods are generally required for plankton. The concurrent use of several frequencies gives information on the size distribution as well as the abundance, provided the model assumptions are reliable. Some progress has been made on the identification of species from their echo characteristics, but in many cases this still depends on the collection of samples by fishing. The development and use of multi-frequency sonars are discussed. These can have as many as 21 frequencies in a hundred-fold band (0.1–10 MHz), although simpler instruments with fewer frequencies are adequate for many applications. Finally, we discuss acoustic methods for observing the behaviour of plankton, particularly the use of multi-beam sonar to provide three-dimensional images.

## 7.2 Acoustic classification of plankton

The echoes returned from a multi-species aggregation, whether it is fish or plankton or a mixture of both, combine to form only one acoustic signal which is measured. This signal can provide the total echo-integral as a function of range from the transducer, and its frequency dependence if the instrumentation is wideband. The acoustic signal determines the backscattering strength in a known volume of water at a particular frequency. By itself, one echo gives us no other information relevant to the identity of the targets which produced the detected echoes. What we really want to know is the composition of the detected targets in terms of species and size distributions, or at least separated into groups which are meaningful in ecological terms. To do that, we need to understand the statistical properties, the frequency dependencies and the spatial variations of the echoes returned from different kinds of targets. We have already discussed how this can be done for large fish targets. The problem is considerably more difficult in the case of plankton due to the small size, high density and variable structure of the targets.

The literature on acoustic scattering covers two rather different questions. The first is the forward problem: given the geometric and acoustic features of a particular target, what echo will be backscattered? The second is the inverse problem: given some echo or backscatter measurements, what kind of target produced them? Not surprisingly, the inverse problem is a lot more difficult. In fisheries applications, the targets are generally identified by other means e.g. fishing on the echo traces. Then we only need to know the target strength by species and size category to solve the inverse problem as an estimate of abundance. It is nevertheless important to deduce as much information as possible about the targets that might be obtained from the acoustic data. To do that, the forward scattering problem must be well understood as a first step. When the sonar detects an assemblage of different sorts of scatterer, we need to know *inter alia* the acoustic characteristics of each type of target, to inform the process of partitioning the echo-integral between its various components. In the case of plankton, even the forward problem is complicated, but much progress has been made in recent years towards a better understanding of the physical processes involved.

The echo returned from a target depends on (a) the modulation frequency, duration and amplitude of the transmitted pulse, (b) transmission losses and secondary scattering in the medium and (c) the size, shape, orientation and material properties of the target. Estimation of the target size is a separate issue which we shall discuss later. As regards other features of biological targets, they may be considered in a few broad groups according to their anatomy which, of course, determines how the echo is formed. Stanton *et al.* (1994a; 1996) adopted this approach in an extensive study of zooplankton. They proposed the following scheme of three anatomical classes:

- (1) Fluid-like (FL, e.g. euphausiid shrimp): the body is roughly cylindrical with length greater than width and weakly-scattering soft tissue; the whole body contributes to the echo.
- (2) Hard elastic shelled (ES, e.g. gastropods): soft tissue surrounded by a hard shell except for a small hole (the opercular opening); may have external soft appendages; the echo comes primarily from the shell.
- (3) Gas bearing (GB, e.g. siphonophores): a soft body together with a gas bubble; the gas provides a strong echo but the body contribution can be important if the gas/tissue volume ratio is small.

Examples of species typical of this classification are illustrated in Fig. 7.2. Clearly there will be many different body shapes and structures among the diverse species assigned to each group. A small fish larva, in which the swimbladder has just begun to develop, does not look at all similar to a siphonophore. Nevertheless, they have comparable acoustic properties, in that the echo is conceived as the sum of contributions from the gas and soft tissue.

Each class of target may be expected to produce different echo strengths for the same volume or mass of reflecting tissue. More importantly, their echoes have different frequency dependencies revealed through resonance patterns in broadband

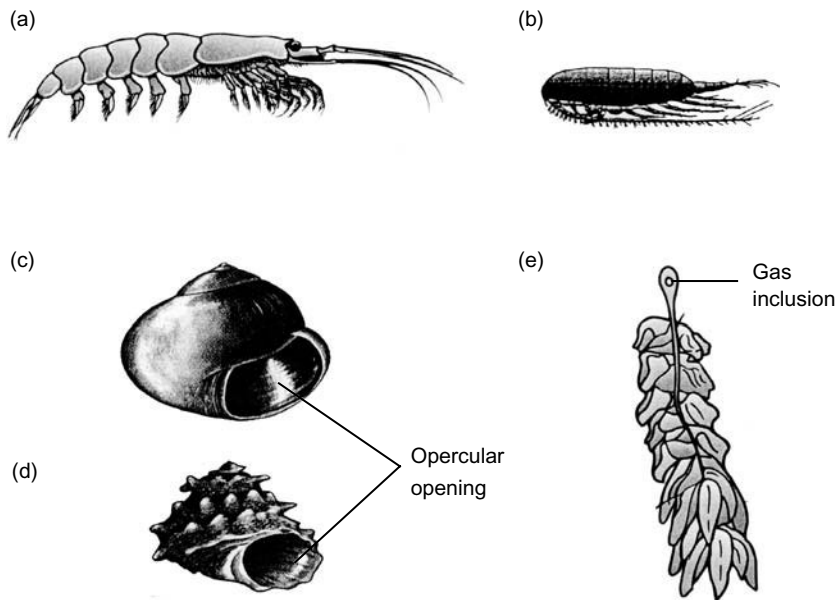


**Fig. 7.2** Illustrations of zooplankton representing the three classes of acoustic target: fluid-like (FL), elastic shelled (ES) and gas bearing (GB). (a) Euphausiid, FL; (b) copepod, FL; (c, d) gastropods, ES; (e) siphonophore, GB.

spectra. Martin *et al.* (1996) have described two algorithms (called MPC and EOFC) developed to classify zooplankton targets, using Stanton's three-class scheme, by reference to the spectra of single-target echoes. MPC depends on comparison of the measurements with theoretical scattering models, while EOFC is a more general approach based on the inherent characteristics of the echoes. From experiments with 18 captive animals, Martin *et al.* (1996) achieved 64% and 77% success in the class identification using, respectively, the MPC and EOFC algorithms. These results are specific to single-target echoes. The exact shape of the echo spectrum (e.g. the spacing of the resonances) depends *inter alia* on the target orientation in the acoustic beam. Zooplankters in an aggregation will have various orientations. Thus the resonance structure of multiple-target echoes is less clear and may not be evident at all (Stanton *et al.* 1998b).

### 7.3 Scattering models

Here we discuss various solutions of the forward scattering problem relevant to plankton, namely the theoretical models which have been used to describe the echo returned by a discrete target whose shape and material properties are known, and how the echo changes with frequency and other factors. As applied to fish or plankton, theoretical scattering models are mostly used to predict the far field back-scattering length,  $L_{bs}$ . This is a complex number (in the mathematical sense), whose

real and imaginary components describe the phase as well as the amplitude of the received echo, while the squared modulus (a real number) is simply the backscattering cross-section i.e.  $\sigma_{bs} = |L_{bs}|^2$ . Analytic expressions for  $L_{bs}$  can be derived for only a few very simple models. The equations generally contain complicated integrals or infinite series which have to be evaluated numerically, although that is not too difficult given the power of modern computers.

In principle, one model based on fundamental acoustic theory should provide all the answers. This is not possible because the wave equations for acoustic scattering cannot be solved with arbitrary boundary conditions. Approximate solutions have to be considered. The approximations may be made either in the theory, by ignoring secondary effects, or in the assumed structure of the target which might be idealized, e.g. as a homogeneous fluid sphere for which there is an exact solution of the wave equations (Anderson 1950; Feuillade and Clay 1999). Theoretical models are useful for demonstrating the principles of echo formation. To that end, approximations can simplify the description of the physical processes which must be understood in order to solve the more difficult inverse scattering problem.

In Chapter 6 we discussed several models relevant to fish. Different methods are required for plankton since they are small targets and the echoes from non-gaseous body tissues are relatively more significant. The simplest model is to suppose that a plankter scatters sound like a fluid sphere of radius ESR, the equivalent spherical radius, such that the volumes of the sphere and the plankter are the same. The target strength depends on  $g$ , the density of the sphere and  $h$ , the sound speed within it, expressed as contrasts, i.e. the proportional difference in each parameter between the scattering body and the surrounding water. Both  $g$  and  $h$  are a few percent for the soft tissue of plankters. However, the fluid-sphere theory is a poor approximation at high frequencies. It shows sharp resonances owing to the perfect symmetry of the sphere. These are not seen in experimental data (Greenlaw 1977), because real plankters have irregular shape, thus the resonance structure (if any) is likely to be less sharp. Early investigators proposed various refinements to overcome this problem, notably the high-pass model (Johnson 1977) and the truncated Anderson model (Pieper and Holliday 1984). In this context, truncation means that the high-order vibrations of the sphere are ignored, with the result that the target strength varies more smoothly with frequency (Fig. 7.3).

The sphere models take no account of the fact that many zooplankters have an elongated shape, in which case the target strength will depend on the orientation of the animal as it does for fish. Stanton (1988a; 1990) proposed a fluid-cylinder model which allowed the orientation to be included as a parameter. Again, high-pass or truncated versions of the cylinder model may be used to improve the representation at high frequencies. The acoustic properties of these early models are compared in Fig. 7.3.

Pieper and Holliday (1984) compared the three versions of the fluid-sphere theory mentioned above. The truncated Anderson model gave the best correlation with biological samples. However, Dalen and Kristensen (1990) considered that

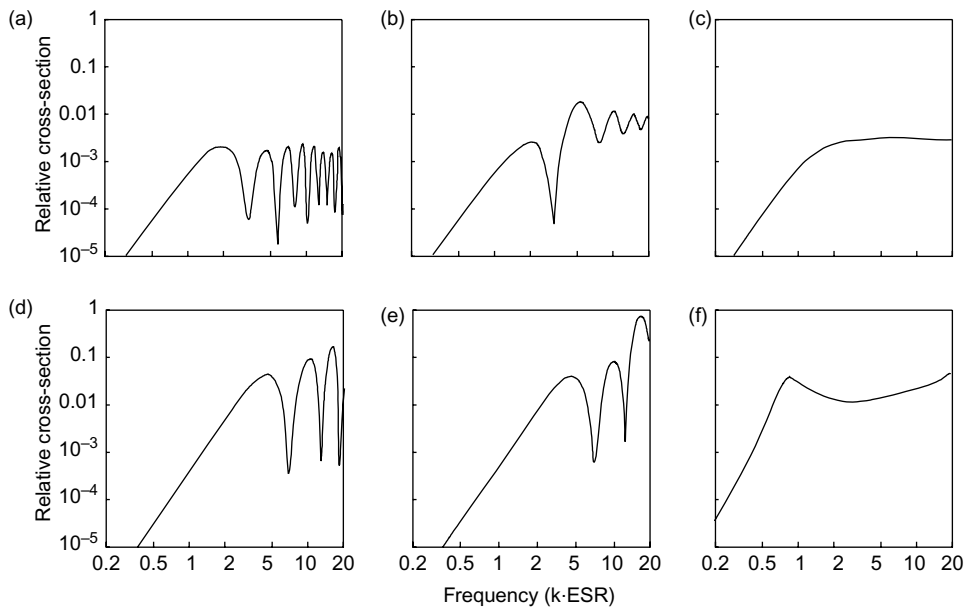


**Fig. 7.3** Predicted  $\sigma_{\text{bs}}$  of plankton modelled as fluid targets with  $(g, h) = (1.041, 1.035)$ . Vertical axes, ratio of backscattering and geometric cross-sections; horizontal axes, dimensionless frequency (wavenumber times equivalent spherical radius). Sphere models: (a) complete Anderson; (b) truncated Anderson; (c) Johnson high-pass. Cylinder models: (d) complete Stanton; (e) truncated Stanton; (f) KRIDA.

a more empirical approach was necessary. They compared various theoretical models with measured target strengths of the krills *Euphausia pacifica*, *Meganyctiphantes norvegica* and *Thysanoessa* spp. This led to a hybrid approach (called KRIDA) in which the basic concept was the fluid cylinder with truncation of high-order modes, but the size and other properties of the cylinder were adjusted to match the observed target strengths. Furthermore, the predicted mean target strength allowed for a stochastic variation of the orientation of the krill with respect to the acoustic beam (Kristensen and Dalen 1986).

There was rapid progress in the 1990s when numerous theoretical investigations greatly improved our understanding of the sound field scattered by plankton. We have already discussed the classification of plankton into three classes according to their acoustic properties (Section 7.2). Below we describe the different modelling approaches which have been developed for each class, mainly through the extensive work of Stanton *et al.* (1996; 1998a; 1998b) in this field.

### 7.3.1 **FL class (soft fluid-like tissues)**

In this case the plankton body is considered to be soft tissue with acoustic properties close to those of water. There can be harder chitinous parts in the exoskeleton, but in

general they have a minor effect which can be ignored. Thus the whole body can be treated as a weakly scattering volume which is nearly homogeneous. The euphausiid shrimps are important members of the FL class, notably the Antarctic krill *Euphausia superba* which has been the subject of many studies.

Furusawa *et al.* (1994) modelled the krill body as a liquid prolate spheroid. Their results showed that 70 kHz would be better than 120 kHz for surveys of *Euphausia superba* in the field, since the variability introduced by the orientation of the targets would be worse at the higher frequency. However, the usual starting point of plankton models is to consider the body as a deformed cylinder of finite length. The axis of this cylinder may be curved, and the geometric cross-section changes along the axis to match the body shape. The body tissue is assumed to be fluid, i.e. it does not support shear waves.

Three types of model have been used to describe the scattering properties of the deformed fluid cylinder, each one involving different assumptions and limitations. Firstly, there is the modal-series-based theory described by Stanton (1988b). This model is applicable to cylinders having a circular cross-section, although the radius can vary along the axis (but only slowly). The acoustic properties of the body are supposed to be homogeneous. The modal solution is correct for strong as well as weak scatterers (unlike the DWBA, see below). However, it is valid only for near-normal angles between the axis and the acoustic beam. This means, in behavioural terms, tilt angles close to zero. Thus the mode model is good for near-spherical bodies and, with other shapes, the special case of normal incidence. It is less useful for elongated forms which could lie at any tilt.

The second approach is to consider the body as many small elements of volume. The complete echo is the sum of contributions from each element, taking account of phase differences as well as the amplitudes. This method is based on the distorted wave Born approximation (DWBA), in which the backscattering length ( $L_{bs}$ ) is expressed mathematically as a three-dimensional integral over the body volume  $V$ . In the ordinary Born approximation, the incident wave is supposed to propagate through the body as it would in empty water. In the ‘distorted wave’ version, phase changes caused by the body tissues are taken into account (Morse and Ingard 1968). Noting that, for consistency with symbols used elsewhere in this book, our notation (especially the subscript convention) is different from the usual formulation in the literature, we write the DWBA equation for far-field backscattering by a body of finite size as:

$$L_{bs} = \frac{k^2}{4\pi} \iiint_V (q - g) \exp[2i(\mathbf{k}_I)_1 \cdot \mathbf{r}_V] dV \quad (7.1)$$

Here, symbols referring to properties of the surrounding medium are unsubscripted, and those with subscript ‘1’ refer to the corresponding values in the body tissue.  $k$  is the wavenumber ( $2\pi/\lambda$ ) of the incident wave in water,  $\mathbf{r}_V$  is the position vector of a body element, and  $(\mathbf{k}_I)_1$  is the incident wave vector evaluated *inside* the body.  $i$  is the usual mathematical shorthand for the complex number  $\sqrt{(-1)}$ .  $q$  and  $g$  are material

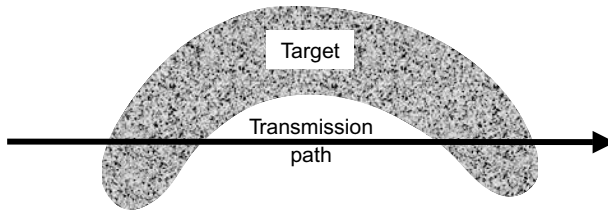


**Fig. 7.4** Illustration of a bent cylindrical target at end-on incidence. The transmission path enters and leaves the body more than once. This causes phase changes which can invalidate scattering predictions made with the DWBA model (Equ. 7.1).

property contrasts, defined by the different compressibilities ( $\kappa$ ) and densities ( $\rho$ ) as the dimensionless ratios:

$$q = (\kappa_1 - \kappa) / \kappa \quad (7.2)$$

$$g = (\rho_1 - \rho) / \rho \quad (7.3)$$

The DWBA-based model has been widely used in studies of plankton (Morse 1948; Martin Traykovski *et al.* 1998; McGehee *et al.* 1998; Stanton *et al.* 1998b; Lavery *et al.* 2002). The model can be applied to any body shape, but it is limited to weak scatterers, since secondary (multiple) scattering and acoustic absorption within the body are ignored. The density and sound speed in the body must be close to the corresponding values in the surrounding water, within 10% or so. Fortunately, that condition is well satisfied in the case of euphausiid shrimp. The model is valid at all frequencies and orientations of the target. There is one exception to this generality. When the incident beam is end-on and the cylinder is bent so that the transmission path enters and leaves the body twice (Fig. 7.4), errors can result from the phase changes along the path (Stanton *et al.* 1998b). The DWBA model can in principle be adjusted to take account of this effect, but the geometry of Fig. 7.4 is perhaps unusual enough to be irrelevant in most applications. There are more important phase-related effects which have led to modified versions of the DWBA, for example the phase-compensated model of Chu and Ye (1999) which accounts for acoustic extinction in the body tissue. Demer and Conti (2003) proposed a stochastic version (the SDWBA) in which random phase shifts are applied to the signals from each body element. Such changes might be associated with variation of acoustic properties between different parts of the body, and/or noise in the signal.

The three-dimensional volume integral can be evaluated numerically for any body shape. Subject to the weak scatterer assumption, it allows arbitrary variation of the acoustic properties from one part of the body to another. It is not always necessary to do the full calculation. If the body has a homogeneous circular cross-section, with only lengthwise variation of the radius and acoustic properties, the volume formula can be reduced to a one-dimensional integration along the body axis. In the case of a uniformly bent cylinder, the formulation of  $L_{bs}$  can be further simplified to an integration over the tilt angles from one end of the body to the other (Stanton *et al.* 1998b).

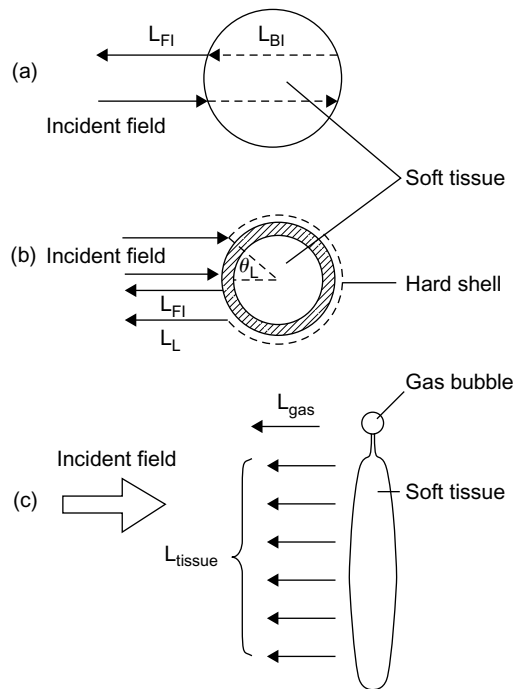


**Fig. 7.5** Ray models of backscattering by three types of plankton. The far field backscattering length ( $L_{bs}$ ) is the sum of components labelled as FI = front interface; BI = back interface; L = Lamb etc. (a) Fluid-like body:  $L_{bs} = L_{FI} + L_{BI}$ ; the front and back surface reflections dominate at near-broadside incidence. (b) Hard elastic shell: the Lamb wave is a circumnavigating vibration of the shell which originates at off-axis angle  $\theta_L$ .  $L_{tissue}$  is negligible so  $L_{bs} = L_{FI} + L_L$ . (c) Gas bearing e.g. a siphonophore:  $L_{bs} = L_{gas} + L_{tissue}$ . (Redrawn from Stanton *et al.* 1998b.)

The third type of model is a relatively simple representation of the scattering as rays reflected from the front and back surfaces of the body. The rays are discrete reflections from the body-medium interfaces which combine to form the echo. Volume scattering within the body is not considered. Formulas for  $L_{bs}$  are expressed in terms of the reflection coefficients at the boundaries. Ray models are generally less accurate than the DWBA or modal analyses. They are more useful for qualitative descriptions of the underlying physics which can be illustrated in an easily understood way (Fig. 7.5). Ray models are generally restricted to applications at higher frequencies, in the transitional or geometric scattering regions for which the wavenumber multiplied by the target size (ESR) is greater than unity.

Stanton *et al.* (1993a) reported successful results with a two-ray model of fluid-like plankton, insonified at normal incidence. Later, a six-ray model was developed to describe the statistical properties of echoes for a variable tilt angle (Stanton *et al.* 1994b). The additional rays took account of reflections from sections of the body which would have different phase relationships when the animal was tilted.

### 7.3.2 ES class (elastic shell)

The outer boundary of the animal is a dense, hard shell which is roughly spherical in shape. There is a hole in the shell called the opercular opening. The internal tissue is soft and weakly reflecting. External tissues (the feet) are likewise soft, thus the

echo comes primarily from the shell. Any contributions from the soft tissues are generally ignored, except for ideal spherical models when the theory is tractable (Stanton 1990). The gastropods are typical examples of the ES class (Fig. 7.2).

Modelling the sound scattered by gastropods is difficult due to the complex boundary of the shell, especially the opercular opening which is a major discontinuity in the hard boundary. Goodman and Stern (1962) give the exact solution for an ideal spherical shell, however, this simplified shape is a poor approximation of the true structure which has surface irregularities and is not closed. The spectrum of the ideal spherical shell has strong resonances which are not seen in the echoes returned by gastropods. More sophisticated theoretical studies have been necessary to explain the experimental observations. The best approach seems to be the analysis of discrete rays which can be associated with particular features of the shell (Stanton *et al.* 1998b).

Measurements of gastropod echoes show two peaks with a lower-amplitude region in between. The initial peak is assumed to come from the immediate reflection of the incident wave by the front of the shell (i.e. the side facing the transducer). The delay between the two peaks is rather long, more than would be expected if the later peak was a simple reflection from the other side of the shell. Stanton *et al.* (1998b) believe this effect is caused by Lamb waves. These are vibrations of the shell which circumnavigate the surface in all directions (meridians) starting from a launch point (Fig. 7.3). The vibrations travel at subsonic speeds, and are mostly contained within the shell material, but some energy leaks into the water. Part of the leaked energy propagates towards the transducer, causing the second peak of the echo, and other amplitude fluctuations through interference with the front-surface reflection.

There are additional effects which might be considered in a complete model. Refractions and reflections in the shell and interior fluid may have some effect on the echo. Then there is the Franz or ‘creeping’ wave which is another circumnavigating vibration. The Franz wave travels in the fluid boundary layer; it does not penetrate the shell surface. See Kargl and Marston (1989) for a ray model of an ideal spherical shell which includes all these effects. However, Stanton *et al.* (1998b) suggest that only the initial specular reflection and the Lamb effect are large enough to warrant attention. Thus they express  $L_{bs}$  as the sum of two components,  $L_{spec}$  and  $L_{Lamb}$ .

$L_{spec}$  is easily described in terms of the reflection coefficient at the shell surface, but formulas for  $L_{Lamb}$  are much more complicated. It is necessary to take some account of the fact that the shell surface is rough, irregular and may be elongated rather than spheroidal. Stanton *et al.* (1998b) start with the ideal spherical-shell model of Kargl and Marston (1989), then they allow the radius of the body to change stochastically over the surface. This leads to a heuristic ray formulation for  $L_{Lamb}$ . Although far from rigorous, this model takes account of dispersion effects, i.e. how the speed of the Lamb wave changes with frequency. It does not take account of the opercular opening, a further complication that has not been successfully modelled so far, except in a qualitative way.

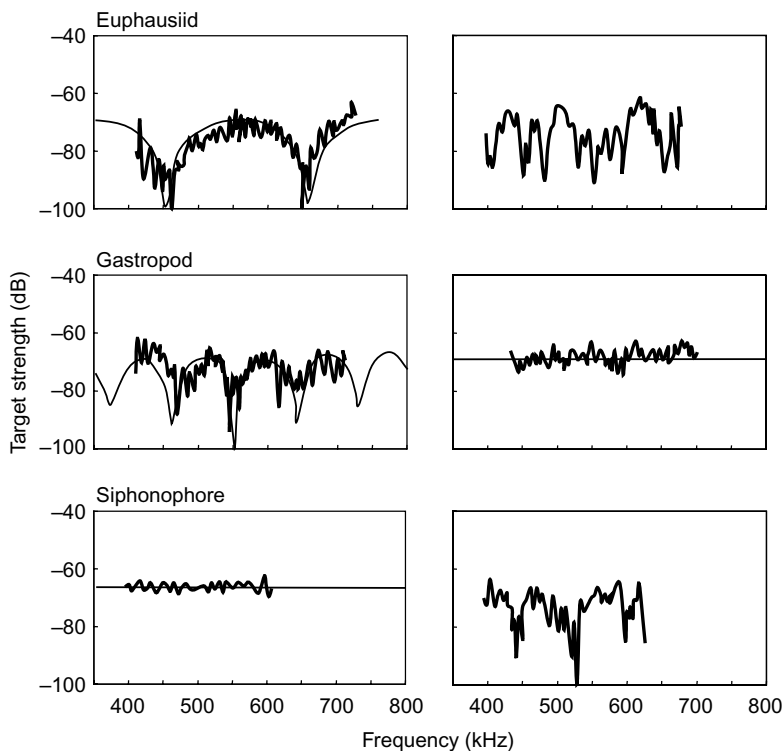


**Fig. 7.6** Examples of single-ping echo spectra from individual zooplankton. The thin lines are theoretical predictions; the thick lines are experimental data. The euphausiid spectra are consistently oscillatory. Those of the other species can be flat or oscillatory. (Redrawn from Stanton *et al.* 1996.)

The spectra of gastropod echoes can be oscillatory or flat (Fig. 7.6). Stanton *et al.* (1996) explain this by the effect of the opercular opening. Depending on the position of the hole relative to the launch point of the Lamb waves, the vibrations may propagate freely or they may be blocked. Stanton's complete model predicts an oscillatory echo spectrum. If the Lamb component of the model is suppressed, however, there is no interference with the initial reflection and the resulting spectrum is flat. The very different gastropod spectra in Fig. 7.6 show that both these conditions can arise in practice.

### 7.3.3 GB class (gas bearing)

Some zooplankton have a gas inclusion which, although small compared to the body volume, is a relatively strong sound reflector. The GB class is typified by siphonophores (Fig. 7.2). The gas inclusion, when present, is in a compartment (the pneumatophore) appended to the main body. The tissues are soft and weakly reflecting. Not all siphonophores have gas inclusions. Those without gas are entirely soft tissue, and should be considered in the FL class. The body shape is highly irregular.

We showed earlier that cylindrical models of the body worked well for targets like shrimp, but such a simple representation is not a good descriptor for the irregular shape of the siphonophore body.

The echo is considered to be the sum of contributions from the gas and the tissue. Thus we start with the formula  $L_{bs} = L_{bubble} + L_{tissue}$  which assumes that any acoustic shadowing by one component does not significantly affect the energy scattered by the other. This assumption is reasonable considering that the tissue is soft and weakly reflecting.  $L_{bubble}$  and  $L_{tissue}$  can be evaluated as though they were isolated scatterers (Stanton *et al.* 1998b).

The gas bubble can be considered as a sphere. It is less deformed by the surrounding tissues than is the case for the swimbladders of fish.  $L_{bubble}$  is obtained as an exact solution of the wave equations, valid for all frequencies, from the fluid-sphere theory described by Anderson (1950). This theory is applicable to the gas bubble, which is acoustically similar to a fluid sphere in that gas does not support shear waves.

The formulation of the tissue contribution is more difficult due to the irregular surface. Simple shape models like the cylinder are not useful here. However, the scattering by an arbitrary body shape can be determined by the DWBA volume-integral approach as described above. This method is suitable for siphonophore tissues since they are weakly reflecting. Stanton *et al.* (1998b) note that the body tissue of the siphonophore grows in long strands, thus  $L_{tissue}$  depends on the body orientation in the incident beam. The gas bubble dominates the mean echo amplitude, while the tissues are responsible for fluctuations in the echo spectrum. These fluctuations are evident in the echoes from single plankters in laboratory experiments. When many animals are observed in the field, we have to consider the average response over a range of body orientations. In that case the spectral fluctuations due to the body tissues tend to cancel out, and the mean target strength is dominated by that of the gas bubble.

### 7.3.4 Acoustic properties of fluid-like bodies

To evaluate the formulas derived from theoretical scattering models, we need to have numerical values for the contrasts which describe the acoustic properties of the body tissues. The compressibility and density contrasts,  $q$  and  $g$  respectively, were defined in connection with the DWBA (p. 269). In the case of fluid-sphere models, the equations are normally written in terms of  $g$  and  $h$ , the latter being the sound-speed contrast which is defined in the same way i.e.:

$$h = (c_1 - c) / c \quad (7.4)$$

As before, subscript '1' refers to the body tissue. Note that the three contrasts ( $q$ ,  $g$  and  $h$ ) are not independent. Since the compressibility depends on the density and sound speed through the formula  $\kappa = (\rho c^2)^{-1}$ , substitution in Equ. (7.2) leads to the relationship:

$$q = 1 / \{(1 + g)(1 + h)^2\} - 1 \quad (7.5)$$

Thus, the body properties in Equ. (7.1) are known if  $g$  and  $h$  can be measured or estimated in some way. This is not necessarily an easy task, particularly for very small animals. Greenlaw (1977) has described experimental techniques which can be applied to plankton.  $\rho_1$  was determined by the density bottle method. The bottles contain water and glycerine solutions with a series of densities at small intervals (about  $5 \text{ g l}^{-1}$ ). A specimen (some fresh, others preserved) was rinsed in distilled water, then placed in each bottle consecutively.  $\rho_1$  was estimated as the average density of the solutions in which the specimen just floated and just sank. This method gives just one numerical result, i.e. the mean density of the immersed body. Greenlaw noted that his specimens of the shrimp *Sergestes similis* floated head up, suggesting that the density was lower in the thorax. Separate measurements of the body parts confirmed that the density was indeed non-uniform, perhaps due to lipid concentrations. Kristensen and Dalen (1986) found that the euphausiid density declined slightly as the animal grew. Again, this effect might be explained by differences in the lipid content of the body.

The sound speed in the body tissue has to be measured indirectly. Consider a mixture of plankton and water in which the sound speed is  $c_{\text{mix}}$ . This can easily be measured given a large enough volume of biota. Let  $\Phi_{\text{pl}}$  be the fraction of the total volume occupied by the plankton. We suppose that  $c_{\text{mix}}$  varies linearly with  $\Phi_{\text{pl}}$ , from  $c$  for empty water to  $c_1$  when the volume is entirely plankton. Thus  $c_1$  can be deduced from one or more measurements of  $c_{\text{mix}}$  and  $\Phi_{\text{pl}}$ .

Greenlaw (1977) conducted experiments with a velocimeter made from two tubes joined in the shape of an inverted 'T'. There were transducers at opposite ends of the horizontal tube.  $c_{\text{mix}}$  was determined from the delay between acoustic pulses being transmitted by one transducer and received by the other. The transparent vertical tube had a scale on which the meniscus showed the total volume of fluid in the velocimeter. The apparatus was initially filled with distilled water. In that case  $\Phi_{\text{pl}}$  is zero and  $c_{\text{mix}}$  is a measure of  $c$ . Specimens were then dropped into the apparatus a few at a time and allowed to spread uniformly through the water. The change in total volume (shown by the scale on the vertical tube) gave the volume of plankters added, thus the  $\Phi_{\text{pl}}$  corresponding to the measured  $c_{\text{mix}}$  could be calculated. This procedure was repeated several times. Finally,  $c_1$  was estimated from the linear regression of  $c_{\text{mix}}$  on  $\Phi_{\text{pl}}$ . See Fig. 7.7 for an illustration of Greenlaw's method, also Foote *et al.* (1990) for a detailed exposition of its application to the krill *Euphausia superba*. Chu *et al.* (2003) used the same techniques to determine the material properties of cod *Gadus morhua* eggs and early-stage larvae. These are fluid-like (FL) plankton up to 5 days post-hatch. After that time, the swimbladder begins to develop and the gas inclusion soon dominates the scattering.

Ye and McClatchie (1998) consider that the results of velocimeter experiments require more careful interpretation. They take account of wave scattering within the mixture, and develop a theory which suggests that Greenlaw's linear volume-fraction approach overestimates  $c_1$ . The two methods agree for weak scatterers at low frequencies (in the Rayleigh region). Otherwise the discrepancy can be large.

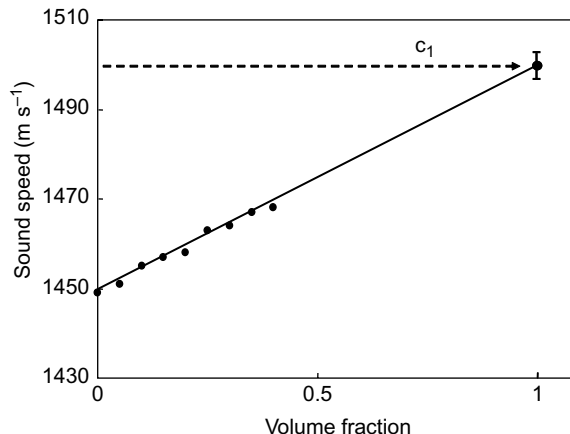


**Fig. 7.7** Measured sound speeds in a mixture of euphausiids and water at 10.4°C, vs the volume fraction occupied by the plankton ( $\Phi_{pl}$ ). The solid line is from least-squares regression. Extrapolation to  $\Phi_{pl} = 1$  predicts  $c_1$ , the sound speed in the body tissue. The vertical bar on  $c_1$  is the 95% confidence interval on the prediction. (Redrawn from Greenlaw 1977.)

Consider a 500 kHz wave passing through a water–plankton mixture, and take 10 mm as the typical animal size. For this example, Ye and McClatchie (1998) suggest that estimates of  $c_1$  by the volume-fraction and wave-scattering methods would be 1.2% different. This may seem small, but given the weak scatterer assumption, it implies a substantial difference in the predicted target strengths.

Various other techniques can be used for the physical measurement of plankton (see for example Coombs 1981; Greenlaw and Johnson 1982; Koegeler *et al.* 1987). Foote (1998b) has reviewed the methodology and practical difficulties with this work. The specimens can deteriorate rapidly after capture, and the observations are made in special liquids rather than sea water. Thus the *ex situ* results might be quite unrepresentative of plankton in the wild. While the density of individual large animals can be determined directly from their mass and volume, the plankton are too small and delicate for that approach. The removal of water clinging to the body surface, even if possible, would destroy or alter the tissues in an unpredictable way.

Collected results from measurements of density and sound speed in plankton are shown in Table 7.1. These have all been obtained from experiments in the laboratory. It is uncertain how representative the results are of plankton in their natural environment. Clearly, further work is needed to provide more accurate data for models and the interpretation of echoes from plankton concentrations in the sea.

## 7.4 Target strength

As discussed in Chapter 6, the target strength (TS) is a measure of how strongly a fish reflects sound. The same principles apply to plankton; however, their small size and

**Table 7.1** Physical properties of zooplankton relevant to acoustic scattering (FL class). Examples of measured densities ( $\rho_1$ ) and sound speeds ( $c_L$ ) in the body tissue. g and h are, respectively, the density and sound-speed contrasts with the surrounding water; T = temperature; S = salinity.

Species	T (°C)	S (ppt)	$\rho_1$ (kg l <sup>-1</sup> )	$c_L$ (m s <sup>-1</sup> )	g	h	Ref. <sup>§</sup>
Amphipods ( <i>Parthenemisto pacifica</i> )	20	29	1.080–1.100	1514	1.055–1.074	1.000	1
Copepods ( <i>Calanus finmarchicus</i> )	15				1.026–1.049	1.015 ± 0.009	1
<i>Calanus plumchrus</i>	20	32	1.070	1546	1.047	1.012	1
25	29						1
Euphausiids ( <i>Euphausia pacifica</i> )	16.2	30	1.060–1.065	1513	1.035–1.040	1.005	1
20	34						1
25	31			1553		1.015	1
<i>Euphausia superba</i>	7.8 <sup>a</sup>	33.2 <sup>a</sup>	1.063 <sup>a</sup>	1521 <sup>a</sup>	1.036 ± 0.007	1.028 ± 0.002	3
<i>Thysanoessa raschii</i>	12.3	34	1.049–1.068		1.021–1.040		1
<i>Thysanoessa</i> sp.			1.055	1511	1.027	1.010	1
<i>Meganyctiphanes</i>			1.071–1.052 <sup>b</sup>		1.044–1.026 <sup>b</sup>	1.025	4
<i>norvegica</i>			1.076–1.056 <sup>c</sup>		1.048–1.029 <sup>c</sup>	1.035	4
Squid							
( <i>Todarodes pacificus</i> )	13	34	1.028	1510	1.003	1.007	5
Cod ( <i>Gadus morhua</i> )							
Days post-hatch							
0 (Eggs)	5.6	30.6	1.003	1492	0.979	1.017	6
1	6.1	31.3	1.007	1498	0.983	1.019	6
5 <sup>d</sup>	9.0	31.2	1.016	1524	0.992	1.026	6

<sup>a</sup> Mean over 17 experiments. <sup>b</sup> g decreases with length, range for TL = 11–25 mm shown. <sup>c</sup> Ditto, TL = 20–46 mm. <sup>d</sup> Contains an embryonic swimbladder ca 1% of total volume.

<sup>§</sup> References: 1, Greenlaw and Johnson (1982); 2, Foote *et al.* (1996); 3, Foote (1998b); 4, Kristensen and Dalen (1986); 5, Arnaya and Sano (1990); 6, Chu *et al.* (2003).

different structure are not amenable to the same methodology as fish. Most investigations of acoustic scattering by plankton have been based on the theoretical models discussed above. The traditional methods of TS measurement are suitable only for the largest zooplankton which are similar in size to the smallest fish. Nevertheless, useful results have been obtained in a few cases, mostly by the *ex situ* method in which a known quantity of the target species is insonified in an enclosure of known volume.

The krill *Euphausia superba* has been the subject of much research due to its ecological importance in the Antarctic seas. This is one of the few species of plankton or micronekton for which the traditional methods of acoustic survey and biomass estimation are useful. For that, of course, the mean target strength must be known (Everson *et al.* 1990; Hewitt and Demer 1991; 1996). Foote *et al.* (1990) investigated the target strength at 38 and 120 kHz, from measurements of live krill in a cage. The observed TS was very small, about  $-86$  dB at 38 kHz for krill 31–38 mm long. The acoustic beam insonifies some of the netting as well as the krill. Because of the low target strength, the echo from the krill is weaker than that from the cage, and it is difficult to determine the cage contribution accurately. This can be done in two ways, firstly by measuring the empty cage and subtracting the mean cage integral from each cage-plus-krill measurement, and secondly, by regressing the cage-plus-krill data on the number of krill and estimating the target strength from the slope of the regression line. Foote *et al.* (1990) found that the two methods for removing the cage contribution gave target strengths which differed by several dB. Pauly and Penrose (1998) avoided this problem by observing their krill in a tank wider than the acoustic beam. This technique works if the krill are evenly distributed across the tank, assuming the beam pattern of the transducer is known or can be measured (cf. Chapter 3).

The krill has an elongated body, thus its orientation (tilt angle) in the acoustic beam has a substantial effect on the target strength. The tilt angle can be determined from photographic or video images, and experiments on captive krill have confirmed the importance of the body orientation in explaining the variability of TS measurements (Miyashita *et al.* 1996). McGehee *et al.* (1998) showed that the mean TS at 120 kHz, averaged over an observed distribution of tilt angles, was about 12 dB lower than the peak (dorsal aspect) value. Stanton *et al.* (1993b) used a cylinder model in a theoretical approach to the problem. They considered an aggregation of krill having a range of tilt angles and body sizes. The resonance structure of the averaged broadband spectra was still evident although less strong than that of a single-target echo. The spectrum depends on the ratio of wavelength to body size. This implies that for the same frequency, TS will change with L in a complicated way. Thus the simple approximation to the length dependence assumed for fish,  $TS = m \log L + b$ , may be unsuitable for plankton. Demer and Martin (1995) discuss this problem in the wider context of whether TS depends on the geometric cross-section or the volume of the body, see also Wiebe *et al.* (1990).

Chu *et al.* (1993) conducted a further analysis of the results reported by Foote *et al.* (1990). They used a deformed cylinder model to predict the mean TS of krill at 38 and 120 kHz, obtaining results for various orientation distributions. By matching

the predicted and observed target strengths at the two frequencies, it was possible to infer the orientation distribution of the caged krill as that of the best fitting prediction. Martin Traykovsky *et al.* (1998) extended this technique to the analysis of broadband echoes. They used measurements as well as models of the echo spectra to infer the orientation distribution. The tilt angles of captive krill were measured from analysis of pictures recorded by a video camera. Thus the method could be validated by comparing the predicted and measured tilt angles of the same target.

Despite the uncertain dependence of echo strength on animal size, the following TS function has been adopted as a standard for multi-national surveys of Antarctic krill:  $TS = -127.45 + 34.85 \log(L)$  at 120 kHz sounder frequency (Greene *et al.* 1991; Hewitt and Demer 1991). Here  $L$  is the standard length in mm, measured from the front of the eye to the tip of the telson. In practice, the target strength per unit weight ( $TS_{kg}$ ) is generally used in survey analysis, since it is less dependent on length measurements. The weight-at-length of *E. superba*, in grams, is  $3.85 \times 10^{-6} L^{3.2}$ . Combining this with the TS-per-krill function gives  $TS_{kg} = -43.3 + 2.85 \log(L)$ .

The Greene *et al.* (1991) function replaced an earlier version that predicted much higher target strengths, which was  $TS = -95.7 + 19.9 \log(L)$  (BIOMASS 1986). There is, however, still some concern that Greene's function may overestimate the TS of krill (McGehee *et al.* 1998; Pauly and Penrose 1998). Note that it has a much higher slope parameter ( $m = 34.85$ ). This reflects the current view that echoes from fluid-like plankton depend on the body volume rather than the cross-sectional area (Wiebe *et al.* 1990; Demer and Martin 1995). The various TS functions for krill are compared in Fig. 7.8.

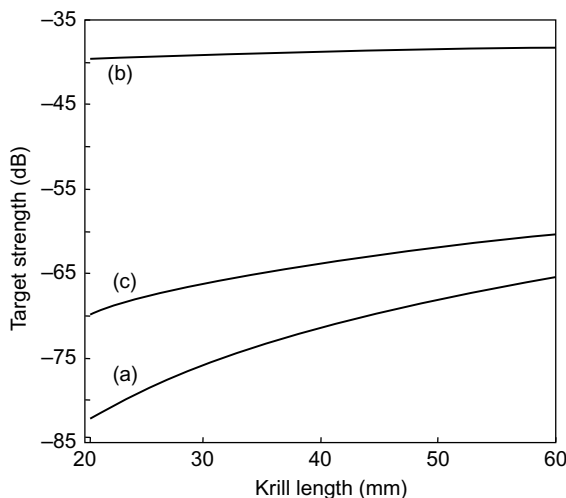


**Fig. 7.8** TS-length relationships for Antarctic krill *Euphausia superba* at 120 kHz. (a) The current standard adopted for multi-national surveys of this species (Greene *et al.* 1991; Hewitt and Demer 1991). (b) The same function normalized to 1 kg of krill. (c) The previous function which predicted much higher target strengths (BIOMASS 1986).

Demer and Conti (2003) describe a novel technique for plankton studies based on acoustic reverberation measurements, see also De Rosny and Roux (2001). Pulses from an omni-directional transducer were transmitted into a glass carboy containing live active krill. At the end of each pulse, receivers in the carboy detect the reverberation which decays with time. The decay rate depends on  $\sigma_t$ , the total scattering cross-section of the krill which takes account of the energy scattered in all directions. The orientations and positions of the animals are immaterial. The main objective of this work was to validate the DWBA scattering model (cf. Section 7.3), which it did since the model predictions were in good agreement with the experimental results over a wide range of frequencies (60–202 kHz). To predict  $\sigma_t$ , Demer and Conti (2003) used a stochastic version of the DWBA model which involves additional integrations over all directions of the incident and scattered sound fields. They suggest that by considering total rather than backscattering cross-sections, their model offers a new approach to the acoustic identification of krill, and prospects for more accurate biomass estimates from acoustic surveys. It is unlikely that this method could be used on its own to predict the correct target strength for survey applications, but it does provide an excellent way of validating the general performance of models such as the DWBA.

There are only a few reports of TS measurements on zooplankton species other than krill. Arnaya *et al.* (1989a; 1989b) studied the surume ika *Todarodes pacificus* which is a small squid. They observed various numbers up to 110 squid in a cage 1.0 m deep and 0.9 m diameter. The dorsal mantle length ranged from 10–20 cm with a mean of 16 cm. The echo energy was found to be proportional to the density of squid in the cage, confirming the linearity of acoustic scattering by this species at the two frequencies investigated, 28.5 and 96.2 kHz. TS measurements have also been made on the common jellyfish *Aurelia aurita* (Mutlu 1996) and the comb-jelly *Belinopsis* sp. (Wiebe *et al.* 1990). For these gelatinous organisms, the size is normally described by the disc diameter rather than the ill-defined length.

Some collected results from TS measurements of macroplankton are shown in Table 7.2.

## 7.5 *In situ* observation techniques

Acoustic methods for the study of plankton in their natural environment have developed rapidly in recent years. They are now well established as a remote-sensing and unobtrusive means of observation in biological oceanography. Applications arise on widely different scales, from large marine ecosystems at one extreme to the behaviour of individual zooplankters at the other (Smith *et al.* 1992; Griffiths *et al.* 2002).

### 7.5.1 Abundance estimation

Early investigators studied the volume scattering strength  $S_v$ , measured by echo-integration at one frequency (e.g. Bary 1966; Peiper 1979; Sameoto 1982). They found

that  $S_v$  correlated well with the zooplankton biomass determined by direct sampling. Thus echo-integration reveals the spatial distribution of the biomass, and a large volume of water may be surveyed acoustically much more rapidly than by mechanical samplers.

In principle, the abundance of plankton may be estimated from the  $S_v$  recorded along transects covering the area of interest. To do this, we must first partition  $S_v$  to exclude the contribution of unwanted targets (which in this case include fish). It is often possible to separate plankton and fish marks from their appearance on the echogram. The plankton give weak diffuse marks while the fish are stronger targets and school structures may be evident. Secondly, the conversion factor between  $S_v$  and the plankton density must be known. This is a more difficult question. In the case of fish, the general approach is to calculate the mean target strength from knowledge of the size and species composition of the animals, and the density follows from linear echo-integration theory (Equ. 5.14). This method is unsuitable for plankton, at least when surveys are conducted with a single-frequency echosounder. Most plankton are too small and their scattering properties are too variable for the traditional idea of TS-length regressions to be useful.

A more direct approach is to calibrate the acoustic data against biological samples caught by a towed net or filtered from pumped water. If the volume of water sampled is known, and assuming there is no avoidance behaviour, the plankton density is determined at a number of stations. Concurrent measurements of  $S_v$  are compared with the observed densities and the relationship is determined by regression. The density may be expressed as the number of animals or simply as the dry weight per unit volume (Pieper 1979; Sameoto 1980). If the same relationship applies throughout the surveyed area, then all the acoustic data can be used to obtain a biomass estimate that should be more precise than one based on the biological samples alone. Whether that is a reasonable assumption depends on how the structure of plankton concentrations changes from one place to another. Hydrographic factors are undoubtedly important in this context. Wiebe *et al.* (1996) found that quite different results were obtained from regions of mixed and stratified water on Georges Bank. There have been several other applications of the direct calibration method, see for example the work of Iida *et al.* (1996) in Japan and Kirsch *et al.* (2000) in Alaska. The technique has proved useful in freshwater as well as marine environments (Morton and MacLellan 1992). See also Greene *et al.* (1998) who compared acoustic and net-sampling methods for assessing the abundance and distribution of zooplankton. They conclude that net sampling is too slow, but it is nevertheless important as a means of ground truthing the results of acoustic surveys.

The single-frequency echosounders used to survey plankton typically operate around 120 kHz, with a few of the cited examples being up to 420 kHz or down to 50 kHz. The 'standard' 38 kHz, popular for surveys of fish, is rather low for plankton, except when the intention is to compare results at different frequencies. The smaller plankton are generally stronger targets at 120 kHz compared to 38 kHz, while the opposite applies to fish. This feature can be a useful criterion for separating

**Table 7.2** Collected results from target strength measurements of macroplankton and microneuston. f is the echosounder frequency. The ‘reduced’ target strength is the mean TS less  $20 * \log(\text{size})$ . It is included only as a standard means of comparing results, and does not imply any particular size-dependence of TS.

Species	Location	Length/size (cm)		f (kHz)	Mean TS (dB)	Reduced TS (dB)	Methods $\perp$	Ref. $^{\$}$
		Mean	St. dev.					
<i>Euphausiids<sup>(1)</sup></i> <i>Euphausia superba</i>	Antarctic	3.27	2.8-4.0	38	-85.1	-95.4	Cage	1
		3.27	2.8-4.0	120	-76.1	-86.4	Cage	1
<i>Tasmania</i>		4.74	0.29	120	-69.0	-82.5	<i>in situ</i> , SB	2
		2.96	0.30	120	-75.5	-84.4	Tank, IND	3
<i>Euphausia pacifica</i>	Washington	3.29	0.15	120	-77.0	-87.3	Tank, IND	3
		3.45	0.20	120	-76.2	-87.0	Tank, IND	3
<i>Euphausia</i> sp. (mostly <i>E. pacifica</i> )	California	2.0	1.9-2.1	420	-72.7	-83.9	Tank, IND	3
		1.65	1.4-1.9	102	-77.5	-83.5	Tether, DB	4
<i>Squid<sup>(2)</sup></i>	Oregon	1.39	1.1-1.9	102	-69.6	-74.0	Comp	5
		11.6	8.0-23.0	120	-71.8	-75.7	Comp	5
<i>Loligo opalescens</i> <i>Ommastrephes bastrami</i>	Japan	23.0	16-42	28.5	-58.6	-79.9	<i>in situ</i> , DB	6
		16.0	10-20	28.5	-40.0	-67.2	Tether	7
<i>Todarodes pacificus</i>	Japan	16.0	10-20	96.2	-51.3	-75.4	Cage	8
					-54.6	-78.7	Cage	8

Jellyfish <sup>(3)</sup>							
<i>Aurelia aurita</i>	Black Sea	9.5	120	-60.2	-79.8	Tank, DB	9
		9.5	200	-64.3	-83.9	Tank, DB	9
		11.5	200	-62.5	-83.7	Tank, DB	9
		15.5	120	-57.1	-80.9	Tank, DB	9
		15.5	200	-56.5	-80.3	Tank, DB	9
<i>Chrysaora hysoscella</i>	South Africa	26.8	18	-51.5	-80.1	Comp	10
			38	-46.6	-75.2	Comp	10
			120	-50.1	-78.7	Comp	10
<i>Aequorea aequorea</i>	South Africa	7.4	18	-68.1	-85.5	Comp	10
			38	-66.3	-83.7	Comp	10
			120	-68.5	-85.9	Comp	10
<i>Aequorea victoria</i>	Washington	4.2	1.9	2.0-5.5	420	-64.8	-77.3
	Bolinopsis sp.	4.5			420	-80.0	-93.1
						Tank, DB	4
						Tank, DB	4

Length/size measurements are <sup>(1)</sup> standard length (front of eyes to tip of telson); <sup>(2)</sup> dorsal mantle length; <sup>(3)</sup> disc diameter.

† Cage, a fully insonified enclosure; Tank, enclosure larger than the beam; Comp, comparison with independent data; Tether, animal restrained by a line; IND, indirect TS measurement; DB, dual-beam echosounder; SB, split-beam echosounder.

§ References: 1, Foote *et al.* (1990); 2, Hewitt and Demer (1991); 3, Pauly and Pentrose (1998); 4, Wiebe *et al.* (1990); 5, Pieper (1979); 6, Jefferts *et al.* (1990); 8, Arriaga *et al.* (1989b); 9, Mutlu (1996); 10, Brieterley *et al.* (2001).

planktonic and fish marks on the echogram. However, there have been reports of echosounder marks, which appear to be entirely plankton, being stronger at 38 kHz than at 120 kHz, suggesting that other scatterers may be contributing apart from those seen in the net samples. While most of these reports are anecdotal and unsupported by good evidence, Mair *et al.* (2004) encountered this anomaly on many occasions in the North Sea. They speculate on the cause, suggesting that gas bubbles within the plankton layer would be an explanation, but they were unable to reach firm conclusions. The source of the gas bubbles (if any) is unknown, though phytoplankton is a candidate. It is therefore necessary to be cautious in applying simple conclusions about how the backscattering changes with frequency, when extracting acoustic data on plankton from the total echo-integral.

The traditional method of acoustic abundance estimation, which assumes knowledge of the target-size distribution and an associated TS function, should be applicable to large zooplankters such as the Antarctic krill *Euphausia superba*. However, early work on this species with single-frequency echosounders gave impossibly small abundances due to the predicted TS being too large. Extensive experimental and theoretical work on the target strength of krill, taking account of the strong variation with the tilt angle demonstrated by McGehee *et al.* (1998), has resulted in a realistic TS function more in line with expectations (Greene *et al.* 1991; Hewitt and Demer 1991). Nevertheless, it has long been recognized that single-frequency surveys of plankton are rather limited. Gross features of the scattering strength and its spatial variation are revealed, but little else. The concurrent use of two or more frequencies can provide additional information on the structure of the surveyed population (Greenlaw 1979).

### **7.5.2 Size determination – the inverse problem**

Some non-acoustic evidence, such as trawl samples, is normally required to determine the species composition of echo traces. However, the size distribution of zooplankters may be determined acoustically by measuring  $S_v$  at several frequencies (Greenlaw and Johnson 1983; Holliday and Pieper 1995). The method depends on the change of scattering strength with frequency which is characteristic of the target size. In particular, Rayleigh scattering applies at low frequencies up to a limit which is inversely proportional to the target size (Section 2.5.1). The target strength is relatively small in the Rayleigh region. This means that the smaller targets are more strongly detected at the higher frequencies. Above the Rayleigh limit, the target strength may still vary with frequency due to resonances. This variation, for a given shape and structure of target, depends on the wavelength–size ratio. Thus the spectrum of echoes from a plankton aggregation should, in principle, provide information on the size distribution of the observed targets.

The usual approach is to express the size distribution in terms of the equivalent spherical radius, ESR. This is the radius of a sphere having the same volume as the zooplankter. Depending on the type of plankton being observed (fluid-like, gas

bearing etc.), scattering models backed by experimental studies show how the target strength changes with frequency and size, as discussed in Section 7.3. This allows the size distribution to be inferred from the  $S_v$  values observed at various frequencies, provided the consequent TS changes are large enough to be observed above random fluctuations of the signal. The frequency range must be sufficient to cover the Rayleigh transition frequencies of all the target sizes being considered. The transition marks the upper limit of the Raleigh scattering region. It occurs when the size-scaled frequency  $ka$  is about 2. Here  $k = 2\pi/\lambda$  and  $a$  is a typical dimension of the target, i.e. the same as ESR in the case of plankton.

Suppose  $S_v$  is determined at  $M$  discrete frequencies written as  $f_i$  for  $i = 1$  to  $M$ . We require linear measures for the calculation, namely the volume backscattering coefficients which are  $s_v = 10^{(S_v/10)}$ . For clarity write  $s_i$  for the measured  $s_v$ . Now consider a set of target sizes  $a_j$ ,  $j = 1$  to  $N$ , covering the range of interest. Each  $a_j$  represents some interval (or bin) of sizes. The size intervals must not overlap but they do not have to be contiguous. Let  $F_j$  be the number of  $j$ -type scatterers per unit volume. The  $F_j$  describe the (unknown) size distribution. The assumed scattering model predicts the  $\sigma_{bs}$  of one target as a function of  $ka$ . Thus for each size and frequency, we know  $\sigma_{ij} = \sigma_{bs}(k_i a_j)$ . Linear echo-integration theory states that  $s_i$  is the sum of contributions from all the sampled targets, and so (Greenlaw 1979):

$$s_i = \sum_{j=1}^N \sigma_{ij} F_j \quad \text{for } i = 1 \text{ to } M \quad (7.6)$$

This is a set of  $M$  simultaneous equations in  $N$  unknowns. It is convenient to express these in matrix notation. Write  $\mathbf{F} = [F_j]$  and  $\mathbf{X} = [s_i]$  as column vectors of the unknowns and the measurements, respectively, and  $\mathbf{R} = [\sigma_{ij}]$  as the matrix of backscattering coefficients ( $M$  rows and  $N$  columns). Equ. (7.6) is now concisely expressed as:

$$\mathbf{RF} = \mathbf{X} \quad (7.7)$$

If  $M = N$ , there is one exact solution of Equ. (7.7) i.e.  $\mathbf{F} = \mathbf{R}^{-1}\mathbf{X}$ . More generally,  $M$  and  $N$  may be different. If  $M > N$ , the equations are said to be over-determined; there is no exact solution but a least-squares best fit can be obtained. If  $M < N$ , the equations are under-determined; there are now many possible solutions, but again there is a best estimate. Writing superscript 'T' for a transposed matrix (i.e. rows and columns interchanged), the best solutions are (Greenlaw and Johnson 1983):

$$\mathbf{F} = (\mathbf{R}^T \mathbf{R})^{-1} \mathbf{R}^T \mathbf{X} \quad \text{for } M > N \quad (7.8a)$$

$$\mathbf{F} = \mathbf{R}^T (\mathbf{R} \mathbf{R}^T)^{-1} \mathbf{X} \quad \text{for } M < N \quad (7.8b)$$

Equation (7.8a) is the solution that minimizes the sum of the squared residuals (i.e. the differences between the right and left hand sides of Equ. (7.6)). The residuals are all zero in the under-determined case, however, Equ. (7.8b) is the solution that minimizes the sum of squares of the  $F_j$ .

Having worked through the above procedure, the results may show negative values for one or more of the  $F_j$ . Densities less than zero are obviously wrong, and what we want is the best solution subject to the constraint  $F_j \geq 0$ . There are several approaches to this problem (Lawson and Hansen 1974). Greenlaw and Johnson (1983) compared the alternatives, and found that the non-negative least-squares method (NNLS) was the most robust for multi-frequency plankton analysis. Essentially, this method repeats the calculation, each time setting the most negative  $F_j$  to zero, continuing until all the  $F_j$  are zero or positive. Good results cannot be expected if there are many more size classes than frequencies ( $N \gg M$ ). However, Holliday and Pieper (1995) suggest that for small zooplankton, NNLS gives useful size distributions when the ratio ( $N/M$ ) is as much as 1.5–2.

The NNLS technique estimates the total plankton density (as the sum of the  $F_j$ ) as well as the size distribution, and the abundance follows by summing these densities multiplied by the relevant sampled volumes. It is important to note that large errors can occur if the frequency range, the size groups and/or the model assumptions are inappropriate for the detected targets. Further, this applies to all species and taxa that contribute to the scattering, not only those of specific interest to the researchers. Equation (7.6) is correct only if it includes all the size groups contributing to  $s_i$ , whether or not they are deemed to be scientifically important.

Multi-frequency studies of plankton are conducted with discrete frequencies which can extend from 0.1 to 10 MHz or more. However, the effective range at 10 MHz is only a few metres (see Section 2.7), which means that the use of data obtained at lower frequencies must be similarly restricted, in order to sample the same volume of water. Thus the volume sampled per ping is rather small. One technique is to deploy several transducers in a probe which is lowered from a stationary ship. The transmissions are repeated as the probe descends, giving a depth profile of targets in the whole water column. The probe may be dropped at a series of stations along a transect, to reveal horizontal changes in the plankton distribution. Alternatively, the probe may be towed at a particular depth to map the horizontal distribution in more detail, or it can be moored on the seabed to record changes with time at a particular location.

Holliday *et al.* (1989) described a sophisticated instrument called the multi-frequency acoustic profiling system (MAPS). It had 21 circular-disc transducers, covering the band 0.1 to 10 MHz, as illustrated in Fig. 7.9. The disc diameter was inversely proportional to the frequency, thus all the transducers had the same beam width. The 21 frequencies were chosen so that the ratio of any two adjacent frequencies was nearly constant. The transducers transmitted 50  $\mu$ s pulses in turn, and the cycle of sequential transmissions through the 100-fold frequency range was repeated in 20–30 s. The sampled volume was about 0.1 m<sup>3</sup> at a distance of 1–2 m from the

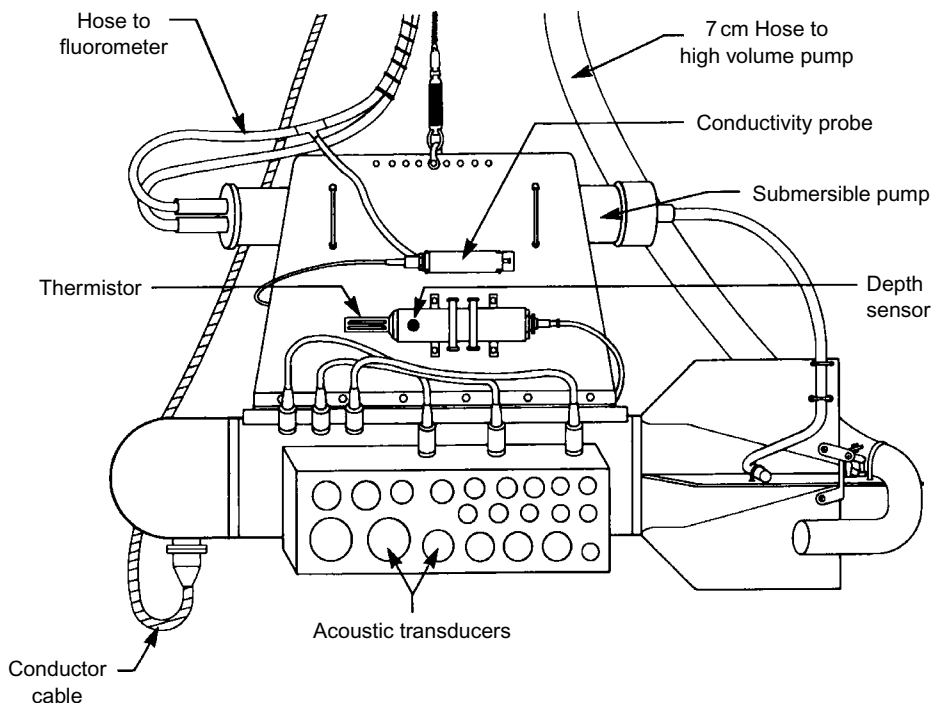


**Fig. 7.9** The MAPS (multi-frequency acoustic profiling system). The probe has 21 transducers operating at discrete frequencies from 0.1–10 MHz, and sensors for temperature, conductivity and depth measurement. A hose is attached for simultaneous pump sampling. (Redrawn from Pieper *et al.* 1990.)

transducer faces. Figure 7.10 illustrates the kind of results provided by MAPS, shown as grey-scale diagrams of the acoustic densities as  $S_v$  values by depth and size class.

Costello *et al.* (1989) tested MAPS against plankton densities determined by pump-sampling. The biological samples were collected by filtering the water from a pump whose inlet was attached to the MAPS probe. The dominant species in the filtrate were the calanoids *Clausocalanus* spp. and *Oikopleura* spp. with modal sizes (ESR) in the range 0.1–0.25 mm. Close agreement was found between the abundances and size distributions indicated by the pump and acoustic measurements. There have been many successful applications of MAPS in field work (e.g. Pieper *et al.* 1990; Napp *et al.* 1993; Buckart *et al.* 1995).

From the experience thus gained, it appeared that simpler (and less expensive) instrumentation might be adequate for some applications. This led to the development of TAPS, the Tracor acoustic profiling sensor (Holliday and Pieper 1995). The frequency band is narrower, 265–3000 kHz, but this is sufficient to measure plankton with ESRs from 50  $\mu$ m to 4 mm (Roman *et al.* 2001). The range resolution is 25 cm or better. Different versions of TAPS provide four, six or eight frequencies depending on the desired target-size resolution. New ways of deploying the instrument have

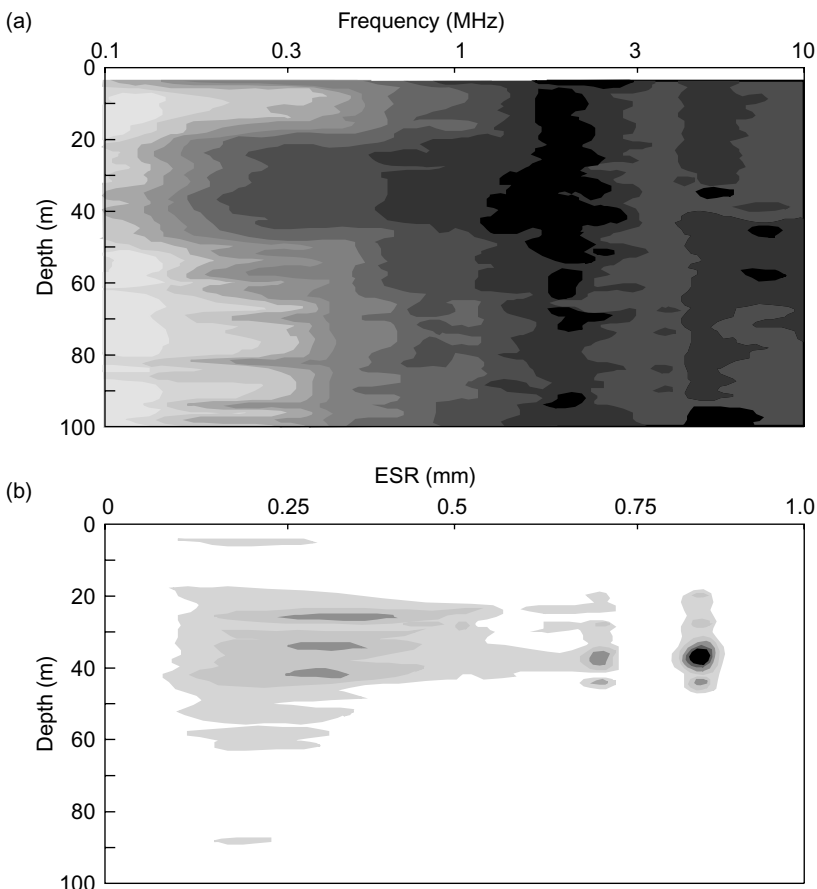


**Fig. 7.10** Examples of results obtained with the MAPS probe. The grey scales indicate relative values; black is high; white is low. (a) Volume backscattering strength vs frequency and depth; (b) biovolume estimates by size class and depth. (Redrawn from Pieper *et al.* 1990.)

been devised, such as mounting it on a vertically-undulating towed body (McGehee *et al.* 2000; Pieper *et al.* 2001) or moored on the seabed with an upward-looking transducer to observe diurnal movements of plankton (Barans *et al.* 1997; Kringel *et al.* 2003).

The six-frequency version of TAPS is illustrated in Plate 7.1a. As shown, the sonar is configured for independent deployment on the seabed. The frequencies are 265, 420, 700, 1100, 1850 and 3000 kHz. The beams are all about 8° wide. The instrument records mean volume backscattering strengths (MVBS, as 24-ping averages) at user-programmable intervals as short as 1 minute and a vertical resolution of 12.5 cm. It transmits the acoustic data to a shore station over a VHF radio link (the antenna is on small spar buoy, partly visible behind the cage). The self-powered version contains three 12-volt batteries and can operate continuously for three weeks. In fixed

installations where it is practical to supply external power via a cable, the limit on the deployment time depends on how fast fouling occurs. Several months of operation in that mode have been achieved.

An echogram for just one frequency (420 kHz) is shown in Plate 7.1b to illustrate the dynamics of high-frequency volume scattering at a site 15 m deep off Goleta Point, Santa Barbara, California. The echogram was recorded over 24 hours on 19 May 2003. The sampling interval was set at 2 minutes to save power. Water currents (from an ADCP mounted on the same cage) and meteorological data were monitored over the same period. These revealed that the changes in scattering were largely caused by the wind driving a stratified water mass into the deployment area just before noon. A combination of currents from a semi-permanent gyre in the Santa Barbara Basin, the weakening of the wind stress on the sea surface after sunset, and the incoming tide allowed the return of less stratified water in the early evening (around 20.00 hours). A thin zooplankton layer is seen a few metres below the surface while the stratified water is present. The fluctuating depth of this layer is associated with large amplitude, high-frequency internal waves near the thermocline. Panels (c) and (d) in Plate 7.1 show the results of a multi-frequency analysis of the thin layer using the NNLS method. This covered two classes of zooplankton believed to be present, distinguished by their shape and size. The classes are described as 'fluid spheres' (e.g. copepods) and 'elongates' (e.g. mysids), reflecting the different models used to define  $\sigma_{ij}$  for each class. The size distributions overlap slightly but are sufficiently different (as are the  $\sigma_{ij}$  functions) to allow a good NNLS solution of Equ. (7.9) (p. 290). The results are presented as biovolume distributions over depth and size ranges for each class (the biovolume is the zooplankton density in  $\text{mm}^3$  of animal per  $\text{m}^3$  of water). The top 5 m of the water column contained both small copepods (*ca* 2 mm length) and a few elongate scatterers of several sizes. The thin layer was dominated by elongate scatterers around 17 mm long, although other sizes were also present. The observed biovolumes were low compared to those seen in previous years. This was consistent with other investigations along the coasts of California and Oregon during the summer of 2003.

Notably, the results shown in Plate 7.1 were obtained solely by acoustic methods, without any net sampling, although there was 'prior knowledge' of the type of zooplankton likely to be in the area coming from many earlier investigations. Multi-frequency techniques are now well established in the study of plankton distributions, their ecology and how they relate to hydrographic features like thermoclines and fronts. This is a fine example of the progress made in solving the inverse scattering problem for biological targets.

If the size distribution consists of one narrow mode, the problem can be solved by measuring  $s_v$  at only two frequencies. The ratio of the two  $s_v$  then has a one-to-one dependence on ESR (Holliday and Pieper 1995). Figure 7.11 shows an example of this method applied to a fluid-like plankter. The frequencies need to be chosen so that the  $s_v$  ratio changes rapidly around the expected ESR. In our example, good results are limited to ESRs in the range 0.05–0.3 mm.

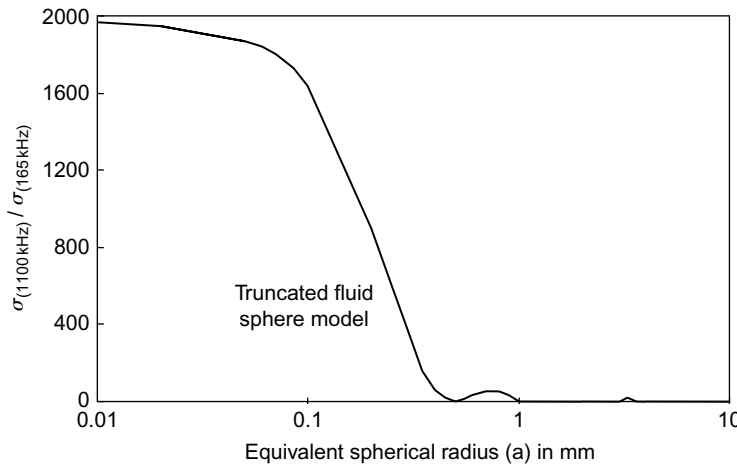


**Fig. 7.11** Ratio of backscattering cross-sections at two frequencies vs size of a fluid-like plankter. The ratio uniquely determines the size except for  $a > 0.3$  mm when there are multiple solutions. Calculations based on the truncated Anderson model. (Redrawn from Holliday and Pieper 1995.)

### 7.5.3 Species identification

The complete identification of detected targets is not possible by acoustic methods alone. Some independent evidence is necessary to know what they might be. This could be net samples collected at the time, or even the experience gained on previous surveys to indicate the sort of echogram marks produced by particular species. Nevertheless, the problem of how to distinguish different species (or broader taxonomic categories) from their echoes has similarities with that of the single-species size distribution. For example, suppose the echoes come from two species one rather larger than the other. They may have different backscattering cross-sections as a function of  $ka$ , say  $\sigma_1$  and  $\sigma_2$ . Equ. (7.6) can now be rewritten as:

$$s_i = \left\{ \sum_{j=1}^{N_1} F_{1,j} \sigma_1(k_i a_{1,j}) + \sum_{j=1}^{N_2} F_{2,j} \sigma_2(k_i a_{2,j}) \right\} \quad \text{for } i = 1 \text{ to } M \quad (7.9)$$

Here subscripts 1 and 2 refer to the respective species; otherwise the symbols are as defined above. There are now  $(N_1 + N_2)$  unknowns, but the NNLS method can still be used to determine the densities at each size of both species, if the equations are well enough determined (i.e.  $M/(N_1 + N_2) < 2$ ). This requires that we know what species are present and their scattering functions, but the relative proportions of each one can be determined from the acoustic data alone.

When the species composition is simple, with a small number of acoustically distinct groups, then echo-integration using two sounder frequencies may provide sufficient information to partition the echo traces (Mitson *et al.* 1996). Madureira *et al.* (1993a) showed that  $\delta S_{V(38-120)}$ , the difference in volume scattering strength

between 38 and 120 kHz, was a useful indicator for identifying krill in the presence of other scatterers found in the Southern Ocean. Selecting  $S_v$  values on the criterion  $2 \text{ dB} < \delta S_{v(38-120)} < 12 \text{ dB}$  eliminated most of the non-krill targets. Further, Madureira *et al.* (1993b) were partially successful in identifying three species of krill from their echo characteristics at 38 and 120 kHz. Frequencies below 100 kHz are not normally considered suitable for surveys directed at plankton. When two or more frequencies are involved, however, having one at e.g. 38 kHz is certainly useful for the primary task of separating plankton and fish marks.

Using more frequencies will in general improve the information that can be extracted from the acoustic records. On the other hand, very high frequency transmissions have a short range. In surveys of Antarctic krill,  $S_v$  has to be measured over tens or hundreds of metres, in which case 120 kHz is about right as the primary frequency and 200 kHz is about the highest that will be useful. Surveys of large areas (like the Southern Ocean) are currently done with sounders operating at two or three frequencies. In that case, Equ. (7.9) is highly under-determined and the NNLS approach is not useful. A more heuristic method of species identification is required. The  $S_v$  at two or three frequencies may be compared in scatter plots of samples at various depths and horizontal locations. Examples are shown in Figs 7.12 and 7.13 for two and three frequencies, respectively. Clusters of points in the scatter plot are assumed to represent particular target categories. Clustering will not occur, of course, unless the target categories are separated in space (by more than the distance over which  $S_v$  has been averaged). In the first instance, the identity of a cluster has to be confirmed by net sampling. Once some experience has been gained, species identification based solely on the acoustic data can succeed in favourable circumstances. This may require additional analysis of, for example, the appearance of marks on the echogram.

Antarctic zooplankton are often found in monospecific aggregations (swarms) or layers, which suggests they are good subjects for acoustic identification. Brierley *et al.* (1998) describe krill surveys in the Antarctic which were done with three frequencies (38, 120 and 200 kHz). Using discriminant function analysis of  $\delta S_v$ , they could distinguish three taxa (euphausiids, amphipods and mysids) with reasonable efficiency. Comparing the results with midwater trawl samples, the acoustic identifications of krill *E. superba* were found to be 77% correct. Woodd-Walker *et al.* (2003) extended this technique to include discrimination based on swarm morphology and  $S_v$  as well as  $\delta S_v$ . This improved the discrimination efficiency, especially between krill and salps. Two species of krill, *E. superba* and *Thysanoessa* sp., could be separated without much difficulty. However, they note that the discrimination of zooplankton other than krill still had to be supported by net sampling.

Most of the work cited above has been on krill, motivated no doubt by its ecological importance in the Antarctic where there are large international research programmes. There has been some interest in other species, notably Goss *et al.* (2001) who discuss the potential of two-frequency surveys (using 38 and 120 kHz) of the squid *Loligo gahi* in the South Atlantic.  $\delta S_{v(38-120)}$  for this species is typically 3.0–5.5 dB and is sufficiently consistent to allow separation of the squid from finfish.

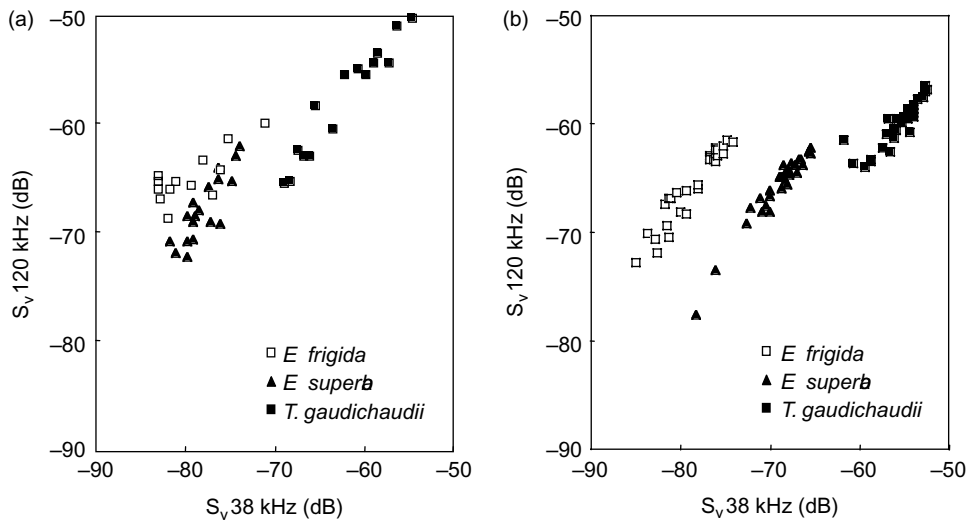


**Fig. 7.12** Scatter plots comparing  $S_v$  at 38 and 120 kHz for three species of Antarctic zooplankton; (a) as measured by Madureira *et al.* (1993b); (b) theoretical predictions for the same animals using the fluid cylinder model of Stanton *et al.* (1994a). (Redrawn from Griffiths *et al.* 2002.)

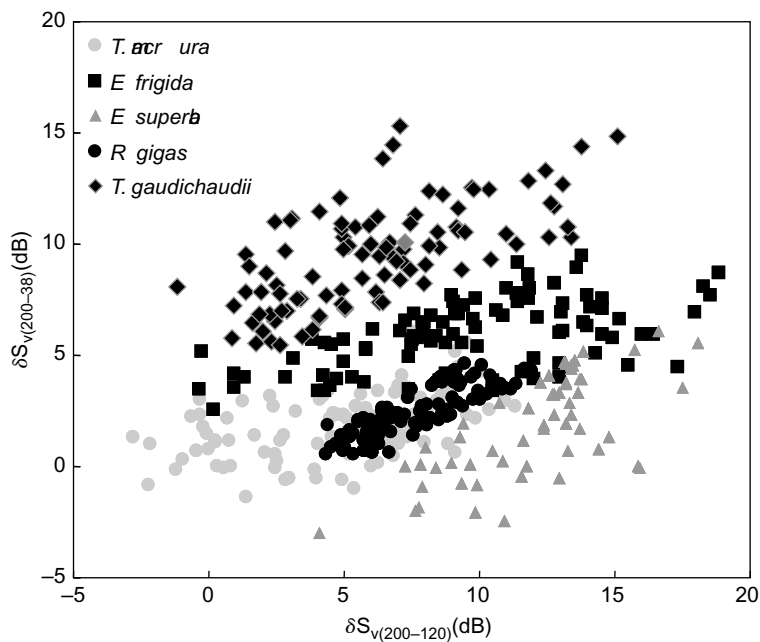


**Fig. 7.13** Scatter plot of  $\delta S_{v(38-200)}$  vs  $\delta S_{v(120-200)}$  for five species of Antarctic zooplankton. Significant clustering of the data is evident. (Redrawn from Brierley *et al.* 1998 with permission from Elsevier.)

However, accurate abundance estimates of *L. gahi* are not yet possible, since the target strength and behaviour of squid are not well enough understood.

#### 7.5.4 Other methods of *in situ* observation

The acoustic Doppler current profiler (ADCP) is an instrument which measures water flows, but it also records the backscattering strength from the sampled volume. Thus information on  $S_v$  can be collected concurrently with hydrographic surveys. This can provide information on the spatial distribution of acoustic scattering over large areas (Roe and Griffiths 1993; Roe *et al.* 1996). The ADCP is a single-frequency device, typically operating at 150–1000 kHz, so there are limited possibilities for identifying the source of echoes. Nevertheless, substantial amounts of data can be obtained through collaboration with hydrographic survey programmes. These can reveal acoustic scattering features relevant to biological oceanography on a large scale.

On a much smaller scale, acoustics can be used to observe the behaviour of large plankters *in situ*. The methods are essentially the same as those discussed in Chapter 5 for fish. Klevjer and Kaartvedt (2003) studied the swimming behaviour of the krill *Meganyctiphanes norvegica* using a split-beam 120 kHz echosounder. The transducer was lowered into scattering layers to allow observations at close range. They measured the swimming speeds which were typically  $4 \text{ cm s}^{-1}$ . The krill swam horizontally with relatively less vertical movements.

Jaffe *et al.* (1995) have described a three-dimensional imaging sonar called FishTV which projects an 8-by-8 raster of beams. Each beam is  $2^\circ$  wide by  $2^\circ$  high. The sonar transmits a swept-frequency pulse (425–465 kHz) which is 0.17 ms long. The transmission is applied sequentially to each element in the raster. The raster provides two coordinates of detected targets while the range measurement (1.5–5.3 m from the transducer) provides the third dimension of the image. Thus the insonified volume is  $4 \text{ m}^3$  and targets stronger than  $-87 \text{ dB}$  are detectable anywhere in this volume. McGehee and Jaffe (1996) used FishTV to study the swimming behaviour of zooplankters. The sonar was deployed at 37 m depth below a moored platform, along with a video camera to identify the detected targets. Many different animals were observed in the field of view (euphausiids, amphipods, small fish etc.) which had very different target strengths ( $-83.0$  to  $-57.7 \text{ dB}$ ) and swimming speeds ( $2$ – $41 \text{ cm s}^{-1}$ ). Despite the variety of targets, a consistent angular turning rate was observed, meaning that the paths of slower targets were more curved. Jaffe *et al.* (1998) have reported further development of FishTV, as part of a combined optical-acoustical imaging system for the study of plankton behaviour.

# Chapter 8

## Survey Design

### 8.1 Introduction

The acoustic estimation of fish abundance has much in common with other survey methods used in fisheries research. It involves the collection of data from the area inhabited by the species of interest, and the analysis of acoustic and other records to provide whatever information is required about the population in the area at the time of the survey. The usual intention is to determine the size of a particular ‘stock’ of fish. The stock is defined by the needs of fishery management, and it is not the same as the biological concept of a ‘population’ (Gulland 1983). Stocks are often defined in terms of the fish resident within artificial boundaries, e.g. national fishery limits, thus excluding any part of the relevant population that is located elsewhere. Many of the issues are discussed in Simmonds *et al.* (1992) which is a review of current practice in acoustic survey design and analysis procedures carried out for the ICES Fisheries Science and Technology Working Group. In this chapter we deal mostly with strategies for surveys of seas or lakes, where the objective is usually to estimate the local fish density and raise this to a stock estimate for the total area. We deal briefly with the sampling of riverine populations, which falls into two categories depending on whether the fish are resident in the area being studied or migrating through it. The objectives of the survey (and the methods employed) will be rather different in each case, the survey of resident populations which is similar to surveys of rivers and lakes and surveys for migrating populations such as salmonids.

Several practical problems have a bearing on the reliability of survey results. Although present-day technology provides acoustic equipment with the accuracy and reliability required, the instrumentation must be used correctly, with a good understanding of the factors which determine its performance. It is particularly important to calibrate the acoustic equipment regularly in accordance with the procedures recommended in Chapter 3. Where the physical properties of the water (such as salinity and temperature) might vary, care should be taken to ensure that the correct values are used; see Chapter 2 for the sound speed and acoustic absorption factors, and Chapter 9 for the extent of resulting errors. Furthermore, the area to be surveyed is often very large, while the volume of water sampled by the acoustic beam is small. There are random errors and biases associated with the sampling strategy, since it is necessary to extrapolate from the observations to estimate the fish abundance and

distribution over the entire area of interest. Similar statistical problems arise in surveys by other methods such as trawling where the volume or area sampled is an even smaller proportion of the total. While only a small proportion of the total area may be sampled, the precision of the results depends more on the variability in the spatial distribution and the number of observations, rather than the proportion of the stock that is sampled.

The purpose of any survey is to provide useful information about the stock of interest. The sampling strategy and the protocols for data collection should be designed to provide the most accurate information that can be obtained within the limits set by the available resources. The first step is to be clear about the objectives of the work. Is the intention to determine the fish abundance in absolute terms, or is it the change since the previous survey that is of most interest? Is it necessary to determine the geographical distribution of the stock, or only an estimate of the total abundance? How much error can be accepted in the abundance estimate, and how should the confidence limits be assessed? These questions must be answered before deciding on the detailed plan for the survey.

The data collected during the survey will come from various sources, notably the echo-integrator, the echogram and/or numbers of fish from single-target counts. The examination of fish catches will indicate the proportion of different species present, and the size distribution of each species, which is important in taking account of the size dependence of the target strength. Independent measurements of the target strength of fish *in situ* may be collected if equipment such as the split-beam echosounder is available. All these data contribute to the analysis which provides quantitative information about the stock, the total abundance and perhaps the structure in terms of the number of individuals at each age.

In this chapter, we discuss practical questions about the use of survey data. We consider how surveys should be planned to meet the objectives set in advance, especially the design of the cruise track and the sampling strategy to make the best use of the time available. The illustrations include examples of cruise tracks which show how the theoretical principles are applied in practice to the design of surveys for open water or areas bounded by irregular coastlines. The analysis of survey data is considered here only to the extent that it has a bearing on the survey design and methods of data collection. A more complete description of the methods used to analyse survey data will be found in the next chapter. The physical calibration of the acoustic equipment has already been described (Section 3.8), but here we cover briefly two additional methods for measuring the overall performance in the field: the live-fish calibration and the inter-ship comparison.

## 8.2 Survey strategic decisions

Acoustic surveys are often conducted to investigate a large volume of water. In practice, owing to the limited time available to perform the survey, only a small proportion

of this volume can be observed acoustically. Thus the acoustic measurements are samples which are assumed to be representative of the wider fish distribution. The survey design is the planning of the cruise track, which needs to be considered well in advance of the survey itself. The object is to ensure that the resources available are adequate for the job to be done, that the resources are used to best effect, and that all the information required for the subsequent analysis is collected. The survey is designed by working through a set procedure along the following lines:

- (1) Define the geographical area to be covered, or if it is intended to employ an adaptive strategy (p. 318), decide on the principles to be applied in adjusting the coverage during the survey.
- (2) Estimate the resources required for an adequate survey of the defined area, principally the (ship) time in relation to the density of sampling.
- (3) Calculate the time available for the survey itself, making due allowance for other activities such as fishing.
- (4) Decide on the sampling strategy and the type of cruise track to be followed, i.e. the shape of the survey grid (triangular, rectangular etc.).
- (5) Lay out the calculated length of cruise track on a map, ensuring that representative samples will be collected from all parts of the area as far as is practicable.

If the survey is well designed, it will be much easier to analyse the data later and to produce satisfactory results. It is not a good idea to begin a survey with no strategy or plan as to how it should be conducted. This would very likely result in wasted time and inefficiency.

Acoustic surveys are similar in some respects to the sighting surveys which are conducted to count animals by visual observation (Quinn 1985; Buckland *et al.* 1993). In both cases, the data are collected while the observer moves along the lines of a grid. The theory of sighting surveys corrects the population count for the probability of detection, which depends on the range and the size of the observed animals. This is important for the horizontal-beaming techniques discussed in Section 5.5.2. However, sighting theory has limited relevance to the conventional acoustic survey done by vertical beaming, because the correction for the range of targets is taken into account by the automatic processing of the signal before the echo is integrated (Chapter 5). There are statistical problems to be considered in the interpretation of acoustic data, but they have more to do with classical sampling theory which is well explained in Cochran (1977) and Thompson (1992).

### **8.2.1 *The geographical area***

The area to be covered by the survey may be obvious, for example when it is bounded by land or national borders. In other cases, the boundaries may be decided by prior knowledge of the likely fish distribution and migration behaviour, or by reference to controlling variables such as the water depth. The survey should be confined to

the area where there is some chance of encountering the species of interest. If the surveyed area includes large regions of empty water, the coverage (sampling intensity) of fish concentrations will be less than optimum; however, missing important parts of a stock can be critical to understanding the population under study. The choice of the correct area is perhaps the most crucial of the design issues.

When the geographical limits of the stock distribution are uncertain, it may be decided to adopt an adaptive strategy, which allows the cruise track to be adjusted during the survey according to where concentrations of fish are observed. In that case, the area to be covered is not specified in detail beforehand, but it is still necessary to consider the range of possible options, so that the available time can be used to the best effect. All regions where fish may be found need to be surveyed to some extent, even though the coverage of some may be minimal. However, adaptive surveys in this context require prior knowledge of the spatial distribution. In the absence of such knowledge, a uniform coverage may deliver more robust information which can be used to design a better survey for another occasion.

## 8.2.2 Working time

The next step is to determine the time available for the collection of acoustic data, which we call the track time. Ideally, this should be decided on the basis of the sampling intensity needed to map the stock with acceptable precision. With information on the statistical properties of the distribution it will be possible to estimate the precision of a survey directly. However, without such information there is still a need for some understanding of how the precision of the results depends on the transect spacing. This statistical problem has been addressed by Aglen (1983; 1989). He expresses his results in terms of the coefficient of variation (CV); however, this measure can be confusing as some authors use it to express the variability in the data and others the variability in the mean. It is the latter measure that Aglen describes, and it is more uniquely described as the standard error divided by the mean. For  $N$  independent samples, the standard error is the precision of the mean calculated as the standard deviation of the data divided by  $\sqrt{N}$ . Here, CV is always the standard error divided by the mean, but readers need to be aware of the two possible interpretations.

Aglen suggests that the CV depends on the degree of coverage, a quantity which he defined as  $\Lambda = D/\sqrt{A}$ . Here  $A$  is the size of the area being surveyed and  $D$  is the total length of the cruise track. The larger  $\Lambda$  is, the smaller is the CV although it depends also on the type of fish distribution. Better results can be expected when the fish are widely distributed as individuals or in layers than when they are concentrated in isolated schools. For planning purposes, we may assume that  $CV = (0.5/\sqrt{\Lambda})$  (cf. p. 359). Thus, for example, if the required precision is  $CV = 0.25$ ,  $\Lambda$  must be at least 4. However, this rough calculation of the standard error is not a substitute for the proper estimation of confidence limits in the post-survey analysis (cf. Section 9.6). In practice, acoustic sampling is often constrained by the availability of the ship or

other resources. Thus we begin with  $t_T$ , the total period within which the survey must be completed. The track-running time is calculated by deducting from  $t_T$  the time required for other activities, such as:

- loading and unloading the ship ( $t_L$ );
- any travelling between the embarkation point and the survey area ( $t_M$ );
- calibrating the acoustic instruments ( $t_C$ );
- fishing to identify the echo traces ( $t_F$ );
- conducting hydrographic stations ( $t_H$ ).

Furthermore, the track time may be restricted to part of each day. If the fish migrate vertically in a diurnal cycle, the survey must be done during the hours when the fish are in midwater. Some surveys will be restricted to the daylight hours when the fish are concentrated in schools. Others may be done only at night when the targets are dispersed. The important point is to ensure that the fish are detected consistently throughout the track time. The planning in advance of the survey must provide for all the ancillary activities as well as the collection of acoustic samples. Some biological sampling through fishing is almost always required; however, it is not essential to conduct hydrographic stations if the environmental conditions are known well enough from other sources.

If  $V$  is the ship speed and  $P_d$  is the proportion of each day that can be used for echo-integration, the total length of the cruise track  $D$  is calculated as:

$$D = (t_T - t_F - t_H - t_L - t_M - t_C)P_dV \quad (8.1)$$

Alternatively, if sufficient resources are available,  $t_T$  may be estimated from the degree of coverage needed to attain a specified precision:

$$t_T = \Lambda\sqrt{A} / (P_dV) + t_F + t_H + t_L + t_M + t_C \quad (8.2)$$

It is necessary to decide in advance on a general scheme for allocating time among the different activities. For example, hydrographic data might be collected at selected positions along the cruise track. Each station might occupy an hour or so, depending on the water depth to be covered and the type of instrumentation available. Calibrations should not be performed in haste, and several hours must be allowed to do the job properly. The need for fishing is more difficult to predict, since the fish samples must be sufficient to partition the acoustic data between species and size groups of fish. However, it may be decided to allow for a certain number of trawl stations each day on average, and then to fish as and when there is doubt about the identity of the echo traces. The proportion of time that should be allocated to trawling is addressed in some detail in Section 8.3. Typically, 25% of the working time might be allowed for fishing on echo traces. It may require 1–3 hours to complete a trawl station on a large ship, and perhaps 30 minutes when using a light gear deployed from a small boat.

## 8.3 Survey design options

There are two fundamentally different approaches to the design of acoustic surveys, according to whether the cruise track is decided in advance (pre-planned) or adjusted on the basis of observations made during the survey (adaptive). The adaptive strategy has the advantage that it allows the geographical distribution of the fish to be explored. However, unless this is done carefully, the non-random sampling which is implied by the adaptive approach may result in bias and uncertain statistical error in the abundance estimate. In most cases, it is better to plan the cruise track in advance, allowing changes during the survey only for practical reasons such as bad weather. The adaptive survey technique may be considered if the main objective is to detect concentrations of fish which might be exploited by commercial fishing, and it is less important to obtain a good unbiased estimate of the stock abundance. The remainder of this section is concerned with pre-planned surveys.

The options chosen in the design of a survey affect both the data collection and the methods that need or can be applied in data analysis. Thus the design must be considered both at the planning stage and again when analysing the data. More correctly, the data analysis options should be included at the planning stage of the design. Surveys may be considered as pre-planned whenever the design is decided in advance, subject only to the uncertainties of practical operation, and they are adaptive when the design is intended to be modified during the survey. The former will be considered first, along with the methods of analysis, followed by a brief consideration of adaptive designs, their general requirements and practical implications. Note that adaptive surveys work best in situations where there is extensive prior knowledge of the properties of the stock being surveyed, and further that the results of an adaptive survey are conditional on the assumptions implied by the adaptive design. Surveyors may often want to solve a problem, if few fish are seen on the pre-planned track for instance, by adapting the survey design. Unfortunately, if prior knowledge of the fish distribution is uncertain, this rarely helps because there will probably not be enough information to know how best to adapt the design. Rather, the less information there is available, the more evenly the survey effort should be spread. These issues will be discussed in more detail in later sections. As a start we consider the general principles of the design of pre-planned surveys.

### 8.3.1 *Survey objectives*

The objectives of the survey and prior knowledge provide the information on which to define the survey design. It is important to have a clear understanding of what are the desired objectives, as this is the basis for choosing between different types of data collection. Survey objectives might cover one or more fish stocks, requiring an estimate of abundance within a defined area together with a map of the spatial distribution. Or, an index of the abundance might be sufficient. The abundance estimate may be required to be unbiased, or the primary need may be results (as indices or

absolute abundances) that have the minimum variance. There may be a requirement to estimate the precision of the survey for which the variance must be determined. Additionally, there may be a need for biological data on the stock, such as the age or size structure or the fraction of the population that is mature. Occasionally it may be important to collect additional information such as hydrographic records. For example, this may be required for use on the survey itself, to determine variable sound-speed profiles, or it may simply be additional data that might correlate with the stock distribution. The user needs to evaluate the importance given to each type of data, and this importance or weighting has a bearing on the balance between the requirements for abundance estimates, mapping the distribution and estimating the variance. These considerations will influence the survey track layout, while the need for biological data, age structure and species composition will influence the allocation of time between acoustic data collection and that spent on other activities such as trawl sampling.

### **8.3.2 *Stratification of effort***

Here stratification means the allocation of survey effort preferentially to one part (stratum) of the survey area compared to another. The survey in each stratum is designed separately. If there is good reason to believe the variance within some part of the survey area is different from elsewhere, division of the total area into two or more strata for design and analysis purposes may improve the precision of the survey results (Cochran 1977). Stratification has often been applied using variables that are surrogates for biological criteria. On bottom trawl surveys for example, water depth may be used as the basis for stratification, on the assumption that the fish size and species composition are more homogeneous at particular depths than they would be in a geographic stratum that included disparate depths. Other variables such as water temperature or prior knowledge of the stock distribution have been used similarly. The data are subsequently analysed by strata, and provided the assumptions about the variance are correct, more precise estimates are obtained. The design and the analysis assume that the strata are independent, and that the variance within each stratum is stationary (in the statistical sense, i.e. it has the same value everywhere within a stratum). The benefits of stratification are more pronounced if the variance is dissimilar among the strata so that different levels of effort in each stratum are indicated. However, the strata-selection criteria need to be independent of the current survey, since it is this independence that distinguishes the pre-planned survey discussed here and the adaptive survey discussed later. It must be remembered that for the precision to be improved it is not the fish abundance *per se* that should differ between the strata, but the variance of its estimate. However, in the case of fish-stock surveys, the abundance may be a very good guide to variance and thus to the best stratification scheme. The ideal approach would be to calculate the rate of change of variance with sampling effort, then the effort would be allocated based on minimization of the variance. In practice it is sufficient to allocate sampling effort

proportional to both the surface area and the variance within the strata. Greater difficulty is encountered when more than one feature of the fish population is required as an output from the survey. This would apply for instance to a species whose spatial distribution was different for certain age groups. Or, two or more species may be of interest but they are differently distributed. Barange and Hampton (1997) give an example of this problem. The solution to the stratification of effort for this multi-objective survey is to determine the variance of each species in each stratum; if the species are of unequal importance, a weighting factor for each species is incorporated. For example if one species is twice as valuable as the other, the factors would be two and one respectively. These weighting factors are used as multipliers for the spatial variance and the survey effort should be allocated in proportion to the combined weighted variance.

### **8.3.3 Proportions of time allocated to transects and trawls**

There is little published information on how best to decide the time allocation. The issue is this: how does the estimate of overall abundance, which is based on biological data from trawl samples as well as the acoustic records, vary as effort is moved from the collection of transect data to trawling? Massé and Retiere (1995) examined data from a survey of an eight-by-eight nautical mile area, conducting eight transects and eight trawl hauls in a 48-hour period. They investigated the precision of the estimates for five main species. One species, the anchovy (*Engraulis encrasicholus*) was dominant and the results for this species were consistent. The variability among the other species depended most heavily on the trawl data which were used to define the species proportions. Massé and Retiere concluded that the number and the location of the hauls had a strong effect on the estimates of the less abundant species. This example relates to a rather small area compared to the typical acoustic survey. Another study of the time allocation problem, concerning the precision of year-class abundance estimates for the North Sea herring (*Clupea harengus*), has been reported by Simmonds (1995). He estimated the precision using a geostatistical estimate of variance based on the variogram derived from a number of annual surveys, and showed how the CV changed with the number of transects in a survey. The influence of the trawl data is more complex, since they are relevant to echo-trace identification and the determination of stock proportions by species, length classes and/or ages.

If the total time is fixed by other considerations, it is three weeks in the case of the North Sea herring survey, the options for the proportions of time allocated to trawling and transect running can be evaluated. Figure 8.1 shows the CV against the numbers of transects and trawls, and the combined curve for a three-week survey. The upper line is the combined CV. The arrows show the points where the CV is 1% above the minimum. The CV is rather insensitive to the precise time allocation, and the 1%-change region of the CV plot lies between the combination to the left of the figure (24 transects with 25 trawls) and that of 17 transects with 51 trawls on the right. This survey is of fish that are seldom found in mixed traces, and 60–90% of

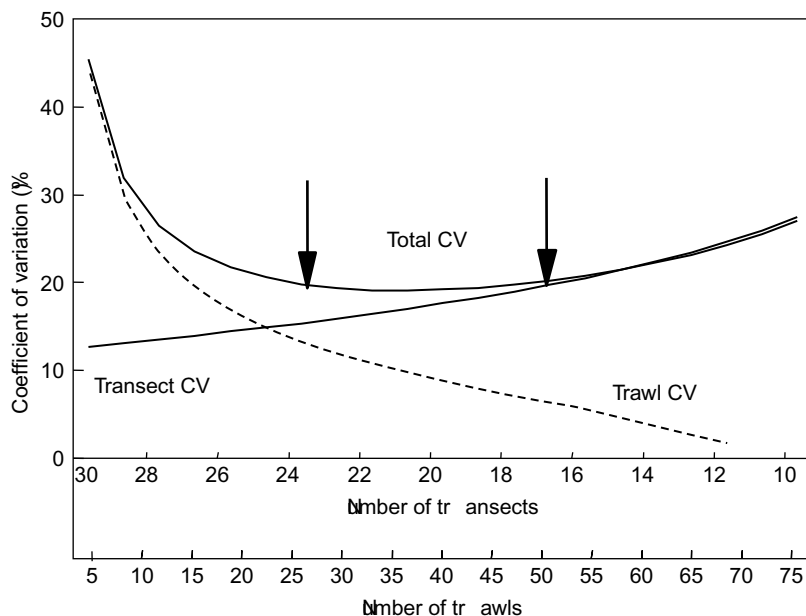


**Fig. 8.1** Example of the precision of an estimated year-class abundance for North Sea herring depending on the time allocated to trawls or transects. The lower lines show the CV for the number of trawls and transects separately. The upper line is the combined CV. The arrows show the points where the CV is 1% above the minimum. The optimum design is rather insensitive to the precise choice and lies between the arrowed limits i.e. 24 transects with 25 trawls on the left to 17 transects with 51 trawls on the right. (From Simmonds 1995.)

the echo abundance is easily allocated directly to the target species. The North Sea herring stock has typically 9 age groups, with ages 2–9 years being found within the survey area. From the results shown in Fig. 8.1, the CV of the age estimates is rather insensitive to the time allocation between trawls and transects. Deriving general rules from the results of one survey is questionable. Different surveys may have CV minima at different time allocations but it seems rather unlikely that the rather shallow minimum seen here is completely atypical. At the time of the Simmonds (1995) study the North Sea herring survey was being conducted with some 30–35 trawl hauls, which was well within the limits for an optimum CV. For many survey designs the precision obtained may be sub-optimal, nevertheless this analysis suggests that a wide range of options would give near-optimal performance and therefore fine-tuning the balance between transects and fishing may not give much improvement. Note that this result applies to a survey where species are allocated through echo-trace identification. When trawl-catch proportions are used directly for this purpose (Massé and Retiere 1995), more fishing will almost certainly be required.

The selectivity of fish-sampling gear is a major topic in its own right and has been mostly studied for demersal trawls (Stewart and Galbraith 1987; Fryer 1991), though the methodology can be applied to any fishing technique. Bethke *et al.* (1999) have

compared the selectivity of pelagic gears. They quantified the mesh selection of small fish which can be corrected, but also report different capture efficiencies on large fish which they could not explain. On the other hand, Fernandes (1998) found little difference in the relative catch rates by size for herring caught in various pelagic gears used throughout a large area. Spatial variation of the catch composition and the relative efficiency between fishing vessels were examined separately. The spatial variation was found to dominate the results. These examples illustrate both the methodology required to estimate the gear-selectivity effect, and the fact that each case may be different.

### **8.3.4 Pre-planned track options: systematic or random designs**

This issue is one of the most hotly debated topics in survey design. The choice is often represented in statistical texts as one between model- and design-based estimates. In this context, the ‘random design’ is one that takes samples with the same probability of being located anywhere in the survey area, in which case each sample represents an independent measure and the precision is simple to calculate (Shotton 1981; Shotton and Bazigos 1984). The ‘model design’ can deploy the sampling in a more structured way; the resulting estimate may be a simple calculation such as the arithmetic mean, or a more complex approach such as a geostatistical kriged estimate (Rivoirard *et al.* 2000). In this modelled case the precision may be more complex to calculate. The simplicity of the calculations for a random design is its main advantage; however, better precision may result from more structured designs. The improvements come from the fact that the distributions of fish (or plankton) are correlated in space. The random survey designs away the correlation problem. The influence of spatial correlation on the estimation of fish abundance, and its variance, was discussed in a workshop on the applicability of spatial techniques to acoustic data in Iceland in 1991. Section 8 of this report deals in detail with the issues (Anon 1993). The important distinction is the source of the correlation. If this is a property of the fish distribution, it is known as process correlation, in contrast to the observation correlation which would be a property of the instrumentation. In acoustic surveys the echosounder responds immediately to changes in the fish density, thus the correlation stems from the process, which in this case is the fish distribution. The model-based survey takes advantage of this correlation and may thus improve the overall precision. The assumption behind the random design is that the survey is randomized over the controlling parameter. In a survey to estimate abundance, the locations of the samples are chosen to be random in space. However, the simple random design becomes more complex if there are additional factors influencing the observations. For example, if the time of day is important, then in theory this should also be taken into account in the random design. It would be necessary to randomize the design both in space and by the time of day. This may lead to quite intractable logistical problems. For simplicity the variability in space is, quite rightly, often assumed to be dominant and other variables are ignored. However, the other option

is to acknowledge that a fully randomized design is impractical, and to choose a model-based approach with a more structured survey design.

Few statistical texts properly illustrate the differences between random and systematic designs, and how the results depend not only on the design but also on the spatial distribution being sampled. We present here a simple simulation to show how the systematic survey can provide more precise estimates. For a stratum with stationary variance, Matheron (1971) showed theoretically that the variance can always be reduced, compared to fully random sampling, by a design which divides the area into equally-spaced strata and provides one observation at a random position within each stratum. In acoustic surveying this would be equivalent to dividing the area into a number of equal-width intervals and placing a single transect randomly within each interval, with the transect extending to the boundaries of the area. It is but one step further to the systematic survey, in which one random location is chosen for the start of a set of transects, and this design often gives even better precision. The performance of different survey designs, contrasting a fully-random design and a systematic survey, is illustrated in Figs 8.2 and 8.3.

Figure 8.2 shows six spatial distributions, each constructed with the same 10 000 randomly selected numbers distributed over a square 100-by-100 units. These 10 000 numbers are reorganized to have increasing spatial correlation (Fig. 8.2a to f), so each

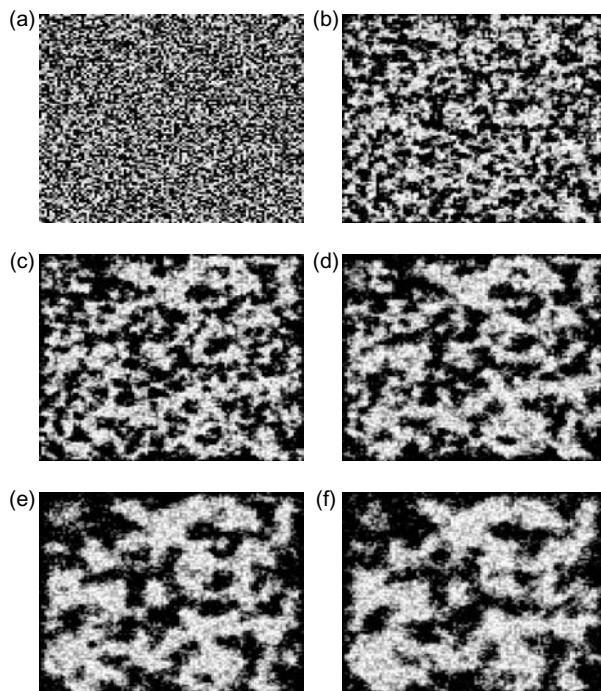


**Fig. 8.2** Illustration of 10 000 random numbers organized in space with increasing spatial correlation from (a) to (f).

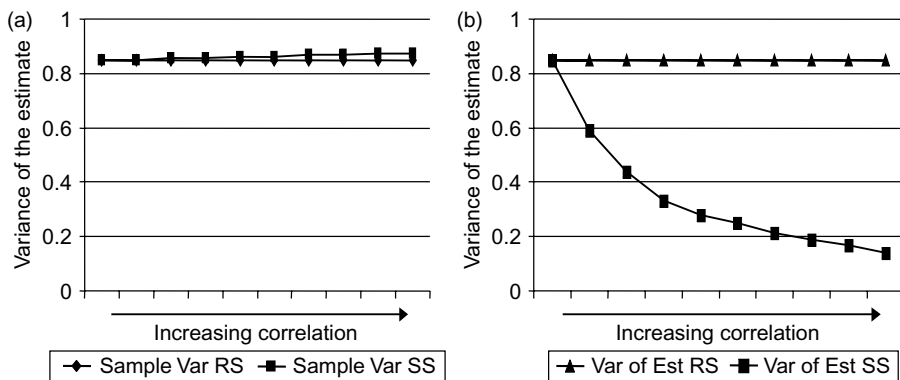


**Fig. 8.3** Comparison of the precision of a random (RS) and a systematic (SS) survey of the spatial distributions shown in Fig. 8.2. (a) The sample variance and (b) the precision of the abundance estimates are compared. The random survey provides an abundance estimate that is independent of the correlation and the sample variance is a good estimate of the precision. The abundance estimate from the systematic survey appears to be more precise as the spatial correlation increases. The sample variance is no longer useful for estimating the precision of the survey.

rectangle does not only have the same distribution of amplitudes with the same mean and variance, but it contains exactly the same numerical values. We can sample these rectangles, i.e. carry out a survey, using two strategies: firstly, a random survey with samples taken at random locations, and secondly a systematic survey with the samples taken on a regular grid that starts at a randomized origin. By simulating many surveys we can then compare the precision with which the arithmetic mean of the samples represents the true mean for the rectangle, and we also see how the sample variance (calculated directly from the observations) changes. The results are shown in Fig. 8.3. The sample variance is  $N$  times larger than the variance of the mean, so for convenience it has been scaled by this factor. Figure 8.3a shows the sample variance divided by  $N$ , while Fig. 8.3b shows the true variance of the estimated mean obtained through repeated evaluations in the simulated surveys. The random survey has a constant precision that is independent of the correlation, and the sample variance provides an unbiased estimate of that precision. In Figs 8.3a and 8.3b the two lines are indistinguishable. However, Fig. 8.3b shows that the systematic survey provides an estimate that becomes more precise as the spatial correlation increases, i.e. the variance of the estimate decreases. This can be considered conceptually in the following way. Each sample contains information about the abundance in the survey area. If there is spatial correlation, then the sample also contains information about nearby locations. The greater the correlation, the greater is the area that the sample represents. By spreading the samples evenly in space we can minimize the overlap in information and thus increase our knowledge. This was the conclusion drawn by Matheron (1971) who showed theoretically that for one random sample per stratum the estimate would always be more precise than that for a more random distribution of samples in the same area. However, Fig. 8.3a shows that the sample variance no

longer provides a direct estimate of the precision of the survey. It is this failure of the sample variance to give a good measure of precision that leads some workers to prefer the simplicity of a fully random survey, while others have sought solutions through the more advanced techniques of spatial statistics (Petitgas 1993; Rivoirard *et al.* 2000). The improvement in the precision of the survey implicit in a regular grid is ignored by some proponents of random designs (Jolly and Hampton 1990). It should be borne in mind that the improved precision of the estimate illustrated in Fig. 8.3 is likely to exceed anything that will be achievable in practice when surveying a fish stock. However, it should be clearly understood that the reason for choosing a random survey is to provide simple variance estimates, but this is achieved at the expense of worse precision of the estimate. Both survey designs shown here provide unbiased estimates of the abundance in the survey area. There are some circumstances, strong periodicity in the fish distribution for instance, when the systematic survey may give higher variance, but in practice these conditions are never observed and such problems can be safely ignored.

Simmonds and Fryer (1996) investigated survey strategies for a variety of simulated populations with properties based on the North Sea herring. The populations had different mixtures of local positive correlation, a short-scale randomness and a non-stationary (or trend) component. Each simulated survey produced the same total of 40 observations, and the simulations were repeated to compare the alternative strategies that might be adopted, as follows:

- random sampling; observations made at random locations anywhere in the survey area;
- stratified random sampling; the survey area was divided into N strata; various levels of stratification tested i.e.  $N = 2, 4, \dots, 40$  (in the latter case there was only one observation per stratum);
- systematic sampling of the 40 observations on a grid with a random starting point;
- systematic sampling on a grid with a centred starting point.

The results from all the populations were broadly similar and are illustrated in Fig. 8.4. The variance of the sample mean always decreased as the amount of stratification increased, with the systematic surveys giving the most precise estimate of the population mean. This finding conforms with the theory of Matheron (1971) who showed that the variance of the sample mean from random sampling is always greater than that obtained by stratified random sampling with the area divided into equally-sized strata and one observation per stratum.

Not only is the precision of the estimated mean likely to be poorer for a fully random survey, so too is the estimate of the precision! Simmonds and Fryer (1996) also considered the statistical properties (precision and bias) of two methods for estimating the variance of the sample mean:

- the usual design-based estimator of the variance (e.g. Thompson 1992) was applied to all the sampling schemes – for the stratified random designs with one

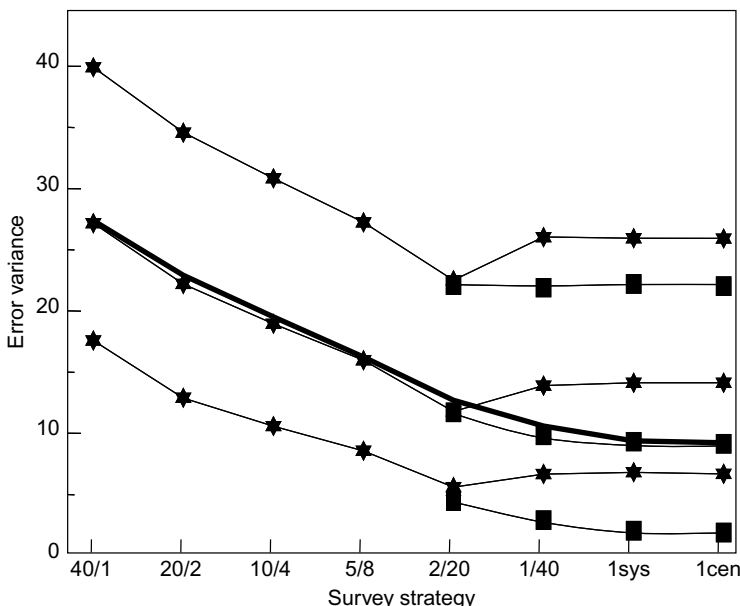


**Fig. 8.4** Comparison of the precision of the estimated abundance (thick line) and percentiles of the estimated variance (5, 50 and 95%, thin lines upwards) from a North Sea herring survey simulated with various survey strategies shown with increasing structure from left to right (see text for details). The precision of the abundance estimate improves with increasing structure in the design. The blocks and stars are, respectively, geostatistical and classical estimators of variance. The interval on the variance is shown in Fig. 8.5. (Redrawn from Simmonds and Fryer 1996 with permission from ICES J. Mar. Sci.)

sample per stratum, and for the systematic designs with the data from adjacent strata combined in pairs (as if they had come from a stratified random design with two samples per stratum);

- a geostatistical estimator was applied to the stratified random designs, with one or two samples per stratum, and also to the systematic designs.

Again, the results were broadly similar across all the populations, although there were some differences that depended on the amount of local correlation. For example, Fig. 8.4 shows the median and 90% intervals of each estimator for each sampling design when the range of the correlation was about 5% of the distance across the survey area. Figure 8.5 shows the width of the 90% intervals for the whole set of populations. Simmonds and Fryer (1996) came to the following conclusions:

- the design-based estimator of the variance was unbiased when there were at least two random samples per stratum (this is always true);
- the design-based estimator of the variance was positively biased for the stratified random design with one sample per stratum and for all the systematic designs;
- the geostatistical estimator of the variance had negligible bias;

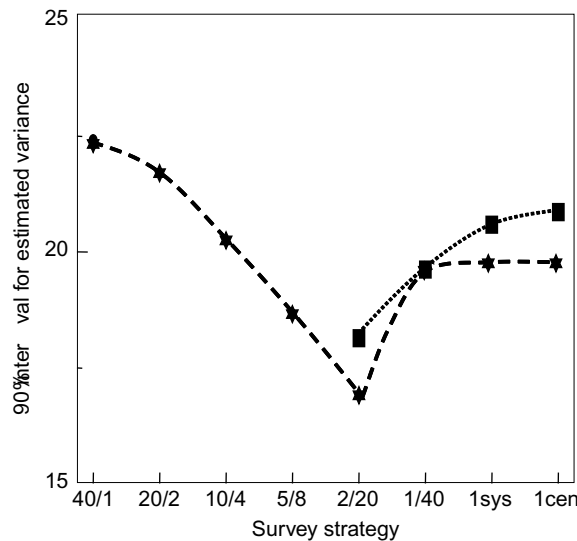


**Fig. 8.5** Confidence interval on the estimate of variance, from Fig. 8.4. The best estimate is obtained when 40 transects are placed randomly in 20 strata (Simmonds and Fryer 1996). The blocks and stars are, respectively, geostatistical and classical estimators of variance.

- the smallest 90% interval on the variance was obtained for the stratified random survey with two samples per stratum (the design-based and the geostatistical estimators both had similar 90% intervals).

In general, more stratification decreases the variance of the sample mean, but it also reduces the degrees of freedom available for estimating that variance. In terms of the variance estimators, this implies that the mean variance decreases, but the width of the 90% interval relative to the mean increases. Thus, the best sampling strategy for variance estimation depends on the balance between these two effects. For the example discussed above, the most precise estimate of variance is obtained with two transects per stratum. As the survey design becomes even more structured (i.e. less random), the precision of the variance deteriorates while that of the abundance estimate still improves. The choice of design must then be based on the relative importance of these two pieces of information, and there is no one design that optimizes the abundance and the variance estimation at the same time. However, in the example presented here, the abundance estimate is required annually while the variance has to be estimated for a series of surveys over several years. Thus more emphasis is placed on the abundance estimate and so the systematic survey with a random start is the preferred choice.

It would be unwise to conclude that this particular simulation is applicable to all fish-stock surveys; however, local positive correlation is a common feature of fish distributions and this leads to the general conclusion that the systematic survey should provide the best results.

The random survey has one strongly redeeming feature; it is difficult to challenge its validity. Random survey designs allow data to be analysed in a simple manner, and the precision (even if poor) can be quantified without controversy and with minimal calculations, thus the random survey is in one sense more defensible. Note, however, that randomization in an acoustic survey is only practical as regards the transect placement in space. There is seldom any temporal randomness, since it is usually far too costly in time to run transects in a random sequence. Furthermore, any other data collected along the transects, for example water temperatures which might be compared with the echo abundance on a local scale (i.e. finer than a transect), does not have random sampling properties because the observations were made systematically along the transect. This issue is further discussed in Chapter 9.

The systematic survey has a grid of evenly spaced transects. This grid has to be mapped onto the area (or stratum) being surveyed. The design prescribes how this is done in the along-transect direction. In the other direction (that of the survey progression), however, it has to be decided how to locate the grid (or specifically the first transect) in relation to the area boundary. There are two options here: firstly, in the centred survey, the first transect is exactly half the transect spacing away from the boundary; secondly, there is the random-start survey. In this case the transect-boundary distance is a random proportion (0–100%) of the transect spacing, and a different starting position is randomly selected on any subsequent survey of the same area.

There is a small but effectively negligible possibility of reducing variance by using the centred survey. The random-start survey has several advantages. It allows powerful statistical methods, such as the geostatistical transitive approach (Petitgas 1993) to be used in analysis. More importantly it ensures that the abundance estimate is unbiased because each part of the area has equal probability of being sampled, in contrast to the centred survey which always samples the same points and takes no account of any spatial trends between those points and the unsampled locations.

### **8.3.5 Pre-planned track options: parallel or triangular designs**

The variances of the alternative parallel ( $V_R$ ) and triangular ( $V_T$ ) estimators can be established for any rectangular area using geostatistics. Rivoirard *et al.* (2000) considered rectangles with length-to-side ratios between 20:1 and 1:1, chosen to provide a useful range of options. The number of locations sampled along each transect was proportional to the time required to run the transect. The estimated variances were weighted by the survey effort, this being the time taken to cross the rectangle corner-to-corner by each method:

$$V_T = \text{var}_T(z - z^*)\sqrt{a_1^2 + a_2^2} \quad (8.3)$$

$$V_R = \text{var}_R(z - z^*)(a_1 + a_2) \quad (8.4)$$

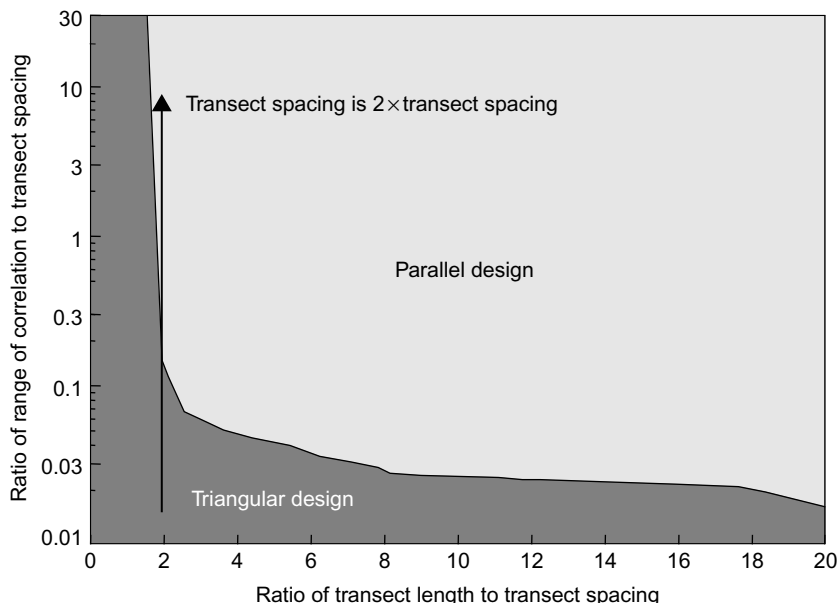


**Fig. 8.6** Comparison of the performance of parallel and triangular transect designs. Shaded areas show where each method provides the most efficient estimation (i.e. minimum variance per unit effort). Except for very short-range correlation of the fish densities, the better method depends on whether the transect length is more or less than twice the spacing.

where  $\text{var}(z - z^*)$  is the geostatistical estimation variance for the section of track and  $a_1$  and  $a_2$  are, respectively, the length and width of the rectangle. The width is the mean distance between transects.

These formulas were evaluated to determine the ratio  $V_R/V_T$  for different ranges of spatial correlation and shapes of rectangle.  $V_R/V_T$  indicates the relative performance of parallel and triangular survey designs. Figure 8.6 illustrates the circumstances under which one or the other is the more efficient. The choice depends almost exclusively on the ratio of the transect length to the transect spacing, and only slightly on the range of the spatial correlation. For transect lengths that are less than twice the transect spacing, the triangular survey track is most efficient. For correlation ranges greater than 0.1 times the transect spacing, parallel designs are superior when the transect length is more than twice the spacing. For very short-range correlations (i.e. essentially random spatial distributions) neither method is clearly superior and it does not matter which type of track design is used.

A simple rule which is correct in almost all cases is to choose a parallel grid when the transect is at least twice as long as the transect spacing, and a triangular design when the transect length is less than twice the spacing. If there is evidence of anisotropic correlation in the fish distribution, however, then the spatial coordinates should be linearly transformed to remove the anisotropy before applying this rule.

### 8.3.6 Number of transects

There have been various studies testing the adequacy of sampling through simulations, for example those of Kalikhman and Ostrovsky (1997). As mentioned earlier, Aglen (1983; 1989) examined the records from many acoustic surveys to obtain an empirical relationship between CV and the sampling effort. However, there is no a priori guidance on the optimum number of acoustic samples that should be recorded; the optimum can only be determined against some other criteria such as cost or in balance with any advantage to be gained by sampling non-acoustic variables. The precision of the abundance estimate will always improve, and reconstruction of the true fish distribution will be more faithful if more samples can be collected; the improvement obtained by increased sampling depends on the spatial correlation and the survey design. In the worst case, just one transect appropriately located will always provide a valid estimate of the abundance, although this could well be rather imprecise. Different considerations arise in sampling to estimate abundance compared to mapping the spatial distribution. If a map of the distribution is required, there is a minimum sampling requirement. This limit can be expressed in two ways, from a statistical or a frequency viewpoint, though the conclusions are the same. In the statistical framework, a good map requires the samples to be at intervals less than the range of the spatial correlation. If more than the basic structure is to be resolved, i.e. the correlation has several spatial components, then sampling must be even more intensive to resolve the smallest components. On the other hand, now considering the properties of a spatial distribution as a set of frequency components, like those of a Fourier-series representation, the minimum level means sampling at a frequency that is more than twice the maximum frequency to be resolved. Both these criteria lead to the same minimum sample spacing. Of course, sampling more intensively than the minimum level will result in a more faithful map.

### 8.3.7 Transect direction

An acoustic survey provides nearly continuous (or exhaustive) sampling along a transect, since there is a very short time between successive measurements. Jolly and Hampton (1990) and Petitgas (1993) describe two approaches to the analysis of exhaustive samples that are based, respectively, on classical statistics and geostatistics. They consider the values recorded along a transect as separate estimates, thus forming a one-dimensional data set. In contrast to this exhaustive sampling along the transect, the sampling intervals in directions across the transects are much greater, and in addition there may be a much longer time between adjacent samples. These properties give us an opportunity for the survey to benefit by arranging to run the transects in the most advantageous way. Consideration of the temporal and spatial properties of the sampling scheme suggests two ideas for improving the survey results in particular circumstances.

If there is no evidence of temporal variability in the fish distribution to be surveyed, the good spatial resolution along the transect should be used to resolve any increased variability in one direction. For example, if the fish are distributed along a depth contour like the edge of a bank or the continental shelf, or they live inshore and are concentrated near the coastline, we might expect more change across the depth contours than along them. This suggests a survey design with each transect lying across the edge or from offshore to inshore i.e. with the along-transect direction experiencing the greatest rate of change. On the other hand, if there is no sign of spatial anisotropy in the distribution, the transects should simply run parallel to the shortest dimension of the survey area, thus minimizing the time between transects.

If there is evidence of temporal change in the population (meaning changes during the survey), this factor may influence the choice of the transect direction. Migration of the stock (Harden Jones 1968) is the most likely cause of temporal problems, and this applies to any survey whether by trawl or acoustic methods. Migration causes a multiplicative error that depends on the speed at which the survey advances (i.e. across the transects) compared to the speed of the migration. Later we provide formulas for correcting this error, assuming uniform fish densities and a known migration speed (cf. Section 9.7.5). However, if the migration speed is unknown, there are strategies to mitigate the problem. If we know the direction of the migration, then the error will be minimized if the transects are run so that the survey advances first with and then against the direction of migration.

In the presence of both an anisotropic distribution and stock migration along the direction with the least variation, the preferred choices are in conflict. In this case a survey progressing in the direction of the migration interlaced with a second survey in the opposite direction (i.e. returning against the migration) would be an option with reduced error. We normally use the arithmetic mean of samples to obtain an unbiased abundance estimate; however, the influence of the migration is best minimized by using the geometric mean. One solution is to estimate each survey in the usual way, based on the arithmetic mean of the samples (or transects), and to compensate for the migration we take the geometric mean of the two survey estimates as the final result. This assumes the migration effect dominates. Unfortunately, there is no perfect solution to this problem without a detailed knowledge of the migration behaviour.

Figure 8.7 illustrates the four main types of pre-defined survey designs, as they might be applied to a single stratum parallel to a coast.

### **8.3.8 *Mapping the cruise track***

Once the type of transect to be followed is decided, the calculated length of track is drawn on a map of the area to be surveyed. When there are several regions to be sampled at different intensities, the mapping calculations need to be performed separately for each region, with the start and end points arranged to ensure continuity of the track at the boundaries.

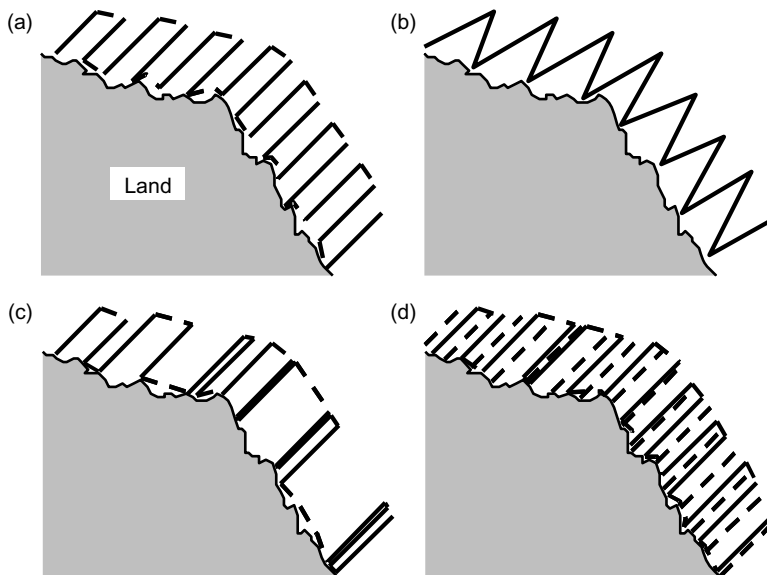


**Fig. 8.7** Four types of cruise track: (a) systematic parallel (data collected along the broken lines joining the transects may not be useful); (b) systematic zig-zag; (c) the fully random design, transects are located completely by chance; and (d) one transect is placed randomly within equally spaced intervals (dashed lines indicate the location of the intervals).

In the case of the systematic triangular grid, the transects run between turning points on opposite sides of the region. The distance between the turning points along a boundary is twice the average spacing of the transects (Fig. 8.7b). If the sampling intensity has been decided, say to be twice that of some other region, this will determine the transect spacing and therefore the distance between the turning points. The turning points are plotted on the map at staggered positions on the opposing boundaries and joined by straight lines to form the grid. If the transect spacing has not been determined explicitly, but a particular length of track has to be fitted into the region, then it is simply a question of adjusting the distance between the turning points (and the number of transects) to achieve the desired result. The number of transects is given approximately by the track length divided by the average width of the region.

The systematic parallel grid (Fig 8.7a) is mapped in much the same way as regards calculating the number and spacing of transects, but there is now the added complication of how to deal with the short portions of track joining the ends. One view is simply to continue each transect to the regional boundary and to ignore data collected along the joining track as not being part of the survey design. This procedure may appear to be wasteful, but it simplifies the analysis of the results and is unbiased. The extent to which the inter-transect data can be usefully employed in the analysis depends on the fish distribution at the regional boundary. If the fish density is likely to change rapidly with position, as might occur at a boundary on a coastline, it is

preferable that the inter-transect data should be ignored. On the other hand, if the boundary is in open water, it may be reasonable to take account of the observations along the joining section. In that case, the transects should not be continued all the way to the boundary. They should end at points short of the boundary by half the transect spacing. This is done to ensure that the centre and the edges of the region are sampled at the same intensity. There may be practical considerations near the coast that result in a lack of coverage in the shallow water. At first sight, excluding the inter-transect data seems the best choice. However, this implies that the average of the transect values is the most appropriate evidence to evaluate the unsurveyed region. This is not the most reasonable solution. The best method would be to extrapolate from the transect data over the unsurveyed region. One way to do this is to map the data by kriging (a geostatistical concept, cf. Chapter 9). Simpler analysis methods might suggest that on a coastal boundary, the inter-transect sections should provide a good estimate by extrapolation. In that case a small section of the inter-transect record, equivalent in length to the distance from the coast, could be used to estimate the unsurveyed region.

If the transects are to be randomized with one transect per zone (Fig. 8.7d), first calculate the average spacing  $D_{tr}$ , for each zone which is equal to that of a systematic parallel grid having the same total track length. Then divide the area into zones of width  $D_{tr}$ . A sequence of numbers  $\xi_1, \xi_2$  etc. is written down, each number having a random value from a uniform distribution on the interval 0 to 1. These numbers can be obtained from mathematical tables or the random-number generator which is provided with most computers. The one transect in the  $i$ 'th zone is placed at the distance  $\xi_i D_{tr}$  from the zone boundary. Thus an adjacent pair of transects may be very close together or as much as  $2D_{tr}$  apart. It may be considered wasteful of survey time to include a pair of transects which are nearly coincident, because the two samples thus obtained may be highly correlated. This problem can be avoided by constraining the transect separation to be no less than some minimum, say 10% of the average spacing, which may be done by deleting from the random number series any of the  $\xi_i$  which are less than 0.05 or greater than 0.95. This procedure could result in bias if the fish distribution were non-stationary, but in practice it is most unlikely that non-stationarity would be evident on the scale of 10% of the transect spacing.

Specimen examples of cruise tracks are shown in Figs 8.8 to 8.11. These illustrate some of the practical problems which have to be solved in survey design, to take account of (a) geographical features such as islands, coastlines and enclosed areas with an irregular boundary, (b) the need for different sampling intensities from place to place and (c) the migration behaviour of the stock.

## 8.4 Riverine surveys

Simple abundance estimates obtained with mobile platforms in rivers follow the same statistical rules as marine surveys of long thin areas. The numerical data may

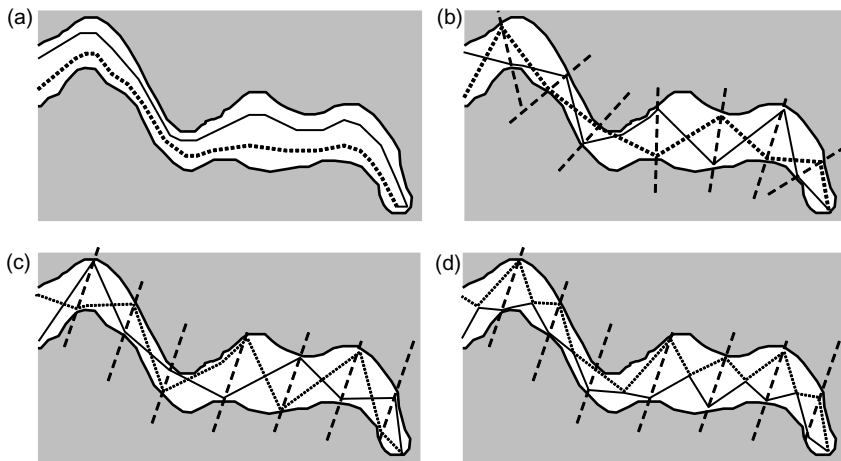


**Fig. 8.8** Examples of cruise tracks covering an area that is long and narrow, e.g. a fjord or lake. (a) In one side, out the other; the area coverage is sensitive to the variable width and crossways migration of fish. (b) Interleaved triangular track in directions determined by normals to the coastline, but this results in biased coverage on the corners. (c) The bias is reduced by regular spacing of the track into equal width segments. (d) Separate in-out triangular designs give the best area coverage but are sensitive to crossways migration.

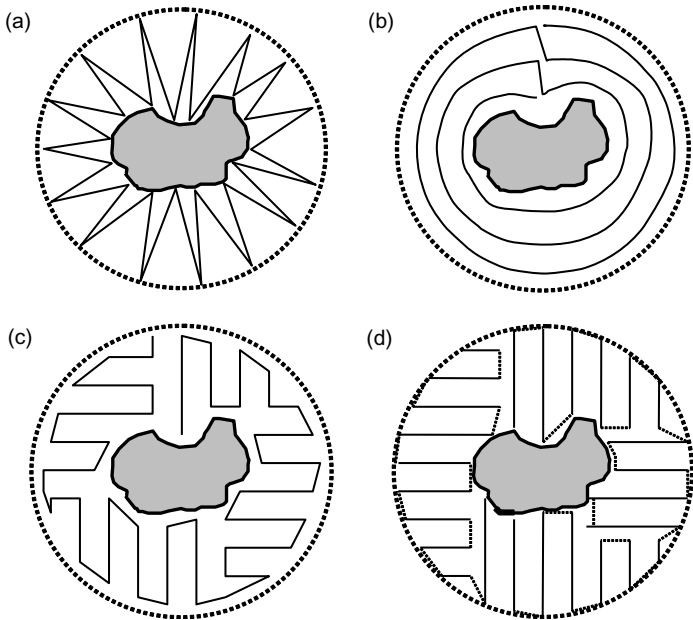


**Fig. 8.9** Examples of cruise tracks in an open area around an island. (a) Triangular, biased due to more intensive sampling inshore; (b) circular grid, gives even intensity but is sensitive to migration in almost any direction; (c) rectangular, all data can be used in the analysis; (d) parallel, data collected along the joining sections (dotted) are not useful.

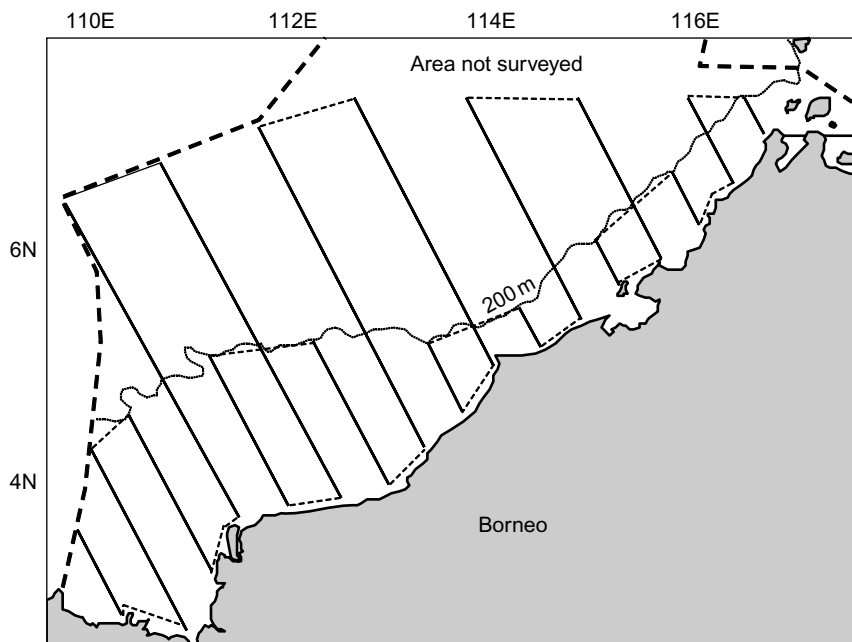


**Fig. 8.10** Systematic parallel grid designed for a survey off Borneo in the South China Sea. This has two levels of stratification, with less coverage in the deeper water ( $>200$  m) and twice the sampling intensity on the continental shelf where higher fish densities are expected.

come from vertical beaming (if the water is deep enough) or side-scan sonar, and is more usually target counts rather than echo-integrals due to the high levels of reverberation. In echo-counting for abundance estimation, the main problem is how to determine unbiased target densities, given that the sampled volume (in relation to fish size) can be uncertain. The degree of coverage is not usually a problem in rivers, indeed the volume of interest may be exhaustively surveyed e.g. by horizontal beaming from one bank to the other. The methods involved are discussed in detail in Chapter 5. Here we deal with aspects of the design decisions relevant to the data collection.

Some riverine methods do have more complex design considerations. The duration-in-beam technique (cf. Section 5.3) has been used for estimating the quantities of sockeye salmon (*Oncorhynchus nerka*) migrating in the Fraser River, using a downward-looking, single-beam sonar. The technique originally proposed by Thorne (1988) and Crittenden *et al.* (1988) was refined by Banneheka *et al.* (1995). Their model estimates daily passage of salmon through the observation site by representing the fish flux as the product of the estimated fish density and the migration speed.

The density estimates come from measurements made from a boat that runs shore-to-shore transects across the river. The migration speeds are determined separately, at times when the boat stops to record duration-in-beam data. This is

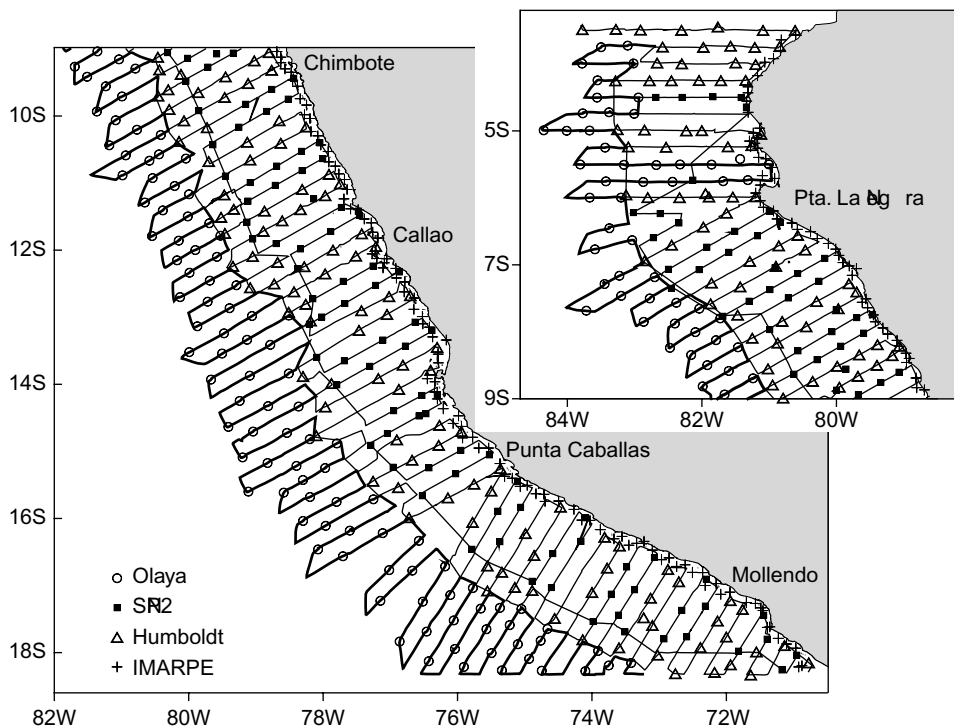


**Fig. 8.11** Systematic parallel grid as used on a Peruvian survey, 7 October to 9 November 2001, involving three research vessels. Transects are normal to the run of the coast in three sections (inset shows northern section). The offshore legs (thick lines) are surveyed by RV 'Olaya', the inshore legs (interlaced in pairs) by RV 'SNP2' and RV 'Humboldt'. Symbols mark the locations of pelagic trawl stations and identify the vessel involved. A fourth vessel (FV 'IMARPE') provides additional trawl samples very close inshore. This was an adaptive survey; the transect length could be adjusted depending on the observed traces or the extent of warm waters. (With thanks to Mariano Gutierrez who constructed the survey design.)

done at randomly chosen locations within the area covered by the transects. The sampling effort must be divided between these two activities, mobile sampling for density and stationary sampling for migration speed. The time available for the whole exercise is limited, so there is a trade-off in the allocation of effort between the density measurements and monitoring the migration speed. Chen *et al.* (2004) investigated an optimal minimum-variance partition of the sampling effort between the stationary and mobile observations i.e. between observations of fish density and migration speed. This study provides a method for optimizing any survey that combines these measures of fish flux to obtain total abundance estimates.

The initial time partition, based on 21 hours being available per day, was to spend 13–15 hours on running transects and 6–8 hours on the stationary sampling. When this strategy was implemented in 1999, the results showed a reduction in CV of about 20%. However, the data from that year suggested that about 1 hour longer

should be spent on collecting the migration speed data. This kind of optimization seems to give an improvement equivalent to the deployment of 40% additional effort, thus it is a valuable contribution. While the results of Chen *et al.* are specific to their survey, the principles of the method should have some general relevance to time-allocation problems.

## 8.5 Adaptive surveys

Adaptive surveys are designed to improve the precision of the results by concentrating effort in areas with higher abundance, or by reducing or removing effort in areas where there are no fish. The theory of adaptive sampling is explained in detail by Thompson and Seber (1996). Adaptive surveys work best when there is extensive knowledge of the properties of the stock being surveyed, as the results are conditional on the assumptions implied by the adaptive design (cf. Section 8.3).

Adaptive surveys fall into two groups, according to whether it is the boundary of the area being surveyed or the sampling scheme (e.g. the transect spacing) that is to be adjusted on the basis of the real-time measurements. Both methods are prone to bias in that they underestimate the true stock when conventional estimators such as the arithmetic mean of the samples are used. Thompson and Seber (1996) have suggested various techniques for compensating this bias. Francis (1984) and Jolly and Hampton (1990) propose two-stage adaptive sampling procedures (see Section 8.5.4 below) which are similar but have minor differences as described by Francis (1991). These authors acknowledge the bias problem but they believe the bias can be estimated (albeit with error) or that it is small. Their methods are design-based and rely on taking all the samples (from both stages of the procedure) randomly from each stratum. We deal first with methods for adapting the boundaries of the area to be surveyed, and then consider how the deployment of effort within the area might also be adapted.

### 8.5.1 *The outline survey*

The survey is conducted in two stages. First, the vessel covers the area of interest on a widely spaced grid, to detect regions of high fish density. This stage should occupy no more than 25% of the time available. The vessel then returns to the regions where fish have been observed, and the remainder of the time is spent in surveying these regions more intensively (Fig. 8.12). This technique is not useful if the fish are likely to migrate or disperse in the time between the initial sweep of the area and the return visit. Furthermore, if the initial sweep is too widely spaced, some localized concentrations may not be detected at all. The outline survey works best when the area to be examined is not too large, within a fjord for example, and the fish are believed to be concentrated in a few large and static schools which can be found on the first pass but measured more accurately on the second.

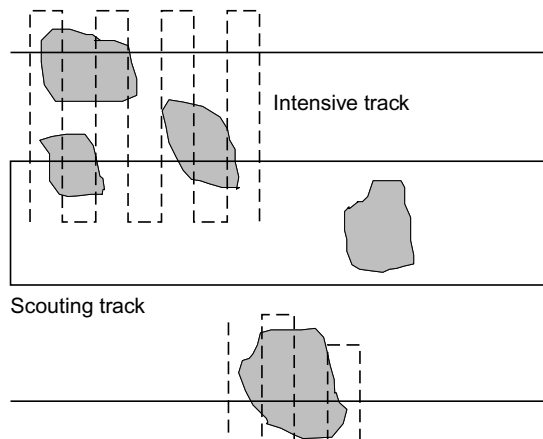


**Fig. 8.12** Illustration of an initial scouting survey followed by more intensive local sampling. The patches found while scouting are later surveyed with higher precision, but some fish concentrations may be missed if the patch size is smaller than the initial transect spacing.

### 8.5.2 Variable transect length

This technique may be applied when the spatial distribution is well defined in one direction. For example, suppose there is a coastline along one edge of the area to be surveyed, and the stock is located mainly in the shallow water near the coast. The survey is designed initially as a grid of transects running between turning points on the inshore and offshore boundaries. During each run in the offshore direction, it may be decided to terminate the transect once the observed fish density has declined to a small proportion of that observed near the coast (Fig. 8.13). The acoustic data may be analysed in the normal way, by calculating the abundance in elements of area, on the assumption that negligible quantities of fish would have been observed along the abandoned parts of the cruise track. To facilitate the analysis, once the decision to turn has been taken, the transect may need to be continued to the edge of the current area element.

### 8.5.3 Increased transect density

Suppose that the fish are expected to occur in local aggregations, but in regions which are unknown in advance, as clusters of migrating schools for example. The general plan is to increase the sampling of any region where the observed fish density is much higher than the average, by reducing the transect spacing. The transects continue to run for the full length to avoid gaps in the coverage.

The transect spacing should be decided on the basis of objective criteria. A simple technique is to observe the mean fish density along each transect, and to make the

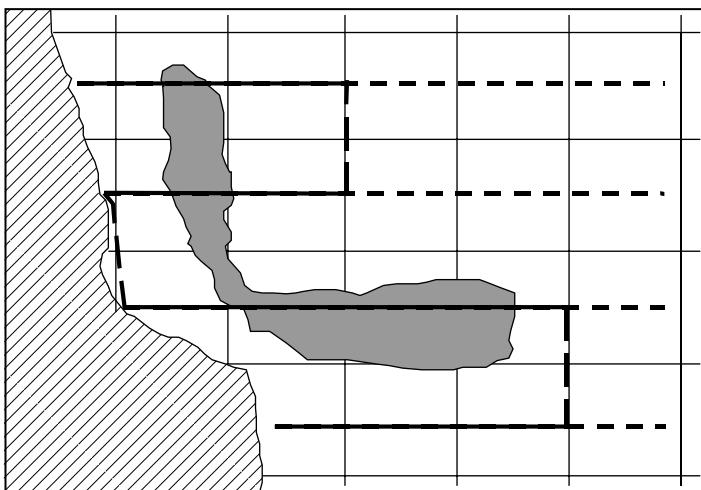


**Fig. 8.13** Adaptive transect lengths. The fish are supposed to be mostly in a zone from the coast to some western limit. The survey progresses from north to south and the east–west transects are terminated early when fish concentrations are no longer encountered. This procedure can be problematic if the western limit is very variable on the scale of the transect spacing.

spacing to the next transect inversely proportional to this, subject to the calculated spacing being contained within practical limits. Alternatively, the variance rather than the mean of the density measurements might be used to determine the spacing, as proposed by Stolyrenko (1988), on the grounds that precision is improved by sampling more intensively in regions of high variance. When few fish are observed, the variance is also small and the effect is to increase the coverage of the main concentrations. The two methods may not be much different in practice. According to Aglen (1989), it is characteristic of natural fish distributions that the standard deviation (square root of the variance) is proportional to the mean of the fish density.

#### 8.5.4 Randomized extra transects

The adaptive methods discussed above all suffer from the problem that the abundance of the stock cannot be estimated reliably, because of the bias introduced by locating the transects with reference to the observed fish densities. The bias may be reduced by randomizing the location of the extra transects. Jolly and Hampton (1990) propose a two-stage survey utilizing most of the effort in the first pass, then allocating the remaining effort on a second or return pass. This method requires the stock to be rather immobile, but it could be modified by taking the decisions during the first pass and conducting the extra transects immediately. In that case, since the decision must be made without knowing what will be seen on the remainder of the first pass, and given the limited time available to complete

the survey, a less than optimal design will almost certainly result. We cannot be sure of the best times and places to apply the additional effort. Sometimes all the spare effort will be used up too early and sometimes there will be spare time at the end.

We begin with a pre-planned set of parallel transects randomly placed in zones, leaving some time for extra transects to be inserted during the survey. When it is decided to increase the sampling intensity, a new transect (also randomly placed) is included within the current zone and, optionally, in those ahead. The new transects may be constrained to be at least 10% of the average spacing from any other. This procedure results in the first additional transect sometimes being out of the normal sequence, when the track progression must reverse to run the extra transect. However, all the transects in each subsequent zone may be taken in the normal progressive sequence. When it is decided to reduce the sampling intensity, all the transects placed in the current zone must be completed first. Alternatively, the transects within each zone may be taken in random order, in which case the sampling intensity may be reduced at any time. Both these procedures introduce a small bias when the arithmetic mean is used to estimate the fish abundance (Francis 1984); in a conventional non-adaptive survey the high estimates will balance the low ones so that the mean is unbiased. However, in a two-stage survey (or in a randomized extra-transect survey), the additional data are collected in strata where the initial catch rates were high. The high values might have occurred because they were drawn from the top end of the catch-rate distribution. They are nevertheless valid samples and (when taken together with the low values) are free of bias. However, the additional data are drawn from the whole of the catch-rate distribution. This reduces the overall mean catch rates in the strata sampled during the second stage, but the other strata (which initially had low catch rates) are unaffected. Consequently, when the results from all the strata are combined, the estimated abundance will be biased low though the bias may be small enough to be acceptable.

Figure 8.14 illustrates the randomized adaptive method. The survey initially progresses from east to west. When the fish concentration is observed on transect 3, the sampling intensity is increased. By chance, transect 4 is back to the east, but the later transects are taken in the normal sequence. The method may appear complicated at first sight, but it is simple to implement in practice. Jolly and Hampton (1990) consider that it provides abundance estimates with low bias and without the need for doubtful assumptions about the spatial distribution of the stock.

The practice of adaptive sampling is described in more detail by Thompson and Seber (1996). Further review of all the methods and problems is beyond the scope of this book. If an adaptive design is to be used, we urge caution and careful matching of the design criteria and the subsequent analysis. Since the conventional estimators when used with an adaptive survey are usually biased, it is recommended that readers who wish to invoke these procedures should consult the above-cited text for more detailed advice on how to avoid the many pitfalls.

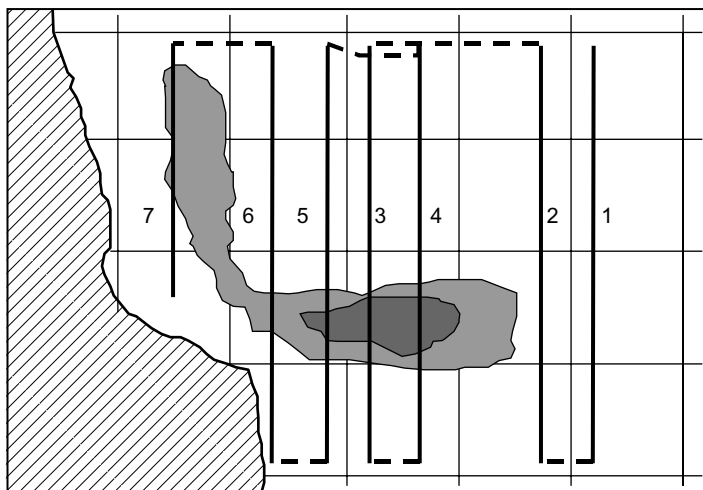


**Fig. 8.14** Randomized additional transects. This method may be employed with the extra transects being allocated at the end of the main survey or, as illustrated here, while the survey progresses.

## 8.6 Multi-ship surveys

Some surveys require more resources than can be provided by any one vessel. These surveys require more work to achieve effective coordination in a survey fleet, starting at the design stage and continuing through to the final report. Each case will be different and the optimal solutions are not necessarily the same, but there are some common problems to be considered. The design issues usually are:

- (1) Predicting the availability of vessels: this depends on the planning cycles of the nations or institutes involved and is often driven by other priorities; it is something to keep in mind but there may not be much that can be altered.
- (2) Allocation of responsibilities for areas to be surveyed: the main solutions are to have separate areas arranged to match local vessel bases, or interlaced areas that are more robust for detecting variable performance between vessels or to maintain coverage in the event that a vessel suddenly becomes unavailable.
- (3) Common sounder and calibration protocols: these should be relatively easy to specify and should accord with international standards such as those described in Chapter 3.
- (4) Common protocols for the acoustic data collection: if data are to be combined from the sample level upwards, then they must be collected in a comparable manner.
- (5) Common procedures for biological sampling and the treatment of samples: standardized sampling gear might be a good idea, though possibly not if the

- vessels have very different capabilities. Where different gears are used, comparison of their performance should be built into the design. However, different methods of fishing may have to be employed, sometimes due to the traditional practices on each vessel and sometimes because the fish distributions are dissimilar in different parts of the area.
- (6) Provision of data in a common format: the formats for acoustic and biological data should be clearly defined if the data are to be combined at the sample level. A less ideal though more manageable method is to conduct the local surveys using the same transect design and stratum definition, then to combine the local abundance estimates taking account of the relative effort provided by each survey vessel.
  - (7) Common reporting style: the professional report on the survey should present text, figures and tables in a uniform style; it is a good idea to prescribe a standard format and details of the information to be provided by each participant.
  - (8) Preparation of combined estimates: combining data from several sources is a skilled task requiring a good intrinsic understanding of the experimental procedures, and the ability to spot errors in the submitted records. Standardized data formats are essential, and an objective method for the analysis (suited to both the aims of the survey and the type of data available) is strongly recommended.

Several internationally coordinated multi-vessel surveys have been running for a number of years, notably the CCAMLR survey for Antarctic krill (Demer 2004), that on the Norwegian spring-spawning herring (Anon 2002) and the North Sea herring survey (Anon 2004) whose time series is now more than 20 years long. Each of these exercises has adopted its own set of agreed sampling methods and data-handling procedures. The written instructions are comprehensive and detailed, as will be seen from the published guidelines in each case.

One aspect of the design that is perhaps most critical for the long-term success of a multi-vessel survey, is the way vessels are deployed to cover the whole area. The simplest approach is to divide the area into regions with one vessel assigned to cover each region. However, there is always the possibility that a particular vessel may break down, be replaced or for some reason it fails to perform consistently. A design that interlaces the regions covered by different vessels will, as a matter of routine, provide data that may be compared later to detect any differences in vessel performance. The redundant data can be ignored to ensure unbiased (if less precise) estimates, but in the event of a vessel breakdown, the interlaced design protects the integrity of the survey to some extent. However, this type of design requires good coordination in transect design, accurate timing to ensure the overlapping parts of regions are surveyed concurrently, and very well integrated data protocols. The latter are essential because if there are few results from one vessel, there will be considerable advantages in combining the available data at the sample level to obtain the best survey estimates.

## 8.7 The EDSU

The elementary distance sampling unit (EDSU) is the length of cruise track along which the acoustic measurements are averaged to give one sample. The survey is conducted by collecting a series of samples from contiguous sections of track, each 1 EDSU long. Each sample is considered to be representative of the fish density at the centre of the corresponding EDSU.

Modern systems for acoustic data analysis, such as the Echo View package supplied by SonarData, allow the EDSU to be selected retrospectively. In the past, the EDSU usually had to be specified before the survey, but there was often doubt as to the most suitable value. If the EDSU is too large, potentially useful information about the geographical distribution of the stock will be lost. If it is much too small, successive samples will be dominated by local variability. In all cases the data from successive EDSUs will be correlated, so that if these are used as the primary samples it is more difficult to determine the confidence limits on the stock-abundance estimate. As a general rule, the EDSU should be small enough to capture the main spatial structure of the stock but not so small that the correlation between pairs of successive samples is rather large. If the along-transect data are to be used to estimate the precision of the stock estimate, appropriate methods such as kriging should be used to estimate the variance.

In practice, the best length for the EDSU may be known from previous surveys of the same area. If not, it may be decided on the basis of normal practice on surveys under similar conditions elsewhere. The EDSU could be as short as 0.1 km, which would be appropriate to dense schools within a fjord, or as much as 5 nmi (9 km) in the case of species that are widely distributed over large areas of ocean. Both extremes are illustrated by the Norwegian spring-spawning herring survey. The fish spend the winter in the Norwegian fjords, while in summer they spread over the North East Atlantic as far as Iceland. More usually, the EDSU might be in the range 1–5 km.

It may also be convenient to organize the data collection within intervals of time rather than distance, as then the number of observations (pings) in each EDSU is constant, maintaining homogeneous statistical properties among the samples. If the vessel travels at 10 knots, then 1 nmi of track is covered in 6 minutes. If it had been decided that the EDSU should be 1 mile, then the samples may be recorded as the average fish density observed in 6-minute intervals. The correspondence between the elapsed time and the distance travelled may not be exact, if the vessel speed is uncertain, but this is not an important source of variability in most analysis procedures, which treat the EDSU as a nominal distance.

## 8.8 More specialized surveys

The discussion above relates specifically to surveys that employ one or at least a limited number of vessels operating independently. The acoustic and biological data are

complementary to one another. However, there are more sophisticated methods for investigating fish stocks, such as the combined trawl and acoustic survey where quantitative data on the fish density come from both fishing and echo-integration (Godø and Wespestad 1993; Aglen 1996; Everson *et al.* 1996). These surveys are specialized applications whose designs will depend on the particular spatial and temporal variability encountered, and there are no really general conclusions to be mentioned. The main advantage is that by combining the information obtained from two kinds of survey, a more precise abundance estimate should be achieved compared to either method applied on its own. However, this is true only if the appropriate weight is given to each source of data. Combing data inappropriately can lead to worse results than might be obtained from the best method alone.

Another technique is the ‘Eureka’ survey (Johannesson and Losse 1977) which has been applied in Peru. Here many vessels (25–50) each run two transects normal to the lie of the coast. The design criteria are very similar to those for a single-vessel survey (Fig. 8.7), with great improvement in the temporal coverage, but there is the disadvantage of the (mostly commercial) vessels having many different kinds of instrumentation. The method has been refined over the years but the fundamentals remain the same. In this case the equipment calibration or the inter-ship comparison (see below) is largely ignored. It is certainly possible to include a requirement for inter-ship comparisons in the survey design, provided the change in availability of vessels occurs slowly enough to allow the determination of relative vessel performances. In this case some randomization in the allocation of transects to vessels would be a useful feature of the design.

## 8.9 Performance tests

In this section we discuss two methods for testing the complete acoustic measurement system as installed on the survey vessel – the live-fish calibration and the inter-ship comparison. These techniques are not a substitute for the physical calibration procedures described in Chapter 3. However, they do allow the overall performance of the equipment to be tested on signals from live targets. Thus the acoustic properties of the fish are included in the measurement. These tests should not be regarded as a precise calibration, but could be useful in revealing any large change in the detectability of fish. Such changes can occur, for instance, if some part of the equipment fails to function properly.

### 8.9.1 Live-fish calibration

Johannesson and Losse (1977) first described this technique in which the performance of the equipment is measured while a known quantity of fish is insonified. The fish are caught locally and then placed in a cage suspended beneath the transducer. In principle, the one measurement determines the conversion factor

for estimating the fish density from the echo-integrals, taking account of the target strength of the fish as well as the physical parameters of the echosounder. The technique is similar to the caged-fish method for measuring target strength (Section 6.2.2).

At first sight, the live-fish calibration may appear to be a simple technique, which obviates the need for the more complicated physical calibration of the acoustic instruments. However, we consider that live-fish calibration is only useful in providing an indication of the mean target strength of the fish. It is not a substitute for the recommended calibration procedure. The signal from the fish may vary for behavioural and physiological reasons to a much greater extent than the physical performance of the equipment. If live-fish calibration is the only measurement made, it will not be possible to say whether a substantial change in the sensitivity is caused by the fish targets, or by the equipment. Furthermore, it is doubtful whether the echoes received from captive fish of uncertain physiological condition will be sufficiently representative of those from free-swimming fish in the wild. We do not recommend live-fish calibration as part of the normal survey procedure, unless there is no other means of estimating the target strength of the species of interest.

### **8.9.2 *Inter-ship comparison***

In the case of the multi-vessel surveys discussed above, each vessel covers part of the area occupied by the stock and the results are combined to produce one estimate of the abundance. A common practice on this kind of survey is to conduct an inter-ship comparison when there are two ships operating in the same area. This technique is not an absolute calibration, but it is a useful means of checking that there is no great difference in the respective measurement capabilities, which might occur for instance if one vessel suffered more fish avoidance due to having a worse noise signature, and thus consistently indicated a lower abundance for the same fish ensemble.

The inter-ship comparison works best when it is done in an area where there are substantial quantities of fish in layers, or dispersed aggregations of varying density. The data are collected by the two ships moving in formation, with one in the lead and the other about 400 m astern, far enough to the side to be clear of the leader's wake (Fig. 8.15). The two ships should take the lead in turns, and Røttingen (1978) suggests they should exchange position at the end of each transect. However, we consider it is preferable to change the lead every two transects, in case one ship is more sensitive to weather than the other.

Both ships record data from their echo-integrators during the comparison. Normally a period of 2–6 hours is required to collect sufficient data, depending on the spatial distribution and the density of fish in the area. It is important to synchronize the integration periods on the two ships, so that they relate to the same portions of cruise track. Thus the following ship must record the echo-integrals over time periods which are delayed relative to those of the leader. Constant radio communication

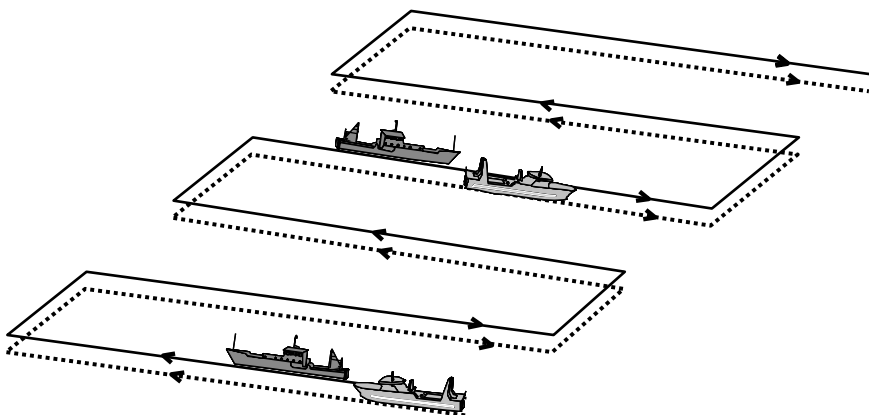


**Fig. 8.15** The inter-ship comparison. Two survey vessels move in formation over typical fish concentrations while their acoustic instruments are operated in the same way as during a survey. Each vessel takes the lead in turn, changing after each pair of transects.

between the ships is essential to ensure satisfactory cooperation and comparability of the results.

The two ships do not move on coincident tracks, because the following ship would then suffer interference from the wake of the lead vessel, but it is assumed that they will nevertheless detect the same density of fish on average. Once the data have been recorded, the two sets of echo-integrator records, expressed in terms of fish density or other comparable units, are plotted against each other. Since we cannot assume that one ship is more liable to error than the other, the functional regression technique is used to fit a straight line to the results (Ricker 1973). If the equipment on both ships is performing correctly, and if they have detected similar fish concentrations, then the regression line should have a slope close to unity, any difference being explained by random sampling error. MacLennan and Pope (1983) have shown how the confidence limits on the slope may be estimated. If the 95% confidence limits do not include unity, as in the example shown in Fig. 8.16a, this suggests that one ship is producing biased results, and the reasons for the discrepancy should be investigated.

Two examples of inter-ship comparisons are cited to illustrate the kind of results obtained, one as described by Foote *et al.* (1987) and a second from Anon (1998b). The first of these (between research vessels 'G.O. Sars' and 'Bjarni Saemundsson') showed a small but significant difference between the echosounder systems on the two vessels. The second comparison, again with 'G.O. Sars' but this time compared against FRV 'Scotia', showed no significant difference (Fig. 8.16b). In the latter case the measurement is less precise even though almost twice the amount of data has been collected. Good inter-ship comparison is dependent on the availability of a reasonable range of smoothly changing densities. If the fish are in small but widely spaced schools, so that each school is seen by only one vessel, the sampling variability will dominate the results.

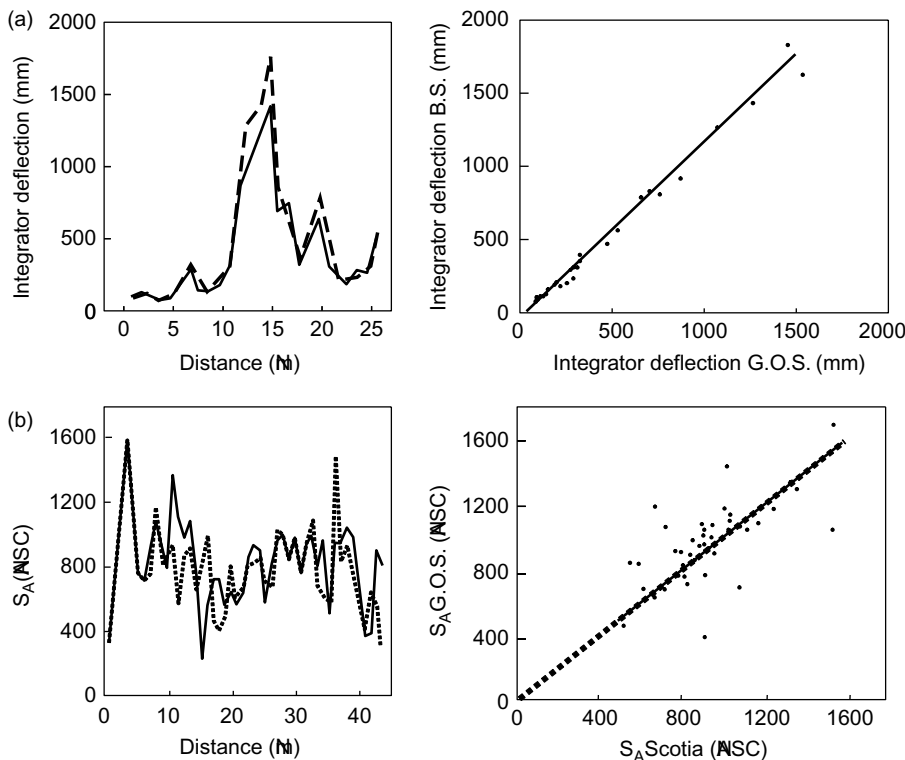


**Fig. 8.16** Results from two inter-ship comparisons. (a) 'G.O. Sars' against 'Bjarni Saemundsson', redrawn from Foote *et al.* (1987); the regression slope is 1.21, indicating a small but significant difference between the vessels. (b) 'G.O. Sars' against 'Scotia', redrawn from Anon (1998b); no significant difference was observed in this case. For each pair, the left panel shows sequential data along the cruise track; the right panel is a scatter plot comparing concurrent measurements on the two vessels.

The advantage of inter-ship comparison is that it will demonstrate any gross difference in acoustic performance. It is not a substitute for the proper calibration of the acoustic equipment, which should be carried out on both ships beforehand. If the comparison nevertheless reveals a large difference, the equipment on both ships should be recalibrated as soon as possible, in accordance with the procedures described in Chapter 3.

# Chapter 9

# Data Analysis

## 9.1 Introduction

After an acoustic survey has been conducted in accordance with the practical guidelines described earlier, the analysis is the stage at which, all being well, useful results are derived from the collected data. Depending on the objectives of the survey, we may wish to estimate the abundance of one or more species of interest, the geographical distribution of fish concentrations and/or the age, sex or maturity structure of the population. In addition, some indication of the accuracy of the results is normally required.

The abundance may be estimated as the quantity of fish in the stock, or as an index which shows how the stock has changed relative to some previous estimate. It is preferable to know the absolute quantity, but if the error in this estimate is very large, the relative index may be more useful since it can be determined more accurately.

The information available from the survey or other sources will include some or all of the following:

- (1) Acoustic data: echograms recorded as volume scattering coefficients, or the same data summarized as echo-integrals or echo-counts accumulated along sections of cruise track, relating to one or more depth channels.
- (2) Calibration results: the echosounder/integrator settings may have been adjusted by calibration before the cruise, or there may be separate measurements, e.g. of transducer sensitivity to indicate how the acoustic data should be scaled.
- (3) Size and species composition, sex, age or maturity stage of biological samples collected by fishing, usually opportunistic fishing on observed echo traces.
- (4) Target strength and its dependence on size (length or weight) for each species detected acoustically.
- (5) Hydrographic data: water temperature and salinity at various depths.
- (6) Geography of the area surveyed, e.g. location of coastlines and islands, the cruise track, fishing and hydrographic stations.

In this chapter, we describe how the analysis is done, working through a series of calculations based on the information collected during the survey, to obtain numerical estimates of the abundance and other parameters of interest. The process is

conceptually quite simple though it may appear complicated in the detail. The first step is to classify the various marks on the echogram which might be identified as (a) individual fish, (b) single species in schools or layers or (c) mixtures of species in aggregations.

Once this is done, the surveyed area is divided into regions which are homogeneous as regards the expected density and size distribution of targets. These regions may be large or small depending on the data available. There may be one or many regions depending on the circumstances. The echo-integrator conversion factor is calculated separately for each region, taking account of the effective target strength therein. These factors are used to convert the acoustic data to estimates of the fish density along the cruise track. The spatial distribution of the stock may be described in contour maps drawn through the observed densities, or by numerical analysis of the acoustic data on a rectangular grid. These preliminary considerations lead to a discussion of methods for estimating the total abundance of the stock.

The key to a good analysis is to determine the appropriate regions that organize the observations to obtain the best estimates. Each type of data, acoustic or biological, has to be considered separately before being combined. Where the data have been collected by stratified sampling on a prescribed spatial design, as is often the case for acoustic measurements, the analysis regions are simply the strata identified in the survey design (cf. Chapter 8). On the other hand, if the sampled locations are opportunistic, as in fishing to identify echo traces, the choice of region is less obvious. Each observation contains information on the fish density or the biological characteristics of a stock at one location, but with some measurement error. The objective is to combine sufficient observations to reduce the measurement error as much as possible, but not to combine so many over an area so large that real spatial differences are obscured. Where the measurement error is large and the spatial change is small, more observations should be combined as averages. Conversely, if the measurements are accurate but the spatial variability is large, the best results will be obtained with little averaging.

We consider the precision of the abundance estimate, namely the statistical uncertainty associated with the sampling strategy. The importance of fish behaviour is discussed, notably problems due to migration, diurnal behaviour rhythms and the reactions of fish to the survey vessel. Several other sources of error are reviewed. Finally we discuss the overall accuracy of the abundance estimate and how it can be assessed in practice.

Figure 9.1 is a flow diagram which illustrates the various steps of the analysis and the order in which the calculations are performed. These procedures are similar in general terms to the analysis methods described by Johannesson and Mitson (1983), Dalen and Nakken (1983) and Simmonds and MacLennan (1988). The top row on the diagram indicates the main sources of information. As a reminder that the data may be subject to behaviour-related biases, particularly in fishing or target-strength measurements, the diagram contains two shaded boxes as optional components. Essentially, the collected data must be organized to represent the abundance and

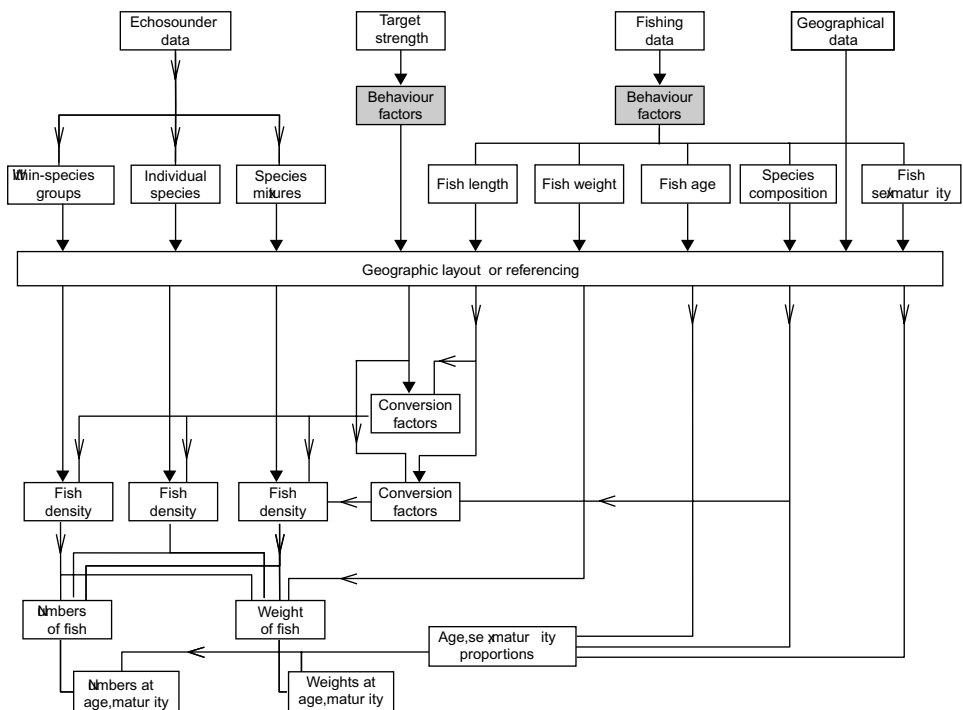


**Fig. 9.1** Flow diagram showing the basic data and analysis procedures for obtaining fish abundance estimates from acoustic and biological data.

biological characteristics of the species of interest in space. In this context, space may be considered as a set of pre-determined strata, a post-stratification scheme, or a regular grid or block representation of an area. Post-stratification is not normally appropriate to acoustic records but it may be helpful in dealing with biological samples. This spatial process is represented as a block running the full width of Fig. 9.1, while the lower half of the figure represents the calculations.

## 9.2 Processing the echograms

### 9.2.1 Classifying or partitioning the echo-integrals

We now come to the problem of assigning or partitioning the echo-integrals into components or classes associated with particular species or, more generally, types of target. Here we introduce the idea of classification or assigning parts of the echogram to a user-defined group or class. This is a broader concept than target identification (review, Horne 2000). The first step is to examine the echograms to see whether any of the marks can be identified as having come from a particular species. It may be known that certain species cause distinctive marks on the

echogram, or they may occur at different depths. This prior knowledge may allow at least some of the marks to be positively identified (Midttun and Nakken 1977). Where single-species marks are identifiable, the class is at species level, but if the species composition is unknown, the class becomes a group of species. Sometimes it may even be possible to classify marks below species level, by the size composition of the fish for example. Suppose there are juveniles and adults in the population whose marks could be separately identified because they are found at different depths. The respective marks should be considered as different classes, since they represent discrete components of the stock.

Assigning a value to each class is done at the simplest level by comparing the echogram and the integrum at corresponding times. The integrum is a graph of the accumulated echo-integral against time. The slope of the integrum depends on the density of detected targets; the greater the density, the steeper is the slope. Figures 9.2, 9.3 and Plate 9.1 show how the acoustic records collected on surveys can be used in different ways when partitioning the echo traces. Figure 9.2 shows the general principle of simple echo-energy allocation. This method is relatively quick and works well in many cases, but it relies on pre-defined depth channels and time or distance intervals. There are various software packages that allow a more flexible approach to the problem through post-processing procedures. Examples in current

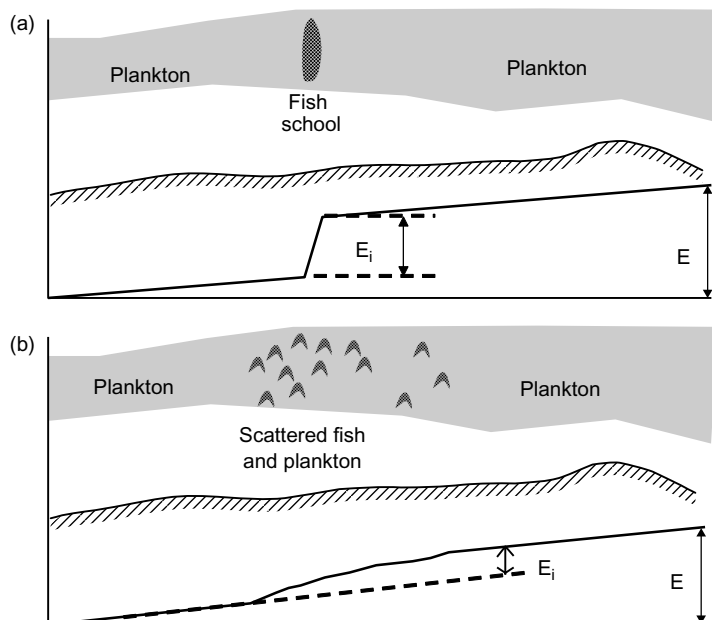


**Fig. 9.2** Illustration of echo-integral partitioning based on the integrum (solid lines, indicating the accumulated echo energy). (a) The contribution of a fish school ( $E_i$ ) is identified from a step change in the integrum; (b) echoes from scattered fish are associated with the change in the integrum gradient.

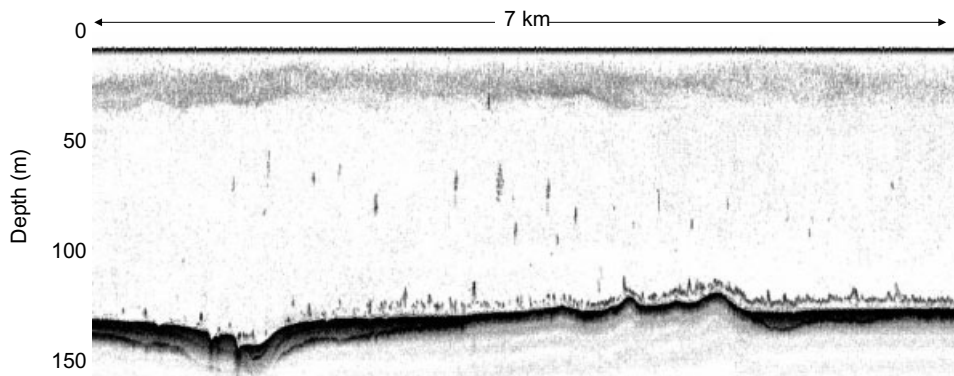


**Fig. 9.3** Echogram (EK500, 38 kHz) from the North Sea displayed in greyscale (original in colour) showing three types of marks at different depths: a near-surface plankton layer (10–40 m), young-of-the-year haddock in small diffuse schools (50–100 m) and 3–4-year-old herring near the seabed (110–130 m). In this case partitioning is achieved by appropriate choice of depth layers for the integration.

use are the EK60 software provided by Simrad, the MOVIES+ package developed by IFREMER, the CH2 from the Canadian Department of Fisheries and Oceans, and Echoview from the Australian company SonarData. In addition to the acoustic data, of course, the partitioning also takes account of the fishing samples, which were obtained to identify particular echo traces.

Figure 9.2 shows a schematic representation of the echogram and the associated integrum. The shallow slope of the integrum (a) is due to plankton and this component of the echo-integral is ignored if the objective is to estimate fish density. The sharp deflection coincident with the school is clearly associated with the stronger fish echoes. Thus the component of the echo-integral attributable to fish is in this case the single sharp deflection. If there were several closely-spaced schools, it would be the sum of the smaller but still sharp deflections seen on the integrum. If required, the remainder of the echo-integral (having subtracted the fish contribution) would be attributed to the plankton. In the case of the more extended marks due to scattered fish, the integrum (b) is less steep and now the change in slope is identified as the contribution of the fish. The partitioned values obtained by this method represent not the total biomass of the school, but the average fish density over the chosen period of the echo-integration (i.e. the EDSU, see Section 8.7).

Thus it is not difficult to partition the echo-integrals between plankton and schooling fish. Partitioning between different fish species is more problematic. Figure 9.3 illustrates an example recorded in the North Sea, where the fish are seen to be in clusters of small schools, one group in midwater and the other near the seabed. Trawl samples identified the schools to species level and provided information on fish size. The midwater schools were found to be young-of-the-year haddock, *Melanogrammus aeglefinus* of about 40–50 mm in length. Those near the seabed were identified as

herring, *Clupea harengus*, of about 260 mm in length. Sections of the echogram containing just one species were analysed separately. In this sample the partitioning is quite straightforward. It is simply a matter of choosing appropriate depth layers for the echo-integration.

While the operator can manually select a group of schools for analysis, in relation to their depth or other criteria, the process may be automated through school-extraction algorithms which have developed over time, e.g. Nunnallee (1983), Souid (1988), Reid and Simmonds (1993), Weill *et al.* (1993), Barange (1994) and Scalabrin *et al.* (1996). Plate 9.1 illustrates the results obtained on fish schools observed in the Bay of Biscay. These have been automatically extracted from the echogram using techniques developed by Weill *et al.* (1993) and implemented in MOVIES+. Each school is labelled with a number and the relevant data can be extracted to a database or viewed on a screen. The details of three schools can be seen in the illustration, one near the surface, one of the small ones near the seabed and a large aggregation that is in contact with the seabed.

Acoustic data processing has become more complex but also much more powerful with the introduction of so-called synthetic or virtual echograms. These are algebraic combinations of several echograms constructed using both arithmetic and logical operators. The results are pictures that look like echograms but the marks are coloured to show the type of target rather than the echo strength. The target classification may be based on decibel differences as suggested by Brierley *et al.* (1998) for discriminating types of zooplankton (which is more difficult than fish-plankton separation), see also Swartzman (1997) and Kang *et al.* (2002). More complex algorithms have been evaluated e.g. Haralabous and Georgakarakos (1993; 1996) who used neural networks for the identification of small pelagic fish in the Mediterranean Sea, while Rose and Leggett (1988) proposed a peak-echo detection method to identify cod near Newfoundland.

Another development is the multi-frequency algorithm that defines echo-classes through the comparison of echo strengths recorded simultaneously at several frequencies (Korneliussen and Ona 2003). Plate 9.2 shows an example of the results that can be achieved. Kloser *et al.* (2002) used a slightly different approach to control the various colours in the display, thus highlighting fish aggregations according to their spectra. Plate 9.3 illustrates this procedure and the resulting display. The multi-frequency algorithm may be implemented at the sample level, or after small-scale spatial averaging to smooth the sampled data, as proposed by Souid (1988) and Reid and Simmonds (1993).

Multi-frequency techniques have been further developed to incorporate school-shape descriptors with discriminant analysis in the classification, see for example LeFeuvre *et al.* (2000), Scalabrin *et al.* (1996), Richards *et al.* (1991) and Korneliussen and Ona (2003). This methodology is now well established and a comprehensive summary will be found in Reid *et al.* (2000). However, good results depend on the volumes insonified by the various transducers overlapping to the greatest extent possible. Thus, the transducers should be located in close proximity, with parallel

axes, to obtain the best horizontal alignment. Further, the pulse lengths and sounder bandwidths should be the same for all the frequencies, to ensure matching samples in the vertical direction.

Plate 9.4 illustrates how the frequency dependence of echo strength can be used to separate plankton and fish schools in the North Sea. Data recorded at three frequencies (38, 120 and 200 kHz) are combined and spatially averaged with a 5-by-5 smoothing matrix applied to the pixels. This is used to create a mask which is applied to the original 38 kHz echogram to extract schools and present them in a new synthetic echogram (Plate 9.4d). If required, the traces identified as plankton could be shown in another synthetic echogram. The use of spatial averaging ensures that the schools are completely extracted and no important parts of the integral are omitted. The significance of simple single-frequency thresholding is illustrated in Plate 9.4e. We can see that parts of the school are missed (suggesting the threshold is too high), but there are scattered pixels outside the schools (suggesting the threshold is too low). In other words, the selected threshold is a compromise. The multi-frequency approach (see below) combined with spatial averaging is preferred since that is a more efficient way to extract whole schools.

There is a large subjective element in the identification of fish species from the appearance of echo traces, but the procedure should be made objective as far as possible. The surveyors have to use their experience as well as the data to hand in deciding how to partition the echo-integrals. They should establish a library of echo traces that have been positively identified by fishing, together with other relevant information such as the location, season and time of day. This will help to ensure that when different people have to identify the echo traces, as might apply when several ships are engaged on the same survey, the partitioning is based on consistent rules. The echo-integration technique depends on the proportion of the echo-integral due to each component (species or species group) in a mixed population being assessed accurately. This is particularly difficult in areas such as tropical seas where many kinds of pelagic fish cohabit and there is the further complication that the echo-integrals are often dominated by plankton.

It must not be forgotten that location (latitude, longitude, depth) and time (hour and date) are often key factors relevant to the classification of echograms. Target identification involves discrimination between alternative categories, and our ability to do this depends on the underlying probability distributions and how they overlap. There will never be just one criterion for identifying a particular species, as the best method will depend not only on that species but also on the other targets whose echoes must be separately identified.

Partitioning is not always a major problem. Off the coast of Morocco, for example, most of the schools are pilchard, *Sardina pilchardus* or the trumpet fish, *Macrorhamphosus scolopax*, the latter being found further from the shore. In the Arabian Sea and the northern part of the Indian Ocean, deep scattering layers of the lantern fish, *Benthosema pterotum*, are easily identified on the echogram, while in shallow waters, *Sardinella aurita* and *Trachurus* spp. may be distinguished from

anchovies (but not from each other) by obvious differences in the school marks seen on the echogram. The anchovies are found in less dense schools and higher in the water column compared to the other species, but only during daylight. The schools dissociate at night, and then the fish are almost uniformly distributed between the surface and the seabed in waters less than 20 m deep.

The partitioning of the echo-integrals is not necessarily done at the species level, but is more generally a matter of classifying targets according to their behaviour and acoustic properties. The subsequent analysis is performed separately for each category of target. For example, if different size classes of one species can be identified, then the abundances of each class can be compared to show the age structure of the stock. At the other extreme, several species may occur in mixed aggregations giving rise to clusters of similar marks which cannot be separately identified with certainty. In that case it would be appropriate to consider a broad category comprising a mixture of species with similar behaviour, and only the total abundance of the mixture would then be estimated. However, the species composition as well as the fish-size distribution must be known to determine the mean target strength, unless all the species concerned can be assumed to have the same length-dependence of the target strength.

Once the partitioning has been done, the result for each species or category is a set of mean echo-integrals, and each mean refers to one EDSU (elementary distance sampling unit, p. 324) along the cruise track.

### **9.2.2 *Quality control of echogram data***

The acoustic data consist of many samples assembled to represent a two-dimensional section of the water volume. Typically, one ping might be transmitted every 5 m along the cruise track and the echoes might be sampled in 2 cm depth bins. For a three-week survey this amounts to some 17 billion samples, or several times that if multiple transducers operating at different frequencies are involved. Ensuring the correct use of all this information is a considerable task. It is advisable to process the data using a dedicated software package of the kind mentioned above. This will ensure proper documentation of the procedure and simplifies the re-analysis of data sets should that be necessary. However, the user must still be aware of the basic checks needed to validate the data and to avoid unnecessary errors in the analysis. We cannot cover every aspect of data management here, but the following items are some of the issues that need careful attention:

- (1) Correct calibration details. Ensure that all the sounder settings are properly applied, where necessary adjusting the records to account for any change in the equipment performance that might have occurred during the survey.
- (2) Correct sound-speed factors. A specific short-range value may be required for the calibration, while a different standard value or a variable profile may be required for the survey itself.

- 
- (3) Correct exclusion of near-surface interference. This can be caused by the wind-induced bubble layer, or the occasional ship's wake that might be confused with a fish school, or the inclusion of part of the transmit pulse (a possibility when motion compensation is used and the transmission is no longer at a fixed depth). While the bubble interference is relatively simple to detect, if time consuming to deal with, the other two effects occur so infrequently that they are easy to miss.
  - (4) Correct exclusion of the seabed. While seabed-following algorithms are reasonably reliable, even the best of them fail sometimes. If there are fish close to the seabed, the user may wish to minimize the safety margin (or back step) needed to exclude the seabed echo. This increases the risk of some seabed returns being wrongly identified as fish. A casual inspection of the echogram may not be sufficient to detect this problem. Preliminary fine-scale extractions may be used to select records with suspicious values for closer scrutiny.
  - (5) Data extractions including recent error corrections. The analysis may involve error checking at an early stage, leading to revised versions of the original data set. Careful documentation of the work done is essential to ensure that the final version with all the relevant corrections included is the one adopted in the subsequent analysis.

Items 1–2 and 5 above are best controlled through documentation protocols. Items 3 and 4 may require preliminary data extraction as part of the quality control. One method of finding occasional near-surface or seabed values that are invalid (i.e. not fish) is to integrate narrow layers at these boundaries, using high thresholds that exclude most (but not all) of the fish traces. Then we extract data on a fine scale, visually inspecting the results to determine if they are valid. If the visual inspection is done on the largest values first, then once a good number of them are found to be correct, the user may feel confident that even if some invalid data are still included, their contribution to the abundance estimate will be small. The visual display of acoustic data is an important part of the quality control. Figure 9.4 shows a bubble plot of EDSU data. This kind of visualization may be used to locate especially large values, pointing the user to records for detailed inspection to ensure that the samples contributing most of the overall abundance are thoroughly checked.

### 9.3 Species composition

Although it may be possible to identify only a small proportion of the marks from the acoustic records alone, it is worthwhile performing a separate analysis of the identified records which will thus not be subject to errors in the interpretation of fishing samples. However, this must not be taken as an excuse to avoid fishing. The collection of biological samples remains an essential part of the survey procedure.

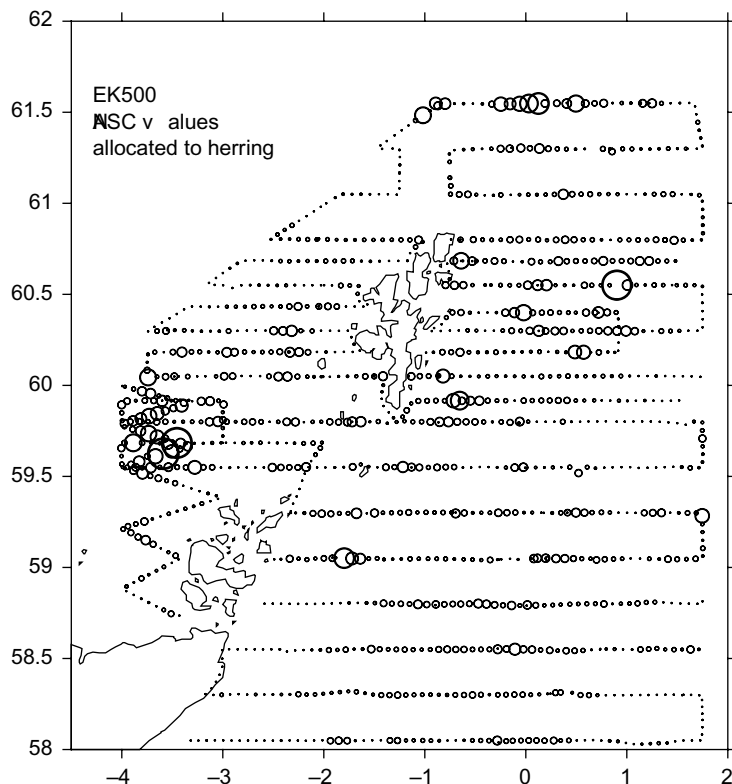


**Fig. 9.4** Bubble plot showing the fish density at intervals along the cruise track of a North Sea herring survey. This type of presentation gives a visual comparison of the observations and is useful when checking the data for quality control purposes.

### 9.3.1 Analysis of fishing samples

Here we consider the interpretation of samples collected by trawling, but the same principles apply to the catches taken by any other kind of gear. Trawling is conducted at a number of positions around the surveyed area, wherever there is doubt as to the identity of echo traces. The object is to determine the species and size composition of the local population which may not be the same over the whole of the surveyed area. We need a map of the species composition and the size (or age) distribution of the fish population. There is currently no standard method for mapping several linked variables in space. Ideally we want a map that reflects real change in the population while smoothing the noise in the observations. Initially we shall consider procedures for evaluating fishing data collected within various strata. Each stratum should be homogeneous in the species and size composition of the fish therein. The analysis strata may be defined at the design stage, if the distribution in relation to e.g. the water depth is well enough known, or they may be based on the biological observations obtained during the survey. Within any part of the area where uniform conditions

are believed to apply, we may have several hauls made at different locations. The compositions indicated by these hauls must be combined to estimate an appropriate mean relevant to the whole stratum. There are several approaches to this problem.

### 9.3.2 Length-frequency distributions

Consider first the length composition of each species represented in the catches. Suppose there are  $M_i$  hauls in which the catch of species  $i$  is sufficient to establish a reasonable length distribution.  $N_{ik}$  is the total number of species  $i$  in haul  $k$  and  $n_{ijk}$  is the number in length class  $j$ . When the catch is large, we normally sample a manageable proportion, in which case  $N_{ik}$  and  $n_{ijk}$  are the observed counts raised to estimates for the whole catch. In the analysis for each species, it is better to ignore any haul in which  $N_{ik}$  is too small to establish a reasonable length distribution. Thus  $M_i$  may not be the same for all species. The duration of haul  $k$  is  $t_k$ . Ideally, the average composition should be calculated by weighting the results from each haul according to the quantity of fish it represents, or the effective area sampled, but it is difficult to say what this is. The catching efficiency of the trawl is highly variable, especially in pelagic fishing, and the observed catch-rates may be quite unrepresentative of the true population densities on a local scale.

When the catches are moderately large, so that a good length distribution can be established for each haul, the best plan is to give equal weight to each distribution, taking no account of differences in the total catch. The mean frequency of species  $i$  and length class  $j$  is  $P_{ij}$ . In this case (Method 1) the estimation formula is:

$$P_{ij} = \sum_{k=1}^{M_i} n_{ijk} / N_{ik} / M_i \quad (9.1)$$

If the catches are small and the length distributions are poorly defined for any one haul, it is better to combine the samples, giving equal weight to each fish but taking account of the haul duration, since it is supposed that, on average, longer hauls will produce more fish. This is Method 2, in which the frequencies are estimated as:

$$P_{ij} = \sum_{k=1}^{M_i} (n_{ijk} / t_k) \left/ \sum_{k=1}^{M_i} N_{ik} / t_k \right. \quad (9.2)$$

A third possibility (Method 3) is to weight the results in proportion to the echo-integrals recorded in the vicinity of the fishing position. This should not be attempted unless each catch consists of one species only, because the echo-integrals give no information as to the species composition of mixed targets. If  $E_{ik}$  is the mean echo-integral for species  $i$  in the vicinity of haul  $k$ , supposed to be proportional to the fish density, the frequencies are estimated as:

$$P_{ij} = \sum_{k=1}^{M_i} (n_{ijk} E_{ik} / N_{ik}) \left/ \sum_{k=1}^{M_i} E_{jk} \right. \quad (9.3)$$

Method 3 is not useful unless the catches are large enough to establish good length distributions. In addition, the frequency estimates may be biased if there is a systematic relationship between fish density and fish size, for example if the young fish are more dispersed than the adults. In essence, Method 3 assigns each haul directly to its local area, a technique known as the nearest-neighbour method where the closest observation is assigned directly without any averaging. For most applications we recommend that Methods 1 or 2 should be used to average the fishing results, depending on the sample sizes and the quality of the length distributions obtained from each haul.

### 9.3.3 *Proportions by species*

The evaluation of species proportions in a mixture is done in a similar way. Suppose again there are M trawl stations in a homogeneous region.  $q_{ik}$  is the quantity of the i'th species caught at station k, and  $q_k$  is the total catch. The weights  $w_i$  are determined by combining the catch compositions, in a similar manner to the treatment of length frequencies. Again, there are three methods to be considered which differ in the weight given to each sample, and the respective formulas are presented below.

Method 1: equal weight is given to proportions in each catch:

$$w_i = \left( \sum_{k=1}^M q_{ik} / q_k \right) / M \quad (9.4)$$

Method 2: equal weight by catch rate:

$$w_i = \left( \sum_{k=1}^M (q_{ik} / t_k) \right) / \left( \sum_{k=1}^M q_k / t_k \right) \quad (9.5)$$

Method 3: the proportions are weighted by the echo-integrals  $E_k$  observed in the vicinity of the trawl stations:

$$w_i = \left( \sum_{k=1}^M (E_k q_{ik} / q_k) \right) / \left( \sum_{k=1}^M E_k \right) \quad (9.6)$$

In each case, the sums are over all the catches from  $k = 1$  to  $M$  whether or not the catch contains species i. We recommend Method 2 as being the most generally applicable. Method 1 is better if the catches are taken from a few schools by aimed fishing, when the catch rate may bear no relation to the mean density. Method 3 might be expected to give the best result when the echo-integrals are highly variable and the catch rate is a worse indicator of the density. However, weighting by the echo-integral is not generally recommended because it depends on the relative target strengths of the species in the mixture. This is not a problem if the species composition is the same everywhere, but otherwise too much weight will be given to those with higher target strengths.

Although it is often the best available, pelagic trawling is a poor method of sampling fish densities, and substantial errors may arise in estimating the proportions of species in mixed aggregations. If there is any possibility of partitioning the echo-integrals to species level from examination of the echograms, this should be attempted in preference to the catch-partitioning technique described by Nakken and Dommasnes (1975). Even if the interpretation of the echogram is uncertain, the error in acoustic partitioning may well be less than that based on the catch analysis (cf. Sections 9.6 and 9.7).

### **9.3.4 Selection of homogeneous regions**

There are several reasons why the size distribution of a fish stock might not be the same over the large area covered in the typical acoustic survey. When the surveyed area is bordered by a coastline, for example, there may be differences in the age structure between inshore fish and those in deeper water. Or the fish may associate with others near the same age, resulting in clusters of fish in particular age groups. If the fishing samples indicate consistent differences between one region and another, size distributions must be determined separately for each region within which the population structure is considered to be homogeneous.

The observed size distributions will vary due to sampling error as well as real changes in the population structure between the trawl stations. To identify the homogeneous regions, we need to consider whether the distributions obtained from any two hauls are significantly different. This might be evident from inspection of the numerical data if there are clear differences between clusters of trawl stations. Alternatively, a more objective approach to the problem is to apply the Kolmogorov–Smirnov (KS) test (Campbell 1974) which is sensitive both to the position of modes and to the shape of the size distributions. The result of the test is a number  $P_{KS}$  in the range 0–1.  $P_{KS} = 0$  when the distributions are identical, and  $P_{KS} = 1$  when there is no similarity at all. If the distributions come from the same population, subject only to sampling error,  $P_{KS}$  is expected to be between 0.1 and 0.3.

It is not suggested that the KS test should be applied as an automatic procedure. A more thoughtful approach is necessary. We might begin by assigning the trawl stations to groups within which  $P_{KS}$  for each pair is less than 0.2, and see whether this suggests a sensible division of the surveyed area into homogeneous regions. The calculations are then repeated for similarity thresholds  $P_{KS} = 0.15$  and  $0.25$ . If the grouping of the trawl stations is sensitive to the threshold value of  $P_{KS}$ , this indicates that the differences in size distribution are small enough to be ignored, and only one region (the surveyed area) needs to be considered. Otherwise, the boundaries between the homogeneous regions are determined by the condition that any part of the surveyed area is assigned to the region corresponding to that of the closest trawl station.

Figure 9.5 shows an example of the  $P_{KS}$  values obtained by comparing samples of herring collected at 40 trawl stations, displayed as a dendrogram. In Fig. 9.6, the distributions are grouped spatially according to the value of  $P_{KS}$ . There is a

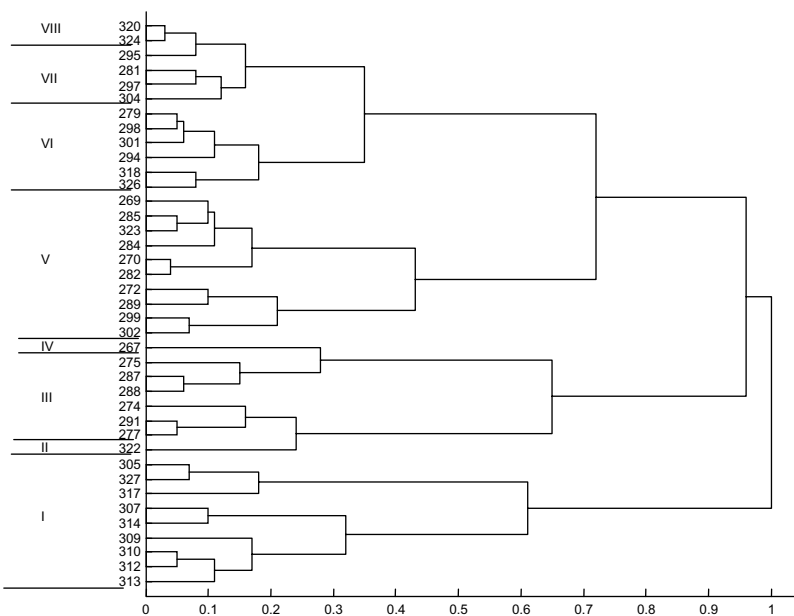


**Fig. 9.5** A dendrogram constructed from the length distributions in trawl catches (ref. numbers of 39 trawl hauls at left) and the eight analysis regions based on statistical consistency and spatial continuity (see map in Fig. 9.6). The horizontal axis is the  $P_{KS}$  value.

clear statistical separation into five groups, with a suggestion of three more which are spatially disparate. This suggests that the surveyed area should be divided into eight regions. The boundaries of these regions in relation to the trawl stations are shown in Fig. 9.6. The mean length of the herring caught at each location is shown as an indication of the spatial variability. Comparison of regions I, III, V and VI shows why the area must be partitioned in this case. The evident local variability suggests that some averaging is better than the nearest-neighbour method, since the latter fits a stepwise surface at each trawl location and implies no error in the fish-size distribution.

It is not useful to divide the surveyed area into a large number of regions. There should normally be more than one trawl station in each region. On the other hand, an average of six hauls per region is probably as many as should be considered. The selection of a few supposedly homogeneous regions is a practical but not ideal way of representing the spatial variability of size distributions which, for fish populations, may change continuously rather than forming discrete clusters. We look forward to the future development of multi-nomial mapping methods which, in principle, should allow more continuous spatial representations of biological attributes and a better solution to this problem.

The KS test can also be used to compare the species mix in different parts of the surveyed area. In this case, the proportion of each species in a sample is treated in the same way as the frequency of a length class in the previous analysis, and the value of  $P_{KS}$  indicates whether or not the species mix is similar between pairs of trawl stations.

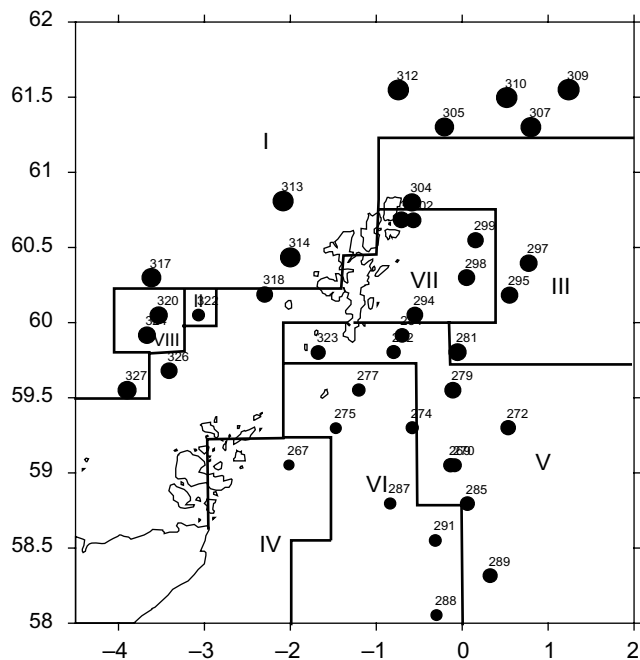


**Fig. 9.6** The distribution of herring by length, showing a clear spatial trend of increasing mean length (dot size for each haul number) from south to north, and the analysis regions selected to provide a stepwise approximation to the (possibly) continuous spatial structure (cf. Fig. 9.5).

## 9.4 The echo-integrator conversion factor

The next step is to estimate the density of targets from the observed echo-integrals. This is done by means of Equ. (5.14), which we repeat here in a slightly different form:

$$F_i = (C_E / \langle \sigma_i \rangle) E_i \quad (9.7)$$

The subscript  $i$  refers to one species or class of target.  $C_E$  is an equipment calibration factor which is the same for all species,  $\langle \sigma_i \rangle$  is the mean backscattering cross-section,  $E_i$  is the mean echo-integral after partitioning and  $F_i$  is the estimated density of species  $i$  per unit area of the integration channel.  $F_i$  is the number or weight of species  $i$ , depending on whether  $\langle \sigma_i \rangle$  is the mean per fish or per unit weight. Note that the echo-integrator conversion factor,  $C_i = (C_E / \langle \sigma_i \rangle)$ , is not the same for all species. Furthermore,  $C_i$  depends on the size distribution of the insonified targets, and if this is not the same over the whole surveyed area, the calculated conversion factors must take regional variation into account.

$C_E$  is determined from the physical calibration of the equipment (Chapter 3); it does not depend on the species or biological parameters. Several calibrations may be performed during a survey. In general, the measured  $C_E$  will differ but should be

within 10% of one another. If two successive measurements are very different, by more than 20% or so, the cause should be investigated because a malfunction of the equipment is indicated. Otherwise,  $C_E$  should be taken as the average of the two measurements before and after the relevant part of the survey. Some instruments (e.g. the Simrad EK500 and EK60 echosounders) have a calibrated output, meaning that the results of a particular calibration are applied internally before the data are recorded, and then  $C_E$  has a known standard value if the particular calibration is correct. Some adjustment of  $C_E$  is necessary, however, if later calibrations produce different results or there are other indications that the sounder settings were incorrect.

#### 9.4.1 Single species

The mean cross-section  $\langle \sigma_i \rangle$  may be determined directly from *in situ* measurements of target strength made during the survey. More usually it is derived from the size distribution of the insonified fish and a function which describes the length dependence of the target strength. There are other approaches involving complex scattering models as discussed in Chapter 6, but here we illustrate the procedure using a simple empirical formulation. This gives the mean target strength of one fish,  $TS_1$ , as a function of its length  $L$ :

$$TS_1 = b_i + m_i \log(L) \quad (9.8)$$

$b_i$  and  $m_i$  are constants for the  $i$ 'th species, assumed to be known from experimental evidence (Chapter 6). The equivalent formula for the backscattering cross-section is:

$$\sigma_i = 10^{(b_i + m_i \log(L) / 10)} \quad (9.9)$$

The appropriate mean is the average of  $\sigma_i$  taken over the size distribution of the insonified fish. Thus:

$$\langle \sigma_i \rangle = \sum_j P_{ij} 10^{(b_i + m_i \log(L_{ij}) / 10)} \quad (9.10)$$

Here  $L_{ij}$  is the midpoint of the  $j$ 'th size class and  $P_{ij}$  is the corresponding frequency, as deduced from the fishing samples by one of the methods described earlier (Section 9.3). The echo-integrator conversion factor is immediately determined as  $C_i = (C_E / \langle \sigma_i \rangle)$ . The calculation is repeated for any species whose target-strength function is known.

Note that it is the backscattering cross-section that is averaged, not the target strength. The arithmetic average of the target strengths calculated from Equ. (9.8) gives a different result which is incorrect. The term ‘mean target strength’ is often seen in the literature, but this is normally the target strength equivalent to  $\langle \sigma_i \rangle$ , namely  $10 \log(\langle \sigma_i \rangle)$ .

### 9.4.2 Mixed species

Sometimes two or more species are found in mixed concentrations and their marks cannot be distinguished on the echogram. The echo-integrals can be partitioned by reference to the acoustic data, with the mixture as one category separated from plankton etc. However, further partitioning to species level is possible by including the composition of the trawl catches (Nakken and Dommasnes 1975). Suppose  $E_m$  is the mean echo-integral of the mixture, and  $w_i$  is the proportion of the  $i$ 'th species, calculated as a weighted average of the catch compositions (see above). It is necessary to know the target-strength function and the size distribution of each species, from which  $\langle \sigma_i \rangle$  is determined as before, and  $C_i = (C_E / \langle \sigma_i \rangle)$ . The echo-integral contributed by each species is proportional to the product of  $w_i$  and  $\langle \sigma_i \rangle$ . Thus the partitioned echo-integrals are now:

$$E_i = w_i \langle \sigma_i \rangle E_m / \left( \sum_j w_j \langle \sigma_j \rangle \right). \quad (9.11)$$

The  $w_i$  are expressed as the proportional number or weight of each species, according to the units used for  $\langle \sigma_i \rangle$  and  $C_i$ . Consistent units must be used throughout the analysis, but the principles are the same whether it is the number of individuals or the total weight that is to be estimated. Note that  $E_i$  depends not only on the proportion of that species ( $w_i$ ) but also on the  $\langle \sigma \rangle$  values of all the species in the mixture.

### 9.4.3 Number–weight relationships

The abundance is expressed either as the total weight or the number of individuals in the stock. When considering the biological structure of the stock, it is convenient to work with the numbers at each age, whereas an assessment of the commercial fishing opportunities would normally be based on the weight of the optimum yield. Consistent units must be used throughout the analysis. So, if the abundance is required as a weight while the target-strength function is for individual fish, the latter must be converted to compatible units. This may be done directly from some estimate of the overall mean weight of the population. Alternatively, the target-strength function may be converted using a length–weight equation in the following manner.

For a fish of length  $L$ , the weight  $W$  is variable but the mean relationship is normally expressed as:

$$W = a_f L^{b_f} \quad (9.12)$$

where  $a_f$  and  $b_f$  are constants for one species. As before, the target strength of one fish is:

$$TS_1 = b_n + m_n \log(L) \quad (9.13)$$

The weight-based function  $TS_w$ , i.e. the target strength of 1 kg of fish, has the same form with different constants:

$$TS_w = b_w + m_w \log(L) \quad (9.14)$$

Since the number of individuals per unit weight of fish is  $(1/W)$ , the constant coefficients are related by the formulas:

$$b_w = b_n - 10 \log(a_f) \quad (9.15)$$

$$m_w = m_n - 10b_f \quad (9.16)$$

The CCAMLR survey of Antarctic krill (Demer 2004) is one application that employs  $TS_w$  rather than  $TS_1$  in the analysis, see Section 7.4 for further details. If required, the individual-based  $TS_1$  can be derived from  $TS_w$ , supposing the latter is the known or assumed function, by inverting the above formulas.

The weight-length relationship is non-linear. This must be taken into account when estimating the total weight from the numbers in discrete size classes. Suppose there are  $n_j$  individuals in the  $j$ 'th class,  $L_j$  is the mean length and  $\Delta L$  is the interval between successive classes. An unbiased estimate of the total weight is:

$$W_t = a_f \sum_j n_j \{ (L_j + \Delta L / 2)^{b_f+1} - (L_j - \Delta L / 2)^{b_f+1} \} / \{(b_f + 1)\Delta L\} \quad (9.17)$$

## 9.5 Abundance estimation

The analysis so far has produced for each EDSU of the cruise track, and for each species and depth-channel considered, an estimate of the mean density of the insonified fish. The next step is to determine the total abundance in the surveyed area. To do this, it is necessary to make some assumptions about the density of fish in places where there are no observations, in zones between the transects which have not been insonified by the acoustic beam. We have to consider the extent to which the observed densities along the cruise track are representative of the surveyed area as a whole. The abundance is calculated independently for each species or category of target for which data have been obtained by partitioning the echo-integrals. In the following discussion, we shall confine attention to the data relating to one species only.

It is an unfortunate fact that the densities observed during an acoustic survey sometimes include a few values much larger than most. It is tempting to ignore unusual observations on the grounds that they are unrepresentative in some way, but this is wrong. While it is reasonable to look for errors or equipment failure as a good cause for rejection, all valid observations should be included in the calculation of abundance, however unusual they may appear at first sight.

Once the total abundance has been calculated (either as numbers or biomass of fish), it may be partitioned according to biological characteristics such as length,

age, sex, maturity stage or indeed any combination of these. The calculations are straightforward if the biological sampling is suitably random. Then, the abundance in any stratum is partitioned in direct proportion to the fractions indicated by the biological samples. However, if the biological data were obtained using a stratified sampling scheme (e.g. by fish length), it is important to ensure that the raising procedures conform to the data collection method. The use of age and maturity data in this way is documented in Simmonds *et al.* (2003) and Anon (2004).

### 9.5.1 Spatial estimates and statistical concepts

Before proceeding, we must introduce a few statistical concepts. The fish density is a stochastic variable, one described by a statistical distribution whose mean is estimated as the average of a large number of measurements. The stochastic nature of the estimate comes from the movements of fish and, on a much finer scale, from the intrinsic variability of acoustic propagation and scattering (cf. Chapters 2 and 5). It is often found that fish tend to concentrate in some localities while they are scarce in others. This kind of spatial distribution is said to be contagious, as opposed to the fish being randomly and independently distributed in space, when the probability of a given density is the same everywhere. In either case, if the density at one position is observed over a period of time, the measurements will cover a range of values owing to the natural movement of fish within the local population.

Thus the observed densities are the result of a stochastic process which may depend on the location and time of the observations. This leads to the concept of stationarity. The process is said to be stationary if all the samples are drawn from the same statistical distribution regardless of time and position. If the statistical distribution changes with time or position, it is then described as non-stationary. This type of stationarity is quite distinct from a lack of mobility. Mobile fish concentrations may well have stationary statistical properties.

We shall now use the term probability density function (PDF) for the statistical distribution which controls the individual observations, to avoid confusion with the spatial distribution, which refers to the location of fish relative to one another. When the fish are randomly and independently distributed, the density PDF is stationary i.e. it has the same properties everywhere. When the distribution is contagious, stationarity depends on the mobility of the concentrations and whether they can occur anywhere. If the fish are in aggregations which can be found anywhere with equal probability, the density PDF is stationary. On the other hand, if the fish are expected to be concentrated in particular localities, inshore as opposed to offshore for example, and are expected to remain so for any realization (see below) of the stochastic process, the PDF is non-stationary. Paradoxically perhaps, when the fish concentrations are less mobile, the density PDF is less likely to be stationary (in the statistical sense).

It is important to understand what is meant by a ‘realization’ in this context. Suppose that surveys were to be conducted in 100 similar lakes. Each lake has the

same topographical features and depth profiles, but the hydrographic conditions and the weather may change. There are identical fish populations in all the lakes, but their mobility ensures that the actual spatial distributions are different. Each survey generates a set of estimates of the fish density at a number of chosen positions in one lake. This set is one realization of the stochastic process which describes the variability arising from the behaviour of the fish, environmental conditions, sampling error and measurement inaccuracy. The 100 surveys should be sufficient to reveal the statistics of this process, in particular whether it is stationary or not. The process is stationary if there is equal probability of finding fish in any part of a lake. However, if the largest concentrations are consistently found in one region but not another, in shallow but not in deep water for example, then the process is non-stationary.

The contagiousness of the distribution depends on the spatial scale of the observations. If a small area is being considered, the mean density might be similar at all points, but this would not be true of an area that is large compared to the size of the fish concentrations (Fig. 9.7).

The densities  $F_i$  recorded at positions along the cruise track are samples of the population in A, the whole area covered by the survey.  $\bar{F}$  is the arithmetic average of all the observations. If there is an equal probability of the fish being at each location,

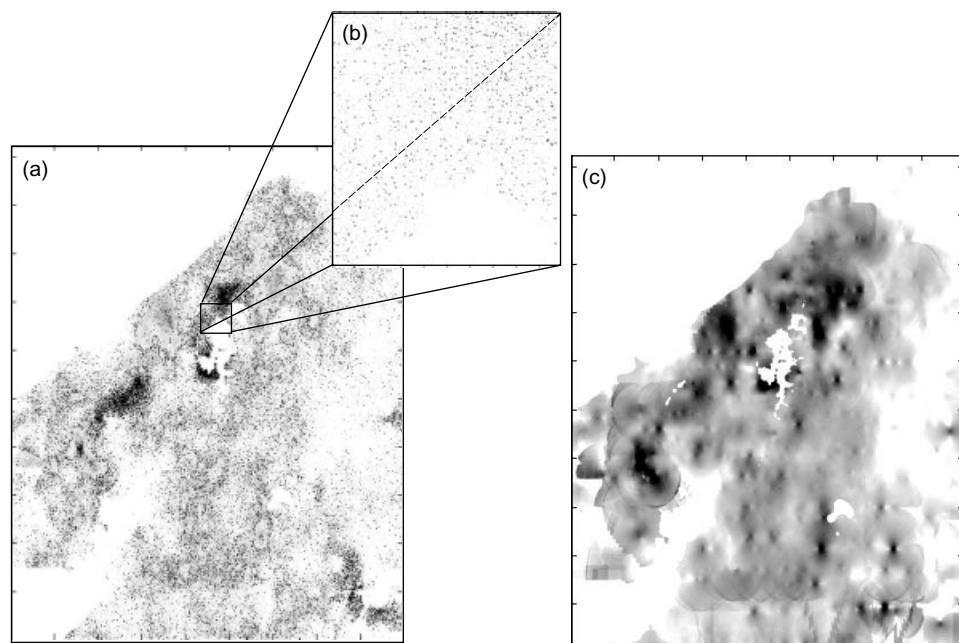


**Fig. 9.7** Spatial distribution of North Sea herring. (a) The full spatial distribution of schools simulated on a 40 m grid, (b) detail showing the small fraction of the area occupied by fish and (c) a map constructed from a simulated survey of (a) showing a smoothed representation of observed fish densities. The latter represents more the probability of fish presence rather than the true distribution.

$\bar{F}$  is an unbiased estimate of the mean density applicable to area A, and an estimate of the total abundance follows immediately as  $\bar{F}$  times the area of A. However, when the distribution is contagious,  $\bar{F}$  although unbiased is not necessarily the best estimator, that is to say it could be very different from the true mean density. To obtain the best estimate, the one likely to be closest to the true value, we must once again consider dividing the surveyed area into strata within which the abundance may be estimated with confidence. These analysis strata are not necessarily the same as the regional divisions considered in the survey design, which allowed for some regions to be sampled more intensively than others, nor those based on the composition of catches that were adopted for the calculation of the conversion factors. It is important to ensure that analysis strata with different levels of survey effort are dealt with separately. While the stratification required for the abundance estimation should take account of the regional boundaries defined earlier, it is likely to be on a smaller scale. Each survey region may be further divided into several analysis strata. Various methods have been employed to estimate the abundance by stratification of the surveyed area, as described below. As a general principle, the analysis strata should comprise the largest non-overlapping contiguous sub-areas such that the density PDF within each sub-area is stationary.

Spatial correlation is another statistical feature that has a bearing on the analysis. When the distribution is contagious, the mean density shows strong local correlations over the surveyed area, meaning that the densities observed at two nearby points are more likely to be similar than those at positions far apart. Thus the sequence of measurements along the cruise track may be serially correlated, which means that the probability of observing  $F_i$  depends on the actual densities close by. Serial correlation may be illustrated by considering the case of a highly contagious population, one in which the fish occur in a few dense concentrations with much empty water in between. The measurement sequence contains strings of consecutive zeros corresponding to the sections of cruise track crossing empty water. Now suppose that the survey is in progress and that a measurement has just been made. If the result is  $F = 0$ , the probability that the next result will be the same is higher than the proportion of zeros in all the measurements. The presence of correlation does not affect the estimate of abundance, provided the cruise track has been designed to give samples which can reasonably be considered as representative of the area in question, but it is important in estimating the variance and the sampling error. We shall return to this problem in Section 9.6.

### 9.5.2 Contour and distribution maps

Figure 9.4 illustrated the raw data from an acoustic survey as a simple bubble plot, and this involved no assumptions about the densities at locations off the track. The distribution of fish in the surveyed area may also be displayed as a contour map. The contours are curves connecting points of equal density, and when they are drawn on a map it is easy to see where the major concentrations of fish are located (Fig. 9.8).

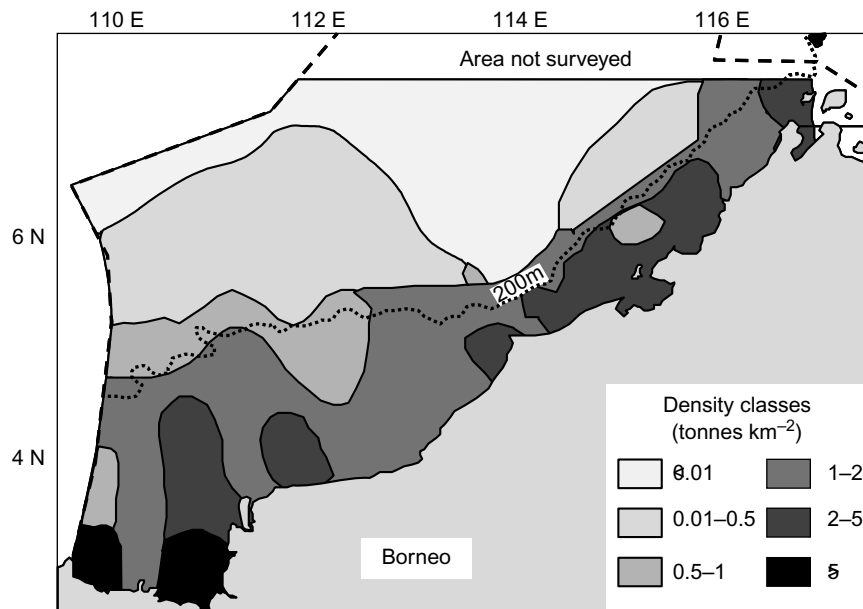


**Fig. 9.8** Contour map of the fish density from an acoustic survey off Borneo, showing higher densities on the continental shelf than in the deeper water.

However, to construct a contour map requires information or assumptions about the spatial statistical properties of the abundance at unsampled locations between the transects.

The contours are constructed by reference to a grid derived from the observed densities along the cruise track. Each observation should be located at the mid-point of the corresponding EDSU. Thus we begin with a number of observations at known positions on a map. It is then necessary to estimate density values on a grid. Gridding is the process of interpolating between the original observations, to deduce the likely densities at regularly-spaced positions. This process is best done using specialized software such as the Surfer package (Golden Software). The choice of gridding method may have a considerable impact on the appearance of the contour map. One of the best methods is kriging which selects an appropriate gridding function according to the spatial properties of the data (Rivoirard *et al.* 2000). Once the grid is created, the contours may be easily constructed as continuous curves on the map.

In principle, the abundance could be determined from the contour map. This is the post-sampling stratification method described by Johannesson and Mitson (1983). In essence, the echo-integrator data are used to define the strata. This approach is an unnecessarily complicated way of deriving an abundance estimate. Post-sampling stratification is not recommended for this purpose. It suffers from fundamental theoretical problems to do with the fact that the same data are used to define the strata

and to calculate the abundance. The measurements cannot be considered as random samples from a defined population because the boundaries of the strata are partly determined by the stochastic variation of the observed densities. Near the boundaries, the measurements are likely to be assigned to the stratum containing the values which are most similar. Thus the apparent variance within each stratum is less than it would be if the boundaries were fixed. Furthermore, the estimated abundance is sensitive to the choice of contour levels and may be biased. It is difficult, if not impossible to determine confidence limits on the abundance estimates obtained by post-sampling stratification. To avoid these problems, it is essential that the strata should be selected by criteria that are independent of the acoustic measurements.

Contouring is most useful as a means of visualizing the important features of fish concentrations. It works best for contagious distributions in which the spatial variations are stronger than the random changes in time. However, contours express more the estimated probability of encountering concentrations in an area rather than the distribution one would expect from actual observations. Various methods have been suggested for constructing density maps from the observations. Brierly *et al.* (2003) propose a Bayesian method; however, this is computationally very demanding and so far has only been used on small data sets. They produced illustrations that reflect local density patterns, but because of the sparse grid are rather like contour maps. Then there is conditional simulation (Gimona and Fernandes 2003; Simard *et al.* 2003) which is a good method for providing plausible abundance distributions based on the survey data. Rather than providing only one outcome, the conditional simulation honours the observations and provides any number of possible realizations that might be valid. Thus, at locations away from any observation, the simulation provides probability distributions of abundance rather than fixed values. These methods work best with smooth PDFs with few zero values. More complex modelling techniques are required for mapping density distributions that include a substantial proportion of zero observations.

For mapping purposes, the method used should reflect the user's requirements: the contour map shows the probability of encountering a particular concentration, while the conditional simulation provides one or more distributions that could occur in reality.

### 9.5.3 Estimation with a rectangular grid

A simple method of stratifying the surveyed area, to provide both an overall abundance estimate and a spatial distribution, is to divide it by equally spaced lines of latitude and longitude (Dalen and Nakken 1983; Simmonds and MacLennan 1988). The strata are the rectangles formed by the intersections of the latitudinal and longitudinal lines. Johannesson and Mitson (1983) refer to this type of stratum as the 'elementary statistical sampling rectangle' or ESSR. The cruise track must pass through each rectangle at least once, which dictates the minimum size of the ESSR. In the case of surveys for herring in the North Sea, it has been found that satisfactory

results are obtained with a rectangular grid spaced at intervals of  $0.5^\circ$  in longitude and  $0.25^\circ$  in latitude. Thus the ESSR is approximately square with a side-length of 26 km, and there are about 100 ESSRs in the surveyed area.

One sample of the fish density is obtained from each EDSU along the cruise track. Suppose there are  $n_k$  samples in the  $k$ 'th ESSR ( $k = 1$  to  $M$ ).  $F_{jk}$  is the  $j$ 'th sample and  $A_k$  is the area of the ESSR which may contain fish.  $A_k$  is not necessarily constant, because part of the ESSR may coincide with islands or the coast or the area may reduce in a northerly direction if the grid is defined in latitude and longitude. The total abundance  $Q$  is estimated from the average density within each ESSR multiplied by the corresponding area.

$$Q = \sum_{k=1}^M \left( A_k \sum_{j=1}^{n_k} F_{jk} / n_k \right) \quad (9.18)$$

The rectangular grid method has a particular advantage in that the geographical basis of the strata allows easy mapping, and the calculations are straightforward.

Anderson and Kirkegaard (1985) have suggested that geographical strata might be bounded partly by depth contours instead of latitudes or longitudes. This approach should be advantageous if different fish densities, size or species compositions are expected according to the water depth. Equation (9.18) is still applicable provided  $A_k$  is the correct area for the  $k$ 'th stratum, whatever type it is.

#### **9.5.4 Transform methods**

The PDF of the fish density is often positively skewed, which means that a large proportion of the observations yield small values, resulting in the characteristic histogram shown in Fig. 9.9. This type of PDF is very different from the symmetrical normal or Gaussian probability function on which much of sampling theory is based. If  $\mu$  is the true mean and  $\sigma^2$  is the true variance of  $F$ , the Gaussian PDF is:

$$P(F) = \exp\{-(F - \mu)^2 / 2\sigma^2\} / \sqrt{2\pi\sigma^2} \quad (9.19)$$

For any stationary PDF, the sample mean and variance (calculated from the observations) are unbiased estimates of the true mean and variance, respectively. But when the PDF is not Gaussian, these estimators although unbiased are not the most precise. They are subject to stochastic variation which may be very large.

More efficient estimators can be derived if the PDF is known. The principle behind this idea is that a new data set is conceived as a one-to-one transformation of the original observations, such that the new PDF is Gaussian. Statistical theory is applied to deduce new estimators of  $\mu$  and  $\sigma^2$  which are more accurate than the original sample mean and variance, respectively.

The first step is to determine the appropriate transformation. It is sufficient for practical purposes to consider only the class of power transformations  $Z_i = (F_i^\Theta - 1)/\Theta$  for  $\Theta$  in the range 0 to 1. The limiting case  $\Theta = 0$  is equivalent

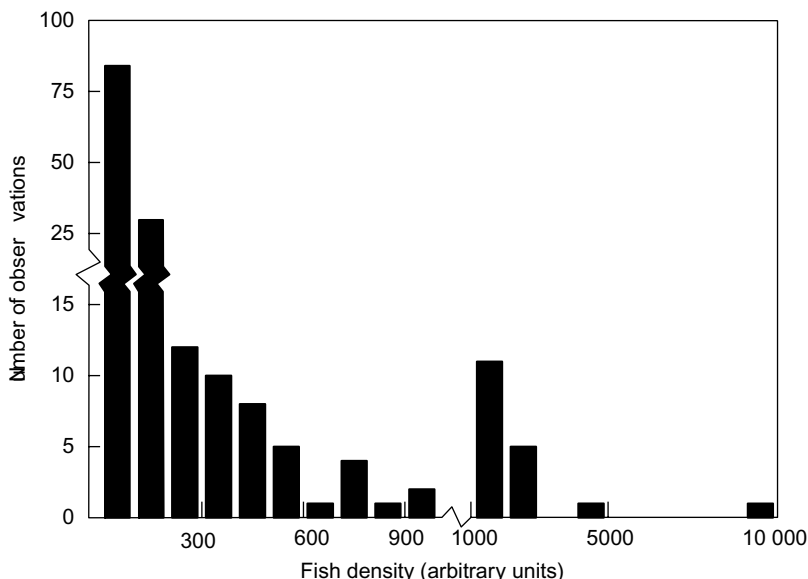


**Fig. 9.9** Histogram of fish densities  $F$  recorded during a herring survey in the North Sea. The class intervals are 100 for  $F < 1000$  and 1000 for  $F > 1000$ . The distribution is positively skewed, most of the values being below the average.

to the log-transform  $Z_i = \ln(F_i)$ . The most likely value of  $\Theta$  may be determined from a test devised by Box and Cox (1964). Estimators for the special cases  $\Theta = 0, 1/6, 1/4, 1/3$  and  $1/2$  have been described by MacLennan and MacKenzie (1988). As far as we know, estimators have not been derived for an arbitrary value of  $\Theta$ , but in practice it is good enough to work with those for which  $\Theta$  is closest to the value indicated by the Box–Cox test.

The transform theory assumes that the samples are drawn from a stationary PDF which is zero for  $F \leq 0$ . Further complications arise when the fish distribution is contagious to the extent that there is a finite probability of observing  $F = 0$ . Aitchison (1955) and Pennington (1983) have considered this problem. It is supposed that the fish occur in patches with empty water in between, but the density PDF is stationary within each patch. Aitchison's method treats the zero values and the others as samples from different PDFs, and the estimators are modified to take account of the proportion of zeros in the data.

In principle, the transform method should provide the best estimates of mean and variance, those most likely to be closest to the true values. However, the method depends on the density PDF being known, and the PDF must be unimodal. If the estimators for the wrong PDF are applied, the results will be biased to an uncertain extent. The contagion which is often a feature of the fish distribution is another practical problem. The transform method is not suitable for contagious distributions unless they conform to the assumptions of Aitchison's technique.

### 9.5.5 Geostatistics

Geostatistics is a family of analytical techniques that covers the mapping, interpolation and variance estimation of a population based on a set of density observations at points within the surveyed area (Matheron 1971; Cressie 1993). Among these, kriging is a powerful interpolation technique which can be used to calculate a surface representing the spatial variation of the expectation of the density. Originally developed for surveys connected with mining operations, hence the commonly adopted term ‘geostatistics’, the merits of this approach were reviewed by an ICES Study Group (Anon 1993) which concluded that the concept was well suited to acoustic observations of fish populations. Essentially, the correlation between samples is interpreted as a property of the underlying process and not of the observation method. In other words, if correlation is observed, this is because the fish population is correlated in space. The observation method (i.e. the echo-integration) provides independent samples along the track (at intervals such that beam overlapping between samples is unimportant) and is capable of responding to very rapid changes in density. Petitgas (1993) has reviewed various applications of geostatistics. Rivoirard *et al.* (2000) present a detailed overview of the theory and a number of examples applied to acoustic survey data along with useful practical guidelines.

The geostatistical technique is based on the variogram. This is a graph of the covariance of paired samples,  $\gamma$ , plotted against the distance  $D_v$  between the sampled locations. If  $(F_i, F_j)$  is the set of paired samples for a given  $D_v$ ,  $\gamma$  is the expected value of  $((F_i - F_j)^2/2)$ . Strictly speaking,  $\gamma$  is the semi-variogram function, but the prefix ‘semi’ is often omitted as we do here. Some examples of variograms derived from fishery data are shown in Fig. 9.10.

When the fish distribution is contagious, the covariance of observations paired at closely spaced points is less than that of the data set as a whole. Thus,  $\gamma$  increases monotonically with  $D_v$ , and for large  $D_v$  it approaches the sample variance of all the observations. A curve is fitted to the empirical  $\gamma$  values in the variogram, and the shape of this curve indicates the spatial characteristics of the fish distribution. If  $\gamma$  remains finite as  $D_v$  tends to zero, this is called the ‘nugget effect’ which implies that there may be two causes of variation. The intercept at  $D_v = 0$  gives the local or point variation caused by measurement error or some very fine spatial variation, and the curve for  $D_v > 0$  describes the broader-scale spatial structure. The size of the nugget effect compared to the sample variance indicates which is the more important cause of variation. To estimate the abundance, the area represented by each sample is calculated, taking account of the other observations in the vicinity and their distance from the point in question. The geostatistical approach does not require the samples to be statistically independent. The effect of serial correlation is explicitly accounted for in the calculations, thus the variance of the abundance estimate is determined without bias.

Over the past decade there has been substantial progress in applying geostatistics to the analysis of acoustic surveys. This technique is now accepted as a reliable way

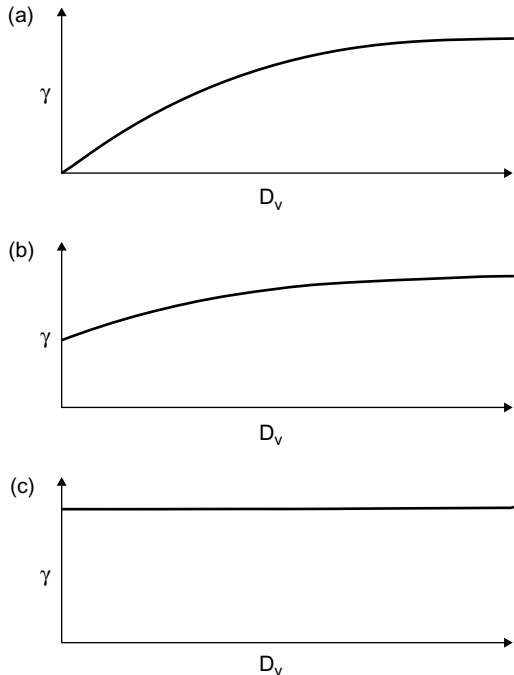


**Fig. 9.10** Examples of variograms.  $\gamma$  is the covariance between fish densities observed at locations separated by a distance  $D_v$ . (a) Contagious distribution,  $\gamma(0) \rightarrow 0$ ; (b) the nugget effect,  $\gamma(0) > 0$  showing some randomness even at a very small scale; (c) a completely random distribution,  $\gamma$  is now independent of  $D_v$ .

to construct contour maps and for estimating the sampling variance when the survey design is not strictly random. The method works best for fish populations having a spatial structure which does not change with time, meaning that the population should be non-mobile. Rivoirard *et al.* (2000) examined the impact of random fish movement on the estimates of variance. They concluded that any effect on the estimate of variance would be negligible. However, if the spatial distribution changes on the time scale of the survey, due to migration of the fish for example, the result will be biased (as would be the case with any classical estimation method). Geostatistical methods have important advantages for the analysis of variance. As far as the abundance estimate itself is concerned, kriging is not particularly sensitive to the assumed form of the variogram, and for uniform survey designs the geostatistical abundance estimate is little different from that obtained by traditional methods.

## 9.6 Precision of the abundance estimate

The densities recorded during an acoustic survey relate to the particular fish detected by the echosounder. We suppose that the stock inhabits a certain volume of water, but only those fish which encounter the acoustic beam are detected. The error in the abundance estimate may be considered as the sum of two components, firstly the sampling error (precision) caused by the measurements being stochastic samples of

the true mean density, and secondly the systematic error (bias) which affects all the observations equally, such as the error in an assumed value of the target strength. The insonified proportion of the total volume indicates the sampled fraction of the stock. This might be as small as 0.01% for a stock spread over a large area of ocean, and seldom exceeds 2% even for small lakes. Estimating the whole population from these samples thus involves some degree of uncertainty. However, it is not the proportion sampled that primarily determines the precision, rather it is a combination of the survey design, the spatial structure of the population and the inherent variability in the densities encountered. In this section we discuss the sampling error and how it can be determined. The magnitude and sources of systematic errors are discussed in Section 9.8.

### 9.6.1 *Repeated surveys*

Suppose that a number of independent surveys have been made of the same stock, by using several ships at the same time or conducting successive surveys of the same area with one ship. There are  $N$  surveys and the abundance estimates are  $Q_1, Q_2, \dots, Q_N$ . If these estimates are believed to be equally precise, the best estimate making use of all the data is the arithmetic average,  $\bar{Q}$ .  $s^2$  is the variance of a single survey and SE (the standard error) is the standard deviation of  $\bar{Q}$ . The well known formulas for these statistics are:

$$\bar{Q} = \sum_{j=1}^N Q_j / N \quad (9.20)$$

$$s^2 = \sum_{j=1}^N (Q_j - \bar{Q})^2 / (N - 1) \quad (9.21)$$

$$SE = s / \sqrt{N} \quad (9.22)$$

It is convenient to describe the precision in terms of confidence limits on the best estimate. The result is given as a statement that  $Q$  is expected to lie in the interval  $(\bar{Q} - t \cdot SE)$  to  $(\bar{Q} + t \cdot SE)$ . The multiplier  $t$  depends on  $N$  and the confidence level. If the PDF of  $Q_j$  is Gaussian (normal),  $t$  is the appropriate percentile from Student's t-distribution. There are  $(N - 1)$  degrees of freedom, and the values given in Table 9.1 are used to determine the confidence limits. It is reasonable to assume normality in this instance, since each abundance estimate is obtained from the average of many density measurements. The central limit theorem provides that whatever the PDF of one observation, the average of many has a PDF much closer to the Gaussian distribution.

There are few reports in the literature of the precision being determined by repeated surveys. Stromme and Saetersdal (1987) have described work on tropical stocks of *Sardinella* spp. The results of independent surveys were generally within 10% of the average. Bailey and Simmonds (1990) compared two surveys conducted

**Table 9.1** Percentile values from Student's t-distribution for various degrees of freedom and levels of confidence.

Degrees of freedom	Confidence level		
	90%	95%	99%
1	6.31	12.71	63.66
2	2.92	4.30	9.92
3	2.35	3.18	5.42
4	2.13	2.78	4.60
6	1.94	2.45	3.70
8	1.86	2.31	3.35
10	1.81	2.23	3.17
15	1.75	2.13	2.95
20	1.72	2.09	2.84
30	1.70	2.04	2.75
$\infty$	1.64	1.96	2.58

by different research vessels working independently but concurrently in the same area of the North Sea. The abundances of herring found by the two vessels differed by 10%. More recently, Wanzenböck *et al.* (2003) made repeated surveys of several lakes. They found the best consistency when the same type of echosounder was used by two different teams, but there was also good agreement between surveys using two systems that had different performance specifications. These results suggest that the precision of a properly designed acoustic survey can be extremely good. However, the cost of repeating the survey several times is often prohibitive. It is normally the case that only one survey of an area can be accomplished in the time available. The precision must then be estimated by reference to the data collected during the one survey, by analysis of the variations observed along the cruise track.

### 9.6.2 Stratified random transects

The analysis of precision is greatly simplified when the survey has been designed as randomly positioned parallel transects. Jolly and Hampton (1990) recommend this approach because simple statistical theory can be applied without too many assumptions, and in particular there is no need to worry about spatial correlation. However, Simmonds and Fryer (1996) maintain that strictly random sampling is not always ideal. In their analysis of North Sea herring surveys, estimates of both the abundance and the precision were shown to improve with more structured designs. Nevertheless, the stratified random design may be advantageous in some circumstances. If the survey area has been stratified into regions by the survey design, the random positioning of transects is done independently for each region. The mean density observed along the whole length of a transect is considered as one sample. Suppose there are  $M$  regions. In the  $i$ 'th region whose area is  $A_i$ , there are  $n_i$  transects and the density samples are  $F_{ji}$  for  $j = 1$  to  $n_i$ . The abundance  $Q_i$  in this region and its

variance  $V_i$  are estimated as:

$$\hat{Q}_i = A_i \sum_{j=1}^{n_i} F_{ji} / n_i \quad (9.23)$$

$$\hat{V}_i = \sum_{j=1}^{n_i} (A_i F_{ji} - \hat{Q}_i)^2 / \{n_i(n_i - 1)\} \quad (9.24)$$

The total abundance and its variance are obtained by summing the results for each region:

$$\hat{Q} = \hat{Q}_1 + \hat{Q}_2 + \hat{Q}_3 + \dots + \hat{Q}_M \quad (9.25)$$

$$\hat{V} = \hat{V}_1 + \hat{V}_2 + \hat{V}_3 + \dots + \hat{V}_M \quad (9.26)$$

The standard error of  $\hat{Q}$  is the square root of  $\hat{V}$ . The confidence limits are once again determined by the standard error and Student's t parameter, the degrees of freedom in this case being the total number of transects less the number of regions. If the design is non-random, however, this method is not rigorous and the predicted confidence limits may be quite wrong.

### 9.6.3 Geostatistical variance

As discussed above, geostatistics is a powerful method for estimating the precision of survey results. The method takes account of the shape of the surveyed area, the sampling design, and the variability of the fish density including spatial correlation. Specialized applications have been reported by Conan *et al.* (1988), Petitgas and Poulard (1989), Petitgas (1990), Simard *et al.* (1993), Williamson and Traynor (1996) and Fernandes and Simmonds (1997). The estimation variance may be calculated from the variogram, examples of which are shown in Fig. 9.10. The formulas for estimating the variance are rather complicated, see Rivoirard *et al.* (2000) for details. Here, we shall avoid the maths and try to explain in a few words how a geostatistical estimation variance is derived.

Suppose a survey has been done of the population in an area A. Samples of the fish density have been collected at a (finite) set of points  $P_{\text{sam}}$ . We also have  $P_{\text{all}}$  which is the (infinite) set of points that includes all the possible locations (both sampled and unsampled) in A. The variogram is constructed from the observed covariances ( $\gamma$ ) between paired points in  $P_{\text{sam}}$  as a function of their distance apart. The curve fitted to the observed  $\gamma$  is assumed to represent the covariance between any point pair in  $P_{\text{all}}$ . The estimation variance is formulated as sums of point-to-point comparisons within and between  $P_{\text{sam}}$  and  $P_{\text{all}}$ . This takes account of the variance of the actual  $P_{\text{sam}}$  locations and the boundaries (shape and area) of A. The survey designer can decide the number and locations of the  $P_{\text{sam}}$ , subject to the constraints discussed in Chapter 8. Thus, repeated calculations of the geostatistical estimation

variance is a convenient way to evaluate the performance of different hypothetical survey designs. Petitgas and Lafont (1997) have provided a geostatistical software package, EVA2, designed for fishery applications. In particular, EVA2 calculates the estimation variance applicable to acoustic survey data. However, this package is only suitable for small areas with few samples, and is best used on a stratum-by-stratum basis.

The geostatistical estimation variance is particularly useful as a description of the survey precision because it allows for any design and any shape of area. It provides a variance that changes appropriately with different areas, survey designs and spatial features of the fish population.

#### **9.6.4 *The degree of coverage***

Another approach is to look for a systematic relationship between the sampling error and the fraction of the stock which has been observed. It may be argued intuitively that the greater the sampling intensity, in terms of the length of cruise track in a particular area, the better the results should be. Aglen (1983; 1989) investigated the precision of surveys made in different circumstances, from confined fjords to large areas of open sea, and in tropical as well as temperate waters. He defined the degree of coverage, a measure of the sampling intensity, to be  $\Lambda = D/\sqrt{A}$  where  $D$  is the total length of the cruise track and  $A$  is the size of the surveyed area. For each survey, Aglen determined the precision of the abundance estimate by comparing results derived from subsets of the transects. Thus every second transect might be used to obtain one estimate, and the intervening transects to provide another. In effect, the two interleaved sets of transects are considered as though they had been covered by different vessels, and the difference between the two results (assumed to be independent estimates of the same stock) is an indication of the sampling error. As a measure of the precision, Aglen used CV, the coefficient of variation which is the standard error of the abundance estimate divided by the mean. The results illustrated in Fig. 9.11 suggest that CV depends on the degree of coverage through a power law of the form:

$$CV = a(D / \sqrt{A})^b \quad (9.27)$$

The coefficients  $a$  and  $b$  may be determined from the function which best fits the results obtained from many surveys. Aglen found that  $b$  is close to  $-0.5$ , the theoretical value predicted on the assumption that the transects provide independent samples. The value of  $a$  is more variable, between  $0.4$  and  $0.8$ . It is reasonable to suppose that  $a$  depends on the contagion of the fish distribution. Higher values of  $a$  would be appropriate in the case of fish concentrated in a few large schools, as opposed to the more uniform distribution of scattering layers.

Another useful conclusion from Aglen's work is that when the degree of coverage is more than  $6$ , the sampling error in the abundance estimate has a PDF which is

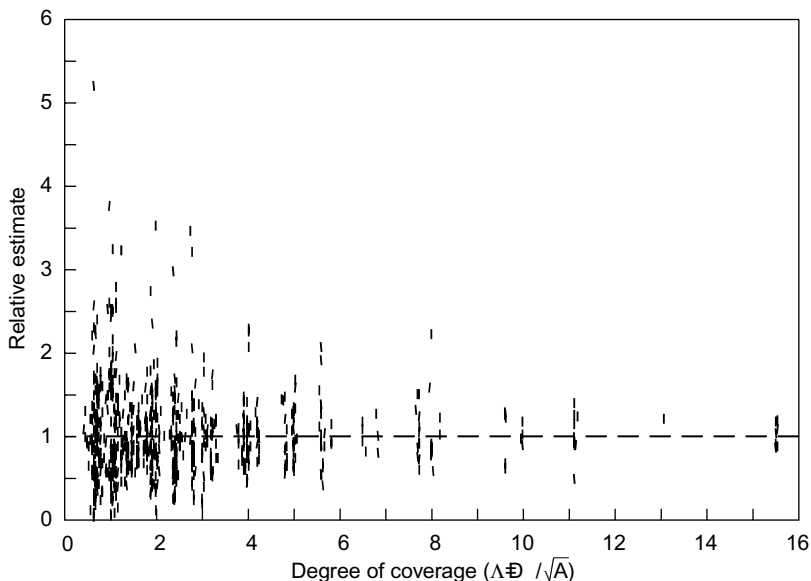


**Fig. 9.11** Variation of the abundance estimate vs the degree of coverage (track length divided by the square root of the area covered). Each point is the ratio of one estimate to the mean of several. (Redrawn from Aglen 1989.)

close to the Gaussian (Fig. 9.12). This simplifies the calculation of confidence limits when  $D$  is large enough.

Kimura and Lemberg (1981) support the use of  $\Lambda = D/\sqrt{A}$  as the determinant of CV, but Francis (1985) suggests that  $D/A$  is more appropriate. To compare the two measures, consider what happens if we combine the results from two surveys conducted in adjacent waters, each covering the same size of area and having the same track design. In the combined survey,  $D$  and  $A$  have each increased by a factor of two. Thus  $D/\sqrt{A}$  has increased by  $\sqrt{2}$ , but  $D/A$  remains the same. If the two surveys have shown abundances  $Q_1$  and  $Q_2$ , the result of the combined survey is  $Q = Q_1 + Q_2$  and the variances are similarly additive (provided they are independent). Thus the combined survey should produce results with a reduced CV. This suggests that  $D/\sqrt{A}$  is the more useful measure, at least for the calculation of confidence limits, since any predictive formula requires a measure of the sampling intensity which changes under circumstances which alter CV.

According to Cochran (1977), the precision depends on  $N$ , the number of independent samples collected from a population of size  $N_0$ , and the sampled fraction  $N/N_0$  is unimportant if  $N_0$  is large. Aglen's interpretation of  $D/\sqrt{A}$  as the sampling intensity may therefore be misleading. Alternatively, we can say that  $N = D/D_I$ , where  $D_I$  is the minimum EDSU which gives independent samples.  $D_I$  may depend on  $A$ , because larger areas are more likely to exhibit contagious distributions. But whatever the explanation, Equ. (9.27) is an empirical result which is helpful in

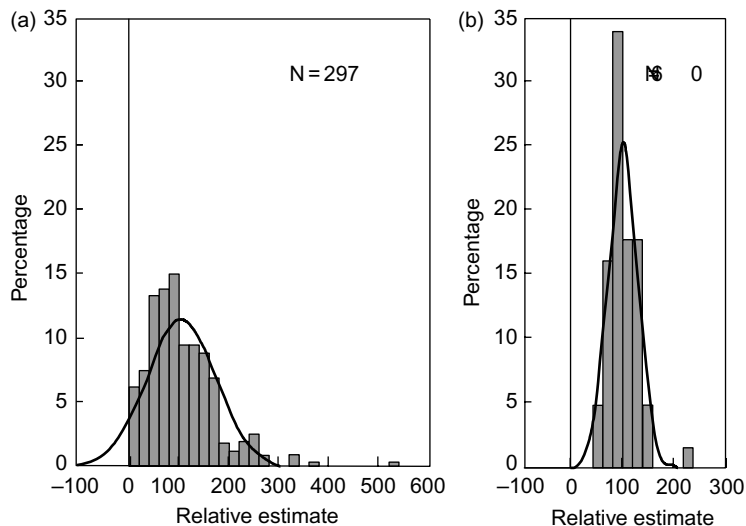


**Fig. 9.12** Histograms of the estimated abundance as a proportion of the true value for degrees of coverage (a)  $\Delta < 2$  and (b)  $\Delta > 6$ . The curves are fitted Gaussian functions. The fit is poor when  $\Delta$  is small. (Redrawn from Aglen 1989.)

designing the survey, since it indicates the track spacing necessary to achieve a given precision.

### 9.6.5 Bootstrap or resampling methods

The bootstrap or jack-knife technique (Efron and Tibshirani 1986) is another approach to the problem of estimating variance. This has been applied to acoustic data by Robotham and Castillo (1990) and Simmonds (2003). The PDF indicated by the observed densities is resampled using a random number generator to produce new sets of simulated data with the same number of samples as were originally collected on the survey. The abundance is estimated for each set and confidence limits are obtained in the manner described for repeated surveys (p. 356). As regards the estimated variance, however, it is implicitly assumed that the sampling design is random. The bootstrap takes no account of the spatial distribution, and each observation is treated as a sample from a stationary PDF. Thus, if there is spatial correlation and the sampling design is non-random, the estimated variance will be wrong. The geostatistical estimation variance described in the previous section does not have this problem. Nevertheless, in some circumstances there are advantages in bootstrapping, because not only the variance but also the PDF may be estimated, and by including catch data within the resampling scheme a more complete analysis of the survey error is possible. Simmonds (2003) showed how a bootstrap analysis of an acoustic survey could be extended to include the correlated errors in the estimation of fish abundances

by age classes. The ability to include correlated errors from different sources is a considerable advantage of the bootstrap technique.

### **9.6.6 *Relative importance of various random errors***

Apart from the primary sampling error associated with the survey design, there are several other factors which cause additional variability in the abundance estimates. It is the total variability that matters and it is important to understand the relative significance of different sources of error. An ICES Working Group (Anon 1998a) considered this problem and concluded that the main sources of variability in acoustic surveying were as follows. They are listed in descending order of importance:

- variation in the mean target strength over the surveyed region;
- species discrimination through echo-integral partitioning;
- diurnal variability affecting fish distribution and target strength;
- spatial sampling error;
- sampling echogram marks by fishing to provide species proportions;
- sudden changes in fish distribution and behaviour due to events such as storms.

This list is a very general guide and is not intended to be exhaustive. The important errors in a particular application might be ranked differently, depending for example on local features of the fish behaviour, species mix and other circumstances. There is an extensive literature which can be consulted for more specific advice on error evaluation. Hazen and Horne (2003) have reviewed the biological causes of target strength variability in a broad range of teleost fishes, see also Kloser and Horne (2003) for a similar study of some deepwater species that do not have air-filled swimbladders, in particular the orange roughy.

Massé and Retiere (1995) and Petitgas *et al.* (2003) consider the errors in echo-integral partitioning when this is done directly (from the echogram) or with reference to the species proportions in trawl hauls. O'Driscoll (2003) describes a model-based partitioning technique which is useful for more complex species assemblages. There are many publications on spatial sampling errors. This topic was addressed in Chapter 8.

Marchal and Petitgas (1993) evaluated the precision of an acoustic survey of sardine. They separately estimated the number of schools and the mean biomass-per-school which were multiplied to obtain the total abundance, and found that the variance of the biomass-per-school was the dominant source of error, while the number of schools could be estimated rather precisely. The underlying problem was the highly skewed distribution of the biomass-per-school. Marchal and Petitgas compared their results with those from MacLennan and MacKenzie (1988) for North Sea herring. Although the latter analysis did not explicitly address spatial correlation in the fish distribution, the conclusions were the same. Thus, in the case of schooling fish, it may generally be true that it is the mean school biomass, not the count of schools per unit area, that dominates the spatial sampling error in the abundance estimate.

## 9.7 Sources of systematic error

So far we have restricted attention to the random error in  $\hat{Q}$  caused by the sampling strategy among other factors. Before the overall accuracy of  $\hat{Q}$  can be assessed, we must include the systematic errors, those that equally affect all the observations and result in  $\hat{Q}$  being a biased estimate of the abundance. Unlike the random error, the bias cannot be reduced by collecting more samples. Here we discuss various sources of the systematic errors liable to occur in acoustic surveys. The target strength is an important factor in this context.  $\hat{Q}$  is inversely proportional to  $\langle \sigma_{bs} \rangle$ , thus any error in the assumed value of  $\langle \sigma_{bs} \rangle$  biases all the observed densities and the abundance. However, the target strength and its determinants have been considered exhaustively in Chapter 6 and elsewhere in this book, and need no further discussion here.

### 9.7.1 Equipment sensitivity

According to Equ. (9.7), the estimated density is proportional to the calibration factor  $C_E$  which describes the physical performance of the echosounder and the echo integrator.  $C_E$  is determined by measuring the signal from a standard target (cf. Chapter 3). The measurement error in  $C_E$ , and any change which occurs between the time of the calibration and the survey, has the same proportional effect on all the density observations and thus contributes to the bias in the abundance estimate.

If the calibration is performed carefully in accordance with the recommended procedure, the precision of  $C_E$  is very good. For scientific echosounders operating in the 30–50 kHz range, Foote *et al.* (1987) say the measurement error in  $C_E$  should be less than 4%. As regards changes in the longer term, Simmonds (1990) examined the calibration history of a 38 kHz Simrad EK400 echosounder and found that  $C_E$  varied by less than 7% over a 5-year period. There is general agreement that this level of precision is achievable, with a few exceptions e.g. Tesler (1989) who found greater variability in his results. We consider that in fishery applications, low-frequency scientific echosounders when properly maintained can perform consistently within 10% in the long term, and they can be calibrated to even better precision. Results at higher frequencies (e.g. 120 kHz) have generally been less good. Little information has been published on the long-term performance of higher frequency echosounders, though Anon (1998a) suggests that inconsistent performance is due to some types of transducer being insufficiently stable, or it may simply be associated with the water temperature and salinity differences encountered in various applications, e.g. between temperate and arctic conditions.

### 9.7.2 Transducer motion

Because of the finite time between the transmitter pulse and the reception of echoes, any movement of the transducer degrades the amplitude of the received signal.

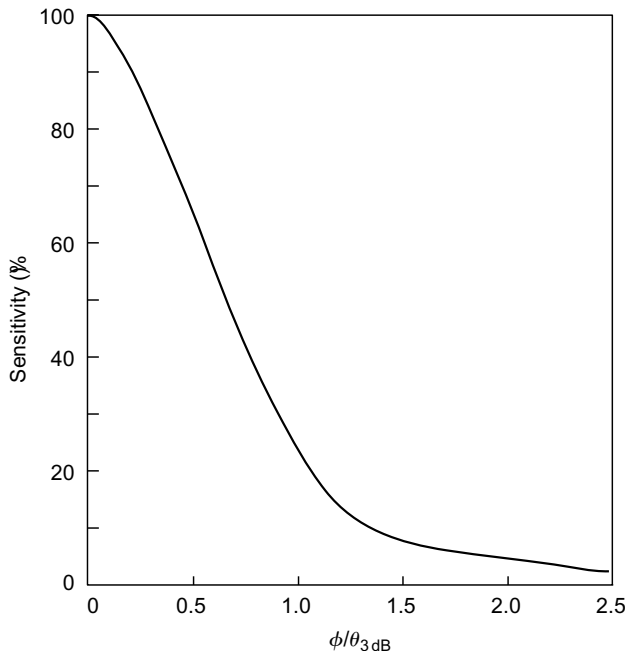


**Fig. 9.13** Reduction of the combined transmit–receive sensitivity (echo intensity) resulting from a rotation  $\phi$  of the transducer (in pitch and/or roll angles) during one ping insonifying randomly distributed targets.  $\theta_{3\text{dB}}$  is the beam width at the  $-3\text{ dB}$  points of the beam pattern.

The transducer moves forward with the vessel, and it also pitches and rolls, so the angular motion is more severe in bad weather. In consequence, there is some fluctuation of the received signal, but more importantly the mean amplitude is reduced. This bias occurs due to the change in the target direction as seen from the transducer (Stanton 1982). In effect, the transmitting and receiving beam patterns have been misaligned by the angle  $\phi$  which is the change in the target direction between transmission and reception. For the same motion, the bias depends on the beam pattern, being greater for narrow-beam transducers (Fig. 9.13).

In the case of pitch and roll,  $\phi = \phi_a$  is simply the angle turned in the time delay of the echo. Thus  $\phi_a$  is proportional to  $\omega_t$ , the rotation rate of the transducer, and it increases with the range of the target. The component owing to the forward motion,  $\phi_f$ , does not depend on the range. When the transducer is transmitting vertically,  $\phi_f$  is a function of  $(v/c)$ , the ratio of the vessel and sound speeds.

$$\phi_f = 2 \tan^{-1}(v/c) \quad (9.28)$$

For example, if  $v = 5.14 \text{ m s}^{-1}$  (10 knots) and  $c = 1500 \text{ m s}^{-1}$ ,  $\phi_f$  is  $0.4^\circ$ . For a transducer whose beam width is  $5^\circ$ , moving at 10 knots without pitching or rolling, the curve in Fig. 9.13 predicts a reduction of 1.5% in the received echo energy compared to the stationary case. For wider beams the effect is smaller. Figure 9.14 illustrates

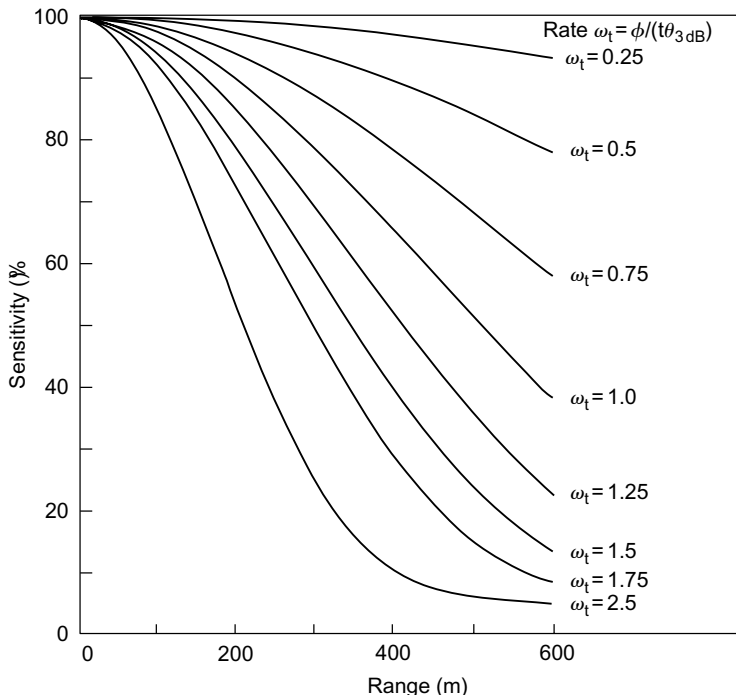


**Fig. 9.14** Relative sensitivity (echo intensity) resulting from pitching/rolling of the transducer through angle  $\phi$ , without horizontal displacement, as a function of the target range and  $\omega_t$  which is the scaled rotation rate  $\phi / (t\theta_{3\text{dB}})$ ;  $t$  is the time delay of the echo and  $\theta_{3\text{dB}}$  is the beam angle between 3 dB points.

the effect of pitching and rolling which is a single-valued function of the target range and the ratio ( $\omega_t/\theta_{3\text{dB}}$ ). The total movement  $\phi$  is somewhere in the interval  $\phi_a \pm \phi_t$ , depending on the direction of the rotation axis.

### 9.7.3 The surface bubble layer

Wind stress on the sea surface induces gas bubbles that increase the attenuation and scattering of sound waves. When the bubble layer extends below the transducer, the echo amplitudes are reduced by the factor  $A_b$ , called the ‘extra attenuation’ which increases with the wind force. The motion of the ship also induces bubbles, as evidenced by the foam seen in the wake. Again, the bubble density and hence the acoustic attenuation are likely to increase in bad weather.

Hall (1989) reviewed the theoretical models which describe firstly the aeration due to wind stress, and secondly the propagation of sound through bubbly water. Weston and Ching (1989) measured the extra attenuation in horizontal propagation at frequencies below 5 kHz. They attributed most of the attenuation to the surface waves; the losses caused by the bubble layer were uncertain. Weston (1989), having

compared measurements with theory for frequencies up to 40 kHz, concluded that the predicted attenuation due to bubbles was typically half that observed. Novarini and Bruno (1982) considered the effect of wind-induced aeration on vertical sound propagation at frequencies up to 150 kHz, see also Bruno and Novarini (1983). They derived empirical equations which expressed  $A_b$  as a function of the wind speed  $v_w$  in knots (1 knot =  $0.514 \text{ m s}^{-1}$ ), the frequency  $f$  in kHz and the transducer depth  $z$  in metres. The equations are valid for wind speeds 6–30 knots,  $z = 1 \text{ m}$  or more, and frequencies as follows.

Low frequencies, 8–60 kHz:

$$A_b = 10^6(0.9754 - 0.0895v_w + 0.002367v_w^2) f^{1.32} e^{(-1616.77zv_w^{-2.36})} \quad (9.29)$$

High frequencies, 70–150 kHz:

$$A_b = 10^6(5.98 - 0.551v_w + 0.0158v_w^2) f^{1.32} e^{(-2756.5zv_w^{-2.579})} \quad (9.30)$$

These equations are based on acoustic propagation theory and early measurement of bubble densities by Johnson and Cooke (1979). Dalen and Løvik (1981) reported experiments with a transducer on the hull of a moving ship. They measured  $A_b$  in two ways, by reference firstly to the volume reverberation from the bubble layer, and secondly to the integral of the seabed echo. There is good agreement between the two methods, but the extra attenuation observed by Dalen and Løvik is much greater than that reported by others (Fig. 9.15). Comparison with the theory of Weston (1989) suggests that the extra attenuation is not all due to bubbles directly induced by the

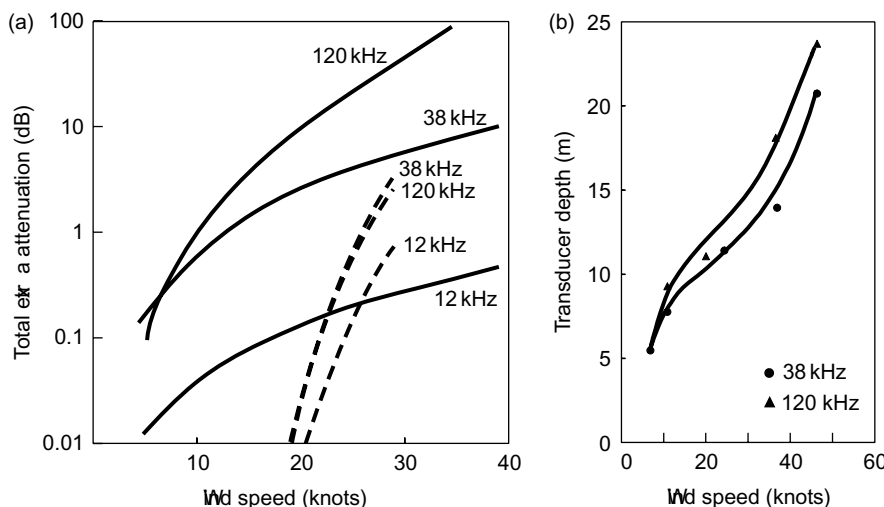


**Fig. 9.15** Extra attenuation caused by wind-induced bubbles for wind speed in knots (1 knot =  $0.514 \text{ m s}^{-1}$ ). (a) Results at 12, 38 and 120 kHz; —— measurements from Dalen and Løvik (1981); ----- predictions after Novarini and Bruno (1982), Bruno and Novarini (1983). (b) Minimum transducer depth for attenuation less than 0.3 dB.

wind. The motion of the ship could be a contributory factor. Apart from the aeration in the wake, water displaced downwards by the ship could enhance the bubble density below a transducer on the hull. Dalen and Løvik note that  $A_b$  depends on the wind direction relative to the ship's track, again suggesting some indirect effect through the weather-induced motion. They suppose that the observed attenuation would apply equally to a transducer in a towed body, but this is unlikely to be true of the component resulting from the ship's motion. More recently, research vessels have been designed with survey transducers housed on drop keels extending up to 3 m below the hull of the vessel. This technique allows the transducer to be deployed at some depth, say 9 m below the surface, considerably reducing the bubble-induced attenuation. In poor weather, however, the bubble layer can extend as far as 20 m below the surface, and while a drop keel does improve matters considerably, it does not completely overcome the problem.

We consider that the Novarini–Bruno equations are a good description of the extra attenuation caused by the natural environment, indicating the minimum level of  $A_b$  which will be greater in the survey application when additional aeration is generated by the ship. Furthermore,  $A_b$  will depend on the weather during the previous few days, and the shelter afforded by the coast if it is nearby, as well as the wind speed at the time. If the survey must continue in bad weather,  $A_b$  should be measured as described by Dalen and Løvik (1981), to allow better compensation of this bias.

There is need for more measurements of the excess attenuation caused by bubble layers. The theory of this effect has been well studied, see for example Feuillade (1996) and Ye (1997), but the relevance of the theoretical predictions to practical survey conditions remains in some doubt.

#### **9.7.4 Hydrographic conditions**

The intensity of the sound wave decreases as it propagates through the water because of beam spreading and absorption. These losses depend on the sound speed  $c$  and the absorption coefficient  $\beta$ . In Chapter 2 we described how  $c$  and  $\beta$  are determined from empirical equations as functions of the water temperature, salinity and depth. Thus it is important to understand the hydrography of the area being surveyed. Ideally, the temperature and salinity should be measured at a number of stations, failing which we must rely on other sources of information such as hydrographic maps.

The prevailing hydrographic conditions can change from place to place and from one season to another. In particular, the position and strength of the thermocline is important in vertical echosounding, causing the average sound speed over the transmission path to change with the depth of targets. The strongest thermoclines occur in tropical seas, where the temperature might be 30°C at the surface but only 12°C at 200 m depth. The change in temperature with depth occurs sharply at the thermocline. In the Persian Gulf for example, the summer temperature can change by 16°C over just 20 m of depth, but the thermocline weakens in winter due to wind-induced

mixing and then the water can be nearly isothermal. Thus local conditions and the seasonal factor need to be considered in estimating the likely values of  $c$  and  $\beta$ .

Suppose that the sound speed and absorption coefficient are assumed or calculated to be  $c_1, \beta_1$ . These estimates may be different from the true values ( $c, \beta$ ) which represent appropriate averages over the transmission path. This error biases the observed fish density through the functional dependence of the equivalent beam angle  $\psi$  and the exact TVG function. According to MacLennan (1990),  $\psi$  is approximately proportional to  $c^2$ . This variation is particularly important for the calibration when the measurement is of a target on the acoustic axis of the transducer. During the survey, when distributed targets are being detected, increases in  $\psi$  are compensated to some extent by decreases in the on-axis sensitivity, the power transmitted into the water and the receiver sensitivity. Errors caused by changes in the radiation impedance and beam focusing are small but they can be quantified.

Errors in estimating the target range are more important. If the actual TVG function is implemented to be exact for the parameter values  $c_1$  and  $\beta_1$ , and  $z_0$  is the depth at the middle of the integration channel, the echo-integral is in error by the factor:

$$\bar{g}_h = (c / c_1)^2 e^{2z_0(\beta - \beta_1 c_1 / c)} \quad (9.31)$$

Since the fish abundance  $\hat{Q}$  is proportional to the ratio  $\bar{g}/\psi$  (Equ. 5.14), the variation of  $\psi$  with  $c$  compensates at least partly for the  $c^2$  dependence of  $\bar{g}$  through the first term of Equ. (9.31). If the water temperature and the salinity are known, MacLennan (1990) suggests that at 38 kHz and  $R_0 = 200$  m, the hydrographic error in  $\hat{Q}$  is less than 3%. Larger errors may occur if the temperature and salinity are very uncertain, see Foote (1981). Figure 9.16 shows how the TVG error depends on the range, the frequency and deviations in the water temperature.

In the case of echo-counting, when the TVG is nominally  $40 \log R$ ,  $\bar{g}_h$  is proportional to  $(c/c_1)^4$ . Consequently, the hydrographic error in echo-counting is greater than it would be in echo-integration.

### 9.7.5 Fish migration

The movements of fish can be conceived as having two components, random motion and migration. In the former case, the fish swim at a particular speed in directions that change randomly with time. In the latter case, the fish swim consistently in the same direction. Simmonds *et al.* (2002) used a fine-scale model of North Sea herring schools, based on a spatial grid covering  $120\,000 \text{ km}^2$  with a node spacing of 40 m, to study the effect of fish movements on the results of simulated surveys. They found that reasonable amounts of random motion were unimportant, but the effect of migration even at a modest speed could not be ignored. It is well known that some fish migrate over long distances on an annual cycle (Harden Jones 1968). One factor in the survey design is the timing in relation to the migration cycle, which should ensure that the surveyed area includes the entire stock. But even if this condition is met, migration

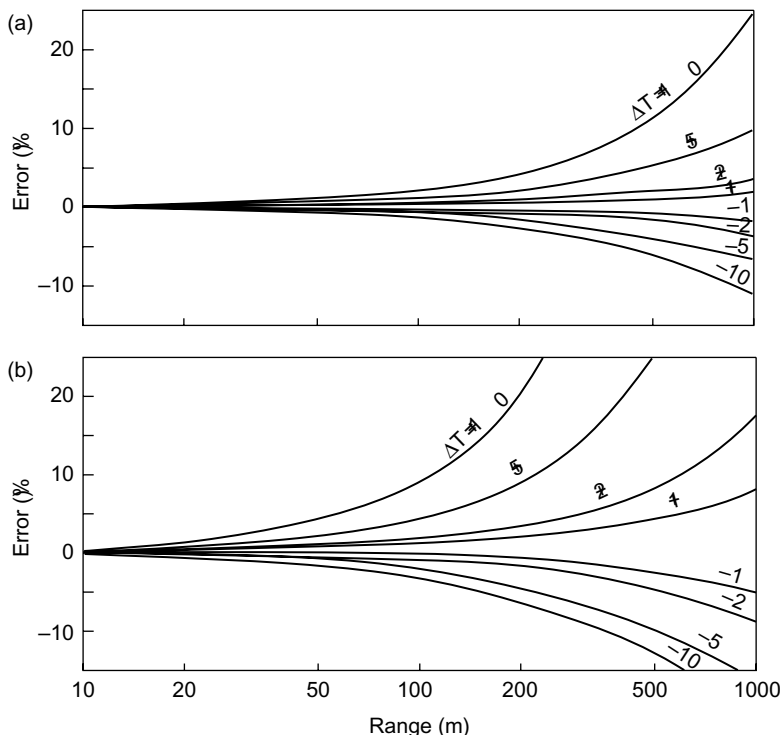


**Fig. 9.16** Error in the estimate of fish density due to the TVG function being based on inaccurate hydrographic data for (a) 38 kHz and (b) 200 kHz sounder frequencies.  $\Delta T$  is the difference between the true and assumed water temperatures ( $^{\circ}\text{C}$ ). The error magnitude increases with the target range. (Redrawn from Foote 1981a.)

of the stock within the surveyed area can bias the abundance estimate. The extent of the bias depends on the direction of the migration in relation to the transects.

Suppose the fish are migrating at speed  $v_f$ , and  $v_s$  is the speed at which the survey progresses in the direction of migration. If  $v_s$  is positive, this means that the fish tend to follow the vessel as it travels along successive transects. If the cruise track were drawn on a map whose frame of reference moved with the fish, the transects would be closer together than those on the geostationary map. Thus the effective area applicable to the analysis is less than the actual area surveyed. The observed densities are unbiased, but since the abundance is the mean density multiplied by the effective area, the estimate  $\hat{Q}$  is biased. The expected value of  $\hat{Q}$  is:

$$E(\hat{Q}) = Q(1 + v_f / v_s) \quad (9.32)$$

Note that when the transects are long and perpendicular to the migration,  $v_s$  is much smaller than the cruising speed of the vessel. For example, if the cruising speed is  $5 \text{ m s}^{-1}$ , and the transect length is 10 times the spacing, then the survey progresses at  $v_s = 0.5 \text{ m s}^{-1}$ , a value which could well be comparable with  $v_f$ . Harden Jones (1968)

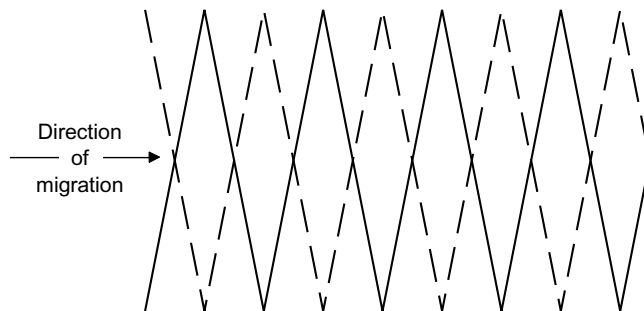


**Fig. 9.17** Cruise track with transects running across the direction of fish migration. The outward section (solid line) is interleaved with the return section (dashed line) so that the track progresses equally with or against the migration.

suggests that herring are capable of migration speeds up to  $0.6 \text{ m s}^{-1}$ . The swimming capability of fish depends on their size, but adult herring and mackerel can sustain speeds around  $1.0 \text{ m s}^{-1}$  for long periods (He and Wardle 1988; Lockwood 1989).

The bias is greatly reduced if the transects run alternately with and against the migration, in which case:

$$E(\hat{Q}) = Q(1 - (v_f / v_s)^2) \quad (9.33)$$

and  $v_s$  is now the cruising speed of the vessel. Taking the worst case as  $v_f = 1 \text{ m s}^{-1}$  and  $v_s = 5 \text{ m s}^{-1}$ , the bias is an underestimate of 4%. In practice, the transect direction may be decided by other factors such as the coastline or depth contours. If the transects must be perpendicular to the migration, we might consider traversing the surveyed area twice, in opposite directions with the outward and return transects interleaved (Fig. 9.17). Thus the survey begins and ends at the same place. This need not be too costly in ship time if the place concerned is the home port. As regards the analysis, the best plan is to treat the outward and return sections as if they were replicate surveys, and to estimate the abundance as the average of the two results.

### 9.7.6 Diurnal behaviour rhythms

The behaviour of many aquatic organisms changes with the time of day, motivated at least in part by the ambient light level. Several writers have discussed the implications for acoustic surveys (e.g. Levenez *et al.* 1990; Thorne *et al.* 1990; Demer and Hewitt 1995; Marchal and Lebourges 1996). Foote (1979b) reported that the abundance estimates from repeated surveys of the same area showed consistent differences between those conducted at night and those by day. There are several reasons why such a bias might occur. Firstly, schools observed during the day are likely to disperse at night, changing the criteria for partitioning the echo-integrals. Secondly, vertical migration could remove a variable proportion of the stock from the sampled

volume, owing to fish rising above the transducer or descending too close to the seabed; furthermore, the target strength will change as the swimbladder expands and contracts in response to the ambient pressure. Thirdly, the orientation of schooling fish may depend on vision and visibility. Thus the mean target strength in daylight and in darkness may not be the same, indeed experimental evidence shows this effect to be rather common (Nakken and Olsen 1977; Sameoto 1980).

The extent of day–night bias may be judged from the comparison of data collected at different times of day, in areas where the fish density is expected to be similar. More generally, it is important to recognize that the bias might suggest spurious changes in the spatial distribution, simply because some regions have been traversed by night and others by day. If the survey is conducted around the clock and all the data are to be used in the analysis, the bias in  $\hat{Q}$  is reduced if the night and day samples represent the fish concentrations in the same (statistical) way, and the effective target strength is calculated as an appropriate diurnal average. Note that the sampling effort might be unevenly divided between night and day for operational reasons. For example, if fishing is conducted only when schools are seen on the echogram, and the schools disperse at night, there will be less time during the day for acoustic data collection. In this context, representative samples can be obtained by random survey designs, or by selecting a subset of the data or weighting the observations so that the day/night samples have the same location and time statistics. It is difficult to organize a survey so that the sampling is random in both space and time. Weighting the observations may be more practical but still requires care at the design stage to ensure that sufficient data are available. Surveys that restart from an overnight inshore anchorage every morning will preferentially sample the coastal zone in the early part of the day. There are several methods for computing estimates that are independent of the time of day, for example kriging with external drift as described by Rivoirard *et al.* (2000) or the so-called generalized additive model (Hastie and Tibshirani 1990). Note that if the data recorded on a survey are themselves used to compensate for the time factor, the corrected abundance estimate will be less biased but also less precise. The variance is increased by the fact that the same data have been used to compute the estimate and the correction factor.

There should be no time-related bias if the abundance is estimated from acoustic data collected under similar light conditions. In high latitudes, it is reasonably efficient to restrict the survey to daytime (in summer) or night time (in winter). In the tropics, of course, there are around 12 hours each of daylight and darkness whatever the season. In that case, the survey must be restricted to 50% of the available time, or separate analyses of the observations by day and by night might be considered if the different mean target strengths are well enough understood.

### 9.7.7 Avoidance reactions

Another behaviour to be considered is the reaction of fish when they are startled by the survey vessel. Olsen *et al.* (1983a; 1983b) showed that herring moved away from

the approaching vessel, so that the density in the acoustic beam was less than the undisturbed value. Furthermore, television and photographic observations showed a change in the mean tilt angle of the reacting fish, thus the target strength would also change. Olsen and Ahlquist (1989) maintain that the noise generated by the vessel is more important than the visual stimulus, and the rate of change of the noise level at a fixed point is especially important. This suggests that the avoidance reaction depends on the vessel speed and the depth of the fish, while the absolute level of the vessel noise may be less important. Diner and Massé (1987) studied the reactions of schools in the Bay of Biscay and the English Channel using an omni-directional sonar to observe the horizontal movement of the schools around the vessel. Complex reactions were observed and few conclusions could be made, but the time of day seemed to be an important factor. Levenez *et al.* (1990) found that on dark nights, fish moved downwards in response to the lights of the survey vessel, although the mean echo-integral was the same whether the lights were on or off.

Much of the experimental work has been descriptive and provides little quantitative evidence to assess the bias due to avoidance. However, Olsen *et al.* (1983b) observed herring at 40 m depth as a vessel approached at 10 knots ( $5 \text{ m s}^{-1}$ ), using a Doppler sonar (cf. Section 3.4.5) which showed that the fish descended at speeds up to  $0.7 \text{ m s}^{-1}$ . They suggested that the change in the mean tilt angle of the reacting fish was inversely proportional to the square of depth, but their results were not consistent between different vessels and species. In another quantitative experiment, Olsen (1990) compared the echo-integrals from two stationary transducers suspended at 10 m depth, one close to the vessel track and the other about 20 m to the side. A much reduced density was observed immediately below the vessel. Again with a stationary transducer, C. Wilson (NMFS Seattle, pers. comm.) observed the reactions of pollack in the Bering Sea close to the passage of a research vessel and a large commercial fishing vessel. The fish reacted more strongly to the commercial vessel.

Olsen's work is a notable contribution to the field, but it has mostly been done in sheltered fjords. It is uncertain to what extent his results are applicable to migrating schools in the open sea. Gerlotto and Fréon (1988) report observations on schools of tropical clupeoids. The structure of the school, notably the height and the fish density within it, changed as the vessel passed by. Schools of *Sardinella aurita* reacted by diving when encountered above 20 m depth, but those in deeper water did not respond. The reactions observed by Gerlotto and Fréon are much less dramatic than those of herring described by Olsen. Gerlotto and Fréon noted that their fish were unexploited and citing the work of Marler and Terrace (1984), they speculate that the stronger reactions observed elsewhere might be conditioned by previous encounters with fishing vessels.

Multi-beam sonar can be used to map the disposition of fish schools near the survey vessel. Using this technique, Soria *et al.* (1996) found significant vessel avoidance by sardine schools. Brehmer and Gerlotto (2001) reported differences in behaviour for the same species between fished and unfished areas. Fernandes *et al.* (2000)

compared the fish densities observed from a low-noise research vessel, one conforming to the ICES recommendations (Mitson 1995), with those from an autonomous underwater vehicle (AUV) using the same 38 kHz echosounder, and found no significant difference.

When the fish react by diving, the target strength alters due to compression of the swimbladder as well as changes in the tilt angle. The swimbladder volume is inversely proportional to the ambient pressure (Boyle's law), and for the same distance descended, the target strength changes more in fish closer to the surface.

There is need for further work to quantify the effect of avoidance reactions. The avoidance bias is most likely to occur in shallow water and with non-migrating fish in sheltered areas, but we can say little more about the magnitude of the effect except that it is likely to be non-linear and dynamic. The noise generated by the survey vessel is clearly an important factor in fish avoidance. This is unlikely to be a problem if the vessel conforms to the recommendations of Mitson (1995).

### 9.7.8 *Precision of the estimated species proportions*

There are essentially two ways of allocating the echo-integrals to species level, firstly by the direct classification of echo traces and secondly by reference to the species proportions observed in trawl samples. Methods for determining the precision of these processes have developed from early bootstrap methods, e.g. Simmonds (1995) which treated each sample as if it were obtained randomly anywhere within the surveyed area. The precisions of length and age determinations were estimated through bootstrap resampling of the trawl-catch data. This showed that the individual trawl haul was the most appropriate sampling unit to consider, and that the within-trawl sampling added little to the variance. Petigas *et al.* (2003) describe how the precision of species allocations can be estimated. Their procedure starts with the automatic classification of identified images, defining groups of images with estimates of the sampling variability in the species identification, while non-identified images are aggregated in a separate group. This procedure results in post-stratification of the data. For each species, the abundance and its variance are derived automatically but are conditioned by the post-stratification. Two methods are proposed based on, respectively, echogram consistency and trawl-catch consistency. All sources of variability are represented as sampling errors, and as the true species composition is unknown it is not possible to test for bias. In the example of a particular multi-species survey analysed by Petigas *et al.* (2003), errors in the species identification contributed 60–80% of the variance and thus were the main source of sampling error in this case.

The standard method for partitioning the echo-integrals based on trawl catches takes account of differences in the target strength (see Section 9.3) but it assumes that the capture efficiency of the gear is the same for all species. Recognizing the doubtful nature of this assumption, O'Driscoll (2003) extended the standard method by including a vulnerability factor for the capture of each species. This leads to a set

of equations expressing the echo-integrals observed while trawling in terms of the backscattering cross-sections, vulnerabilities and catch proportions of each species. These equations are solved by the non-negative least-squares method (NNLS) which we described in Chapter 7. O'Driscoll used a bootstrap analysis (p. 361) to determine confidence intervals on the vulnerabilities (and hence on the species proportions). Some 20 species were included in the analysis and, perhaps unsurprisingly, the confidence intervals on the relative proportions were rather large.

In summary, we consider that the method of Petitgas *et al.* is a good choice when direct classification of the echo traces is feasible. Otherwise, the partitioning has to be based on trawl sampling, in which case O'Driscoll's method is preferred. It is better than the traditional analysis since it allows for differences in the capture efficiency between species.

## 9.8 Accuracy of the abundance estimate

It is difficult to assess the overall accuracy of the abundance estimate, but it is nevertheless essential to consider how good or bad the results are. This demonstrates the validity of the results but may also show where it is possible to make improvements. There are two approaches to the problem. The intrinsic method is an error analysis of the survey itself. Alternatively, the acoustic abundance may be compared with independent estimates of the same stock, if any are available.

The abundance may be expressed as an absolute quantity of fish, or as an index proportional to the quantity by a factor which is unknown but supposed to be constant from one survey to the next. The accuracy of the index depends mainly on the sampling errors discussed in Section 9.6. The larger systematic errors, notably those associated with fish behaviour, may reasonably be expected not to change between surveys conducted in comparable circumstances, for example at the same time of year. Thus the accuracy of the index should be much better than that of the absolute abundance. The arguments in favour of using indices or absolute abundances are complex. For some fishery management purposes, an index may be sufficient since it shows whether the stock is increasing or decreasing. However, the value of an index depends on how constant is the (unknown) ratio between it and the absolute abundance. Any variability in this ratio adds to the error in the index. Furthermore, fishery assessment models which use absolute estimates of the yield combined with absolute abundances from a survey are subject to other kinds of error. Unknown biases in the survey results and the yield determination have different consequences over a time series; the yields influence the history while the survey has more bearing on the current state of the stock. Thus the choice between using the absolute abundance or the relative index obtained by acoustic survey should be made after examining both the acoustic data and any other information that is to be included in the stock assessment. Analysis of the sources of error in the survey will help to inform these decisions.

### 9.8.1 Intrinsic error analysis

Assessments of the total error in acoustic abundance estimates have been presented by Demer (1994; 2004) for Antarctic krill (*Euphausia superba*), Rose *et al.* (2000) for Atlantic cod (*Gadus morhua*) and redfish (*Sebastes* sp.), and O'Driscoll (2003) for spawning hoki (*Macruronus novaezelandiae*). The total error is estimated as the combination of several components whose magnitudes are known or may be calculated on reasonable assumptions. The cited investigations illustrate two approaches to the problem. Rose *et al.* (2000) and O'Driscoll (2003) considered a limited set of error factors constructed to be statistically independent. Where two or more error sources were known to be correlated, they were treated as a combined effect described by a single error factor. Thus simple statistics could be used to calculate the total error (see below). Demer (1994; 2004) incorporated a wider range of error sources but then was obliged to make assumptions about the extent of correlations. The complexity of addressing this problem in totality should not be underestimated. Some sources of error may be negatively correlated. For example, the variability in transmission sensitivity due to hydrographic factors is negatively correlated with corresponding changes in the beam angle. Care should be taken to ensure that such compensating errors are properly evaluated. Importantly, all the studies cited above succeeded in identifying the main sources of error for their particular circumstances. They are undoubtedly important contributions in a difficult field; however, further development of intrinsic error analysis is needed to resolve some outstanding issues. Rose *et al.* (2000) assumed uncorrelated errors where this may be inappropriate and selected error models with limited scope for validation. Demer *et al.* (1999) considered observations made at different frequencies and assumed that the variability between frequencies indicated the overall error. This assumption reduces the influence of errors driven by hydrographic variation which will affect different frequencies in the same direction though perhaps with different magnitudes.

The many factors which contribute individual errors have been discussed in Sections 9.6 and 9.7. They are summarized in Table 9.2 which indicates how much error might be expected under the conditions typically encountered on acoustic surveys, assuming that the survey has been well designed and competently conducted with properly calibrated scientific instruments. The errors are listed in two groups, (a) those which apply equally to the absolute abundance and the index, and (b) those applicable to the absolute abundance only. These error magnitudes are purely indications based on general experience in the field. The errors obviously depend on the particular circumstances encountered in specific applications. It is not recommended that the total error should be calculated from Table 9.2 without more detailed consideration of how the individual errors depend on, for example, the species being surveyed, the equipment being used (including the vessel) and the hydrographic conditions (which may or may not have been monitored). Further guidance on the errors relevant to particular surveys will be found in (Anon 1998a; Kloser *et al.* 2000; Rose *et al.* 2000; O'Driscoll 2003; Demer 2004).

**Table 9.2** Sources of error in acoustic surveys.

Source of error	Random error	Bias	Comment
<i>Error in an acoustic index</i>			
Physical calibration	±2 to 5%	±2 to 5%	Lower frequencies can be measured more reliably
Transducer motion		0 to -25%	Narrow beams are more sensitive to motion
Bubble attenuation		0 to -90%	Keel mounted and deep towed systems are less sensitive
Hydrographic conditions	±2 to 5%	0 to 25%	Long range (deep water) and high frequencies suffer from uncertainty in absorption coefficients
Target strength	±5 to 25%		Due to uncertainties in size of targets and orientation
Species identification	0 to 50%		Depends on species mix and target strength differences among species
Random sampling	5 to 20%		Depends on spatial distribution; layers can be estimated precisely; highly variable school sizes are the most difficult scenario
Migration		0 to 30%	
Diurnal behaviour	0 to 50%		Greatest for major vertical migration with changes in target strength due to ambient pressure variation
Avoidance		0 to 50%	Low with quiet ship in open deep water, worse in confined areas with shallow schooling species
<i>Absolute abundance errors</i>			
Physical calibration		±3 to 10%	Worse at higher frequencies and with very narrow beams
Hydrographic conditions		±2 to 25%	Worse at high frequencies and long ranges due to uncertain absorption coefficients
Target strength	0 to 50%		Best for well established swimbladdered species, worst for deepwater species

Each factor contributes an error which is random, systematic or both. The distinction was explained in Section 9.7. The random errors may be reduced by collecting more samples, which means spending more time on the survey or moving effort from one activity to another. This is not true of the systematic errors since they bias all the observations equally.

To calculate the accuracy of an abundance estimate, we must first determine the individual error magnitudes. We suppose that the results have been corrected for the

biases in so far as they are known. Thus the individual errors are random variables, each of which has an associated PDF, assumed to be Gaussian, with an expectation of zero. Most of them are statistically independent. There is no reason to suppose, for example, that the equipment performance should have any bearing on the fish behaviour. Some errors are correlated and they require special treatment. Referring to Table 9.2, we note that the transducer motion is correlated with the bubble-layer attenuation, since both increase in magnitude as the weather gets worse. Also, changes in the equivalent beam angle and the on-axis sensitivity of the transducer are correlated through their mutual dependence on the hydrographic conditions; however, the effect on the estimated fish density is minimal because these changes act in opposite directions (p. 120). It is reasonable to suppose that the other factors listed in Table 9.2 are statistically independent. There may be correlation between some of the behavioural errors, but they are poorly understood and the assumption of independence is as good as any. The errors within any correlated set are summed and the result is treated as one independent error in the subsequent analysis.

The individual errors are expressed as percentages though they have a multiplicative effect on the abundance estimate. The model is:

$$\hat{Q} = X_1 X_2 X_3, \dots, X_n \quad (9.34)$$

Each variable  $X_i$  includes an error  $\Delta X_i$ . There is a simple formula for the total error which is valid if  $\Delta X_i \ll X_i$ . While some  $\Delta X_i/X_i$  may not be small, the more complicated theory required to deal with large but uncertain errors is unlikely to be worthwhile. If  $\varepsilon_i^2$  is the expected value of  $(\Delta X_i/X_i)^2$ , i.e. the variance of the proportional error, and the  $\Delta X_i$  are uncorrelated, the variance of  $\hat{Q}$  is estimated as:

$$\hat{V} = \hat{Q}^2 \sum_{i=1}^n \varepsilon_i^2 \quad (9.35)$$

### 9.8.2 Comparison with other methods

The ultimate test of the acoustic survey technique is to compare estimates of the same stock obtained by acoustic and other methods. Suppose that methods A and B give the abundance estimates  $Q_a$  and  $Q_b$  with variances  $V_a$  and  $V_b$  respectively. The variances may be unknown, but the differences  $(Q_a - Q_b)$  incorporate the combined error of both methods. If the errors are independent, the variance of  $(Q_a - Q_b)$  is  $V = V_a + V_b$ . Given two series of comparable abundance measurements, from annual surveys of the same stock conducted over several years for example,  $V$  is estimated as the sample variance of  $(Q_a - Q_b)$ . The simple comparison does not indicate which method is more accurate, but the variance is a positive quantity and so  $V$  is an upper bound on the variances of both  $Q_a$  and  $Q_b$ .

Jacobsson (1983) compared acoustic abundances of the Icelandic summer-spawning herring against estimates from virtual population analysis (VPA). This is a retrospective calculation based on the catches taken in the fishery which is explained

in Gulland (1983). While there was good agreement between the two methods, the comparison was not strictly valid because the acoustic data had been used to 'tune' the VPA, thus the most recent VPA and the acoustic estimates were not completely independent. Nakken and Ulltang (1983) conducted a similar study of cod and haddock in the north-east Arctic. In this case the VPA and the acoustic estimates were independent. When the cod and haddock were considered as one stock, the estimates agreed within 10%, but much larger differences were found in the results for each species. The problem appeared to be due to the trawl catches, which did not reflect the true proportion of cod and haddock in the sea. Hampton (1996) compared 10-year time series of acoustic and egg surveys of the anchovy *Engraulis capensis*. Both surveys reflected the same major changes in abundance. Hampton analysed the random and systematic errors in the abundance estimates, and concluded that the accuracy of both surveys depended primarily on the sampling error. This finding adds considerably to the confidence in survey results and provides a good basis for deciding how to allocate resources to achieve a desired accuracy. Simmonds (2003) examined acoustic, trawl and larval surveys of the North Sea herring stock. Correlations were determined (by a bootstrap analysis) between estimates of the same age class (a) in the same year by different methods and (b) in different years by the same method. The various indices were then compared in a stock-assessment model. Simmonds showed that all the surveys produced useful data and could be combined in the model to improve the assessment, with the most weight being given to the acoustic survey which was evidently the most reliable of the three techniques.

Røttingen and Tjelmeland (2003) compared various estimates of the 1983 year class of the Norwegian spring-spawning herring, namely absolute acoustic abundances, VPA calculations and a 'minimum' stock size indicated by the fishery yield. They concluded that the acoustic survey underestimated the stock by 50%, and this error had unfortunate consequences for the management of the fishery. However, we suggest that if management measures are to be based on uncertain abundance estimates, it is better they should be too low than too high. In the former case, there is less risk of overexploitation to the point of stock collapse. Furthermore, it is inadvisable to change the standard methodology of a survey unless this is very well justified. For example, in 1987 it was decided to revise the target-strength function applicable to the North Sea herring. In retrospect it seems that the earlier version was more accurate. This suggests a cautious approach to innovation.

In freshwater environments, electrical counters are often used to monitor the run of migrating fish. Nunnalee (1983) compared the count of sockeye salmon, *Oncorhynchus nerka*, observed passing a weir, against the population indicated by acoustic surveys of Cultus Lake in British Columbia. The acoustic estimates were obtained by a combination of echo-counting and echo-integration, surveying only at night when the juvenile sockeye were distributed in the upper part of the water column, mainly at depths 20–25 m. Several other species were present in the lake, but they did not migrate, so the sockeye population was estimated from the change in the acoustic abundance after the start of the sockeye run. The weir-count and

the acoustic abundance differed by only 2.5%, much less than the 95% confidence interval suggested by intrinsic error analysis. Another approach is comparison with the fish densities indicated by trawl samples. Thorne (1983) discussed the accuracy of acoustic surveys of salmonid populations in North American lakes. He obtained independent abundance estimates from the catches of a large midwater trawl towed at night. The acoustic estimates were made by echo-integration using either 105 or 120 kHz echosounders, giving 19 valid comparisons of juvenile sockeye salmon populations. Regression of the acoustic and trawl estimates showed a systematic difference of 4%, and a correlation coefficient of 0.73 which suggests the random sampling error was somewhat greater. Ransom *et al.* (1996) compared fyke-net catches with acoustic data recorded at fixed installations (420 kHz transducers) near four dams in the Columbia river basin. Estimates of the passage of sockeye smolts were highly correlated ( $r = 0.96$ ) and the two methods revealed very similar vertical distributions of the fish. In a separate investigation to determine the efficiency of a fish guidance device, however, the efficiencies indicated by the net samples and the acoustic data were similar on average but less well correlated ( $r = 0.36$ ).

Although it is not often that two independent assessment methods give satisfactory results for the same stock, the comparisons which have been made suggest that for the assessment of pelagic fish stocks, the acoustic technique is at least as good as, and probably better than, any other. Furthermore, the sources of error in acoustic abundance estimates have been more extensively investigated than appears to be the case for other methods, at least as regards the assessment of pelagic stocks in the sea. The most poorly understood errors are those related to fish behaviour and the partitioning of the echo-integrals between species. These errors apply to the absolute abundance estimates, but in a well-designed series of surveys, they should be less important in the precision of the acoustic index. Again, the index may be converted to an absolute abundance by calibration against any independent measure of the stock that is considered to be reliable enough. Even if that is not possible, the use of an abundance index may be good enough for some purposes in fishery management.

All survey techniques have their own advantages and disadvantages, and we would not claim that the acoustic method is the best in every case. The important point is that the sources of error in any method should be well enough understood to judge the best approach to the problem of fish-stock estimation. The acoustic survey has become well established as a useful technique in fishery research. There are many applications in which it is the only practical means of assessment available to fishery managers, but there are others in which no one method is satisfactory. Sometimes we have no choice but to apply different methods in parallel, to produce an average result whose confidence interval is acceptably small. When independent results are to be combined, a good understanding of the error factors in each method is critical to obtaining the best overall estimate. The acoustic survey, if carefully designed and analysed, can provide good estimates of the fish abundance together with confidence limits that are soundly based.

# References

- Abramowitz, M. and Stegun, I.A. (1964) *Handbook of Mathematical Functions*. Dover Publications Inc., New York.
- Aglen, A. (1983) Random errors of acoustic fish abundance estimates in relation to the survey grid density applied. *FAO Fish. Rep.* **300**, 293–8.
- Aglen, A. (1989) Empirical results on precision-effort relationships for acoustic surveys. ICES CM 1989/B:30, 28 pp. (mimeo).
- Aglen, A. (1996) Impact of fish distribution and species composition on the relationship between acoustic and swept-area estimates of fish density. *ICES J. Mar. Sci.* **53**, 501–6.
- Aglen, A., Engås, A., Huse, I., Michalsen, K. and Stensholt, B.K. (1999) How vertical fish distribution may affect survey results. *ICES J. Mar. Sci.* **56**, 345–60.
- Ainslie, M.A. and McColm, J.G. (1998) A simplified formula for viscous and chemical absorption in sea water. *J. Acoust. Soc. Am.* **103**, 1671–2.
- Aitcheson, J. (1955) On the distribution of a positive random variable having a discrete probability mass at the origin. *J. Am. Stat. Soc.* **90**, 901–8.
- Akopian, A.I. and Ivanov, M.P. (2001) Ranging of the moving target by the Black Sea dolphin *Tursiops truncatus*. *Proc. Inst. Acoust.* **23** (4), 87–92.
- Aksland, M. (1986) Estimating numbers of pelagic fish by echo integration. *J. Cons. Int. Explor. Mer* **43**, 7–25.
- Amorim, M.C.P., Stratoudakis, Y. and Hawkins, A.D. (2004) Sound production during competitive feeding in the grey gurnard. *J. Fish Biol.* **65**, 182–93.
- Anderson, K.P. and Kirkegaard, E. (1985) Sources and magnitude of random errors in acoustic fish abundance estimate. ICES CM 1985/B:40 (mimeo).
- Anderson, V.T. (1950) Sound scattering from a fluid sphere. *J. Acoust. Soc. Am.* **22**, 426–31.
- Andreeva, I. (1964) Scattering of sound by air bladders of fish in deep sound scattering layers. *Sov. Phys. Acoust.* **10**, 17–20.
- Andreeva, I.B. and Belousov, A.V. (1996) Multiple sound scattering by densely packed shoals of marine animals. *ICES J. Mar. Sci.* **53**, 323–8.
- Anon (1925) Echo sounding. *Nature* **115**, 689–90.
- Anon (1934) Forsøkene med ekkolodd ved Brislingfisket (Trials with an echosounder during the sprat fishery). *Tidsskrift for Hermetikindustri (Bulletin of the Canning Industry)*, July **1934**, 222–3. (In Norwegian)
- Anon (1993) Report of the workshop on the applicability of spatial statistical techniques to acoustic survey data. *ICES Coop. Res. Rep.* **195**, 87 pp.
- Anon (1998a) Report of the Working Group on Fisheries Acoustics, Science and Technology. ICES CM 1998/B:4, 23–37.
- Anon (1998b) Report of the Planning Group for Herring Surveys. ICES CM 1998/G:04, 89 pp. (mimeo).

- Anon (2002) The Planning Group on Surveys of Pelagic Fish in the Norwegian Sea. ICES CM 2003/D:07.
- Anon (2003) *Ocean Noise and Marine Mammals*. The National Academies Press, Washington, DC.
- Anon (2004) Report of the Planning Group for Herring Surveys. ICES CM 2004/G:05 Ref. D, 207 pp.
- Aplin, J.A. (1947) The effect of explosives on marine life. *California Fish and Game* **33**, 23–30.
- Armstrong, F. (1986) Target strength of sandeels. ICES CM 1986/B:5, 6 pp. (mimeo).
- Arnaya, I.N. and Sano, N. (1990) Studies on acoustic target strength of squid VI. Simulation of squid target strength by prolate spheroidal model. *Bull. Fac. Fish. Hokkaido Univ.* **41**, 32–42.
- Arnaya, I.N., Sano, N. and Iida, K. (1989a) Studies on acoustic target strength of squid II: Effect of behaviour on averaged dorsal aspect target strength. *Bull. Fac. Fish. Hokkaido Univ.* **40**, 83–99.
- Arnaya, I.N., Sano, N. and Iida, K. (1989b) Studies on acoustic target strength of squid III: Measurement of the mean target strength of small live squid. *Bull. Fac. Fish. Hokkaido Univ.* **40**, 100–15.
- Arnold, G.P., Greer Walker, M. and Holford, B.H. (1990) Fish behaviour, achievement and potential of high-resolution sector scanning sonar. *Rapp. P.-v. Reun. Cons. Explor. Mer* **189**, 112–22.
- Aroyan, J.L. (2001) Three-dimensional modeling of hearing in *Delphinus delphis*. *J. Acoust. Soc. Am.* **110**, 3305–18.
- Aroyan, J.L., Cranford, T.W., Kent, J. and Norris, K.S. (1992) Computer modeling of acoustic beam formation in *Delphinus delphis*. *J. Acoust. Soc. Am.* **92**, 2539–45.
- Arrhenius, F., Benneheij, B.J.A.M., Rudstam, L.G. and Boisclair, D. (2000) Can stationary bottom split-beam hydroacoustics be used to measure fish swimming speed in situ? *Fish. Res.* **45**, 21–30.
- Astrup, J. and Møhl, B. (1993) Detection of intense ultrasound by the cod, *Gadus morhua*. *J. Exp. Biol.* **182**, 71–80.
- Astrup, J. and Møhl, B. (1998) Discrimination between high and low repetition rates of ultrasonic pulses by the cod. *J. Fish. Biol.* **52**, 205–8.
- Au, W.W.L. (1980) Echolocation signals of the Atlantic Bottlenose dolphin (*Tursiops truncatus*) in open waters. In: *Animal Sonar Systems* (eds R.G. Busnel and J.F. Fish), pp. 251–82. Plenum Press, New York.
- Au, W.W.L. (1992) Application of the reverberation-limited form of the sonar equation to dolphin echolocation. *J. Acoust. Soc. Am.* **92**, 1822–6.
- Au, W.W.L. (1993) *The Sonar of Dolphins*. Springer Verlag, New York.
- Au, W.W.L. and Banks, K. (1998) The acoustics of the snapping shrimp *Synalpheus paraneomeris* in Kaneohe Bay. *J. Acoust. Soc. Am.* **103**, 41–8.
- Au, W.W.L. and Herzing, D.L. (2003) Echolocation signals of wild Atlantic spotted dolphin (*Stenella frontalis*). *J. Acoust. Soc. Am.* **113**, 598–604.
- Au, W.W.L. and Martin, D.W. (1989) Insights into dolphin sonar discrimination capabilities from human listening experiments. *J. Acoust. Soc. Am.* **86**, 1662–70.
- Au, W.W.L. and Moore, P.W.B. (1990) Critical ratio and critical bandwidth for the Atlantic bottlenose dolphin. *J. Acoust. Soc. Am.* **88**, 1635–8.
- Au, W.W.L. and Pawloski, D.A. (1991) Cylinder wall thickness difference discrimination by an echolocating Atlantic bottlenose dolphin. *J. Comp. Physiol. A* **170**, 41–7.

- Au, W.W.L. and Pawloski, J.L. (1989) Detection of noise with rippled spectra by the Atlantic bottlenose dolphin. *J. Acoust. Soc. Am.* **86**, 591–6.
- Au, W.W.L. and Turl, C.W. (1991) Material composition discrimination of cylinders at different aspect angles by an echolocating dolphin. *J. Acoust. Soc. Am.* **90**, 2448–51.
- Au, W.W.L., Floyd, R.W., Penner, R.H. and Murchison, A.E. (1974) Measurement of echo-location signals of the Atlantic bottlenose dolphin, *Tursiops truncatus* Montagu, in open waters. *J. Acoust. Soc. Am.* **56**, 1180–90.
- Au, W.W.L., Schusterman, R.J. and Kersting, D.A. (1980) Sphere-cylinder discrimination via echolocation by *Tursiops truncatus*. In: *Animal Sonar Systems* (eds R.G. Busnel and J.F. Fish), pp. 859–62. Plenum Press, New York.
- Au, W.W.L., Penner, R.H. and Kadane, J. (1982) Acoustic behaviour of echolocating Atlantic bottlenose dolphin. *J. Acoust. Soc. Am.* **71**, 1269–75.
- Au, W.W.L., Kastelein, R.A., Rippe, T. and Schooneman, N.M. (1999) Transmission beam pattern and echolocation signals of a harbor porpoise (*Phocoena phocoena*). *J. Acoust. Soc. Am.* **106**, 3699–705.
- Aubauer, R. and Au, W.W.L. (1998) Phantom echo generation: a new technique for investigating dolphin echolocation. *J. Acoust. Soc. Am.* **104**, 1165–70.
- Bach, P., Dagorn, I., Bertrand, A., Josse, E. and Misselis, C. (2003) Acoustic telemetry versus longline fishing for studying the vertical distribution of pelagic fish: bigeye tuna (*Thunnus obesus*) in French Polynesia. *Fish. Res.* **60**, 281–92.
- Bailey, M.C., Maravelias, C.D. and Simmonds, E.J. (1998) Changes in the spatial distribution of autumn spawning herring (*Clupea harengus* L) derived from annual acoustic surveys during the period 1984–1996. *ICES J. Mar. Sci.* **55**, 545–55.
- Bailey, R.S. and Simmonds, E.J. (1990) The use of acoustic surveys in the assessment of North Sea herring stocks and a comparison with other methods. *Rapp. P.-v. Reun. Cons. Int. Explor. Mer* **189**, 9–17.
- Balls, R. (1946) *Fish on the Spotline*. Marconi International Marine Communication Company Ltd, London, 37 pp.
- Balls, R. (1948) Herring fishing with the echometer. *J. Cons. Int. Explor. Mer* **15**, 193–206.
- Banneheka, S.G., Routledge, R.D., Guthrie, I.C. and Woodey, J.C. (1995) Estimation of in-river passage using a combination of transect and stationary acoustic sampling. *Can. J. Fish. Aquat. Sci.* **52**, 335–43.
- Barange, M. (1994) Acoustic identification, classification and structure of biological patchiness on the edge of the Agulhas Bank and its relation to frontal features. *South African J. Mar. Sci.* **14**, 333–47.
- Barange, M. and Hampton, I. (1997) Spatial structure of co-occurring anchovy and sardine populations from acoustic data: implications for survey design. *Fish. Oceanog.* **6** (2), 94–108.
- Barange, M., Hampton, I. and Soule, M.E. (1996) Empirical determination of in situ target strengths of three loosely aggregated pelagic fish species. *ICES J. Mar. Sci.* **53**, 225–32.
- Barans, C.A., Stender, B.W. and Holliday, D.V. (1997) Variation in the vertical distribution of zooplankton and fine particles in an estuarine inlet of South Carolina. *Estuaries* **20**, 467–82.
- Bary, B.M. (1966) Backscattering at 12 kc/s in relation to biomass and numbers of zooplanktonic organisms in Saanich Inlet, British Columbia. *Deep Sea Res.* **13**, 655–66.
- Baxter, L. (1985) Mortality of fish subjected to explosive shock as applied to oil well severance on Georges Bank. In: *Proceedings of the Workshop on Effects of Explosive Use in the Marine Environment*, 29–31 January 1985, Halifax (eds G.D. Greene, F.R. Engelhardt and

- R.J.E. Paterson). *Tech. Rep. Canada Oil and Gas Lands Administration, Ottawa*, No. 5, 119–35.
- Bell, J.M., Chantler, M.J. and Wittig, T. (1999) Sidescan sonar: a directional filter of seabed texture. *Sonar and Navigation* **146**, 65–72.
- Benoit-Bird, K.J. and Au, W.W.L. (2001) Target strength measurements of Hawaiian mesopelagic boundary community animals. *J. Acoust. Soc. Am.* **110**, 812–19.
- Berka, R. (1986) The transport of live fish: a review. *European Inland Fish. Advisory Comm. Tech. Pap.* **48**, 52 pp.
- Bethke, E., Arrhenius, F., Cardinale, M. and Hakansson, N. (1999) Comparison of the selectivity of three pelagic sampling trawls in a hydroacoustic survey. *Fish. Res.* **44**, 15–23.
- Beverton, R.J. (1990) Small marine pelagic fish and the threat of fishing: are they endangered? *J. Fish Biol.* **37** (Suppl. A), 5–16.
- BIOMASS (1986) Post-FIBEX Acoustic Workshop. *BIOMASS Rep. Ser. No. 40*, 1–106.
- Blaxter, J.H.S. and Batty, R.S. (1984) The herring swimbladder: loss and gain of gas. *J. Mar. Biol. Assn. UK* **64**, 441–59.
- Blaxter, J.H.S. and Batty, R.S. (1990) Swimbladder behaviour and target strength. *Rapp. P.-v. Reun. Cons. Int. Explor. Mer* **189**, 233–44.
- Blaxter, J.H.S. and Hunter, J.R. (1982) The biology of the clupeoid fishes. *Adv. Mar. Biol.* **20**, 1–223.
- Blue, J.E. (1984) Physical calibration. *Rapp. P.-v. Reun. Cons. Int. Explor. Mer* **184**, 19–24.
- Bodholt, H. (1977) Variance error in echo-integrator output. *Rapp. P.-v. Reun. Cons. Int. Explor. Mer* **170**, 196–204.
- Borisenko, E.S., Gusar, A.G. and Goncharov, S.M. (1989) The target strength dependence of some freshwater species on their length-weight characteristics. *Proc. Inst. Acoust.* **11** (3), 27–34.
- Box, G.E.P. and Cox, D.R. (1964) An analysis of transformations. *J. Roy. Stat. Soc. B* **26**, 211–52.
- Brede, R., Kristensen, F.H., Solli, H. and Ona, E. (1990) Target tracking with a split-beam echosounder. *Rapp. P.-v. Reun. Cons. Int. Explor. Mer* **189**, 254–63.
- Brehmer, P. and Gerlotto, F. (2001) Comparative analysis of swimming behaviour in different populations of *Sardinella aurita*: influence of environment and exploitation; effect on catchability. ICES CM 2001/Q:04.
- Brensing, K., Linke, K. and Todt, D. (2001) Sound source location by difference of phase on a hydrophone array with small dimensions. *J. Acoust. Soc. Am.* **109**, 430–33.
- Brierley, A.S., Ward, P., Watkins, J.L. and Goss, C. (1998) Acoustic discrimination of Southern Ocean zooplankton. *Deep Sea Res. II* **45**, 1155–73.
- Brierley, A.S., Axelsen, B.A., Buecher, E., Sparks, C.A.J., Boyer, H. and Gibbons, M.J. (2001) Acoustic observations of jellyfish in the Namibian Benguela. *Mar. Ecol. Prog. Ser.* **210**, 55–66.
- Brierley, A.S., Gull, S.F. and Wafey, M.H. (2003) A Bayesian maximum entropy reconstruction of stock distribution and inference of stock density from line-transect acoustic-survey data. *ICES J. Mar. Sci.* **60**, 446–52.
- Bruno, D.R. and Novarini, J.C. (1983) High frequency sound attenuation caused by the wind-generated bubble layer in the open sea. *J. Acoust. Soc. Am.* **73**, 1064–5.
- Buck, J.R., Morgenbesser, H.B. and Tyack, P.L. (2000) Synthesis and modification of the whistles of the bottlenose dolphin, *Tursiops truncatus*. *J. Acoust. Soc. Am.* **108**, 407–16.

- Buckart, C.A., Kleppel, G.S., Brander, K., Holliday, D.V. and Pieper, R.E. (1995) Copepod and barnacle nauplius distributions in the Irish Sea: relation to springtime hydrographic variability. *J. Plankton Res.* **17**, 1177–88.
- Buckland, S.T., Anderson, D.R., Burnham, K.P. and Laake, J.L. (1993) *Distance Sampling: Estimating Abundance of Biological Populations*. Chapman & Hall, London.
- Burczynski, J. (1982) Introduction to the use of sonar systems for estimating fish biomass. *FAO Fish. Tech. Pap.* No. 191 (Rev. 1), 89 pp.
- Burczynski, J.J. and Johnson, R.L. (1986) Application of dual-beam acoustic survey techniques to limnetic populations of juvenile sockeye salmon, *Oncorhynchus nerka*. *Can. J. Fish. Aquat. Sci.* **43**, 1776–88.
- Burczynski, J.J., Johnson, R.L. and Kirchner, W.B. (1990) Acoustic estimation of dense aggregations of fish in sea pens. *Rapp. P.-v. Reun. Cons. Int. Explor. Mer* **189**, 54–64.
- Burwen, D.L., Fleischman, S.J., Miller, J.D. and Jensen, M.E. (2003) Time-based signal characteristics as predictors of fish size and species for a side-looking hydroacoustic application in a river. *ICES J. Mar. Sci.* **60**, 662–8.
- Campbell, R.C. (1974) *Statistics for Biologists*, 2nd edn. Cambridge University Press, Cambridge, 383 pp.
- Carlson, T.J. and Jackson, D.R. (1980) Empirical evaluation of the feasibility of split beam methods for direct *in situ* target strength measurement of single fish. Seattle Applied Physics Laboratory, University of Washington, 43 pp.
- Cato, D. (1993) The biological contribution to the ambient noise in waters near Australia. *Acoust. Australia* **20**, 76–80.
- Cech, M. and Kubecka, J. (2002) Sinusoidal cycling swimming pattern of reservoir fishes. *J. Fish Biol.* **61**, 456–71.
- Chapman, C.J. and Hawkins, A.D. (1973) A field study of hearing in the cod, *Gadus morhua*. *J. Comp. Physiol.* **85**, 147–67.
- Chapman, C.J. and Johnstone, A.D.F. (1974) Some auditory discrimination experiments on marine fish. *J. Exp. Biol.* **61**, 521–8.
- Chapman, C.J. and Sand, O. (1974) Field studies of hearing in two species of flatfish, *Pleuronectes platessa* and *Limanda limanda*. *Comp. Biochem. Physiol.* **47A**, 371–85.
- Chapman, N.R. (1985) Measurements of the waveform parameters of shallow explosive charges. *J. Acoust. Soc. Am.* **78**, 672–81.
- Chapman, N.R. (1988) Source levels of shallow explosive charges. *J. Acoust. Soc. Am.* **84**, 697–702.
- Chen, C. and Millero, F.J. (1977) Speed of sound in seawater at high pressures. *J. Acoust. Soc. Am.* **62**, 1129–35.
- Chen, D.G., Xie, Y., Mulligan, T.J. and MacLennan, D.N. (2004) Optimal partition of sampling effort between observations of fish density and migration speed for a riverine hydroacoustic duration-in-beam method. *Fish. Res.* **67**, 275–82.
- Chu, D. and Ye, Z. (1999) A phase-compensated distorted wave Born approximation representation of the bistatic scattering by weakly scattering objects: application to zooplankton. *J. Acoust. Soc. Am.* **106**, 1732–43.
- Chu, D., Foote, K.G. and Stanton, T.K. (1993) Further analysis of target strength measurements of Antarctic krill at 38 and 120 kHz: comparison with deformed cylinder model and inference of orientation distribution. *J. Acoust. Soc. Am.* **93**, 2985–8.

- Chu, D., Wiebe, P.H., Copley, N.J., Lawson, G.L. and Puvanendran, V. (2003) Material properties of North Atlantic cod eggs and early-stage larvae and their influence on acoustic scattering. *ICES J. Mar. Sci.* **60**, 508–15.
- Clark, C.W. (1990) Acoustic behavior of mysticete whales. In: *Sensory Abilities of Cetaceans* (eds J.A. Thomas and R.A. Kastelein), pp. 571–83. Plenum, New York.
- Clark, C.W. (1994) Application of U.S. Navy underwater hydrophone arrays for scientific research on whales. *Sci. Rep. Int. Whal. Comm.* **44**, 1–12.
- Clay, C.S. (1983) Deconvolution of the fish scattering PDF from the echo PDF for a single transducer sonar. *J. Acoust. Soc. Am.* **73**, 1989–94.
- Clay, C.S. (1992) Composite ray-mode approximations for backscattered sound from gas-filled cylinders and swimbladders. *J. Acoust. Soc. Am.* **92**, 2173–80.
- Clay, C.S. and Heist, B.G. (1984) Acoustic scattering by fish: acoustic models and a two-parameter fit. *J. Acoust. Soc. Am.* **75**, 1077–83.
- Clay, C.S. and Horne, J.K. (1994) Acoustic models of fish: the Atlantic cod (*Gadus morhua*). *J. Acoust. Soc. Am.* **96**, 1661–8.
- Clay, C.S. and Medwin, H. (1977) *Acoustical Oceanography: Principles and Applications*. John Wiley & Sons, New York.
- Cochran, W.G. (1977) *Sampling Techniques*, 3rd edn. John Wiley & Sons, New York, 428 pp.
- Cole, R.H. (1948) *Underwater Explosions*. Princeton University Press, Princeton, 436 pp.
- Conan, G., Buerkle, U., Wade, E., Chadwick, M. and Comeau, M. (1988) Geostatistical analysis of spatial distribution in a school of herring. ICES CM 1988/D:21, 19 pp.
- Connelly, P.R., Woodward, B. and Goodson, A.D. (1997) A non intrusive tracking technique for dolphins interacting with a pelagic trawl using a sparse array of hydrophones. *Proc. Inst. Acoust.* **19**, 193–8.
- Conti, S. and Demer, D.A. (2003) Wide-bandwidth acoustical characterization of anchovy and sardine from reverberation measurements in an echoic tank. *ICES J. Mar. Sci.* **60**, 617–24.
- Coombs, S.H. (1981) A density-gradient column for determining the specific gravity of fish eggs, with particular reference to eggs of mackerel *Scomber scombrus*. *Mar. Biol.* **63**, 101–6.
- Coombs, S. and Fay, R.R. (1989) The temporal evolution of masking and frequency selectivity in the goldfish (*Carassius auratus*). *J. Acoust. Soc. Am.* **86**, 925–33.
- Coombs, S. and Popper, A.N. (1979) Hearing differences among Hawaiian squirrelfish (Holocentridae) related to differences in the peripheral auditory system. *J. Comp. Physiol.* **132**, 203–7.
- Costello, J.H., Pieper, R.E. and Holliday, D.V. (1989) Comparison of acoustic and pump sampling techniques for the analysis of zooplankton distributions. *J. Plankton Res.* **11**, 703–9.
- Craig, R.E. (1983) Re-definition of sonar theory in terms of energy. *FAO Fish. Rep.* **300**, 1–3.
- Craig, R.E. and Forbes, S.T. (1969) A sonar for fish counting. *FiskDir. Skr. Ser. Havunders.* **15**, 210–19.
- Cressie, N. (1993) *Statistics for Spatial Data*. John Wiley & Sons, New York.
- Crittenden, R.N. and Thomas, G.L. (1992) A comparison of four duration-in-beam estimators for the sine of the half angle of the effective conical volume sampled. *Fish. Res.* **14**, 197–208.
- Crittenden, R.N., Thomas, G.C., Marino, D.A. and Thorne, R.E. (1988) A weighted duration-in-beam estimator for the volume sampled by a quantitative echosounder. *Can. J. Fish. Aquat. Sci.* **45**, 1249–56.
- Curtis, K.R., Howe, B.M. and Mercer, J.A. (1999) Low frequency ambient sound in the North Pacific: long time series observations. *J. Acoust. Soc. Am.* **106**, 3189–200.

- Cushing, D.H. (1977) Observations on fish shoals with the ARL scanner. *Rapp. P.-v. Reun. Cons. Int. Explor. Mer* **170**, 15–20.
- Dagorn, I., Bach, P. and Josse, E. (2000a) Movement patterns of large bigeye tuna (*Thunnus obesus*) in the open ocean determined using ultrasonic telemetry. *Mar. Biol.* **136**, 361–71.
- Dagorn, I., Bach, P. and Josse, E. (2000b) Individual differences in horizontal movements of yellowfin tuna (*Thunnus albacores*) in nearshore areas in French Polynesia. *Aqu. Living Resources* **13**, 193–202.
- Dalen, J. and Bodholt, H. (1991) Deep-towed vehicle for fish abundance estimation: concept and testing. ICES CM 1991/B:53, 13 pp.
- Dalen, J. and Kristensen, K.E. (1990) Comparative studies of theoretical and empirical target-strength models of euphausiids (krill) in relation to field-experiment data. *Rapp. P.-v. Reun. Cons. Int. Explor. Mer* **189**, 336–44.
- Dalen, J. and Løvik, A. (1981) The influence of wind induced bubbles on echo integration surveys. *J. Acoust. Soc. Am.* **69** (6), 1653–9.
- Dalen, J. and Nakken, O. (1983) On the application of the echo integration method. ICES CM 1983/B:19, 30 pp. (mimeo).
- Dalen, J. and Smedstad, O.M. (1983) Abundance estimation of demersal fish in the Barents Sea by an extended acoustic method. *FAO Fish. Rep.* **300**, 232–9.
- Dalen, J., Nedreaas, K. and Pedersen, R. (2003) A comparative acoustic-abundance estimation of pelagic redfish (*Sebastes mentella*) from hull-mounted and deep-towed acoustic systems. *ICES J. Mar. Sci.* **60**, 472–9.
- de Munck, J.C. and Schellart, N.A.M. (1987) A model for the nearfield acoustics of the fish swimbladder and its relevance for directional hearing. *J. Acoust. Soc. Am.* **81**, 556–60.
- De Rosny, J. and Roux, P. (2001) Multiple scattering in a reflecting cavity: application to fish counting in a tank. *J. Acoust. Soc. Am.* **109**, 2587–97.
- Degnbol, P. and Lewy, P. (1990) Interpretation of target-strength information from split-beam data. *Rapp. P.-v. Reun. Cons. Int. Explor. Mer* **189**, 274–82.
- Degnbol, P., Lassen, H. and Staehr, K.J. (1985) In-situ determination of target strength of herring and sprat at 38 and 120 kHz. *Dana* **5**, 45–54.
- Del Grosso, V.A. (1974) New equation for the speed of sound in natural waters (with comparison with other equations). *J. Acoust. Soc. Am.* **56**, 1084–91.
- Del Grosso, V.A. and Mader, C.W. (1972) Speed of sound in pure water. *J. Acoust. Soc. Am.* **52**, 1442–6.
- Demer, D.A. (1994) Accuracy and precision of echo integration surveys of Antarctic krill. Ph.D. Thesis, University of California, San Diego.
- Demer, D.A. (2004) An estimate of error for the CCAMLR 2000 survey estimate of krill biomass. *Deep Sea Res. II* **51**, 1237–51.
- Demer, D.A. and Conti, S. (2003) Validation of the stochastic distorted-wave Born approximation model with broad bandwidth total target-strength measurements of Antarctic krill. *ICES J. Mar. Sci.* **60**, 625–35.
- Demer, D.A. and Hewitt, R.P. (1995) Bias in acoustic estimates of *Euphausia superba* due to diel vertical migration. *Deep Sea Res. I* **42**, 455–75.
- Demer, D.A. and Martin, L.V. (1995) Zooplankton target strength: volumetric or areal dependence? *J. Acoust. Soc. Am.* **98**, 1111–18.
- Demer, D.A., Soule, M.A. and Hewitt, R.P. (1999) A multiple-frequency method for potentially improving the accuracy and precision of in situ target strength measurements. *J. Acoust. Soc. Am.* **105**, 2359–76.

- Demer, D.A., Barange, M. and Boyd, A.J. (2000) Measurements of three-dimensional fish school velocities with an acoustic Doppler current profiler. *Fish. Res.* **47**, 201–14.
- Denbigh, P., Smith, Q. and Hampton, I. (1991) Determination of fish number density by a statistical analysis of backscattered sound. *J. Acoust. Soc. Am.* **90**, 457–69.
- Diachok, O. (1999) Effects of absorptivity due to fish on transmission loss in shallow water. *J. Acoust. Soc. Am.* **105**, 2107–28.
- Diercks, J.J., Trochta, R.T., Greenlaw, R.L. and Evans, W.E. (1971) Recording and analysis of dolphin echolocation signals. *J. Acoust. Soc. Am.* **49**, 1729–32.
- Diner, N. (1999) Correction of school geometry and density: an approach based on acoustic image simulation. *ICES Coop. Res. Rep.* **238**, 27–51.
- Diner, N. and Massé, J. (1987) Fish school behaviour during echo survey observed by acoustic devices. Presented at the International Symposium on Fisheries Acoustics, Seattle, USA, 22–26 June 1987, Paper No. 30, 28 pp. (mimeo).
- Ding, L. (1997) Direct laboratory measurement of forward scattering by individual fish. *J. Acoust. Soc. Am.* **101**, 3398–404.
- Do, M.A. and Surti, A.M. (1990) Estimation of dorsal aspect target strength of deep-water fish using a simple model of swimbladder backscattering. *J. Acoust. Soc. Am.* **87**, 1588–96.
- Dobbins, P.F. (2001) Modelling dolphin echolocation reception. *Proc. Inst. Acoust.* **23** (4), 123–32.
- Dragesund, O. and Olsen, S. (1965) On the possibility of estimating year-class strength by measuring echo-abundance of 0-group fish. *FiskDir. Skr. Ser. Havunders.* **13**, 47–75.
- Dragonette, L.R., Vogt, R.H., Flax, L. and Neubauer, W.G. (1974) Acoustic reflection from elastic spheres and rigid spheres and spheroids. II Transient analysis. *J. Acoust. Soc. Am.* **55**, 1130–7.
- Duncan, A. and Kubecka, J. (1996) Patchiness of longitudinal fish distribution in a river as revealed by a continuous hydroacoustic survey. *ICES J. Mar. Sci.* **53**, 161–5.
- Duncan, P.M. (1985) Seismic sources in a marine environment. In: *Proceedings of the Workshop on Effects of Explosive Use in the Marine Environment*, 29–31 January 1985, Halifax (eds G.D. Greene, F.R. Engelhardt and R.J.E. Paterson). *Tech. Rep. Canada Oil and Gas Lands Administration, Ottawa*, No. 5, pp. 56–87.
- Dunshaw, B.D., Worcester, P.F., Cornuelle, B.D. and Howe, B.M. (1993) On equations for the speed of sound in seawater. *J. Acoust. Soc. Am.* **93**, 255–75.
- Edwards, J.I. and Armstrong, F. (1983) Measurement of the target strength of live herring and mackerel. *FAO Fish. Rep.* **300**, 69–77.
- Edwards, J.I. and Armstrong, F. (1984) Target strength experiments on caged fish. *Scot. Fish. Bull.* **48**, 12–20.
- Edwards, J.I., Armstrong, F., Magurran, A.E. and Pitcher, T.J. (1984) Herring, mackerel and sprat target strength experiments with behavioural observations. ICES CM 1984/B:34 (mimeo).
- Efron, B. and Tibshirani, R. (1986) Bootstrap methods for standard errors, confidence intervals and other measures of statistical accuracy. *Statistical Science* **2**, 54–77.
- Ehrenberg, J.E. (1972) A method for extracting the fish target strength distribution from acoustic echoes. *Proc. 1972 IEEE Conf. Eng. Ocean Environ.* **1**, 61–4.
- Ehrenberg, J.E. (1973) Estimation of the intensity of a filtered Poisson process and its application to acoustic assessment of marine organisms. *Univ. Wash. Sea Grant Publ. WSG* **73-2**, 135 pp.

- Ehrenberg, J.E. (1974a) Two applications for a dual-beam transducer in hydroacoustic fish assessment systems. *Proceedings of the IEEE International Conference on Engineering in the Ocean Environment*, 21–23 August 1974, IEEE 1974, pp. 152–5.
- Ehrenberg, J.E. (1974b) Recursive algorithm for estimating the spatial density of acoustic point scatterers. *J. Acoust. Soc. Am.* **56**, 542–7.
- Ehrenberg, J.E. (1979) A comparative analysis of in situ methods for directly measuring the acoustic target strength of individual fish. *IEEE J. Oceanics Engineering* **OE-4**, 141–52.
- Ehrenberg, J.E. (1983) A review of in situ target strength estimation techniques. *FAO Fish. Rep.* **300**, 85–90.
- Ehrenberg, J.E. and Steig, T.W. (2003) Improved techniques for studying the temporal and spatial behaviour of fish in a fixed location. *ICES J. Mar. Sci.* **60**, 700–6.
- Ehrenberg, J.E. and Torkelson, T.C. (1996) Application of dual-beam and split-beam target tracking in fisheries acoustics. *ICES J. Mar. Sci.* **53**, 329–34.
- Ehrenberg, J.E. and Torkelson, T.C. (2000) FM slide (chirp) signals: a technique for significantly improving the signal-to-noise performance in hydroacoustic assessment systems. *Fish. Res.* **47**, 193–9.
- Ehrenberg, J.E., Carlson, T.J., Traynor, J.J. and Williamson, N.J. (1981) Indirect measurement of the mean acoustic backscattering cross-section of fish. *J. Acoust. Soc. Am.* **69**, 955–62.
- Engås, A., Misund, O.A., Soldal, A.V., Horvei, B. and Solstad, A. (1995) Reactions of penned herring and cod to playback of original, frequency-filtered and time-smoothed vessel sound. *Fish. Res.* **22**, 243–54.
- Engås, A., Lokkeborg, L., Ona, E. and Soldal, A.V. (1996) Effects of seismic shooting on local abundance and catch rates of cod (*Gadus morhua*) and haddock (*Melanogrammus aeglefinus*). *Can. J. Fish. Aquat. Sci.* **53**, 2238–49.
- Enger, P.S. (1967) Hearing in herring. *Comp. Biochem. Physiol.* **22**, 527–38.
- Enger, P.S. and Anderson, R. (1967) An electrophysiological field study of hearing in fish. *Comp. Biochem. Physiol.* **22**, 517–25.
- Enger, P.S., Karlsen, H.E., Knudsen, F.R. and Sand, O. (1993) Detection and reaction of fish to infrasound. *ICES Mar. Sci. Symp.* **196**, 108–12.
- Erbe, C. and Farmer, D.M. (2000a) A software model to estimate zones of impact on marine mammals around anthropogenic noise. *J. Acoust. Soc. Am.* **108**, 1327–31.
- Erbe, C. and Farmer, D.M. (2000b) Zones of impact around icebreakers affecting beluga whales in the Beaufort Sea. *J. Acoust. Soc. Am.* **108**, 1332–40.
- Ermolchev, V. and Zaferman, M. (2003) Results of experiments on the video-acoustic estimation of fish target strength in situ. *ICES J. Mar. Sci.* **60**, 544–7.
- Evans, W.E. (1973) Echolocation by marine delphinids and one species of fresh-water dolphin. *J. Acoust. Soc. Am.* **54**, 191–9.
- Everest, F.A., Yound, R.W. and Johnson, M.W. (1948) Acoustical characteristics of noise produced by snapping shrimp. *J. Acoust. Soc. Am.* **20**, 137–42.
- Everson, I., Watkins, J.L., Bone, D.G. and Foote, K.G. (1990) Implications of a new acoustic strength for abundance estimates of Antarctic krill. *Nature* **345**, 338–40.
- Everson, I., Goss, C. and Murray, A.W.A. (1993) Comparison of krill (*Euphausia superba*) density estimates using 38 and 120 kHz echosounders. *Marine Biology* **116**, 269–75.
- Everson, I., Bravington, M. and Goss, C. (1996) A combined acoustic and trawl survey for efficiently estimating fish abundance. *Fish. Res.* **26**, 75–92.

- Farmer, D.M., Trevorow, M.V. and Pedersen, B. (1999) Intermediate range fish detection with a 12-kHz sidescan sonar. *J. Acoust. Soc. Am.* **106**, 2481–90.
- Fay, R.R. (1988) *Hearing in Vertebrates: A Psychophysics Databook*. Hill-Fay Associates, Winnetka, IL.
- Fay, R.R. and Popper, A.N. (1980) Structure and function in teleost auditory systems. In: *Comparative Studies of Hearing in Vertebrates* (eds A.N. Popper and R.R. Fay), pp. 1–42. Springer-Verlag, New York.
- Fedotova, T.A. and Shatoba, O.E. (1983) Acoustic backscattering cross-section of cod averaged by sizes and inclination of fish. *FAO Fish. Rep.* **300**, 63–8.
- Ferguson, B.G. and Cleary, J.L. (2001) In situ source level and source position estimates of biological transient signals produced by snapping shrimp in an underwater environment. *J. Acoust. Soc. Am.* **109**, 3031–7.
- Fernandes, P.G. (1998) A spatial analysis of trawl variability in the 1995 North Sea herring acoustic survey. ICES CM 1998/J:6, 17 pp.
- Fernandes, P.G. and Simmonds, E.J. (1997) Variographic refinement of North Sea herring acoustic survey data. In: *GeoENV I – Geostatistics for Environmental Applications* (eds A. Soares, J. Gomez-Hernandez and R. Froidevaux), pp. 451–62. Kluwer, Dordrecht.
- Fernandes, P.G., Brierley, A.S., Simmonds, E.J., Millard, N.W., McPhail, S.D., Armstrong, F., Stevenson, P. and Squires, M. (2000) Fish do not avoid survey vessels. *Nature* **404**, 35–6.
- Fernandes, P.G., Gerlotto, F., Holliday, D.V., Nakken, O. and Simmonds, E.J. (2002) Acoustic applications in fisheries science: the ICES contribution. *ICES Mar. Sci. Symp.* **215**, 483–92.
- Feuillade, C. (1996) The attenuation and dispersion of sound in water containing multiply interacting air bubbles. *J. Acoust. Soc. Am.* **99**, 3412–30.
- Feuillade, C. and Clay, C.S. (1999) Anderson (1950) revisited. *J. Acoust. Soc. Am.* **106**, 553–64.
- Feuillade, C. and Nero, R.W. (1998) A viscous-elastic swimbladder model for describing enhanced-frequency resonance scattering from fish. *J. Acoust. Soc. Am.* **103**, 3245–55.
- Feuillade, C., Nero, R.W. and Love, R.H. (1996) A low-frequency acoustic scattering model for small schools of fish. *J. Acoust. Soc. Am.* **99**, 196–208.
- Fine, M.L., Winn, H.E. and Olla, B.L. (1977) Communication in fishes. In: *How Animals Communicate* (ed. T.A. Sebeok), pp. 472–518. Indiana University Press, Bloomington.
- Finneran, J.J., Carder, D.A. and Ridgway, S.H. (2002) Low-frequency acoustic pressure, velocity and intensity thresholds in a bottlenose dolphin (*Tursiops truncatus*) and white whale (*Delphinapterus leucas*). *J. Acoust. Soc. Am.* **111**, 447–56.
- Fish, M.P. (1964) Biological sources of sustained ambient sea noise. In: *Marine Bio-acoustics* (ed. W.N. Tavolga), pp. 175–94. Pergamon Press, New York.
- Fisher, F.H. and Simmons, V.P. (1977) Sound absorption in sea water. *J. Acoust. Soc. Am.* **62**, 558–64.
- Fleischman, S.J. and Burwen, D.L. (2003) Mixture models for species apportionment of hydroacoustic data, with echo-envelope length as the discriminatory variable. *ICES J. Mar. Sci.* **60**, 592–8.
- Fletcher, H. (1940) Auditory patterns. *Rev. Mod. Phys.* **12**, 47–56.
- Flint, J.A., Goodson, A.D. and Pomeroy, S.C. (1997) Visualising wave propagation in bio-acoustic lens structures using the transmission line modelling method. *Proc. Inst. Acoust.* **19** (9), 29–37.
- Foldy, L.L. and Primakoff, H. (1945) General theory of passive linear electroacoustic transducers and the electroacoustic reciprocity theorem I. *J. Acoust. Soc. Am.* **17**, 109–20.

- Foldy, L.L. and Primakoff, H. (1947) General theory of passive linear electroacoustic transducers and the electroacoustic reciprocity theorem II. *J. Acoust. Soc. Am.* **19**, 50–8.
- Foote, A.D., Osborne, R.W. and Hoelzel, A.R. (2004) Whale-call response to masking boat noise. *Nature* **428**, 910.
- Foote, K.G. (1978) Analyses of empirical observations on the scattering of sound by encaged aggregations of fish. *FiskDir. Skr. Ser. Havunders*. **16**, 422–55.
- Foote, K.G. (1979a) On representing the length dependence of acoustic target strengths of fish. *J. Fish. Res. Board Can.* **36** (12), 1490–6.
- Foote, K.G. (1979b) Evidence for the influence of fish behaviour on echo energy. In: *Meeting on Hydroacoustical Methods for the Estimation of Marine Fish Populations*, 25–29 June 1979, Vol. 2 (ed. J.B. Suomala), pp. 201–28. The Charles Stark Draper Laboratory, Cambridge, Mass., USA.
- Foote, K.G. (1980a) Effect of fish behaviour on echo energy: the need for measurements of orientation distributions. *J. Cons. Int. Explor. Mer* **39**, 193–201.
- Foote, K.G. (1980b) Importance of the swimbladder in acoustic scattering by fish: a comparison of gadoid and mackerel target strengths. *J. Acoust. Soc. Am.* **67** (6), 2084–9.
- Foote, K.G. (1981) Absorption term in time-varied-gain functions. *FiskDir. Skr. Ser. Havunders*. **17**, 191–213.
- Foote, K.G. (1982a) Optimising copper spheres for precision calibration of hydroacoustic equipment. *J. Acoust. Soc. Am.* **71**, 742–7.
- Foote, K.G. (1982b) Energy in acoustic echoes from fish aggregations. *Fisheries Research* **1**, 129–40.
- Foote, K.G. (1983) Linearity of fisheries acoustics, with addition theorems. *J. Acoust. Soc. Am.* **73**, 1932–40.
- Foote, K.G. (1985) Rather-high-frequency sound scattering by swimbladdered fish. *J. Acoust. Soc. Am.* **68**, 688–700.
- Foote, K.G. (1986) A critique of Goddard and Welsby's paper 'The acoustic target strength of live fish'. *J. Cons. Int. Explor. Mer* **42**, 212–20.
- Foote, K.G. (1987) Fish target strengths for use in echo integrator surveys. *J. Acoust. Soc. Am.* **82** (3), 981–7.
- Foote, K.G. (1990) Correcting acoustic measurements of scatterer density for extinction. *J. Acoust. Soc. Am.* **88** (3), 1543–6.
- Foote, K.G. (1991a) Acoustic sampling volume. *J. Acoust. Soc. Am.* **90**, 959–64.
- Foote, K.G. (1991b) Summary of methods for determining fish target strength at ultrasonic frequencies. *ICES J. Mar. Sci.* **48**, 211–17.
- Foote, K.G. (1996) Coincidence echo statistics. *J. Acoust. Soc. Am.* **99**, 266–71.
- Foote, K.G. (1998a) Broadband Acoustic Scattering Signatures of Fish and Zooplankton (BASS) Third Marine Science and Technology Conference, Lisbon 23–27 May 1998. In: *Vol. III, Generic Technologies*, pp. 1012–25. European Commission, Brussels, EUR 18220EN.
- Foote, K.G. (1998b) Measurement of morphology and physical properties of zooplankton. Recent advances in sonar applied to biological oceanography. Institute of Electrical Engineers, London, IEE Rep. 1998/227, 3/1–3/6.
- Foote, K.G. (1999) Extinction cross-section of Norwegian spring-spawning herring. *ICES J. Mar. Sci.* **56**, 606–12.
- Foote, K.G. (2000) Standard calibration of broadband sonars. *J. Acoust. Soc. Am.* **108**, 2484.

- Foote, K.G. and Francis, D.T.I. (2002) Comparing Kirchoff-Approximation and boundary-element-models for computing gadoid target strengths. *J. Acoust. Soc. Am.* **111**, 1644–54.
- Foote, K.G. and MacLennan, D.N. (1984) Comparison of copper and tungsten carbide calibration spheres. *J. Acoust. Soc. Am.* **75**, 612–16.
- Foote, K.G. and Nakken, O. (1978) Dorsal aspect target strength functions of six fishes at two ultrasonic frequencies. *Fisker. og Hvet. Ser. B* **1978** (3), 95 pp.
- Foote, K.G. and Ona, E. (1985) Swimbladder cross sections and acoustic target strengths of 13 pollack and 2 saithe. *FiskDir. Skr. Ser. Havunders.* **18**, 1–57.
- Foote, K.G. and Traynor, J.J. (1988) Comparison of walleye pollock target strength estimates determined from in situ measurements and calculations based on swimbladder form. *J. Acoust. Soc. Am.* **83**, 9–17.
- Foote, K.G., Knudsen, H.P. and Vestnes, G. (1983) Standard calibration of echosounders and integrators with optimal copper spheres. *FiskDir. Skr. Ser. Havunders.* **17**, 335–46.
- Foote, K.G., Aglen, A. and Nakken, O. (1986) Measurements of fish target strength with a split-beam echo sounder. *J. Acoust. Soc. Am.* **80** (2), 612–21.
- Foote, K.G., Knudsen, H.P., Vestnes, G., MacLennan, D.N. and Simmonds, E.J. (1987) Calibration of acoustic instruments for fish density estimation: a practical guide. *ICES Coop. Res. Rep.* **144**, 57 pp.
- Foote, K.G., Everson, I., Watkins, J.L. and Bone, D.G. (1990) Target strengths of Antarctic krill (*Euphausia superba*) at 38 and 120 kHz. *J. Acoust. Soc. Am.* **87**, 16–24.
- Foote, K.G., Ona, E. and Toresen, R. (1992) Determining the extinction cross section of aggregating fish. *J. Acoust. Soc. Am.* **91**, 1983–9.
- Foote, K.G., Knutsen, T., Baekkevold, A.E., Dalpado, P. and Johannessen, S.E. (1996) Initial, collateral measurements of some properties of *Calanus finmarchicus*. *ICES CM 1996/L:21*, 23 pp.
- Foote, K.G., Francis, D.T.I., Furset, H. and Hobaek, H. (1999) Spheres for calibrating high-frequency broadband echosounders. *Acta Acustica* **85**, S186–7.
- Forbes, S.T. (1985) Progress in dual-beam target-strength measurement on herring and blue whiting. *ICES CM1985/B:22*, 5 pp. (mimeo).
- Forbes, S.T. and Nakken, O. (1972) (eds) *Manual of Methods for Fisheries Resource Survey and Appraisal. Part 2: The Use of Acoustic Instruments for Fish Detection and Abundance Estimation*. FAO Man. Fish. Sci., Food and Agriculture Organisation, Rome.
- Francis, D.T.I. (1993) A gradient formulation of the Helmholtz integral equation for acoustic radiation and scattering. *J. Acoust. Soc. Am.* **93**, 1700–09.
- Francis, R.I.C.C. (1984) An adaptive strategy for random trawl surveys. *New Zealand J. Mar. Freshwat. Res.* **18**, 57–91.
- Francis, R.I.C.C. (1985) Two acoustic surveys of pelagic fish in Hawke Bay, New Zealand, 1980. *New Zealand J. Mar. Freshwat. Res.* **19**, 375–89.
- Francis, R.I.C.C. (1991) Statistical properties of two-phase surveys: comment. *Can. J. Fish. Aquat. Sci.* **48**, 1228.
- Francois, R.E. and Garrison, G.R. (1982a) Sound absorption based on ocean measurements. Part I: Pure water and magnesium sulphate contributions. *J. Acoust. Soc. Am.* **72**, 896–907.
- Francois, R.E. and Garrison, G.R. (1982b) Sound absorption based on ocean measurements. Part II: Boric acid contributions and equation for total absorption. *J. Acoust. Soc. Am.* **72**, 1879–90.
- Frankel, A.S. (1995) Individual variation in the songs of humpback whales. *J. Acoust. Soc. Am.* **99**, 2556.

- Fréon, P. and Misund, O.A. (1999) *Dynamics of Pelagic Fish Distribution and Behaviour: Effects on Fisheries and Stock Assessment*. Fishing News Books, Oxford.
- Fréon, P., Gerlotto, F. and Soria, M. (1992) Changes in school structure according to external stimuli: description and influence on acoustic assessment. *Fish. Res.* **15**, 45–66.
- Fréon, P., Gerlotto, F. and Soria, M. (1996) Diel variability of school structure with special reference to transition periods. *ICES J. Mar. Sci.* **53**, 459–64.
- Fryer, R.J. (1991) A model of between-haul variation in selectivity. *ICES J. Mar. Sci.* **48**, 281–90.
- Furusawa, M. (1988) Prolate spheroidal models for predicting general trends of fish target strength. *J. Acoust. Soc. Japan (E)* **9**, 13–24.
- Furusawa, M., Ishii, K., Miyanohana, Y. and Maniwa, Y. (1984) Experimental investigation of an acoustic method to estimate fish abundance using culture nets. *Jpn J. Appl. Phys.* **23** (Suppl. 23), 101–3.
- Furusawa, M., Ishii, K. and Miyanohana, Y. (1992) Attenuation of sound by schooling fish. *J. Acoust. Soc. Am.* **92**, 987–94.
- Furusawa, M., Miyanohana, Y., Ariji, M. and Sawada, Y. (1994) Prediction of krill target strength by liquid prolate spheroid model. *Fish. Sci.* **60**, 261–5.
- Furusawa, M., Hamada, M. and Aoyama, C. (1999) Near range errors in sound scattering measurements of fish. *Fish. Sci. (Japan)* **65**, 109–16.
- Garnier, B.E., Beltri, P., Marchand, P. and Diner, N. (1992) Noise signature management of fisheries research vessels. In: *Proceedings of European Conference on Underwater Acoustics* (ed. M. Weydert), pp. 210–15. Elsevier.
- Gaudet, D.M. (1990) Enumeration of migrating salmon populations using fixed location sonar counters. *Rapp. P.-v. Reun. Cons. Int. Explor. Mer* **189**, 197–209.
- Gauthier, S. and Rose, G.A. (2002) Acoustic observation of diel vertical migration and shoaling behaviour in Atlantic redfishes. *J. Fish Biol.* **61**, 1135–53.
- Gauthier, S., Boisclair, D. and Legendre, P. (1997) Evaluation of a variable angle scanning method to estimate relative abundance and distribution of fish using a single-beam echosounder in shallow lakes. *J. Fish. Biol.* **50**, 208–21.
- Gerlotto, F. and Fréon, P. (1988) Influence of the structure and behaviour of fish schools on acoustic assessment. ICES CM1988/B:53, 31 pp.
- Gerlotto, F. and Paramo, J. (2003) The three-dimensional morphology and internal structure of clupeid schools as observed using vertical scanning multibeam sonar. *Aqu. Living Resources* **16**, 113–22.
- Gerlotto, F., Fréon, P., Soria, P., Cottais, P.H. and Ronzier, L. (1994) Exhaustive observation of 3D school structure using multibeam side scan sonar, potential use for school classification, biomass estimation and behaviour studies. ICES CM 1994/B:26, 12 pp.
- Gerlotto, F., Hernandez, C. and Linares, E. (1998) Experiences with multibeam sonar in shallow tropical waters. *Fish. Res.* **35**, 143–8.
- Gerlotto, F., Soria, M. and Fréon, P. (1999) From two dimensions to three: the use of multibeam sonar for a new approach in fisheries acoustics. *Can. J. Fish. Aquat. Sci.* **56**, 6–12.
- Gerstein, E.R., Gerstein, L., Forsythe, S.E. and Blue, J.E. (1999) The underwater audiogram of the West Indian manatee (*Trichechus manatus*). *J. Acoust. Soc. Am.* **105**, 3575–83.
- Getabu, A., Tumwebaze, R. and MacLennan, D.N. (2003) Spatial distribution and temporal changes in the fish populations of Lake Victoria. *Aqu. Living Resources* **16**, 159–65.

- Gimona, A. and Fernandes, P.G. (2003) A conditional simulation of acoustic survey data: advantages and potential pitfalls. *Aqu. Living Resources* **16**, 113–22.
- Godø, O.R. and Wespestad, V.G. (1993) Monitoring changes in abundance of gadoids with varying availability to trawl and acoustic surveys. *ICES J. Mar. Sci.* **50**, 39–51.
- Goertner, J.F. (1978) Dynamical model for explosion injury to fish, Naval Surface Weapons Center, White Oak Laboratory, Tech. Rep. NSWC/WO2/TR76-155, 136 pp.
- Goodman, R.R. and Stern, R. (1962) Reflection and transmission of sound by elastic spherical shells. *J. Acoust. Soc. Am.* **34**, 338–44.
- Goodson, A.D. (1997) Developing deterrent devices designed to reduce the mortality of small cetaceans in commercial fishing nets. *Mar. Freshwat. Behav. Physiol.* **29**, 211–36.
- Goodson, A.D. and Klinowska, M. (1990) A proposed echolocation receptor for the bottlenose dolphin (*Tursiops truncatus*): modelling the receive directivity from tooth and lower jaw geometry. In: *Sensory Abilities of Cetaceans: Laboratory and Field Evidence* (eds J.A. Thomas and R.A. Kastelein), pp. 255–68. Plenum Press, New York.
- Goodson, A.D. and Sturtivant, C.R. (1996) Sonar characteristics of the harbour porpoise (*Phocoena phocoena*): source levels and spectrum. *ICES J. Mar. Sci.* **53**, 465–72.
- Goold, J.C. and Fish, P.J. (1998) Broadband spectra of seismic survey air-gun emissions with reference to dolphin auditory thresholds. *J. Acoust. Soc. Am.* **103**, 2177–84.
- Gorska, N. and Ona, E. (2003) Modelling the acoustic effect of swimbladder compression in herring. *ICES J. Mar. Sci.* **60**, 548–54.
- Goss, C., Middleton, D. and Rodhouse, P. (2001) Investigations of squid stocks using acoustic survey methods. *Fish. Res.* **54**, 111–21.
- Greene, C.H., Stanton, T.K., Wiebe, P.H. and McClatchie, S. (1991) Acoustic estimates of Antarctic krill. *Nature* **349**, 110.
- Greene, C.H., Wiebe, P.H., Pershing, A.J., Gal, G., Popp, J.M., Copley, N.J., Austin, T.C., Bradley, A.M., Goldsborough, R.G., Dawson, J., Hendershott, R. and Kaartvedt, S. (1998) Assessing the distribution and abundance of zooplankton: a comparison of acoustic and net sampling methods with D-BAD MOCNESS. *Deep Sea Res. II* **45**, 1219–37.
- Greene, G.D., Engelhardt, F.R. and Paterson, R.J.E. (1985) (eds) *Proceedings of the Workshop on Effects of Explosive Use in the Marine Environment*, 29–31 January 1985, Halifax. Tech. Rep. Canada Oil and Gas Lands Administration, Ottawa, No. 5, 383 pp.
- Greenlaw, C.F. (1977) Backscattering spectra of preserved zooplankton. *J. Acoust. Soc. Am.* **62**, 44–52.
- Greenlaw, C.F. (1979) Acoustical estimation of zooplankton populations. *Limnology and Oceanography* **24**, 226–42.
- Greenlaw, C.F. and Johnson, R.K. (1982) Physical and acoustical properties of zooplankton. *J. Acoust. Soc. Am.* **72**, 1706–10.
- Greenlaw, C.F. and Johnson, R.K. (1983) Multiple frequency acoustical estimation. *Biological Oceanography* **2**, 227–52.
- Gregory, J. and Clabburn, P. (2003) Avoidance behaviour of *Alosa fallax fallax* to pulsed ultrasound as a technique for monitoring clupeid spawning migration in a shallow river. *Aqu. Living Resources* **16**, 313–16.
- Griffiths, G., Fielding, S. and Roe, H.S.J. (2002) Biological–physical–acoustical interactions. In: *The Sea*, Vol. 12 (eds A.R. Robinson, J.J. McCarthy and B.J. Rothschild), pp. 441–74. John Wiley & Sons, New York.
- Gulland, J.A. (1983) *Fish Stock Assessment: A Manual of Basic Methods*. FAO Food and Agriculture Series, John Wiley & Sons Ltd, Chichester.

- Gunderson, D.R. (1993) *Surveys of Fisheries Resources*. John Wiley & Sons, New York.
- Gutierrez, M. and MacLennan, D.N. (1998) Preliminary results of determination of in situ target strength of main pelagic species: Cruise of RV Humboldt 9803-05 from Tumbes to Tacna (in Spanish, English abstract). *Inf. Inst. Mar Peru* **135**, 16–19.
- Hall, J.D. and Johnson, C.S. (1972) Auditory thresholds of a killer whale, *Orcinus orca*. *J. Acoust. Soc. Am.* **51**, 515–17.
- Hall, M.V. (1989) A comprehensive model of wind-generated bubbles in the ocean and predictions of the effects on sound propagation at frequencies up to 40 kHz. *J. Acoust. Soc. Am.* **86**, 1103–17.
- Halldorsson, O. and Reynisson, P. (1983) Target strength measurements of herring and capelin in situ at Iceland. *FAO Fish. Rep.* **300**, 78–84.
- Hamilton, D., Lozow, J., Suomala Jr, J. and Werner, R. (1977) A hydroacoustic measurement program to examine target quantification methods. *Rapp. P.-v. Reun. Cons. Int. Explor. Mer* **170**, 105–21.
- Hamilton, M.F. and Blackstock, D.T. (1997) *Nonlinear Acoustics*. Academic Press, London.
- Hampton, I. (1996) Acoustic and egg-production estimates of South African anchovy biomass over a decade: comparisons, accuracy, and utility. *ICES J. Mar. Sci.* **53**, 493–500.
- Haralabous, J. and Georgakarakos, S. (1993) Fish-school species identification using a neural network. *ICES CM 1993/B:9*.
- Haralabous, J. and Georgakarakos, S. (1996) Artificial neural networks as a tool for species identification of fish schools. *ICES J. Mar. Sci.* **53**, 173–80.
- Harden Jones, F.R. (1968) *Fish Migration*. Edwards Arnold, London. 325 pp.
- Harris, G.G. (1964) Considerations on the physics of sound production by fishes. In: *Marine Bio-acoustics* (ed. W.N. Tavolga), pp. 233–47. Pergamon Press, Oxford.
- Haslett, R.W.G. (1970) Acoustic echoes from targets underwater. In: *Underwater Acoustics* (ed. R.W.B. Stephens), pp. 129–97. John Wiley & Sons Ltd, Chichester.
- Hastie, T.J. and Tibshirani, R.J. (1990) *Generalized Additive Models*. Chapman & Hall, London.
- Hastings, M.C., Popper, A.N., Finneran, J.J. and Lanford, P.J. (1996) Effect of low frequency underwater sound on hair cells of the inner ear and lateral line of the teleost fish *Astronotus ocellatus*. *J. Acoust. Soc. Am.* **99**, 1759–66.
- Hawkins, A.D. (1977) Fish sizing by means of swimbladder resonance. *Rapp. P.-v. Reun. Cons. Int. Explor. Mer* **170**, 122–9.
- Hawkins, A.D. (1981) Some biological sources of error in the hydroacoustical methods for the estimation of marine fish populations. In: *Meeting on Hydroacoustical Methods for the Estimation of Marine Fish Populations*, 25–29 June 1979, Vol. 2 (ed. J.B. Suomala), pp. 183–200. The Charles Stark Draper Laboratory, Cambridge, Mass., USA.
- Hawkins, A.D. (1993) Underwater sound and fish behaviour. In: *Behavior of Teleost Fishes* (ed. T.J. Pitcher), pp. 129–69. Chapman & Hall, London.
- Hawkins, A.D. and Amorim, M.C.P. (2000) Spawning sounds of the male haddock, *Melanogrammus aeglefinus*. *Env. Biol. Fishes* **59**, 29–41.
- Hawkins, A.D. and Chapman, C.J. (1975) Masked auditory thresholds in the cod, *Gadus morhua*. *J. Comp. Physiol.* **103A**, 209–26.
- Hawkins, A.D. and Johnstone, A.D.F. (1978) The hearing of the Atlantic salmon, *Salmo salar*. *J. Fish. Biol.* **13**, 655–73.

- Hawkins, A.D. and MacLennan, D.N. (1976) An acoustic tank for hearing studies on fish. In: *Sound Reception in Fish* (eds A. Schuijff and A.D. Hawkins), pp. 149–70. Elsevier, Amsterdam.
- Hawkins, A.D. and Myrberg Jr, A.A. (1983) Hearing and sound communication under water. In: *Bioacoustics: A Comparative Approach* (ed. B. Lewis), pp. 347–405. Academic Press, London.
- Hawkins, A.D. and Sand, O. (1977) Directional hearing in the median vertical plane by the cod. *J. Comp. Physiol.* **122**, 1–8.
- Hawkins, A.D., MacLennan, D.N., Urquhart, G.G. and Robb, C. (1974) Tracking cod (*Gadus morhua* L.) in a Scottish sea loch. *J. Fish Biol.* **6**, 225–36.
- Hazen, E.L. and Horne, J.K. (2003) A method for evaluating the effects of biological factors on fish target strength. *ICES J. Mar. Sci.* **60**, 555–62.
- He, P. and Wardle, C.S. (1988) Endurance at intermediate swimming speed of Atlantic mackerel, *Scomber scombrus* L., herring, *Clupea harengus* L. and saithe, *Pollachius virens* L. *J. Fish Biol.* **33** (2), 255–66.
- Heathershaw, A.D., Ward, P.D. and David, A.M. (2001) The environmental impact of underwater sound. *Proc. Inst. Acoust.* **23** (4), 1–12.
- Hedgepeth, J.B., Gallucci, F.V., O'Sullivan, F. and Thorne, R.E. (1999) An expectation maximization and smoothing approach for indirect acoustic estimation of fish size and density. *ICES J. Mar. Sci.* **56**, 36–50.
- Hedgepeth, J.B., Furiman, D., Cronkite, G.M.W., Xie, Y. and Mulligan, T. (2000) A tracking transducer for following fish movement in shallow water and at close range. *Aqua. Living Resources* **13**, 305–11.
- Helweg, D.A., Franklin, A.S., Mobley, J.R. and Herman, L.M. (1992) Humpback whale song: our current understanding. In: *Marine Mammal Sensory Systems* (eds J.A. Thomas, R.A. Kastelein and A. Ya Supin), pp. 459–83. Plenum, New York.
- Hersey, J.B., Backus, R.H. and Hellwig, J. (1962) Sound-scattering spectra of deep scattering layers in the western North Atlantic Ocean. *Deep Sea Res.* **8**, 196–210.
- Hester, F.J. (1967) Identification of biological sonar targets from body motion Doppler shifts. In: *Symposium on Marine Bioacoustics*, Vol. 2 (ed. W.N. Tavolga), pp. 59–74. Pergamon Press, New York.
- Hewitt, R.P. and Demer, D.A. (1991) Krill abundance. *Nature* **353**, 310.
- Hewitt, R.P. and Demer, D.A. (1996) Lateral target strength of Antarctic krill. *ICES J. Mar. Sci.* **53**, 297–302.
- Hewitt, R.P., Smith, P.E. and Brown, J.C. (1976) Development and use of sonar mapping for pelagic stock assessment in the California current area. *Fishery Bulletin (USA)* **74** (2), 281–300.
- Hickling, R. (1962) Analysis of echoes from a solid elastic sphere in water. *J. Acoust. Soc. Am.* **34**, 1582–92.
- Hodgson, W.C. (1950) Echosounding and the pelagic fisheries. *Fishery Investigations, Series 2*, **17** (4). 25 pp.
- Hodgson, W.C. and Fridriksson, A. (1955) Report on echo-sounding and Asdic for fishing purposes. *Rapp. P.-v. Reun. Cons. Int. Explor. Mer* **139**, 1–45.
- Holliday, D.V. (1974) Doppler structure in schools of pelagic fish. *J. Acoust. Soc. Am.* **55**, 1313–22.
- Holliday, D.V. (1977a) Two applications of the Doppler effect in the study of fish schools. *Rapp. P.-v. Reun. Cons. Int. Explor. Mer* **170**, 21–30.

- Holliday, D.V. (1977b) The use of swimbladder resonance in the sizing of schooled pelagic fish. *Rapp. P.-v. Reun. Cons. Int. Explor. Mer* **170**, 130–35.
- Holliday, D.V. and Pieper, R.E. (1995) Bioacoustical oceanography at high frequencies. *ICES J. Mar. Sci.* **52**, 279–96.
- Holliday, D.V., Pieper, R.E. and Kleppel, G.S. (1989) Determination of zooplankton size and distribution with multifrequency acoustic technology. *J. Cons. Int. Explor. Mer* **46**, 52–61.
- Horne, J.K. (2000) Acoustic approaches to remote species identification: a review. *Fish. Oceanog.* **9**, 356–71.
- Horne, J.K., Walline, P.D. and Jech, J.M. (2000) Comparing acoustic model predictions to in situ backscatter measurements of fish with dual-chambered swimbladders. *J. Fish Biol.* **57**, 1105–21.
- Huang, K. and Clay, C.S. (1979) Backscattering cross-sections of live fish: PDF and aspect. *J. Acoust. Soc. Am.* **67**, 795–802.
- Hubbs, C.L. and Rechnitzer, A.B. (1952) Report on experiments designed to determine effects of underwater explosions on fish life. *California Fish and Game* **38**, 333–66.
- Hughes, S. (1998) A mobile horizontal hydroacoustic fisheries survey of the river Thames, United Kingdom. *Fish. Res.* **35**, 91–7.
- Hurst, D.H. and Karlson, J.A. (2004) Side-scan sonar along the north wall of the Hess Deep Rift: processing, texture analysis and geological ground truth on an oceanic escarpment. *J. Geophys. Res.* **109**, B02107.
- Huse, I. and Ona, E. (1996) Tilt angle distribution and swimming speed of overwintering Norwegian spring spawning herring. *ICES J. Mar. Sci.* **53**, 863–73.
- Hwang, D., Sano, N., Iida, K., Mukai, T., Masuda, K. and Sasaki, S. (1993) Target strength of demersal fish calculated from echo integration and bottom trawl in the East China Sea. *Bull. Fac. Fish. Hokkaido Univ.* **44**, 197–208.
- Iida, K., Mukai, T. and Ishii, K. (1991) Application of a dual beam echo-sounder to measuring fish length. *Nippon Suisan Gakkaishi* **57**, 623–7.
- Iida, K., Mukai, T. and Hwang, D. (1996) Relationship between acoustic backscattering strength and density of zooplankton in the sound-scattering layer. *ICES J. Mar. Sci.* **53**, 507–12.
- Jacobs, D.W. and Hall, J.D. (1972) Auditory thresholds of a freshwater dolphin, *Inia geoffrensis*. *J. Acoust. Soc. Am.* **51**, 530–3.
- Jacobs, J.E. (1965) The ultrasound camera. *Science (London)* **1** (4), 60–65.
- Jacobson, P.T., Clay, C.S. and Magnusson, J.J. (1990) Size, distribution and abundance of pelagic fish by deconvolution of single-beam acoustic data. *Rapp. P.-v. Reun. Cons. Int. Explor. Mer* **189**, 304–11.
- Jaffe, J.S. (1999) Target localisation for a three-dimensional multibeam sonar imaging system. *J. Acoust. Soc. Am.* **105**, 3168–75.
- Jaffe, J.S., Reuss, E., McGehee, D. and Chandran, G. (1995) FTV, a sonar for tracking macrozooplankton in three dimensions. *Deep Sea Res.* **45**, 1495–512.
- Jaffe, J.S., Ohman, M.D. and De Robertis, A. (1998) OASIS in the sea: measurement of the acoustic reflectivity of zooplankton with concurrent optical imaging. *Deep Sea Res.* **45**, 1239–53.
- Jakobsson, J. (1983) Echo surveying of the Icelandic summer spawning herring 1973–1982. *FAO Fish. Rep.* **300**, 240–8.
- Jech, J.M., Schael, D.M. and Clay, C.S. (1995) Application of three sound scattering models to threadfin shad (*Dorosoma petenense*). *J. Acoust. Soc. Am.* **98**, 2262–9.

- Jefferts, K., Burczynski, J.J. and Pearcy, W.G. (1987) Acoustical assessment of squid, *Loligo opalescens*, off the Central Oregon coast. *Can. J. Fish. Aquat. Sci.* **44**, 1261–7.
- Jensen, F.B., Kuperman, W.A., Porter, M.B. and Schmidt, H. (1994) *Computational Ocean Acoustics*. American Institute of Physics Press, New York.
- Jerkø, H., Turunen-Rise, I., Enger, P.S. and Sand, O. (1989) Hearing in the eel (*Anguilla anguilla*). *J. Comp. Physiol. A* **165**, 455–69.
- Johannesson, K.A. and Losse, G.F. (1977) Methodology of acoustic estimations of fish abundance in some UNDP/FAO resource survey projects. *Rapp. P.-v. Reun. Cons. Int. Explor. Mer* **170**, 296–318.
- Johannesson, K.A. and Mitson, R.B. (1983) Fisheries acoustics: a practical manual for biomass estimation. *FAO Fish. Tech. Pap.* **240**, 249 pp.
- Johnson, B.D. and Cooke, R.C. (1979) Bubble population and spectra in coastal waters: a photographic approach. *J. Geophys. Res.* **84**, 3761–6.
- Johnson, C.G. (1967) Sound detection thresholds in marine mammals. In: *Marine Bio-acoustics* (ed. W.N. Tavolga), pp. 247–60. Pergamon Press, Oxford.
- Johnson, C.S., McManus, M.W. and Skaar, D. (1989) Masked tonal hearing thresholds in the beluga whale. *J. Acoust. Soc. Am.* **85**, 2651–4.
- Johnson, R.K. (1977) Sound scattering from a fluid sphere revisited. *J. Acoust. Soc. Am.* **61**, 375–7.
- Johnston, S.V. and Hopelain, J.S. (1990) The application of dual-beam target tracking and Doppler shifted echo processing to assess upstream salmonid migration in the Klamath River, California. *Rapp. P.-v. Reun. Cons. Int. Explor. Mer* **189**, 210–22.
- Jolly, G.M. and Hampton, I. (1990) A stratified random transect design for acoustic surveys of fish stocks. *Can. J. Fish. Aquat. Sci.* **47**, 1282–91.
- Jones, R.H. (1993) *Longitudinal Data with Serial Correlation: A State Space Approach*. Chapman & Hall, London.
- Kajiwara, Y., Iida, K. and Kamei, Y. (1990) Measurement of target strength for the flying squid (*Ommastrephes bartrami*). *Bull. Fac. Fish. Hokkaido Univ.* **41**, 205–12.
- Kalikhman, I. and Ostrovsky, I. (1997) Patchy distribution fields: survey design and adequacy of reconstruction. *ICES J. Mar. Sci.* **54** (5), 809–18.
- Kang, D. and Hwang, D. (2003) Ex situ target strength of rockfish (*Sebastodes schlegeli*) and red seabream (*Pagrus major*) in the Northwest Pacific. *ICES J. Mar. Sci.* **60**, 538–43.
- Kang, M., Furusawa, M. and Miyashita, K. (2002) Effective and accurate uses of difference in mean volume backscattering strength to identify fish and plankton. *ICES J. Mar. Sci.* **59**, 794–804.
- Kargl, S.G. and Marston, P.L. (1989) Observation and modeling of the backscattering of short tone bursts from a spherical shell: Lamb wave echoes, glory, and axial reverberations. *J. Acoust. Soc. Am.* **85**, 1014–28.
- Karlsen, H.E. (1992a) The inner ear is responsible for detection of infrasound in the perch (*Perca fluviatilis*). *J. Exp. Biol.* **171**, 163–72.
- Karlsen, H.E. (1992b) Infrasound sensitivity in the plaice (*Pleuronectes platessa*). *J. Exp. Biol.* **171**, 173–87.
- Kastak, D. and Schusterman, R.J. (1996) Temporary threshold shift in a harbor seal (*Phoca vitulina*). *J. Acoust. Soc. Am.* **100**, 1905–8.
- Kendall, M.G. and Buckland, W.R. (1971) *A Dictionary of Statistical Terms*, 3rd edn. Longman, London.

- Kenyon, T.N., Ladich, F. and Yan, H.Y. (1998) A comparative study of hearing ability in fishes: the auditory brainstem response approach. *J. Comp. Physiol. A* **182**, 307–18.
- Kieser, R. and Ehrenberg, J.E. (1990) An unbiased stochastic echo counting model. *Rapp. P.-v. Reun. Cons. Int. Explor. Mer* **189**, 65–72.
- Kieser, R. and Mulligan, T.J. (1984) Analysis of echo-counting data: a model. *Can. J. Fish. Aquat. Sci.* **41**, 451–8.
- Kieser, R., Mulligan, T. and Ehrenberg, J.E. (2000) Observation and explanation of systematic split-beam angle measurement errors. *Aqu. Living Resources* **13**, 275–81.
- Kimura, D.K. and Lemberg, N.A. (1981) Variability of line intercept density estimates (a simulation study of the variance of hydroacoustic biomass estimates). *Can. J. Fish. Aquat. Sci.* **38**, 1141–52.
- Kimura, K. (1929) On the detection of fish-groups by an acoustic method. *J. Imp. Fish. Inst., Tokyo* **24**, 41–5.
- Kinsler, L.E. and Frey, A.R. (1951) *Fundamentals of Acoustics*. John Wiley & Sons, New York.
- Kirsch, J., Thomas, G.L. and Cooney, R.T. (2000) Acoustic estimates of zooplankton distributions in Prince William Sound, Spring 1996. *Fish. Res.* **47**, 245–60.
- Klevjer, T.A. and Kaartvedt, S. (2003) Split-beam target tracking can be used to study the swimming behaviour of deep-living plankton in situ. *Aqu. Living Resources* **16**, 293–8.
- Kloser, R.J. (1996) Improved precision of acoustic surveys of benthopelagic fish by means of a deep-towed transducer. *ICES J. Mar. Sci.* **53**, 407–14.
- Kloser, R.J. and Horne, J.K. (2003) Characterizing uncertainty in target-strength measurements of a deepwater fish, orange roughy (*Hoplostethus atlanticus*). *ICES J. Mar. Sci.* **60**, 516–23.
- Kloser, R.J., Ryan, T.E., Williams, A. and Soule, M. (2000) *Development and Implementation of an Acoustic Survey of Orange Roughy in the Chatham Rise Spawning Box from a Commercial Factory Trawler, FV Amal'tal Explorer*. CSIRO, Melbourne.
- Kloser, R.J., Ryan, T., Sakov, P., Williams, A. and Koslow, J.A. (2002) Species identification in deep water using multiple acoustic frequencies. *Can. J. Fish. Aquat. Sci.* **59**, 1065–77.
- Knudsen, F.R. and Saegrov, H. (2002) Benefits from horizontal beaming during acoustic survey: application to three Norwegian lakes. *Fish. Res.* **56**, 205–11.
- Knudsen, F.R., Enger, P.S. and Sand, O. (1994) Avoidance responses to low frequency sound in downstream migrating Atlantic salmon smolt, *Salmo salar*. *J. Fish Biol.* **45**, 227–34.
- Koegeler, J.W., Falk-Petersen, S., Kristensen, A., Pettersen, F. and Dalen, J. (1987) Density and sound speed contrasts in sub-Arctic zooplankton. *Polar Biol.* **7**, 231–5.
- Korneliussen, R.J. (2000) Measurement and removal of echo integration noise. *ICES J. Mar. Sci.* **57**, 1204–17.
- Korneliussen, R.J. and Ona, E. (2003) Synthetic echograms generated from the relative frequency response. *ICES J. Mar. Sci.* **60**, 636–40.
- Kostyuchenko, L.P. (1971) Effects of elastic waves generated in marine seismic prospecting on fish eggs in the Black Sea. *Hydrobiological Journal* **9**, 45–8.
- Kraus, S.D., Read, A.J., Solow, A., Baldwin, K., Spradlin, T., Anderson, E. and Williamson, J. (1997) Acoustic alarms reduce porpoise mortality. *Nature* **388**, 525.
- Kringel, K., Jumars, P.A. and Holliday, D.V. (2003) A shallow scattering layer: high-resolution acoustic analysis of nocturnal vertical migration from the seabed. *Limnol. Oceanogr.* **48**, 1223–34.
- Kristensen, A. and Dalen, J. (1986) Acoustic estimation of size distribution and abundance of zooplankton. *J. Acoust. Soc. Am.* **80**, 601–11.

- Kubecka, J. (1994) Simple model on the relationship between fish acoustical target strength and aspect for high-frequency sonar in shallow waters. *J. Appl. Ichthyol.* **10**, 75–81.
- Kubecka, J. and Duncan, A. (1998) Diurnal changes of fish behaviour in a lowland river monitored by a dual-beam echosounder. *Fish. Res.* **35**, 55–63.
- Kubecka, J. and Wittingerova, M. (1998) Horizontal beaming as a crucial component of acoustic fish stock assessment in freshwater reservoirs. *Fish. Res.* **35**, 99–106.
- Kubecka, J., Duncan, A. and Butterworth, A. (1992) Echo counting or echo integration for fish biomass assessment in shallow water. In: *Proceedings of the European Conference on Underwater Acoustics* (ed. M. Weydert), pp. 129–32. Elsevier, Amsterdam.
- Kubecka, J., Duncan, A., Duncan, W.M., Sinclair, D. and Butterworth, A.J. (1994) Brown trout populations of three Scottish lochs estimated by horizontal sonar and multimesh gill nets. *Fish. Res.* **20**, 29–48.
- Lavery, A.C., Stanton, T.K., McGhehee, D.E. and Chu, D. (2002) Three-dimensional modeling of acoustic backscattering from fluid-like zooplankton. *J. Acoust. Soc. Am.* **111**, 1197–210.
- Lawson, C.L. and Hansen, R.J. (1974) *Solving Least Squares Problems*. Prentice-Hall, Englewood Cliffs, New Jersey.
- LeFeuvre, P., Rose, G.A., Gosine, R., Hale, R., Pearson, W. and Khan, R. (2000) Acoustic species identification in the Northwest Atlantic using digital image processing. *Fish. Res.* **47**, 137–47.
- Leroy, C.C. (1969) Development of simple equations for accurate and more realistic calculation of the speed of sound in sea water. *J. Acoust. Soc. Am.* **46**, 216–26.
- Levenez, J.-J., Gerlotto, F. and Petit, D. (1990) Reactions of tropical coastal pelagic species to artificial lighting and implications for the assessment of abundance by echo integration. *Rapp. P.-v. Reun. Cons. Int. Explor. Mer* **189**, 128–314.
- Lillo, S., Cordova, J. and Paillaman, A. (1996) Target-strength measurements of hake and jack mackerel. *ICES J. Mar. Sci.* **53**, 267–72.
- Lindem, T. (1981) The application of hydroacoustical methods in monitoring the spawning migration of whitefish *Coregonus lavaretus* in Lake Randsfjorden, Norway. In: *Meeting on Hydroacoustical Methods for the Estimation of Marine Fish Populations*, 25–29 June 1979, Vol. 2 (ed. J.B. Suomala), pp. 925–40. The Charles Stark Draper Laboratory, Cambridge, Mass., USA.
- Lockwood, S.J. (1989) *The Mackerel: Its Biology, Assessment and Management of a Fishery*. Fishing News Books, Oxford.
- Love, R.H. (1971) Dorsal aspect target strength of an individual fish. *J. Acoust. Soc. Am.* **49**, 816–23.
- Love, R.H. (1977) Target strength of an individual fish at any aspect. *J. Acoust. Soc. Am.* **62**, 1397–403.
- Løvik, A. and Hovem, J.M. (1979) An experimental investigation of swimbladder resonance in fishes. *J. Acoust. Soc. Am.* **66**, 850–4.
- Lytle, D.W. and Maxwell, D.R. (1983) Hydroacoustic assessment in high density fish schools. *FAO Fish. Rep.* **300**, 157–71.
- Mackenzie, K.V. (1981) Nine-term equation for speed of sound in the oceans. *J. Acoust. Soc. Am.* **70**, 807–12.
- MacLennan, D.N. (1981a) The theory of solid spheres as sonar calibration targets. *Scot. Fish. Res. Rep.* No. 22, 17 pp.

- MacLennan, D.N. (1981b) The target strength of cod at 38 kHz as a function of fish length. ICES CM 1981/B:27, 11 pp. (mimeo).
- MacLennan, D.N. (1982) Target strength measurements on metal spheres. *Scot. Fish. Res. Rep.* No. 25, 20 pp.
- MacLennan, D.N. (1986) Time-varied-gain functions for pulsed sonars. *J. Sound Vib.* **110**, 511–22.
- MacLennan, D.N. (1990) Acoustical measurement of fish abundance. *J. Acoust. Soc. Am.* **87**, January 15.
- MacLennan, D.N. and Armstrong, F. (1984) Tungsten carbide calibration spheres. *Proc. Inst. Acoust.* **6**, 68–75.
- MacLennan, D.N. and Dunn, J. (1984) Estimation of sound velocities from resonance measurements on tungsten carbide calibration spheres. *J. Sound Vib.* **97**, 321–31.
- MacLennan, D.N. and Forbes, S.T. (1984) Fisheries acoustics: a review of general principles. *Rapp. P.-v. Reun. Cons. Int. Explor. Mer* **184**, 7–18.
- MacLennan, D.N. and Forbes, S.T. (1987) Acoustic methods of fish stock estimation. In: *Developments in Fisheries Research in Scotland* (eds R.S. Bailey and B.B. Parrish), pp. 40–50. Fishing News Books, Oxford.
- MacLennan, D.N. and MacKenzie, I.G. (1988) Precision of acoustic fish stock estimates. *Can. J. Fish. Aquat. Sci.* **45**, 605–16.
- MacLennan, D.N. and Menz, A. (1996) Interpretation of in situ target-strength data. *ICES J. Mar. Sci.* **53**, 233–6.
- MacLennan, D.N. and Pope, J.A. (1983) Analysis procedure for the inter-ship calibration of echo integrators. ICES CM 1983/B:22, 7 pp. (mimeo).
- MacLennan, D.N. and Simmonds, E.J. (1992) *Fisheries Acoustics*. Chapman & Hall, London.
- MacLennan, D.N. and Svellingen, I. (1989) Simple calibration technique for the split-beam echosounder. *FiskDir. Skr. Ser. Havunders.* **18**, 365–79.
- MacLennan, D.N., Hollingworth, C.E. and Armstrong, F. (1989) Target strength and the tilt angle distribution of caged fish. *Proc. Inst. Acoust.* **11** (3), 11–20.
- MacLennan, D.N., Armstrong, F. and Simmonds, E.J. (1990a) Further observations on the attenuation of sound by aggregations of fish. *Proc. Inst. Acoust.* **12**, 99–106.
- MacLennan, D.N., Magurran, A.E., Pitcher, T.J. and Hollingworth, C.E. (1990b) Behavioural determinants of fish target strength. *Rapp. P.-v. Reun. Cons. Int. Explor. Mer* **189**, 245–53.
- MacLennan, D.N., Fernandes, P.G. and Dalen, J. (2002) A consistent approach to definitions and symbols in fisheries acoustics. *ICES J. Mar. Sci.* **59**, 365–9.
- MacLennan, D.N., Copland, P.J., Armstrong, E. and Simmonds, E.J. (2004) Experiments on the discrimination of fish and seabed echoes. *ICES J. Mar. Sci.* **61**, 201–10.
- Madureira, L.S.P., Everson, I. and Murphy, E.J. (1993a) Interpretation of acoustic data at two frequencies to discriminate between Antarctic krill (*Euphausia superba* Dana) and other scatterers. *J. Plankton Res.* **15**, 787–802.
- Madureira, L.S.P., Ward, P. and Atkinson, A. (1993b) Differences in backscattering strength determined at 120 and 38 kHz for three species of Antarctic macroplankton. *Mar. Ecol. Prog. Ser.* **93**, 17–24.
- Maes, J., Turnpenny, A.W.H., Lambert, D.R., Nedwell, J.R., Parmentier, A. and Ollevier, F. (2004) Field evaluation of a sound system to reduce estuarine fish intake rates at a power plant cooling water inlet. *J. Fish Biol.* **64**, 938–46.
- Mair, A.M., Fernandes, P.G. and Brierley, A.S. (2004) Examination of North Sea plankton samples in relation to multifrequency echograms. ICES CM 2004/R:13.

- Mann, D.A., Lu, Z. and Popper, A.N. (1997) A clupeid fish can detect ultrasound. *Nature* **389**, 341.
- Mann, D.A., Lu, Z., Hastings, M.C. and Popper, A.N. (1998) Detection of ultrasonic tones and simulated dolphin echolocation clicks by a teleost fish, the American shad (*Alosa sapidissima*). *J. Acoust. Soc. Am.* **104**, 562–8.
- Mann, D.A., Higgs, D.M., Tavolga, W.N., Souza, M.J. and Popper, A.N. (2001) Ultrasound detection by clupeiform fishes. *J. Acoust. Soc. Am.* **109**, 3048–54.
- Marchal, E. and Lebourges, A. (1996) Acoustic evidence for unusual diel behaviour of a mesopelagic fish (*Vinciguerria nimbaria*) exploited by tuna. *ICES J. Mar. Sci.* **53**, 443–8.
- Marchal, E. and Petitgas, P. (1993) Precision of acoustic fish abundance estimates: separating the number of schools from the biomass in the schools. *Aqu. Living Resources* **6** (3), 211–19.
- Marler, P. and Terrace, H.S. (1984) *The Biology of Learning*, Dahlem Konferenzen. Springer-Verlag, Berlin, 740 pp.
- Marshall, W.J. (1996) Descriptors of impulsive signal levels commonly used in underwater acoustics. *IEEE J. Oceanic Eng.* **20**, 108–10.
- Marshall, W.J. (1998) Acoustical properties of end-initiated explosive line charges. *J. Acoust. Soc. Am.* **103**, 2365–76.
- Martin, L.V., Stanton, T.K., Lynch, J.F. and Wiebe, P.H. (1996) Acoustic classification of zooplankton based on single-ping broadband insonifications. *ICES J. Mar. Sci.* **53**, 217–24.
- Martin Traykovski, L.V., O'Driscoll, R.L. and McGehee, D.E. (1998) Effect of orientation on broadband acoustic scattering of Antarctic krill (*Euphausia superba*): implications for inverting zooplankton spectral acoustic signatures for angle of orientation. *J. Acoust. Soc. Am.* **104**, 2121–35.
- Mason, W.P. (1964) *Physical Acoustics, Principles and Methods*. Academic Press, London.
- Massé, J. and Retiere, N. (1995) Effect of the number of transects and identification hauls on acoustic biomass estimates under mixed species conditions. *Aqu. Living Resources* **8**, 195–9.
- Massé, J., Koutsikopoulos, C. and Patty, W. (1996) The structure and spatial distribution of pelagic fish schools in multispecies clusters: an acoustic study. *ICES J. Mar. Sci.* **53**, 155–60.
- Matheron, G. (1971) The theory of regionalized variables and its application. Les Cahiers du Centre de Morphologie Mathématique de Fontainebleau, Fasc. 5, Ecole Nat. Sup. des Mines de Paris.
- McCauley, R.D., Fewtrell, J. and Popper, A.N. (2003) High intensity anthropogenic sound damages fish ears. *J. Acoust. Soc. Am.* **113**, 638–42.
- McClatchie, S., Macaulay, G., Hanchet, S. and Coombs, R.F. (1998) Target strength of southern blue whiting (*Micromesistius australis*) using swimbladder modelling, split beam and deconvolution. *ICES J. Mar. Sci.* **55**, 482–93.
- McClatchie, S., Macaulay, G., Coombs, R.F., Grimes, P. and Hart, A. (1999) Target strength of an oily deep-water fish, orange roughy (*Hoplostethus atlanticus*) I. Experiments. *J. Acoust. Soc. Am.* **106**, 131–42.
- McClatchie, S., Macaulay, G.J. and Coombs, R.F. (2003) A requiem for the use of  $20 \log_{10}$  Length for acoustic target strength with special reference to deep-sea fishes. *ICES J. Mar. Sci.* **60**, 419–28.
- McGehee, D. (1994) A three-dimensional acoustical imaging system for zooplankton observations. PhD Thesis, University of California, San Diego.
- McGehee, D. and Jaffe, J.S. (1996) Three-dimensional swimming behaviour of individual zooplankters: observation using the acoustical imaging system FishTV. *ICES J. Mar. Sci.* **53**, 363–9.

- McGehee, D.M., O'Driscoll, R.L. and Martin Traykovski, L.V. (1998) Effects of orientation on acoustic scattering from Antarctic krill. *Deep Sea Res.* **45**, 1273–94.
- McGehee, D.M., Greenlaw, C.F., Holliday, D.V. and Pieper, R.E. (2000) Multifrequency acoustical volume backscattering patterns in the Arabian Sea – 265 kHz to 3 MHz. *J. Acoust. Soc. Am.* **107**, 193–200.
- McQuinn, I.H. and Winger, P.D. (2003) Tilt angle and target strength: target tracking of Atlantic cod (*Gadus morhua*) during trawling. *ICES J. Mar. Sci.* **60**, 575–83.
- Medwin, H. and Clay, C.S. (1998) *Fundamentals of Acoustical Oceanography*. Academic Press, New York.
- Melvin, G., Li, Y., Mayer, L. and Clay, A. (1998) The development of an automated sounder/sonar acoustic logging system for deployment on commercial fishing vessel. ICES CM 1998/S:14.
- Melvin, G.D., Cochrane, N.A. and Li, Y. (2003) Extraction and comparison of acoustic backscatter from a calibrated multi- and single-beam sonar. *ICES J. Mar. Sci.* **60**, 669–77.
- Mesiar, D.C., Eggers, D.M. and Gaudet, D.M. (1990) Development of techniques for the application of hydroacoustics to counting migratory fish in large rivers. *Rapp. P.-v. Reun. Cons. Int. Explor. Mer* **189**, 223–32.
- Midttun, L. (1984) Fish and other organisms as acoustic targets. *Rapp. P.-v. Reun. Cons. Int. Explor. Mer* **184**, 25–33.
- Midttun, L. and Hoff, I. (1962) Measurements of the reflection of sound by fish. *FiskDir. Skr. Ser. Havunders.* **13** (3), 1–18.
- Midttun, L. and Nakken, O. (1977) Some results of abundance estimation studies with echo integrators. *Rapp. P.-v. Reun. Cons. Int. Explor. Mer* **170**, 253–8.
- Midttun, L. and Saetersdal, G. (1957) On the use of echo sounder observations for estimating fish abundance. Paper 29 presented at the Joint Scientific Meeting of ICNAF, ICES and FAO, Lisbon 1957. *Spec. Publ. Int. Comm. NW Atlant. Fish.* **2**, 4 pp. (mimeo).
- Minnaert, F. (1933) On musical air bubbles and the sounds of running water. *Philos. Mag.* **16**, 235–48.
- Misund, O.A. and Beltestad, A.K. (1989) School sizing of small pelagic species off Mozambique by density estimation and acoustic dimensioning. *Proc. Inst. Acoust.* **11**, 260–6.
- Misund, O.A. and Beltestad, A.K. (1996) Target-strength estimates of schooling herring and mackerel using the comparison method. *ICES J. Mar. Sci.* **53**, 281–4.
- Misund, O.A. and Øvredal, J.T. (1988) Acoustic measurements of schooling herring: estimation of school biomass and target strength. ICES CM 1988/B:26, 16 pp. (mimeo).
- Misund, O.A., Aglen, A., Beltestad, A.K. and Dalen, J. (1992) Relationships between the geometric dimensions and biomass of schools. *ICES J. Mar. Sci.* **49**, 305–15.
- Misund, O.A., Aglen, A. and Frønæs, E. (1995) Mapping the shape, size, and density of fish schools by echo integration and a high-resolution sonar. *ICES J. Mar. Sci.* **52**, 11–20.
- Misund, O.A., Aglen, A., Hamre, J., Ona, E., Røttingen, I., Skagen, D. and Valdemarsen, J.W. (1996) Improved mapping of schooling fish near the surface: comparison of abundance estimates obtained by sonar and echo integration. *ICES J. Mar. Sci.* **53**, 383–8.
- Mitson, R.B. (1983) *Fisheries Sonar*. Fishing News Books Ltd, Farnham.
- Mitson, R.B. (1995) Underwater noise of research vessels: review and recommendations. *ICES Coop. Res. Rep.* **209**, 61 pp.
- Mitson, R.B. and Knudsen, H.P. (2003) Causes and effects of underwater noise on fish abundance estimation. *Aqu. Living Resources* **16**, 255–63.
- Mitson, R.B. and Wood, R.J. (1962) An automatic method of counting fish echoes. *J. Cons. Int. Explor. Mer* **26**, 281–91.

- Mitson, R.B., Simard, Y. and Goss, C. (1996) Use of a two-frequency algorithm to determine size and abundance of plankton in three widely spaced locations. *ICES J. Mar. Sci.* **53**, 209–16.
- Miyanohana, Y., Ishii, K. and Furusawa, M. (1986) Effect of beam pattern and fish behaviour on averaged target strength. *Bull. Fish. Soc. Jpn.* (in Japanese with English summary and figure legends) **7**, 87–96.
- Miyashita, K., Aoki, I. and Inagaki, T. (1996) Swimming behaviour and target strength of isada krill (*Euphausia pacifica*). *ICES J. Mar. Sci.* **53**, 303–8.
- Møhl, B. and Andersen, S. (1973) Echolocation: high frequency component in the click of the harbour porpoise (*Phocoena ph.* L.). *J. Acoust. Soc. Am.* **54**, 1368–72.
- Møhl, B., Wahlberg, M., Madsen, P.T., Miller, L.A. and Surlykke, A. (2000) Sperm whale clicks: directionality and source level revisited. *J. Acoust. Soc. Am.* **107**, 638–48.
- Møhl, B., Wahlberg, M. and Heerfordt, A. (2001) A large-aperture array of nonlinked receivers for acoustic positioning of biological sound sources. *J. Acoust. Soc. Am.* **109**, 434–7.
- Monstad, T. (1992) Report of the joint Norwegian–Russian acoustic survey on blue whiting, Spring 1992. ICES CM 1992/H:6.
- Moose, P.H. and Ehrenberg, J.E. (1971) An expression for the variance of abundance estimates using a fish echo integrator. *J. Fish. Res. Bd Can.* **28**, 1293–301.
- Morphett, N., Woodward, B. and Goodson, A.D. (1993) Tracking dolphins by detecting their sonar clicks. *Proc. Inst. Acoust.* **15**, 50–6.
- Morse, P.M. (1948) *Vibration and Sound*, 2nd edn. McGraw-Hill, New York.
- Morse, P.M. and Ingard, K.U. (1968) *Theoretical Acoustics*, Chapter 8. Princeton University Press, Princeton, New Jersey.
- Morton, K.F. and MacLellan, S.G. (1992) Acoustics and freshwater zooplankton. *J. Plankton Res.* **14**, 1117–27.
- Moursund, R.A., Carlson, T.J. and Peters, R.D. (2003) A fisheries application of a dual-frequency identification sonar acoustic camera. *ICES J. Mar. Sci.* **60**, 678–83.
- Mous, P.J., Kemper, J. and Schelvis, A. (1999) A towed body designed for side-scanning hydroacoustic surveying of fish stocks in shallow waters. *Fish. Res.* **40**, 97–8.
- Mozgovoy, V.A. (1986) Determining the parameters of fish in sound scattering layer and their behaviour during migration based on scattered acoustic signal spectra. *Oceanology* **26**, 567–74.
- Mukai, T. and Iida, K. (1996) Depth dependence of target strength of live kokanee salmon in accordance with Boyle's law. *ICES J. Mar. Sci.* **53**, 245–8.
- Mulligan, T.J. and Chen, D.G. (1998) A split-beam echo counting model: development of statistical procedures. *ICES J. Mar. Sci.* **55**, 905–17.
- Mulligan, T.J. and Chen, D.G. (2000) Comment: Can stationary bottom split-beam hydroacoustics be used to measure fish swimming speed in-situ? *Fish. Res.* **49**, 93–6.
- Mulligan, T.J. and Kieser, R. (1986) Comparison of acoustic population estimates of salmon in a lake with a weir count. *Can. J. Fish. Aquat. Sci.* **43**, 1373–85.
- Mulligan, T.J. and Kieser, R. (1996) A split-beam echo-counting model for riverine use. *ICES J. Mar. Sci.* **53**, 403–6.
- Mutlu, E. (1996) Target strength of the common jellyfish (*Aurelia aurita*): a preliminary experimental study with a dual-beam acoustic system. *ICES J. Mar. Sci.* **53**, 309–12.
- Myrberg Jr, A.A., Ha, S.J., Walewski, S. and Banburg, J.C. (1972) Effectiveness of acoustic signals in attracting epipelagic sharks to an underwater sound source. *Bull. Mar. Sci.* **22**, 926–49.

- Myrberg Jr, A.A., Gordon, C.R. and Klimley, A.P. (1976) Attraction of free ranging sharks by low frequency sound, with comments on its biological significance. In: *Sound Reception in Fish* (eds A. Schuijf and A.D. Hawkins), pp. 205–28. Elsevier, Amsterdam.
- Nachtigall, P.E. (2000) Psychoacoustic studies of dolphins and whales. In: *Hearing by Dolphins and Whales* (eds W.W.L. Au, A.N. Popper and R.R. Fay), pp. 330–63. Springer, New York.
- Nachtigall, P.W. (1980) Odontocete echolocation performance on object size, shape and material. In: *Animal Sonar Systems* (eds R.G. Busnel and J.F. Fish), pp. 71–95. Plenum, New York.
- Nakken, O. and Dommasnes, A. (1975) The application of an echo integration system in investigations of the stock strength of the Barents Sea capelin 1971–1974. ICES CM 1975/B:25, 20 pp. (mimeo).
- Nakken, O. and Olsen, K. (1977) Target strength measurements of fish. *Rapp. P.-v. Reun. Cons. Int. Explor. Mer* **170**, 52–69.
- Nakken, O. and Ulltang, O.A. (1983) Comparison of the reliability of acoustic estimates of fish stock abundance and estimates obtained by other assessment methods in the northeast Atlantic. *FAO Fish. Rep.* **300**, 249–61.
- Napp, J.M., Ortner, P.B., Pieper, R.E. and Holliday, D.V. (1993) Biovolume-size spectra of epipelagic zooplankton using a multi-frequency acoustic profiling system (MAPS). *Deep Sea Res. I* **40**, 445–59.
- Nealson, P.A. and Gregory, J. (2000) Hydroacoustic differentiation of adult salmon and aquatic macrophytes in the River Wye, Wales. *Aqu. Living Resources* **13**, 331–9.
- Nestler, J.M., Ploskey, G.R., Pickens, J., Menezes, J. and Schilt, C. (1992) Responses of blueback herring to high-frequency sound and implications for reducing entrainment at hydropower dams. *N. Am. J. Fish. Man.* **12**, 667–83.
- Neubauer, W.G., Vogt, R.H. and Dragonette, L.R. (1974) Acoustic reflection from elastic spheres. *J. Acoust. Soc. Am.* **55**, 1123–9.
- Nielsen, J.R. and Lundgren, B. (1999) Hydroacoustic ex situ target strength measurements on juvenile cod (*Gadus morhua* L.). *ICES J. Mar. Sci.* **56**, 627–39.
- Novarini, J.C. and Bruno, D.R. (1982) Effects of the sub-surface bubble layer on sound propagation. *J. Acoust. Soc. Am.* **72**, 501–14.
- Nunnallee, E.P. (1983) Scaling of an echo integrator using echo counts, and a comparison of acoustic and weir count estimates of a juvenile sockeye salmon population. *FAO Fish. Rep.* **300**, 262–8.
- Nunnallee, E.P. (1990) An alternative method to thresholding during echo-integration data collection. *Rapp. P.-v. Reun. Cons. Int. Explor. Mer* **189**, 92–4.
- O'Driscoll, R.L. (2003) Determining species composition in mixed-species marks: an example from the New Zealand hoki (*Macruronus novaezealandiae*) fishery. *ICES J. Mar. Sci.* **60**, 609–16.
- O'Driscoll, R.L. and McClatchie, S. (1998) Spatial distribution of planktivorous fish schools in relation to krill abundance and local hydrography off Otago, New Zealand. *Deep Sea Res. II* **45**, 1295–325.
- Officer, C.B. (1958) *Introduction to the Theory of Sound Transmission*. McGraw-Hill, New York.
- Offutt, C.G. (1970) Acoustic stimulus perception by the American lobster, *Homarus americanus*. *Experientia* **26**, 1276–8.

- O'Keefe, D. (1985) A computer model for predicting the effects of underwater explosions on swimbladder fish and marine mammals. In: *Proceedings of the Workshop on Effects of Explosive Use in the Marine Environment*, 29–31 January 1985, Halifax (eds G.D. Greene, F.R. Engelhardt and R.J.E. Paterson). *Tech. Rep. Canada Oil and Gas Lands Administration, Ottawa*, No. 5, pp. 324–53.
- Olsen, K. (1969) Directional response in herring for sound and noise stimuli. ICES CM 1969/B:20, 8 pp. (mimeo).
- Olsen, K. (1990) Fish behaviour and acoustic sampling. *Rapp. P.-v. Reun. Cons. Explor. Mer* **189**, 147–58.
- Olsen, K. and Ahlquist, I. (1989) Target strength of fish at various depths, observed experimentally. ICES CM 1989/B:53, 8 pp.
- Olsen, K., Angell, J. and Løvik, A. (1983a) Quantitative estimations of the influence of fish behaviour on acoustically determined fish abundance. *FAO Fish. Rep.* **300**, 139–49.
- Olsen, K., Angell, J., Pettersen, E. and Løvik, A. (1983b) Observed fish reactions to a surveying vessel with special reference to herring, cod, capelin and polar cod. *FAO Fish. Rep.* **300**, 131–8.
- Olsen, S. (1969) A note on estimating school size from echo traces. *FAO Fish. Rep.* **78**, 37–48.
- Ona, E. (1990) Physiological factors causing natural variations in acoustic target strength of fish. *J. Mar. Biol. Ass. UK* **70**, 107–27.
- Ona, E. (1994) Detailed in situ target strength measurements of O-group cod. ICES CM 1994/B:30, 9 pp.
- Ona, E. (2001) Herring tilt angles measured through target tracking. In: *Herring: Expectations For a New Millennium* (eds F. Funk *et al.*). Alaska Sea Grant College Program AK-SG-01-04, 509–20.
- Ona, E. (2003) An expanded target-strength relationship for herring. *ICES J. Mar. Sci.* **60**, 493–9.
- Ona, E. and Barange, M. (1999) Single target recognition. *ICES Coop. Res. Rep.* **235**, 28–43.
- Ona, E. and Eger, K. (1987) Sonar observations of trawl performance. Paper No. 99, Int. Symp. Fisheries Acoustics, Seattle, WA, 22–26 June 1987, 10 pp. (mimeo).
- Ona, E. and Hansen, K. (1986) In-situ target strength observations on haddock. ICES CM 1986/B:39, 13 pp. (mimeo).
- Ona, E. and Mitson, R.B. (1996) Acoustic sampling and signal processing near the seabed: the dead zone revisited. *ICES J. Mar. Sci.* **53**, 677–90.
- Otis, L.S., Cerf, J.A. and Thomas, G.J. (1957) Conditioned inhibition of respiration and heart rate in the goldfish. *Science (N.Y.)* **126**, 263–4.
- Pauly, T. and Penrose, J.D. (1998) Laboratory target strength measurements of free-swimming Antarctic krill (*Euphausia superba*). *J. Acoust. Soc. Am.* **103**, 3268–80.
- Payne, R.S. and McVay, S. (1971) Songs of the humpback whales. *Science* **173**, 587–97.
- Pearson, W.H., Skalski, J.R. and Malme, C.I. (1992) Effects of sounds from a geophysical survey device on behavior of captive rockfish (*Sebastes* spp.). *Can. J. Fish. Aquat. Sci.* **49**, 1343–56.
- Pedersen, B. and Trevorow, M.V. (1999) Continuous monitoring of fish in a shallow channel using a fixed horizontal sonar. *J. Acoust. Soc. Am.* **105**, 3126–35.
- Pedersen, J. (1996) Discrimination of fish layers using the three-dimensional information obtained by a split-beam echo-sounder. *ICES J. Mar. Sci.* **53**, 371–6.
- Pedersen, J. (2001) Hydroacoustic measurement of swimming speed of North Sea saithe in the field. *J. Fish Biol.* **57**, 1073–85.

- Pennington, M. (1983) Efficient estimators for fish and plankton surveys. *Biometrics* **39**, 281–6.
- Petitgas, P. (1990) Geostatistics for fish acoustic surveys: precision of the abundance estimate and survey efficiency. ICES CM 1990/D:12, 27 pp.
- Petitgas, P. (1993) Geostatistics for fish stock assessments: a review and an acoustic application. *ICES J. Mar. Sci.* **50**, 285–98.
- Petitgas, P. and Lafont, T. (1997) EVA2 (Estimation Variance – Version 2): a geostatistical software on Windows 95 for the precision of fish stock assessment surveys. ICES CM 1997/Y:22, 22 pp. (mimeo).
- Petitgas, P. and Poulard, J.C. (1989) Applying stationary geostatistics to fisheries: a study on hake in the Bay of Biscay. ICES CM 1989/G:62, 21 pp. (mimeo).
- Petitgas, P., Massé, J., Beillois, P., Lebarbier, E. and Le Cann, A. (2003) Sampling variance of species identification in fisheries acoustic surveys based on automated procedures associating acoustic images and trawl hauls. *ICES J. Mar. Sci.* **60**, 437–45.
- Pieper, R.E. (1979) Euphausid distribution and biomass determined acoustically at 102 kHz. *Deep Sea Res.* **26**, 687–702.
- Pieper, R.E. and Holliday, D.V. (1984) Acoustic measurement of zooplankton distributions in the sea. *J. Cons. Int. Explor. Mer* **41**, 226–38.
- Pieper, R.E., Holliday, D.V. and Kleppel, G.S. (1990) Quantitative zooplankton distributions from multifrequency acoustics. *J. Plankton Res.* **12**, 433–41.
- Pieper, R.E., McGehee, D.E., Greenlaw, C.F. and Holliday, D.V. (2001) Acoustically measured seasonal patterns of zooplankton in the Arabian Sea. *Deep Sea Res. II* **48**, 1325–43.
- Pilleri, G., Zbinden, K., Gehr, M. and Kraus, C. (1976) Sonar clicks, directionality of the emission field and echolocating behaviour of the Indus river dolphin (*Platirista indi*) In: *Investigations on Cetacea*, Vol. 7 (ed. G. Pilleri), pp. 13–43. Brain Anatomy Institute, Berne.
- Pilleri, G., Zbinden, K. and Kraus, C. (1979) The sonar field of *Inia geoffrensis*. In: *Investigations on Cetacea*, Vol. 10 (ed. G. Pilleri), pp. 157–78. Brain Anatomy Institute, Berne.
- Pitcher, T.J. and Partridge, B.L. (1979) Fish school density and volume. *Mar. Biol.* **54**, 383–94.
- Popper, A.N. (1972) Pure tone auditory thresholds for the carp, *Cyprinus carpio*. *J. Acoust. Soc. Am.* **52**, 1714–17.
- Popper, A.N. and Clarke, N.I. (1976) The auditory system of the goldfish (*Carassius auratus*): effects of intense acoustic stimulation. *Comp. Biochem. Physiol.* **53A**, 11–18.
- Portier, P. (1924) Sur l'application des ondes ultra-sonores aux recherches d'océanographie biologique. *C.R. Soc. Biol., Paris*, 91.
- Purves, P.E. and Pilleri, G.E. (1983) *Echolocation in Whales and Dolphins*. Academic Press, San Diego.
- Quinn, T.J. (1985) Line transect estimators for schooling populations. *Fish. Res.* **3**, 189–99.
- Raitt, R.W. (1948) Sound scatterers in the sea. *J. Mar. Res.* **7**, 393–409.
- Rallier du Baty, R. (1927) La peche sur le banc de Terre-Neuve et autour des îles Saint-Pierre et Miquelon, Office Scientifique et Technique des Peches Maritimes. Memoires (Serie Speciale), 7, 142 pp.
- Ransom, B.H., Johnston, S.V. and Steig, T.W. (1992) Review on monitoring adult salmonid (*Onchorhynchus* and *Salmo* spp.) escapement using fixed-location split-beam hydroacoustics. *Fish. Res.* **35**, 33–42.
- Ransom, B.H., Steig, T.W. and Nealson, P.A. (1996) Comparison of hydroacoustic and net catch estimates of Pacific salmon smolt (*Onchorhynchus* spp.) passage at hydro-power dams in the Columbia River Basin, USA. *ICES J. Mar. Sci.* **53**, 477–82.

- Rayleigh, L. (1945) *Theory of Sound*. Dover Publications, New York.
- Readhead, M.L. (1997) Snapping shrimp noise near Gladstone, Queensland. *J. Acoust. Soc. Am.* **101**, 1718–22.
- Reeder, D.B. and Stanton, T.K. (2004) Acoustic scattering by axisymmetric finite-length bodies: an extension of a two-dimensional conformal mapping method. *J. Acoust. Soc. Am.* **116**, 729–46.
- Reeder, D.B., Jech, J.M. and Stanton, T.K. (2004) Broadband acoustic backscatter and high-resolution morphology of fish: measurement and modeling. *J. Acoust. Soc. Am.* **116**, 747–61.
- Reid, D., Scalabrin, C., Petitgas, P., Massé, J., Aukland, R., Carrera, P. and Georgakarakos, S. (2000) Standard protocols for the analysis of school based data from echo sounder surveys. *Fish. Res.* **47**, 125–36.
- Reid, D.G. and Simmonds, E.J. (1993) Image analysis techniques for the study of school structure from acoustic survey data. *Can. J. Fish. Aquat. Sci.* **50**, 1264–72.
- Reut, Z., Pace, N.G. and Heaton, M.J.P. (1985) Computer classification of sea beds by sonar. *Nature* **314**, 426–8.
- Reynisson, P. (1996) Evaluation of threshold-induced bias in the integration of single-fish echoes. *ICES J. Mar. Sci.* **53**, 345–50.
- Richards, L.J., Kieser, R., Mulligan, T.J. and Candy, J.R. (1991) Classification of fish assemblages based on echo integration surveys. *Can. J. Fish. Aquat. Sci.* **48**, 886–93.
- Richardson, I.D., Cushing, D.H., Harden Jones, F.R., Beverton, R.J. and Blacker, R.W. (1959) Echo sounding experiments in the Barents Sea. *Fishery Investigations* **22**, 55 pp.
- Richardson, W.J. (1997) Marine mammals and man-made noise: current issues. *Proc. Inst. Acoust.* **19** (9), 39–50.
- Richardson, W.J. and Wurtz, B. (1997) Influences of man-made noise and other human activities on cetacean behaviour. *Mar. Freshwat. Behav. Physiol.* **29**, 183–209.
- Richardson, W.J., Greene, C.R., Malme, C.I. and Thomson, D.H. (1995) *Marine Mammals and Noise*. Academic Press, San Diego.
- Ricker, W.E. (1973) Linear regressions in fishery research. *J. Fish. Res. Bd Can.* **30**, 409–34.
- Ridgway, S.H., Carder, D.A., Smith, R.R., Kamolnik, T., Schlundt, E. and. Elsberry, W.R. (1997) Behavioral responses and temporary shift in masked hearing threshold of bottlenose dolphins, *Tursiops truncatus*, to 1-second tones of 141 to 201 dB re 1 micro Pa. San Diego, CA, Naval Command Control and Ocean Surveillance Center, 27 pp.
- Rivoirard, J., Simmonds, E.J., Foote, F., Fernandes, P.G. and Bez, N. (2000) *Geostatistics for Estimating Fish Abundance*. Blackwell Science Ltd, Oxford.
- Robinson, B.J. (1982) An in-situ technique to determine fish target strength with results for blue whiting, *Micromesistius poutassou* (Risso). *J. Cons. Int. Explor. Mer* **40**, 153–60.
- Robinson, B.J. (1983) In situ measurements of the target strength of pelagic fishes. *FAO Fish. Rep.* **300**, 99–103.
- Robotham, V.H. and Castillo, J. (1990) The bootstrap method: an alternative for estimating confidence intervals of resources surveyed by hydroacoustic techniques. *Rapp. P.-v. Reun. Cons. Int. Explor. Mer* **189**, 421–4.
- Roe, H.S.J. and Griffiths, G. (1993) Biological information from an acoustic Doppler current profiler. *Mar. Biol.* **115**, 339–46.
- Roe, H.S.J., Griffiths, G., Hartman, M. and Crisp, N. (1996) Variability in biological distributions and hydrography from concurrent Acoustic Doppler Current Profiler and SeaSoar surveys. *ICES J. Mar. Sci.* **53**, 131–8.
- Rogers, P.H. and Van Buren, A.L. (1978) A new approach to constant beam width transducers. *J. Acoust. Soc. Am.* **64**, 38–43.

- Roman, M.R., Holliday, D.V. and Sanford, L.P. (2001) Temporal and spatial patterns of zooplankton in the Chesapeake Bay turbidity maximum. *Mar. Ecol. Prog. Ser.* **213**, 215–27.
- Romare, P. (2001) An evaluation of horizontal echosounding as a method for behavioural studies of 0+ fish in field experiments. *J. Fish Biol.* **57**, 1512–23.
- Rose, G.A. (1998) Acoustic target strength of capelin in Newfoundland waters. *ICES J. Mar. Sci.* **55**, 918–23.
- Rose, G.A. (2003) Monitoring coastal Northern cod: towards an optimal survey of Smith Sound, Newfoundland. *ICES J. Mar. Sci.* **60**, 453–62.
- Rose, G.A. and Leggett, W.C. (1988) Hydroacoustic signal classification of fish schools by species. *Can. J. Fish. Aquat. Sci.* **50**, 597–604.
- Rose, G.A. and Porter, D.R. (1996) Target-strength studies on Atlantic cod (*Gadus morhua*) in Newfoundland waters. *ICES J. Mar. Sci.* **53**, 259–66.
- Rose, G.A., Gauthier, S. and Lawson, G.L. (2000) Acoustic surveys in the full monte: simulating uncertainty. *Aqu. Living Resources* **13**, 367–72.
- Ross, D. (1976) *Mechanics of Underwater Sound*. Pergamon Press, New York.
- Røttingen, I. (1976) On the relation between echo intensity and fish density. *FiskDir. Skr. Ser. Havunders.* **16** (9), 301–14.
- Røttingen, I. (1978) Field intercalibrations of echo integrator systems. ICES CM 1978/B:25 (mimeo).
- Røttingen, I. and Tjelmeland, S. (2003) Evaluation of the absolute levels of acoustic estimates of the 1983 year class of Norwegian spring-spawning herring. *ICES J. Mar. Sci.* **60**, 480–5.
- Rozwadowski, H.M. (2002) *The Sea Knows No Boundaries: A Century of Marine Science under ICES*. International Council for the Exploration of the Sea, in association with University of Washington Press, Seattle.
- Rschekvian, S.N. (1963) *A Course of Lectures in the Theory of Sounds*. Pergamon Press, London.
- Rudstam, L.G., Clay, C.S. and Magnuson, J.J. (1987) Density and size estimates of Cisco (*Coregonus artedii*) using analysis of echo peak PDF from a single-transducer sonar. *Can. J. Fish. Aquat. Sci.* **44**, 811–21.
- Rudstam, L.G., Lindem, T. and Hansson, S. (1988) Density and in-situ target strength of herring and sprat: a comparison between two methods of analysing single-beam sonar data. *Fish. Res.* **6**, 305–15.
- Rudstam, L.G., Hansson, S., Lindem, T. and Einhouse, D.W. (1999) Comparison of target strength distributions and fish densities obtained with split and single beam echo sounders. *Fish. Res.* **42**, 207–14.
- Rudstam, L.G., Parker, S.L., Einhouse, D.W., Witzel, L.D., Warner, D.M., Stritzel, J.L., Parrish, D.L. and Sullivan, P.J. (2003) Application of in situ target-strength estimations in lakes: examples from rainbow-smelt surveys in Lakes Erie and Champlain. *ICES J. Mar. Sci.* **60**, 500–07.
- Runnstrom, S. (1937) A review of Norwegian herring investigations in recent years. *J. Cons. Int. Explor. Mer* **12**, 123–43.
- Rusby, J.S.M. (1977) Long range survey of a herring fishery by side-scan sonar. *Rapp. P.-v. Reun. Cons. Int. Explor. Mer* **170**, 7–14.
- Sakaguchi, S., Fukuhara, O., Umezawa, S., Fuhiya, M. and Ogawa, T. (1976) The influence of underwater explosions on fishes. *Bull. Nansei Reg. Fish. Res. Lab.* (in Japanese, summary and figure legends in English) **9**, 33–56.

- Sameoto, D. (1980) Quantitative measurements of euphausids using a 120 kHz sounder and their in-situ orientation. *Can. J. Fish. Aquat. Sci.* **37**, 693–702.
- Sameoto, D. (1982) Zooplankton and micronekton abundance on the Nova Scotian slope. *Can. J. Fish. Aquat. Sci.* **39**, 760–77.
- Sand, O. (1974) Directional sensitivity of microphonic potentials from the perch ear. *J. Exp. Biol.* **60**, 881–99.
- Sand, O. and Hawkins, A.D. (1973) Acoustic properties of the cod swimbladder. *J. Exp. Biol.* **58**, 797–820.
- Sand, O. and Karlsen, H.E. (1986) Detection of infrasound by the Atlantic cod. *J. Exp. Biol.* **125**, 449–60.
- Sawada, K., Furusawa, M. and Williamson, N.J. (1993) Conditions for the precise measurement of fish target strength in situ. *J. Mar. Acoust. Soc. Japan* **2**, 73–9.
- Scalabrin, C., Diner, N., Weill, A., Hillion, A. and Mouchot, M.-C. (1996) Narrowband acoustic identification of monospecific fish shoals. *ICES J. Mar. Sci.* **53**, 181–8.
- Scherbino, M. and Truskanov, M.D. (1966) Determination of fish concentration by means of acoustic apparatus. ICES CM 1966/F:3, 6 pp.
- Schevill, W.E., Watkins, W.A. and Backus, R.H. (1964) The 20-cycle signals and Balaenoptera (fin whales). In: *Marine Bio-Acoustics* (ed. W.N. Tavolga), pp. 147–52. Pergamon Press, New York.
- Schlundt, C.E., Finneran, J.J., Carder, D.A. and Ridgway, S.H. (2000) Temporary shift in masked hearing thresholds of bottlenose dolphins, *Tursiops truncatus*, and white whales, *Delphinapterus leucas*, after exposure to intense tones. *J. Acoust. Soc. Am.* **107**, 3496–508.
- Scholik, A.R. and Yan, H.Y. (2001) Effect of underwater noise on auditory sensitivity of a cyprinid fish. *Hear. Res.* **152**, 17–24.
- Scholik, A.R. and Yan, H.Y. (2002) The effects of noise on the auditory sensitivity of the bluegill sunfish, *Lepomis macrochirus*. *Comp. Biochem. Physiol.* **133A**, 43–52.
- Schuijf, A. and Buwalda, R.J.A. (1980) Underwater localisation – a major problem in fish acoustics. In: *Comparative Studies of Hearing in Vertebrates* (eds A.N. Popper and R.R. Fay), pp. 43–77. Springer-Verlag, New York.
- Selivanovsky, D.A., Stunzhas, P.A. and Didenkulov, I.N. (1996) Acoustical investigation of phytoplankton. *ICES J. Mar. Sci.* **53**, 313–16.
- Shenderov, E.L. (1998) Some physical models for estimating scattering of underwater sound by algae. *J. Acoust. Soc. Am.* **104**, 791–800.
- Shibata, K. (1972) Experimental measurement of target strength of fish. In: *Modern Fishing Gear of the World*, Vol. 2 (ed. H. Kristjonsson), pp. 104–8. Fishing News Books, London.
- Shooter, J.A., Muir, T.G. and Blackstock, D.T. (1974) Acoustic saturation of spherical waves in water. *J. Acoust. Soc. Am.* **55**, 54–62.
- Shotton, R. (1981) Acoustic survey design. In: *Meeting on Hydroacoustical Methods for the Estimation of Marine Fish Populations*, 25–29 June 1979, Vol. 2 (ed. J.B. Suomala), pp. 629–87. The Charles Stark Draper Laboratory, Cambridge, Mass., USA.
- Shotton, R. and Bazigos, G.P. (1984) Techniques and considerations in the design of acoustic surveys. *Rapp. P.-v. Reun. Cons. Int. Explor. Mer* **184**, 34–57.
- Shulkin, M. and Marsh, H.W. (1963) Absorption of sound in sea water. *J. Brit. Inst. Radio Eng.* **25**, 493–99.
- Siler, W. (1969) Near and far fields in a marine environment. *J. Acoust. Soc. Am.* **46**, 483–84.

- Simard, Y., Marcotte, D. and Bourgault, G. (1993) Exploration of geostatistical methods for mapping and estimating acoustic biomass of pelagic fish in the Gulf of St. Lawrence, Size of echo-integration unit and auxiliary environmental variables. *Aqu. Living Resources* **6**, 185–99.
- Simard, Y., Marcotte, D. and Naraghi, K. (2003) Three-dimensional acoustic mapping and simulation of krill distribution in the Saguenay-St. Lawrence Marine Park whale feeding ground. *Aqu. Living Resources* **16**, 137–44.
- Simmonds, E.J. (1984a) A comparison between measured and theoretical equivalent beam angles for seven similar transducers. *J. Sound Vib.* **97**, 117–28.
- Simmonds, E.J. (1984b) The effect of mounting on the equivalent beam angle of acoustic survey transducers. ICES CM 1984/B, 32 (mimeo).
- Simmonds, E.J. (1990) Very accurate calibration of vertical echosounders, a five-year assessment of performance and accuracy. *Rapp. P.-v. Reun. Cons. Int. Explor. Mer* **189**, 183–91.
- Simmonds, E.J. (1995) Survey design and effort allocation: a synthesis of choices. ICES CM 1995/B, 9.
- Simmonds, E.J. (2003) Weighting of acoustic- and trawl-survey indices for the assessment of North Sea herring. *ICES J. Mar. Sci.* **60**, 463–71.
- Simmonds, E.J. and Copland, P.J. (1989) Species recognition: results from a wide band echosounder 27–54 kHz. *Proc. Inst. Acoust.* **11**, 54–60.
- Simmonds, E.J. and Fryer, R.J. (1996) Which are better, random or systematic acoustic surveys? A simulation using North Sea herring as an example. *ICES J. Mar. Sci.* **53**, 39–50.
- Simmonds, E.J. and MacLennan, D.N. (1988) Survey and data analysis procedures. ICES CM1988/B:58, 15 pp. (mimeo).
- Simmonds, E.J., Petrie, I.B., Armstrong, F. and Copland, P.J. (1984) High precision calibration of a vertical sounder system for use in fish stock estimation. *Proc. Inst. Acoust.* **6**, 129–38.
- Simmonds, E.J., Williamson, N.J., Gerlotto, F. and Aglen, A. (1992) Acoustic survey design and analysis procedure: a comprehensive review of current practice. *ICES Coop. Res. Rep.* **187**, 112 pp.
- Simmonds, E.J., Armstrong, F. and Copland, P.J. (1996) Species identification using wide-band backscatter with neural network and discriminant analysis. *ICES J. Mar. Sci.* **53**, 189–96.
- Simmonds, E.J., Gerlotto, F., Fernandes, P.G. and MacLennan, D.N. (2000) Observation and extraction of three dimensional information on fish schools. ASA Annual Conference, Berlin, June 2000.
- Simmonds, E.J., Fernandes, P.G. and Reid, D.G. (2002) School based model of the spatial distribution and dynamics of an acoustically surveyed herring distribution in the North Sea. ICES Symposium on Acoustics in Fisheries and Aquatic Ecology, Montpellier, June 2002.
- Simmonds, E.J., Zimmermann, S., Jansen, S., Götze, E., Torstensen, E., Staehr, K.-J., Couperus, A.S. and Fernandes, P.G. (2003) 2003 ICES co-ordinated acoustic survey of ICES Divisions IIIa, IVa, IVb and VIa (North): results and long term trends. ICES CM 2003/Q:20.
- Skalski, J.R., Hoffman, A., Ransom, B.H. and Steig, T.W. (1993) Fixed-location hydroacoustic monitoring designs for estimating fish passage using stratified random and systematic sampling. *Can. J. Fish. Aqu. Sci.* **50**, 1208–21.
- Skudrzyk, E. (1971) *The Foundations of Acoustics*. Springer-Verlag, New York.

- Slotte, A., Hansen, K., Dalen, J. and Ona, E. (2004) Acoustic mapping of pelagic fish distribution and abundance in relation to a seismic shooting area off the Norwegian west coast. *Fish. Res.* **67**, 143–50.
- Smith, G.W., Urquhart, G.G., MacLennan, D.N. and Sarno, B. (1998) A comparison of theoretical estimates of the errors associated with ultrasonic tracking using a fixed hydrophone array and field measurements. *Hydrobiologia* **371/372**, 9–17.
- Smith, P.E. (1970) The horizontal dimensions and abundance of fish schools in the upper mixed layer as measured by sonar. International Symposium on Biological Sound Scattering in the Ocean, March 31–April 2, 1970, Maury Ocean Science Center, Warrenton, USA, Dep. Navy, Washington, DC.
- Smith, P.E. (1977) The effect of internal waves on fish school mapping with sonar in the California Current area. *Rapp. P.-v. Cons. Int. Explor. Mer* **170**, 223–31.
- Smith, S.L., Pieper, R.E., Moore, M.V., Rudstam, L.G., Greene, C.H., Zamon, J.E., Flagg, C.N. and Williamson, C.E. (1992) Acoustic techniques for the in situ observation of zooplankton. *Arch. Hydrobiol. Beih. Ergebn. Limnol.* **36**, 25–43.
- Smith, W.J. (1991) Singing is based on two markedly different kinds of signaling. *J. Theor. Biol.* **152**, 241–53.
- Smyth, C.N., Poynton, F.Y. and Sayers, J.F. (1963) The ultrasound image camera. *Proc. IEE* **110**, 16–28.
- Solomon, D.J. and Hawkins, A.D. (1981) Fish capture and transport. In: *Aquarium Systems* (ed. A.D. Hawkins), pp. 197–221. Academic Press, London.
- Soria, M., Fréon, P. and Gerlotto, F. (1996) Analysis of vessel influence on spatial behaviour of fish schools using a multi-beam sonar and consequences for biomass estimates by echosounder. *ICES J. Mar. Sci.* **53**, 453–8.
- Sorokin, M.A., Perkin, S.I. and Lebedeva, A.N. (1988) On the distance of directional sound discrimination by fishes (in Russian). *Voprosy Ikhtiologii* **2**, 341–3.
- Soudi, P. (1988) Automatisation de la description et de la classification des détections acoustiques de bancs de poissons pélagiques pour leur identification – Thèse Dr. Univ. Aix-Marseille-II, France, décembre 1988.
- Soule, M., Barange, M. and Hampton, I. (1995) Evidence of bias in estimates of target strength obtained with a split-beam echosounder. *ICES J. Mar. Sci.* **52**, 139–44.
- Soule, M., Barange, M. and Hampton, I. (1996) Potential improvements to current methods of recognizing single targets with a split-beam echosounder. *ICES J. Mar. Sci.* **53**, 237–43.
- Southall, B.L., Schusterman, R.J. and Kastak, D. (2000) Masking in three pinnipeds: underwater, low-frequency critical ratios. *J. Acoust. Soc. Am.* **108**, 1322–6.
- Speisberger, J.L. and Metzger, K. (1991) A new algorithm for sound speed in seawater. *J. Acoust. Soc. Am.* **89**, 2677–88.
- Spindel, R.C. and McElroy, P.T. (1973) Level and zero crossings in volume reverberation signals. *J. Acoust. Soc. Am.* **53**, 1417–26.
- Squire, J.L. (1978) Northern anchovy school shapes as related to problems in school size estimation. *Fish. Bull.* **76**, 443–8.
- Staal, P.R. (1985) Acoustic effects of underwater explosive discharges. In: *Proceedings of the Workshop on Effects of Explosive Use in the Marine Environment*, 29–31 January 1985, Halifax (eds G.D. Greene, F.R. Engelhardt and R.J.E. Paterson). *Tech. Rep. Canada Oil and Gas Lands Administration*, Ottawa, No. 5, pp. 89–110.

- Stables, T.B. and Kautsky, G.A. (2000) Evaluation of a stimulus response method for distinguishing out-migrant salmonids from drifting debris for sonar counts in the Trinity river, California. *Aqu. Living Resources* **13**, 341–7.
- Stafford, K.M., Nieuirk, S.L. and Fox, C.G. (1999) Low-frequency whale sounds recorded on hydrophones moored in the eastern tropical Pacific. *J. Acoust. Soc. Am.* **106**, 3687–98.
- Stansfield, D. (1991) *Underwater Electroacoustic Transducers: A Handbook for Users and Designers*. Institute of Acoustics, Bath University Press.
- Stanton, T.K. (1982) Effects of transducer motion on echo-integration techniques. *J. Acoust. Soc. Am.* **72** (3), 947–9.
- Stanton, T.K. (1983) Multiple scattering with applications to fish-echo processing. *J. Acoust. Soc. Am.* **73**, 1164–9.
- Stanton, T.K. (1984) Effects of second-order scattering on high resolution sonars. *J. Acoust. Soc. Am.* **76**, 861–6.
- Stanton, T.K. (1985) Volume scattering: echo peak PDF. *J. Acoust. Soc. Am.* **77**, 1358–66.
- Stanton, T.K. (1988a) Sound scattering by cylinders of finite length I: fluid cylinders. *J. Acoust. Soc. Am.* **83**, 55–63.
- Stanton, T.K. (1988b) Sound scattering by cylinders of finite length III: deformed cylinders. *J. Acoust. Soc. Am.* **86**, 691–705.
- Stanton, T.K. (1990) Sound scattering by spherical and elongated shelled bodies. *J. Acoust. Soc. Am.* **88**, 1619–33.
- Stanton, T.K. and Clay, C.S. (1986) Sonar echo statistics as a remote sensing tool: volume and seafloor. *IEEE J. Oceanic Eng.* **11**, 79–99.
- Stanton, T.K., Chu, D., Wiebe, P.H. and Clay, C.S. (1993a) Average echoes from randomly orientated random-length finite cylinders: zooplankton models. *J. Acoust. Soc. Am.* **94**, 3463–72.
- Stanton, T.K., Clay, C.S. and Chu, D. (1993b) Ray representation of sound scattering by weakly scattering deformed fluid cylinders: simple physics and applications to zooplankton. *J. Acoust. Soc. Am.* **94**, 3454–62.
- Stanton, T.K., Wiebe, P.H., Chu, D., Benfield, M., Scanlon, L., Martin, L. and Eastwood, R.L. (1994a) On acoustic estimates of zooplankton biomass. *ICES J. Mar. Sci.* **51**, 505–12.
- Stanton, T.K., Wiebe, P.H., Chu, D. and Goodman, L. (1994b) Acoustic characterization and discrimination of marine zooplankton and turbulence. *ICES J. Mar. Sci.* **51**, 469–79.
- Stanton, T.K., Chu, D. and Wiebe, P.H. (1996) Acoustic scattering characteristics of several zooplankton groups. *ICES J. Mar. Sci.* **53**, 289–302.
- Stanton, T.K., Chu, D., Wiebe, P.H., Martin, L. and Eastwood, R.L. (1998a) Sound scattering by several zooplankton groups I: experimental determination of dominant scattering mechanisms. *J. Acoust. Soc. Am.* **103** (1), 225–35.
- Stanton, T.K., Chu, D. and Wiebe, P.H. (1998b) Sound scattering by several zooplankton groups II: scattering models. *J. Acoust. Soc. Am.* **103** (1), 236–53.
- Steig, T.W. and Johnston, S.V. (1996) Monitoring fish movement patterns in a reservoir using horizontally scanning split-beam techniques. *ICES J. Mar. Sci.* **53**, 435–42.
- Stewart, P.A.M. and Galbraith, R.D. (1987) Investigating the capture efficiency of survey gears. ICES CM 1987/B:7 (mimeo).
- Stolyrenko, D.A. (1988) Local integral measurement: an advanced spline approximation method for trawl, echosounding and television surveys. ICES CM 1988/D:1 (mimeo).

- Stromme, T. and Saetersdal, G. (1987) Consistency of acoustic biomass estimates tested by repeated survey coverages. Paper presented at the International Symposium on Fisheries Acoustics, Seattle, USA, 22–26 June 1987. No. 126 (mimeo).
- Sund, O. (1935) Echo sounding in fishery research. *Nature* **135**, 953.
- Swartzman, G. (1997) Analysis of the summer distribution of fish schools in the Pacific Eastern Boundary Current. *ICES J. Mar. Sci.* **54**, 105–16.
- Swingler, N. and Hampton, I. (1981) Investigation and comparison of current theories for the echo-integration technique of investigating fish abundance and of their verification by experiment. In: *Meeting on Hydroacoustical Methods for the Estimation of Marine Fish Populations*, 25–29 June 1979, Vol. 2 (ed. J.B. Suomala), pp. 97–156. The Charles Stark Draper Laboratory, Cambridge, Mass., USA.
- Tarbox, K.E. and Thorne, R.E. (1996) Assessment of adult salmon in near-surface waters of Cook Inlet, Alaska. *ICES J. Mar. Sci.* **53**, 397–402.
- Tavolga, W.N. (1962) Mechanisms of sound production in the ariid catfishes, *Galeichthys* and *Bagre*. *Bull. Amer. Mus. Nat. Hist.* **124**, 1–30.
- Tavolga, W.N. (1974) Signal/noise ratio and the critical band in fishes. *J. Acoust. Soc. Am.* **55**, 1323–33.
- Tavolga, W.N. (1976) Acoustic obstacle detection in the sea catfish, *Arius felis*. In: *Sound Reception in Fish* (eds A. Schuijf and A.D. Hawkins), pp. 185–204. Elsevier, Amsterdam.
- Tavolga, W.N., Popper, A.N. and Fay, R.R. (1981) (eds) *Hearing and Sound Communication in Fishes*. Springer-Verlag, New York.
- Teleki, G.C. and Chamberlain, A.J. (1978) Acute effects of underwater construction blasting on fishes in Long Point Bay, Lake Erie. *J. Fish. Res. Bd Can.* **35**, 1191–8.
- Terhune, J.M. and Ronald, K. (1975) Underwater hearing sensitivity of two ringed seals. *Can. J. Zool.* **53**, 227–31.
- Tesler, W.D. (1989) Bias and precision in acoustic biomass estimation. *Proc. Inst. Acoust.* **11** (3), 202–11.
- Thomas, J., Moore, P., Withrow, R. and Stoermer, M. (1990) Underwater audiogram of a Hawaiian monk seal (*Monachus schauinslandi*). *J. Acoust. Soc. Am.* **87**, 417–19.
- Thompson, C.H. and Love, R.H. (1996) Determination of fish size distributions and areal densities using broadband low-frequency measurements. *ICES J. Mar. Sci.* **53**, 197–202.
- Thompson, J.K. (1992) *Sampling*. John Wiley & Sons, New York.
- Thompson, P., Findlay, L., Vidal, O. and Cummings, W. (1996) Underwater sounds of blue whales, *Balaenoptera musculus*, in the Gulf of California, Mexico. *Marine Mammal Sci.* **12**, 288–93.
- Thompson, P.O., Cummings, W.C. and Ha, S.J. (1986) Sounds, source levels and associated behaviors of humpback whales, southeast Alaska. *J. Acoust. Soc. Am.* **80**, 735–40.
- Thompson, P.O., Findlay, L.T. and Vidal, O. (1992) 20-Hz pulses and other vocalizations of fin whales, *Balaenoptera physalus*, in the Gulf of California, Mexico. *J. Acoust. Soc. Am.* **92**, 3051–7.
- Thompson, S.K. and Seber, G.A.F. (1996) *Adaptive Sampling*. John Wiley & Sons, New York.
- Thomsen, F., Franck, D. and Ford, J.K.B. (2001) Characteristics of whistles from the acoustic repertoire of resident killer whales (*Orcinus orca*) off Vancouver Island, British Columbia. *J. Acoust. Soc. Am.* **109**, 1240–6.
- Thorne, R.E. (1971) Investigations into the relation between integrated echo voltage and fish density. *J. Fish. Res. Bd Can.* **28**, 1269–73.

- Thorne, R.E. (1979) Hydroacoustic estimates of adult sockeye salmon (*Onchorhynchus nerka*) in Lake Washington 1972–1975. *J. Fish. Res. Bd Can.* **36**, 1145–9.
- Thorne, R.E. (1983) Application of hydroacoustic assessment techniques to three lakes with contrasting fish distributions. *FAO Fish. Rep.* **300**, 269–77.
- Thorne, R.E. (1988) An empirical evaluation of the duration-in-beam technique for hydroacoustic estimation. *Can. J. Fish. Aquat. Sci.* **45**, 1244–8.
- Thorne, R.E. (1998) Review: Experiences with shallow water acoustics. *Fish. Res.* **35**, 137–41.
- Thorne, R.E., Hedgepeth, J. and Campos, J. (1990) The use of stationary hydroacoustic transducers to study diel and tidal influences on fish behaviour. *Rapp. P.-v. Reun. Cons. Int. Explor. Mer* **189**, 167–75.
- Tichy, F.E., Solli, H. and Klaveness, H. (2003) Nonlinear effects in a 200-kHz sound beam and the consequences for target-strength measurement. *ICES J. Mar. Sci.* **60**, 571–4.
- Tollefson, C.D.S. and Zedel, L. (2003) Evaluation of a Doppler sonar system for fisheries applications. *ICES J. Mar. Sci.* **60**, 692–9.
- Toresen, R. (1991) Absorption of acoustic energy in dense herring schools studied by the attenuation in the bottom echo signal. *Fish. Res.* **10**, 317–27.
- Toresen, R., Gjøsaeter, H. and de Barros, P. (1998) The acoustic method as used in the abundance estimation of capelin (*Mallotus villosus* Muller) and herring (*Clupea harengus* Linne) in the Barents Sea. *Fish. Res.* **34**, 27–38.
- Traynor, J.J. (1996) Target-strength measurements of walleye pollock and Pacific whiting. *ICES J. Mar. Sci.* **53**, 253–8.
- Traynor, J.J. and Williamson, N.J. (1983) Target strength measurements of walleye pollock (*Theragra chalcogramma*) and a simulation study of the dual beam method. *FAO Fish. Rep.* **300**, 112–24.
- Trevorrow, M.V. (1996) Multifrequency acoustic investigations of juvenile and adult fish in Lake Biwa, Japan. *J. Acoust. Soc. Am.* **100**, 3042–52.
- Trevorrow, M.V. (1998) Salmon and herring school detection in shallow waters using sidescan sonars. *Fish. Res.* **35**, 5–14.
- Trevorrow, M.V. (2001) An evaluation of a steerable sidescan sonar for surveys of near-surface fish. *Fish. Res.* **50**, 221–34.
- Trevorrow, M.V. and Pedersen, B. (2000) Detection of migratory herring in a shallow channel using 12 and 100 kHz sidescan sonars. *Aqu. Living Resources* **13**, 395–401.
- Trout, G.C., Lee, A.J., Richardson, I.D. and Harden Jones, F.R. (1952) Recent echosounder studies. *Nature* **170**, 4315, 71–2.
- Tucker, D.G. and Gazey, B.K. (1966) *Applied Underwater Acoustics*. Pergamon Press, London.
- Tungate, D.S. (1958) Echo-sounder surveys in the autumn of 1956. *Fishery Investigations, Series 2* **12**, 3–17.
- Turl, C.W. and Penner, R.H. (1989) Differences in echolocation click patterns of the beluga (*Delphinapterus leucas*) and the bottlenose dolphin (*Tursiops truncatus*). *J. Acoust. Soc. Am.* **86**, 497–502.
- Tyack, P.L. (1999) Communication and cognition. In: *The Biology of Marine Mammals* (eds J.E. Reynolds III and S.A. Rommel), pp. 287–323. Smithsonian Institute Press, Washington, DC.
- Urick, R.J. (1967) *Principles of Underwater Sound for Engineers*. McGraw-Hill Book Company, New York.

- Urick, R.J. (1975) *Principles of Underwater Sound*, 2nd edn. McGraw-Hill Book Company, New York, 384 pp.
- Urick, R.J. (1983) *Principles of Underwater Sound*, 3rd edn. Peninsula Publishing, Los Altos, California.
- Urick, R.J. (1986) *Ambient Noise in the Sea*. Peninsula Publishing, California.
- Vabø, R., Olsen, K. and Huse, I. (2002) The effect of vessel avoidance of wintering Norwegian spring spawning herring. *Fish. Res.* **58**, 59–77.
- Venema, S.C. (1985) A selected bibliography of acoustics in fisheries research and related fields. FAO Fish. Circ. 748 (Revision 1) FIRM/C748. Food and Agriculture Organisation, Rome.
- Wahlberg, M., Møhl, B. and Madsen, P.T. (2001) Estimating source position accuracy of a large-aperture hydrophone array for bioacoustics. *J. Acoust. Soc. Am.* **109**, 397–406.
- Walker, R.A. (1963) Some intense low frequency underwater sounds of wide geographic distribution, apparently of biological origin. *J. Acoust. Soc. Am.* **35**, 1816.
- Walline, P.D., Pisanty, S. and Lindem, T. (1992) Acoustic assessment of the number of pelagic fish in Lake Kinneret, Israel. *Hydrobiologia* **231**, 153–63.
- Wanzenböck, J., Mehner, T., Schulz, M., Gassner, H. and Winfield, I. (2003) Quality assurance of hydroacoustic surveys: the repeatability of fish-abundance and biomass estimates in lakes within and between hydroacoustic systems. *ICES J. Mar. Sci.* **60**, 486–92.
- Warner, D.M., Rudstam, L.G. and Klumb, R.A. (2002) In situ target strength of alewives in freshwater. *Trans. Am. Fish. Soc.* **131**, 212–23.
- Watkins, J.L. and Brierley, A.S. (1996) A post-processing technique to remove background noise from echo integration data. *ICES J. Mar. Sci.* **53**, 339–44.
- Watkins, W.A., Tyack, P., Moore, K.E., and Bird, J.E. (1987) The 20 Hz signals of finback whales (*Balaenoptera physalus*). *J. Acoust. Soc. Am.* **82**, 1901–12.
- Weill, A., Scalabrin, C. and Diner, N. (1993) MOVIES B: an acoustic detection description software. Application to shoal species classification. *Aqu. Living Resources* **6** (3), 255–67.
- Weimer, R.T. and Ehrenberg, J.E. (1975) Analysis of threshold-induced bias inherent in acoustic scattering cross-section estimates of individual fish. *J. Fish. Res. Bd Can.* **32**, 2547–51.
- Welsby, V.G. and Hudson, J.E. (1972) Standard small targets for calibrating underwater sonars. *J. Sound Vib.* **20**, 399–406.
- Wenz, G.M. (1962) Acoustic ambient noise in the ocean: spectra and sources. *J. Acoust. Soc. Am.* **34**, 1936–56.
- Wenz, G.M. (1972) Reviews of underwater acoustics: noise. *J. Acoust. Soc. Am.* **51**, 1010–24.
- Weston, D.E. (1960) Underwater explosions as acoustic sources. *Proc. Phys. Soc. London B* **76**, 233–49.
- Weston, D.E. (1967) Sound propagation in the presence of bladder fish. In: *Underwater Acoustics 2* (ed. V.M. Albers), pp. 55–88. Plenum Press, New York.
- Weston, D.E. (1989) On the losses due to storm bubbles in oceanic sound transmission. *J. Acoust. Soc. Am.* **86**, 1546–53.
- Weston, D.E. and Andrews, H.W. (1988) Seasonal sonar observations of the diurnal shoaling times of fish. *J. Acoust. Soc. Am.* **87**, 673–80.
- Weston, D.E. and Andrews, H.W. (1990) Monthly estimates of fish numbers using a long-range sonar. *J. Cons. Int. Explor. Mer* **47**, 104–11.

- Weston, D.E. and Ching, P.A. (1989) Wind effects in shallow water acoustic transmission. *J. Acoust. Soc. Am.* **86**, 1530–45.
- Whitehead, P.J.P. and Blaxter, J.H.B. (1989) Swimbladder form in the clupeoid fishes. *Zool. J. Linnean Soc.* **97**, 299–372.
- Wiebe, P.H., Greene, C.H., Stanton, T.K. and Burczynski, J. (1990) Sound scattering by live zooplankton and microneuston: empirical studies with a dual-beam acoustical system. *J. Acoust. Soc. Am.* **88**, 2346–60.
- Wiebe, P.H., Mountain, D.G., Stanton, T.K., Greene, C.H., Lough, G., Kaartvedt, S., Dawson, J. and Copley, N. (1996) Acoustical study of the spatial distribution of plankton on Georges Bank and the relationship between volume backscattering strength and the taxonomic composition of the plankton. *Deep Sea Res. II* **43**, 1971–2001.
- Wiley, M.L., Gaspin, J.B. and Goertner, J.F. (1981) Effects of underwater explosions on fish with a dynamical model to predict fish kill. *Ocean Sci. Eng.* **6**, 223–84.
- Williamson, N.J. and Traynor, J.J. (1996) Application of a one-dimensional geostatistical procedure to fisheries acoustic surveys of Alaskan pollock. *ICES J. Mar. Sci.* **53**, 423–8.
- Wong, G.S.K. and Zhu, S. (1995) Sound speed in seawater as a function of salinity. *J. Acoust. Soc. Am.* **97**, 1732–6.
- Wood, A.B., Smith, F.D. and McGeachy, J.A. (1935) A magnetostriction echo depth-recorder. *J. Inst. Elect. Eng.* **76**, 550–67.
- Woodd-Walker, R.S., Watkins, J.L. and Brierley, A.S. (2003) Identification of Southern Ocean acoustic targets using aggregation backscatter and shape characteristics. *ICES J. Mar. Sci.* **60**, 641–9.
- Yasuma, H., Sawada, K., Ohshima, T., Miyashita, K. and Aoki, I. (2003) Target strength of mesopelagic lanternfishes (family Myctophidae) based on swimbladder morphology. *ICES J. Mar. Sci.* **60**, 584–91.
- Ye, Z. (1995) Theoretical description of possible detection of swimbladdered fish in forward scatter. *J. Acoust. Soc. Am.* **98**, 2717–25.
- Ye, Z. (1996) On acoustic attenuation by swimbladder fish. *J. Acoust. Soc. Am.* **100**, 669–72.
- Ye, Z. (1997) Acoustic dispersion and attenuation in many spherical scatterer systems and the Kramers–Kronig relations. *J. Acoust. Soc. Am.* **101**, 3299–305.
- Ye, Z. and Farmer, D.M. (1994) Acoustic scattering from swim-bladder fish at low frequencies. *J. Acoust. Soc. Am.* **96**, 951–6.
- Ye, Z. and Farmer, D.M. (1996) Acoustic scattering by fish in the forward direction. *ICES J. Mar. Sci.* **53**, 249–52.
- Ye, Z. and McClatchie, S. (1998) On inferring speed of sound in aquatic organisms. *J. Acoust. Soc. Am.* **103**, 1667–70.
- Yelverton, J.T., Richmond, D.R., Hicks, W., Saunders, K. and Fletcher, E.R. (1975) The relationship between fish size and their response to underwater blast. Rep. DNA 3677 T. Defense Nuclear Agency, Washington, DC. 39 pp.
- Yule, D.L. (2000) Comparison of horizontal acoustic and purse seine estimates of salmonid densities and sizes in eleven Wyoming waters. *North Am. J. Fish. Man.* **20**, 759–75.
- Zakharia, M., Corgiatti, J.P., Joly, F. and Person, R. (1989). Wide-band sounder for fisheries. *Proc. Inst. Acoust.* **11**, 274–81.
- Zakharia, M.E., Magand, F., Hetroit, F. and Diner, N. (1996) Wideband sounder for fish species identification at sea. *ICES J. Mar. Sci.* **53**, 203–8.

# Species Index

- Aequorea aequorea* (jellyfish), 283  
*Aequorea victoria* (jellyfish), 283  
*Alosa fallax fallax*, 137, 156  
*Alosa sapidissima* (American shad), 132, 137, 138  
*Ammodytes* sp. (sandeel), 236, 237, 260  
Amphipods, 277, 291, 293  
Anchovies, 2, 161, 162, 173, 174, 197, 258, 301, 336, 378  
*Argentina silus* (great silver smelt), 256  
*Arius felis* (catfish), 139  
*Astronotus ocellatus* (oscar), 132  
*Aurelia aurita* (common jellyfish), 280, 283
- Benthosema fibulatum* (myctophid), 260  
*Benthosema pterotum* (lantern fish), 335  
*Bolinopsis* sp. (jellyfish), 283  
*Brevoortia patronus* (menhaden), 138
- Calanus finmarchicus* (copepod), 277  
*Calanus plumchrus* (copepod), 277  
*Caradina nilotica* (freshwater shrimp), Plate 5.1  
*Carassius auratus* (goldfish), 132, 137  
Cetaceans, 13, 129, 132, 140, 142, 144  
*Chrysaora hysoscella* (jellyfish), 283  
*Clausocalanus* spp. (calanoid copepods), 287  
*Clupea harengus* (herring), 2, 3, 5, 72, 73, 78, 79, 87, 99, 108, 132, 160, 161, 167, 174, 175, 194, 198, 204, 208, 223, 226, 230, 236, 237, 238, 239, 244, 249, 250, 251, 253, 254, 258, 263, 301, 302, 303, 306, 307, 323, 324, 333, 334, 338, 341, 342, 343, 348, 351, 353, 357, 362, 368, 370, 371, 372, 377, 378, Plate 3.2
- Clupeidae, 2  
*Coregonus artedii* (cisco), 259, Plate 3.5  
Crangonidae (snapping shrimp), 128  
*Cyprinus carpio* (carp), 131, 132, 152
- Delphinapterus leucas* (beluga whale), 140  
*Delphinus delphis* (common dolphin), 142, 144  
*Diaphus theta* (myctophid), 260  
*Diplotaxodon* spp., 242, 259  
*Dorosoma petenense* (threadfin shad), 230
- Engraulidae, 2  
*Engraulis capensis* (anchovy), 258, 378  
*Engraulis encrasicolus* (anchovy), 301  
*Engraulis mordax* (northern anchovy), 161, 162, 174, 197  
*Engraulis ringens* (anchoveta), 258  
*Euphausia frigida* (krill), 292  
*Euphausia pacifica* (krill), 268  
*Euphausia* spp., 263, 265, 266, 269, 270, 273, 275  
*Euphausia superba* (Antarctic krill), 263, 269, 278, 284, 292, 375
- Fundulus heteroclitus* (mummichog), 235
- Gadus morhua* (Atlantic cod), 4, 96, 99, 131, 132, 133, 134, 135, 136, 137, 138, 139, 159, 160, 161, 221, 227, 230, 232, 235, 236, 237, 239, 245, 248, 249, 251, 252, 256, 275, 277, 334, 375, 378, Plate 3.8, Plate 6.1
- Galeichthys felis* (catfish), 129  
*Gambusia affinis* (minnow), 152  
Gastropods, 265, 266, 272, 273
- Homarus americanus* (lobster), 131, 132  
*Hoplostethus atlanticus* (orange roughy), 235, 249, 260, Plate 9.3
- Ictalurus punctatus* (channel catfish), 152  
*Inia geoffrensis* (Amazon dolphin), 132, 140, 142
- Jellyfish, 280, 283
- Katsuwonus pelamis* (skipjack tuna), 83, Plate 3.4
- Krill, 8, 263, 264, 265, 266, 268, 269, 270, 273, 275, 277, 278, 279, 280, 284, 291, 292, 293, 323, 346, 375
- Lates niloticus* (Nile perch), 259, Plate 5.1  
*Leiostomous xanthurus* (spot), 152  
*Lepomis macrochirus* (bluegill), 152

- Limanda limanda* (dab), 132  
*Loligo gahi* (squid), 291  
*Loligo opalescens* (squid), 282
- Mackerels, 2, 99, 161, 162, 226, 235, 236, 237, 238, 239, 249, 256, 260, 335, 370
- Macrorhamphosus scolopax* (trumpet fish), 335
- Macruronus novaezelandiae* (hoki), 260, 375
- Mallotus villosus* (capelin), 256
- Maurolicus muelleri* (myctophid), 240
- Meganyctiphanes norvegica* (krill), 268, 277
- Megaptera novaeangliae* (humpback whale), 129
- Melanogrammus aeglefinus* (haddock), 238, 239, 256, 333, 378
- Merluccius australis* (southern hake), 256
- Merluccius gayi* (Chilean hake), 256
- Merluccius productus* (Pacific whiting), 256
- Microchiroptera (bats), 139
- Micromesistius australis* (southern blue whiting), 256
- Micromesistius poutassou* (blue whiting), 99, 240, 241, 242, 256, 263
- Micropterus salmoides* (black bass), 152
- Monachus schauinslandi* (Hawaiian monk seal), 132
- Morone americana* (white perch), 152
- Myctophids, 235, 240, 241, 242, 260, 335
- Myripristis kuhnei* (soldier fish), 131, 132
- Mysids, 289, 291
- Notoscopulus japonicus* (myctophid), 260
- Notropis cornutus* (common shiner), 235
- Oikopleura* spp. (calanoid copepods), 287
- Oncorhynchus nerka* (sockeye salmon, kokanee), 226, 239, 259, 316, 378
- Oncorhynchus* spp., 174
- Oncorhynchus tshawytscha* (chinook salmon), 94
- Orcinus orca* (killer whale), 132, 140
- Osmerus mordax* (rainbow smelt), 259
- Pagrosomus major*, 3
- Pagrus auratus* (pink snapper), 154
- Pagrus major* (sea bream), 235, 260
- Parathemisto pacifica* (amphipod), 277
- Perca fluviatilis* (perch), 139
- Phoca vitulina* (harbor seal), 137
- Phocoena phocoena* (harbour porpoise), 140, 142
- Physeter catodon* (sperm whale), 140
- Platinista indi* (Indus river dolphin), 140, 142, 144
- Pleuronectes platessa* (plaice), 139
- Pollachius pollachius* (pollack), 161, 194, 231, 245, 246, 372
- Pollachius virens* (saithe), 161, 256
- Pusa hispida* (ringed seal), 132, 137
- Rastrineobola argentea* (dagaa), 259, Plate 5.1
- Rhincalanus gigas* (copepod), 292
- Salmo salar* (Atlantic salmon), 131, 132, 137
- Salmo trutta* (trout), 161
- Salmonidae, 2, 93, 94, 98, 131, 132, 137, 138, 157, 174, 207, 208, 226, 259, 316, 378, 379
- Sardina pilchardus* (pilchard), 204, 335
- Sardine, 133, 137, 197, 204, 211, 234, 258, 335, 356, 362, 372, Plate 3.6
- Sardinella aurita* (Spanish sardine), 137, 372, Plate 3.6
- Sardinella* spp., 356
- Sardinops ocellatus* (pilchard), 258
- Sardinops sagax* (sardine), 133, 197, 258
- Sardinops sagax caerulea* (sardine), 197
- Sardinops sagax melanosticta* (sardine), 133
- Scardinius erythrophthalmus* (rudd), 234
- Scomber japonicus* (horse mackerel, caballa), 260
- Scomber scombrus* (Atlantic mackerel), 235, 237, 239, 249, 260
- Scombridae (mackerels), 2
- Sebastes marinus* (redfish), 256
- Sebastes schlegeli* (lawnun, rockfish), 259, 260
- Sebastes* sp. (redfish), 375
- Seriola quinqueradiata* (yellowtail), 235
- Sharks, 133, 139
- Siphonophores*, 265, 266, 271, 273, 274
- Sprattus sprattus* (sprat), 4, 53, 161, 196, 197, 250, 251, 258
- Squid, 277, 280, 282, 291, 293
- Stenella frontalis* (Atlantic spotted dolphin), 140
- Symbolophorus californiensis* (myctophid), 260
- Synalpheus parneomeris* (snapping shrimp), 128
- Themisto gaudichaudii* (amphipod), 292
- Theragra chalcogramma* (walleye pollock), 228, 244, 256
- Thunnus obesus* (bigeye tuna), 101
- Thysanoessa macrura* (krill), 292
- Thysanoessa* spp. (krill), 268
- Todarodes pacificus* (squid, surume ika), 277, 280, 282

- Trachurus japonicus* (Japanese horse mackerel), 235  
*Trachurus picturatus* (jurel), 256  
*Trachurus* spp., 335  
*Trachurus symmetricus* (jack mackerel), 161, 162, 256  
*Trachurus trachurus capensis* (Cape horse mackerel), 256  
*Trichechus manatus* (West Indian manatee), 132
- Trisopterus esmarkii* (Norway pout), 256  
Tuna, 53, 83, 84, 95, 101, 129, Plate 3.4,  
Plate 3.7  
Whales, 45, 53, 64, 128, 129, 132, 139, 140, 154,  
155, 157
- Zalophus californianus*  
(California sea lion), 13

# Author Index

- Abramowitz, M., 29  
Aglen, A., 167, 170, 174, 175, 201, 202, 240,  
    244, 257, 294, 297, 311, 320, 325, 359,  
    360, 361  
Ainslie, M. A., 41  
Aitchesson, J., 353  
Aksland, M., 187, 202  
Amorim, M. C. P., 129  
Andersen, S., 140, 142  
Anderson, D. R., 296  
Anderson, E., 157  
Anderson, K. P., 352  
Anderson, R., 130  
Anderson, V. T., 267, 274  
Andreeva, I. B., 159, 197, 229  
Andrews, H. W., 203  
Angell, J., 371, 372  
Aoki, I., 232, 260, 278  
Aoyama, C., 180, 191  
Aplin, J. A., 150  
Ariji, M., 269  
Armstrong, E., 53, 99, 108, 196, 198, 201, 221,  
    224, 235, 238, 246, 250, 251, 253, 255,  
    258, 260, 372  
Arnaya, I. N., 277, 280, 283  
Arnold, G. P., 90, 100  
Aroyan, J. L., 142, 144  
Arrhenius, F., 209, 302  
Astrup, J., 137, 138  
Atkinson, A., 291, 292  
Au, W. W. L., 128, 135, 137, 139, 140, 141, 142,  
    143, 235, 260  
Aubauer, R., 141  
Aukland, R., 92, 334  
Austin, T. C., 281  
Axelsen, B. A., 283
- Bach, P., 101  
Backus, R. H., 45, 129, 160  
Baekkevold, A. E., 277  
Bailey, M. C., 202  
Bailey, R. S., 356  
Baldwin, K., 157  
Balls, R., 3  
Banburg, J. C., 133
- Banks, K., 128  
Bannehaka, S. G., 186, 316  
Barange, M., 80, 84, 211, 227, 240, 257, 258,  
    301, 334  
Barans, C. A., 288  
Bary, B. M., 280  
Batty, R. S., 160, 249  
Baxter, L., 153  
Bazigos, G. P., 303  
Beillois, P., 362, 373  
Bell, J. M., 87  
Belousov, A. V., 197  
Belttestad, A. K., 170, 174, 226, 258, 260  
Beltri, P., 107  
Benfield, M., 265, 292  
Benneheij, B. J. A. M., 209  
Benoit-Bird, K. J., 235, 260  
Berka, R., 224  
Bertrand, A., 101  
Bethke, E., 302  
Beverton, R. J., 1, 5  
Bez, N., 303, 306, 309, 350, 354, 355, 358, 371  
Bird, J. E., 129, 235, 260  
Blacker, R. W., 5  
Blackstock, D. T., 37, 38  
Blaxter, J. H. B., 159, 160, 170, 249  
Blue, J. E., 110, 130, 132  
Bodholt, H., 105, 187  
Boisclair, D., 186, 209  
Bone, D. G., 275, 278, 283  
Borisenko, E. S., 235  
Bourgault, G., 358  
Box, G. E. P., 353  
Boyd, A. J., 211  
Boyer, H., 283  
Bradley, A. M., 281  
Brander, K., 287  
Bravington, M., 325  
Brede, R., 209  
Brehmer, P., 372  
Brensing, K., 102  
Brierley, A. S., 108, 186, 283, 291, 292, 334,  
    351, 372  
Brown, J. C., 171  
Bruno, D. R., 366

- Buck, J. R., 139  
 Buckart, C. A., 287  
 Buckland, S. T., 296  
 Buckland, W. R., 191  
 Buecher, E., 283  
 Buerkle, U., 358  
 Burczynski, J., 21, 105, 191, 196, 259, 277, 278,  
     279, 280, 283  
 Burnham, K. P., 296  
 Burwen, D. L., 186  
 Butterworth, A. J., 186, 205  
 Buwalda, R. J. A., 133  
 Campbell, R. C., 341  
 Campos, J., 370  
 Candy, J. R., 334  
 Carder, D. A., 133, 135, 155  
 Cardinale, M., 302  
 Carlson, T. J., 80, 93, 240  
 Carrera, P., 92, 334  
 Castillo, J., 361  
 Cato, D., 128  
 Cech, M., 209  
 Cerf, J. A., 130  
 Chadwick, M., 358  
 Chamberlain, A. J., 151  
 Chandran, G., 96, 293  
 Chantler, M. J., 87  
 Chapman, C. J., 130, 131, 132, 133, 134, 135,  
     136, 137  
 Chapman, N. R., 149  
 Chen, C., 42, 69  
 Chen, D. G., 177, 205, 210, 317  
 Ching, P. A., 365  
 Chu, D., 255, 257, 262, 265, 266, 268, 270, 271,  
     272, 273, 274, 275, 277, 278, 292  
 Clabburn, P., 137, 156  
 Clark, C. W., 129  
 Clarke, N. I., 155  
 Clay, A., 91  
 Clay, C. S., 2, 21, 51, 123, 179, 182, 184, 218,  
     224, 228, 229, 230, 235, 241, 242, 245,  
     259, 267, 271, 278  
 Cleary, J. L., 128  
 Cochran, W. G., 296, 300, 360  
 Cochrane, N. A., 91, 124  
 Cole, R. H., 145, 147, 148, 150  
 Comeau, M., 358  
 Conan, G., 358  
 Connelly, P. R., 102  
 Conti, S., 197, 270, 280  
 Cooke, R. C., 366  
 Coombs, R. F., 235, 252, 255, 257, 260  
 Coombs, S. H., 276  
 Cooney, R. T., 281  
 Copland, P. J., 99, 198, 201  
 Copley, N. J., 255, 257, 275, 277, 281  
 Cordova, J., 240, 257  
 Cornuelle, B. D., 42  
 Costello, J. H., 287  
 Cottais, P. H., 91  
 Couperus, A. S., 347  
 Cox, D. R., 353  
 Craig, R. E., 23, 177, 182, 228  
 Cranford, T. W., 142  
 Cressie, N., 354  
 Crittenden, R. N., 185, 316  
 Cronkite, G. M. W., 209  
 Cummings, W. C., 129  
 Curtis, K. R., 154  
 Cushing, D. H., 5, 90  
 Dagorn, I., 101  
 Dalen, J., 9, 51, 60, 105, 106, 107, 154, 174,  
     202, 267, 268, 275, 276, 277, 330, 351,  
     366, 367  
 Dalpado, P., 277  
 David, A. M., 2, 145, 155, 156  
 Dawson, J., 281  
 de Barros, P., 202  
 de Munck, J. C., 133  
 De Robertis, A., 293  
 De Rosny, J., 197, 280  
 Degnbol, P., 122, 258  
 Del Gross, V. A., 42, 69  
 Demer, D. A., 84, 197, 211, 227, 270, 278, 279,  
     280, 283, 284, 323, 346, 370, 375  
 Denbigh, P., 98  
 Diachok, O., 160  
 Didenkulov, I. N., 263  
 Diercks, J. J., 139, 140  
 Diner, N., 92, 99, 107, 108, 167, 168, 170,  
     334, 372  
 Ding, L., 212  
 Do, M. A., 260  
 Dobbins, P. F., 144  
 Dommasnes, A., 341, 345  
 Dragesund, O., 5, 187  
 Dragonette, L. R., 53  
 Driscoll, R. L., 87, 171, 270, 278, 279, 284, 362,  
     373, 375  
 Duncan, A., 186, 202, 205  
 Duncan, P. M., 146, 148  
 Duncan, W. M., 186  
 Dunn, J., 55  
 Dunshaw, B. D., 42  
 Eastwood, R. L., 265, 268, 272, 292  
 Edwards, J. I., 221, 224, 235, 238, 250, 251,  
     258, 260  
 Efron, B., 361  
 Eger, K., 77  
 Eggers, D. M., 186  
 Ehrenberg, J. E., 80, 101, 177, 182, 183, 185,  
     187, 188, 201, 209, 210, 240, 241, 248  
 Einhouse, D. W., 202, 240, 259

- Elsberry, W. R., 155  
Engås, A., 154, 156, 202  
Engelhardt, F. R., 145  
Enger, P. S., 130, 132, 138, 157  
Erbe, C., 155, 156, 157  
Ermolchev, V., 224, 252, 257  
Evans, W. E., 139, 140  
Everest, F. A., 128  
Everson, I., 202, 275, 278, 283, 290, 325
- Falk-Petersen, S., 276  
Farmer, D. M., 155, 157, 159, 204, 207, 212, 218  
Fay, R. R., 128, 129, 130, 134  
Fedotova, T. A., 235, 253  
Ferguson, B. G., 128  
Fernandes, P. G., 6, 9, 51, 60, 105, 108, 124,  
125, 284, 303, 306, 309, 347, 350, 351,  
354, 355, 358, 368, 371, 372, 406  
Feuillade, C., 159, 229, 267, 367  
Fewtrell, J., 154  
Fielding, S., 280, 292  
Findlay, L. T., 129  
Fine, M. L., 129  
Finneran, J. J., 133, 135, 154, 155, 156  
Fish, M. P., 128  
Fish, P. J., 146  
Fisher, F. H., 41  
Flagg, C. N., 280  
Flax, L., 53  
Fleischman, S. J., 186  
Fletcher, E. R., 151, 152  
Fletcher, H., 135  
Flint, J. A., 144  
Foldy, L. L., 111  
Foote, A. D., 157  
Foote, K. G., 5, 27, 28, 52, 53, 55, 56, 110, 111,  
112, 117, 177, 185, 187, 191, 194, 195,  
196, 201, 218, 219, 220, 222, 227, 228,  
229, 230, 231, 232, 233, 234, 235, 240,  
244, 245, 246, 250, 251, 252, 255, 257,  
258, 275, 276, 277, 278, 283, 303, 306,  
309, 327, 350, 354, 355, 358, 363, 368,  
369, 370, 371  
Forbes, S. T., 21, 52, 177, 182, 228, 240, 241, 242  
Ford, J. K. B., 139  
Forsythe, S. E., 130, 132  
Fox, C. G., 129  
Francis, D. T. I., 55, 230, 231, 232  
Francis, R. I. C. C., 318, 321, 360  
Franck, D., 139  
Francois, R. E., 41, 67  
Frankel, A. S., 129  
Franklin, A. S., 129  
Fréon, P., 1, 91, 169, 171, 176, 372  
Frey, A. R., 98  
Fridriksson, A., 5  
Frinaes, E., 167, 170, 174, 175  
Fryer, R. J., 302, 306, 307, 308, 357
- Fuhiya, M., 151  
Fukuhara, O., 151  
Furiman, D., 209  
Furset, H., 55  
Furusawa, M., 180, 191, 195, 196, 218, 235,  
269, 334
- Gal, G., 281  
Galbraith, R. D., 302  
Gallucci, F. V., 228  
Garnier, B. E., 107  
Garrison, G. R., 41, 67  
Gassner, H., 357  
Gaudet, D. M., 186  
Gauthier, S., 170, 186, 375  
Gazey, B. K., 21, 25, 29, 48, 89, 90  
Georgakarakos, S., 92, 334  
Gerlotto, F., 6, 91, 124, 125, 169, 171, 176, 207,  
208, 294, 370, 372
- Gerstein, E. R., 130, 132  
Gerstein, L., 130, 132  
Getabu, A., 202, 259  
Gibbons, M. J., 283  
Gihr, M., 139, 140, 143, 144  
Gimona, A., 351  
Gjøsaeter, H., 202  
Godø, O. R., 325  
Goertner, J. F., 152  
Goldsborough, R. G., 281  
Goncharov, S. M., 235  
Goodman, L., 271, 272  
Goodson, A. D., 102, 140, 142, 144, 157  
Goold, J. C., 146  
Gordon, C. R., 139  
Gorska, N., 230  
Gosine, R., 334  
Goss, C., 202, 290, 291, 292, 325, 334  
Götze, E., 347  
Greene, C. H., 277, 278, 279, 280, 281, 283, 284  
Greene, C. R., 2, 65, 154, 156, 157  
Greene, G. D., 145  
Greenlaw, C. F., 267, 275, 276, 277, 284, 285,  
286, 288  
Greenlaw, R. L., 139, 140  
Greer Walker, M., 90, 100  
Gregory, J., 137, 156, 186  
Griffiths, G., 280, 292, 293  
Grimes, P., 235, 260  
Gull, S. F., 351  
Gulland, J. A., 2, 294, 378  
Gunderson, D. R., 1, 2, 164  
Gusar, A. G., 235  
Guthrie, I. C., 186, 316  
Gutierrez, M., 257, 258, 260
- Ha, S. J., 129, 133  
Hakansson, N., 302  
Hale, R., 334

- Hall, J. D., 132  
 Hall, M. V., 365  
 Halldorsson, O., 240, 257  
 Hamada, M., 180, 191  
 Hamilton, D., 194  
 Hamilton, M. F., 38  
 Hampton, I., 80, 98, 194, 227, 240, 257, 258,  
     301, 306, 311, 318, 320, 357, 378  
 Hanchet, S., 257  
 Hansen, K., 154, 257  
 Hansen, R. J., 286  
 Hansson, S., 184, 202, 228, 240, 258  
 Haralabous, J., 334  
 Harden Jones, F. R., 5, 176, 312, 368, 369  
 Harris, G. G., 23  
 Hart, A., 235, 260  
 Hartman, M., 293  
 Haslett, R. W. G., 219  
 Hastie, T. J., 371  
 Hastings, M. C., 132, 138, 154, 156  
 Hawkins, A. D., 2, 100, 128, 129, 130, 131, 132,  
     133, 134, 135, 136, 137, 160, 224, 253  
 Hazen, E. L., 247, 362  
 He, P., 370  
 Heathershaw, A. D., 2, 145, 155, 156  
 Heaton, M. J. P., 87  
 Hedgepeth, J. B., 209, 228, 370  
 Heerfordt, A., 102  
 Heist, B. G., 218, 241, 242  
 Hellwig, J., 160  
 Helweg, D. A., 129  
 Hendershott, R., 281  
 Herman, L. M., 129  
 Hernandez, C., 91, 207, 208  
 Hersey, J. B., 160  
 Herzing, D. L., 140  
 Hester, F. J., 210  
 Detroit, F., 99  
 Hewitt, R. P., 84, 171, 227, 278, 279, 283,  
     284, 370  
 Hickling, R., 53  
 Hicks, W., 151, 152  
 Higgs, D. M., 137, 138  
 Hillion, A., 92, 334  
 Hobæk, H., 55  
 Hodgson, W. C., 5  
 Hoelzel, A. R., 157  
 Hoff, I., 5, 219  
 Hoffman, A., 186  
 Holford, B. H., 90, 100  
 Holliday, D. V., 6, 98, 161, 162, 210, 267, 284,  
     286, 287, 288, 289, 290, 411  
 Hollingsworth, C. E., 218, 246, 253, 255  
 Hopelain, J. S., 98, 187, 210  
 Horne, J. K., 218, 224, 230, 232, 245, 247,  
     331, 362  
 Horvei, B., 156  
 Hovem, J. M., 160, 161  
 Howe, B. M., 42, 154  
 Huang, K., 235  
 Hubb, C. L., 150  
 Hudson, J. E., 53  
 Hughes, S., 205, 209  
 Hunter, J. R., 170  
 Hurst, D. H., 87  
 Huse, I., 202, 209, 253  
 Hwang, D., 226, 260, 281  
 Iida, K., 226, 235, 239, 259, 280, 281, 283  
 Inagaki, T., 278  
 Ingard, K. U., 269  
 Ishii, K., 195, 196, 235, 259  
 Jackson, D. R., 80  
 Jacobs, D. W., 132  
 Jacobs, J. E., 92  
 Jacobson, P. T., 184  
 Jaffe, J. S., 96, 293  
 Jakobsson, J., 377  
 Jansen, S., 347  
 Jech, J. M., 218, 224, 230, 232, 245  
 Jefferts, K., 283  
 Jensen, F. B., 157  
 Jensen, M. E., 186  
 Jerkø, H., 130  
 Johansson, K. A., 221, 325  
 Johannessen, S. E., 277  
 Johannesson, K. A., 21, 330, 350, 351  
 Johnson, B. D., 366  
 Johnson, C. G., 130, 132  
 Johnson, C. S., 132, 135  
 Johnson, M. W., 128  
 Johnson, R. K., 267, 276, 277, 284, 285, 286  
 Johnson, R. L., 196, 259  
 Johnston, S. V., 98, 186, 187, 208, 210  
 Johnstone, A. D. F., 130, 132, 133, 137  
 Jolly, G. M., 306, 311, 318, 320, 357  
 Jones, R. H., 5, 176, 210, 312, 368, 369  
 Josse, E., 101  
 Jumars, P. A., 288  
 Kaartvedt, S., 281, 293  
 Kajiwara, Y., 283  
 Kalikhman, I., 311  
 Kamei, Y., 283  
 Kamolnik, T., 155  
 Kang, D., 260  
 Kang, M., 334  
 Kargl, S. G., 272  
 Karlsen, H. E., 138, 139  
 Karlson, J. A., 87  
 Kastak, D., 135, 137, 155  
 Kastelein, R. A., 140, 143  
 Kautsky, G. A., 187  
 Keefe, D., 153  
 Kemper, J., 105

- Kendall, M. G., 191  
Kent, J., 142  
Kenyon, T. N., 130, 132  
Kersting, D. A., 142  
Kieser, R., 177, 185, 202, 208, 210, 226, 241, 334  
Kimura, D. K., 360  
Kimura, K., 3, 4  
Kinsler, L. E., 98  
Kirchner, 196  
Kirkegaard, 352  
Kirsch, J., 281  
Klaveness, H., 38  
Kleppel, G. S., 286, 287, 288  
Klevjer, T. A., 293  
Klimley, A. P., 139  
Klinowska, M., 144  
Kloser, R. J., 106, 107, 202, 334, 362, 375,  
    Plate 9.3  
Klumb, R. A., 259  
Knudsen, F. R., 138, 157, 186, 205  
Knudsen, H. P., 5, 55, 110, 111, 117, 156,  
    327, 363  
Knutsen, T., 277  
Koegeler, J. W., 276  
Korneliussen, R. J., 186, 334, Plate 9.2  
Koslow, J., Plate 9.3  
Kostyuchenko, L. P., 154  
Koutsikopoulos, C., 171  
Kraus, C., 139, 140, 142, 143, 144, 157  
Kraus, S. D., 157  
Kringel, K., 288  
Kristensen, A., 209, 267, 268, 275, 276, 277  
Kristensen, F. H., 209  
Kristensen, K. E., 267  
Kubecka, J., 186, 202, 205, 206, 209, 224, 234  
Kuperman, W. A., 157
- Laake, J. L., 296  
Ladich, F., 130, 132  
Lafont, T., 359  
Lambert, D. R., 157  
Lanford, P. J., 154, 156  
Lassen, H., 258  
Lavery, A. C., 270  
Lawson, C. L., 255, 257, 275, 277, 286, 375  
Lawson, G. L., 255, 257, 275, 277, 375  
Le Cann, A., 362, 373  
Lebarbier, E., 362, 373  
Lebedeva, A. N., 133  
Lebourges, A., 370  
Lee, A. J., 176  
LeFeuvre, P., 334  
Legendre, P., 186  
Leggett, W. C., 98, 257, 334  
Lemberg, N. A., 360  
Leroy, C. C., 42, 68  
Levenez, J.-J., 370, 372  
Lewy, P., 122
- Li, Y., 91, 124  
Lillo, S., 240, 257  
Linares, E., 91, 207, 208  
Lindem, T., 184, 186, 202, 228, 240, 258, 259  
Linke, K., 102  
Lockwood, S. J., 370  
Lokkeborg, L., 154  
Losse, G. F., 221, 325  
Lough, G., 281  
Love, R. H., 99, 159, 162, 219, 229, 233, 234  
Løvik, A., 160, 161, 366, 367, 371, 372  
Lozow, J., 194  
Lu, Z., 132, 137, 138  
Lundgren, B., 252, 257  
Lynch, J. F., 266  
Lytle, D. W., 194, 195
- Macaulay, G., 235, 257, 260  
Macaulay, G. J., 252, 255  
MacKenzie, I. G., 353, 362  
MacLellan, S. G., 281  
MacLennan, D. N., 5, 6, 9, 51, 52, 53, 55, 60,  
    100, 110, 111, 112, 117, 118, 119, 122,  
    124, 125, 131, 180, 190, 196, 198, 201,  
    202, 205, 218, 241, 242, 243, 246, 252,  
    253, 255, 257, 258, 259, 260, 317, 327,  
    330, 351, 353, 362, 363, 368
- Mader, C. W., 69  
Madsen, P. T., 102, 140  
Madureira, L. S. P., 290, 291, 292  
Maes, J., 157  
Magand, F., 99  
Magnuson, J. J., 259  
Magnusson, J. J., 184  
Magurran, A. E., 218, 235, 250, 251, 253,  
    258, 260  
Mair, A. M., 284  
Malme, C. I., 2, 65, 154, 156, 157  
Maniwa, Y., 196  
Mann, D. A., 132, 137, 138  
Maravelias, C. D., 202  
Marchal, E., 362, 370  
Marchand, P., 107  
Marcotte, D., 351, 358  
Marino, D. A., 185, 316  
Marler, P., 372  
Marsh, H. W., 41  
Marshall, W. J., 147, 150  
Marston, P. L., 272  
Martin Traykovski, L. V., 270, 278, 279, 284  
Martin, D. W., 142, 265, 266, 268, 272, 278,  
    279, 292  
Martin, L. V., 266, 268, 278, 279  
Mason, W. P., 20  
Massé, J., 92, 108, 171, 301, 302, 334, 362,  
    372, 373  
Masuda, K., 226  
Matheron, G., 304, 305, 306, 354

- Maxwell, D. R., 194, 195  
 Mayer, L., 91  
 McCauley, R. D., 154  
 McClatchie, S., 87, 171, 235, 252, 255, 257, 260,  
     275, 276, 279, 284  
 McColm, J. G., 41  
 McElroy, P. T., 179  
 McGeachy, J. A., 3  
 McGehee, D. E., 96, 270, 278, 279, 284,  
     288, 293  
 McManus, M. W., 135  
 McPhail, S. D., 108, 372  
 McQuinn, I. H., 209, 248  
 McVay, S., 129  
 Medwin, H., 2, 21, 51, 230  
 Mehner, T., 357  
 Melvin, G. D., 91, 124  
 Menezes, J., 137, 138  
 Menz, A., 241, 242, 243, 259  
 Mercer, J. A., 154  
 Mesiar, D. C., 186  
 Metzger, K., 42  
 Michalsen, K., 202  
 Middleton, D., 291  
 Midttun, L., 176, 219, 224, 251, 332  
 Millard, N. W., 108, 372  
 Miller, J. D., 140, 186  
 Miller, L. A., 140  
 Millero, F. J., 42, 69  
 Minnaert, F., 158  
 Misselis, C., 101  
 Misund, O. A., 1, 156, 167, 170, 174, 175, 226,  
     258, 260  
 Mitson, R. B., 1, 5, 21, 62, 89, 90, 108, 156, 163,  
     198, 199, 200, 201, 290, 330, 350, 351,  
     373  
 Miyanohana, Y., 195, 196, 235, 269  
 Miyashita, K., 232, 260, 278, 334  
 Mobley, J. R., 129  
 Møhl, B., 102, 137, 138, 140, 142  
 Monstad, T., 257  
 Moore, K. E., 129, 132, 135, 137, 280  
 Moore, M. V., 280  
 Moore, P., 132, 135, 137  
 Moore, P. W. B., 135, 137  
 Moose, P. H., 187  
 Morgenbesser, H. B., 139  
 Morphett, N., 102  
 Morse, P. M., 20, 48, 269, 270  
 Morton, K. F., 281  
 Mouchot, M.-C., 92, 334  
 Mountain, D. G., 281  
 Moursund, R. A., 93  
 Mous, P. J., 105  
 Mozgovoy, V. A., 160  
 Muir, T. G., 37, 38  
 Mukai, T., 226, 235, 239, 259, 281  
 Mulligan, T. J., 177, 202, 205, 208, 209, 210,  
     226, 317, 334  
 Murphy, E. J., 290  
 Murray, A. W. A., 202  
 Mutlu, E., 280, 283  
 Myrberg Jr, A. A., 128, 129, 133, 139  
 Nachtigall, P. E., 130  
 Nachtigall, P. W., 142  
 Nakken, O., 6, 21, 194, 201, 219, 220, 221, 234,  
     235, 240, 244, 252, 257, 330, 332, 341,  
     345, 351, 371, 378  
 Napp, J. M., 287  
 Naraghi, K., 351  
 Nealson, P. A., 186, 379  
 Nedreaas, K., 105, 106, 107  
 Nedwell, J. R., 157  
 Nero, R. W., 159, 229  
 Nestler, J. M., 137, 138  
 Neubauer, W. G., 53  
 Nielsen, J. R., 252, 257  
 Nieukirk, S. L., 129  
 Norris, K. S., 142  
 Novarini, J. C., 366  
 Nunnalee, E. P., 334, 378  
 O'Driscoll, R. L., 87, 171, 270, 278, 279, 284,  
     362, 373, 375  
 Officer, C. B., 20, 48  
 Offutt, C. G., 131, 132  
 Ogawa, T., 151  
 Ohman, M. D., 293  
 Ohshima, T., 232, 260  
 O'Keefe, D., 153  
 Olla, B. L., 129  
 Ollevier, F., 157  
 Olsen, K., 5, 166, 187, 194, 219, 220, 221, 234,  
     235, 252, 253, 371, 372  
 Olsen, S., 5, 166, 187  
 Ona, E., 77, 84, 154, 195, 198, 199, 200, 201,  
     209, 218, 223, 227, 230, 239, 253, 257,  
     334, Plate 9.2  
 Ortner, P. B., 287  
 Osborne, R. W., 157  
 Ostrovsky, I., 311  
 O'Sullivan, F., 228, 240, 259  
 Otis, L. S., 130  
 Øvredal, J. T., 258  
 Pace, N. G., 87  
 Paillaman, A., 240, 257  
 Paramo, J., 176  
 Parker, S. L., 240, 259  
 Parmentier, A., 157  
 Parrish, D. L., 240, 259  
 Partridge, B. L., 170, 176, 196  
 Paterson, R. J. E., 145

- Pauly, T., 278, 279, 283  
Pawloski, D. A., 142  
Pawloski, J. L., 142  
Payne, R. S., 129  
Pearcy, W. G., 283  
Pearson, W. H., 154  
Pedersen, B., 171, 186, 204, 206, 207, 208, 209  
Pedersen, J., 209  
Pedersen, R., 105, 106, 107  
Penner, R. H., 140, 141  
Pennington, M., 353  
Penrose, J. D., 278, 279, 283  
Perkin, S. I., 133  
Pershing, A. J., 281  
Peters, R. D., 93  
Petit, D., 370, 372  
Petitgas, P., 92, 306, 309, 311, 334, 354, 358,  
    359, 362, 373  
Pettersen, E., 276, 371, 372  
Pettersen, F., 276  
Pickens, J., 137, 138  
Pieper, R. E., 226, 267, 280, 281, 283, 284, 286,  
    287, 288, 289, 290  
Pilleri, G. E., 139, 140, 142, 143, 144, 145  
Pisanty, S., 259  
Pitcher, T. J., 170, 176, 196, 218, 235, 250, 251,  
    253, 258, 260  
Ploskey, G. R., 137, 138  
Pomeroy, S. C., 144  
Pope, J. A., 327  
Popp, J. M., 281  
Popper, A. N., 128, 129, 131, 132, 137, 138, 154,  
    155, 156  
Porter, D. R., 157, 252, 256  
Porter, M. B., 157  
Portier, P., 3  
Poulard, J. C., 358  
Poynton, F. Y., 92  
Primakoff, H., 111  
Purves, P. E., 139, 140, 142, 144, 145  
Puvanendran, V., 255, 257, 275, 277
- Quinn, T. J., 296
- Raitt, R. W., 182  
Rallier du Baty, R., 3  
Ransom, B. H., 186, 379  
Rayleigh, L., 20, 58  
Read, A. J., 157  
Readhead, M. L., 128  
Rechnitzer, A. B., 150  
Reeder, D. B., 231, 232, 245  
Reid, D. G., 92, 334, 368  
Retiere, N., 301, 302, 362  
Reuss, E., 96, 293  
Reut, Z., 87  
Reynisson, P., 202, 233, 240, 257  
Richards, L. J., 334
- Richardson, I. D., 2, 5, 65, 154, 155, 156, 157,  
    158, 176  
Richardson, W. J., 2, 65, 154, 155, 156, 157, 158  
Richmond, D. R., 151, 152  
Ricker, W. E., 327  
Ridgway, S. H., 133, 135, 155  
Rippe, T., 140, 143  
Rivoirard, J., 303, 306, 309, 350, 354, 355,  
    358, 371  
Robb, C., 100  
Robinson, B. J., 184, 257, 258  
Robotham, V. H., 361  
Rodhouse, P., 291  
Roe, H. S. J., 280, 292, 293  
Rogers, P. H., 99  
Roman, M. R., 287  
Romare, P., 186  
Ronald, K., 130, 132, 137  
Ronzier, L., 91  
Rose, G. A., 98, 170, 202, 252, 256, 334, 375  
Ross, D., 154  
Røttingen, I., 194, 196, 326, 378  
Routledge, R. D., 186, 316  
Roux, P., 197, 280  
Rozwadowski, H. M., 6  
Rschevkin, S. N., 40  
Rudstam, L. G., 184, 202, 209, 228, 240, 258,  
    259, 280  
Runnstrom, S., 5  
Rusby, J. S. M., 87  
Ryan, T. E., 106, 334, 375, Plate 9.3
- Saegrov, H., 186, 205  
Saetersdal, G., 176, 356  
Sakaguchi, S., 151  
Sameoto, D., 226, 280, 281, 371  
Sand, O., 130, 132, 133, 138, 139, 157, 160  
Sanford, L. P., 287  
Sano, N., 226, 277, 280, 283  
Sarno, B., 100  
Sasaki, S., 226  
Saunders, K., 151, 152  
Sawada, K., 227, 232, 260, 269  
Sawada, Y., 269  
Sayers, J. F., 92  
Scalabrin, C., 92, 334  
Scanlon, L., 265, 292  
Schael, D. M., 218, 224, 230, 245  
Schellart, N. A. M., 133  
Schelvis, A., 105  
Scherbino, M., 5, 187  
Schevill, W. E., 45, 129  
Schilt, C., 137, 138  
Schlundt, C. E., 135, 155  
Schmidt, H., 157  
Scholik, A. R., 155  
Schooneman, N. M., 140, 143  
Schuijf, A., 133

- Schulz, M., 357  
 Schusterman, R. J., 135, 137, 142, 155  
 Seber, G. A. F., 318, 321  
 Selivanovsky, D. A., 263  
 Sessarego, J. P., 99  
 Shatoba, O. E., 235, 253  
 Shenderov, E. L., 263  
 Shibata, K., 219  
 Shooter, J. A., 37, 38  
 Shotton, R., 303  
 Shulkin, M., 41  
 Siler, W., 23  
 Simard, Y., 290, 351, 358  
 Simmonds, E. J., 5, 6, 9, 32, 99, 108, 110, 111,  
     117, 119, 124, 125, 126, 196, 198, 201,  
     202, 294, 301, 302, 303, 306, 307, 308,  
     309, 327, 330, 334, 347, 350, 351, 354,  
     355, 356, 357, 358, 361, 363, 368, 371,  
     372, 373, 378  
 Simmons, V. P., 41  
 Sinclair, D., 186  
 Skaar, D., 135  
 Skagen, D., 174  
 Skalski, J. R., 154, 186  
 Skudrzyk, E., 192  
 Slotte, A., 154  
 Smedstad, O. M., 202  
 Smith, F. D., 3, 86, 98, 100, 129, 155, 171, 173,  
     174, 280  
 Smith, G. W., 100  
 Smith, P. E., 86, 171, 173, 174  
 Smith, Q., 98  
 Smith, R. R., 155  
 Smith, S. L., 280  
 Smith, W. J., 129  
 Smyth, C. N., 92  
 Soldal, A. V., 154, 156  
 Solli, H., 38, 209  
 Solomon, D. J., 224  
 Solow, A., 157  
 Solstad, A., 156  
 Soria, M., 91, 169, 171, 176, 372  
 Sorokin, M. A., 133  
 Souid, P., 334  
 Soule, M. A., 80, 84, 106, 227, 240, 257, 258,  
     334, 375  
 Southall, B. L., 135, 137  
 Souza, M. J., 137, 138  
 Sparks, C. A. J., 283  
 Speisberger, J. L., 42  
 Spindel, R. C., 179  
 Spradlin, T., 157  
 Squire, J. L., 173  
 Squires, M., 108, 372  
 Staal, P. R., 147  
 Stables, T. B., 187  
 Staehr, K. J., 258, 347  
 Stafford, K. M., 129  
 Stansfield, D., 25, 27  
 Stanton, T. K., 179, 184, 193, 194, 197, 198, 229,  
     231, 232, 245, 262, 265, 266, 267, 268,  
     269, 270, 271, 272, 273, 274, 277, 278,  
     279, 280, 281, 283, 284, 292, 364  
 Stegun, I. A., 29  
 Steig, T. W., 101, 186, 208, 379  
 Stender, B. W., 288  
 Stensholz, B. K., 202  
 Stevenson, P., 108, 372  
 Stewart, P. A. M., 302  
 Stoermer, M., 132  
 Stolyrenko, D. A., 320  
 Stratoudakis, Y., 129  
 Stritzel, J. L., 240, 259  
 Stromme, T., 356  
 Stunzhas, P. A., 263  
 Sturtivant, C. R., 140, 142  
 Sullivan, F., 228, 240, 259  
 Sullivan, P. J., 228, 240, 259  
 Sund, O., 4  
 Suomala Jnr, J., 194  
 Surlykke, A., 140  
 Surti, A. M., 260  
 Svellingen, I., 122  
 Swartzman, G., 334  
 Swingler, N., 194  
 Tarbox, K. E., 174, 205  
 Tavolga, D. N., 128, 129, 134, 137, 138, 139  
 Teleki, G. C., 151  
 Terhune, J. M., 130, 132, 137  
 Terrace, H. S., 372  
 Tesler, W. D., 363  
 Thomas, G. C., 130, 132, 185, 281, 316  
 Thomas, G. J., 130  
 Thomas, G. L., 185, 281  
 Thomas, J., 132  
 Thompson, C. H., 99, 129, 162, 296, 306,  
     318, 321  
 Thompson, J. K., 296, 306  
 Thompson, P., 129  
 Thompson, P. O., 129  
 Thompson, S. K., 318, 321  
 Thomsen, F., 139  
 Thomson, D. H., 2, 65, 154, 156, 157  
 Thorne, R. E., 174, 185, 186, 187, 205, 228, 316,  
     370, 379  
 Tibshirani, R. J., 361, 371  
 Tichy, F. E., 38  
 Tjelmeland, S., 378  
 Todt, D., 102  
 Tollefson, C. D. S., 98, 210  
 Toresen, R., 195, 202  
 Torkelson, T. C., 101, 209  
 Torstensen, E., 347  
 Traynor, J. J., 185, 228, 240, 244, 358

- Trevorow, M. V., 87, 171, 174, 186, 204, 205, 206, 207, 208  
Trochta, R. T., 139, 140  
Trout, G. C., 176  
Truskanov, M. D., 5, 187  
Tucker, D. G., 21, 25, 29, 48, 89, 90  
Tumwebaze, R., 202, 259  
Tungate, D. S., 5  
Turl, C. W., 140, 141, 142  
Turnpenny, A. W. H., 157  
Turunen-Rise, I., 130  
Tyack, P. L., 129, 139
- Ulltang, O. A., 378  
Umezawa, S., 151  
Urwick, R. J., 2, 20, 31, 32, 63  
Urquhart, G. G., 100
- Vabø, R., 253  
Valdemarsen, J. W., 174  
Van Buren, A. L., 99  
Venema, S. C., 9  
Vestnes, G., 5, 55, 110, 111, 117, 327, 363  
Vidal, O., 129  
Vogt, R. H., 53
- Wade, E., 358  
Wafey, M. H., 351  
Wahlberg, M., 102, 140  
Walewski, S., 133  
Walker, R. A., 90, 100, 129, 291  
Walline, P. D., 224, 232, 259  
Wanzenböck, J., 357  
Ward, P. D., 2, 145, 155, 156, 291, 292, 334  
Wardle, C. S., 370  
Warner, D. M., 240, 259  
Watkins, J. L., 45, 129, 186, 275, 278, 283, 291, 292, 334  
Watkins, W. A., 45, 129  
Weill, A., 92, 334  
Weimer, R. T., 185, 201  
Welsby, V. G., 53  
Wenz, G. M., 64, 155  
Werner, R., 194
- Wespestad, V. G., 325  
Weston, D. E., 146, 158, 203, 365, 366  
Whitehead, P. J. P., 159, 249  
Wiebe, P. H., 255, 257, 262, 265, 266, 268, 270, 271, 272, 273, 274, 275, 278, 279, 280, 281, 283, 284, 292  
Wiley, M. L., 151, 152  
Williams, A., 106, 334, 375, Plate 9.3  
Williamson, C. E., 157, 185, 227, 240, 280, 294, 358  
Williamson, J., 157  
Williamson, N. J., 185, 227, 240, 294, 358  
Winfield, I., 357  
Winger, P. D., 209, 248  
Winn, H. E., 129  
Withrow, R., 132  
Wittig, T., 87  
Wittingerova, M., 205, 206  
Witzel, L. D., 240, 259  
Wong, G. S. K., 42  
Wood, A. B., 3, 5  
Wood, R. J., 5  
Woodd-Walker, R. S., 291  
Woodey, J. C., 186, 316  
Woodward, B., 102  
Worcester, P. F., 42  
Wurtsig, B., 157
- Xie, Y., 205, 209, 317
- Yan, H. Y., 130, 132, 155  
Yasuma, H., 232, 260  
Ye, Z., 159, 160, 212, 218, 270, 275, 276, 367  
Yelverton, J. T., 151, 152  
Yound, R. W., 128  
Yule, D. L., 209
- Zaferman, M., 224, 252, 257  
Zakharia, M. E., 99  
Zamon, J. E., 280  
Zbinden, K., 139, 140, 142, 143, 144  
Zedel, L., 98, 210  
Zhu, S., 42  
Zimmermann, S., 347

# Subject Index

- Absorption of sound  
calculation of, 67  
causes of, 40, 67  
coefficient of, 10, 18, 20, 40–42, 61, 67, 68,  
118, 120, 180, 191, 367, 368, 376  
with frequency, 41  
process of, 40
- Abundance  
absolute, 295, 300, 374–6, 379  
estimation of, 5, 8, 104, 164, 187, 203, 205,  
212, 264, 265, 280, 284, 299, 316, 330,  
346, 349, 363, 374  
precision of estimate, 295, 297, 300, 302, 303,  
305–7, 318, 324, 355  
relative, 329, 374  
spatial variation, 40, 264, 284, 303, 351, 354  
temporal variation, 309, 312, 325
- Acclimatization of fish, 237
- Acoustic  
axis, 11, 15, 28–32, 34, 77, 81, 110, 111,  
115–17, 122, 124, 125, 181, 183, 211,  
220, 253, 368  
camera, 92–4, 203  
cross-section (*see also* main entry), 52  
extinction, 58, 193, 270  
fish tag (*see also* tag), 101  
impedance, 10, 11, 23, 26, 27, 48, 50, 132  
instruments, 1, 6, 7, 17, 20, 55, 70, 79, 93, 106,  
108, 110, 126, 164, 217, 248, 298,  
326, 327  
link, 76, 77  
propagation, 38, 127, 157, 203, 206, 207,  
347, 366  
reflectivity (*see also* Target strength), 9, 25,  
166, 223, 237
- Acoustic profiling  
Doppler (ADCP), 70, 97, 98, 187, 210, 211,  
289, 293, 372  
multi-frequency, general, 7, 16, 84, 262, 264,  
289, 334, 335, Plate 7.1, Plate 9.3,  
Plate 9.4  
multi-frequency (MAPS), 286–8  
Tracor (TAPS), 287, 288, Plate 7.1
- Acoustic survey  
design, 176, 294–6, 299, 302–4, 306, 308–14,  
317, 325, 330, 349, 355–9, 362, 368  
equipment, 8  
vessel, 17, 18, 90, 91, 166, 172, 253, 261, 323,  
325, 327, 330, 371–3
- Active sonar, 84, 100, 127, 139, 163, 203
- Age class, 240–42, 362, 378
- Aggregation of fish (*see also* contagious  
distribution), 16, 83, 121, 191, 193–7,  
232, 233, 239, 247, 253, 264, 266, 278,  
284, 334, Plate 3.4
- Airgun, 26, 133, 146, 148, 154
- Ambient  
noise, 6, 64, 108, 157  
pressure, 11, 22, 148, 151, 153, 158, 159, 161,  
238, 239, 247–9, 371, 373
- Amplifier (*see also* Time-varied gain), 25, 61,  
62, 180
- Analogue echo integrator, 74
- Angle  
of attack, 15, 167, 168  
detection, 15, 167  
of incidence, 49, 199, 269–71  
of reflection, 49, 149, 271
- Animal sonar, 13, 127, 139–41, 145
- Antarctic, 8, 263, 264, 269, 278, 279, 284, 291,  
292, 323, 346, 375
- Arctic, 202, 363, 378
- Array  
end fire, 35, 144, 149  
hydrophone, 100, 101, 128, 141, 203  
shading, 33, 34, 96, 99  
transducer, 26, 34, 35
- Attenuation (*see also* Absorption), 17, 37, 38,  
195, 196, 365–7, 376, 377
- Audiogram, 130, 133, 136–8
- Auditory threshold, 130–36, 138, 155–7
- Autonomous underwater vehicle (AUV), 373
- Avoidance reactions, 2, 91, 138, 156, 157, 171,  
205, 209, 226, 281, 326, 371–3, 376
- Backscattering  
alternative measures,  $s_{bs}$  and TS, 9, 51  
coefficient, area, 9, 59

- Backscattering (*continued*)  
  coefficient, volume, 9, 59, 285  
  length, 9, 16, 266, 269, 271  
  strength, 9, 59, 212, 264, 288, 293, Plate 9.2  
Bandwidth, 10, 13, 22, 37, 46, 52, 55, 58, 62–5,  
  73, 90, 98, 99, 102, 112, 113, 117–19, 134,  
  135, 162, 177  
critical, 12, 127, 133–7  
noise, 135  
transducer, 25–8  
Baxter model, 153  
Beam  
  angle, 12, 119, 167, 365, 375  
  factor, 81, 82, 123, 124, 228  
  pattern, 10, 13, 15, 28–34, 66, 80–82, 85, 110,  
    119, 120, 123–5, 143, 144, 167, 177,  
    181, 183–6, 190, 197, 201, 222, 227,  
    233, 278, 364  
  spreading, 20, 23, 35, 38, 51, 61, 74, 121, 141,  
    180, 195, 305, 367  
  width, 15, 31, 33, 34, 39, 66, 71, 76, 85, 99,  
    103, 119, 120, 167–9, 171, 172, 175,  
    190, 200, 203, 204, 209, 286, 364  
  *see also* Equivalent beam angle  
Behaviour of fish, 56, 93, 101, 156  
Bessel function, 29  
Biomass, 59, 91, 163, 173, 229, 252, 262, 278,  
  280, 281, 333, 346, 362  
Bladder oscillation parameter, 152  
Bootstrap technique, 362  
Boric acid, 40, 67  
Bottom reflection, 50, 149, 150  
Box-Cox test, 353  
Boyle's Law, 158, 373  
Bubble  
  elimination from standard target  
    support, 113  
  induced attenuation, 17, 103, 337, 365–7  
  pulses, 13, 146–8  
  resonance frequency, 12, 13, 50, 158, 159  
Cage, 151, 194, 196, 217, 219, 221–5, 234, 235,  
  237–9, 251, 253, 254, 278, 280, 282, 283,  
  288, 289, 325  
Calibration  
  beam pattern, 119  
  transducer sensitivity, 111  
  TVG, 118  
  *see also* Standard target  
CCAMLR, 323, 346  
Ceramic transducer, 25, 119  
Chirp (swept frequency transmission), 56, 101  
Click (*see also* Echo location), 13, 128, 138,  
  139, 140, 141  
Colour sonar display, 166  
Communication, acoustic, 2, 127, 128, 140,  
  160, 326  
Compensation for range dependence, 11, 62,  
  118, 119, 180, 189, 190  
Confidence limits, 8, 18, 295, 297, 324, 327, 351,  
  356, 358, 360, 361, 379  
Contagious distribution, 16, 83, 121, 191,  
  193–7, 232, 233, 239, 247, 253, 264, 266,  
  278, 284, 334, 351, 353, 355, 360,  
  Plate 3.4  
Continuous waves, 23, 24, 52  
Contours  
  calculating and mapping, 350  
  fish density, 349  
  mortality, 154  
Contrasts (of plankton bodies)  
  compressibility, 16, 274  
  density, 16, 158, 249  
  sound speed, 8, 16, 264, 277  
Conversion factor, echo integrator, 8, 17, 330,  
  343, 344  
Copper sphere (*see also* Sphere), 54, 112  
Correlation, 153, 246, 253, 267, 310, 311, 324,  
  375, 377–9  
  serial, 19, 349, 354  
  spatial, 8, 18, 303–8, 310, 311, 349, 354, 357,  
    358, 361, 362  
Coverage, 17, 18, 175, 296–8, 314–16, 319, 320,  
  322, 325, 359, 360, 361  
Craig-Forbes algorithm, 182, 184  
Cristae maxillares, 142, 144  
Critical  
  bandwidth, 12, 127, 133–7  
  fish density, 186  
  ratio, 12, 135, 137  
Cross-section  
  average, 172, 194, 344  
  backscattering, 10, 12, 13, 15, 16, 19, 51–3,  
    79, 81, 110, 111, 123, 124, 177, 181,  
    190, 218, 219, 221, 233, 241, 246, 249,  
    267, 280, 290, 343, 344, 374  
  definitions, 9  
  differential scattering, 10, 51  
  extinction, 15, 195  
  spherical scattering, 9, 10, 51, 52  
  total, 280  
Cruise track, 8, 14, 16, 17, 85–7, 170, 295–9,  
  312–15, 319, 324, 326, 328–30, 336, 338,  
  346, 348–52, 357, 359, 369, 370  
Cumulative distribution, 169  
Cycle, 23, 24, 237, 286, 298, 368  
  
Data collection, 87, 93, 295, 299, 300, 316, 322,  
  324, 347, 371  
Dead zone, 199, 200, 201  
Decibel, 24, 25, 53, 61, 334  
Deconvolution, 123, 184, 209, 228  
Delay, 2, 3, 47, 111, 116, 117, 140, 141, 148, 180,  
  206, 364, 365  
Dendrogram for area selection, 341, 342

- Density  
 contrasts, 16, 158, 249  
 critical, of fish, 186  
 fish by area, 17, 195, 196, 200  
 fish by volume, 196, 200  
 gas, 159  
 packing in schools, 204  
 water, 10, 112, 159
- Depth  
 dependence, 69, 121, 238  
 effect on sound speed, 69  
 measurement, 3
- Detection threshold, 81, 123, 201
- Digital echo integrator, 74, 75, 110, 187, 189, 226
- Directivity, 32, 33, 143, 167, 226
- Displacement, 22, 23, 365
- Diurnal rhythms, 129, 160, 237, 253, 254, 288, 298, 330, 362, 370, 371, 376
- Doppler effect, 97, 98, 187, 210
- Doppler log (*see also* Acoustic profiling systems), 98
- Drift net, 3
- Dual-beam sonar, 12, 80, 82, 121, 123, 124, 185, 227, 228, 240, 241, 257, 259, 283
- Duration-in-beam technique, 185, 316
- EBA, *see* Equivalent beam angle
- Echo  
 amplitude, 5, 12, 14, 15, 57, 83, 84, 98, 116, 118, 121, 124, 177, 180, 181, 189, 192, 228, 241, 242, 274, 365  
 boundary, 205  
 counter/counting, 5, 121, 164, 174, 185, 187, 189, 202, 203, 262, 316  
 energy, 7, 14, 24, 57, 62, 75, 115–17, 122, 123, 182, 183, 191–3, 226, 248, 280, 332, 364  
 envelope, 177  
 fluctuation, 58  
 identification/classification, 100, 142, 202, 331, 334–5, 373–4  
 integration, 5, 7, 17, 23, 32, 72, 74, 75, 110, 118, 121, 126, 164, 167, 170, 185, 187, 188, 191, 194, 196, 197, 199, 200–203, 261, 280, 281, 298, 368, 378, 379  
 integrator, 5, 24, 70, 74, 115, 118, 163, 187, 190, 191, 200, 202, 226, 295, 326, 327, 363  
 integrator conversion factor, 12, 17, 121  
 integrator equation, 110, 119, 164, 189, 190, 215  
 location, 127, 129, 138, 140  
 multi-path, 206–9  
 multiple targets, 58, 227  
 overlapping, 84, 178, 179, 186, 187, 191  
 second-order, 193
- single target, 65, 116, 121, 180, 184, 185, 188, 227  
 trace, 8, 72, 187, 207, 265, 284, 298, 333, 335, 338
- Echogram, 3, 5, 7, 14, 70, 71–8, 83–6, 163–6, 168–71, 176, 197, 201, 212, 263, 281, 284, 289, 290, 291, 295, 330, 331, 332–7, 341, 345, 362, 371, 373, Plate 3.1, Plate 3.2, Plate 3.3, Plate 3.4, Plate 5.1, Plate 7.1, Plate 9.2, Plate 9.3
- Echogram mark or sign, 72, 73, 76, 86, 115, 164, 166, 168–71, 197, 207, 209, 317
- Echosounder  
 colour, 72, 165, Plate 3.1  
 direction-sensing, 121, 123, 184  
 dual-beam, 12, 80, 82, 121, 123, 124, 185, 227, 228, 240, 241, 256, 259, 283  
 scientific, 5, 55, 73, 74, 118, 363  
 single-beam, 70, 79, 110, 122, 123, 164, 177, 181, 182, 227, 228, 240  
 split-beam, 5, 34, 70, 74, 80, 82–4, 89, 93, 103, 123, 125, 184, 185, 209, 210, 244, 248, 257–61, 283, 295, Plate 3.2
- Edge effect, 173
- EDSU, 17, 324, 333, 336, 337, 346, 350, 352, 360
- Ehrenberg's method, 183
- Energy  
 echo, 7, 14, 24, 57, 62, 75, 115–17, 122, 123, 182, 183, 191–3, 226, 248, 280, 332, 364  
 flux, 23, 147–9, 153
- Ensemble, 14, 15, 172, 191–4, 227
- Environmental impacts of sound  
 behavioural disturbance, 157  
 hearing threshold shifts, 13, 155, 157  
 mitigation measures, 154, 157, 158
- Equivalent beam angle, 9, 10, 31, 32, 47, 111, 119, 120, 126, 190, 191, 368, 377
- Error  
 random, 294, 362, 363, 376  
 sources of, 330, 362, 374–6, 379  
 stochastic, 182, 185  
 systematic, 356, 363, 374, 376, 378
- ESSR, 17, 351, 352
- Explosives as sound sources  
 biological damage, 7, 127, 154  
 linear explosion, 149  
 pentolite, 147–9, 151  
 prediction of fish mortality, 153  
 pressure signature, 148, 150, 153  
 propellants, 147  
 shock front, 13, 146–52  
 TNT, 147–9, 153
- Exponential distribution, 192, 241, 242
- Extinction, acoustic, 58, 193, 270

- FAD (fish aggregating device), 83, Plate 3.4  
Field  
  far, 11, 35, 38–40  
  free, 22, 44, 131, 132, 146–9, 152  
  near, 39, 40, 51, 114, 171  
Filter, Kalman (for fish tracking), 210  
Fish  
  behaviour, 1, 7, 90, 95, 97, 100, 162, 170, 195,  
    204, 209, 210, 217, 218, 234, 237, 330,  
    362, 374, 377, 379  
  catch composition, 303, 340, 345  
  hearing, 24, 108, 137  
  migration, 368, 370  
  school, 3–5, 13–15, 35, 71–3, 76, 86, 87, 91–3,  
    163, 166, 167, 172, 176, 194, 198, 207,  
    208, 210, 212, 263, 332, 334, 335, 337,  
    372, Plate 3.3, Plate 3.5, Plate 9.1,  
    Plate 9.4  
  sizing, 162  
  sounds, 128  
  stock (*see also* main entry), 1, 5, 162, 228,  
    294, 295, 297, 299–302, 306, 308, 312,  
    314, 318–21, 324–6, 329, 330, 332, 336,  
    341, 345, 355, 356, 359, 368–70, 374,  
    377–9  
  target classification, 142, 334  
  target strength, 237, 239, 250, 261  
  tracking, Plate 3.8  
  transport, 224  
Fishermen, 85, 146  
Fishery scientists, 146  
Fishing gear  
  bottom trawl, 86, 95–6, 154, 226, 295, 300,  
    302, 312, 325, 378, Plate 3.8  
  drift net, 3  
  pelagic trawl, 1, 17, 18, 76–9, 103, 166, 203,  
    228, 240, 241–2, 244, 284, 291, 298,  
    301, 317, 333, 339–42, 345, 362,  
    373–4, 379  
  purse seine, 95, 170, 226, 228, Plate 3.7  
  selectivity, 302, 303  
FishTV, 293  
Fluctuations of echoes, 58  
Foote's experiment, 194  
Form function, 10, 54, 55  
Forward scatter, 48, 163, 211, 212, 264, 265, 266  
Fraunhofer zone, 39  
Free-field propagation, 132, 147  
Frequency  
  operating, 46, 65, 67, 92, 176, 203  
  optimum, 74  
  response, 52, 58, 62, 112, Plate 9.2  
  spectrum, 62, 90  
  sweep, 56, 101  
Fresnel zone, 39  
Gain, time-varied, 9, 11–14, 61, 62, 110, 111,  
  118–20, 122, 180, 182, 188–91, 202, 207,  
  215, 368, 369  
Gaussian distribution, 242, 356  
Gear (*see also* Fishing), 70, 93, 96, 102, 138,  
  156, 157, 226, 228  
Generic Threshold Value (GTV), 155  
Geographical boundaries, influence on survey  
  design, 295, 299, 324, 329  
Geometric scattering, 50, 271  
Geostatistics, 8, 309, 311, 354, 358  
Ghost echo, 207, 208  
Goertner model, 152, 153  
Gradient of sound speed, 44  
Grid  
  parallel, 310, 313, 314, 316, 317  
  randomized, 303, 305, 306, 308, 309, 371  
  rectangular, 8, 330, 351, 352  
  systematic, 304–6, 308, 309  
  triangular, 296, 309, 315  
  *see also* Transect  
Gulf of Oman, 45, 100  
  
Hearing  
  capability, 7, 13, 23, 60–61, 108–9, 127,  
    136–9, 144, 154–8  
  specialists, 131, 133  
  threshold shifts (TTS/PTS), 13, 155, 157  
Heave compensation, 91  
Homogeneity, 20, 53, 111, 206, 229, 230, 242,  
  267, 269, 270, 300, 324, 330, 338, 340–42  
Hull-mounted transducer, 65, 103  
Hydrography, 367  
Hydrophone, 28, 76, 100–102, 111, 128, 140,  
  141, 203, 211  
  
ICES, 5, 6, 108, 109, 294, 354, 362, 373  
Identification of echo traces, 301, 302, 333–5,  
  Plate 9.1  
Impedance, acoustic, 10, 11, 23, 26, 27, 48, 50,  
  132  
Impulse of shock wave, 7, 9, 10, 13, 35, 127,  
  133, 146–53, 158  
In situ TS measurement (*see also* Target  
  strength), 5, 105, 141, 195, 219, 225–9,  
  239–43, 247, 248, 250, 251, 256, 258–61,  
  280, 282, 293, 295, 299, 344  
Incident wave, 10, 11, 16, 48, 50, 51, 56, 58, 60,  
  133, 160, 197, 218, 230, 269, 272  
Incoherence of phases, 85, 192, 197, 210  
Infrasound, 137, 138, 139  
Integral, 332, 333, Plate 3.3  
Intensity of sound waves, 5, 9, 12, 23, 32, 59,  
  105, 161, 165, 200, 208, 233, 364, 365  
Interference of waves, 28, 30, 48, 57, 58, 63,  
  102, 106, 157, 204, 227, 253, 272, 273,  
  327, 337  
Inter-ship comparison, 8, 295, 325–8

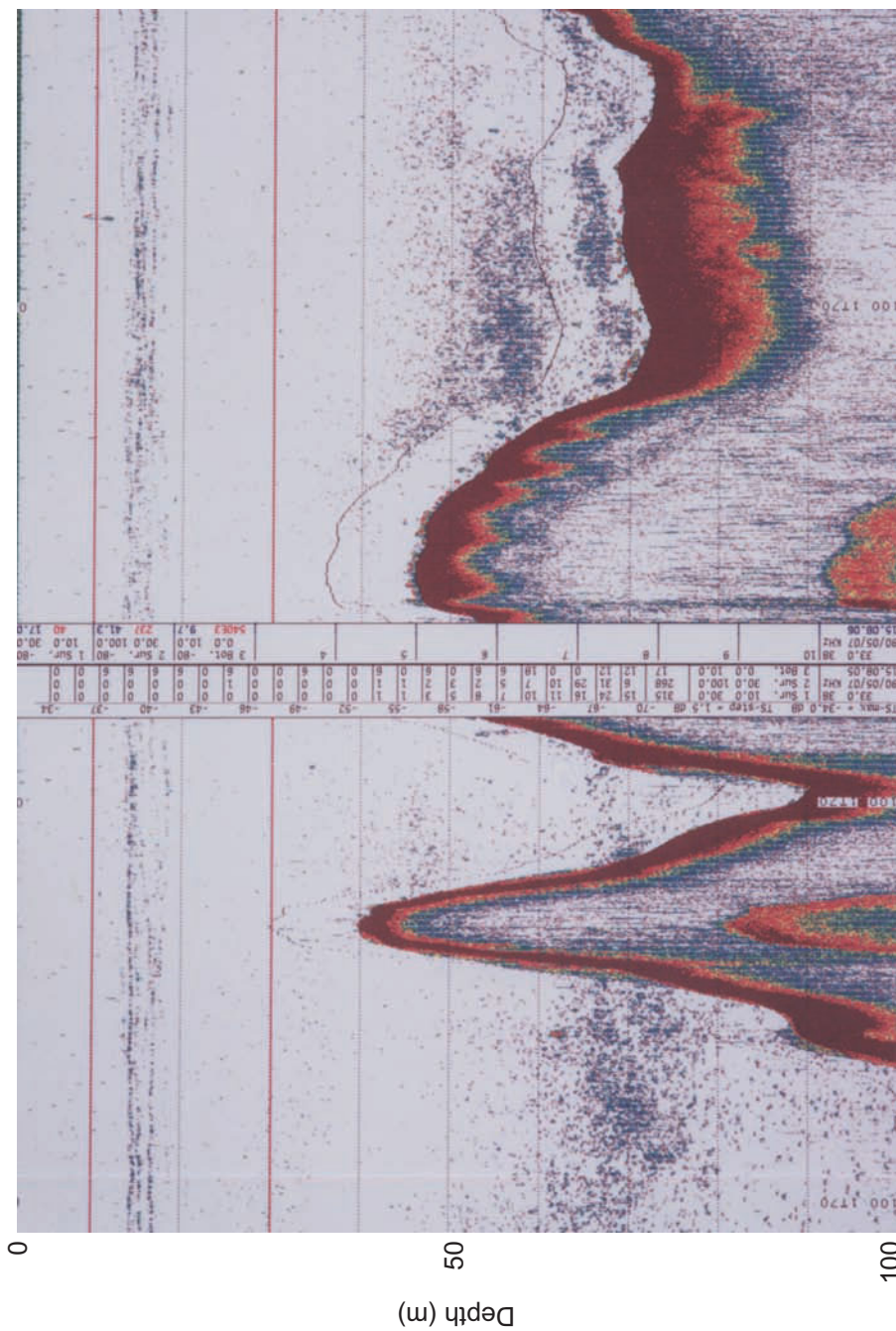
- Inverse scattering problem, 61, 163, 267, 289  
 Inverse square law, 39
- Jack-knife technique, 361
- Kolmogorov-Smirnov (KS) test, how and when to use, 18, 341
- Kriging, 314, 324, 350, 354, 355, 371
- Krill, 8, 263, 264, 268, 269, 275, 278–80, 284, 291, 293, 323, 346, 375
- Length  
 backscattering, 9, 16, 266, 269, 271  
 distribution, 339, 340, 342  
 fork, 244, 256, 258, 259, 260  
 total, 9, 16, 17, 244, 256, 258, 259, 260, 297, 298, 359
- Leonardo da Vinci, 2
- Linearity principle, 7, 164, 191–4, 234
- Link, acoustic, 76, 77
- Lobe  
 main, 30–35, 37, 81, 82, 119, 181, 186, 197, 222  
 side, 30–34, 80, 81, 82, 119, 190
- Log, ship's speed, 15, 18, 98, 298, 312, 369
- Longitudinal sound wave, 10
- Long-range sonar, 160
- Machinery noise, 63–6, 107, 108
- Magnesium sulphate, 40, 67
- Magnetostrictive transducer, 4, 25, 26
- Mammals  
 aquatic, 1, 2, 7, 24, 64, 101, 102, 127–33, 135, 153–6  
 dolphins, 35, 102, 138, 139, 141, 157  
 seals, 132, 137, 155, 157  
 whales, 45, 53, 64, 129, 139, 157
- Mapping  
 echosounder, 6, 166  
 sonar, 86, 171
- Masking, 12, 127, 133–7, Plate 9.4
- Migration  
 horizontal, 18, 90, 98, 172, 205, 296, 312, 314–17, 330, 355, 368–70, 376  
 vertical, 160, 162, 249, 263, 370, 376
- Mile, nautical, 60, 301
- Modulation scanner, *see* Scanner
- Molecular relaxation, 40, 41
- Morocco, 335
- Multi-beam sonar, *see* Sonar
- Multi-frequency acoustic profiling, *see* Acoustic profiling systems
- Multiple scattering, 14, 58, 159, 193, 194, 197, 198
- Nautical area scattering coefficient (NASC), 9, 60
- Nautical mile, *see* Mile, nautical
- Near-field effect, 23, 31, 38, 39, 115, 131, 132
- Neper, 10, 18, 40, 68
- Net, fishing gear, 1, 5, 17, 18, 76–9, 93, 95, 96, 103, 166, 203, 226, 228, 240–42, 244, 281, 284, 289, 290, 291, 298, 300–302, 312, 317, 325, 333, 339, 340–42, 345, 362, 373, 374, 378, 379, Plate 3.8
- Netsonde  
 conventional, 77  
 scanning, 77, 79
- Noise  
 ambient, 6, 64, 108, 157  
 electrical, 63, 201  
 machinery, 65  
 masking, 12, 127, 133–7, Plate 9.4  
 pollution, 7, 127, 154  
 self, 62, 63  
 shipping, 64, 145, 154  
 signal threshold, use of to reduce noise, 14, 81, 82, 123, 130, 132, 134–8, 155, 156, 167, 168, 177, 178, 181, 185, 186, 201, 202, 206, 209, 227, 233, 335, 341, Plate 3.5, Plate 5.1, Plate 9.3, Plate 9.4  
 thermal, 64  
 weather, 64  
 white, 134, 135  
*see also* Signal-to-noise ratio
- Non-linear effects, 20, 35, 36–8, 74, 194, 195, 202, 346, 373
- Non-negative least-squares method (NNLS), 286, 374
- North Sea, 167, 198, 258, 260, 284, 301, 302, 306, 307, 323, 333, 335, 338, 348, 351, 353, 357, 362, 368, 378
- Norwegian fjord, 72, 256, 258, 324
- Nugget effect, 354, 355
- Null (of beam pattern), 29, 30, 142, 144
- Observation band, 13, 171, 172, 173
- Omni-sonar, 94–6, Plate 3.7
- Optical thickness, 195
- Otolith, 133
- Overlapping echoes, 84, 178, 179, 186, 187, 191
- Packing densities, 98, 170, 194
- Particle  
 displacement, 21, 22, 23, 138  
 velocity, 10, 11, 20, 22, 23, 131–3, 230
- Partitioning of the echo integral, 265, 331–3, 335, 336, 341, 343, 345, 346, 362, 370, 373, 374, 379
- Passive sonar, 84, 85
- PDF (probability density function), 15, 18, 58, 179, 202, 241, 347, 349, 352, 353, 356, 359, 361, 377

- Pentolite (*see also* Explosives), 147–9, 151  
Persian Gulf, 44, 45, 367  
Peru, 256, 258, 260, 325  
Phase  
    difference, 10, 12, 28, 29, 58, 82, 83, 89, 102,  
        133, 192, 210, 269  
    incoherence, 85, 192, 197, 210  
Physoclist, 151, 152, 159, 160, 161, 251, 255, 256  
Physostome, 151, 152, 159, 160, 249, 250, 258  
Piezo-electric transducer material, 25, 28  
Ping (*see also* Pulse), 14, 25, 46, 59  
Pinger, 100, 101  
Plankton  
    body tissue properties, 265, 267, 268,  
        271, 274  
    density estimation, 276  
    effect of shape on target strength, 265  
    physical properties tabulated, 277  
    target classification, 265, 276, 282  
    target strength, 267, 268, 274  
    TS-length functions, 264  
Point source, 28, 30, 31, 39, 48  
Power  
    engine, 128  
    response, of sonar, 11, 52  
    transformations, 352  
    transmitter, 65, 112, 118  
Pressure  
    ambient, 11, 22, 148, 151, 153, 158, 159, 161,  
        238, 239, 247–9, 371, 373  
    peak, of explosive, 13, 148  
    radiation, 11, 13, 20, 60, 61, 138  
    signature, 148, 150, 153  
    sound, 11, 13, 22–5, 28, 40, 48, 131–3, 138,  
        143, 155  
Probability Density Function, *see* PDF  
Projector, 3, 141, 142  
Propagation of sound, 23, 24, 25, 365, 366  
Pulse  
    duration, 22–3, 34, 46–7, 55, 62–3, 65, 73, 86,  
        88–9, 98, 101, 118–19, 168, 171, 188,  
        198–9  
    envelope, 60  
    length, 10, 22, 46, 47, 58, 111, 118, 120, 121,  
        146, 178–80, 186, 188, 191, 215, 335  
    shell, 191  
    spectrum, 22  
Purse seine, 95, 170, 226, 228, Plate 3.7  
  
Quality factor (Q), 13  
  
Randomized transect, 303, 305, 306, 308,  
    309, 371  
Randomness of target distribution, 32, 58, 59,  
    111, 123, 191, 192, 213  
  
Range  
    compensation, 11, 62, 118, 119, 180, 189, 190  
    measurement, 293  
    resolution, 73, 89, 125, 287  
Rarefaction, 13, 146, 147, 149, 151  
Rayleigh  
    distribution, 58, 192, 193, 241, 242  
    scattering region, 50, 66  
Ray tracing, 44, 206, 207  
Realization, of stochastic process, 192, 347, 348  
Receiver, 3, 10, 12, 28, 33, 34, 51, 52, 61, 63, 72,  
    73, 76, 88, 99, 100, 110, 112, 113, 116–19,  
    128, 141, 164, 177, 180, 188–90, 206, 217,  
    221, 368  
Reciprocity calibration method, 111  
Reflected wave, 47, 48, 50, 57, 58, 60  
Reflection coefficient, 11, 271, 272  
Refraction, 38, 42–4, 121, 142  
Region (of survey), 349  
Relaxation, molecular, 40, 41  
Resolution  
    angle, 6, 144, 207, 208  
    range, 73, 89, 125, 287  
    target, 22, 66, 80, 84  
Resonance  
    for fish sizing, 162  
    gas bubble, 16, 265  
    solid sphere, 54  
    swimbladder, 7, 13, 67, 127, 161, 229  
Reverberation 63, 97, 201–3, 205–7, 209, 280,  
    316, 366  
    angle (*see* Equivalent beam angle), 9, 32, 33  
Rician distribution, 241, 242  
  
Salinity, 9, 22, 40–43, 67, 68, 224, 277, 294, 329,  
    363, 367, 368  
Sampled volume, 11, 15, 47, 58, 59, 65–7, 98,  
    105, 167, 176, 181, 184–6, 191, 201, 205,  
    209, 211, 227, 233, 286, 293, 316  
Sampling  
    error, 327, 341, 348, 349, 355, 356, 359, 362,  
        373, 374, 378, 379  
    intensity, 297, 313, 316, 321, 359, 360  
    strategy, 8, 294, 295, 296, 308, 330, 363  
Scanner  
    modulation, 12, 89, 90  
    time-delay, 12  
    *see also* Sector-scanning sonar  
Scattering  
    acoustic, 7, 9, 20, 47, 51, 53, 56, 111, 217, 229,  
        233, 245, 265, 267, 277, 278, 280, 293  
    back-, 9, 10, 12, 13, 15, 16, 19, 51–3, 59, 81,  
        110, 111, 123, 124, 177, 181, 190, 212,  
        218, 219, 221, 233, 241, 246, 249, 264,  
        266–9, 271, 280, 284, 285, 288, 290,  
        293, 343, 344, 374, Plate 3.6, Plate 9.2  
    coherent, 193

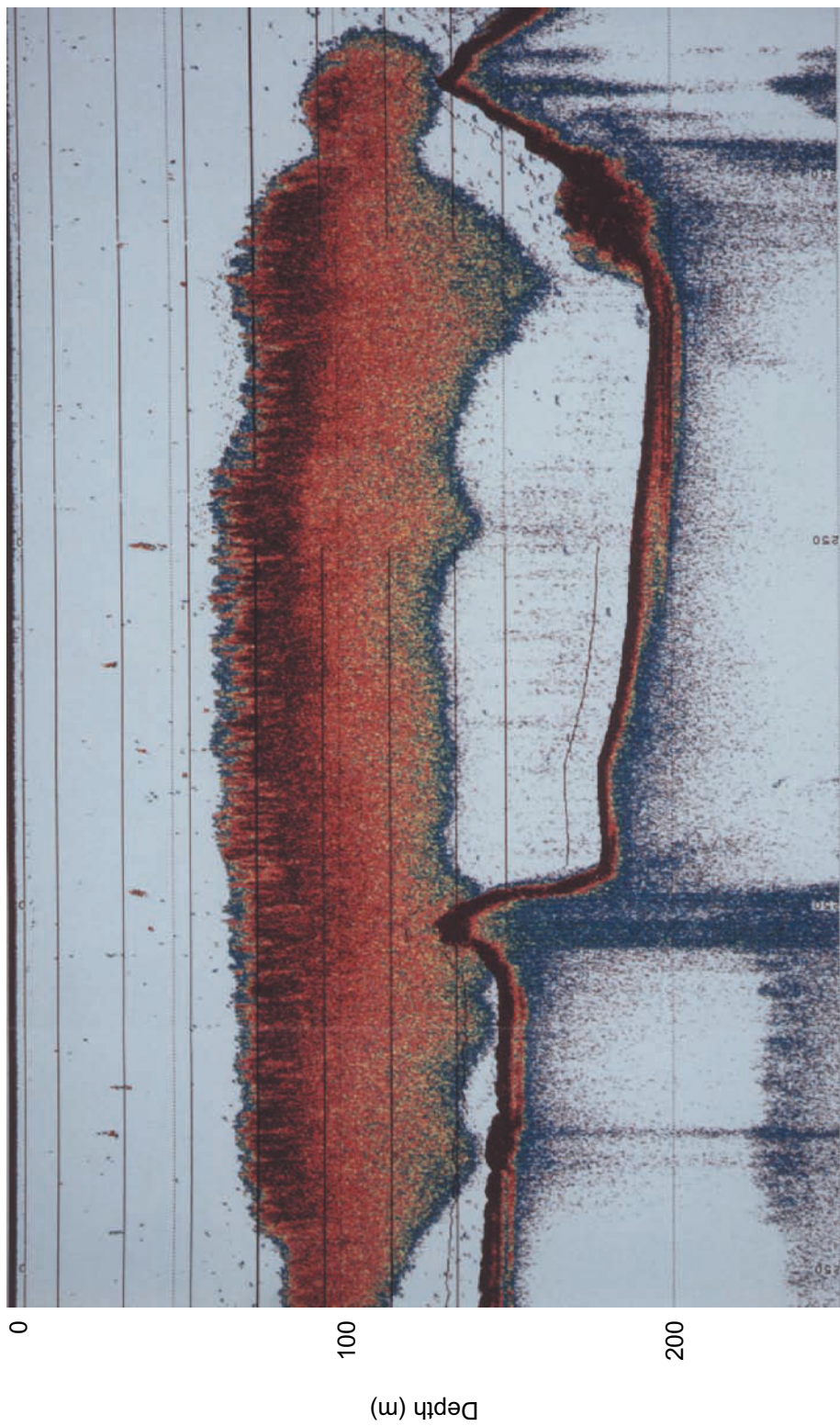
- forward, 163, 211, 212, 264–6  
geometric, 50, 271  
multiple, 14, 58, 159, 193, 194, 197, 198  
problem, forward, 163, 264–6  
problem, inverse, 61, 163, 267, 289  
specular, 16
- Scattering models, 8, 99, 229, 245, 262, 266, 274, 280, 285, 344  
boundary element method (BEM), 230, 232  
deformed cylinder (DCM), 229, 269, 278  
distorted-wave born approximation (DWBA), 269  
fluid sphere (Anderson), 267, 274, 289  
Fourier matching method (FMM), 231  
high pass, 267  
Kirchoff ray-mode (KRM), 230, 232, 245, Plate 6.1  
modal-series-based, 269  
prolate spheroid, 229, 230, 232, 269  
truncated Anderson, 267, 268, 290
- School  
counting, 13  
dimensions, 166, 174  
packing density, 98, 170, 174, 176, 195, 197  
shapes/morphology, 172, 174  
structure (nuclei, vacuoles), 169, 176, 281, Plate 9.4
- Sea bed, 1, 71, 73, 77, 86, 100, 149, 158  
classification, 87
- Sector-scanning sonar, 70, 88–90, 94, 97, 207
- Seine, (*see also* Purse seine), 4, 95, 209, 226
- Seismic survey, 145, 146, 154, 158
- Sensitivity, on-axis, 11, 34, 82, 110, 111, 115, 116, 120, 121, 368, 377
- Shading of arrays, 33, 34, 96, 99
- Shadow effect, 164, 193, 195–7
- Sharks, 133, 139
- Ship (*see also* Vessel), 12, 15, 17, 66, 71, 76, 77, 83, 85, 86, 94–6, 108, 113, 114, 158, 164–6, 168, 171, 189, 203, 228, 286, 296–8, 322, 325–7, 337, 356, 365–7, 370, 376
- Shock  
front, 13, 146–52  
wave, 7, 9, 10, 35, 127, 133, 146, 147, 149, 150, 151, 158
- Side lobe, 30–34, 80–82, 119, 190
- Side-scan sonar, 85–8, 171–4, 204, 206
- Signal-to-noise ratio (SNR), 10, 56, 65, 97, 104, 106, 168, 186, 202, 233
- Signature (*see also* Pressure), 148, 150, 153
- Similarity principle, 150
- Simulation, 304, 308, 351
- Sine wave, 10, 13, 21, 22, 36, 89, 192
- Single target, 65, 116, 121, 180, 184, 185, 188, 227
- Single-beam sonar, 207, 316
- Size distribution, calculation of true value, 163, 168, 169, 212
- Sizing of fish, 7, 67, 99, 152, 160, 177, 209, 217, 243, 250, 255, 256, 258–60, 300, 316, 333, 340
- SOFAR channel, 44, 45
- Solid  
angle, 12, 15, 32, 183, 190  
spheres (*see also* Sphere), 53
- Sonar  
active, 84, 100, 127, 139, 163, 203  
biological, 139, 144  
Doppler, 70, 98, 210, 372  
horizontal, 205, 206, 234  
long-range, 160  
mapping, 171  
multi-beam, 8, 70, 95, 103, 110, 124, 126, 163, 174–6, 207, 208, 226, 264, 372, Plate 3.6  
multi-frequency, 7, 16, 264, Plate 7.1
- omni, Plate 3.7
- passive, 84, 85
- scanning netsonde, 77, 79
- searchlight, 77, 85, 86
- sector-scanning, 6, 174
- single-beam, 207, 316
- split-beam, 209
- wide-band, 70, 99
- Songs of whales, 129
- Sound  
dosage, 155, 156  
field, 23, 28, 38, 48, 52, 54, 56, 133, 144, 157, 211, 245, 268, 280
- Sound waves, *see* Waves
- Source level (SL), 10, 25, 26, 37, 38, 61, 128, 140, 141, 158
- South China Sea, 316
- Sparker, 148
- Species identification, 99, 100, 105, 290, 291, 373, 376
- Specific heat, 13, 159
- Specular reflection, 49, 272
- Speed of sound, 36, 68, 69, 112, 118
- Sphere  
copper, 54, 112  
determination of optimal size, 55  
tungsten carbide, 55, 56, 112, 113, 221
- Spherical spreading, 39, 218
- Split-beam sonar, 5, 34, 70, 74, 80, 82–4, 89, 93, 103, 123, 125, 184, 185, 209, 210, 244, 248, 257–61, 283, 295, Plate 3.2
- Standard target (*see also* Target), 11, 12, 53, 55, 111–14, 117, 120, 122–5, 189, 363
- Stationary process, 8, 314, 347
- Stochastic variable, 177, 182, 184, 185, 219, 241, 246, 347

- Stock  
  assessment, 5, 374, 378, 379  
  estimation, 8, 110, 200, 261, 293–5, 299–301,  
    305, 307–9, 311, 314, 317, 321, 323–5,  
    330, 331, 337, 351, 354–6, 359, 360,  
    362, 363, 369–71, 374–9  
location, 330  
management, 1, 2, 294, 374, 379
- Stratification  
  effort, 8, 306, 316  
  water, 206, 281, 289
- Stridulation, 128, 129
- Student's t-statistic, 356, 357, 358
- Surface reflection, 149–51, 271, 272
- Survey  
  adaptive, 297, 299, 300, 317, 318, 321  
  cruise track, 8, 16, 17, 85, 86, 170, 295–9,  
    312–15, 319, 324, 326, 328–30, 336,  
    338, 346, 348–52, 357, 359, 369, 370  
  data collection, 87, 93, 295, 299, 300, 316,  
    322, 324, 347, 371  
  objectives, 299  
  outline, 318  
  planning, 296  
  reliability, 294  
  riverine, 294, 314, 316  
  sampling strategy, 8, 294–6, 306–8, 330,  
    357, 363  
  tests for performance, 356–9, 361, 362  
  *see also* Acoustic survey; Seismic survey
- Swept frequency transmission, *see* Chirp
- Swimbladder  
  absence and consequences thereof, 84, 151,  
    223, 237, 239, 249  
  contraction-rate factor (g), 239  
  gas replenishment, 237  
  influence on target strength, 218, 247, 362  
  oscillation parameter, 13  
  resonance, 7, 13, 67, 127, 161, 229  
  shape/morphology, 231, 232  
  physoclistous, 151, 152, 159, 160, 161, 251,  
    255, 256  
  physostomous, 151, 152, 159, 160, 249,  
    250, 258  
  wax or ester filled, 249
- Tag, acoustic (*see also* Pinger), 101
- Target  
  moving (*see also* Doppler effect), 97, 142  
  multiple, 58, 59, 84, 179, 184, 227, 247  
  standard, 54–6, 112, 113, 221  
  tracking, 70, 95, 96, 101, 102, 185, 209
- Target strength  
  depth dependence, 238  
  estimation, 182, 228  
  fish, 237, 239, 250, 261  
  in situ measurement, 225
- indirect measurement of, 226  
length dependence, 242, 250, 344
- physoclists, 151, 152, 159, 160, 161, 251,  
  255, 256
- physostomes, 151, 152, 159, 160, 249,  
  250, 258
- plankton, 267, 268, 274
- reduced, 245, 255
- shellfish, 282
- size dependence, 8, 250
- as a stochastic variable, 7, 177, 182, 184, 185,  
  219, 241, 243, 246, 255, 347
- surface-adapted, 15, 240
- Temperature, 10, 22, 35, 41–4, 55, 67–9, 74, 77,  
  100, 120, 159, 191, 277, 287, 294, 300,  
  329, 363, 367, 368
- effect on acoustic absorption, 40, 41, 67
- effect on sound speed, 42, 68
- see also* Thermocline
- Thermocline, 42, 44, 72, 77, 205, 289, 367
- Threshold  
  auditory, 130–36, 138, 155–7  
  bias engendered by, 185, 201  
  signal, 167, 168, 181, 185, 201, 202, 233
- Tilt angle, 56, 57, 194, 220–22, 225, 228, 229,  
  231–4, 245–8, 251, 253, 255, 269–71, 278,  
  279, 284, 372, 373
- Time-constant, 13, 147, 148, 149
- Time-delay scanner, *see* Scanner
- Time-varied gain (TVG), 61, 110, 118, 182,  
  202, 207  
  correction factor, 9, 110, 111, 190, 215, 368  
  distributed targets, 118, 188, 189  
  function, 11, 13, 118, 180, 189, 368  
  optimum start time, 12, 118, 119  
  single targets, 122, 180
- TNT (*see also* Explosives), 147, 148, 149, 153
- Towed transducer body  
  deep-towed, 104  
  shallow-towed, 70, 103–5  
  sidescan, 85
- Track (of survey vessel; *see also* Cruise track),  
  14, 85, 87, 90, 91, 95, 166, 168, 170, 171,  
  172, 176, 209, 210, 212, 213, 228, 253,  
  297–300, 310, 312–15, 321, 324, 346, 349,  
  354, 359, 360, 361, 367, 370, 372,  
  Plate 3.5, Plate 3.7
- Transducer  
  array, 26, 34, 35  
  beam pattern, 15, 33, 80, 81, 190, 222,  
    228, 233  
  ceramic (piezo-electric), 25–8, 119  
  effect of motion on data collected, 363,  
    376, 377  
  element, 27, 34, 35, 39, 89, 90, 91  
  gain, 12, 120, 121  
  magnetostrictive, 4, 25, 26

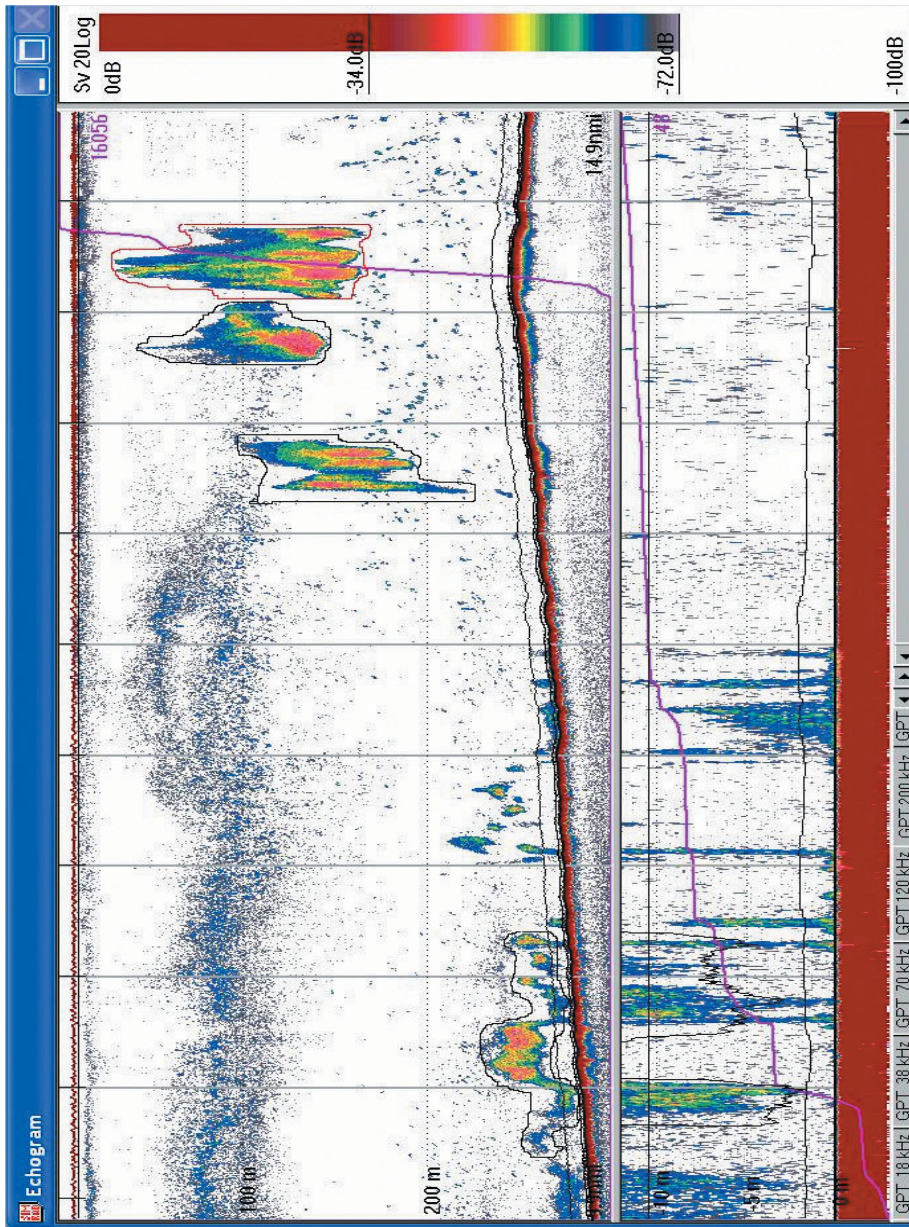
- mounting, 103, 105, 110, 288, 376  
 size, relationship to beam width or frequency, 63, 99
- Transect  
 adaptive, 320  
 completely random, 303, 305, 306, 308, 309, 371  
 length, 310, 317, 319, 369  
 parallel, 321, 357  
 pre-planned, 303, 309  
 randomized, 313  
 spacing of, and choice of direction, 297, 309–14, 318–20, 370  
 stratified, 300  
 time allocation cf. trawling, 301, 302  
 triangular, 17, 36, 38, 100, 309, 310, 313, 315  
*see also* Grid
- Transmission loss, 160, 188, 265
- Transmitter, 3, 11, 12, 15, 31, 46, 51, 63, 65, 71–3, 81, 88, 112, 116, 118, 177, 178, 180, 188, 202, 212, 215, 218, 221, 230, 363
- Transponder, 100
- Transverse sound wave, 10, 11, 23, 53, 112, 113
- Trawling, pelagic  
 in acoustic surveying, 301, 302  
 aimed, 340  
 role of netsonde, 70, 76–8
- TS (*see also* Target strength), 10, 16, 25, 52, 53, 66, 82, 112, 113, 120, 123, 124, 155, 182, 206, 207, 209, 220, 222, 223, 233, 235, 240–46, 249, 250–53, 255, 256, 258–61, 264, 276, 278–85
- Tungsten carbide sphere (*see also* Sphere), 55, 56, 112, 113, 221
- TVG (*see also* Time-varied gain), 9, 11–14, 61, 62, 110, 111, 118–20, 122, 180, 188–91, 202, 207, 215, 368, 369
- Ultrasound, 137, 138
- Variance, 12, 17–19, 100, 122, 123, 300, 301, 303–10, 317, 320, 324, 349, 351–6, 358, 359, 361, 362, 371, 373, 377
- Variance, precision of, 308
- Variogram, 18, 301, 354, 355, 358
- Vertical migration, 160, 162, 249, 263, 370, 376
- Vessel, 4, 6, 65, 72, 76, 77, 83, 85, 86, 88, 90–93, 95–7, 102–4, 106–9, 114, 156, 171, 175, 176, 201, 226, 239, 253, 317, 318, 322–7, 364, 367, 369, 370, 373, 375, Plate 3.4, Plate 3.6, Plate 3.7, Plate 3.8, Plate 5.1
- noise, 62, 102, 109
- speed, 324, 372, Plate 5.1
- Viscosity, 67
- VPA, 377, 378
- Wave  
 backscattered, 10, 51, 58, 218  
 Franz, 272  
 incident, 10, 11, 16, 48, 50, 51, 56, 58, 60, 133, 160, 197, 218, 230, 269, 272  
 Lamb, 16, 271, 272, 273  
 longitudinal, 10, 11, 23, 53, 112  
 plane, 21–3, 40, 230  
 reflected, 47, 48, 50, 57, 58, 60  
 shear, 269, 274  
 sine, 10, 13, 21, 22, 36, 89, 192  
 sound, 1, 6, 9, 10, 20–23, 27, 28, 43, 127, 129, 131, 133, 139, 146, 180, 218, 365, 367  
 spherical, 22, 23, 39, 48, 218  
 transverse, 10, 11, 23, 53, 112, 113
- Waveform, 36, 47, 56, 58, 117, 125, 146, 147, 149, 152, 190
- Wave-front, 21–3, 28, 31, 38, 39, 42, 43
- Wavelength, 10, 21–3, 27, 28, 30, 31, 34–6, 39, 48, 50, 54, 56–8, 66, 120, 131, 193, 229, 250, 278, 284
- Wavenumber, 9, 16, 22, 268, 269, 271
- Whale songs, 129
- Whistle, *see* Echo location, 139
- Wide-band sonar, 70, 99
- Working time (*see also* Track), 297, 298
- Year class, 240–42, 378
- Zooplankton, 229, 263, 265, 266, 273, 277, 278, 280, 281, 286, 289, 291, 292, 334, Plate 7.1



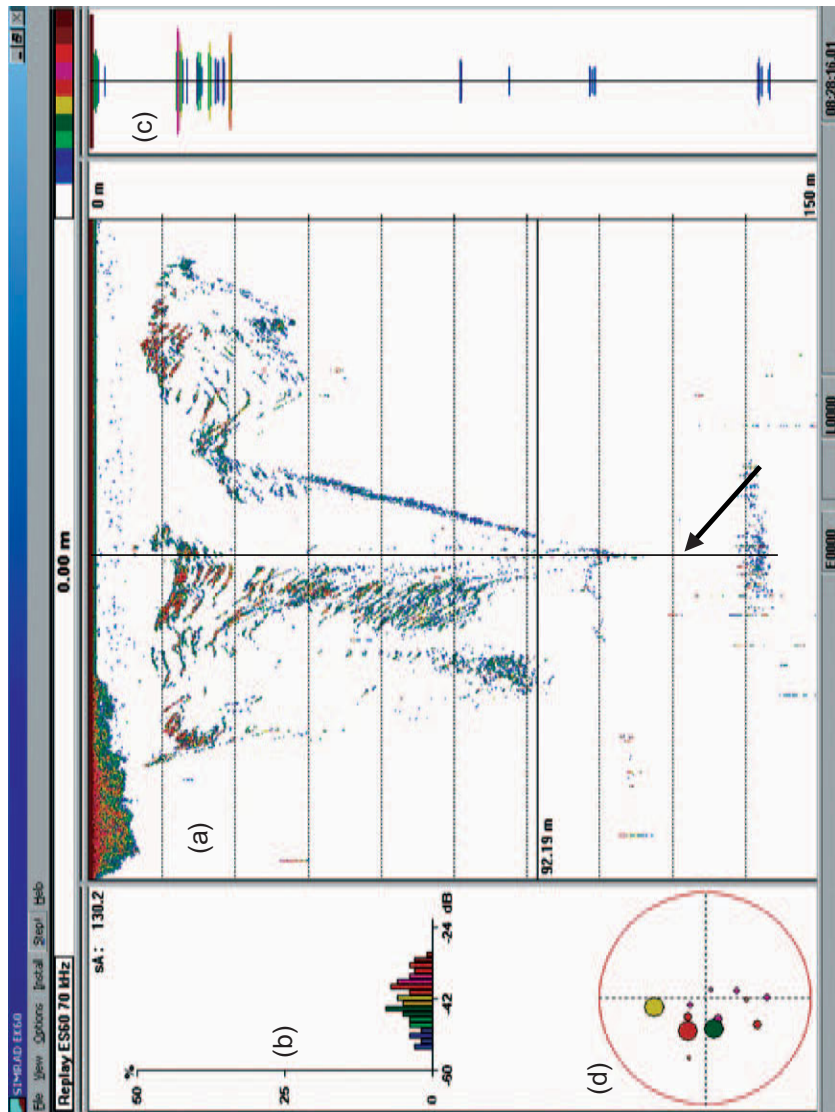
**Plate 3.1** Echogram displayed on a colour printer showing low density aggregations of small fish in Oslo Fjord, Norway. Simrad EK500 echosounder, 38 kHz frequency and 40 log R time-varied-grain. Vertical scale 0–100 m depth. Numbers printed on the echogram show (left column) measured target strengths of individual scatterers and (right column) echo-integrals in three depth layers. (Reproduced with permission from Simrad Norge AS.)



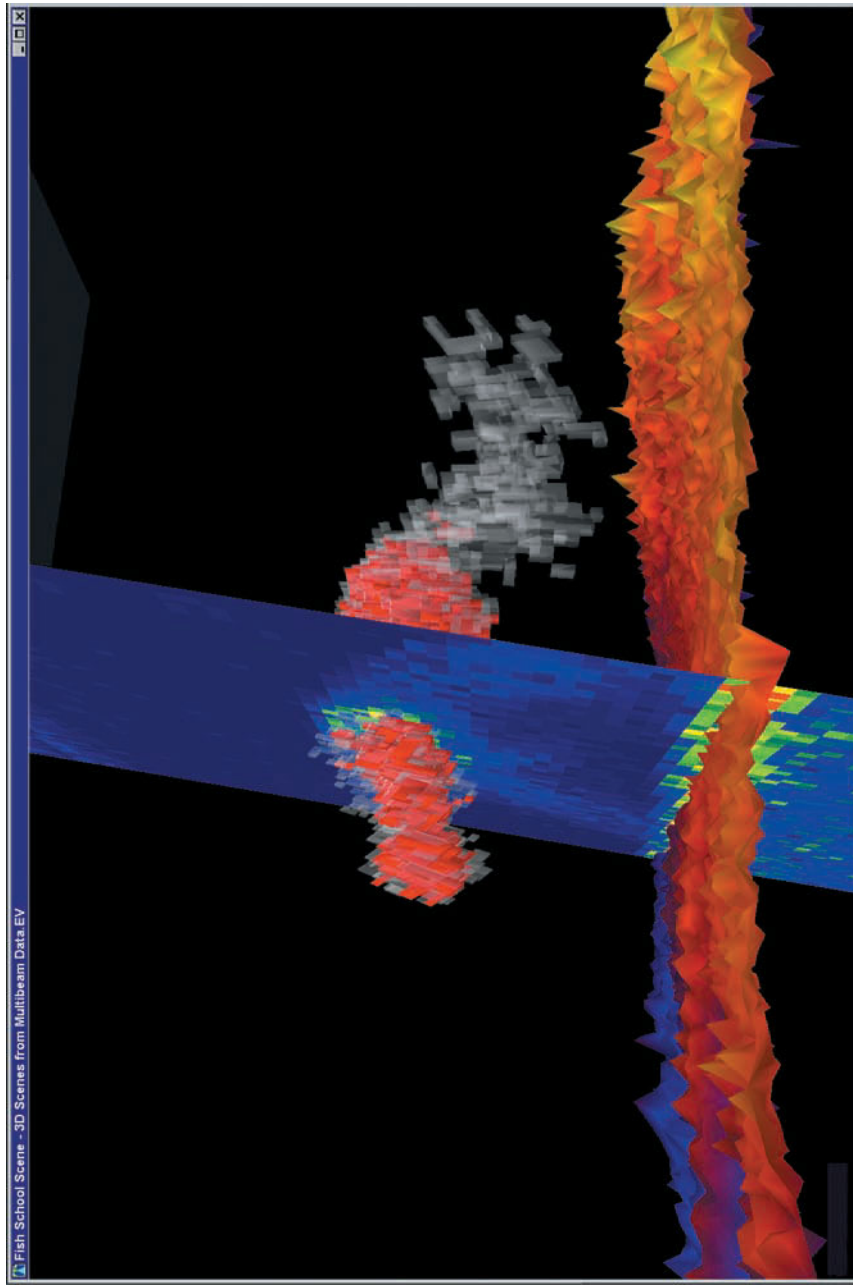
**Plate 3.2** Echogram of a large herring school in Gratangen Fjord, Norway, recorded on RV 'Michael Sars' using a Simrad EK500 split-beam echosounder operating at 38 kHz. The school is about 5.5 km long and 60 m deep on average.



**Plate 3.3** Example of a post-processed echogram. Upper panel shows four groups of fish schools selected by the manually-drawn black outlines, and an integrgram (red line) for the 150–200 m depth interval. Lower panel shows a bottom-following channel (10 m deep, also shown in the upper panel) and the integrgram for this channel over the full width of the echogram. (Reproduced with permission from Simrad Norge AS.)

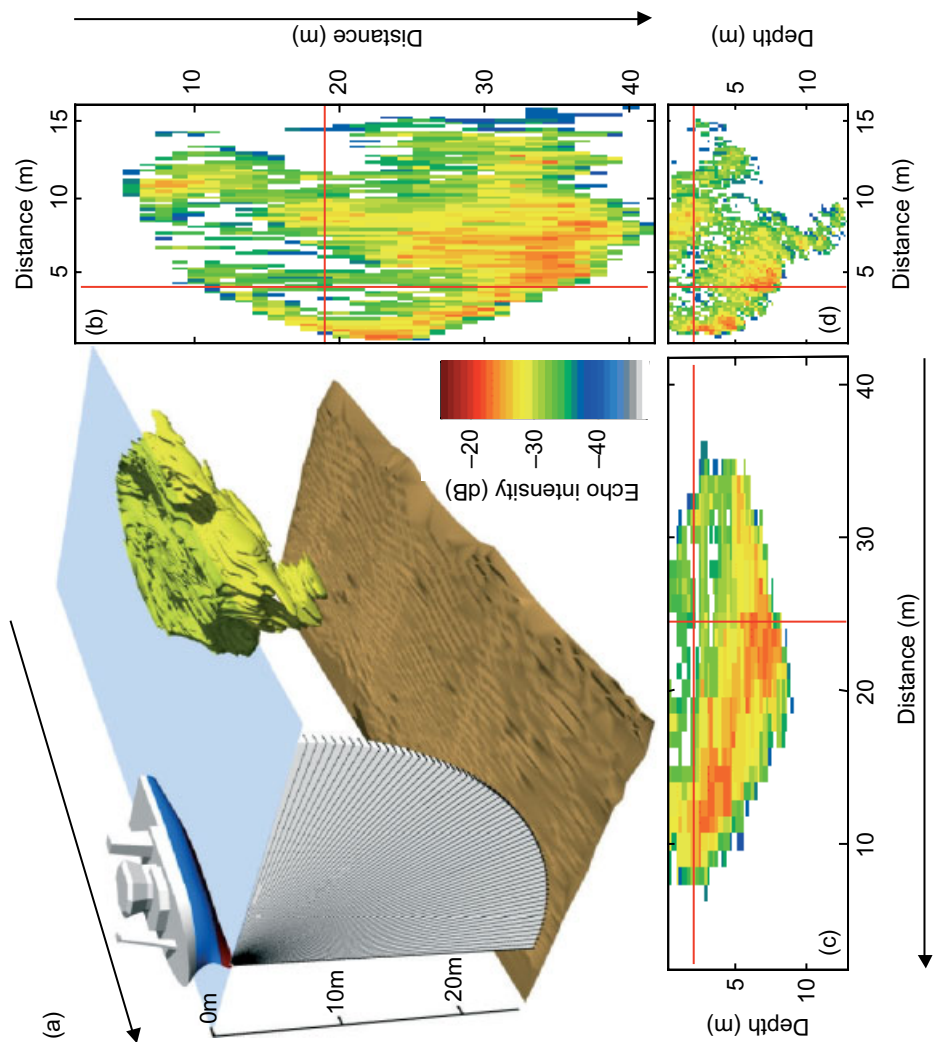


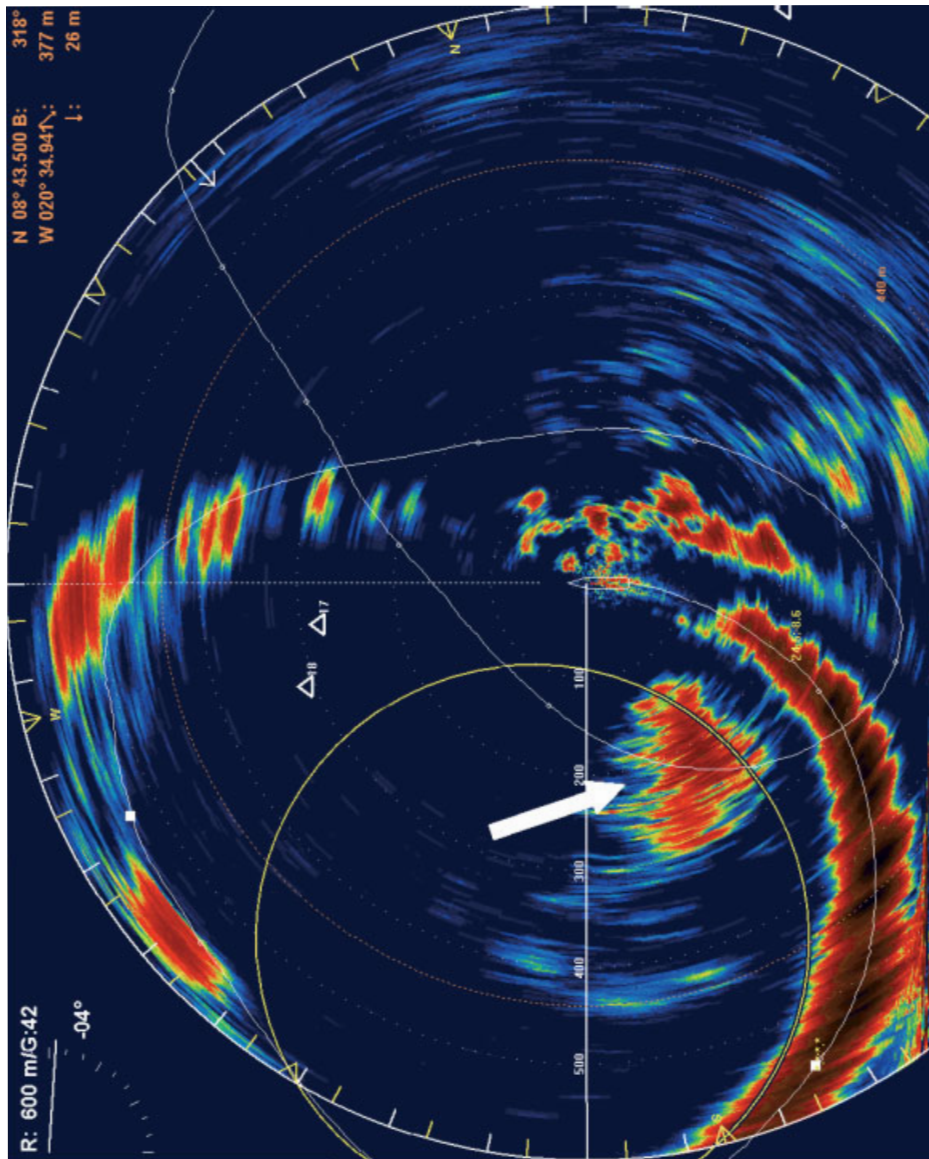
**Plate 3.4** Target strength measurements. The display shows an EK60 echogram (a) recorded in the Indian Ocean ( $3^{\circ} 2.5'N$ ,  $53^{\circ} 47.6'W$ ) on fishing vessel 'Kersaint de Coetnempren' at approx 10.30 local time. The vessel is moving slowly past a fish aggregation device (FAD). 50 tonnes of fish (95% skipjack, *Katsuwonus pelamis*, 40–70 cm and 5% bigeye, *Thunnus obesus*, 40–60 cm) were caught at the FAD. The target strength histogram (b) contains values mostly from the skipjack, but the larger values are probably from the bigeye which are the stronger targets. The vertical display (c) and the horizontal distribution of detected targets (d) come from the location arrowed. The vertical excursion illustrated in the echogram is typical of tuna in this situation. (With thanks to Erwin Josse who provided this recording.)



**Plate 3.5** Three-dimensional representation of a fish school (in red, *Coregonus artedii*) at 16 m depth in Lake Opeongo, Canada. The school is 30 by 15 m across and 4 m high. The grey area represents the same school detected with a lower threshold. Average seabed depth is 24 m. Data obtained with a 128-beam Simrad SM2000 swathe sounder and displayed using SonarData Echoview software. Beam 50 is shown as the blue 'curtain' along the track (into the picture). Schools are detected and extracted after thresholding and a 3 by 3 'closure' operation giving two-dimensional (ping-based) smoothing. (With thanks to SonarData pty, Kongsberg Simrad Mesotech, the Ontario Ministry of Natural Resources and the Scientific Assessment Technology Laboratory.)

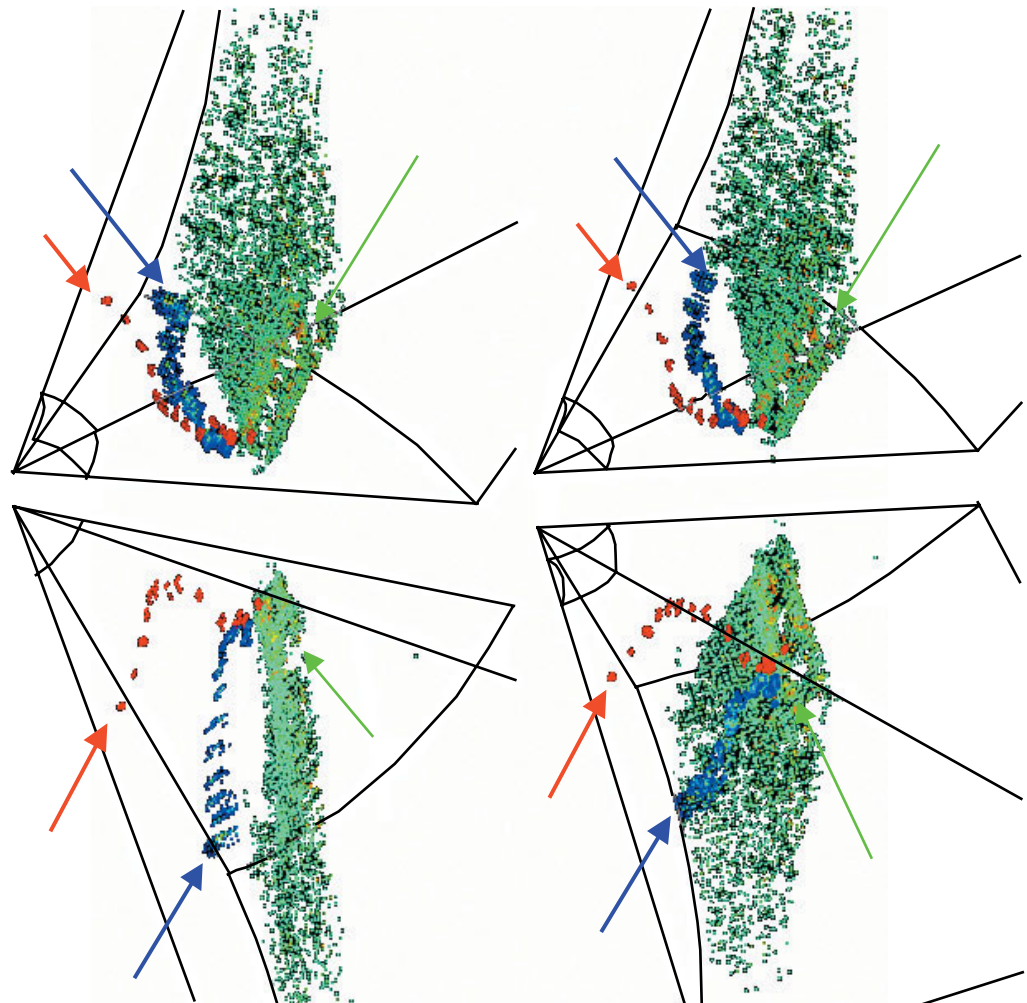
**Plate 3.6** Images of a *Sardinella aurita* school. Data collected with a 455 kHz Reson Seabat multi-beam sonar. Arrows indicate the vessel route. (a) The 3D reconstruction allows determination of school parameters (volume 2260 m<sup>3</sup>, surface area 5796 m<sup>2</sup>, overall length 41.6 m, width 16.7 m, height 14.9 m, MVBS –26 dB) and locates the school relative to the seabed (12 m) and the vessel route (8 m). The fan of 60 receiving beams for one ping is illustrated at the front of the vessel. The panels show cross-sections of the backscattering intensity in three planes: (b) horizontal; (c) vertical alongships; (d) vertical athwartships. Red cross-hairs in each panel indicate the locations of the other two cross-sections. (Reproduced with permission from Paul Fernandes, Fisheries Research Services.)





**Plate 3.7** Omni-sonar display as a purse seiner circles a school of yellowfin tuna (arrowed). Simrad omni-sonar. The vessel track is shown by the thin white line; the propeller wake can be seen as the irregular red/brown arc at the bottom left of the picture. (Reproduced with permission from Simrad Norge AS.)

**Plate 3.8** Four views of a single 3D image of fish entering a demersal trawl, from data obtained with the Omnitech sonar and viewed using the OpenGL software package. The images were recorded in the Barents Sea during November 2003 on board the Norwegian research vessel 'Sarsen'. The sonar was mounted on the headline looking backwards into the mouth of the trawl. The footrope of the trawl can be seen as a raised ridge along the lower leading edge of the images (arrowed in green). The post-processed tracks of two fish (probably cod) entering the trawl just in front of the footrope can be seen; one fish is moving upwards (arrowed in red) while the other remains closer to the belly of the trawl (arrowed in blue). This kind of fish tracking is used to investigate species-specific behaviour for the development of more selective trawl gears. (Reproduced with permission from Norman Graham, Institute of Marine Research, Bergen.)



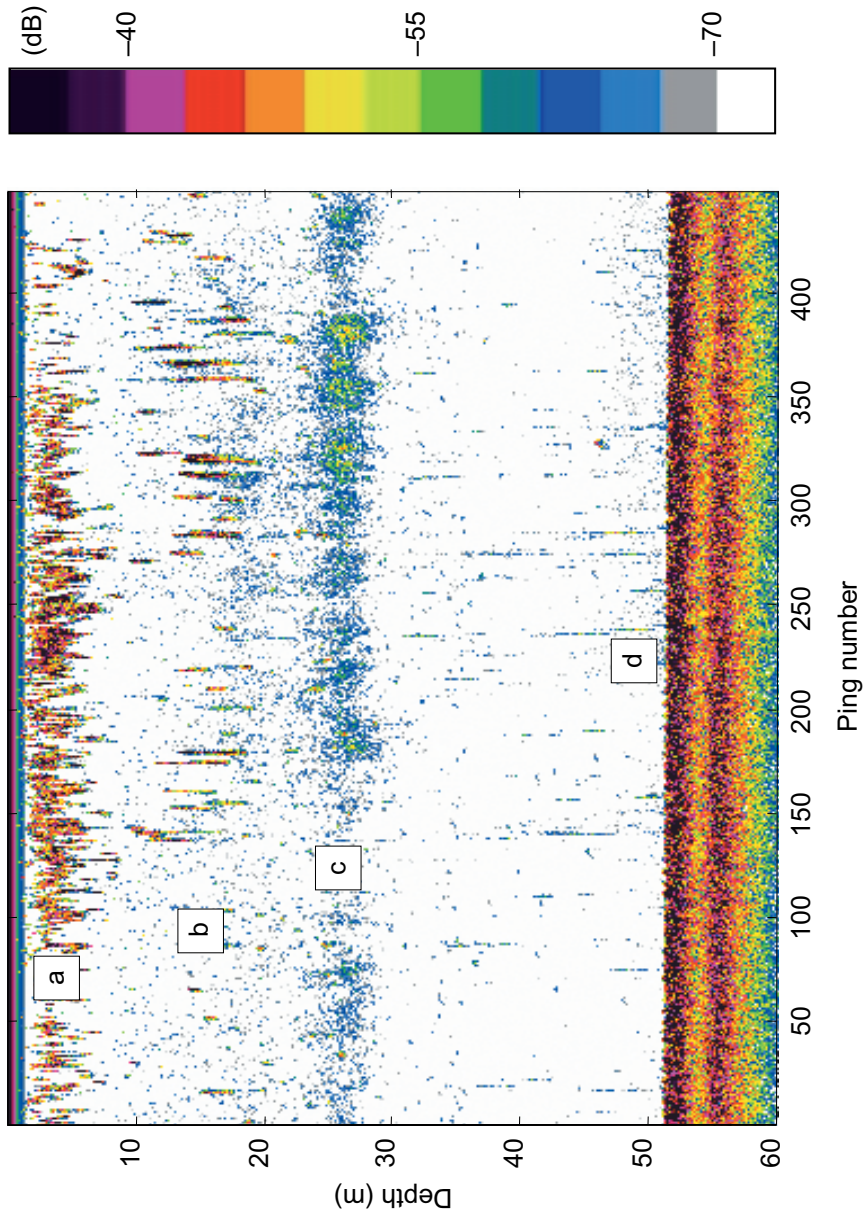


**Plate 5.1** The colour echogram displays the volume scattering strength ( $S_v$ ) by the colour of each pixel. This example, recorded in Lake Victoria (East Africa) at 09:40 on 5 September 2001, shows four target layers distinguished by their  $S_v$  composition as well as depth. Sounder frequency 120 kHz; ping rate  $1\text{ s}^{-1}$ ; vessel speed 10 knots ( $5.14\text{ m s}^{-1}$ ). The colour scale is on the right. Colours change in 3 dB intervals from grey (weakest) to black (strongest). The layers are: (a) dense schools of dagaa *Rastrineobola argentea*; (b) a mixture of Nile perch *Lates niloticus*, haplochromines and other species; (c) medium density of small pelagics; (d) weak scattering just above the  $-70\text{ dB}$  threshold, plankton and/or the shrimp *Caridina nilotica*.

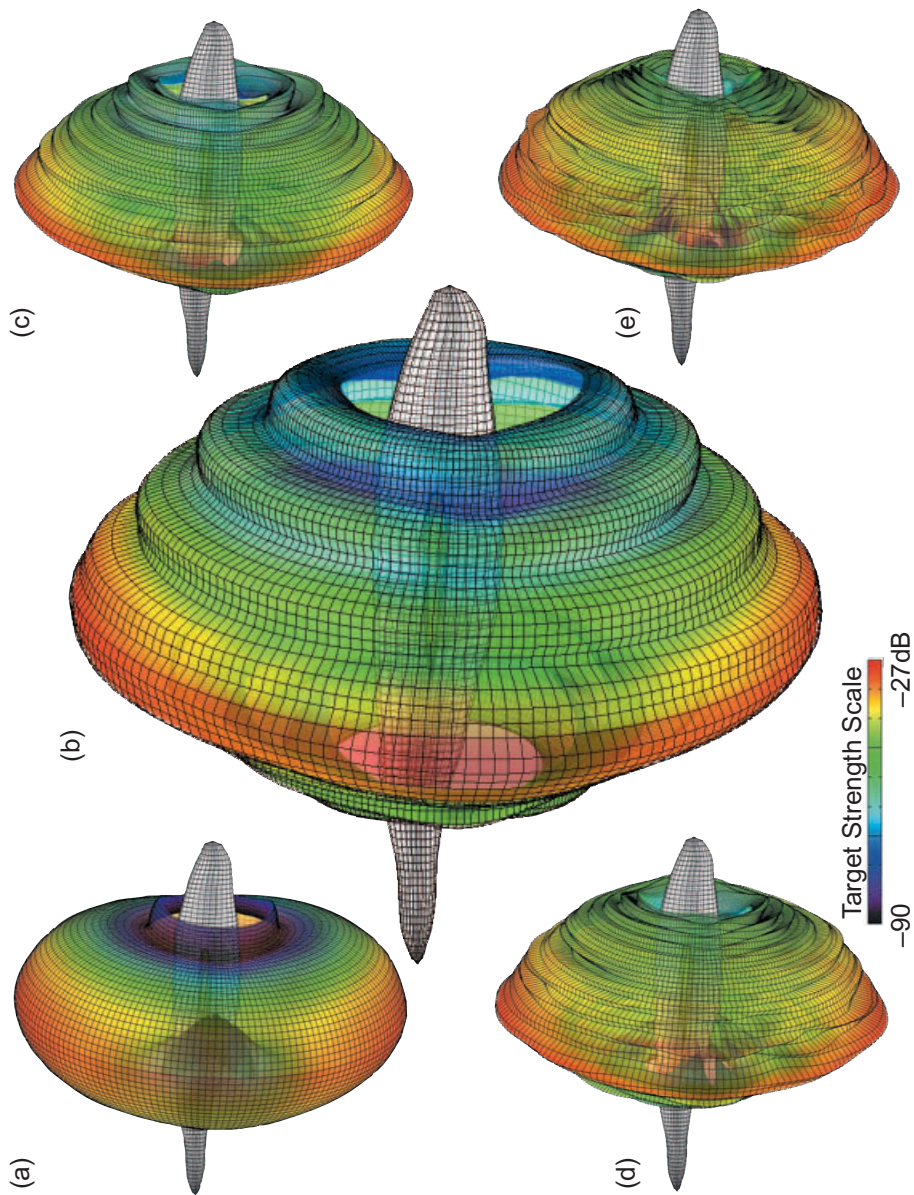


**Plate 6.1** Visualization of the target strength of a 34.4 cm cod at 5 frequencies (a) 12 kHz, (b) 38 kHz, (c) 70 kHz, (d) 120 kHz and (e) 200 kHz. Computed values based on the KRM model. Results are shown for incidence angles from 90° down to 15° off the long axis of the fish. The modelled swimbladder is visible as the small structure in the centre of the fish. (Reproduced with permission from John Horne and Rick Towler, University of Washington, Seattle.)

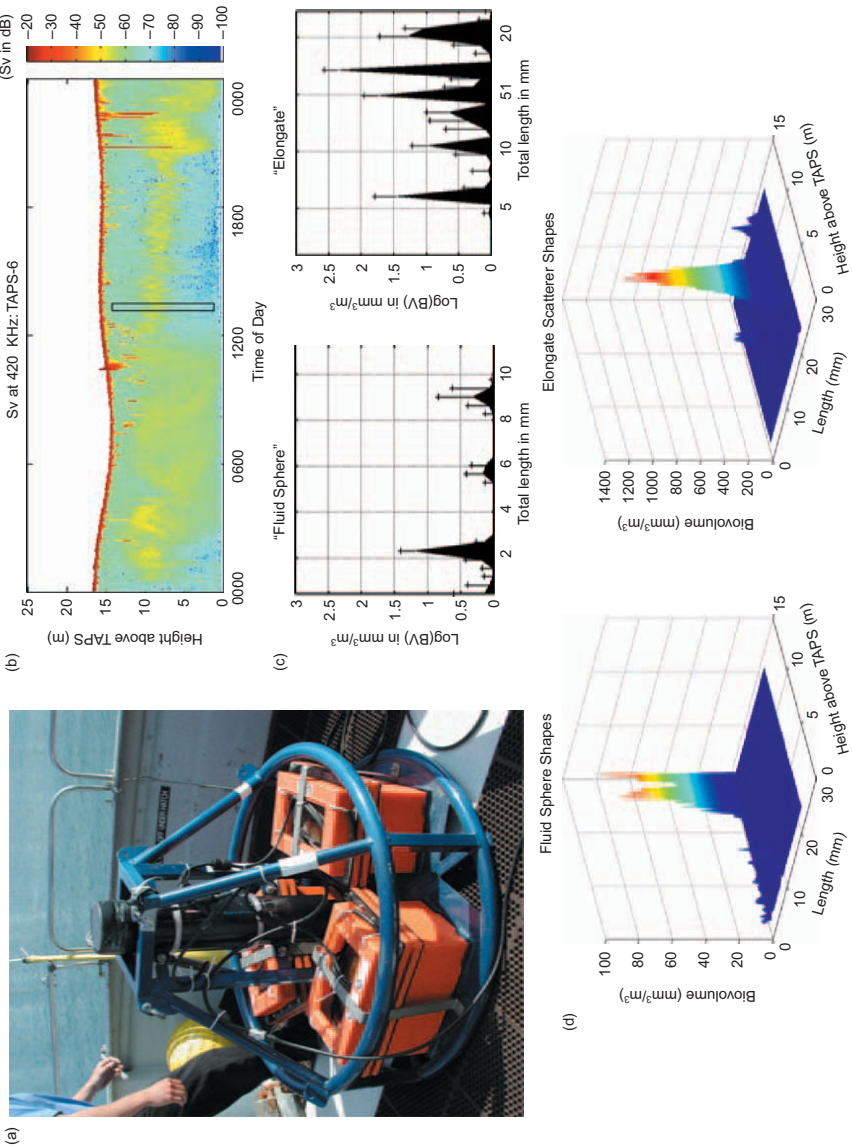


**Plate 7.1** (a) The TAPS-6 multi-frequency sonar configured for upward beaming from a fixed seabed installation with six frequencies from 265 to 3000 kHz. (b) Echogram at 420 kHz recorded over 24 hours; the transducer is on the bottom and the undulating red line is the water surface; the volume scattering is predominantly from zooplankton; the rectangle indicates the zone selected for multi-frequency analysis leading to (c) biovolume distributions for two types of zooplankton; the filled bars and + show, respectively, the mean and maximum biovolumes in each size mode. (d) The same results in 3D plots showing variations with depth as well as size. (Reproduced with permission from Van Holliday, Tracor Inc.)

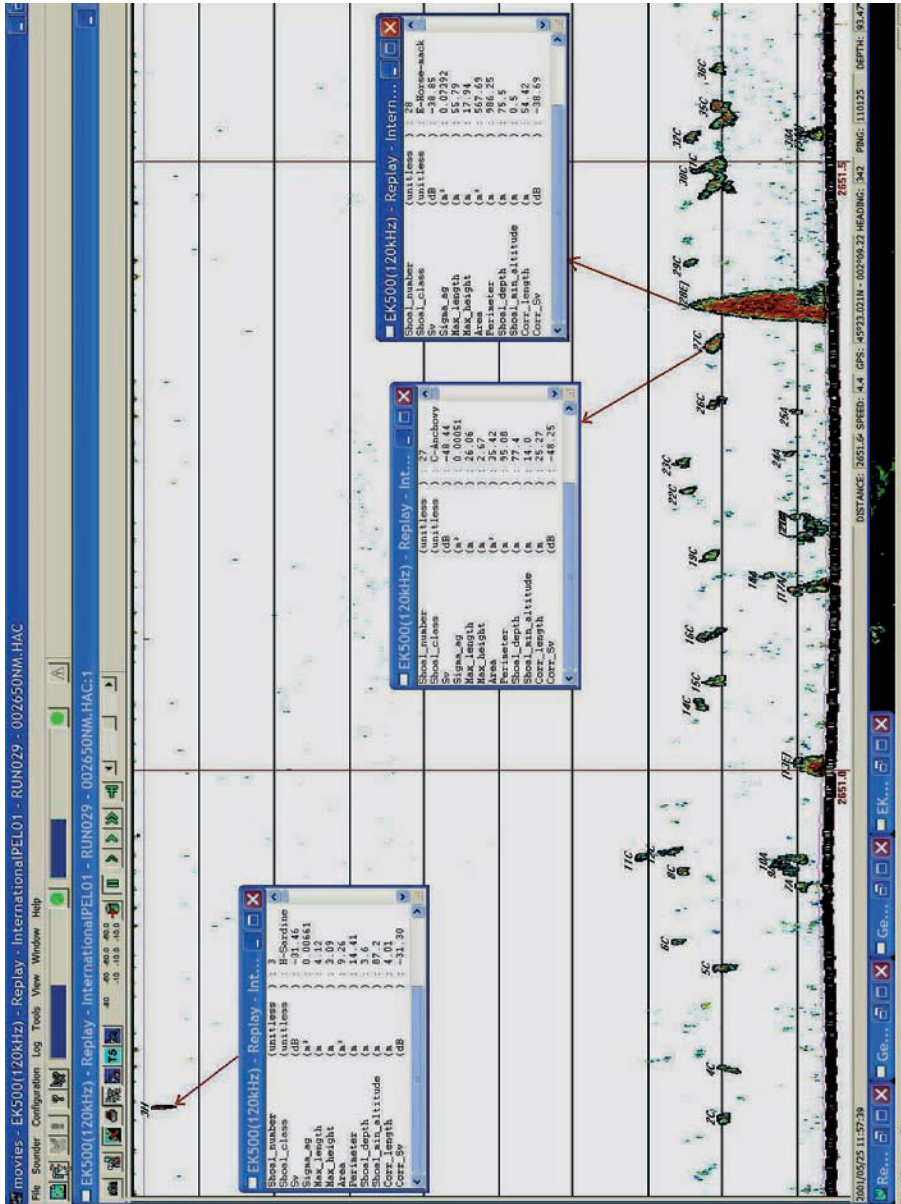


**Plate 9.1** Illustration of the extraction and labelling of fish schools using the MOVIES+ software. This automatically extracts objects and assigns these to identification categories based on extracted parameters. The panels show various attributes of the extracted schools. (Reproduced with permission from Noel Diner and Laurent Berger, Ifremer, France.)

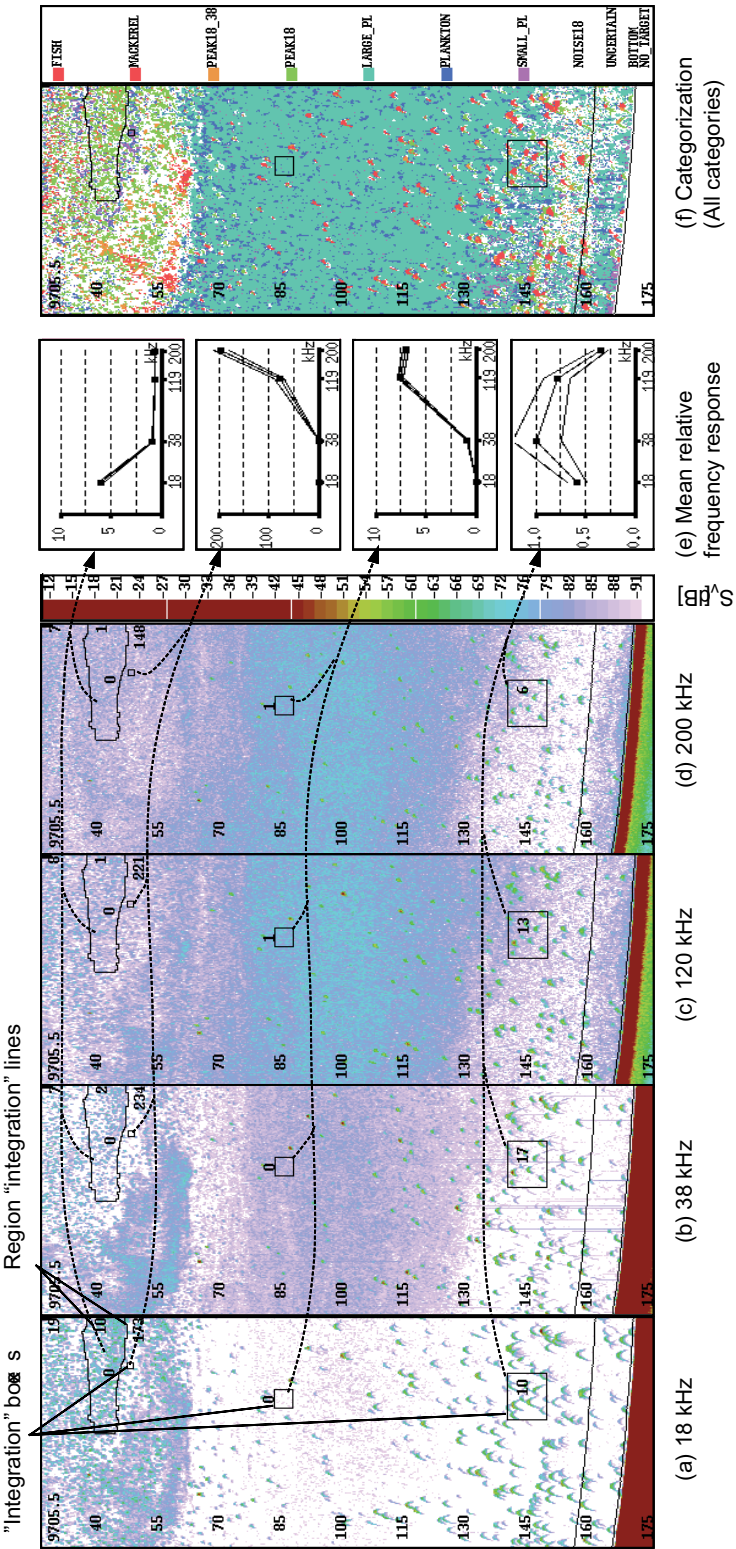


**Plate 92** The synthetic echogram. (a–d) show conventional echograms at four frequencies, recorded over 0.5 nmi distance in Balsfjorden, Norway. (e) Four classes of target are identified by their relative frequency response. The classification is used to derive a synthetic echogram (f) which still locates the echoes in space but the colours now indicate the target category, not the backscattering strength. The colour scale beside (f) shows the correspondence between the acoustic categories and the colours. (Reproduced with permission from Korneliussen and Oma 2003.)

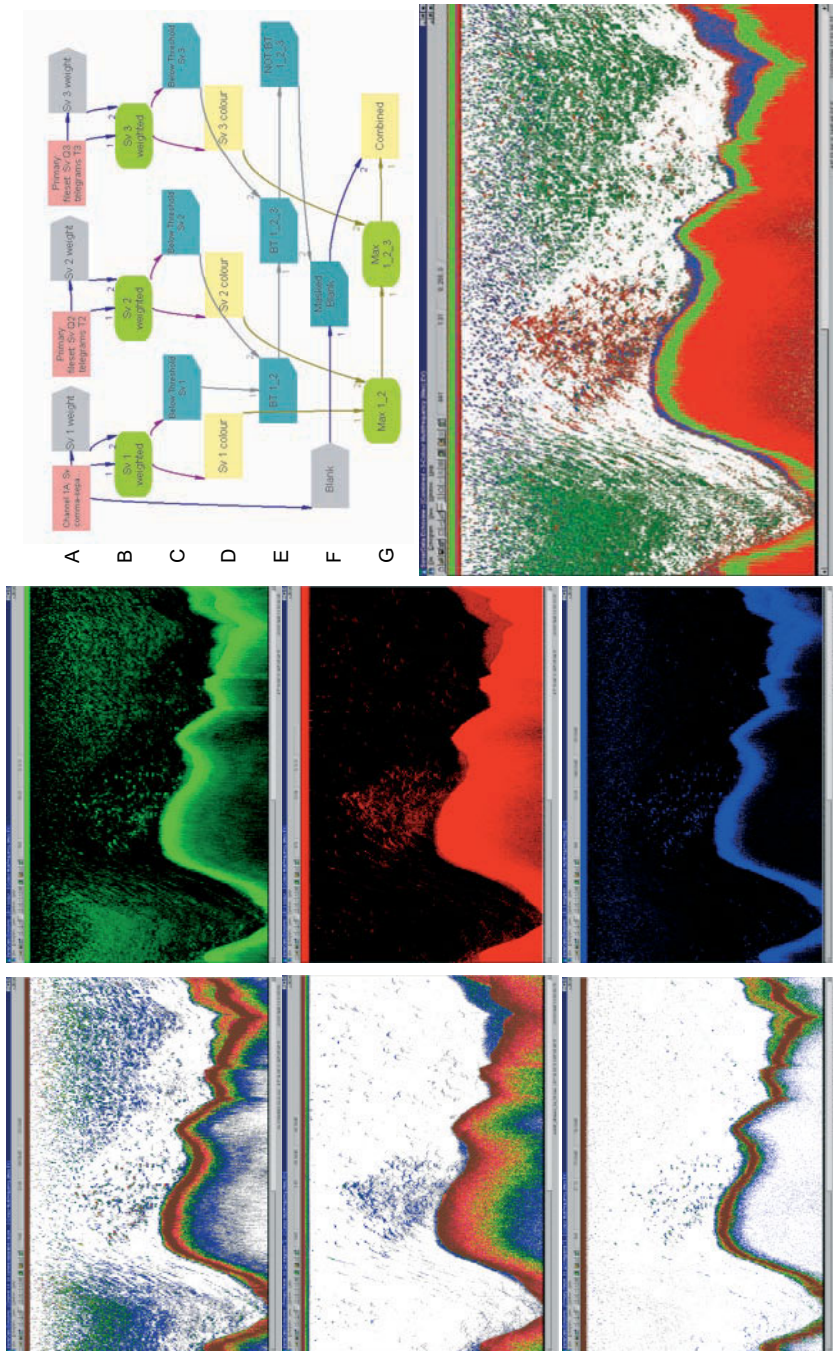


**Plate 9.3** Multi-frequency synthetic echogram (bottom right) constructed in the manner described by Kloser *et al.* (2002). Red, green and blue are assigned to 12, 38 and 120 kHz respectively. The echogram shows St Helens Hill seamount, Tasmania, July 1996 during an orange roughy (*Hoplostethus atlanticus*) spawning event. Seabed depth approximately 800 m. Data recorded from three transducers mounted on a deep-towed body. The method is illustrated in the flow diagram (top right). Rows A and B weight the three echograms; rows C and E threshold the combined echogram; row D assigns colour to each frequency; rows F and G construct the final echogram. (Reproduced with permission from an image prepared by SonarData using Echoview. With thanks to Mathew Wilson, Tim Ryan and Rudy Kloser.)

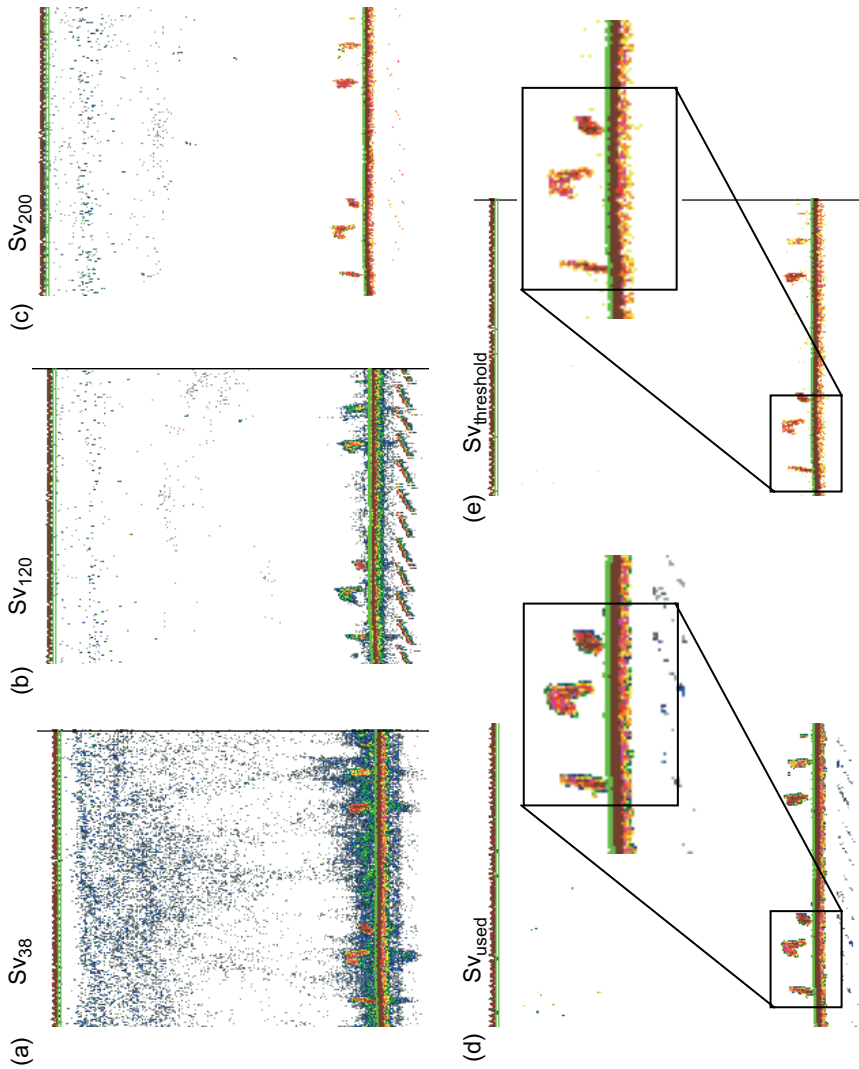


**Plate 9.4** Multi-frequency extraction of fish schools. Panels (a–c) are echograms of the same fish recorded at 38, 120 and 200 kHz. The higher frequency measurements are used to mask those at 38 kHz, thus removing the plankton echoes and extracting the fish schools without the need for any threshold on the 38 kHz signals. (d) The outcome of the masking procedure shows clearly defined schools. (e) When the extraction is done by conventional thresholding, the school structure is eroded; some fish as well as plankton echoes are evidently removed.